

INTERNATIONAL COUNCIL FOR BUILDING RESEARCH STUDIES AND DOCUMENTATION

WORKING COMMISSION W18 - TIMBER STRUCTURES

CIB - W18

MEETING TWENTY - Nine

BORDEAUX

FRANCE

AUGUST 1996

Lehrstuhl für Ingenieurholzbau und Baukonstruktionen
Universität Karlsruhe
Germany
Compiled by Rainer Görlacher
1996

ISSN 0945-6996

CONTENTS

- 0 List of Participants
 - 1 Chairman's Introduction
 - 2 Cooperation With Other Organisations
 - 3 Strength Grading
 - 4 Stresses for Solid Timber
 - 5 Timber Joints and Fasteners
 - 6 Laminated Members
 - 7 Environmental Conditions
 - 8 Timber Beams
 - 9 Structural Stability
 - 10 Structural Design Codes
 - 11 Any Other Business
 - 12 Venue for the Next Meeting
 - 13 Close
 - 14 List of CIB W18 Papers/Bordeaux, France 1996
 - 15 Current List of CIB W18 Papers
- CIB-W18 Papers 29-5-1 up to 29-102-1

0 List of Participants

**INTERNATIONAL COUNCIL FOR BUILDING RESEARCH STUDIES
AND DOCUMENTATION**

WORKING COMMISSION W18 - TIMBER STRUCTURES

MEETING TWENTY-NINE

BORDEAUX, FRANCE, 26-29 AUGUST 1996

LIST OF PARTICIPANTS

AUSTRALIA

R Leicester DBCE, CSIRO, Victoria

AUSTRIA

G Schickhofer Techn. University of Graz

CANADA

E Karacabeyli Forintek Canada Corp., Vancouver
F Lam Departement of Wood Science UBC, Vancouver
H G L Prion Departement of Civil Eng. UBC, Vancouver
I Smith University of New Brunswick

CZECH REPUBLIC

P Kuklik Czech Technical University in Prague

DENMARK

H J Larsen Danish Building Research Institute, Hørsholm

FINLAND

J Kangas VTT Building Technology, Espoo
T Poutanen Tampere University of Technology
A Ranta-Maunus VTT Building Technology, Espoo

FRANCE

L Daudeville LMT, Cachan
L Davenne LMT, Cachan
E Fourneley C.U.S.T. Aubière Cedex
P Galimard LRBB, Bordeaux
P Morlier LRBB, Bordeaux
P Racher C.U.S.T. Aubière Cedex
F Rouger CTBA, Paris

GERMANY

H J Blaß	University of Karlsruhe
N Burger	University of Munich
J Ehlbeck	University of Karlsruhe
R Görlacher	University of Karlsruhe

JAPAN

M Yasumura	Shizuoka University, Shizuoka
------------	-------------------------------

NETHERLANDS

A D Leijten	Delft University of Technology
-------------	--------------------------------

NORWAY

K H Solli	Norwegian Institute of Wood Technology, Oslo
-----------	--

POLAND

B Szyperska	Building Research Institute. Warszawa
-------------	---------------------------------------

SWEDEN

C J Johansson	Swedish National Testing and Research Institute, Borås
B Källsner	Swedish Institute for Wood Technology Research, Stockholm
J König	Swedish Institute for Wood Technology Research, Stockholm

SWITZERLAND

E Gehri	ETH, Zürich
A U Meierhofer	EMPA, Dübendorf

UK

R J Bainbridge	TRADA Technology Limited, High Wycombe
T D G Canisius	Building Research Establishment, Watford
D R Griffiths	University of Surrey, Guildford
C Holland	Building Research Establishment, Watford
J Marcroft	Eleco Technology, Aldershot
C J Mettem	TRADA Technology Limited, High Wycombe
R Marsh	Consultant - TRADA, London
A P Reffold	Eleco Technology, Aldershot
L R J Whale	Eleco Technology, Aldershot

USA

B Weeks	American Forestry & Paper Association, Washington D.C
S Zylkowski	APA - The Engineered Wood Association, Tacoma

- 1. Chairman's Introduction**
- 2. Cooperation With Other Organisations**
- 3. Strength Grading**
- 4. Stresses for Solid Timber**
- 5. Timber Joints and Fasteners**
- 6. Laminated Members**
- 7. Environmental Conditions**
- 8. Timber Beams**
- 9. Structural Stability**
- 10. Structural Design Codes**
- 11. Any other Business**
- 12. Venue for Next Meeting**
- 13. Close**

**INTERNATIONAL COUNCIL FOR BUILDING RESEARCH,
STUDIES AND DOCUMENTATION**

WORKING COMMISSION W18 - TIMBER STRUCTURES

MEETING TWENTY-NINE

BORDEAUX, FRANCE, 26 - 29 AUGUST 1996

MINUTES

1. CHAIRMAN'S INTRODUCTION

The chairman **H J Blass** welcomed the delegates to the 29th meeting of CIB - W18 in Bordeaux and thanked CTBA and LRBB for their organisational work.

G-H Florentin then welcomed delegates on behalf of CTBA and thanked local industries who had supported the meeting. He noted the importance of Bordeaux to the French timber industry and explained the work of CTBA which will move its operation to Bordeaux in 1998. He then introduced the visits linked to the meeting.

The chairman specially welcomed **H-J Larsen** and **R H Leicester**. He then described arrangements for the meeting.

2. CO-OPERATION WITH OTHER ORGANISATIONS

(a) CIB - W18B

R H Leicester presented a report. He noted the work of the group related to hardwoods and tropical countries. Little of the work scheduled has been achieved due to lack of funding in the developing countries represented. He outlined solutions to the problem for discussions.

- (i) dissolve CIB - W18B and bring their work very loosely under CIB - W18 and IUFRO groups.
- (ii) dissolve the group but keep the work programme going in CIB - W18.
- (iii) keep going as before but work to gain sponsorship for developing countries so they could become part of CIB and attract funding to allow their delegates to attend conferences.

Comments from the audience suggested the third solution was not practicable and the chairman noted the main topic areas of work to be appropriate to CIB - W18 showing preference for option (ii).

(b) **ISO TC165**

Chairman **C Stieda** is now unable to attend CIB meetings. The chairman noted a meeting of the ISO group in Kyoto in November and **M Yasamura** gave further details.

(c) **RILEM**

S Thelandersson could not be present and the chairman presented a report on his behalf. RILEM had contributed to the development of timber technology with five technical committees completing their work successfully since the late 1980's. Two TC's are at present active.

W Rug had started a programme of work in TC149 - HTS on "Diagnosis and repair of historic load - bearing timber structures" but had now been replaced as chairman by **L Uzielli**.

A new group TC-MTE had been set up to be chaired by **J Ehlbeck** on "Test methods for load transferring metalwork used in timber engineering". **J Ehlbeck** then explained the proposed work load and invited initial contributions from different countries, either directly to himself or through national representatives.

(d) **CEN**

H-J Larsen gave a report on two areas of work:

(i)TC 250 responsible for drafting Eurocodes. EC5, at present a prestandard, had been voted on and it was expected that support would be given to transform it into a full standard. A group had already been set up to cover the redrafting work. The code on fire was now complete and the final draft on bridges was almost ready for voting.

(ii)TC 124 responsible for materials and product standards for timber structures. Of 42 standards half were published and the rest were in advanced stages of drafting or were being voted on. Only three standards were causing problems and they should be completed within a year. New work is due to start redrafting standards to new European requirements.

H-J Larsen is to be replaced as chairman of TC 250/SC5 by **H J Blass**.

(e) **IABSE**

No report

U Meierhofer noted that there would be a meeting in Innsbruck in September 1997 mainly on composite structures.

(f) IUFRO

No report

(g) CIB - W85

No report

3. STRENGTH GRADING

Before taking the first paper **H J Blass** introduced **P Morlier** Head of LRBB, co-hosts of the meeting.

*Paper 29-5-1 The effect of edge knots on the strength of SPF MSR Lumber -
T Courchene, F Lam and J D Barrett*

H J Blass asked for classification of the visual grade results and how much VQL material was fed back for MSR; about 50% but a quality assurance tension testing would be needed for this in practice.

*Paper 29-5-2 Determination of moment configuration factors using grading
machine readings - T D G Canisius and T Isaksson*

R H Leicester commented that testing modes had not been based on test data when data was available from Leicester and Madsen. It is necessary to define what is meant by strength; using CEN rules would make moment configuration factors unnecessary. **H J Larsen** commented that the work seemed to concentrate on low level distributions which necessarily had to be arbitrarily fixed and could not be treated too scientifically.

4. STRESSES FOR SOLID TIMBERS

Paper 29-6-1 Effect of size on tensile strength of timber - N Burger and P Glos

R H Leicester thought that if specimens were tested to CEN rules there would not be a size factor because the worst apparent defect would be in the centre. In practice a factor would be needed. **U Meierhofer** asked if specimens were hinged or clamped; clamped as required by EN 508. **F Rouger** commented that a length effect would be included for tensile stresses for glulam laminates based on Norwegian and Austrian work. **F Lam** asked when was grading of specimens done; before testing. He was also worried by the sample size for species. **C Mettem** queried on what factor test length should be standardised; a constant length. How could results be related to work on other European standards; a conversion factor would be needed.

*Paper 29-6-2 Equivalence of in-grade testing standards - R H Leicester,
H O Breitingner and H F Fordham*

H-J Larsen noted it was a pity that there were different test methods. Comparison is needed between US and EN methods but Australasian work is of little importance to Europe. Perhaps the European method of choosing the worst defect is wrong. In summary; a lot of useful work but not useable data for Europe. **R H Leicester** replied

that it was the technical viewpoint that was important not the commercial market and that Australasia tested timber in the way it is used. **F Lam** supported findings related to European and N. American test method. **H-J Larsen** came back to say research should be related to trade. Changes cannot be made too often to test methods as then data is wasted. He commented that there are groups of species that are similar but that there are materials that are different in behaviour. This makes global comparison difficult and explains differences in research data from different countries. **E Gehri** commented that the goal for design in terms of stiffness should be on the whole beam. Local stiffness is perhaps only useful to stress rating. Thus for the stiffness the US method is better.

5. TIMBER JOINTS AND FASTENERS

Paper 29-7-1 A simple method for lateral load-carrying capacity of dowel-type fasteners - J Kangas and J Kurkela

H-J Larsen commented that no new methods had been added so the nomograph method must be identical to the EC5 rules. EC5 is not a handbook it is the law so it is not the place for nomographs. **J Ehlbeck** commented the authors were right to wish to extend information to designers as well as students.

Paper 29-7-2 Nail plate joint behaviour at low versus high load level - T Poutanen

H-J Larsen summarised the meaning of the work to be that manufacturers would use larger plates and less or lower grade timber. There was disagreement concerning the acceptability of plastic design to such trusses. **L Whale** felt that the conclusion of the paper should be to ask for more guidance from the Code as to the position of node points for design.

Paper 29-7-4 A critical review of the moment rotation test method proposed in prEN 1075 - M Bettison, B S Choo and L R J Whale

J Ehlbeck commented that the shear test is at present in an informal annex. **A Leijten** queried the measurement of rotations and measurements. **L Whale** noted that inclinometer readings agreed with transducer readings. **B Kallsner** felt that stiffness results in two transitional directions could be used to derive rotational stiffness as done by Foschi. **T Poutanen** queried steel stresses; basically they were within the elastic region.

Paper 29-7-3 The moment resistance of tee and butt joint nail plate test specimens - a comparison with current design methods - A Reffold, L R J Whale and B S Choo

The chairman asked if characteristic conservatism ratios had been calculated as well as mean ratios. **L Whale** explained why this was not necessary. **T Poutanen** queried how the work could be related to practical accuracies. He commented on the merit of using larger plates.

Paper 29-7-5 Explanation of the translation and rotational behaviour of prestressed moment timber joints - A J M Leijten

No questions or comments.

Paper 29-7-6 Design of joints and frame corners using dowel-type fasteners - E Gehri

C Mettem showed work he had undertaken comparing EC5 values with test results relating to spacing and number of connectors. **M Yasumura** queried the deflection at failure; often very ductile up to six times elastic prediction. **E Gehri** noted the importance of this to design. **L Whale** noted the important point on fabrication tolerance, what should be done; if tolerances are poor a factor of 0.8 was suggested but it was noted that higher tolerances could be achieved and a value nearer unity would then be appropriate. **H Prion** queried the difference in results between hand drilled and machine drilled dowels.

Paper 29-7-7 Quasi-static reversed-cyclic testing of nailed joints - E Karacabeyli and A Ceccotti

F Lam queried graphs on energy dissipation for earthquake results. **R H Leicester** stated that the test must simulate the earthquake resistance. **H-J Larsen** wished to see conclusions related to the reduction of the test results, he was unhappy with the ASTM method. The author replied that it was still favoured in the US. **H Prion** related the work to his shear wall tests and commented on his worries concerning the number of cycles. In an earthquake there would be very few cycles in the ductile range. **E Gehri** queried the use of common nails in shear walls. The author noted that many failures were pull through and edge distance which did not benefit from improved nails.

Paper 29-7-8 Failure of bolted joints loaded parallel to the grain: experiment and simulation - L Davenne, L Daudeville and M Yasumura

H Blass asked how plastic deformation due to embedding would affect results.

E Gehri asked what was the orientation of the bolt to the lamination; parallel thus the crack was in one lamella. He then commented on the combination of results for different diameters in figure 7 which did not make sense. **H Blass** asked how loads determined would compare with Johansen's values; the author noted this comparison should be carried out. **H J Larsen** queried the angle for crack propagation, his work showed cracks would be at quarter points of bolt diameter. **H Blass** checked that friction had been considered in the finite element model. **M Yasumura** explained some of the experimental results associated with the project.

6. LAMINATED MEMBERS

Paper 29-12-1 Development of efficient glued laminated timber - G Schickhofer

R H Leicester asked for clarification regarding European testing standards. **H-J Larsen** queried the gradings and how the samples could be so different for the same grades; this was due to adjustments which had to be made to the grading machine. He then queried the overall modulus of elasticity results for some of the combined grade beams. **N Burger** queried the derivation of the width factor; this was needed to allow comparison

with, and use of, Norwegian results. **H-J Larsen** commented on the work in relationship to the last meeting on pr EN 1194. The author and **E Gehri** commented that it was important to take advantage of this comprehensive piece of work but that manipulation in the use of tensile strength data would have to be considered to prove the CEN rules. **H-J Larsen** replied that all European work must be considered. **H Prion** noted that in Canada a finite element programme had been written to predict Glulam performance. The programme would be commercially available for use with test results. **R H Leicester** noted that in Australia finger joints are much closer, could this affect the application of the results; no because normally finger joints would not be critical.

7. ENVIRONMENTAL CONDITIONS

Paper 29-11-1 Load duration effect on structural beams under varying climate - influence of size and shape - P Galimard and P Morlier

H-J Larsen commented that the results concerning moisture variations were very interesting but he wished for care in linking results to EC5 because of differences in moisture class classifications. He asked for clarification of the loading procedure for the time to failure and commented on the care needed in interpretation. **C J Mettem** commented that the discrepancies would only relate to Service Class 3. **F Lam** suggested a damage accumulation model could be used. He also noted that the differences between sawn timber and low COV materials in the frequency of times to failure. **E Gehri** commented that direction of load depends on the level of characteristic values used and comparison is not easy. The author agreed but noted the problem of using characteristic values when the samples were necessarily small. **H-J Larsen** commented that the results had not been expected, to which the author agreed. **E Karacabeyli** asked for clarification on the “forcing” of the data through fixed points which he could not accept. **U Meierhofer** encouraged the measurement of moisture gradient through the wood because it induces secondary stresses; he therefore preferred the use of larger specimens. **R H Leicester** suggested data should be checked against different models in particular one he had designed.

8. TIMBER BEAMS

Paper 29-10-1 Time dependent lateral buckling of timber beams - F Rouger

J Ehlbeck queried the equations used in the modified EC5 approach; the author explained his approach which was a proposal linked to his findings. **H-J Larsen** asked if the work could be linked to less slender columns; this was work to be done. **H J Blass** queried the fit of results in Figure 2. The author preferred his solution as it was simpler. **R H Leicester** noted the differences in the Australian procedures.

Paper 29-10-2 Determination of modulus of elasticity in bending according to EN 408 - K H Solli

N Burger agreed but commented that the other effects of position were important, e.g. depth. The author agreed and stated again that standardisation was essential. **H-J Larsen** commented that in EN 408 they had wanted to give flexibility and they did not think differences would be a problem. **E Gehri** noted that the problems were not so great in glulam, but for sawn timber with twist, etc. differences would be significant. **B**

Kallsner commented on the importance of putting the measuring points in a constant vertical plane.

Paper 29-10-4 Relation of moduli of elasticity in flatwise and edgewise bending of solid timber - C J Johansson, A Steffen and E W Wormuth

E Gehri commented on the difference between small test samples and structural sections where wood could be considered a composite; this could also be related to tension effects.

Paper 29-10-3 On determination of modulus of elasticity in bending - L Bostrom, S Ormarsson and O Dahlblom

L Whale commented on the commercial effect of using different E values, but more important than standardization, was achieving the correct value. **B Kallsner** commented that it was better to measure on the tension side.

9. STRUCTURAL STABILITY

Paper 29-15-1 Lateral resistance of wood based shear walls with oversized sheathing materials - F Lam, H G L Prion and M He

D R Griffiths checked that the sheathing was fully free to rotate and commented on the likely high variability between panels which would make conclusions a little difficult from one replicate. He also noted the benefits of this sheathing system to panels with opening and variable nail spanning. **H-J Larsen** commented that the shaking table work might not be appropriate.

Paper 29-15-3 The racking resistance of timber frame walls: design by test and calculation - D R Griffiths, V Enjily, C J Mettem and P J Steer

B Kallsner appreciated the background but could not accept that EC5 oversimplifies the design. **D R Griffiths** replied noting that EC5 did not examine the internal behaviour of the wall panels, nor the stiffness and that some equations in EC5 gave silly results. It was agreed that the two approaches could be linked. **R H Leicester** commented that walls are only 50% efficient when testing whole houses and that walls do not pick up load at the same time. The author noted the high stiffness of internal “non structural” walls. **E Karacabeyli** noted work on 4.8m x 2.4m walls in Canada with hold down of studs so that the influence of vertical load was small. The author explained why this approach was not used in the UK and discussed the limited performance of short wall panels with **F Lam**.

Paper 29-15-4 Current developments in medium-rise timber frame buildings in the UK - C J Mettem, G C Pitts, P J Steer and V Enjily

U Meierhofer asked what lay-up of floors will be used, compartment floors and innovative ones relocating layers for fire and sound resistance. **H-J Larsen** commented on five storey buildings in Scandinavia and the problem of competition from steel. In recent exhibitions much more interest had been expressed in steel because of the architecture and finishes. He noted that we do not do justice to the potential of timber and this was shown in the poor architecture of the designs put forward. **R Marsh** noted

that UK buyers have little appreciation of house architecture, but that design detail is important.

*Paper 29-15-2 Damage of wooden buildings caused by the 1995 Hyogo-Ken
Nanbu earthquake - M Yasumura, N Kawai, N Yamaguch and
S Nakajima*

F Lam asked what acceleration is used in Japan; 0.2g. If the peak acceleration is 0.8g is this accommodated in design; peak acceleration taken in Japan to be 0.4 - 0.5g and in buildings designed using a code based on this there was very little damage.

*Paper 29-15-5 Natural frequency prediction for timber floors - R J Bainbridge
and C J Mettem*

R H Leicester queried supports of floors; two edges only, and location of accelerometers grid of locations used, he was also interested in what was done with the lowest frequency. **H-J Larsen** commented that the system tested was simple and that this could be easily calculated there being no need therefore to test further structures. **C Mettem** explained that the theory behind the correction related to a tee-beam. Full reliance could not be put on a finite element model and a correction factor was needed. **J Konig** could not understand the use of a support system on two sides. He noted the tee beam effect to be appropriate but that it would introduce other problems. He recommended work by Ohlsson. In orthotropic plates the lowest frequency is not the only importance, secondary frequencies are also important. This comment and its relevance to EC5 led to discussions including **C J Mettem** and **H-J Larsen**. The latter commented that the floor was not practical because the ceiling would have an influence and that the test must be related to theory. **R H Leicester** noted Australian work in this area and the problems relating to a damping factor the author agreed the need for a damping ratio.

10. STRUCTURAL DESIGN CODES

*Paper 29-102-1 Model code for the probabilistic design of timber structures -
H-J Larsen, T Isaksson and S Thelandersson*

The purpose of the paper is to gain interest to set up an ad hoc working party to study this area of work ready for the next CIB meeting in Vancouver. **J Ehlbeck** queried why engineers were being asked to produce a probabilistic code for timber structures. The first reason was for completeness with other materials and then for simplified values, and finally for refined determination of γ factors. **J Ehlbeck** was unhappy that there would be great difficulty in selling another new method to designers. **H-J Larsen** commented that the work was needed for code writers not designers, again this related to the evaluation of γ values. **R H Leicester** commented on the tail distribution; rogue results do happen so it may not be practical to truncate the curve. He noted this study could be useful in a teaching environment and should be linked to work in other materials. **H-J Larsen** commented that Foschi's method could not work without the truncation. **E Gehri** stated it was not just academic work it was very important to system behaviour. The discussion was very relevant to earlier discussions on Glulam.

11. ANY OTHER BUSINESS

- (a) Master copies of reports or changes must be sent to Karlsruhe by the end of September.
- (b) **R H Leicester** suggested that much work was related in detail to CEN standards. It would help for those not familiar with CEN standards if the relevant parts could be included in the papers. **H J Blass** agreed with this and urged members to include relevant information.
- (c) **J Ehlbeck** queried the proposed merger of CIB W18 and CIB W18 B discussed earlier. **R H Leicester** commented that the merger was the best way forward but that he should first check this would be acceptable to the other members of CIB W18 B. **C J Mettem** asked if the classification of papers could be re-analysed and then it would be easy to include the area of simplified or appropriate codes.

12. VENUE AND PROGRAMME FOR NEXT MEETING

Meeting 30: Vancouver, within the period 25th-29th August 1997. F Lam will make the necessary arrangements and the meeting will be in downtown Vancouver. H J Larsen suggested visits should be at the end of the meeting and not within it.

Meeting 31 in 1998: an offer had been received from Finland. Suitable dates were 17-20th August to best fit with another meeting in Lausanne.

Meeting 32 in 1999: there was a possibility of holding the meeting in Austria.

13. CLOSE

The chairman thanked everyone for their attendance and contributions and wished them a pleasant journey home.

**14. List of CIB-W18 Papers,
Bordeaux, France 1996**

List of CIB-W18 Papers, Bordeaux, France 1996

- 29-5-1 The Effect of Edge Knots on the Strength of SPF MSR Lumber -
T Courchene, F Lam and J D Barrett
- 29-5-2 Determination of Moment Configuration Factors using Grading Machine
Readings - T D G Canisius and T Isaksson
- 29-6-1 Effect of Size on Tensile Strength of Timber - N Burger and P Glos
- 29-6-2 Equivalence of In-Grade Testing Standards - R H Leicester, H O Breitingner
and H F Fordham
- 29-7-1 A Simple Method for Lateral Load-Carrying Capacity of Dowel-Type
Fasteners - J Kangas and J Kurkela
- 29-7-2 Nail Plate Joint Behaviour at Low Versus High Load Level - T Poutanen
- 29-7-3 The Moment Resistance of Tee and Butt - Joint Nail Plate Test Specimens -
A Comparison with Current Design Methods - A Reffold, L R J Whale and
B S Choo
- 29-7-4 A Critical Review of the Moment Rotation Test Method Proposed in prEN
1075 - M Bettison, B S Choo and L R J Whale
- 29-7-5 Explanation of the Translation and Rotation Behaviour of Prestressed
Moment Timber Joints - A J M Leijten
- 29-7-6 Design of Joints and Frame Corners using Dowel-Type Fasteners - E Gehri
- 29-7-7 Quasi-Static Reversed-Cyclic Testing of Nailed Joints - E Karacabeyli and
A Ceccotti
- 29-7-8 Failure of Bolted Joints Loaded Parallel to the Grain: Experiment and
Simulation - L Davenne, L Daudeville and M Yasumura
- 29-10-1 Time Dependent Lateral Buckling of Timber Beams - F Rouger
- 29-10-2 Determination of Modulus of Elasticity in Bending According to EN 408 -
K H Solli

- 29-10-3 On Determination of Modulus of Elasticity in Bending - L Boström, S Ormarsson and O Dahlblom
- 29-10-4 Relation of Moduli of Elasticity in Flatwise and Edgewise Bending of Solid Timber - C J Johansson, A Steffen and E W Wormuth
- 29-11-1 Load Duration Effect on Structural Beams under Varying Climate Influence of Size and Shape - P Galimard and P Morlier
- 29-12-1 Development of Efficient Glued Laminated Timber - G Schickhofer
- 29-15-1 Lateral Resistance of Wood Based Shear Walls with Oversized Sheathing Panels - F Lam, H G L Prion and M He
- 29-15-2 Damage of Wooden Buildings Caused by the 1995 Hyogo-Ken Nanbu Earthquake - M Yasumura, N Kawai, N Yamaguch and S Nakajima
- 29-15-3 The Racking Resistance of Timber Frame Walls: Design by Test and Calculation - D R Griffiths, C J Mettem, V Enjily, P J Steer
- 29-15-4 Current Developments in Medium-Rise Timber Frame Buildings in the UK - C J Mettem, G C Pitts, P J Steer, V Enjily
- 29-15-5 Natural Frequency Prediction for Timber Floors - R J Bainbridge, C J Mettem
- 29-102-1 Model Code for the Probabilistic Design of Timber Structures - H J Larsen, T Isaksson and S Thelandersson

15. Current List of CIB-W18(A) Papers

CURRENT LIST OF CIB-W18(A) PAPERS

Technical papers presented to CIB-W18(A) are identified by a code CIB-W18(A)/a-b-c, where:

- a denotes the meeting at which the paper was presented.
Meetings are classified in chronological order:

- 1 Princes Risborough, England; March 1973
- 2 Copenhagen, Denmark; October 1973
- 3 Delft, Netherlands; June 1974
- 4 Paris, France; February 1975
- 5 Karlsruhe, Federal Republic of Germany; October 1975
- 6 Aalborg, Denmark; June 1976
- 7 Stockholm, Sweden; February/March 1977
- 8 Brussels, Belgium; October 1977
- 9 Perth, Scotland; June 1978
- 10 Vancouver, Canada; August 1978
- 11 Vienna, Austria; March 1979
- 12 Bordeaux, France; October 1979
- 13 Otaniemi, Finland; June 1980
- 14 Warsaw, Poland; May 1981
- 15 Karlsruhe, Federal Republic of Germany; June 1982
- 16 Lillehammer, Norway; May/June 1983
- 17 Rapperswil, Switzerland; May 1984
- 18 Beit Oren, Israel; June 1985
- 19 Florence, Italy; September 1986
- 20 Dublin, Ireland; September 1987
- 21 Parksville, Canada; September 1988
- 22 Berlin, German Democratic Republic; September 1989
- 23 Lisbon, Portugal; September 1990
- 24 Oxford, United Kingdom; September 1991
- 25 Åhus, Sweden; August 1992
- 26 Athens, USA; August 1993
- 27 Sydney, Australia; July 1994
- 28 Copenhagen, Denmark, April 1995
- 29 Bordeaux, France, August 1996

b denotes the subject:

- 1 Limit State Design
- 2 Timber Columns
- 3 Symbols
- 4 Plywood
- 5 Stress Grading
- 6 Stresses for Solid Timber
- 7 Timber Joints and Fasteners
- 8 Load Sharing
- 9 Duration of Load
- 10 Timber Beams
- 11 Environmental Conditions
- 12 Laminated Members
- 13 Particle and Fibre Building Boards
- 14 Trussed Rafters
- 15 Structural Stability
- 16 Fire
- 17 Statistics and Data Analysis
- 18 Glued Joints
- 19 Fracture Mechanics
- 20 Serviceability
- 100 CIB Timber Code
- 101 Loading Codes
- 102 Structural Design Codes
- 103 International Standards Organisation
- 104 Joint Committee on Structural Safety
- 105 CIB Programme, Policy and Meetings
- 106 International Union of Forestry Research Organisations

c is simply a number given to the papers in the order in which they appear:

Example: CIB-W18/4-102-5 refers to paper 5 on subject 102 presented at the fourth meeting of W18.

Listed below, by subjects, are all papers that have to date been presented to W18. When appropriate some papers are listed under more than one subject heading.

LIMIT STATE DESIGN

- 1-1-1 Limit State Design - H J Larsen
- 1-1-2 The Use of Partial Safety Factors in the New Norwegian Design Code for Timber Structures - O Brynildsen
- 1-1-3 Swedish Code Revision Concerning Timber Structures - B Noren
- 1-1-4 Working Stresses Report to British Standards Institution Committee BLCP/17/2
- 6-1-1 On the Application of the Uncertainty Theoretical Methods for the Definition of the Fundamental Concepts of Structural Safety - K Skov and O Ditlevsen
- 11-1-1 Safety Design of Timber Structures - H J Larsen
- 18-1-1 Notes on the Development of a UK Limit States Design Code for Timber - A R Fewell and C B Pierce
- 18-1-2 Eurocode 5, Timber Structures - H J Larsen
- 19-1-1 Duration of Load Effects and Reliability Based Design (Single Member) - R O Foschi and Z C Yao
- 21-102-1 Research Activities Towards a New GDR Timber Design Code Based on Limit States Design - W Rug and M Badstube
- 22-1-1 Reliability-Theoretical Investigation into Timber Components Proposal for a Supplement of the Design Concept - M Badstube, W Rug and R Plessow
- 23-1-1 Some Remarks about the Safety of Timber Structures - J Kuipers
- 23-1-2 Reliability of Wood Structural Elements: A Probabilistic Method to Eurocode 5 Calibration - F Rouger, N Lheritier, P Racher and M Fogli

TIMBER COLUMNS

- 2-2-1 The Design of Solid Timber Columns - H J Larsen
- 3-2-1 The Design of Built-Up Timber Columns - H J Larsen
- 4-2-1 Tests with Centrally Loaded Timber Columns - H J Larsen and S S Pedersen
- 4-2-2 Lateral-Torsional Buckling of Eccentrically Loaded Timber Columns - B Johansson
- 5-9-1 Strength of a Wood Column in Combined Compression and Bending with Respect to Creep - B Källsner and B Norén
- 5-100-1 Design of Solid Timber Columns (First Draft) - H J Larsen
- 6-100-1 Comments on Document 5-100-1, Design of Solid Timber Columns - H J Larsen and E Theilgaard
- 6-2-1 Lattice Columns - H J Larsen
- 6-2-2 A Mathematical Basis for Design Aids for Timber Columns - H J Burgess
- 6-2-3 Comparison of Larsen and Perry Formulas for Solid Timber Columns - H J Burgess
- 7-2-1 Lateral Bracing of Timber Struts - J A Simon
- 8-15-1 Laterally Loaded Timber Columns: Tests and Theory - H J Larsen
- 17-2-1 Model for Timber Strength under Axial Load and Moment - T Poutanen
- 18-2-1 Column Design Methods for Timber Engineering - A H Buchanan, K C Johns, B Madsen
- 19-2-1 Creep Buckling Strength of Timber Beams and Columns - R H Leicester

- 19-12-2 Strength Model for Glulam Columns - H J Blaß
- 20-2-1 Lateral Buckling Theory for Rectangular Section Deep Beam-Columns-
H J Burgess
- 20-2-2 Design of Timber Columns - H J Blaß
- 21-2-1 Format for Buckling Strength - R H Leicester
- 21-2-2 Beam-Column Formulae for Design Codes - R H Leicester
- 21-15-1 Rectangular Section Deep Beam - Columns with Continuous Lateral Restraint -
H J Burgess
- 21-15-2 Buckling Modes and Permissible Axial Loads for Continuously Braced Columns -
H J Burgess
- 21-15-3 Simple Approaches for Column Bracing Calculations - H J Burgess
- 21-15-4 Calculations for Discrete Column Restraints - H J Burgess
- 22-2-1 Buckling and Reliability Checking of Timber Columns - S Huang, P M Yu and
J Y Hong
- 22-2-2 Proposal for the Design of Compressed Timber Members by Adopting the
Second-Order Stress Theory - P Kaiser

SYMBOLS

- 3-3-1 Symbols for Structural Timber Design - J Kuipers and B Norén
- 4-3-1 Symbols for Timber Structure Design - J Kuipers and B Norén
- 28-3-1 Symbols for Timber and Wood-Based Materials - J Kuipers and B Noren
- 1 Symbols for Use in Structural Timber Design

PLYWOOD

- 2-4-1 The Presentation of Structural Design Data for Plywood - L G Booth
- 3-4-1 Standard Methods of Testing for the Determination of Mechanical Properties of
Plywood - J Kuipers
- 3-4-2 Bending Strength and Stiffness of Multiple Species Plywood - C K A Stieda
- 4-4-4 Standard Methods of Testing for the Determination of Mechanical Properties of
Plywood - Council of Forest Industries, B.C.
- 5-4-1 The Determination of Design Stresses for Plywood in the Revision of CP 112 -
L G Booth
- 5-4-2 Veneer Plywood for Construction - Quality Specifications - ISO/TC 139.
Plywood, Working Group 6
- 6-4-1 The Determination of the Mechanical Properties of Plywood Containing Defects -
L G Booth
- 6-4-2 Comparison of the Size and Type of Specimen and Type of Test on Plywood
Bending Strength and Stiffness - C R Wilson and P Eng
- 6-4-3 Buckling Strength of Plywood: Results of Tests and Recommendations for
Calculations - J Kuipers and H Ploos van Amstel
- 7-4-1 Methods of Test for the Determination of Mechanical Properties of Plywood -
L G Booth, J Kuipers, B Norén, C R Wilson
- 7-4-2 Comments Received on Paper 7-4-1

- 7-4-3 The Effect of Rate of Testing Speed on the Ultimate Tensile Stress of Plywood - C R Wilson and A V Parasin
- 7-4-4 Comparison of the Effect of Specimen Size on the Flexural Properties of Plywood Using the Pure Moment Test - C R Wilson and A V Parasin
- 8-4-1 Sampling Plywood and the Evaluation of Test Results - B Norén
- 9-4-1 Shear and Torsional Rigidity of Plywood - H J Larsen
- 9-4-2 The Evaluation of Test Data on the Strength Properties of Plywood - L G Booth
- 9-4-3 The Sampling of Plywood and the Derivation of Strength Values (Second Draft) - B Norén
- 9-4-4 On the Use of the CIB/RILEM Plywood Plate Twisting Test: a progress report - L G Booth
- 10-4-1 Buckling Strength of Plywood - J Dekker, J Kuipers and H Ploos van Amstel
- 11-4-1 Analysis of Plywood Stressed Skin Panels with Rigid or Semi-Rigid Connections - I Smith
- 11-4-2 A Comparison of Plywood Modulus of Rigidity Determined by the ASTM and RILEM CIB/3-TT Test Methods - C R Wilson and A V Parasin
- 11-4-3 Sampling of Plywood for Testing Strength - B Norén
- 12-4-1 Procedures for Analysis of Plywood Test Data and Determination of Characteristic Values Suitable for Code Presentation - C R Wilson
- 14-4-1 An Introduction to Performance Standards for Wood-base Panel Products - D H Brown
- 14-4-2 Proposal for Presenting Data on the Properties of Structural Panels - T Schmidt
- 16-4-1 Planar Shear Capacity of Plywood in Bending - C K A Stieda
- 17-4-1 Determination of Panel Shear Strength and Panel Shear Modulus of Beech-Plywood in Structural Sizes - J Ehlbeck and F Colling
- 17-4-2 Ultimate Strength of Plywood Webs - R H Leicester and L Pham
- 20-4-1 Considerations of Reliability - Based Design for Structural Composite Products - M R O'Halloran, J A Johnson, E G Elias and T P Cunningham
- 21-4-1 Modelling for Prediction of Strength of Veneer Having Knots - Y Hirashima
- 22-4-1 Scientific Research into Plywood and Plywood Building Constructions the Results and Findings of which are Incorporated into Construction Standard Specifications of the USSR - I M Guskov
- 22-4-2 Evaluation of Characteristic values for Wood-Based Sheet Materials - E G Elias
- 24-4-1 APA Structural-Use Design Values: An Update to Panel Design Capacities - A L Kuchar, E G Elias, B Yeh and M R O'Halloran

STRESS GRADING

- 1-5-1 Quality Specifications for Sawn Timber and Precision Timber - Norwegian Standard NS 3080
- 1-5-2 Specification for Timber Grades for Structural Use - British Standard BS 4978
- 4-5-1 Draft Proposal for an International Standard for Stress Grading Coniferous Sawn Softwood - ECE Timber Committee
- 16-5-1 Grading Errors in Practice - B Thunell

- 16-5-2 On the Effect of Measurement Errors when Grading Structural Timber-
L Nordberg and B Thunell
- 19-5-1 Stress-Grading by ECE Standards of Italian-Grown Douglas-Fir Dimension
Lumber from Young Thinnings - L Uzielli
- 19-5-2 Structural Softwood from Afforestation Regions in Western Norway - R Lackner
- 21-5-1 Non-Destructive Test by Frequency of Full Size Timber for Grading - T Nakai
- 22-5-1 Fundamental Vibration Frequency as a Parameter for Grading Sawn Timber -
T Nakai, T Tanaka and H Nagao
- 24-5-1 Influence of Stress Grading System on Length Effect Factors for Lumber Loaded
in Compression - A Campos and I Smith
- 26-5-1 Structural Properties of French Grown Timber According to Various Grading
Methods - F Rouger, C De Lafond and A El Quadrani
- 28-5-1 Grading Methods for Structural Timber - Principles for Approval - S Ohlsson
- 28-5-2 Relationship of Moduli of Elasticity in Tension and in Bending of Solid Timber -
N Burger and P Glos
- 29-5-1 The Effect of Edge Knots on the Strength of SPF MSR Lumber - T Courchene,
F Lam and J D Barrett
- 29-5-2 Determination of Moment Configuration Factors using Grading Machine
Readings - T D G Canisius and T Isaksson

STRESSES FOR SOLID TIMBER

- 4-6-1 Derivation of Grade Stresses for Timber in the UK - W T Curry
- 5-6-1 Standard Methods of Test for Determining some Physical and Mechanical
Properties of Timber in Structural Sizes - W T Curry
- 5-6-2 The Description of Timber Strength Data - J R Tory
- 5-6-3 Stresses for EC1 and EC2 Stress Grades - J R Tory
- 6-6-1 Standard Methods of Test for the Determination of some Physical and Mechanical
Properties of Timber in Structural Sizes (third draft) - W T Curry
- 7-6-1 Strength and Long-term Behaviour of Lumber and Glued Laminated Timber under
Torsion Loads - K Möhler
- 9-6-1 Classification of Structural Timber - H J Larsen
- 9-6-2 Code Rules for Tension Perpendicular to Grain - H J Larsen
- 9-6-3 Tension at an Angle to the Grain - K Möhler
- 9-6-4 Consideration of Combined Stresses for Lumber and Glued Laminated Timber -
K Möhler
- 11-6-1 Evaluation of Lumber Properties in the United States - W L Galligan and
J H Haskell
- 11-6-2 Stresses Perpendicular to Grain - K Möhler
- 11-6-3 Consideration of Combined Stresses for Lumber and Glued Laminated Timber
(addition to Paper CIB-W18/9-6-4) - K Möhler
- 12-6-1 Strength Classifications for Timber Engineering Codes - R H Leicester and
W G Keating
- 12-6-2 Strength Classes for British Standard BS 5268 - J R Tory
- 13-6-1 Strength Classes for the CIB Code - J R Tory

- 13-6-2 Consideration of Size Effects and Longitudinal Shear Strength for Uncracked Beams - R O Foschi and J D Barrett
- 13-6-3 Consideration of Shear Strength on End-Cracked Beams - J D Barrett and R O Foschi
- 15-6-1 Characteristic Strength Values for the ECE Standard for Timber - J G Sunley
- 16-6-1 Size Factors for Timber Bending and Tension Stresses - A R Fewell
- 16-6-2 Strength Classes for International Codes - A R Fewell and J G Sunley
- 17-6-1 The Determination of Grade Stresses from Characteristic Stresses for BS 5268: Part 2 - A R Fewell
- 17-6-2 The Determination of Softwood Strength Properties for Grades, Strength Classes and Laminated Timber for BS 5268: Part 2 - A R Fewell
- 18-6-1 Comment on Papers: 18-6-2 and 18-6-3 - R H Leicester
- 18-6-2 Configuration Factors for the Bending Strength of Timber - R H Leicester
- 18-6-3 Notes on Sampling Factors for Characteristic Values - R H Leicester
- 18-6-4 Size Effects in Timber Explained by a Modified Weakest Link Theory- B Madsen and A H Buchanan
- 18-6-5 Placement and Selection of Growth Defects in Test Specimens - H Riberholt
- 18-6-6 Partial Safety-Coefficients for the Load-Carrying Capacity of Timber Structures - B Norén and J-O Nylander
- 19-6-1 Effect of Age and/or Load on Timber Strength - J Kuipers
- 19-6-2 Confidence in Estimates of Characteristic Values - R H Leicester
- 19-6-3 Fracture Toughness of Wood - Mode I - K Wright and M Fonselius
- 19-6-4 Fracture Toughness of Pine - Mode II - K Wright
- 19-6-5 Drying Stresses in Round Timber - A Ranta-Maunus
- 19-6-6 A Dynamic Method for Determining Elastic Properties of Wood - R Görlacher
- 20-6-1 A Comparative Investigation of the Engineering Properties of "Whitewoods" Imported to Israel from Various Origins - U Korin
- 20-6-2 Effects of Yield Class, Tree Section, Forest and Size on Strength of Home Grown Sitka Spruce - V Picardo
- 20-6-3 Determination of Shear Strength and Strength Perpendicular to Grain - H J Larsen
- 21-6-1 Draft Australian Standard: Methods for Evaluation of Strength and Stiffness of Graded Timber - R H Leicester
- 21-6-2 The Determination of Characteristic Strength Values for Stress Grades of Structural Timber. Part 1 - A R Fewell and P Glos
- 21-6-3 Shear Strength in Bending of Timber - U Korin
- 22-6-1 Size Effects and Property Relationships for Canadian 2-inch Dimension Lumber - J D Barrett and H Griffin
- 22-6-2 Moisture Content Adjustements for In-Grade Data - J D Barrett and W Lau
- 22-6-3 A Discussion of Lumber Property Relationships in Eurocode 5 - D W Green and D E Kretschmann
- 22-6-4 Effect of Wood Preservatives on the Strength Properties of Wood - F Ronai
- 23-6-1 Timber in Compression Perpendicular to Grain - U Korin

- 24-6-1 Discussion of the Failure Criterion for Combined Bending and Compression - T A C M van der Put
- 24-6-3 Effect of Within Member Variability on Bending Strength of Structural Timber - I Czmocho, S Thelandersson and H J Larsen
- 24-6-4 Protection of Structural Timber Against Fungal Attack Requirements and Testing- K Jaworska, M Rylko and W Nozynski
- 24-6-5 Derivation of the Characteristic Bending Strength of Solid Timber According to CEN-Document prEN 384 - A J M Leijten
- 25-6-1 Moment Configuration Factors for Simple Beams- T D G Canisius
- 25-6-3 Bearing Capacity of Timber - U Korin
- 25-6-4 On Design Criteria for Tension Perpendicular to Grain - H Petersson
- 25-6-5 Size Effects in Visually Graded Softwood Structural Lumber - J D Barrett, F Lam and W Lau
- 26-6-1 Discussion and Proposal of a General Failure Criterion for Wood - T A C M van der Put
- 27-6-1 Development of the "Critical Bearing": Design Clause in CSA-086.1 - C Lum and E Karacabeyli
- 27-6-2 Size Effects in Timber: Novelty Never Ends - F Rouger and T Fewell
- 27-6-3 Comparison of Full-Size Sugi (*Cryptomeria japonica* D.Don) Structural Performance in Bending of Round Timber, Two Surfaces Sawn Timber and Square Sawn Timber - T Nakai, H Nagao and T Tanaka
- 28-6-1 Shear Strength of Canadian Softwood Structural Lumber - F Lam, H Yee and J D Barrett
- 28-6-2 Shear Strength of Douglas Fir Timbers - B Madsen
- 28-6-3 On the Influence of the Loading Head Profiles on Determined Bending Strength - L Muszyński and R Szukala
- 28-6-4 Effect of Test Standard, Length and Load Configuration on Bending Strength of Structural Timber- T Isaksson and S Thelandersson
- 28-6-5 Grading Machine Readings and their Use in the Calculation of Moment Configuration Factors - T Canisius, T Isaksson and S Thelandersson
- 28-6-6 End Conditions for Tension Testing of Solid Timber Perpendicular to Grain - T Canisius
- 29-6-1 Effect of Size on Tensile Strength of Timber - N Burger and P Glos
- 29-6-2 Equivalence of In-Grade Testing Standards - R H Leicester, H O Breitingner and H F Fordham

TIMBER JOINTS AND FASTENERS

- 1-7-1 Mechanical Fasteners and Fastenings in Timber Structures - E G Stern
- 4-7-1 Proposal for a Basic Test Method for the Evaluation of Structural Timber Joints with Mechanical Fasteners and Connectors - RILEM 3TT Committee
- 4-7-2 Test Methods for Wood Fasteners - K Möhler
- 5-7-1 Influence of Loading Procedure on Strength and Slip-Behaviour in Testing Timber Joints - K Möhler
- 5-7-2 Recommendations for Testing Methods for Joints with Mechanical Fasteners and Connectors in Load-Bearing Timber Structures - RILEM 3 TT Committee

- 5-7-3 CIB-Recommendations for the Evaluation of Results of Tests on Joints with Mechanical Fasteners and Connectors used in Load-Bearing Timber Structures - J Kuipers
- 6-7-1 Recommendations for Testing Methods for Joints with Mechanical Fasteners and Connectors in Load-Bearing Timber Structures (seventh draft) - RILEM 3 TT Committee
- 6-7-2 Proposal for Testing Integral Nail Plates as Timber Joints - K Möhler
- 6-7-3 Rules for Evaluation of Values of Strength and Deformation from Test Results - Mechanical Timber Joints - M Johansen, J Kuipers, B Norén
- 6-7-4 Comments to Rules for Testing Timber Joints and Derivation of Characteristic Values for Rigidity and Strength - B Norén
- 7-7-1 Testing of Integral Nail Plates as Timber Joints - K Möhler
- 7-7-2 Long Duration Tests on Timber Joints - J Kuipers
- 7-7-3 Tests with Mechanically Jointed Beams with a Varying Spacing of Fasteners - K Möhler
- 7-100-1 CIB-Timber Code Chapter 5.3 Mechanical Fasteners;CIB-Timber Standard 06 and 07 - H J Larsen
- 9-7-1 Design of Truss Plate Joints - F J Keenan
- 9-7-2 Staples - K Möhler
- 11-7-1 A Draft Proposal for International Standard: ISO Document ISO/TC 165N 38E
- 12-7-1 Load-Carrying Capacity and Deformation Characteristics of Nailed Joints - J Ehlbeck
- 12-7-2 Design of Bolted Joints - H J Larsen
- 12-7-3 Design of Joints with Nail Plates - B Norén
- 13-7-1 Polish Standard BN-80/7159-04: Parts 00-01-02-03-04-05.
"Structures from Wood and Wood-based Materials. Methods of Test and Strength Criteria for Joints with Mechanical Fasteners"
- 13-7-2 Investigation of the Effect of Number of Nails in a Joint on its Load Carrying Ability - W Nozynski
- 13-7-3 International Acceptance of Manufacture, Marking and Control of Finger-jointed Structural Timber - B Norén
- 13-7-4 Design of Joints with Nail Plates - Calculation of Slip - B Norén
- 13-7-5 Design of Joints with Nail Plates - The Heel Joint - B Källsner
- 13-7-6 Nail Deflection Data for Design - H J Burgess
- 13-7-7 Test on Bolted Joints - P Vermeyden
- 13-7-8 Comments to paper CIB-W18/12-7-3 "Design of Joints with Nail Plates"- B Norén
- 13-7-9 Strength of Finger Joints - H J Larsen
- 13-100-4 CIB Structural Timber Design Code. Proposal for Section 6.1.5 Nail Plates - N I Bovim
- 14-7-1 Design of Joints with Nail Plates (second edition) - B Norén
- 14-7-2 Method of Testing Nails in Wood (second draft, August 1980) - B Norén
- 14-7-3 Load-Slip Relationship of Nailed Joints - J Ehlbeck and H J Larsen
- 14-7-4 Wood Failure in Joints with Nail Plates - B Norén

- 14-7-5 The Effect of Support Eccentricity on the Design of W- and WW-Trussed with Nail Plate Connectors - B Källsner
- 14-7-6 Derivation of the Allowable Load in Case of Nail Plate Joints Perpendicular to Grain - K Möhler
- 14-7-7 Comments on CIB-W18/14-7-1 - T A C M van der Put
- 15-7-1 Final Recommendation TT-1A: Testing Methods for Joints with Mechanical Fasteners in Load-Bearing Timber Structures. Annex A Punched Metal Plate Fasteners - Joint Committee RILEM/CIB-3TT
- 16-7-1 Load Carrying Capacity of Dowels - E Gehri
- 16-7-2 Bolted Timber Joints: A Literature Survey - N Harding
- 16-7-3 Bolted Timber Joints: Practical Aspects of Construction and Design; a Survey - N Harding
- 16-7-4 Bolted Timber Joints: Draft Experimental Work Plan - Building Research Association of New Zealand
- 17-7-1 Mechanical Properties of Nails and their Influence on Mechanical Properties of Nailed Timber Joints Subjected to Lateral Loads - I Smith, L R J Whale, C Anderson and L Held
- 17-7-2 Notes on the Effective Number of Dowels and Nails in Timber Joints - G Steck
- 18-7-1 Model Specification for Driven Fasteners for Assembly of Pallets and Related Structures - E G Stern and W B Wallin
- 18-7-2 The Influence of the Orientation of Mechanical Joints on their Mechanical Properties - I Smith and L R J Whale
- 18-7-3 Influence of Number of Rows of Fasteners or Connectors upon the Ultimate Capacity of Axially Loaded Timber Joints - I Smith and G Steck
- 18-7-4 A Detailed Testing Method for Nailplate Joints - J Kangas
- 18-7-5 Principles for Design Values of Nailplates in Finland - J Kangas
- 18-7-6 The Strength of Nailplates - N I Bovim and E Aasheim
- 19-7-1 Behaviour of Nailed and Bolted Joints under Short-Term Lateral Load - Conclusions from Some Recent Research - L R J Whale, I Smith and B O Hilson
- 19-7-2 Glued Bolts in Glulam - H Riberholt
- 19-7-3 Effectiveness of Multiple Fastener Joints According to National Codes and Eurocode 5 (Draft) - G Steck
- 19-7-4 The Prediction of the Long-Term Load Carrying Capacity of Joints in Wood Structures - Y M Ivanov and Y Y Slavic
- 19-7-5 Slip in Joints under Long-Term Loading - T Feldborg and M Johansen
- 19-7-6 The Derivation of Design Clauses for Nailed and Bolted Joints in Eurocode 5 - L R J Whale and I Smith
- 19-7-7 Design of Joints with Nail Plates - Principles - B Norén
- 19-7-8 Shear Tests for Nail Plates - B Norén
- 19-7-9 Advances in Technology of Joints for Laminated Timber - Analyses of the Structural Behaviour - M Piazza and G Turrini
- 19-15-1 Connections Deformability in Timber Structures: A Theoretical Evaluation of its Influence on Seismic Effects - A Ceccotti and A Vignoli

- 20-7-1 Design of Nailed and Bolted Joints-Proposals for the Revision of Existing Formulae in Draft Eurocode 5 and the CIB Code - L R J Whale, I Smith and H J Larsen
- 20-7-2 Slip in Joints under Long Term Loading - T Feldborg and M Johansen
- 20-7-3 Ultimate Properties of Bolted Joints in Glued-Laminated Timber - M Yasumura, T Murota and H Sakai
- 20-7-4 Modelling the Load-Deformation Behaviour of Connections with Pin-Type Fasteners under Combined Moment, Thrust and Shear Forces - I Smith
- 21-7-1 Nails under Long-Term Withdrawal Loading - T Feldborg and M Johansen
- 21-7-2 Glued Bolts in Glulam-Proposals for CIB Code - H Riberholt
- 21-7-3 Nail Plate Joint Behaviour under Shear Loading - T Poutanen
- 21-7-4 Design of Joints with Laterally Loaded Dowels. Proposals for Improving the Design Rules in the CIB Code and the Draft Eurocode 5 - J Ehlbeck and H Werner
- 21-7-5 Axially Loaded Nails: Proposals for a Supplement to the CIB Code - J Ehlbeck and W Siebert
- 22-7-1 End Grain Connections with Laterally Loaded Steel Bolts A draft proposal for design rules in the CIB Code - J Ehlbeck and M Gerold
- 22-7-2 Determination of Perpendicular-to-Grain Tensile Stresses in Joints with Dowel-Type Fasteners - A draft proposal for design rules - J Ehlbeck, R Görlacher and H Werner
- 22-7-3 Design of Double-Shear Joints with Non-Metallic Dowels A proposal for a supplement of the design concept - J Ehlbeck and O Eberhart
- 22-7-4 The Effect of Load on Strength of Timber Joints at high Working Load Level - A J M Leijten
- 22-7-5 Plasticity Requirements for Portal Frame Corners - R Gunnewijk and A J M Leijten
- 22-7-6 Background Information on Design of Glulam Rivet Connections in CSA/CAN3-086.1-M89 - A proposal for a supplement of the design concept - E Karacabeyli and D P Janssens
- 22-7-7 Mechanical Properties of Joints in Glued-Laminated Beams under Reversed Cyclic Loading - M Yasumura
- 22-7-8 Strength of Glued Lap Timber Joints - P Glos and H Horstmann
- 22-7-9 Toothed Rings Type Bistyp 075 at the Joints of Fir Wood - J Kerste
- 22-7-10 Calculation of Joints and Fastenings as Compared with the International State - K Zimmer and K Lissner
- 22-7-11 Joints on Glued-in Steel Bars Present Relatively New and Progressive Solution in Terms of Timber Structure Design - G N Zubarev, F A Boitemirov and V M Golovina
- 22-7-12 The Development of Design Codes for Timber Structures made of Composite Bars with Plate Joints based on Cylindrical Nails - Y V Piskunov
- 22-7-13 Designing of Glued Wood Structures Joints on Glued-in Bars - S B Turkovsky
- 23-7-1 Proposal for a Design Code for Nail Plates - E Aasheim and K H Solli
- 23-7-2 Load Distribution in Nailed Joints - H J Blass
- 24-7-1 Theoretical and Experimental Tension and Shear Capacity of Nail Plate Connections - B Källsner and J Kangas

- 24-7-2 Testing Method and Determination of Basic Working Loads for Timber Joints with Mechanical Fasteners - Y Hirashima and F Kamiya
- 24-7-3 Anchorage Capacity of Nail Plate - J Kangas
- 25-7-2 Softwood and Hardwood Embedding Strength for Dowel type Fasteners - J Ehlbeck and H Werner
- 25-7-4 A Guide for Application of Quality Indexes for Driven Fasteners Used in Connections in Wood Structures - E G Stern
- 25-7-5 35 Years of Experience with Certain Types of Connectors and Connector Plates Used for the Assembly of Wood Structures and their Components- E G Stern
- 25-7-6 Characteristic Strength of Split-ring and Shear-plate Connections - H J Blass, J Ehlbeck and M Schlager
- 25-7-7 Characteristic Strength of Tooth-plate Connector Joints - H J Blass, J Ehlbeck and M Schlager
- 25-7-8 Extending Yield Theory to Screw Connections - T E McLain
- 25-7-9 Determination of k_{def} for Nailed Joints - J W G van de Kuilen
- 25-7-10 Characteristic Strength of UK Timber Connectors - A V Page and C J Mettem
- 25-7-11 Multiple-fastener Dowel-type Joints, a Selected Review of Research and Codes - C J Mettem and A V Page
- 25-7-12 Load Distributions in Multiple-fastener Bolted Joints in European Whitewood Glulam, with Steel Side Plates - C J Mettem and A V Page
- 26-7-1 Proposed Test Method for Dynamic Properties of Connections Assembled with Mechanical Fasteners - J D Dolan
- 26-7-2 Validatory Tests and Proposed Design Formulae for the Load-Carrying Capacity of Toothed-Plate Connected Joints - C J Mettem, A V Page and G Davis
- 26-7-3 Definitions of Terms and Multi-Language Terminology Pertaining to Metal Connector Plates - E G Stern
- 26-7-4 Design of Joints Based on in V-Shape Glued-in Rods - J Kangas
- 26-7-5 Tests on Timber Concrete Composite Structural Elements (TCCs) - A U Meierhofer
- 27-7-1 Glulam Arch Bridge and Design of its Moment-Resisting Joints - K Komatsu and S Usuku
- 27-7-2 Characteristic Load - Carrying Capacity of Joints with Dowel - type Fasteners in Regard to the System Properties - H Werner
- 27-7-3 Steel Failure Design in Truss Plate Joints - T Poutanen
- 28-7-1 Expanded Tube Joint in Locally DP Reinforced Timber - A J M Leijten, P Ragupathy and K S Virdi
- 28-7-2 A Strength and Stiffness Model for the Expanded Tube Joint - A J M Leijten
- 28-7-3 Load-carrying Capacity of Steel-to Timber Joints with Annular Ring Shanked Nails. A Comparison with the EC5 Design Method - R Görlacher
- 28-7-4 Dynamic Effects on Metal-Plate Connected Wood Truss Joints - S Kent, R Gupta and T Miller
- 28-7-5 Failure of the Timber Bolted Joints Subjected to Lateral Load Perpendicular to Grain - M Yasumura and L Daudeville
- 28-7-6 Design Procedure for Locally Reinforced Joints with Dowel-type Fasteners - H Werner

- 28-7-7 Variability and Effects of Moisture Content on the Withdrawal Characteristics for Lumber as Opposed to Clear Wood - J D Dolan and J W Stelmokas
- 28-7-8 Nail Plate Capacity in Joint Line - A Kevarinmäki and J Kangas
- 28-7-9 Axial Strength of Glued-In Bolts - Calculation Model Based on Non-Linear Fracture Mechanics - A Preliminary Study - C J Johansson, E Serrano, P J Gustafsson and B Enquist
- 28-7-10 Cyclic Lateral Dowel Connection Tests for seismic and Wind Evaluation - J D Dolan
- 29-7-1 A Simple Method for Lateral Load-Carrying Capacity of Dowel-Type Fasteners - J Kangas and J Kurkela
- 29-7-2 Nail Plate Joint Behaviour at Low Versus High Load Level - T Poutanen
- 29-7-3 The Moment Resistance of Tee and Butt - Joint Nail Plate Test Specimens - A Comparison with Current Design Methods - A Reffold, L R J Whale and B S Choo
- 29-7-4 A Critical Review of the Moment Rotation Test Method Proposed in prEN 1075 - M Bettison, B S Choo and L R J Whale
- 29-7-5 Explanation of the Translation and Rotation Behaviour of Prestressed Moment Timber Joints - A J M Leijten
- 29-7-6 Design of Joints and Frame Corners using Dowel-Type Fasteners - E Gehri
- 29-7-7 Quasi-Static Reversed-Cyclic Testing of Nailed Joints - E Karacabeyli and A Ceccotti
- 29-7-8 Failure of Bolted Joints Loaded Parallel to the Grain: Experiment and Simulation - L Davenne, L Daudeville and M Yasumura

LOAD SHARING

- 3-8-1 Load Sharing - An Investigation on the State of Research and Development of Design Criteria - E Levin
- 4-8-1 A Review of Load-Sharing in Theory and Practice - E Levin
- 4-8-2 Load Sharing - B Norén
- 19-8-1 Predicting the Natural Frequencies of Light-Weight Wooden Floors - I Smith and Y H Chui
- 20-8-1 Proposed Code Requirements for Vibrational Serviceability of Timber Floors - Y H Chui and I Smith
- 21-8-1 An Addendum to Paper 20-8-1 - Proposed Code Requirements for Vibrational Serviceability of Timber Floors - Y H Chui and I Smith
- 21-8-2 Floor Vibrational Serviceability and the CIB Model Code - S Ohlsson
- 22-8-1 Reliability Analysis of Viscoelastic Floors - F Rouger, J D Barrett and R O Foschi
- 24-8-1 On the Possibility of Applying Neutral Vibrational Serviceability Criteria to Joisted Wood Floors - I Smith and Y H Chui
- 25-8-1 Analysis of Glulam Semi-rigid Portal Frames under Long-term Load - K Komatsu and N Kawamoto

DURATION OF LOAD

- 3-9-1 Definitions of Long Term Loading for the Code of Practice - B Norén

- 4-9-1 Long Term Loading of Trussed Rafters with Different Connection Systems - T Feldborg and M Johansen
- 5-9-1 Strength of a Wood Column in Combined Compression and Bending with Respect to Creep - B Källsner and B Norén
- 6-9-1 Long Term Loading for the Code of Practice (Part 2) - B Norén
- 6-9-2 Long Term Loading - K Möhler
- 6-9-3 Deflection of Trussed Rafters under Alternating Loading during a Year - T Feldborg and M Johansen
- 7-6-1 Strength and Long Term Behaviour of Lumber and Glued-Laminated Timber under Torsion Loads - K Möhler
- 7-9-1 Code Rules Concerning Strength and Loading Time - H J Larsen and E Theilgaard
- 17-9-1 On the Long-Term Carrying Capacity of Wood Structures - Y M Ivanov and Y Y Slavic
- 18-9-1 Prediction of Creep Deformations of Joints - J Kuipers
- 19-9-1 Another Look at Three Duration of Load Models - R O Foschi and Z C Yao
- 19-9-2 Duration of Load Effects for Spruce Timber with Special Reference to Moisture Influence - A Status Report - P Hoffmeyer
- 19-9-3 A Model of Deformation and Damage Processes Based on the Reaction Kinetics of Bond Exchange - T A C M van der Put
- 19-9-4 Non-Linear Creep Superposition - U Korin
- 19-9-5 Determination of Creep Data for the Component Parts of Stressed-Skin Panels - R Kliger
- 19-9-6 Creep an Lifetime of Timber Loaded in Tension and Compression - P Glos
- 19-1-1 Duration of Load Effects and Reliability Based Design (Single Member) - R O Foschi and Z C Yao
- 19-6-1 Effect of Age and/or Load on Timber Strength - J Kuipers
- 19-7-4 The Prediction of the Long-Term Load Carrying Capacity of Joints in Wood Structures - Y M Ivanov and Y Y Slavic
- 19-7-5 Slip in Joints under Long-Term Loading - T Feldborg and M Johansen
- 20-7-2 Slip in Joints under Long-Term Loading - T Feldborg and M Johansen
- 22-9-1 Long-Term Tests with Glued Laminated Timber Girders - M Badstube, W Rug and W Schöne
- 22-9-2 Strength of One-Layer solid and Lengthways Glued Elements of Wood Structures and its Alteration from Sustained Load - L M Kovaltchuk, I N Boitemirova and G B Uspenskaya
- 24-9-1 Long Term Bending Creep of Wood - T Toratti
- 24-9-2 Collection of Creep Data of Timber - A Ranta-Maunus
- 24-9-3 Deformation Modification Factors for Calculating Built-up Wood-Based Structures - I R Kliger
- 25-9-2 DVM Analysis of Wood. Lifetime, Residual Strength and Quality - L F Nielsen
- 26-9-1 Long Term Deformations in Wood Based Panels under Natural Climate Conditions. A Comparative Study - S Thelandersson, J Nordh, T Nordh and S Sandahl

- 28-9-1 Evaluation of Creep Behavior of Structural Lumber in Natural Environment - R Gupta and R Shen

TIMBER BEAMS

- 4-10-1 The Design of Simple Beams - H J Burgess
- 4-10-2 Calculation of Timber Beams Subjected to Bending and Normal Force - H J Larsen
- 5-10-1 The Design of Timber Beams - H J Larsen
- 9-10-1 The Distribution of Shear Stresses in Timber Beams - F J Keenan
- 9-10-2 Beams Notched at the Ends - K Möhler
- 11-10-1 Tapered Timber Beams - H Riberholt
- 13-6-2 Consideration of Size Effects in Longitudinal Shear Strength for Uncracked Beams - R O Foschi and J D Barrett
- 13-6-3 Consideration of Shear Strength on End-Cracked Beams - J D Barrett and R O Foschi
- 18-10-1 Submission to the CIB-W18 Committee on the Design of Ply Web Beams by Consideration of the Type of Stress in the Flanges - J A Baird
- 18-10-2 Longitudinal Shear Design of Glued Laminated Beams - R O Foschi
- 19-10-1 Possible Code Approaches to Lateral Buckling in Beams - H J Burgess
- 19-2-1 Creep Buckling Strength of Timber Beams and Columns - R H Leicester
- 20-2-1 Lateral Buckling Theory for Rectangular Section Deep Beam-Columns - H J Burgess
- 20-10-1 Draft Clause for CIB Code for Beams with Initial Imperfections - H J Burgess
- 20-10-2 Space Joists in Irish Timber - W J Robinson
- 20-10-3 Composite Structure of Timber Joists and Concrete Slab - T Poutanen
- 21-10-1 A Study of Strength of Notched Beams - P J Gustafsson
- 22-10-1 Design of Endnotched Beams - H J Larsen and P J Gustafsson
- 22-10-2 Dimensions of Wooden Flexural Members under Constant Loads - A Pozgai
- 22-10-3 Thin-Walled Wood-Based Flanges in Composite Beams - J König
- 22-10-4 The Calculation of Wooden Bars with flexible Joints in Accordance with the Polish Standart Code and Strict Theoretical Methods - Z Mielczarek
- 23-10-1 Tension Perpendicular to the Grain at Notches and Joints - T A C M van der Put
- 23-10-2 Dimensioning of Beams with Cracks, Notches and Holes. An Application of Fracture Mechanics - K Riipola
- 23-10-3 Size Factors for the Bending and Tension Strength of Structural Timber - J D Barret and A R Fewell
- 23-12-1 Bending Strength of Glulam Beams, a Design Proposal - J Ehlbeck and F Colling
- 23-12-3 Glulam Beams, Bending Strength in Relation to the Bending Strength of the Finger Joints - H Riberholt
- 24-10-1 Shear Strength of Continuous Beams - R H Leicester and F G Young
- 25-10-1 The Strength of Norwegian Glued Laminated Beams - K Solli, E Aasheim and R H Falk

- 25-10-2 The Influence of the Elastic Modulus on the Simulated Bending Strength of Hyperstatic Timber Beams - T D G Canisius
- 27-10-1 Determination of Shear Modulus - R Görlacher and J Kürth
- 29-10-1 Time Dependent Lateral Buckling of Timber Beams - F Rouger
- 29-10-2 Determination of Modulus of Elasticity in Bending According to EN 408 - K H Solli
- 29-10-3 On Determination of Modulus of Elasticity in Bending - L Boström, S Ormarsson and O Dahlblom
- 29-10-4 Relation of Moduli of Elasticity in Flatwise and Edgewise Bending of Solid Timber - C J Johansson, A Steffen and E W Wormuth

ENVIRONMENTAL CONDITIONS

- 5-11-1 Climate Grading for the Code of Practice - B Norén
- 6-11-1 Climate Grading (2) - B Norén
- 9-11-1 Climate Classes for Timber Design - F J Keenan
- 19-11-1 Experimental Analysis on Ancient Downgraded Timber Structures - B Leggeri and L Paolini
- 19-6-5 Drying Stresses in Round Timber - A Ranta-Maunus
- 22-11-1 Corrosion and Adaptation Factors for Chemically Aggressive Media with Timber Structures - K Erler
- 29-11-1 Load Duration Effect on Structural Beams under Varying Climate Influence of Size and Shape - P Galimard and P Morlier

LAMINATED MEMBERS

- 6-12-1 Directives for the Fabrication of Load-Bearing Structures of Glued Timber - A van der Velden and J Kuipers
- 8-12-1 Testing of Big Glulam Timber Beams - H Kolb and P Frech
- 8-12-2 Instruction for the Reinforcement of Apertures in Glulam Beams - H Kolb and P Frech
- 8-12-3 Glulam Standard Part 1: Glued Timber Structures; Requirements for Timber (Second Draft)
- 9-12-1 Experiments to Provide for Elevated Forces at the Supports of Wooden Beams with Particular Regard to Shearing Stresses and Long-Term Loadings - F Wassipaul and R Lackner
- 9-12-2 Two Laminated Timber Arch Railway Bridges Built in Perth in 1849 - L G Booth
- 9-6-4 Consideration of Combined Stresses for Lumber and Glued Laminated Timber - K Möhler
- 11-6-3 Consideration of Combined Stresses for Lumber and Glued Laminated Timber (addition to Paper CIB-W18/9-6-4) - K Möhler
- 12-12-1 Glulam Standard Part 2: Glued Timber Structures; Rating (3rd draft)
- 12-12-2 Glulam Standard Part 3: Glued Timber Structures; Performance (3 rd draft)
- 13-12-1 Glulam Standard Part 3: Glued Timber Structures; Performance (4th draft)
- 14-12-1 Proposals for CEI-Bois/CIB-W18 Glulam Standards - H J Larsen

- 14-12-2 Guidelines for the Manufacturing of Glued Load-Bearing Timber Structures - Stevin Laboratory
- 14-12-3 Double Tapered Curved Glulam Beams - H Riberholt
- 14-12-4 Comment on CIB-W18/14-12-3 - E Gehri
- 18-12-1 Report on European Glulam Control and Production Standard - H Riberholt
- 18-10-2 Longitudinal Shear Design of Glued Laminated Beams - R O Foschi
- 19-12-1 Strength of Glued Laminated Timber - J Ehlbeck and F Colling
- 19-12-2 Strength Model for Glulam Columns - H J Blaß
- 19-12-3 Influence of Volume and Stress Distribution on the Shear Strength and Tensile Strength Perpendicular to Grain - F Colling
- 19-12-4 Time-Dependent Behaviour of Glued-Laminated Beams - F Zaupa
- 21-12-1 Modulus of Rupture of Glulam Beam Composed of Arbitrary Laminae - K Komatsu and N Kawamoto
- 21-12-2 An Appraisal of the Young's Modulus Values Specified for Glulam in Eurocode 5- L R J Whale, B O Hilson and P D Rodd
- 21-12-3 The Strength of Glued Laminated Timber (Glulam): Influence of Lamination Qualities and Strength of Finger Joints - J Ehlbeck and F Colling
- 21-12-4 Comparison of a Shear Strength Design Method in Eurocode 5 and a More Traditional One - H Riberholt
- 22-12-1 The Dependence of the Bending Strength on the Glued Laminated Timber Girder Depth - M Badstube, W Rug and W Schöne
- 22-12-2 Acid Deterioration of Glulam Beams in Buildings from the Early Half of the 1960s - Preliminary summary of the research project; Overhead pictures - B A Hedlund
- 22-12-3 Experimental Investigation of normal Stress Distribution in Glue Laminated Wooden Arches - Z Mielczarek and W Chanaj
- 22-12-4 Ultimate Strength of Wooden Beams with Tension Reinforcement as a Function of Random Material Properties - R Candowicz and T Dziuba
- 23-12-1 Bending Strength of Glulam Beams, a Design Proposal - J Ehlbeck and F Colling
- 23-12-2 Probability Based Design Method for Glued Laminated Timber - M F Stone
- 23-12-3 Glulam Beams, Bending Strength in Relation to the Bending Strength of the Finger Joints - H Riberholt
- 23-12-4 Glued Laminated Timber - Strength Classes and Determination of Characteristic Properties - H Riberholt, J Ehlbeck and A Fewell
- 24-12-1 Contribution to the Determination of the Bending Strength of Glulam Beams - F Colling, J Ehlbeck and R Görlacher
- 24-12-2 Influence of Perpendicular-to-Grain Stressed Volume on the Load-Carrying Capacity of Curved and Tapered Glulam Beams - J Ehlbeck and J Kürth
- 25-12-1 Determination of Characteristic Bending Values of Glued Laminated Timber. EN-Approach and Reality - E Gehri
- 26-12-1 Norwegian Bending Tests with Glued Laminated Beams-Comparative Calculations with the "Karlsruhe Calculation Model" - E Aasheim, K Solli, F Colling, R H Falk, J Ehlbeck and R Görlacher
- 26-12-2 Simulation Analysis of Norwegian Spruce Glued-Laminated Timber - R Hernandez and R H Falk

- 26-12-3 Investigation of Laminating Effects in Glued-Laminated Timber - F Colling and R H Falk
- 26-12-4 Comparing Design Results for Glulam Beams According to Eurocode 5 and to the French Working Stress Design Code (CB71) - F Rouger
- 27-12-1 State of the Art Report: Glulam Timber Bridge Design in the U.S. - M A Ritter and T G Williamson
- 27-12-2 Common Design Practice for Timber Bridges in the United Kingdom - C J Mettem, J P Marcroft and G Davis
- 27-12-3 Influence of Weak Zones on Stress Distribution in Glulam Beams - E Serrano and H J Larsen
- 28-12-1 Determination of Characteristic Bending Strength of Glued Laminated Timber - E Gehri
- 28-12-2 Size Factor of Norwegian Glued Laminated Beams - E Aasheim and K H Solli
- 28-12-3 Design of Glulam Beams with Holes - K Riipola
- 28-12-4 Compression Resistance of Glued Laminated Timber Short Columns- U Korin
- 29-12-1 Development of Efficient Glued Laminated Timber - G Schickhofer

PARTICLE AND FIBRE BUILDING BOARDS

- 7-13-1 Fibre Building Boards for CIB Timber Code (First Draft)- O Brynildsen
- 9-13-1 Determination of the Bearing Strength and the Load-Deformation Characteristics of Particleboard - K Möhler, T Budianto and J Ehlbeck
- 9-13-2 The Structural Use of Tempered Hardboard - W W L Chan
- 11-13-1 Tests on Laminated Beams from Hardboard under Short- and Longterm Load - W Nozynski
- 11-13-2 Determination of Deformation of Special Densified Hardboard under Long-term Load and Varying Temperature and Humidity Conditions - W Halfar
- 11-13-3 Determination of Deformation of Hardboard under Long-term Load in Changing Climate - W Halfar
- 14-4-1 An Introduction to Performance Standards for Wood-Base Panel Products - D H Brown
- 14-4-2 Proposal for Presenting Data on the Properties of Structural Panels - T Schmidt
- 16-13-1 Effect of Test Piece Size on Panel Bending Properties - P W Post
- 20-4-1 Considerations of Reliability - Based Design for Structural Composite Products - M R O'Halloran, J A Johnson, E G Elias and T P Cunningham
- 20-13-1 Classification Systems for Structural Wood-Based Sheet Materials - V C Kearley and A R Abbott
- 21-13-1 Design Values for Nailed Chipboard - Timber Joints - A R Abbott
- 25-13-1 Bending Strength and Stiffness of Izopanel Plates - Z Mielczarek
- 28-13-1 Background Information for "Design Rated Oriented Strand Board (OSB)" in CSA Standards - Summary of Short-term Test Results - E Karacabeyli, P Lau, C R Henderson, F V Meakes and W Deacon
- 28-13-2 Torsional Stiffness of Wood-Hardboard Composed I-Beam - P Olejniczak

TRUSSED RAFTERS

- 4-9-1 Long-term Loading of Trussed Rafters with Different Connection Systems - T Feldborg and M Johansen
- 6-9-3 Deflection of Trussed Rafters under Alternating Loading During a Year - T Feldborg and M Johansen
- 7-2-1 Lateral Bracing of Timber Struts - J A Simon
- 9-14-1 Timber Trusses - Code Related Problems - T F Williams
- 9-7-1 Design of Truss Plate Joints - F J Keenan
- 10-14-1 Design of Roof Bracing - The State of the Art in South Africa - P A V Bryant and J A Simon
- 11-14-1 Design of Metal Plate Connected Wood Trusses - A R Egerup
- 12-14-1 A Simple Design Method for Standard Trusses - A R Egerup
- 13-14-1 Truss Design Method for CIB Timber Code - A R Egerup
- 13-14-2 Trussed Rafters, Static Models - H Riberholt
- 13-14-3 Comparison of 3 Truss Models Designed by Different Assumptions for Slip and E-Modulus - K Möhler
- 14-14-1 Wood Trussed Rafter Design - T Feldborg and M Johansen
- 14-14-2 Truss-Plate Modelling in the Analysis of Trusses - R O Foschi
- 14-14-3 Cantilevered Timber Trusses - A R Egerup
- 14-7-5 The Effect of Support Eccentricity on the Design of W- and WW-Trusses with Nail Plate Connectors - B Källsner
- 15-14-1 Guidelines for Static Models of Trussed Rafters - H Riberholt
- 15-14-2 The Influence of Various Factors on the Accuracy of the Structural Analysis of Timber Roof Trusses - F R P Pienaar
- 15-14-3 Bracing Calculations for Trussed Rafter Roofs - H J Burgess
- 15-14-4 The Design of Continuous Members in Timber Trussed Rafters with Punched Metal Connector Plates - P O Reece
- 15-14-5 A Rafter Design Method Matching U.K. Test Results for Trussed Rafters - H J Burgess
- 16-14-1 Full-Scale Tests on Timber Fink Trusses Made from Irish Grown Sitka Spruce - V Picardo
- 17-14-1 Data from Full Scale Tests on Prefabricated Trussed Rafters - V Picardo
- 17-14-2 Simplified Static Analysis and Dimensioning of Trussed Rafters - H Riberholt
- 17-14-3 Simplified Calculation Method for W-Trusses - B Källsner
- 18-14-1 Simplified Calculation Method for W-Trusses (Part 2) - B Källsner
- 18-14-2 Model for Trussed Rafter Design - T Poutanen
- 19-14-1 Annex on Simplified Design of W-Trusses - H J Larsen
- 19-14-2 Simplified Static Analysis and Dimensioning of Trussed Rafters - Part 2 - H Riberholt
- 19-14-3 Joint Eccentricity in Trussed Rafters - T Poutanen
- 20-14-1 Some Notes about Testing Nail Plates Subjected to Moment Load - T Poutanen
- 20-14-2 Moment Distribution in Trussed Rafters - T Poutanen

- 20-14-3 Practical Design Methods for Trussed Rafters - A R Egerup
- 22-14-1 Guidelines for Design of Timber Trussed Rafters - H Riberholt
- 23-14-1 Analyses of Timber Trussed Rafters of the W-Type - H Riberholt
- 23-14-2 Proposal for Eurocode 5 Text on Timber Trussed Rafters - H Riberholt
- 24-14-1 Capacity of Support Areas Reinforced with Nail Plates in Trussed Rafters - A Kevarinmäki
- 25-14-1 Moment Anchorage Capacity of Nail Plates in Shear Tests - A Kevarinmaki and J. Kangas
- 25-14-2 Design Values of Anchorage Strength of Nail Plate Joints by 2-curve Method and Interpolation - J Kangas and A Kevarinmaki
- 26-14-1 Test of Nail Plates Subjected to Moment - E Aasheim
- 26-14-2 Moment Anchorage Capacity of Nail Plates - A Kevarinmäki and J Kangas
- 26-14-3 Rotational Stiffness of Nail Plates in Moment Anchorage - A Kevarinmäki and J Kangas
- 26-14-4 Solution of Plastic Moment Anchorage Stress in Nail Plates - A Kevarinmäki
- 26-14-5 Testing of Metal-Plate-Connected Wood-Truss Joints - R Gupta
- 26-14-6 Simulated Accidental Events on a Trussed Rafter Roofed Building - C J Mettem and J P Marcroft

STRUCTURAL STABILITY

- 8-15-1 Laterally Loaded Timber Columns: Tests and Theory - H J Larsen
- 13-15-1 Timber and Wood-Based Products Structures. Panels for Roof Coverings. Methods of Testing and Strength Assessment Criteria. Polish Standard BN-78/7159-03
- 16-15-1 Determination of Bracing Structures for Compression Members and Beams - H Brüninghoff
- 17-15-1 Proposal for Chapter 7.4 Bracing - H Brüninghoff
- 17-15-2 Seismic Design of Small Wood Framed Houses - K F Hansen
- 18-15-1 Full-Scale Structures in Glued Laminated Timber, Dynamic Tests: Theoretical and Experimental Studies - A Ceccotti and A Vignoli
- 18-15-2 Stabilizing Bracings - H Brüninghoff
- 19-15-1 Connections Deformability in Timber Structures: a Theoretical Evaluation of its Influence on Seismic Effects - A Ceccotti and A Vignoli
- 19-15-2 The Bracing of Trussed Beams - M H Kessel and J Natterer
- 19-15-3 Racking Resistance of Wooden Frame Walls with Various Openings - M Yasumura
- 19-15-4 Some Experiences of Restoration of Timber Structures for Country Buildings - G Cardinale and P Spinelli
- 19-15-5 Non-Destructive Vibration Tests on Existing Wooden Dwellings - Y Hirashima
- 20-15-1 Behaviour Factor of Timber Structures in Seismic Zones. - A Ceccotti and A Vignoli
- 21-15-1 Rectangular Section Deep Beam - Columns with Continuous Lateral Restraint - H J Burgess

- 21-15-2 Buckling Modes and Permissible Axial Loads for Continuously Braced Columns-
H J Burgess
- 21-15-3 Simple Approaches for Column Bracing Calculations - H J Burgess
- 21-15-4 Calculations for Discrete Column Restraints - H J Burgess
- 21-15-5 Behaviour Factor of Timber Structures in Seismic Zones (Part Two)
- A Ceccotti and A Vignoli
- 22-15-1 Suggested Changes in Code Bracing Recommendations for Beams and Columns -
H J Burgess
- 22-15-2 Research and Development of Timber Frame Structures for Agriculture in Poland-
S Kus and J Kerste
- 22-15-3 Ensuring of Three-Dimensional Stiffness of Buildings with Wood Structures -
A K Shenghelia
- 22-15-5 Seismic Behavior of Arched Frames in Timber Construction - M Yasumura
- 22-15-6 The Robustness of Timber Structures - C J Mettem and J P Marcroft
- 22-15-7 Influence of Geometrical and Structural Imperfections on the Limit Load of Wood
Columns - P Dutko
- 23-15-1 Calculation of a Wind Girder Loaded also by Discretely Spaced Braces for Roof
Members - H J Burgess
- 23-15-2 Stability Design and Code Rules for Straight Timber Beams -
T A C M van der Put
- 23-15-3 A Brief Description of Formula of Beam-Columns in China Code - S Y Huang
- 23-15-4 Seismic Behavior of Braced Frames in Timber Construction - M Yasumara
- 23-15-5 On a Better Evaluation of the Seismic Behavior Factor of Low-Dissipative Timber
Structures - A Ceccotti and A Vignoli
- 23-15-6 Disproportionate Collapse of Timber Structures - C J Mettem and J P Marcroft
- 23-15-7 Performance of Timber Frame Structures During the Loma Prieta California
Earthquake - M R O'Halloran and E G Elias
- 24-15-2 Discussion About the Description of Timber Beam-Column Formula - S Y Huang
- 24-15-3 Seismic Behavior of Wood-Framed Shear Walls - M Yasumura
- 25-15-1 Structural Assessment of Timber Framed Building Systems - U Korin
- 25-15-3 Mechanical Properties of Wood-framed Shear Walls Subjected to Reversed Cyclic
Lateral Loading - M Yasumura
- 26-15-1 Bracing Requirements to Prevent Lateral Buckling in Trussed Rafters -
C J Mettem and P J Moss
- 26-15-2 Eurocode 8 - Part 1.3 - Chapter 5 - Specific Rules for Timber Buildings in Seismic
Regions - K Becker, A Ceccotti, H Charlier, E Katsaragakis, H J Larsen and
H Zeitter
- 26-15-3 Hurricane Andrew - Structural Performance of Buildings in South Florida -
M R O'Halloran, E L Keith, J D Rose and T P Cunningham
- 29-15-1 Lateral Resistance of Wood Based Shear Walls with Oversized Sheathing Panels -
F Lam, H G L Prion and M He
- 29-15-2 Damage of Wooden Buildings Caused by the 1995 Hyogo-Ken Nanbu Earthquake
- M Yasumura, N Kawai, N Yamaguchi and S Nakajima
- 29-15-3 The Racking Resistance of Timber Frame Walls: Design by Test and Calculation -
D R Griffiths, C J Mettem, V Enjily, P J Steer

- 29-15-4 Current Developments in Medium-Rise Timber Frame Buildings in the UK - C J Mettem, G C Pitts, P J Steer, V Enjily
- 29-15-5 Natural Frequency Prediction for Timber Floors - R J Bainbridge, and C J Mettem

FIRE

- 12-16-1 British Standard BS 5268 the Structural Use of Timber: Part 4 Fire Resistance of Timber Structures
- 13-100-2 CIB Structural Timber Design Code. Chapter 9. Performance in Fire
- 19-16-1 Simulation of Fire in Tests of Axially Loaded Wood Wall Studs - J König
- 24-16-1 Modelling the Effective Cross Section of Timber Frame Members Exposed to Fire - J König
- 25-16-1 The Effect of Density on Charring and Loss of Bending Strength in Fire - J König
- 25-16-2 Tests on Glued-Laminated Beams in Bending Exposed to Natural Fires - F Bolonius Olesen and J König
- 26-16-1 Structural Fire Design According to Eurocode 5, Part 1.2 - J König

STATISTICS AND DATA ANALYSIS

- 13-17-1 On Testing Whether a Prescribed Exclusion Limit is Attained - W G Warren
- 16-17-1 Notes on Sampling and Strength Prediction of Stress Graded Structural Timber - P Glos
- 16-17-2 Sampling to Predict by Testing the Capacity of Joints, Components and Structures - B Norén
- 16-17-3 Discussion of Sampling and Analysis Procedures - P W Post
- 17-17-1 Sampling of Wood for Joint Tests on the Basis of Density - I Smith, L R J Whale
- 17-17-2 Sampling Strategy for Physical and Mechanical Properties of Irish Grown Sitka Spruce - V Picardo
- 18-17-1 Sampling of Timber in Structural Sizes - P Glos
- 18-6-3 Notes on Sampling Factors for Characteristic Values - R H Leicester
- 19-17-1 Load Factors for Proof and Prototype Testing - R H Leicester
- 19-6-2 Confidence in Estimates of Characteristic Values - R H Leicester
- 21-6-1 Draft Australian Standard: Methods for Evaluation of Strength and Stiffness of Graded Timber - R H Leicester
- 21-6-2 The Determination of Characteristic Strength Values for Stress Grades of Structural Timber. Part 1 - A R Fewell and P Glos
- 22-17-1 Comment on the Strength Classes in Eurocode 5 by an Analysis of a Stochastic Model of Grading - A proposal for a supplement of the design concept - M Kiesel
- 24-17-1 Use of Small Samples for In-Service Strength Measurement - R H Leicester and F G Young
- 24-17-2 Equivalence of Characteristic Values - R H Leicester and F G Young
- 24-17-3 Effect of Sampling Size on Accuracy of Characteristic Values of Machine Grades - Y H Chui, R Turner and I Smith
- 24-17-4 Harmonisation of LSD Codes - R H Leicester
- 25-17-2 A Body for Confirming the Declaration of Characteristic Values - J Sunley

- 25-17-3 Moisture Content Adjustment Procedures for Engineering Standards - D W Green and J W Evans
- 27-17-1 Statistical Control of Timber Strength - R H Leicester and H O Breitingen

GLUED JOINTS

- 20-18-1 Wood Materials under Combined Mechanical and Hygral Loading - A Martensson and S Thelandersson
- 20-18-2 Analysis of Generalized Volkersen - Joints in Terms of Linear Fracture Mechanics - P J Gustafsson
- 20-18-3 The Complete Stress-Slip Curve of Wood-Adhesives in Pure Shear - H Wernersson and P J Gustafsson
- 22-18-1 Perspective Adhesives and Protective Coatings for Wood Structures - A S Freidin

FRACTURE MECHANICS

- 21-10-1 A Study of Strength of Notched Beams - P J Gustafsson
- 22-10-1 Design of Endnotched Beams - H J Larsen and P J Gustafsson
- 23-10-1 Tension Perpendicular to the Grain at Notches and Joints - T A C M van der Put
- 23-10-2 Dimensioning of Beams with Cracks, Notches and Holes. An Application of Fracture Mechanics - K Riipola
- 23-19-1 Determination of the Fracture Energie of Wood for Tension Perpendicular to the Grain - W Rug, M Badstube and W Schöne
- 23-19-2 The Fracture Energy of Wood in Tension Perpendicular to the Grain. Results from a Joint Testing Project - H J Larsen and P J Gustafsson
- 23-19-3 Application of Fracture Mechanics to Timber Structures - A Ranta-Maunus
- 24-19-1 The Fracture Energy of Wood in Tension Perpendicular to the Grain - H J Larsen and P J Gustafsson
- 28-19-1 Fracture of Wood in Tension Perpendicular to the Grain: Experiment and Numerical Simulation by Damage Mechanics - L Daudeville, M Yasumura and J D Lanvin
- 28-19-2 A New Method of Determining Fracture Energy in Forward Shear along the Grain - H D Mansfield-Williams
- 28-19-3 Fracture Design Analysis of Wooden Beams with Holes and Notches. Finite Element Analysis based on Energy Release Rate Approach - H Petersson
- 28-19-4 Design of Timber Beams with Holes by Means of Fracture Mechanics - S Aicher, J Schmidt and S Brunold

SERVICEABILITY

- 27-20-1 Codification of Serviceability Criteria - R H Leicester
- 27-20-2 On the Experimental Determination of Factor k_{def} and Slip Modulus k_{ser} from Short- and Long-Term Tests on a Timber-Concrete Composite (TCC) Beam - S Capretti and A Ceccotti
- 27-20-3 Serviceability Limit States: A Proposal for Updating Eurocode 5 with Respect to Eurocode 1 - P Racher and F Rouger

27-20-4 Creep Behavior of Timber under External Conditions - C Le Govic, F Rouger, T Toratti and P Morlier

CIB TIMBER CODE

- 2-100-1 A Framework for the Production of an International Code of Practice for the Structural Use of Timber - W T Curry
- 5-100-1 Design of Solid Timber Columns (First Draft) - H J Larsen
- 5-100-2 A Draft Outline of a Code for Timber Structures - L G Booth
- 6-100-1 Comments on Document 5-100-1; Design of Solid Timber Columns - H J Larsen and E Theilgaard
- 6-100-2 CIB Timber Code: CIB Timber Standards - H J Larsen and E Theilgaard
- 7-100-1 CIB Timber Code Chapter 5.3 Mechanical Fasteners; CIB Timber Standard 06 and 07 - H J Larsen
- 8-100-1 CIB Timber Code - List of Contents (Second Draft) - H J Larsen
- 9-100-1 The CIB Timber Code (Second Draft)
- 11-100-1 CIB Structural Timber Design Code (Third Draft)
- 11-100-2 Comments Received on the CIB Code
 - a U Saarelainen
 - b Y M Ivanov
 - c R H Leicester
 - d W Nozynski
 - e W R A Meyer
 - f P Beckmann; R Marsh
 - g W R A Meyer
 - h W R A Meyer
- 11-100-3 CIB Structural Timber Design Code; Chapter 3 - H J Larsen
- 12-100-1 Comment on the CIB Code - Sous-Commission Glulam
- 12-100-2 Comment on the CIB Code - R H Leicester
- 12-100-3 CIB Structural Timber Design Code (Fourth Draft)
- 13-100-1 Agreed Changes to CIB Structural Timber Design Code
- 13-100-2 CIB Structural Timber Design Code. Chapter 9: Performance in Fire
- 13-100-3a Comments on CIB Structural Timber Design Code
- 13-100-3b Comments on CIB Structural Timber Design Code - W R A Meyer
- 13-100-3c Comments on CIB Structural Timber Design Code - British Standards Institution
- 13-100-4 CIB Structural Timber Design Code. Proposal for Section 6.1.5 Nail Plates - N I Bovim
- 14-103-2 Comments on the CIB Structural Timber Design Code - R H Leicester
- 15-103-1 Resolutions of TC 165-meeting in Athens 1981-10-12/13
- 21-100-1 CIB Structural Timber Design Code. Proposed Changes of Sections on Lateral Instability, Columns and Nails - H J Larsen
- 22-100-1 Proposal for Including an Updated Design Method for Bearing Stresses in CIB W18 - Structural Timber Design Code - B Madsen
- 22-100-2 Proposal for Including Size Effects in CIB W18A Timber Design Code - B Madsen

- 22-100-3 CIB Structural Timber Design Code - Proposed Changes of Section on Thin-Flanged Beams - J König
- 22-100-4 Modification Factor for "Aggressive Media" - a Proposal for a Supplement to the CIB Model Code - K Erler and W Rug
- 22-100-5 Timber Design Code in Czechoslovakia and Comparison with CIB Model Code - P Dutko and B Kozelouh

LOADING CODES

- 4-101-1 Loading Regulations - Nordic Committee for Building Regulations
- 4-101-2 Comments on the Loading Regulations - Nordic Committee for Building Regulations

STRUCTURAL DESIGN CODES

- 1-102-1 Survey of Status of Building Codes, Specifications etc., in USA - E G Stern
- 1-102-2 Australian Codes for Use of Timber in Structures - R H Leicester
- 1-102-3 Contemporary Concepts for Structural Timber Codes - R H Leicester
- 1-102-4 Revision of CP 112 - First Draft, July 1972 - British Standards Institution
- 4-102-1 Comparison of Codes and Safety Requirements for Timber Structures in EEC Countries - Timber Research and Development Association
- 4-102-2 Nordic Proposals for Safety Code for Structures and Loading Code for Design of Structures - O A Brynildsen
- 4-102-3 Proposal for Safety Codes for Load-Carrying Structures - Nordic Committee for Building Regulations
- 4-102-4 Comments to Proposal for Safety Codes for Load-Carrying Structures - Nordic Committee for Building Regulations
- 4-102-5 Extract from Norwegian Standard NS 3470 "Timber Structures"
- 4-102-6 Draft for Revision of CP 112 "The Structural Use of Timber" - W T Curry
- 8-102-1 Polish Standard PN-73/B-03150: Timber Structures; Statistical Calculations and Designing
- 8-102-2 The Russian Timber Code: Summary of Contents
- 9-102-1 Svensk Byggnorm 1975 (2nd Edition); Chapter 27: Timber Construction
- 11-102-1 Eurocodes - H J Larsen
- 13-102-1 Program of Standardisation Work Involving Timber Structures and Wood-Based Products in Poland
- 17-102-1 Safety Principles - H J Larsen and H Riberholt
- 17-102-2 Partial Coefficients Limit States Design Codes for Structural Timberwork - I Smith
- 18-102-1 Antiseismic Rules for Timber Structures: an Italian Proposal - G Augusti and A Ceccotti
- 18-1-2 Eurocode 5, Timber Structures - H J Larsen
- 19-102-1 Eurocode 5 - Requirements to Timber - Drafting Panel Eurocode 5
- 19-102-2 Eurocode 5 and CIB Structural Timber Design Code - H J Larsen
- 19-102-3 Comments on the Format of Eurocode 5 - A R Fewell

- 19-102-4 New Developments of Limit States Design for the New GDR Timber Design Code - W Rug and M Badstube
- 19-7-3 Effectiveness of Multiple Fastener Joints According to National Codes and Eurocode 5 (Draft) - G Steck
- 19-7-6 The Derivation of Design Clauses for Nailed and Bolted Joints in Eurocode5 - L R J Whale and I Smith
- 19-14-1 Annex on Simplified Design of W-Trusses - H J Larsen
- 20-102-1 Development of a GDR Limit States Design Code for Timber Structures - W Rug and M Badstube
- 21-102-1 Research Activities Towards a New GDR Timber Design Code Based on Limit States Design - W Rug and M Badstube
- 22-102-1 New GDR Timber Design Code, State and Development - W Rug, M Badstube and W Kofent
- 22-102-2 Timber Strength Parameters for the New USSR Design Code and its Comparison with International Code - Y Y Slavik, N D Denesh and E B Ryumina
- 22-102-3 Norwegian Timber Design Code - Extract from a New Version - E Aasheim and K H Solli
- 23-7-1 Proposal for a Design Code for Nail Plates - E Aasheim and K H Solli
- 24-102-2 Timber Footbridges: A Comparison Between Static and Dynamic Design Criteria - A Ceccotti and N de Robertis
- 25-102-1 Latest Development of Eurocode 5 - H J Larsen
- 25-102-1A Annex to Paper CIB-W18/25-102-1. Eurocode 5 - Design of Notched Beams - H J Larsen, H Riberholt and P J Gustafsson
- 25-102-2 Control of Deflections in Timber Structures with Reference to Eurocode 5 - A Martensson and S Thelandersson
- 28-102-1 Eurocode 5 - Design of Timber Structures - Part 2: Bridges - D Bajolet, E Gehri, J König, H Kreuzinger, H J Larsen, R Mäkipuro and C Mettem
- 28-102-2 Racking Strength of Wall Diaphragms - Discussion of the Eurocode 5 Approach - B Källsner
- 29-102-1 Model Code for the Probabilistic Design of Timber Structures - H J Larsen, T Isaksson and S Thelandersson

INTERNATIONAL STANDARDS ORGANISATION

- 3-103-1 Method for the Preparation of Standards Concerning the Safety of Structures (ISO/DIS 3250) - International Standards Organisation ISO/TC98
- 4-103-1 A Proposal for Undertaking the Preparation of an International Standard on Timber Structures - International Standards Organisation
- 5-103-1 Comments on the Report of the Consultion with Member Bodies Concerning ISO/TC/P129 - Timber Structures - Dansk Ingeniorforening
- 7-103-1 ISO Technical Committees and Membership of ISO/TC 165
- 8-103-1 Draft Resolutions of ISO/TC 165
- 12-103-1 ISO/TC 165 Ottawa, September 1979
- 13-103-1 Report from ISO/TC 165 - A Sorensen
- 14-103-1 Comments on ISO/TC 165 N52 "Timber Structures; Solid Timber in Structural Sizes; Determination of Some Physical and Mechanical Properties"

- 14-103-2 Comments on the CIB Structural Timber Design Code - R H Leicester
21-103-1 Concept of a Complete Set of Standards - R H Leicester

JOINT COMMITTEE ON STRUCTURAL SAFETY

- 3-104-1 International System on Unified Standard Codes of Practice for Structures -
Comité Européen du Béton (CEB)
7-104-1 Volume 1: Common Unified Rules for Different Types of Construction and
Material - CEB

CIB PROGRAMME, POLICY AND MEETINGS

- 1-105-1 A Note on International Organisations Active in the Field of Utilisation of Timber
- P Sonnemans
5-105-1 The Work and Objectives of CIB-W18-Timber Structures - J G Sunley
10-105-1 The Work of CIB-W18 Timber Structures - J G Sunley
15-105-1 Terms of Reference for Timber - Framed Housing Sub-Group of CIB-W18
19-105-1 Tropical and Hardwood Timbers Structures - R H Leicester
21-105-1 First Conference of CIB-W18B, Tropical and Hardwood Timber Structures
Singapore, 26 - 28 October 1987 - R H Leicester

INTERNATIONAL UNION OF FORESTRY RESEARCH ORGANISATIONS

- 7-106-1 Time and Moisture Effects - CIB W18/IUFRO 55.02-03 Working Party

**INTERNATIONAL COUNCIL FOR BUILDING RESEARCH STUDIES AND DOCUMENTATION
WORKING COMMISSION W18 - TIMBER STRUCTURES**

THE EFFECT OF EDGE KNOTS ON THE STRENGTH OF SPF MSR LUMBER

by

T Courchene

F Lam

J D Barrett

Department of Wood Science

Faculty of Forestry

University of British Columbia

Canada

MEETING TWENTY - NINE

BORDEAUX

FRANCE

AUGUST 1996

THE EFFECT OF EDGE KNOTS ON THE STRENGTH OF SPF MSR LUMBER

by

Terry Courchene¹, Frank Lam² and J.D. Barrett³

ABSTRACT

An experimental program has been performed to evaluate the impact of edge knot visual quality level on the tension and bending strengths of 1650f-1.5E 38 x 89 mm Spruce-Pine-Fir machine stress rated lumber. A closed form solution has been developed to establish the strength property probability distribution of a new combined grade containing visual quality level knots. Simulations have been conducted verifying the closed form solution. The results indicate that the amount of visual quality level material to be included in the new grade is important. In this study, the new grade exceeded the bending strength and edge-wise modulus of elasticity requirements but failed to meet the tension strength requirement due to the quality and quantity of visual quality level material included in the grade mix.

INTRODUCTION

In North America, machine stress rated (MSR) lumber was introduced in the early 1960's when the well-known principle of positive correlation between the bending strength and stiffness of lumber was used to develop commercial grading machines such as the Continuous Lumber Tester (CLT). During production each piece of lumber passes lengthwise through the grading machine. As the piece travel through the machine, it is deflected on the flat into an S-shape by a series of rollers (Figure 1).

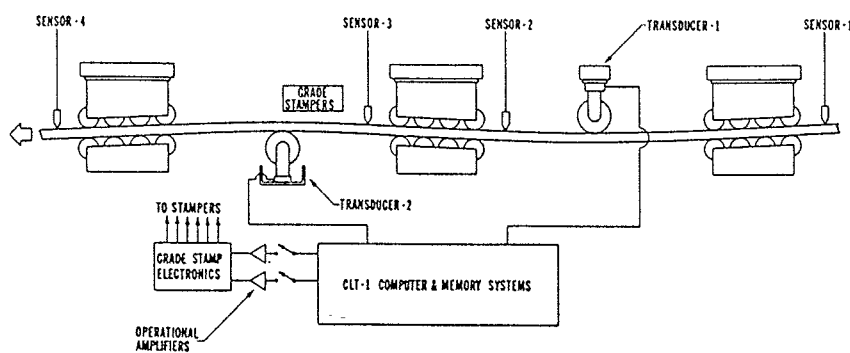


Figure 1. - Illustration of a CLT machine. (from Galligan *et al.* 1977: Machine Stress Rating: Practical Concerns for Lumber Producers. USDA General Technical Report FPL 7.)

¹Graduate Res. Assistant, Dept. of Wood Sci., Univ. of British Columbia, Van., B.C. Canada V6T 1Z4.

²Assistant Prof., Dept. of Wood Sci., Univ. of British Columbia, Van., B.C. Canada V6T 1Z4.

³Professor, Dept. of Wood Sci., Univ. of British Columbia, Van., B.C. Canada V6T 1Z4.

The forces required to deform the piece are continuously monitored and converted into flat-wise modulus of elasticity (MOE) estimates along the member. Based on the within member minimum and average MOE readings, the board is put into a preliminary grade or MOE class.

Past research has shown that lumber strength properties are affected by knot size, knot location and slope of grain more than any other common defect (Littleford 1966, 1978, Orosz 1977, Bolger and Rasmussen 1962, and Cramer and Goodman 1983). Based on these results, visual quality level (VQL) restrictions have been established to reduce the variability in strength by excluding oversized edge knots and some non-structural appearance characteristics such as wane, warp, and general appearance from different grades of MSR lumber even though the material met the flat-wise MOE requirements.

Littleford (1978) studied visual restrictions on the size of edge knots on unseasoned Douglas-fir and western hemlock nominal 38 x 140 mm lumber. The material was graded by a CLT-1 stress rating machine. Littleford (1978) showed that lumber below the average strength, for any MOE, can be attributed to edge knots. He stated that "edge knot restrictions arise to eliminate those pieces where the flat-wise stiffness measured by the machine might not be a good index of the actual strength for use on edge as, for example, joists and rafters". Further, he stated that with respect to "restrictions on the maximum size of edge knots to be allowed in Douglas-fir and western hemlock grades...it is debatable that such a restriction will prove to be so useful for lodgepole pine and western white spruce".

In Canada the majority of MSR production is Spruce-Pine-Fir (SPF) material. Results from the Canadian Lumber Properties In-grade Program indicate that SPF MSR material tends to be governed by bending stiffness rather than strength. Therefore, the current VQL restriction, based on Douglas Fir-Larch and Hem-Fir data, may not be suitable for the Canadian SPF material.

The objectives of this study are: 1) to quantify the frequency of visual downgrading of SPF MSR lumber resulting from edge knot restrictions, 2) to evaluate the relationship between knot size and lumber strength, and 3) to provide guidance for establishing alternate VQL rules for SPF MSR lumber.

IMPACT OF VQL ON PRODUCTION

Mill visits were conducted to quantify the impact of edge knot restriction on MSR lumber production and to evaluate the mill practices of edge knot size determination. MSR lumber production facilities from the following regions in British Columbia were studied: Interior, Cariboo, and Kooteney or Rocky Mountain. These areas provide a good representation of the SPF timber supply.

Finished packages of lumber were inspected. The original machine grade, the final grade, and the visual restriction that caused downgrading were recorded. Table 1 shows the summary results which indicate that wane and edge knots are two of the most frequent

reasons for downgrading with relative percentages of downgrade of 31.76% and 18.15%, respectively. These levels of downgrade are significant to the mills from the viewpoint of production and the impact is most evident in the 1650f-1.5E grade.

Downgrading Characteristics	Percentage of Total
Edge Knots	18.15
Other Knots	8.35
Wane	31.76
Shake	13.25
Slope of Grain	2.54
Manufacturing	10.16
Natural	6.72
Drying	9.07

Table 1. Summary Information for all Regions.

MATERIAL AND METHODS

The testing material was sampled from a MSR lumber sawmill from the Interior Region of British Columbia. The material was 4.8 m long 1650f-1.5E 38 x 89 mm kiln dried SPF lumber. This grade permits a maximum edge knot displacement of 1/4 of the net cross section (NLGA, 1994). The sample was separated into two different types: 1) visual quality level (VQL) and 2) on-grade or 1650. The VQL material had at least one edge defect with a displacement greater than 1/4 of the net cross section as defined by the NLGA current lumber grading rules and practices (NLGA, 1994). The VQL material contained approximately 450 specimens. The on-grade material consisted of one package of lumber, 294 specimens, which was on-grade for all characteristics including current visual override rules.

All material was sampled during a continuous production run during which the CLT was set to classify lumber into three grades; 2400f-2.0E, 2100f-1.8E and 1650f-1.5E. Information on the volume of production for all grades after visual grading was recorded. Production figures such as total number of boards processed by the CLT and the number of pieces assigned by the CLT in each grade were also recorded.

The specimens were shipped to the University of B.C. where the following physical properties were measured and recorded: species, CLT machine grade, specimen dimension and number. The largest strength reducing edge defect was visually determined. Its location and size (to the nearest 1.6 mm) were measured and recorded.

A two-pass Cook Bolinders SG-AF grading machine was used to determine the flat-wise MOE profile of each board. The machine measured and recorded the varying load along the board length required to achieve a flat-wise deflection of 4.5 mm over a span of 900 mm. The load profile for each specimen was converted to a MOE profile assuming simple supports and center point loading.

A 224 kN bending machine was used to determine the edge-wise MOE of all specimens. The machine was setup in a third point loading configuration with a span to depth ratio of 21:1. All specimens were longitudinally centered within the machine configuration. A yoke was suspended between nails spaced at a distance of 7 times the sample depth. A linear variable differential transducer was centered within the yoke and measured mid-depth displacement to the nearest 0.025 mm. This yoke displacement, the actuator stroke displacement and the applied load were recorded. The machine was set so that the loading time was approximately 1 minute.

Within the VQL and on-grade groups, specimens were randomly assigned to destructive testing in either tension or bending mode. The sample size for tension testing from the on-grade and VQL group was 144 and 220, respectively. A Metriguard Model 403 Tension Proof Tester was used in the tension testing. The lumber was lightly sanded for 61 cm on the ends to ensure that they did not slip within the machine grips. Since 61 cm on both ends were within the grips, the test gauge length was 3.7 m. Moisture content, peak load, cause and location of the failure were recorded.

A 224 kN bending machine was used to determine the bending strength of 148 on-grade specimens and 220 VQL specimens. The machine was setup in the third point loading configuration with a span to depth ratio of 21:1. Samples were trimmed to 2.04 meters, to ensure adequate coverage of the end supports and to ensure the worst defect in a specimen could be placed within the middle third of the test length or as close to this as possible. The actuator stroke displacement and the applied load were recorded. The stroke actuator rate was set at 23 mm/min. to achieve failure in approximately one minute. The moisture content, failure location and failure cause were recorded.

ANALYSIS AND RESULTS

KNOT AREA RATIO

The manual knot measurements were analyzed to: 1) determine the knot size as a percentage of the cross sectional area, and 2) classify a knot as either an edge knot or otherwise based on current grading practices. The determination of knot area ratio (KAR) showed that many of the knots that were manually measured did not meet the criteria for MSR edge knots. From a total of 440 VQL specimens selected by mill personal during material sampling only 263 specimens actually contained edge knots greater than 25%, as determined by manual measurements in the laboratory.

In this particular case, the lumber grader felt that he could only achieve 75-80% accuracy in selecting VQL samples for edge knots alone during production. This would mean that approximately 340 specimens should have had large edge knots which is substantially above the actual number of 263 large edge knots. Some of this discrepancy can be explained by the fact that there was more time and accuracy involved in the manual measurements in the laboratory than the visual assessment done by lumber graders in the mill.

Figures 2 and 3 show the relationship between edge knot KAR for the VQL specimens with bending and tension strengths, respectively. The relationship between KAR and strength seems to be weaker when comparing bending to tension strength. This results from the nature of the bending test where the worst defect is randomly selected to either the tension or the compression edge. Furthermore, it was not always possible to get the worst defect within the middle third of the test span for every specimen.

MODULUS OF ELASTICITY

For each specimen, the within board flat-wise average and minimum MOE values were calculated. The cumulative probability distributions of the within board average and minimum MOE are shown in Figure 4. The summary statistics for the within board flat-wise MOE values are given in Table 2.

	MOE Flat-wise		MOE Edge-wise	
	VQL	1650	VQL	1650
Mean (MPa)	11065	11375	10124	11258
Median (MPa)	11000	11372	10096	11197
Standard Deviation (MPa)	1139	1062	2032	1535
Coefficient of Variation (%)	10.3	9.3	20.0	13.6
Minimum (MPa)	5780	8755	4339	6694
Maximum (MPa)	14800	15662	16604	15786
Count	440	294	442	294
Fifth Percentile (MPa)	9271	9741	6734	9068

Table 2. Summary Statistics for MOE by Group.

For each specimen, the load versus yoke displacement in the edge-wise MOE tests were analyzed. A linear regression of load data in the range of 0.448 to 1.556 kN was performed to estimate the slope of the load-deflection curve where the deflection is the relative deformation between the load point and the mid span. With this slope value, MOE on edge was calculated. Summary statistics of the edge-wise MOE results are presented in Table 2. The cumulative probability distributions for each grade are provided in Figure 5.

BENDING AND TENSION STRENGTHS

Based on the peak load information, the bending and tension strengths were calculated with standard engineering formulae. Figure 6 shows the cumulative probability distributions of bending strength for both VQL and 1650 groups. Figure 7 shows the cumulative probability distributions of tension strength for both VQL and 1650 groups. Summary statistical information on the bending and tension strengths are shown in Table 3.

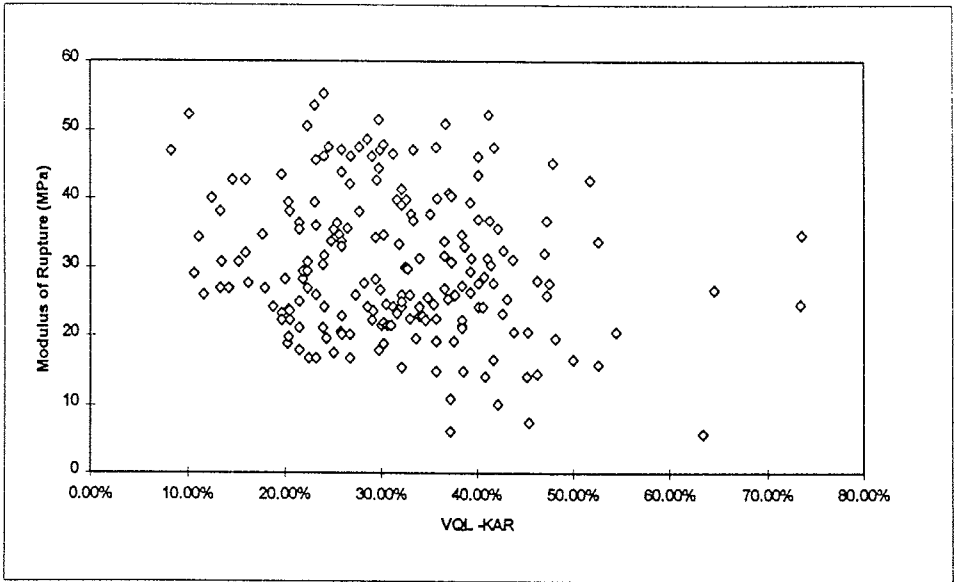


Figure 2. Relationship between Bending Strength and Knot Area Ratio of VQL Specimens.

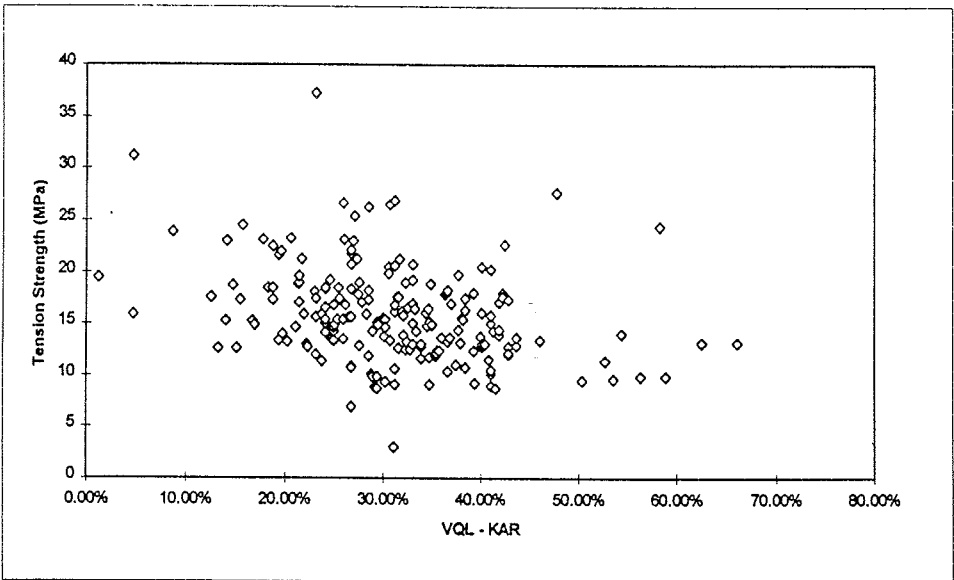


Figure 3. Relationship between Tension Strength and Knot Area Ratio of VQL Specimens.

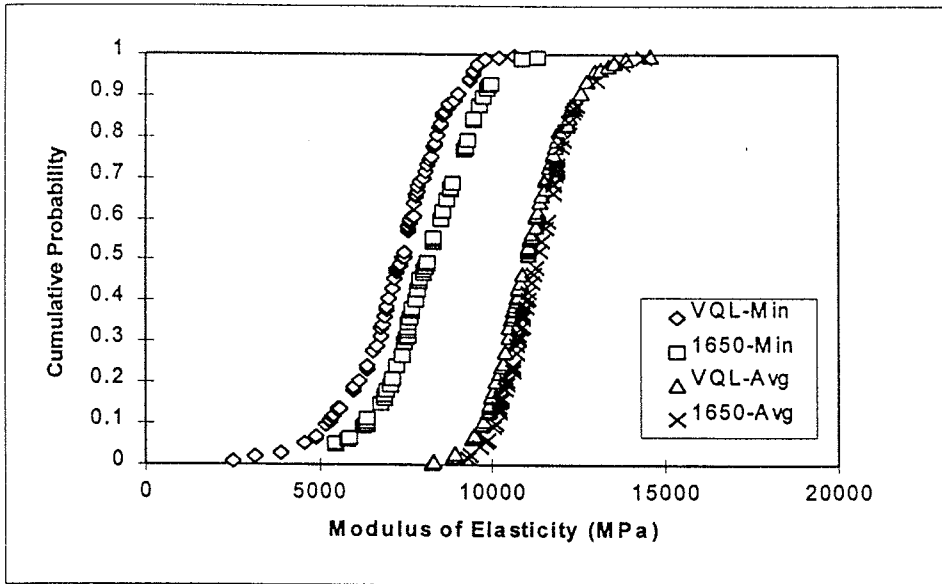


Figure 4. Cumulative Probability Distributions of Flat-wise MOE (every fifth point shown).

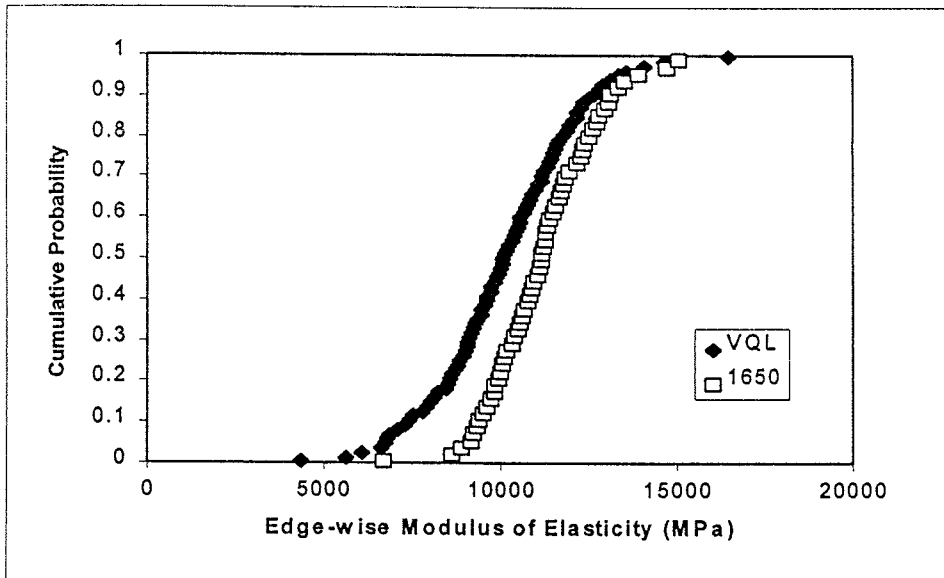


Figure 5. Cumulative Probability Distributions of Edge-wise MOE (every fifth point shown).

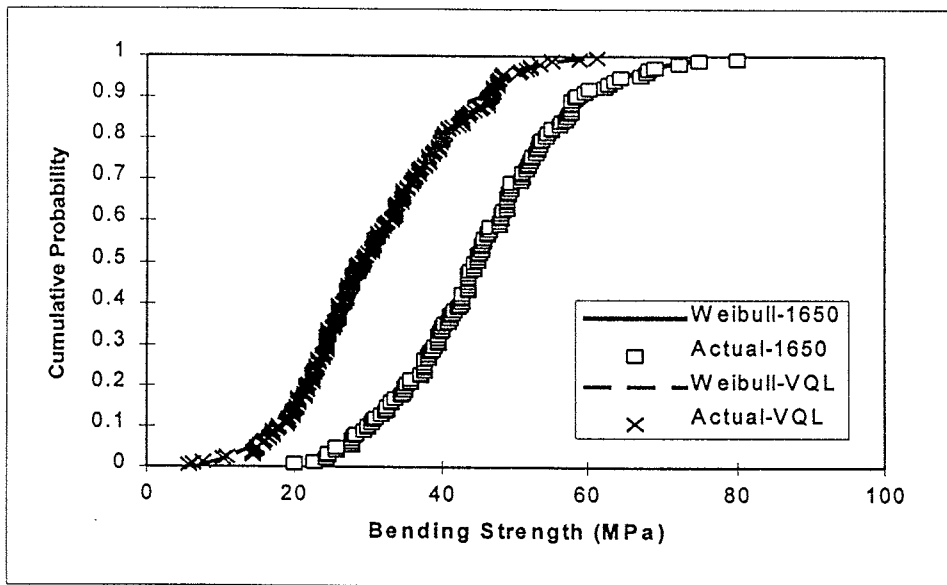


Figure 6. Cumulative Probability Distributions of Bending Strength for Both Groups.

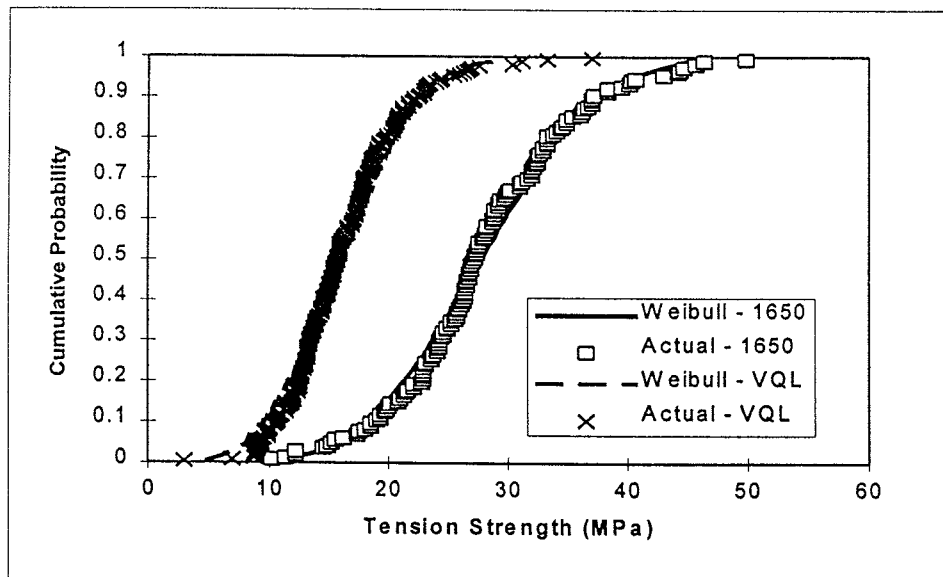


Figure 7. Cumulative Probability Distributions of Tension Strength for Both Groups.

	Bending		Tension	
	VQL	1650	VQL	1650
Mean (MPa)	30.66	45.06	16.23	27.91
Median (MPa)	29.12	44.61	15.63	27.11
Standard Deviation (MPa)	10.59	11.33	4.80	7.41
Coefficient of Variation (%)	34.54	25.15	29.59	26.57
Minimum (MPa)	5.72	19.86	3.02	10.24
Maximum (MPa)	61.27	80.12	37.17	49.77
Count	220	148	220	146
Fifth Percentile (MPa)	14.85	26.49	9.33	15.24

Table 3. Summary Statistics for Bending and Tension Strength by Group.

WEIBULL ANALYSIS

Based on maximum likelihood procedures, tension and bending strength data of both lumber grades were fitted with 3-parameter (3-P) Weibull distributions. The 3-P Weibull was chosen because it was judged to be the best at fitting the data amongst the various distributions tried, including 2-parameter Weibull and lognormal. The distribution takes on the following form:

$$X = m\{-\ln(1-P_f)\}^{1/K} + \text{Loc} \quad [1]$$

where

- X = the strength level for a particular P_f
- m = scale parameter
- K = shape parameter
- Loc = location parameter
- P_f = probability of failure

Knowing the distribution parameters, the probability of failure for a given X (strength level) can be determined. Figures 6 and 7 show the fitted 3-P Weibull distribution to the various groups of strength data.

CLOSED FORM SOLUTION

A closed form solution was used to determine the strength attributes of a new combined grade which is a mixture of both 1650 and VQL groups. In the new combined grade, a portion of the total is VQL material and the remaining proportion is 1650 material. For a given strength level, the probability of failure for the new grade (P_{fr}) was determined by these proportions and their associated P_f as:

$$P_{fT} = P_{f/1650}p_{1650} + P_{f/VQL}p_{VQL}$$

[2]

where

- P_{fT} = probability of failure of combined grades
 $P_{f/1650}$ = probability of failure for 1650 grade
 p_{1650} = proportion of 1650 material
 $P_{f/VQL}$ = probability of failure for VQL grade
 p_{VQL} = proportion of VQL material
 $p_{1650} + p_{VQL} = 1$

Given a strength level X, the associated $P_{f/1650}$ and $P_{f/VQL}$ were estimated from the respective probability distributions. With the portion of VQL (p_{VQL}) known, equation 2 was used to establish the associated probability of failure. The strength property probability distribution of the combined grade was established when a range of strength levels were considered. Figure 8 shows a schematic illustration of the procedures.

The amount of VQL material in the new grade combination was determined by evaluation of different knot area ratios. In essence, boundaries were placed on the VQL group resulting in separation of the VQL into different groups based on KAR. These group characteristics, the amount of material in each group, and its corresponding percentage are summarized in Table 4. The percentage was calculated from the total production of 2642 pieces of 1650f-1.5E material produced during VQL collection.

To produce a MSR lumber grade, the material fifth percentile tension and bending strengths are required to equal or exceed the grade threshold value (NLGA, 1994). Therefore, the strength level for the combined grade at the 5% probability of failure was calculated for different combinations of p_{1650} and p_{VQL} in the various KAR groups. Tables 5 and 6 contain summary information on tension and bending strengths of the combined grade considering all material with a KAR of greater than 25%.

These results reveal that the new combined grade meets the requirements for bending strength but does not meet the requirements for tension strength. The exercise was repeated with the additional KAR groups shown in Table 4 to study the influence of various levels of VQL on the strength properties. The results indicate that although the tension strength requirements cannot be met by any of these groups, both KAR group 4 and 5 narrowly missed the target of 14.8 MPa. The resulting fifth percentile tension strength levels were 14.67 MPa and 14.71 MPa for KAR groups 4 and 5, respectively.

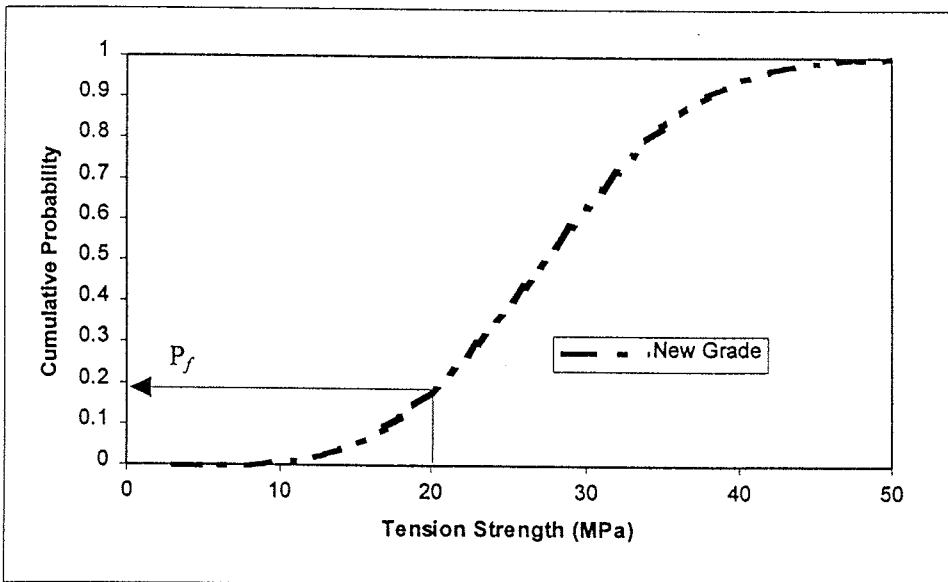
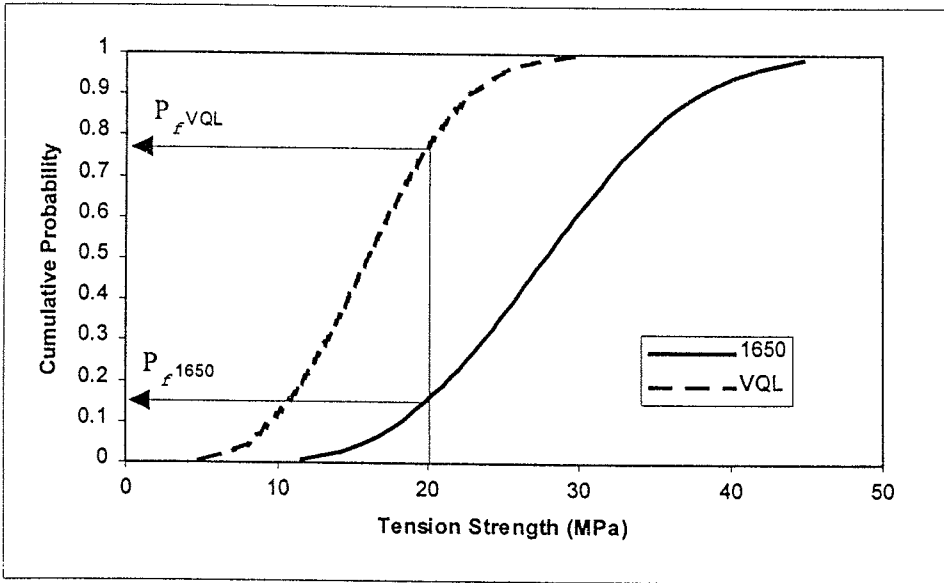


Figure 8. Graphical Illustration of Close Form Solution Procedures.

KAR Group Name	Group Characteristics	Number of Specimens Containing Group Characteristics	Percentage or Portion of Specimens Containing Group Characteristics
KAR 1	KAR >25%	263 / 2642	9.05 %
KAR 2	50 % > KAR ≥ 25%	246 / 2642	8.52 %
KAR 3	40% > KAR ≥ 25%	197 / 2642	6.94 %
KAR 4	33.3% >KAR ≥ 25%	128 / 2642	4.62 %
KAR 5	33.3% ≥ KAR > 25%	124 / 2642	4.48 %

Table 4. Statistics of VQL Breakdown into KAR Groups.

	1650 Group	KAR Group 1	Combined Grade
Average (MPa)	45.06	29.07	
Median (MPa)	44.78	26.60	
Standard Deviation (MPa)	11.33	10.69	
Coefficient of Variation (%)	25.15	36.78	
Count	148	130	
Weibull Parameters			
Shape	2.70	2.77	
Scale	31.89	60.61	
Location	16.68	1.83	
Proportion	0.91	0.09	
P_f	0.02	0.35	0.05
Fifth Percentile Strength (MPa)			24.26
Requirement* (MPa)			23.90

* Fifth percentile strength requirement specified by NLGA for 1650f-1.5E.

Table 5. Closed Form Solution Results for Bending Strength using KAR Group 1.

	1650 Group	KAR Group 1	Combined Grade
Average (MPa)	27.91	15.24	
Median (MPa)	27.19	14.84	
Standard Deviation (MPa)	7.41	4.15	
Coefficient of Variation (%)	26.57	27.25	
Count	146	133	
Weibull Parameters			
Shape	3.00	2.21	
Scale	23.11	9.82	
Location	7.24	6.55	
Proportion	0.91	0.09	
P_f	0.02	0.36	0.05
Fifth Percentile Strength (MPa)			13.40
Requirement* (MPa)			14.80

*Fifth percentile strength requirement specified by NLGA for 1650f-1.5E.

Table 6. Closed Form Solution Results for Tension Strength using KAR Group 1.

The KAR group 5 contained 68 specimens in tension compared to the 71 specimens for KAR group 4. Originally it was thought that the reduction of a few low tension strength specimens with a KAR of 25% was responsible for the increase in strength for the new combined grade. Careful inspection of the tension strength CDF's of both KAR groups revealed that the difference between the groups was insignificant; therefore, the increased tension strength of the new combined grade must be a result of the slightly lower proportion of material included. The proportions of KAR material was 4.62% and 4.48% respectively for KAR groups 4 and 5. This slight difference in proportion of KAR material allowed for KAR group 5 in combination with on-grade material to achieve the slightly higher tension strength.

The fifth percentile and median strength levels for the MOE on edge were determined nonparametrically. For the 1650f-1.5E grade, the MOE on edge is required to have a minimum fifth percentile and mean strengths of 8481 MPa and 10342 MPa, respectively. The results reveal that for all of the KAR groups the MOE on edge exceeded both requirements. Edgewise MOE results of KAR cases 1 and 4 are summarized in Table 7.

Percentile	Grade	KAR 1	Both	KAR 4
5 th (MPa)	1650		9068	
	VQL	6687		6703
	Combined Requirement	8763		8896
		8481		8481
50 th (MPa)	1650		11197	
	VQL	10074		9822
	Combined	11166		11182
	Requirement	10342		10342

Table 7. Summary of Closed Form Solution for MOE on Edge of cases KAR 1 and 4.

SIMULATION STUDIES

Simulations were also performed to represent the lumber strength properties of MSR material in production and to verify the closed form solution method. Again, the goal was to determine the characteristics of a new lumber grade that contains a mixture of both 1650 and VQL groups. Based on 3-P Weibull distributions of the tension and bending strengths of the 1650 and VQL groups, a database of lumber strength properties was randomly generated. From the simulated populations a new grade combination consisting of 5,000 specimens was created where a percentage of the samples was drawn from the VQL group and a corresponding percentage from the 1650 group. The simulated results and the P_f/VQL are in excellent agreement with the results from the closed form solution method (see Table 8).

5th Percentile		KAR Group 1		KAR Group 4	
Test Type	Grade	Simulation	Proportion	Simulation	Proportion
Bending (MPa)	1650	27.07	27.28	27.44	27.28
	VQL	12.09	12.30	17.93	17.85
	Combined	24.67	24.26	26.16	25.96
Tension (MPa)	1650	15.90	15.82	15.93	15.82
	VQL	9.15	9.11	9.32	9.27
	Combined	13.45	13.39	14.56	14.67

Table 8. Comparisons of 5th Percentile Strength Values.

ALTERNATE VQL QUALIFICATION

The current qualification for alternate VQL in the SPS-2 guidelines (NLGA, 1994) requires testing 6 samples that contain the large VQL of which none can fail to meet the required fifth percentile bending strength. Simulated trials of the new combined grade revealed that on average 36.53% and 29.20% of the 6 samples failed for KAR 1 and 4 proportions, respectively. In both the simulation and closed form solution, tension strength was shown to be more important and restrictive than bending strength. While it is difficult to meet the bending requirement, tension strength is a more appropriate measure for qualification and quality control associated with the large VQL. To qualify large VQL, it is recommended that a similar approach, as used in this study, be followed where the strengths and proportions of both large VQL and on-grade material were determined. With these parameters and using equation 2, it is possible to determine the amount of VQL material that can be included into the current production while still meeting the grade requirements.

CONCLUSIONS

The determination of knot area ratio showed that many of the knots that were manually measured did not meet the criteria for MSR edge knots. This fact must be addressed by the MSR producing mills to increase lumber grader accuracy in the determination of MSR edge knots.

A closed form solution was developed to assess the strength properties of a new grade of MSR lumber with inclusion of a proportion of large VQL material. The results indicate that the new combined grade exceeds the requirements in bending strength (23.9 MPa) for KAR groups 1 to 5 but fails to meet the tension strength criteria (14.8 MPa) for KAR groups 1 to 5. When considering KAR groups 4 and 5, the new combined grade just fails to meet the tension strength requirements.

The tension strength of the new combined grade is very sensitive to the amount of KAR material included. However, it should be noted that the frequency of large VQL is a function of the raw material and the manufacturing process. The testing program

conducted here is in effect a snapshot in time where large VQLs were evaluated during a moment of production. This picture corresponds to a certain timber resource from a particular location with specific growing conditions influencing the resulting lumber strengths and large edge knot frequency. Therefore, if a mill wishes to qualify a larger VQL than currently allowed, representative testing of regional conditions must be performed to assess lumber strength characteristics. Daily quality control procedures, including tension strength proof testing may be needed to ensure product performance.

REFERENCES

Bolger, R.J. and C.A. Rasmussen. 1962. Stress-O-Matic Stress rating System. American Society of Testing and Materials Special Publication No. 353. pp19-27.

Cramer, S.M. and J.R. Goodman. 1983. Model for stress analysis and strength prediction of lumber. Wood and Fiber Science. 15(4):330-349

Littleford, T.W. 1966. Visual restrictions on size of edge-knots as an aid to machine stress rating of Western Canadian species. Western Forest Products Laboratory. Information report VP-X-5, Vancouver, B.C.

Littleford, T.W. 1978. Flexural properties of dimension lumber from Western Canada. Western Forest Products Laboratory. Information report VP-X-179, Vancouver, B.C.

National Lumber Grades Authority (NLGA). 1994. NLGA special products standard for machine stress-rated lumber SPS2-94. National Lumber Grades Authority, Burnaby, B.C. 18pp.

Orosz, I. 1977. Relationships between transverse free vibration E and other properties as affected by knots. Forest Products Journal. 27(1):23-27.

ACKNOWLEDGMENTS

The authors gratefully acknowledgment the funding support received from the National Lumber Grades Authority, Forestry Canada, and NSERC.

INTERNATIONAL COUNCIL FOR BUILDING RESEARCH STUDIES AND DOCUMENTATION

WORKING COMMISSION W18 - TIMBER STRUCTURES

**DETERMINATION OF MOMENT CONFIGURATION FACTORS USING GRADING
MACHINE READINGS**

by

T D G Canisius

Building Research Establishment

Garston, Watford,

The United Kingdom

T Isaksson

Department of Structural Engineering

Lund University

Sweden

MEETING TWENTY - NINE

BORDEAUX

FRANCE

AUGUST 1996

Determination of moment configuration factors using grading machine readings

T. D. G. Canisius

*Timber Structures Section, Building Research Establishment,
Bucknals Lane, Garston, Watford WD2 7JR, The United Kingdom
and*

T. Isaksson

*Department of Structural Engineering, Lund University,
PO Box 118, S-221 00, Lund, Sweden*

Abstract

A method to determine moment configuration factors using currently available data from the Lund University test programme on along-member strength variation in timber beams is presented. The grading machine readings for the beams and the statistical data on weak-section strengths are used in the study. Although sufficient data are not available, and more research is needed, the method presented here may be considered to provide the required information in a conservative manner. The moment configuration factors determined for some typical loading cases are also presented.

1 Introduction

The variation of mechanical properties along timber beams is a topic which has interested many researchers. With this information timber structures can be made more efficient, and thus more economical. Also such information makes it possible to determine reliability levels of structures more accurately.

An important benefit of information on the along-beam variation of flexural properties is the possible introduction of a Moment Configuration Factor (MCF) into the limit state design procedure. This strength conversion factor would help to narrow the difference between reliability levels of different structures, while improving their efficiency. Such a possibility occurs for the design of timber structures because, when the along member strength varies randomly, the maximum bending moment resistable by a given beam depends on the bending moment diagram. This can be understood with the help of Figures 1 and 2. Figure 1 shows a possible hypothetical idealisation of bending strengths along a beam. Figure 2 shows how the 'strength' of a beam, in terms of the maximum possible bending moment in it, can be different under two forms of loading. A detailed descriptions of this phenomenon

has already been made in previous papers by the authors and others[1]-[13]. The reader is referred to these documents for a better understanding of the issues involved.

The procedure used to simulate beam strengths using Lund University test data has been presented in [13] together with some preliminary results. The current report, which uses all the available test data, presents the method adopted for determining MCFs from the computer simulated strengths. Also MCFs results for a simply supported beam with a uniformly distributed load and a concentrated load are derived and compared with those obtained from direct test results.

1.1 The concept of moment configuration factors

The meaning of MCFs can be understood through the beam shown in Figure 2. Let the maximum bending moment that can be applied to it under the non-uniform moment profile be M_1 . Also, let the maximum uniform bending moment that can be applied be M_2 . That is, under the given non-uniform and uniform bending moment profiles, the strengths of the beam are M_1 and M_2 , respectively. Then, for this beam, the moment configuration factor (MCF) under the given non-uniform moment is given by

$$\text{MCF} = \frac{M_1}{M_2} . \quad (1)$$

However, it is not a moment configuration factor based on a single beam which is needed in design, but one which considers the total population or representative samples of beams. That is MCFs need to be determined in relation to the cumulative distribution functions(CDFs) of strength and the applied loads, and based on a structural reliability criterion[9].

1.2 The Lund University study

This section provides a summary of results from the Lund University tests. As this programme of work is well documented in [11], only the briefest and essential information is provided.

The currently available strength data are with respect to weak sections of beams as predicted by significant depressions in the Cook-Bolinder grading machine reading profiles. The sample of beams consisted of 131 beams of nominal cross section $45 \times 145 \text{mm}^2$ and lengths of between 5.1 and 5.4m. The grading machine readings for all these beams were obtained, and at least four weak sections of each beam were directly tested for strength.

The grading machine readings at the weak sections were converted to a modulus of elasticity (MOE) value E using the formula

$$E = 840 + 1.21 \frac{PL^3}{48I\delta} \quad (2)$$

where P is the grading machine reading in Newtons, δ is the grading machine deflection setting, I is the second moment of area of the beam cross-section, and L is the grading machine span. In Equation 2 all the length dimensions are in mm and the unit of E is N/mm²(MPa).

A regression analysis was carried out between the determined MOE values(E) and the directly measured strengths(S) of the weak sections, giving

$$S = 0.0048E - 13.47 \quad (3)$$

where S is the strength of the weak section.

The above information is used in this paper to simulate the strengths of *all* weak sections of a beam, as observed from its Cook-Bolinder grading machine reading profile.

2 Method of beam strength simulation

2.1 Assumptions and idealisation

A brief description of the idealisation used to simulate the lengthwise variation of beam strengths and the assumption involved are given here. Additional details can be obtained from [13].

- Any defectless(clear) beam is assumed to possess infinite strength. This assumption is unavoidable because no information on clear area strengths of tested beams is currently available. The importance of the strength of clear regions lies mainly with bending moment configurations having high intensity localised peaks.
- A reduction in strength is assumed to occur at each cross-section deemed to have a defect through the examination of the grading machine data profile.
- Based on Equations 2 and 3, *i.e.* using the E value for this cross section obtained from the grading machine readings, the corresponding mean strength value can be determined for the cross-section.

- Assuming a normal distribution with the above determined mean strength and the experimentally determined coefficient of variation (COV), a random strength value can be generated for the particular cross-section. Here, the COV of strength is assumed to be independent of the MOE value and the determined mean strength of the section. This assumption is made based on the fact that the determined COVs have been similar (0.24) for both the strengths of all weak sections in beams and the strengths of only the weakest section of each beam.
- The above determined strength is assumed either as localised in a cross-section of infinitesimal width or to be influencing the strength of an adjoining region of finite length. The importance of such a spread of influence would depend on the bending moment profile and on the width of the region of reduced strength relative to the span: *i.e.* it is important when the beam span is short or when the bending moment profile has high intensity localised peaks.
- Due to the current lack of information, it is approximately assumed that the strength reduction at a cross section spreads symmetrically to an adjoining region of width L , such that

$$L = 2nD \left(\frac{G_m}{G} \right)^k, \quad (4)$$

where D is the beam depth, G is the grading machine reading at the considered weak cross section, and G_m is the maximum grading machine reading for the beam. In addition, n and k are parameters which are assumed to take values such as 0, 1 and 2, with the $n=0$ indicating no spread of influence. The strength reduction is considered to vary parabolically within this region, such that

$$S(y) = \frac{(1 - \tilde{R})}{n^2 D^2} \tilde{R}^{2k} y^2 + \tilde{R} \quad (5)$$

where $S(y)$ is the strength at a distance $-0.5L \geq y \leq 0.5L$ from the weak section and \tilde{R} denotes G/G_m . The complete details of these can be found in [13].

2.2 Beam simulation procedure

The simulation procedure for along-member variation of beam strength, based on the above described assumptions, can be summarised as follows.

1. Plot a graph of grading machine readings against the respective distances along the beam.
2. Determine the positions and the machine readings at the valleys in the graph, independently of any other information on the beam. These valleys are considered to depict weak sections.
3. Using Equation 2 determine the modulus of elasticity (MOE).
4. Using the MOE value and Equation 3, predict the mean strength of each weak section.
5. Generate a random strength value from an assumed normal distribution with the determined mean strength and a COV of 0.24.

If spread of strength reduction is used:

6. Obtain the assumed approximate strength reduction ratio $\tilde{R} = G/G_m$, using the grading machine readings.
7. Using Equation 5, obtain the strengths in the region adjoining the weak section.

3 Stress Analysis of beams

On having simulated the cross sectional strength profile of a beam, to obtain the 'beam strength', it is necessary to analyse it under the relevant bending moment profile. Here the 'beam strength' under a given moment profile refers to the bending moment at the position of maximum moment when the beam fails at any position(see Figure 2). This bending moment can then be converted to a bending stress.

A linear elastic beam finite element program, based on the two-noded cubic element, is used for structural analysis. This program is connected to a program which simulates the random cross-sectional strengths and then allocates them to the relevant finite elements. Within each finite element the beam strength is assumed to be constant and to be equal to the minimum value simulated within the corresponding portion of the beam. The details of the finite element program and the associated strength determination routines are available in its users' manual[14].

The current results are based on analyses which used 140 finite elements to discretise the complete beam. A comparison of beam strength results obtained with 70 and 140 finite element discretisations for the central concentrated load case showed that the maximum error was less than 1.5% of the value for the latter for all n and k combinations. Thus, the concentrated load

case being the most critical with respect to discretisation, 70 finite elements were considered sufficient for the analyses presented earlier in [13]. However, in the current analyses, where all the 131 of beams were used, it was discovered that the higher differences between results from the two analyses were more concentrated at the lower end of the strength CDF. It is this area of the CDF which is relevant for MCF determination. Hence, it was decided to use 140 elements in the full analysis. Although not necessary, this number of elements was used also for uniform moment and uniformly distributed load analyses.

4 Calculations and Results

4.1 Comparison of generated and measured strengths

Figures 3 to 5 show comparisons of generated beam strengths with the measured (tested) strength of each beam. The measured (tested) strengths have been determined by testing at least four weak cross sections in each beam. Shown in each figure are the simulated strengths for no spread of defect influence ($ND=0$) and the largest spread defect influence [$ND(=n) = NP(=k)=2$]. From the results for the three load cases, it can be seen that the simulated strengths are often lower than the tested values. Among the lower values of simulated strengths, the results for the above two extremes of defect spreads differ from each other only in a very small number of occasions. Thus, considering that it is the lower strength values which contribute towards MCFs, the spread of defect influence could be neglected for these bending moment diagrams.

Figure 6 shows the CDFs for the above three load cases, under the two extremes of defect spreads, drawn for the range of strengths below the 40th percentile. The maximum difference at the lower tail is provided by the concentrated load case, which has the sharpest peaking of bending moment diagram (for the cases considered). The difference at the lowest available fractile ($1/131 = 0.0076$) is 0.125 of the lower value of the two cases which was obtained with $ND=NP=2$. This points to the need, until relevant information is available, to consider the extreme spread as the conservative one for cases such as continuous beams where its influence may be large. Due to the many approximations involved, and considering that $ND=2$ considers a basic initial width of $4d$ (for $NP=0$), the above possible error is considered acceptable for bending moment profiles considered here.

Figure 7 shows the simulated and tested beam strengths under different conditions, plotted against the ordered ranks of strengths. The rank, given

in the X-axis, corresponds to the CDF by the relation

$$\text{CDF} = \frac{\text{RANK}}{131}$$

where 131 is the total number of beams used in this study. This figure shows, for any rank, the CDFs from tests are consistently higher than the corresponding simulated ones. The lower strengths of simulated results may be mainly attributed to the fact that simulations consider all possible defects in a beam, whereas test results consider only a limited number of defects as allowed for by the test procedure. It is to be noted that, as the presented graphs refer to the sorted strength ranks, the strengths for a given rank value need not correspond to the same beam physically.

4.2 Derived moment configuration factors

Figure 8 shows the MCFs from both the simulated and test results, plotted against the respective strength ranks. In the case of the simulated beams, the extremes have some undulations, with especially large values at the very lowest rank. Such undulations at the extremes, although not severe, can be observed with test results too. The simulated beams, which depend on the generated random numbers, could reasonably produce a freak case whose influence will be eliminated only when the sample size is large. In the present case, the fact that both load cases have these extremely large MCFs for the first rank indicates that the error is mainly due to a large reduction in the strength under the uniform moment. This could be seen to be the case by examining Figure 7. Figure 9 shows the MCFs with the results for the Rank 1 beams eliminated. It is this set of 130 beams which is used for the calculations carried out below. The general undulations at the two extremes of ranks in both simulated and tested results can be attributed the smallness of the sample.

In a previous paper[9] it was shown that the phenomenon of moment configuration factors could be also explained as occurring because of the non-coincidence of strength CDFs under different bending moment diagrams. It was shown there that it was the behaviour of the lower tails of the distributions which affect the values of the MCFs. It was also observed that the use of characteristic strength based MCFs for ultimate limit state design could be too optimistic than reliability based values. This was explained as due to the gradual increase of MCFs with the increase of the strength fractile. The correctness of this conclusion, which was originally based on an assumed approximate strength model, could be evaluated through Figure 9. The figure shows that the simulated MCFs generally increase in value with the strength rank. This increase is very small for the tested concentrated load case, while it is almost non-existent for the uniformly distributed load case. This slight

β	3.0	3.8
Approx. prob. of failure	0.001	0.0001
Design Pt. Fractile	0.0082	0.0012

Table 1: Design point fractile in terms of reliability index.

difference between simulated and test results could be due to the smaller number of weak sections that could be tested in laboratory, but no conclusive statement can be made in this regard at present. If it is assumed that due to the larger number of weak sections considered, the simulated values provide a better picture of the phenomena than the test results, the need for the use of reliability-based methods for the determination of MCFs can be justified here.

4.2.1 Reliability-based MCFs

Reliability-based MCFs have to be determined through statistical analyses which involve the statistics of both the beam strengths and the relevant actions. In the case of beam strengths, it is the lower portion of the tail of the strength distribution which is relevant. The extent of the relevant section of the tail depends on the target reliability index (β): lower the β value, larger is the relevant area of the strength distribution.

The undulations of strength CDFs at the lower fractile end (see Figure 9) indicate that the direct use of these CDFs would not have sufficient accuracy for a reliability-based study. While the reason for this non-convergence was the small sample size, the smallness of the sample meant the non-availability of fractiles in the range important for reliability studies. Unfortunately, the sample size was also too small to obtain a good regression fit to the lower tails of strength distributions such that the low fractiles could be adequately assessed. Thus, it was decided to not carry out reliability studies, but to base the MCFs on the strengths at the design values, which themselves had to be approximated. The possible use of design values in an MCF study was previously proposed as an approximate method in [10].

The design point for the material strength in a two variable (i.e one action and one material) structural reliability problem could be derived from elementary reliability theory[15] as the strength fractile value $\Phi^{-1}(-\beta)$, where Φ is the cumulative distribution function of the standard normal distribution, β is the reliability index and α is the FORM factor for strength. For a single material variable case or for a dominant material, α takes the value

of -0.8 . For different β values the design point fractiles will take values as given in Table 1. The β value of 3.8 refers to the life-time reliability level specified against the ultimate limit state of failure[15].

4.3 Moment configuration factors based on the design point

4.3.1 The need to fit regression curves

In Figure 9, the least available strength fractile is 0.015. This fractile is larger than the design point fractile required (see Table 1). Thus, it is necessary to extrapolate data to obtain the design point strength or MCF. However, the CDF curves are not sufficiently smooth for such direct extrapolation. Hence, the solution was deemed to be either to fit a regression curve to the obtained CDF graphs, or to fit a curve to the derived MCF graph itself. The former method was chosen here as the undulations in MCFs occurred because of the non-smoothness of the strength CDF curves. (A later fitting of a curve to directly determined MCFs showed that the differences in results from these methods were not significant.)

As fitting of curves to the whole range of fractiles (ranks) would reduce the fit of the curves, it was confined to the first 65 members in rank, *i.e.* approximately the lowest 50% of rankings. Using MATHCAD[16] computer package curves were fitted to both the simulated and tested strength CDFs.

4.3.2 Fitted curves

After several trials at curve fitting, it was observed that the sum of a truncated geometric series and a truncated reciprocal geometric series would provide a good fit to the data. No statistical test of fit in terms of R^2 was carried out, but the fit was tested through eye observation of the lower strength(rank) portion of the data. The truncation points for the series were obtained by observing the changes in the fit due to the presence of additional terms. The obtained regression formulae, $F(X)$, for each of the six cases, are given below in terms of the dot product of two vectors such that

$$F(X) = \{C\}^T \{S\} \quad (6)$$

where $\{C\}$ is the set of multiplicative coefficients for the (algebraic) terms of the series $\{S\}$. These regression curves are also plotted in Figures 10 to 15 which show the respective CDFs.

Concentrated load(Tests):

$$\{S\} = (X^{-3}, X^{-2}, X^{-1}, 1, X, X^2)^T \quad (7)$$

$$\{C\} = (12.68, -9.008, -14.082, 36.42, 0.475, -0.001)^T \quad (8)$$

Uniformly distributed load(Tests):

$$\{S\} = (X^{-3}, X^{-2}, X^{-1}, 1, X, X^2)^T \quad (9)$$

$$\{C\} = (-12.30, 32.56, -28.21, 32.48, 0.492, -0.002)^T \quad (10)$$

Uniform moment(Tests):

$$\{S\} = (X^{-2}, X^{-1}, 1, X, X^2, X^3, X^4)^T \quad (11)$$

$$\{C\} = (-0.818, -0.536, 19.92, 1.522, -0.057, 0.001, -6.93 \times 10^{-6})^T \quad (12)$$

Concentrated load (Simulations):

$$\{S\} = (X^{-2}, X^{-1}, 1, X, X^2, X^3)^T \quad (13)$$

$$\{C\} = (2.865, -9.234, 20.21, 0.585, -0.003, 8.31 \times 10^{-6})^T \quad (14)$$

Uniformly distributed load (Simulations):

$$\{S\} = (X^{-2}, X^{-1}, 1, X, X^2, X^3)^T \quad (15)$$

$$\{C\} = (3.682, -8.122, 17.00, 0.67, -0.009, 6.791 \times 10^{-5})^T \quad (16)$$

Uniform moment (Simulations):

$$\{S\} = (X^{-3}, X^{-2}, X^{-1}, 1, X, X^2, X^3)^T \quad (17)$$

$$\{C\} = (-14.00, 22.52, -22.64, 20.05, 0.141, 0.004, -3.913 \times 10^{-5})^T \quad (18)$$

The moment configuration factors, determined using the curves fitted to the test data, are shown in Figure 16. In the figure, 'T' refers to test results while 'S' refers to simulated results. For example, TCONC and SCONC refer to the concentrated load case with test and simulated results, respectively. Due to the fitting of curves to CDFs, the MCF curves are much smoother now than those shown in Figures 8 and 9. However, the very high MCFs at the first rank are still present in the simulated MCFs. The very high increase of the factor at the lowest available fractile in the simulated results can be again considered as a freak result due to the small sample size used in the

statistical simulation. In addition, as the lower ends of strength distributions lack accuracy due to the small sample size in both tests and simulations, the (standard) errors in the MCFs at those places should be much higher. Figure 17 shows these MCF results at a higher scale after eliminating the lowest strength fractile's results. The MCFs calculated with test results, although similar to those determined with simulated data, tend to show a decrease in value with the decrease of strength fractiles below approximately 0.03.

If the lower fractile portions of the MCF curves, which may be considered unreliable, are eliminated then the MCFs calculated with test results can be seen to be more conservative than those obtained with simulated results. This could be a result of the different numbers of weak sections considered in the tests and simulations: greater the number of weak sections considered, more will be the randomness of along-member strength and hence higher will be the MCFs.

Comparisons of MCFs determined with curves fitted to strength CDFs, and those determined directly without fitted curves are presented in Figures 18 and 19, for concentrated load and uniformly distributed load cases, respectively. From these it can be seen that the MCFs determined from the fitted curve data could be considered to provide approximate fitted curves for the MCFs determined without fitting curves to the strength CDFs. That is, for the cases considered, fitting of curves to either CDFs or MCFs would provide similar results.

4.3.3 Selected procedure for MCF calculations

As mentioned previously, the design point method was adopted for the determination of MCFs. The design point values were obtained from the graphs of MCFs determined with curve fitted CDF data shown in Figure 17. However, considering the possible errors in the lower fractiles, and the need for an approximation was made as follows. Consider Figure 20 where the strength fractile range from zero to approximately 0.15 (rank of 20) are shown. Tangential straight lines were fitted to the MCF curves as shown so that the least possible intercepts of the $y(=MCF)$ axis could be obtained. These tangents could now be considered to provide sufficiently conservative MCFs. As the design point fractile is very small a conservative result, without loss of meaning, could now be obtained by considering the y -axis intercept as the required MCF.

Through the above procedure, the values of MCFs for central concentrated load and uniformly distributed load cases were obtained as 1.20 and 1.05, respectively (see Figure 20). These are lower than those obtained with the test results, which have their own limitations, and those obtained previously with approximate methods[9]. Hence, until more test data are available, these results could be adopted as a set of safe and conservative estimates

based on actual test data. The presented procedure could be adopted as the method to follow in determining MCFs for other moment configurations.

5 Discussion

In Figures 3 to 5, it was observed that there are differences in the predicted and measured strengths of beams. This difference needs to be accepted as a part of the present limited nature of the analysis. When individual beams are considered it would never be possible to predict the exact strength under the current method of statistical simulation. It is only the statistical parameters which could be expected to be predicted, and this too is possible only with sufficiently large sample sizes. A particular observation that could be made from Figure 7 for CDFs is that the simulated strengths are statistically lower than the test strengths. This could be attributed to the larger number of weak sections considered in a simulation, whereas only a limited number of weak sections with a certain minimum distance between them could be tested in laboratory. Thus, this difference, in fact, points to the correctness of the simulation procedure.

The current simulation procedure and the method adopted to determine design point MCFs have provided results which are conservative than the direct test results. However, there still are unknown parameters and shortcomings in the current procedure. One shortcoming, which may be eliminated in the future, is the small sample size. As both the design point and ultimate limit state reliability analysis (for high β) deal with very low fractiles, the required sample size for reliable results is large. A large sample size might also have eliminated possible statistical freaks, as happened with the lowest strength member. The use of different sets of random numbers, obtained through different SEEDs for the initiation of the random number generator, may have eliminated the above problem. However, this alternative was not followed as it cannot be considered as reasonable. Another current shortcoming is the non-consideration of clear section strengths. However, this will disappear when the results from current test on such sections become available. The effect of this on the bending moment diagrams considered here should be insignificant. However, until clear section strengths are available, the use of the current method for bending moment diagrams with localised high peaks should be done with care, and may need more conservatism. A parametric simulation with assumed clear section strengths may help to shed light to the relative size of errors.

The effect of the width of the region of influence of weak sections is to reduce the strength of an individual beam. Its effect is more for bending moment diagrams with high localised peaks. It becomes of lesser importance with the increase of uniformity of the bending moment diagram, with no effect at the extreme of a uniform bending moment. Hence, the

non-consideration of width of influence of weak sections can only result in non-conservative answers. This makes it necessary to consider them with continuous beams or to provide some additional measure of conservatism.

In current analyses, the width of influence of weak sections is based on assumptions. Also the manner in which the strength varies within these regions is assumed. In the analyses, the ratio of strength of weak sections and of clear sections, which is used for the above purpose, is approximated with a ratio of grading machine readings. This approximation could be eliminated only when clear area strengths are available. Thus, for more accurate results it will be required to study this phenomenon in detail.

In the current simulation procedure it is assumed that the bending strengths in positive and negative directions remain the same at all cross sections. This, of course, is not true for solid timber beams. The effect of this assumption would be important for beams with both negative and positive bending, such as those clamped at both ends and those continuous over supports. The effect of this, in terms of possible errors, remains unknown and need to be addressed sometime. If experimental data could not be found, a preliminary study may be carried out through computer simulations based on assumed variations of strengths.

In the case of indeterminate beams such as continuous beams, an important aspect which need to be considered is the influence of the elasticity modulus on MCFs[6]. Although grading machine readings refer to a weighted average of elasticity modulus about the grading machine span, while structural analysis requires the cross-sectional values, the problem may be addressed approximately with the results of Equation 2.

There are several improvements to be made to the simulation procedure itself. At present the manual procedure to determine weak sections from grading machine readings involves some subjectivity[13]. There is a need to make this procedure more objective. If objective criteria for selection of weak sections can be developed, then the procedure may be automated to be carried out in a computer, thus saving a considerable amount of time.

The current MCF calculations are based on results obtained from a sample of structural timber of Norway spruce. Hence, there is the question on whether MCF's could be significantly different for different grades of different species of timber. This possibly could be answered only through further tests.

The current derivation of MCFs did not consider the possible importance of size effects. This needs to be addressed in the future. The consideration of depth effect needs results on other cross-sections, and these could be obtained only from further laboratory tests. A length effect study could be carried out with current results by considering beam lengths smaller than the currently considered 4200mm span.

6 Conclusions

The following conclusions can be made with respect to moment configuration factor(MCF) determination procedure presented in this report.

- The presented procedure is able to provide, for the cases considered, MCFs which may be considered as reasonable and conservative.
- The accuracy of the determined results were assessed through a comparison with the results determined through laboratory tests. As the latter itself possesses some uncertainty due to the limited number of weak sections that could be tested, a comparison of the relative sizes were made, and found to be satisfactory.
- The present method has some shortcomings, mainly due to the unavailability of data. More research, as described in the discussion, is needed to eliminated these unknowns. Until then, when using the presented method for other moment configurations such as those present in continuous beams, it may be prudent to make the MCF results more conservative through some form of artificial reduction.
- Test data are available only with respect to a single species, grade and cross-section of timber. It is necessary to carry out tests with respect to other species, grades and cross-sectional sizes of timber so that the currently derived factors could be confidently used with them.
- The current derivation of MCFs did not consider the possible importance of size effects. This needs to be addressed in the future.
- In order to carry out proper reliability based studies, it is necessary to carry out tests with samples larger than the currently used 131 beams.
- The currently derived MCFs, *viz.* 1.05 uniformly distributed load on a simply supported beam and 1.20 for a central concentrated load on a similar beam, can be recommended for use in designs until more reliable results become available through further research. The above MCF of 1.05 for uniformly distributed loads on simply supported beams may also be used with continuous beams until the results for them are derived in the future.

References

- [1] Riberholt, H. and Madsen, P.H.; *Strength distribution of timber structures. Measured variation of cross sectional strengths of lumber*, Struct. Res. Lab., Tech. University of Denmark, Rept. R114, 1979.

- [2] Riberholt, H.; *Safety of timber structures*, Struct. Research Lab., Tech. University of Denmark, June 1979.
- [3] Czmocho, I., Thelanderson, S. and Larsen, H.J.; *Effect of within member variability on bending strength of structural timber*, Proc. Intl. Council for Building Research Studies and Documentation, Working Commission W18A, Meeting 24, Oxford, UK, Sept. 1991.
- [4] Madsen, B.; *Structural behaviour of timber*, Timber Engineering Ltd., North Vancouver, BC, Canada, 1992.
- [5] T.D.G. Canisius, *Moment Configuration Factors for Simple Beams*, Proc., Int'l Council for Building Research Studies and Documentation, Working Commission W18A, Meeting 25, Ahus, Sweden. August 1992.
- [6] T.D.G. Canisius, *Effect of the Elasticity Modulus on the Simulated Bending Strength of Hyperstatic Timber Beams*, Proc., Int'l Council for Building Research Studies and Documentation, Working Commission W18A, Meeting 25, Ahus, Sweden. August 1992.
- [7] Canisius, T.D.G.; *Reliability-based moment configuration factors: a parametric study*, BRE Clinet Report, Proj GD263, Garston, UK, August 1993.
- [8] Canisius, T.D.G.; *Variation of moment configuration factors with the strength quantile* BRE Internal Report, Proj GD263, Garston, UK, March 1994.
- [9] Canisius, T.D.G.; *Reliability-based configuration factors for timber beams*, Structural Safety, **16**, pp. 215-226, 1994.
- [10] Canisius, T.D.G.; *Changes in material strength and Level I designs*, Report PD302/93, Building Research Establishment, Oct. 1993.
- [11] Isaksson, T., Thelandersson, S., and Moller-Pederson, T.; *Within member variability of bending strength of timber*, Proc., Pacific Timber Eng. Conf., Gold Coast, Australia, pp.634-641, July 1994.
- [12] Kallsner, B. and Ditlevsen, O.; *Lengthwise bending strength of variation of structural timber*, Proc., IUFRO Timber engineering meeting, Sydney, Australia, July, 1994.
- [13] Canisius, T.D.G., Isaksson, T., and Thelandersson, S.; *Grading machine readings and their use in the calculation of moment configuration factors*, Paper No. 28-6-6, Proc., Int'l Council for Building Research Studies and Documentation, Working Commission W18A, Meeting 28, Copenhagen, Denmark. April 1995.

- [14] Canisius, T.D.G.; Manual for beam simulation program BEAMSIM, BRE, Garston, April 1995.
- [15] CEN: Eurocode 1, Part 1: Basis of Design, The CEN/CS version, August 1994.
- [16] MATHCAD 5.0, MathSoft Inc., USA.

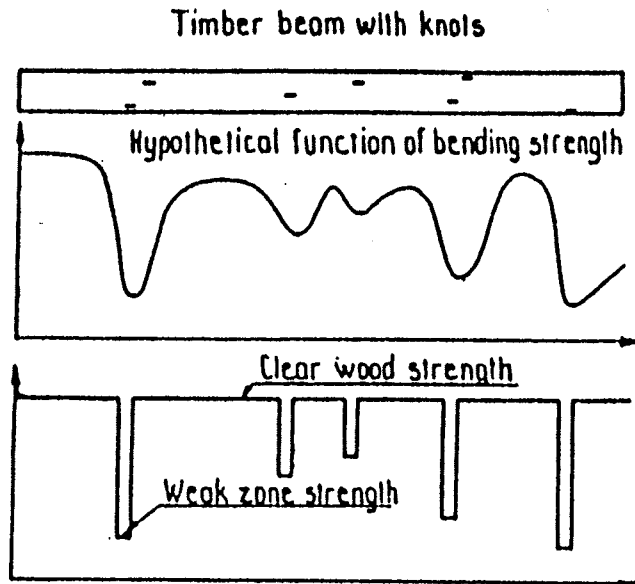


Figure 1: Modelling of lengthwise variation of bending strength

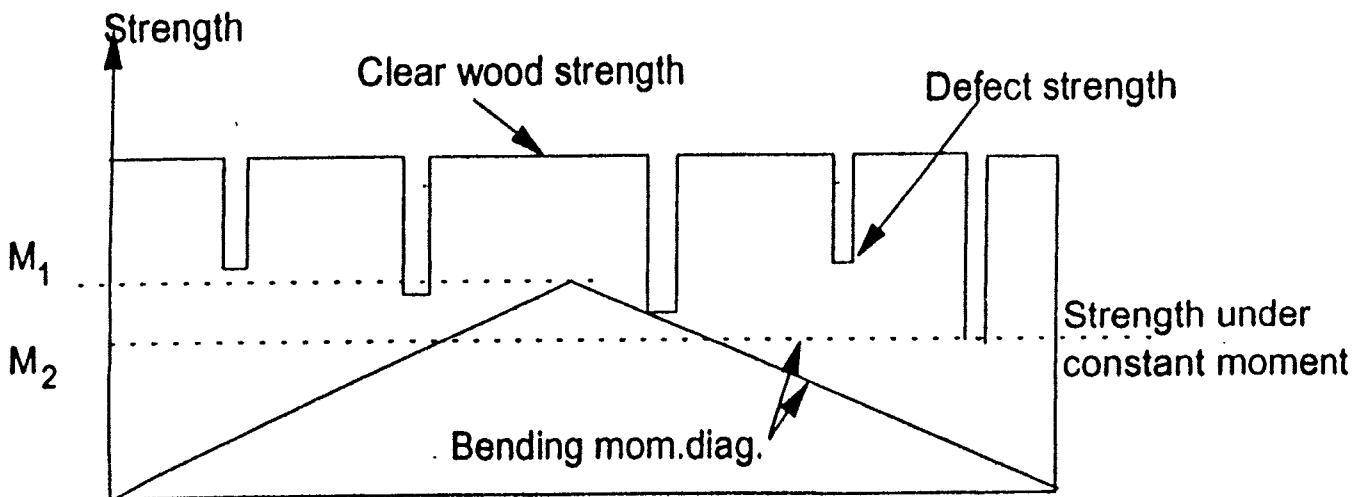


Figure 2: Differences in bending strength due to moment configuration

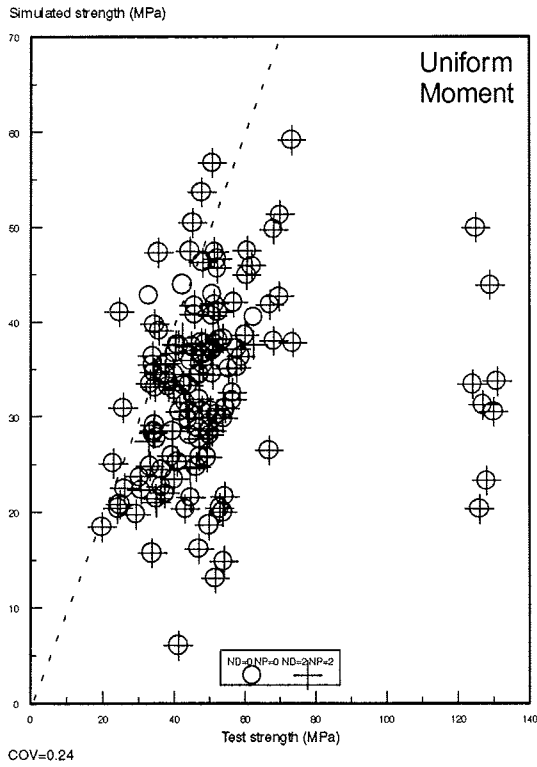


Figure 3: Comparison of simulated and tested strengths of all beams under a uniform moment.

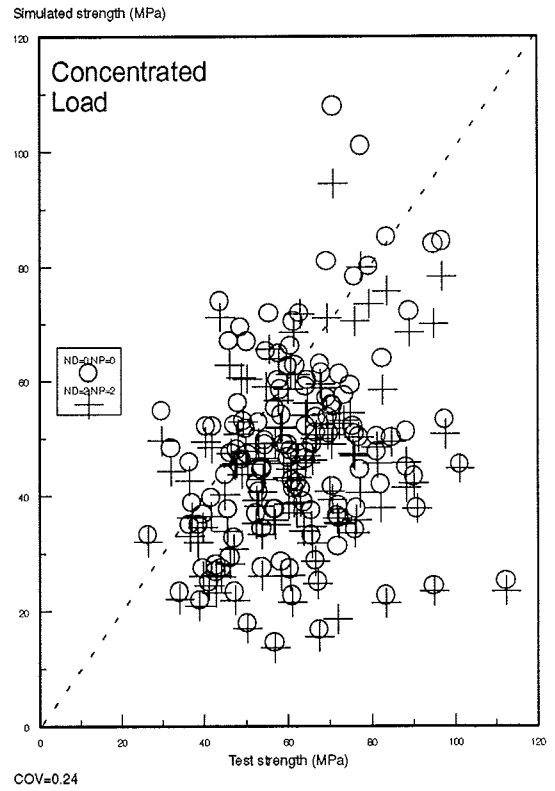


Figure 4: Comparison of simulated and tested strengths of all beams under a central concentrated load.

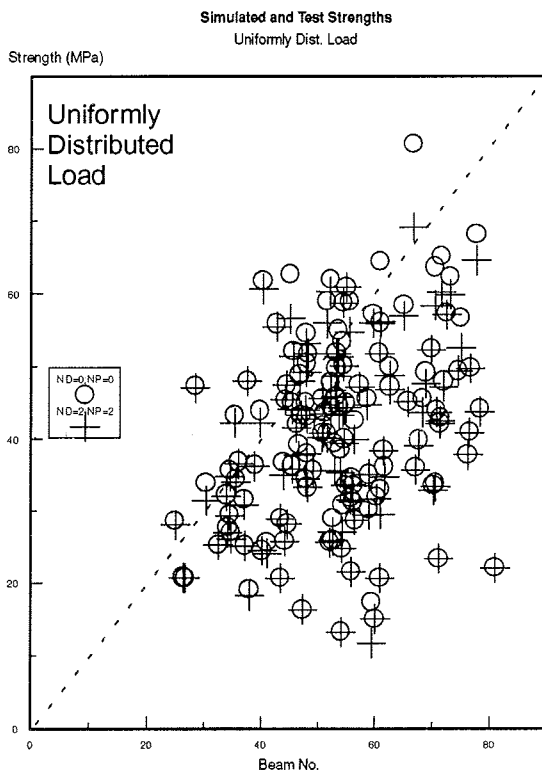


Figure 5: Comparison of simulated and test strengths of all beams under a uniformly distributed load.

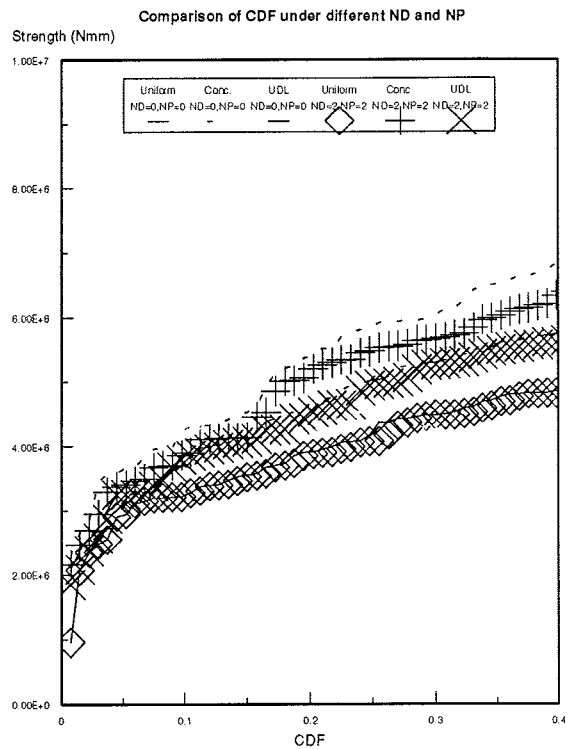


Figure 6: Comparison of simulated strengths of beams under different widths of weak-section influence.

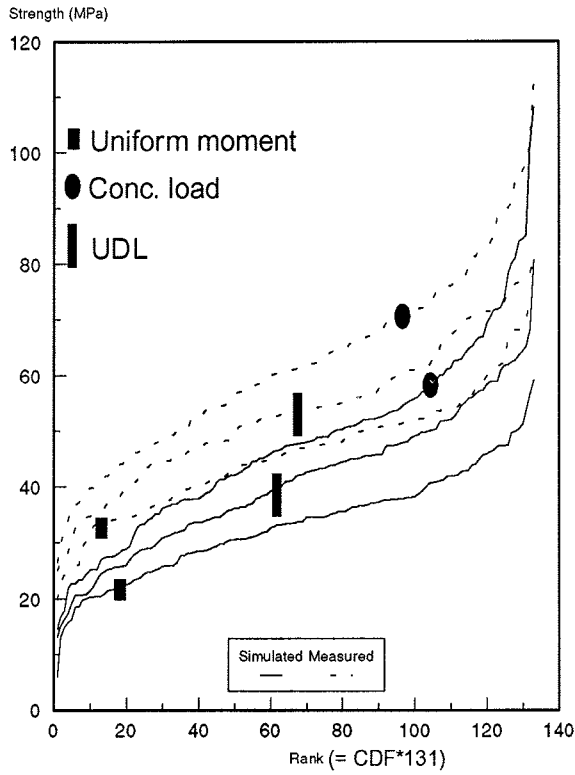


Figure 7: Comparison of simulated and tested strength cumulative distribution functions

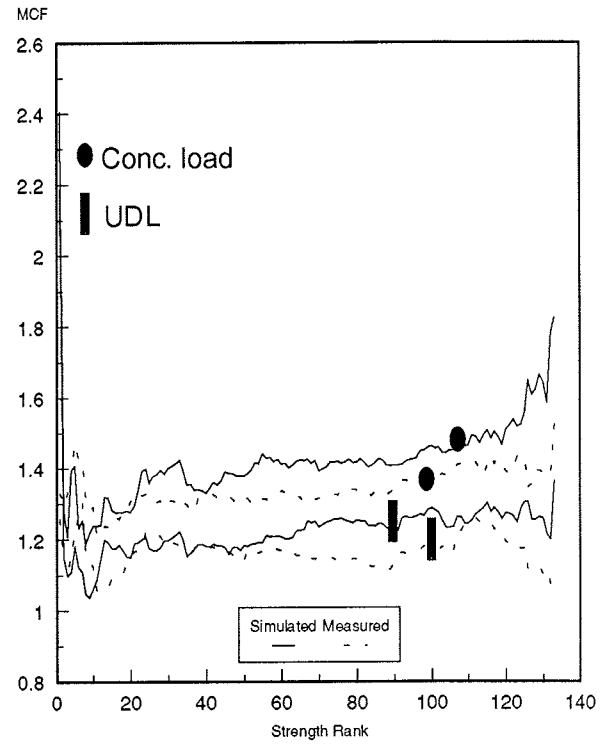


Figure 8: Comparison of MCFs determined with simulated and tested strength data.

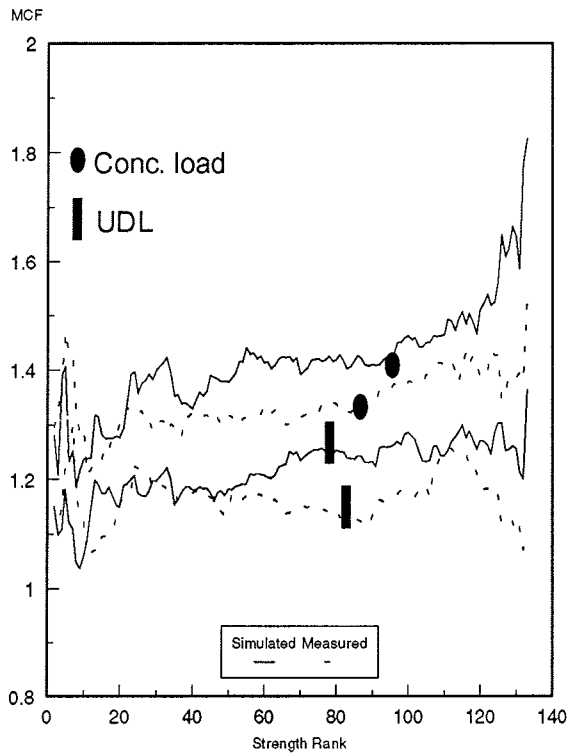


Figure 9: Comparison of MCFs determined with simulated and tested strength data, but with Rank 1 eliminated.

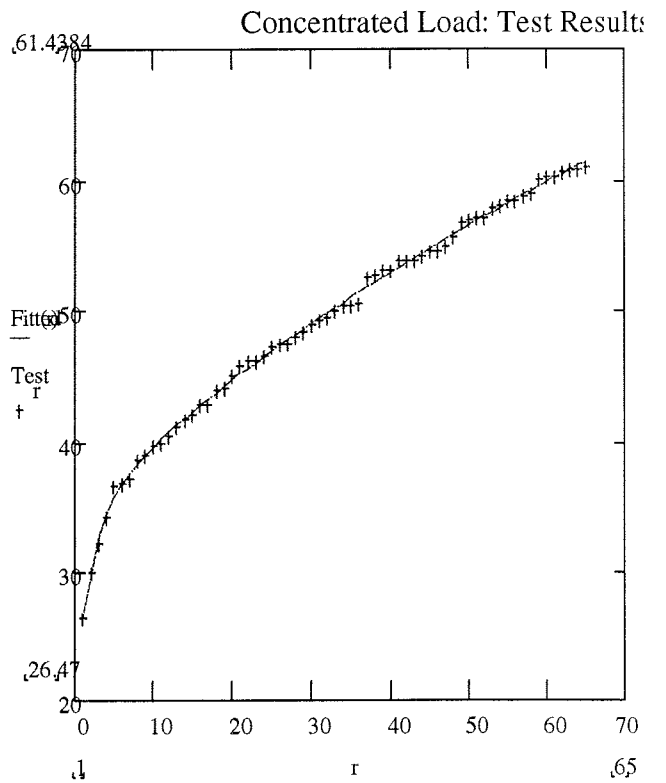


Figure 10: CDF for concentrated load case: Test results and fitted curve.

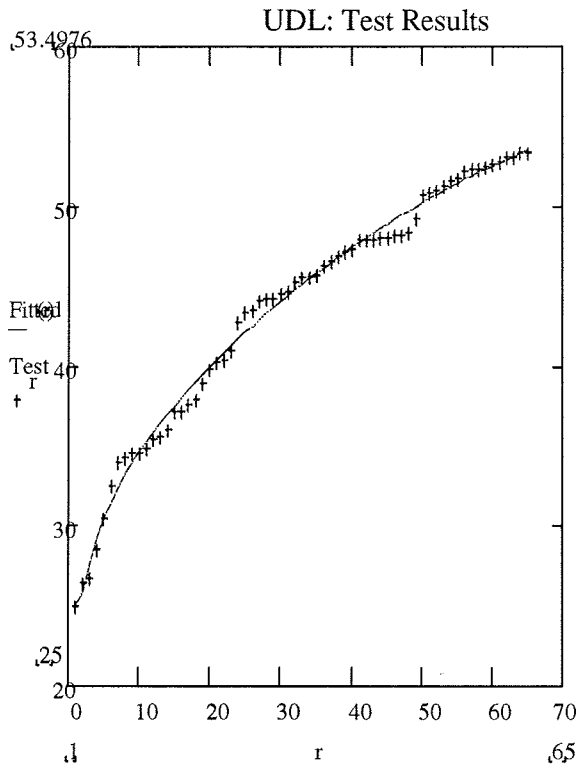


Figure 11: CDF for uniformly distributed load case: Test results and fitted curve.

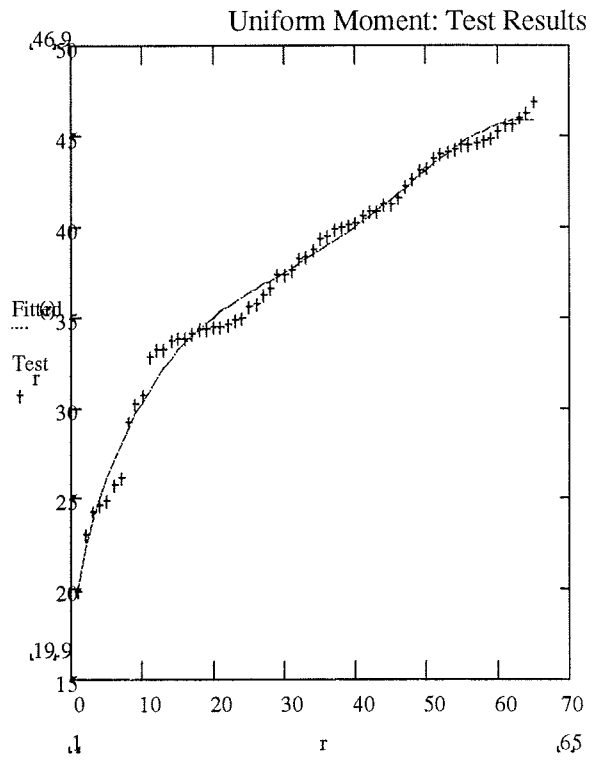


Figure 12: CDF for uniform moment case: Test results and fitted curve.

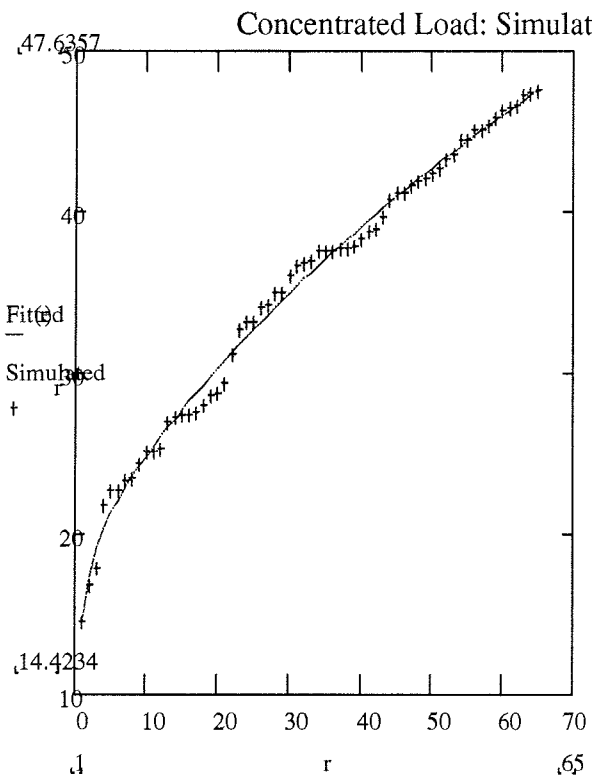


Figure 13: CDF for concentrated load case: Simulated results and fitted curve.

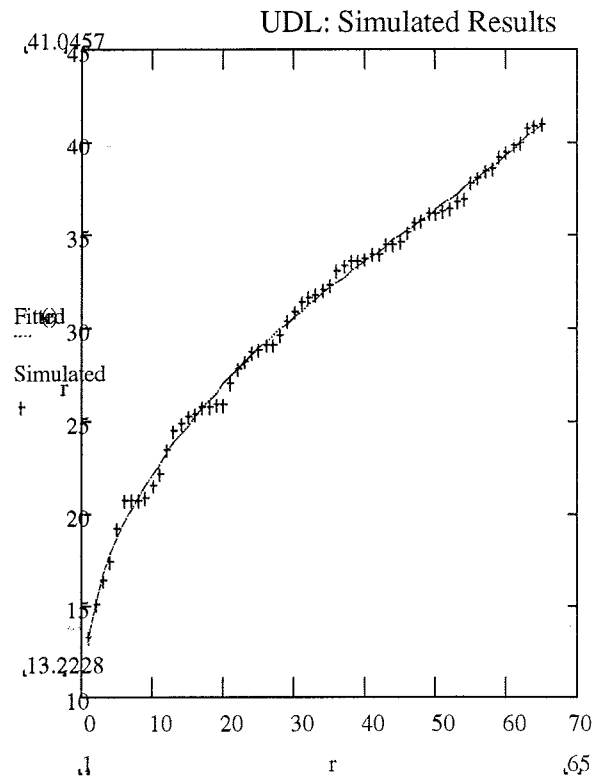


Figure 14: CDF for uniformly distributed load case: Simulated results and fitted curve.

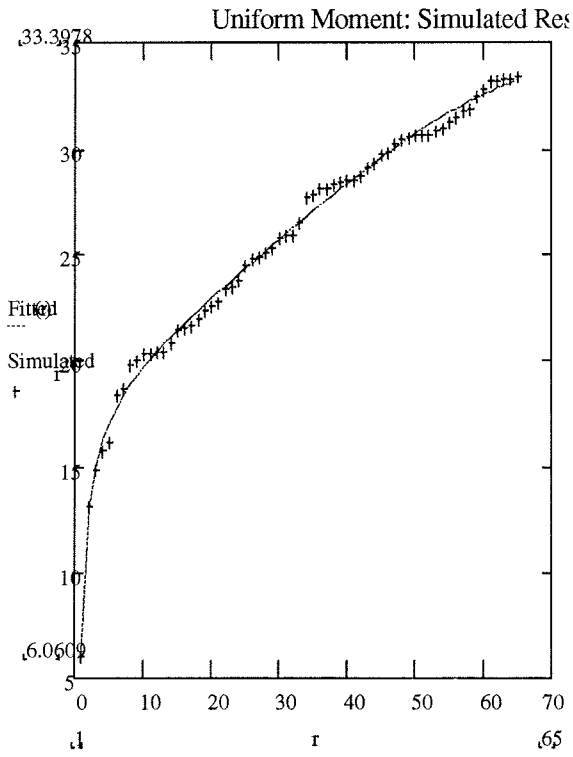


Figure 15: CDF for uniform moment case: Simulated results and fitted curve.

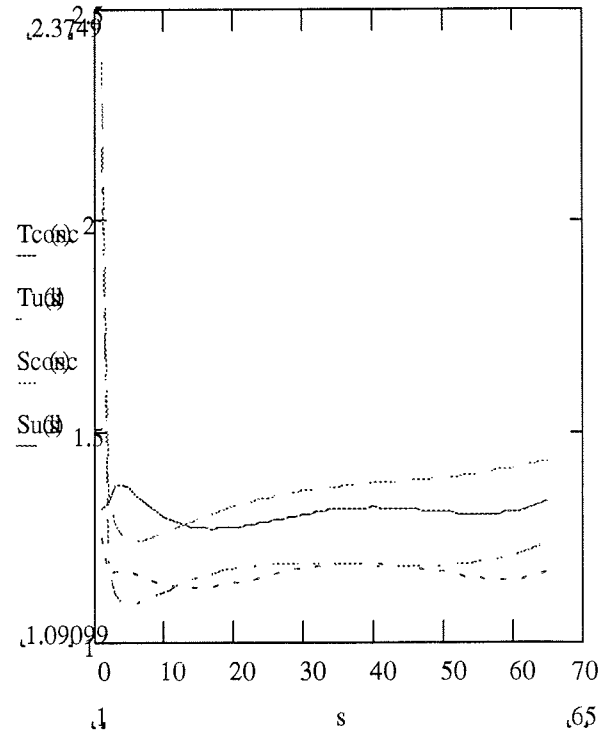


Figure 16: MCFs determined with fitted curves for test results (e.g. Tconc) and simulated results (e.g. Sconc).

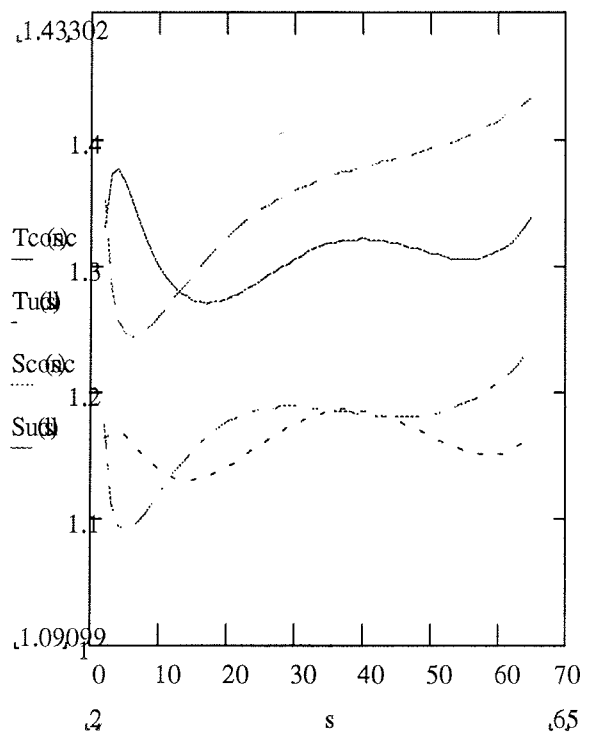


Figure 17: MCFs determined with fitted curves for test results (e.g. Tconc) and simulated results (e.g. Sconc), but with Rank 1 results eliminated.

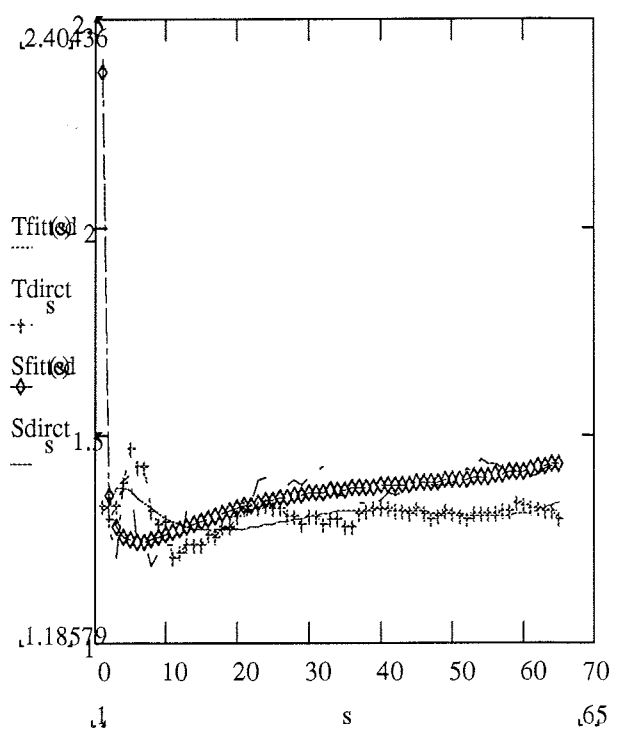


Figure 18: Comparison of MCFs for concentrated load case determined directly with test results and simulated results, and also through the use of fitted curves. 'S' = simulated, 'T' = tested.

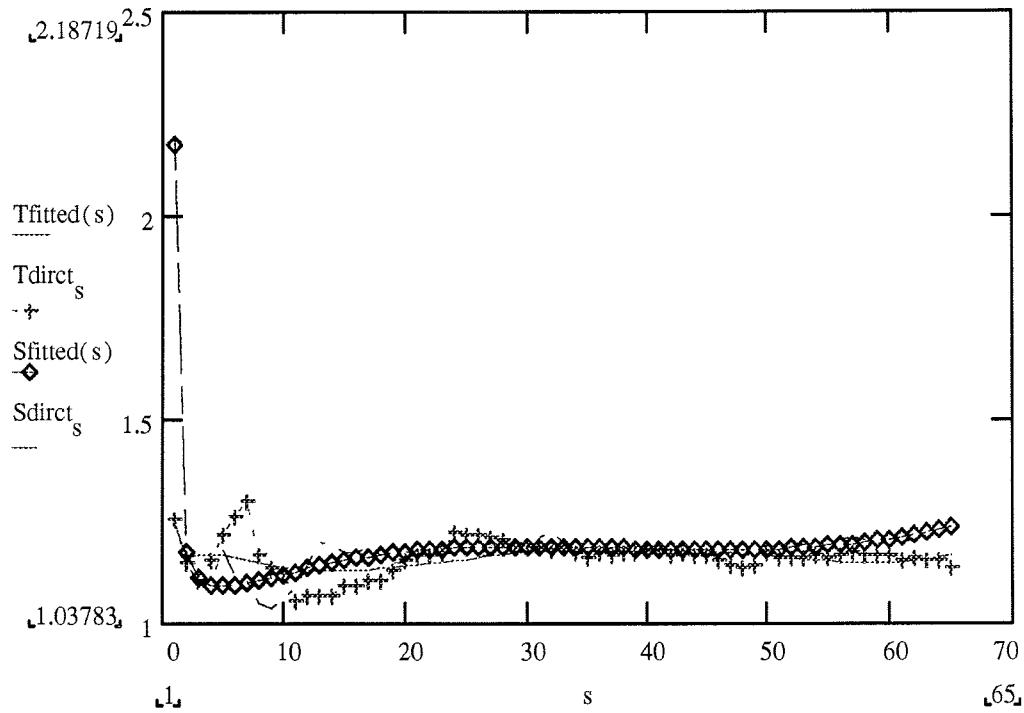


Figure 19: Comparison of MCFs for uniformly distributed load case determined directly with test results and simulated results, and also through the use of fitted curves. 'S' = simulated, 'T' = tested.

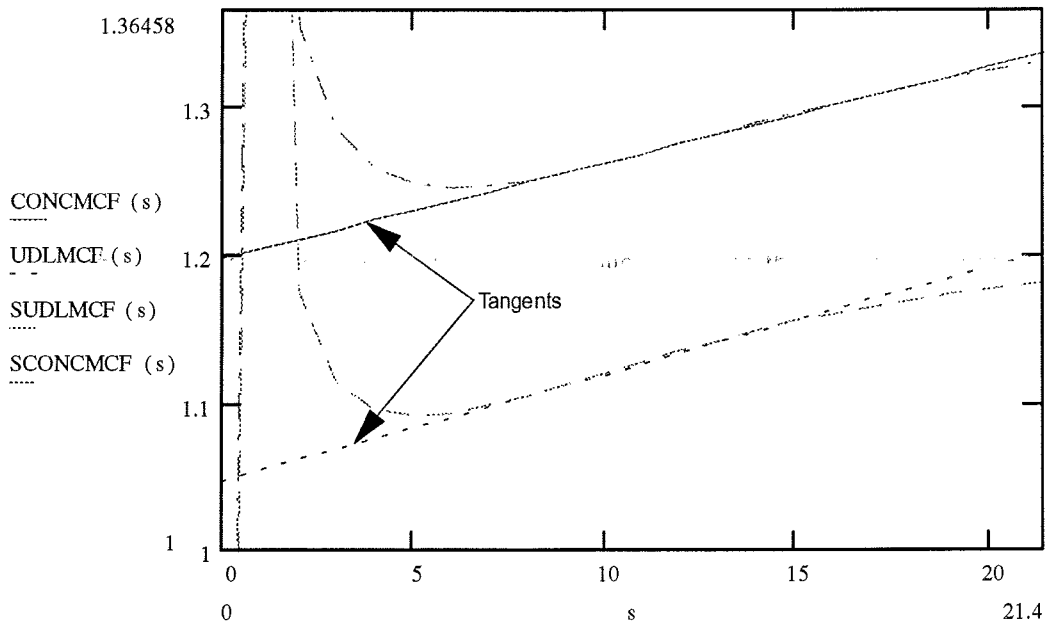


Figure 20: Fitting of tangents to extrapolate MCF curves to obtain conservative 'zero-fractile' values.

**INTERNATIONAL COUNCIL FOR BUILDING RESEARCH STUDIES AND DOCUMENTATION
WORKING COMMISSION W18 - TIMBER STRUCTURES**

EFFECT OF SIZE ON TENSILE STRENGTH OF TIMBER

by

N Burger
P Glos
Institute for Wood Research
University of Munich
Germany

MEETING TWENTY - NINE

BORDEAUX

FRANCE

AUGUST 1996

Effect of size on tensile strength of timber

N. Burger and P. Glos

Institute for Wood Research, University of Munich

1. Introduction

When designing timber members according to Eurocode 5 the size of the member has to be taken into account by means of size factors. These factors were derived from investigations mainly carried out in North America and Great Britain using wood species and grading rules common in these countries. Since it is most likely that size effects may also depend on wood quality, grading rules and, perhaps, wood species, the purpose of this study was to investigate whether these size factors also apply to wood species and grading rules currently in use in Germany.

Towards this end the influence of specimen size on the tensile strength was investigated using 750 specimens from timber of native spruce and 200 specimens from timber of native Douglas fir, with varying cross-sectional dimensions and lengths.

2. Current State-of-the-Art

Indications that strength decreases with increasing cross-sectional dimensions were first published at the beginning of the 20th century (Schneeweiß 1969 quoting Tanaka 1909 and Cline and Heim 1912). Causes were initially attributed to the compression zone. The tension zone, at the time, was considered not critical according to results from tests which used small clear specimens. Newlin and Trayer (1924) developed the fiber support theory. Basically, this involves the idea that highly stressed fibres at the periphery of the cross-section of bending members are being supported by fibres situated further towards the centre which are subjected to less stress. The size effect was quantified in bending tests using clear specimens of Sitka spruce by means of a form factor related to cross-sectional form and size (see Buchanan 1983). Tensile strength, in this theory, is considered a material property independent of size. This model therefore does not explain size effects in tension parallel to grain.

The basis for later models was the weakest link theory put forward by Pierce (1926) and Tucker (1927) which evolved from cotton yarn and concrete tests. This theory is based upon the assumption that the strength of a structural element is defined by its weakest point (chain model).

By dividing a continuum into individual elements the one-dimensional model of a chain can be transferred to three-dimensional bodies. Given brittle material conditions the entire structural element will fail as soon as the critical load of its weakest element is surpassed. A potential size effect can be explained by the fact that with increasing volume the occurrence of weak elements becomes increasingly probable. Since wood loaded in tension is generally assumed to exhibit brittle material behaviour, this model appears applicable to wood. In this case it is assumed that the cause for a potential size effect must be sought in the tension zone of bending members. Thus the theory is also applicable to tension members.

Weibull (1939a,b) developed the mathematical basis for the application of the weakest link theory from considerations based on probability theory. The failure probability of the member may be calculated from that of its elements, provided the strength distribution for these elements is known. Assuming the statistical independence of the part elements the following distribution function of the failure probability for structural elements evolves:

$$S = 1 - e^{-V \left(\frac{\sigma - \sigma_u}{\sigma_m} \right)^k} \quad (1)$$

where V volume of the structural element
 σ existing stress within the structure
 σ_u lower limit of material strength
 σ_m scale parameter of the distribution
 k form parameter of the distribution

This leads to a specific form of distribution, called Weibull-distribution in honour of its developer. The statistical strength theory on which it is based is known as Weibull-theory, weakest link theory or brittle fracture theory. For a two-parameter Weibull-distribution in which the lower limit of material strength is set at $\sigma_u = 0$, the strength ratio of two structures with different dimensions in relation to its volumes is obtained by equating the strength distribution functions of the two structures:

$$\frac{\sigma_2}{\sigma_1} = \left(\frac{V_1}{V_2} \right)^{\frac{1}{k}} = \left(\frac{V_1}{V_2} \right)^m \quad (2)$$

In most investigations published after 1939 the influence of dimensions was determined using this model and the size factor quantified by the exponent m . The size factor proposed in EN 384 and Eurocode 5 to cover the height or width of a structural element is also based on the relationship given in equation (2).

Madsen and Buchanan (1986) suggested a modification of equation (2), which permitted the determination of a size factor specifically for each dimension (see Eq. 3).

$$\frac{\sigma_2}{\sigma_1} = \left(\frac{V_1}{V_2} \right)^m \cong \left(\frac{l_1}{l_2} \right)^{m_l} \cdot \left(\frac{b_1}{b_2} \right)^{m_b} \cdot \left(\frac{d_1}{d_2} \right)^{m_d} \quad (3)$$

Mistler (1979), in extending the above theory, developed the so-called rope-chain-model. The cross-section is treated as a multi-wire rope which remains intact for as long as at least one wire keeps on transferring the load from all the other failed wires. In contrast to the original brittle fracture theory by Weibull this makes it possible to take load rearrangements within the cross-section into account.

Later studies increasingly deal with the application of fracture mechanics to wood, which also indicate a size factor (Aicher et al. 1993; Aicher and Reinhardt 1993). So far this approach has mainly been used in studies dealing with load in tension perpendicular to grain.

A number of further investigations are concerned with variations in local tensile strength along the length of structural timber (Showalter et al. 1987; Bechtel 1988; Taylor and Bender 1991; Zhao and Woeste 1991). Generally, this involved the development of statistical models.

Large test series to study the influence of wood dimensions on strength have to date mainly been done in North America. Only in the recent past and even then only sporadically was this subject studied in Europe. The majority of these papers deals with size effects in bending.

A study to determine test specimen geometry for tension tests by Graf and Egner (1938) was the first instance, in Germany, of tests indicating size effects on specimens under tension load. The test material consisted largely of clear specimens, with a sample size of 4 to 5 specimens per dimension. Hence, by present-day standards these results cannot be considered conclusive.

The most comprehensive investigation, to date, on the influence of dimensions on tensile strength was carried out in a Canadian test program to determine strength determining factors and design values. These tests involved various wood species and species combinations in different grades (Madsen 1992). The following factors were proposed:

effect of length:	50 percentile	$m_l = 0.20$
	10 percentile	$m_l = 0.15$
effect of width:	50 percentile	$m_b = 0.15$
	10 percentile	$m_b = 0.10$

In a subsequent test program American wood species were studied (Barrett and Griffin 1989). Using the factor $m_l = 0.15$ various test lengths were converted into uniform length. Irrespective of wood species and wood quality an effect of width of $m_b = 0.22$ was determined.

Barrett and Fewell (1990), combined Canadian and American test results with English data and proposed the values $m_l = 0.17$ and $m_b = 0.23$ for the consideration of specimen length and width respectively. Glos (1990), in a report on the determination of characteristic values suggests the factor $m_l = 0.15$ for the conversion of specimen length, based on a reference length of 2,000 mm. Rouger and Fewell (1994) point out that the size effect may be influenced by timber quality.

Glos and Burger (1995) provide an overview of published test results.

3. Test program

The study reported here involved tests of 750 specimens of European spruce (*Picea abies*), the main species used for structural timber in Germany. For comparison, further tests were carried out using 200 specimens of Douglas fir (*Pseudotsuga menziesii*). Table 1 provides an overview of the test program, the various dimensions investigated and the sample size for each dimension.

The specimen cross-sections were selected, based on typical dimensions of structural elements subjected to tension load (e.g. glulam laminates, chords and diagonal members of trusses). A maximum test length of 2,500 mm was chosen, under the assumption that no great variations in strength determining characteristics of a specimen are to be expected beyond this length.

Length	Depth	Width		
		50 mm	120 mm	200 mm
European spruce (<i>Picea abies</i>)				
150 mm	30 mm	49	50	50
	50 mm	50	50	49
1090 mm	30 mm	-	50	-
	50 mm	-	49	-
	70 mm	-	50	-
2500 mm	30 mm	48	49	45
	50 mm	48	50	46
Douglas fir (<i>Pseudotsuga menziesii</i>)				
2500 mm	50 mm	49	51 (sapwood) 50 (heartwood)	50

Table 1: Test program of the investigation. Number of specimens for each size.

4. Material and methods

Timber properties, including strength and stiffness, are known to vary greatly, making it imperative that, in order to reduce statistical uncertainties, a great number of individual tests for each specimen dimension be done. Madsen (1978) called for at least 200 specimens per sample, when the test material encompasses the entire range of wood quality. To keep the number of the tests at a minimum the size factor was studied using specially cut test specimens with little variation in growth rate, density and knot ratio. The effect of wood quality was moreover tested using existing data from over 2,000 tension tests on timber carried out earlier.

Test specimens were produced according to the sawing pattern shown in Figure 1 in such a manner that uniform density distributions and similar density ranges for the individual samples as well as comparable patterns of annual rings and knots were achieved. Since density increases with the distance from the pith a uniform distance from the pith was chosen and logs with approximately equal diameters were used.

The spruce and Douglas fir logs were each taken from a single growth area. All test specimens were consistently produced from the butt log. For Douglas fir an additional sample, for comparison, was taken from the heartwood. To guarantee the independence of the individual tests only one test specimen per sample was taken from each log. Given these preconditions it appeared justifiable to use a sample size of 50 for each dimension.

As far as possible the test length was kept clear of unusual defects such as ingrowths. To prevent fracture at the grips care was taken that no large knots occurred at the transition from test length to the clamped section. Efforts were made to make sure that specimens with test lengths of 150 mm and 1,090 mm from the same stem had also originated from the same stem height.

The test specimens were kiln-dried to a moisture content of 10 %. After drying they were planed to the required test dimensions. Thus the test specimens did not exhibit any significant bow or distortion.

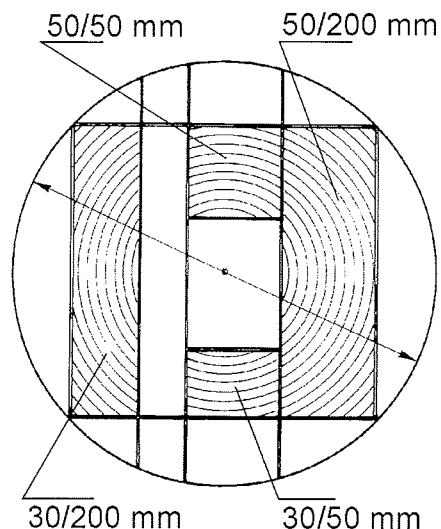


Fig. 1: Sawing pattern of the specimens (exemplary 4 out of 15 sizes).

Specimens were then stored for at least 4 weeks under standard climate conditions (20°C, 65 % rel. humidity) so that on average a moisture content of about 12 % (14 % for Douglas fir) had been reached at the time of the strength tests. During conditioning all knots in the specimens were measured and recorded according to the German grading rule DIN 4074, part 1, while for spruce specimens an additional record of measurements was made according to the UN/ECE grading rules.

The tension tests were carried out according to EN 408. The 10.000 MN tension testing machine used permits testing of full-size specimens at constant strain rate. On both narrow sides the strain on specimens in the course of the tension test was recorded. The modulus of elasticity was then calculated by linear regression of the two stress-strain curves. After the test a sample section was cut out near the failure point to determine moisture content, oven-dry density, average annual ring width and portion of compression wood.

Having planed the specimens it became apparent that 17 specimens showed some compression failure or fibre deviations above 5° and they were therefore not used in the evaluation. This brought the number of specimens to be analysed down to 733.

Tensile strength is described by the 5 percentile (characteristic strength value) and the 50 percentile (median) values. Preference was given to the 50 percentile value rather than the mean value as strength values for wood tend to have skewed distributions and the mean value is strongly affected by a few extremely high values, especially when small sample sizes are used.

According to EN 384 the 5 percentile values for strength have to be determined from at least 40 tests using order statistics, i.e. by a non-parametric method and, where necessary, by interpolation. However, with decreasing sample size this method becomes increasingly less accurate, as random extreme values may have a disproportionate effect on results. Due to the small size of the sample the calculation of 5 percentile values in this investigation was based on a three-parametric Weibull distribution. The 50 percentile values were determined by ranking.

In accordance with the formula used in the European standards the size factor was quantified by determining the exponents of a modified Weibull-equation (see Eq. 3). Exponents were determined by regression equations according to equation (4), without taking specimen thickness into account (see section 5.2).

$$f_t = f_{t,r} \cdot \left(\frac{l_r}{l}\right)^{m_l} \cdot \left(\frac{b_r}{b}\right)^{m_b} \quad \text{or} \quad f_t = f_{t,r} \cdot \left(\frac{l_r \cdot b_r}{l \cdot b}\right)^{m_{ak}} \quad (4)$$

where f_t , l , b tensile strength, length and width of specimens
 $f_{t,r}$, l_r , b_r tensile strength, length and width of reference specimen

In analogy to European standards the reference dimensions were set at $b_r = 150$ mm and $l_r = 9 \cdot b_r = 1,350$ mm.

To eliminate the effects of density and knot-ratio individual test values were converted into reference strength and stiffness values by relating them to reference density and knot values (Burger 1995). For this conversion a regression curve with linear variable residual standard deviation was used. For each test value a reference value was calculated by taking into account the respective residual deviation.

5. Results

5.1. Wood characteristics

The mean values and coefficients of variation for density, knot ratio, tensile strength and modulus of elasticity in tension for each sample are compiled in Tables 2 and 3 for spruce and Douglas fir respectively. Figures 2 and 3 show the tensile strength of spruce specimens in relation to oven-dry density and knot ratio according to DIN 4074.

Due to the manner in which specimens had been cut from the logs comparable density distributions and annual ring widths were obtained.

Density values for the Douglas fir specimens were, on average, about 30 % higher than those for spruce, with the exception of the sample taken from the heartwood. The density of Douglas fir specimens cut from near the pith was about 10 % lower than that for specimens taken from farther away from the pith.

The Douglas fir samples generally had wider annual rings and a greater number of specimens with compression wood than the spruce collectives.

Cross-section [mm]		50/50	50/120 (sapwood)	50/200	50/120 (heartwood)
Number of specimens		49	51	50	50
Density	$\rho_{0,mean}$	0.552	0.566	0.558	0.504
	V [%]	11.6	9.5	9.3	10.3
Knot ratio acc. to DIN 4074	\overline{DAB}	0.55	0.30	0.21	0.48
	V [%]	53.9	49.3	53.1	32.7
Tensile strength	$f_{t,mean}$	40.7	48.7	52.0	34.3
	V [%]	38.3	34.1	29.1	37.1
Modulus of elasticity	$E_{t,mean}$	15000	15100	16500	12200
	V [%]	33.3	21.0	17.9	26.7

Table 3: Results of the tested specimens of Douglas fir. ρ_0 in [g/cm³], DAB, ET, EM [-], f_t and E_t in [N/mm²].

Length Cross-section [mm]	$l_0 = 150$ mm				$l_0 = 1090$ mm				$l_0 = 2500$ mm						
	30/50	50/50	30/120	50/120	30/200	50/200	30/120	50/120	70/120	30/50	48	50/50	30/120	50/120	30/200
Number of specimens	49	50	50	50	49	49	50	49	50	48	48	49	50	45	46
Density $\rho_{0,mean}$ V [%]	0.416	0.414	0.421	0.407	0.423	0.426	0.439	0.440	0.427	0.416	0.416	0.413	0.410	0.429	0.430
Knot ratio DAB V [%]	0.35	0.36	0.16	0.25	0.16	0.17	0.23	0.27	0.31	0.56	0.61	0.27	0.31	0.24	0.26
Knot ratio ET V [%]	0.24	0.16	0.13	0.14	0.11	0.11	0.14	0.15	0.14	0.33	0.29	0.17	0.18	0.16	0.17
Knot ratio EM V [%]	0.35	0.21	0.24	0.24	0.19	0.17	0.29	0.33	0.32	0.69	0.64	0.50	0.44	0.38	0.33
ECE	96.0	63.6	108.5	86.8	84.7	94.2	72.1	64.3	65.0	35.0	37.7	40.4	40.8	39.7	44.5
Tensile strength $f_{t,mean}$ $f_{t,50}$ $f_{t,05}$ V [%]	50.0	52.6	59.8	50.7	57.9	59.5	49.2	46.1	44.4	28.9	30.0	38.3	36.9	40.1	39.6
	43.6	48.8	57.5	48.7	56.5	57.0	50.1	44.6	45.8	26.7	28.9	38.1	37.3	37.2	39.2
	21.1	23.2	32.7	22.2	33.2	31.4	18.4	19.9	18.4	9.0	13.1	11.7	16.5	17.6	17.1
	42.9	36.0	30.7	34.7	30.6	32.4	39.2	33.2	34.0	50.6	38.1	51.6	38.5	40.7	37.1
Modulus of elasticity $E_{t,mean}$ V [%]	10100 ¹⁾	11200 ¹⁾	12100 ¹⁾	11300 ¹⁾	12800 ¹⁾	12900 ¹⁾	13000	13200	13000	12600	11700 ²⁾	12400	11900	13700	13500
	31.4	24.1	24.7	25.3	20.5	20.2	21.0	18.9	18.4	36.4	46.3	25.5	21.6	19.9	20.5

1) Gauge length for measurement of modulus of elasticity: 133,5 mm

2) Gauge length for measurement of modulus of elasticity: 600 mm

Table 2: Results of the tested specimens of Spruce. ρ_0 in [g/cm³], DAB, ET, EM [-], f_t and E_t in [N/mm²].

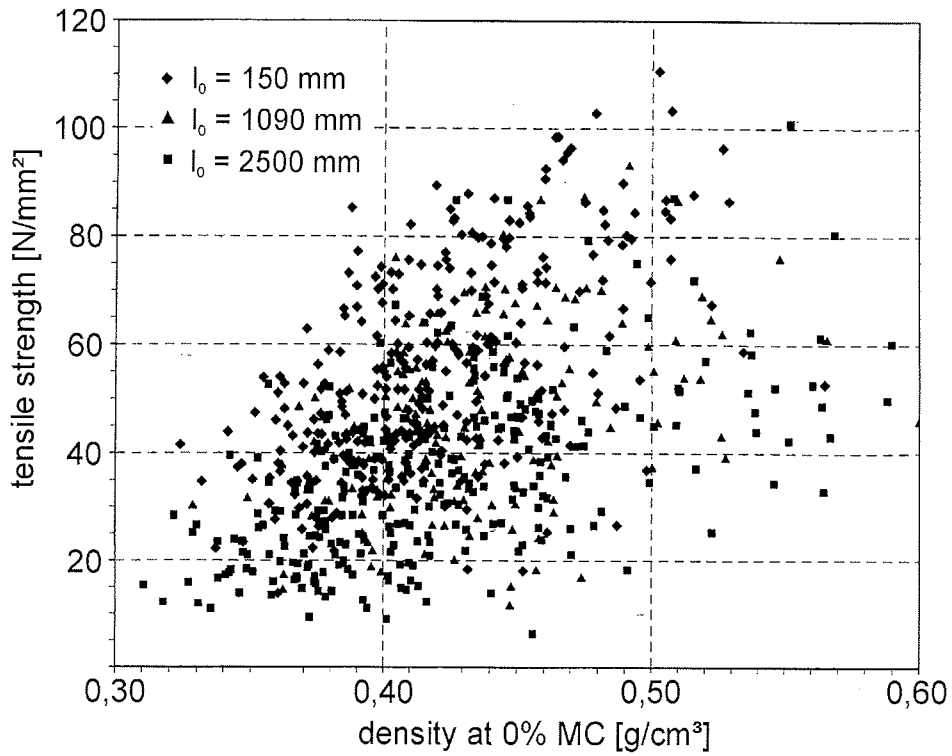


Fig. 2: Tensile strength of the 733 tested spruce specimens as related to density.

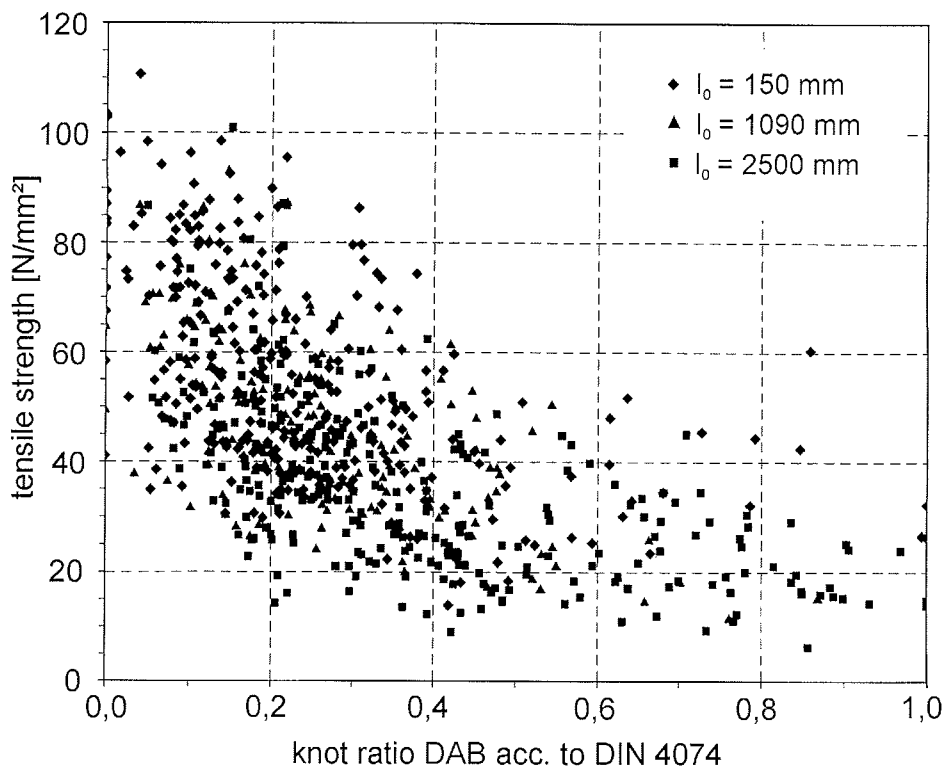
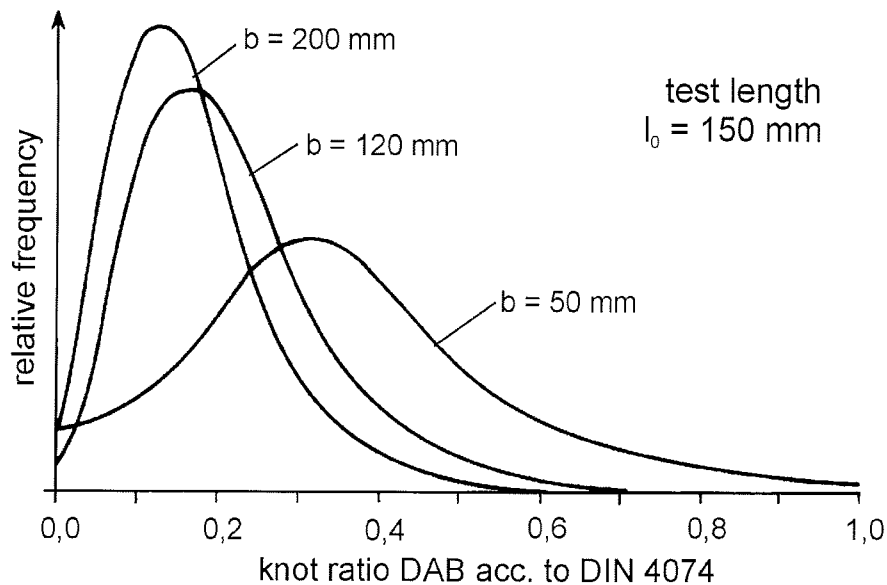


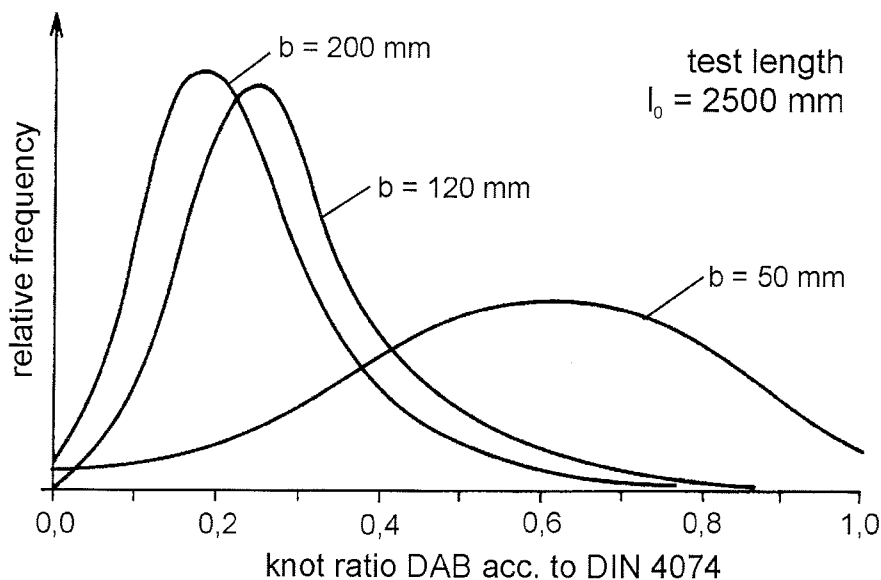
Fig. 3: Tensile strength of the 733 tested spruce specimens as related to knot ratio acc. to DIN 4074, criterion boards, knot cluster (DAB).

Due to the variations in dimensions there were considerable differences regarding the knot ratio of the individual samples:

Knots comparable in size result in a greater knot ratio in smaller cross-sections than in larger ones. Knot-ratio therefore decreases with increasing specimen width while with increasing length the probability of larger knot clusters in a specimen tends to rise. Mainly, however, the maximum knot ratio occurring in specimens is related to specimen width. Furthermore there was evidence of a decrease in knot ratio variation with increasing specimen width as well as length because of the lesser portion of particularly low knot ratios and, with increasing width, of very high knot ratios (see Figures 4 and 5). Specimen thickness has a comparably negligible influence, as was also demonstrated by the regression equation (see 5.2).



a) Test length $l_0 = 150$ mm.



b) Test length $l_0 = 2500$ mm.

Fig. 4: Distribution of knot ratio acc. to DIN 4074 as dependent on specimen width b .

In the tests the significance of knot position within the cross-section in triggering failure and hence in affecting tensile strength became apparent. Excentric knots have an unfavourable effect on tensile strength, as became apparent in the deformations recorded in the strain graphs. The strength reducing effect of edge knots increases with decreasing specimen width.

5.2 Tensile strength

There is great variation in the tensile strength of the individual samples. This goes for mean values and 50 percentiles as well as for 5 percentiles. With increasing specimen width and concomitant decreasing variation tensile strength rises, while an increase in specimen length leads to a reduction in strength. Since there is a strong dependence of tensile strength on knot ratio (see Fig. 3) this is mainly due to the different knot ratios of the samples and is true for both spruce and Douglas fir specimens. Low tensile strength of Douglas fir specimens from heartwood can be attributed to distinctly lower density as well as to a higher knot ratio.

A stepwise regression analysis was done for the purpose of evaluating which parameters and combinations of parameters have the greatest influence on tensile strength. To account for the interaction of parameters various parameter combinations involving knot ratio, thickness, width and length, were used as regression parameters in addition to density, knot ratio and specimen dimensions. In the following the statistically significant influencing parameters at the 5 percentile level are listed in the sequence in which they were included in the regression equation, along with the corresponding multiple correlation coefficient:

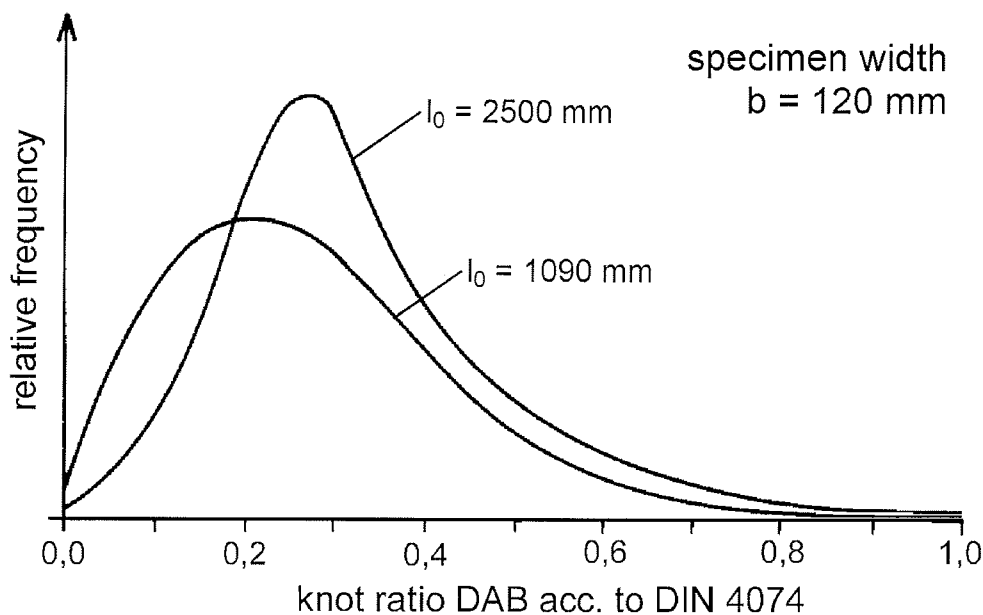


Fig. 5: Distribution of knot ratio acc. to DIN 4074 as dependent on test length l_0 .

1.	DAB	$r = 0.62$
2.	ρ_0	$r = 0.70$
3.	l_0	$r = 0.76$
4.	$DAB \cdot b$	$r = 0.77$
5.	$DAB \cdot l_0$	$r = 0.77$
6.	$l_0 \cdot b$	$r = 0.78$
7.	$DAB \cdot d$	$r = 0.78$
8.	d	$r = 0.78$
9.	$b \cdot d$	$r = 0.78$

Specimen width b and the parameter $l_0 \cdot d$ combining test length and specimen thickness were not included in the equation. The result indicates that tensile strength is predominantly being affected by test length, apart from the effects of knot ratio and density. Moreover, a relationship between knot ratio and specimen width is apparent. Further variables from the 5th step onwards, inter alia specimen thickness, contribute very little towards improving the correlation and can be considered negligible.

The regression equation for tensile strength after the first four regression steps is shown in equation (5), which demonstrates the well-known linear relationship with the parameters density and knot ratio as well as the most important effects of specimen dimensions.

$$f_t = 9.7 - 34.3 \cdot DAB + 138.9 \cdot \rho_0 - 0.0054 \cdot l_0 - 0.177 \cdot (DAB \cdot b) \quad (5)$$

For the Douglas fir tests a corresponding analysis gave the following sequence:

1.	DAB	$r = 0.58$
2.	ρ_0	$r = 0.71$
3.	$DAB \cdot b$	$r = 0.72$
4.	b	$r = 0.73$

The results, too, show the established relationship between knot ratio and specimen width, which has a stronger effect on tensile strength than specimen width by itself. As the Douglas fir specimens were tested at uniform length the influence of length could not be determined here.

Figure 6 shows the influence of the length of spruce specimens on tensile strength. The curves were obtained by means of regression analysis using the Weibull formula according to equation (4). Standardized curves in which test values were converted into reference values of oven-dry density and knot ratio are shown next to the regression curve with the original test data. The standardized curves give little evidence of an effect of specimen length, which can be attributed to the compensating effect of higher knot ratios in specimens of greater length. Table 4 compiles the exponents of the size factors from the regression analyses using equation (4).

For a study of the effect of wood quality on size factor a further evaluation was made of 2,000 earlier tensile tests from other research projects involving European spruce specimens. Specimen cross-sectional dimensions ranged from 20 to 50 mm thickness and 80 to 260 mm width. In all tests specimen lengths corresponding to 9 times the respective specimen widths had been used. Here too, regression analyses using these data gave evidence of the relationship between specimen width and knot ratio and their influence on tensile strength.

Because the density values of the individual samples varied greatly, the strength values were adapted to reference density values for each grade. Since all these tests had been conducted according to EN 408 and all specimens hence showed a constant ratio of length to width for all tested cross-sectional dimensions, no separate study of the effect of each parameter was possible but only of the combined effect. The exponents m_{ak} for the combined effect of length and width determined according to equation (4) are given in Table 5. Figure 7 is an example of this effect using grade S 10 specimens.

The influence of wood quality differs for visually and machine graded timber. While visually graded timber (Table 5: grades S 7 to S 13) exhibits an increasingly greater size factor with decreasing wood quality, the effect of wood quality in machine graded wood (Table 5: Grades MS 10 to MS 17) is unrecognizable for the range of both the 5 percentiles and 50 percentiles. For visually graded wood of grades S 7 to S 13 with low specimen widths and lengths relatively few data are available. Hence, the values for the 5 percentiles can only be used as a rough estimate.

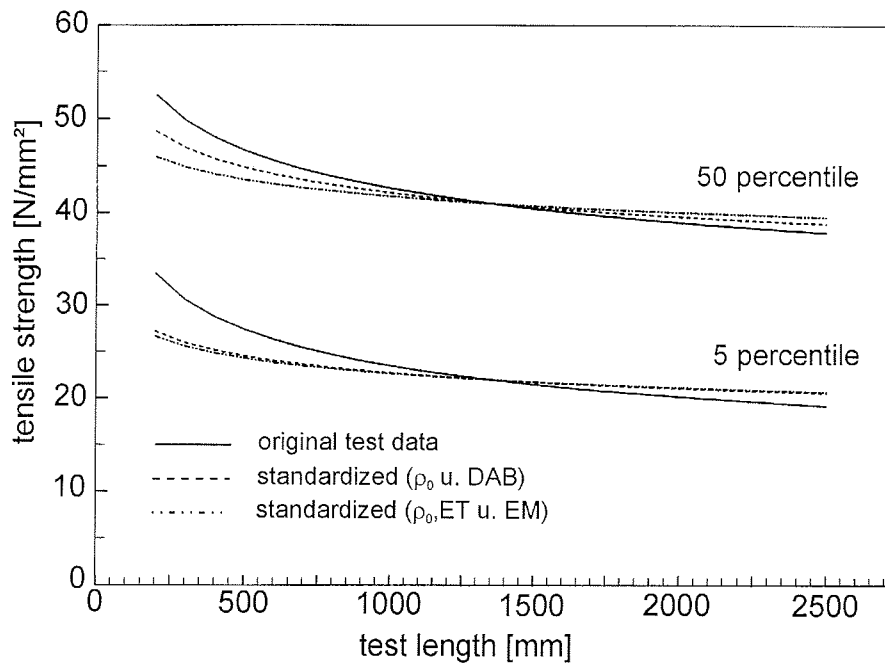


Fig. 6: Effect of length on tensile strength of the 733 tested spruce specimens.

Tensile strength		Spruce		Douglas fir
		m_l	m_b	m_b
measured	50 %	0.13	-0.17	-0.17
	5 %	0.22	-0.29	-0.16
standardized (ρ_0 and <i>DAB</i>)	50 %	0.09	0.09	0.01
	5 %	0.11	0.01	-0.15
standardized (ρ_0 , <i>ET</i> and <i>EM</i>)	50 %	0.06	0.04	-
	5 %	0.10	0.00	-

Table 4: Exponents of the size factors. Test results for spruce and Douglas fir.

The mean values for all grades correlate with the results of the present investigation. This permits the conclusion that for these tests, too, specimen length is the major influence on the size factor.

Figure 8 shows the effect of specimen width on the tensile strength of the 733 spruce specimens of this study from the regression analysis using equation (4), again separated into original test data and standardized values for density and knot ratio. For comparison the curve for the Eurocode 5 size factor $k_h = (150/b)^{0.2}$ has also been included in the graph. The exponents m_b of the size factors for spruce and Douglas fir are provided in Table 4. The conversion into reference values clearly shows the following relationship between specimen width, knot ratio and tensile strength: The increase in tensile strength with increasing specimen width is caused by the relationship between specimen width and knot ratio and is being compensated or even overcompensated when the knot ratio is included in the regression equation. The tests involving Douglas fir timber show the same results.

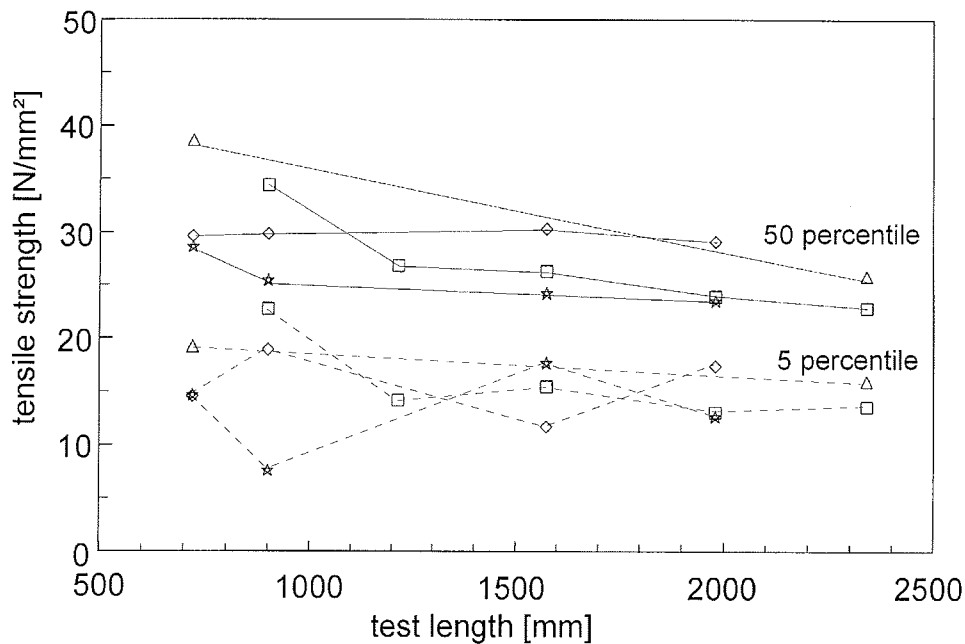


Fig. 7: Effect of length on tensile strength. Test results from the institute's data base. Grade S 10. 15 sub-samples totalling 866 tests.

	Visual grading		Machine grading		
	50 %	5 %	50 %	5 %	
S 13	0.01	(- 0.09)	MS 17	0.00	0.08
S 10	0.11	0.06	MS 13	0.01	0.06
S 7	0.16	(0.35)	MS 10	0.02	0.09

Table 5: Exponents m_{ak} of the combined size factors for visually and machine graded timber. Available tests of the data base.

As far as the effect of specimen thickness is concerned a comparison of the samples revealed no distinct tendencies. Since specimen thickness also proved of little significance in the regression analysis its influence was not studied in greater detail in this investigation.

5.3 Modulus of elasticity in tension

Test values for modulus of elasticity showed a slight decrease with increasing length and decreasing specimen width. These results are again overlapped by density and knot ratio, with evidence of a more pronounced effect of density on the modulus of elasticity ($r = 0.70$) compared with that of knot ratio ($r = 0.49$).

Upon standardization of the modulus of elasticity in tension values and conversion into reference values for oven-dry density and knot ratio DAB no further influence of size on modulus of elasticity is apparent.

6. Discussion of Results

Results from the tension tests conducted in the course of this study reveal systematic effects of specimen dimensions on tensile strength. On the one hand tensile strength decreases with increasing test length, which corresponds to the statistical approach according to the Weibull theory. On the other hand an increase in tensile strength with increasing specimen width was apparent. This observation contradicts the Weibull theory and can be attributed to the influence of decreasing knot ratio concomitant with the increase in specimen width.

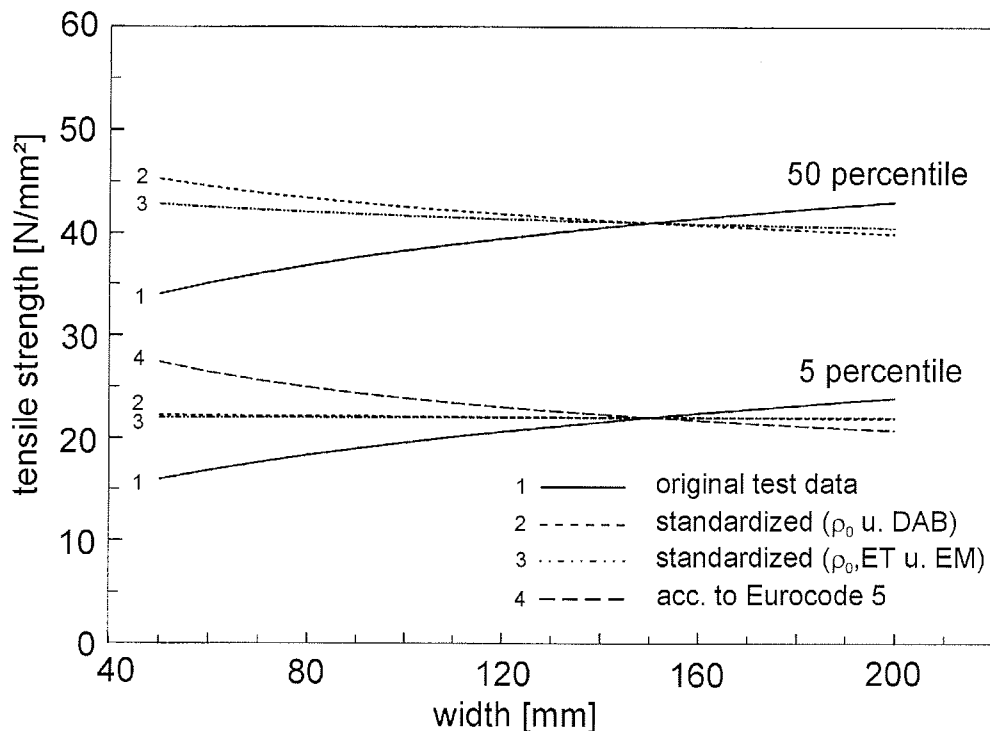


Fig. 8: Effect of width on tensile strength of the 733 tested spruce specimens.

The dependence of tensile strength on specimen dimensions is thus being determined by two different influences, both of a statistical nature and both related to specimen size. They can be characterized, on the one hand, as effects based on microscopic defects (classic statistical size effect) and, on the other, as effects based on macroscopic defects (knots, structural size effect). Structural size effects on tensile strength are based on an increase in knot ratio with increasing length and decreasing width.

While the probability of the occurrence of knots is known to rise with increasing specimen width, the strength-affecting knot ratio related to the overall cross-section was shown to decrease.

As regards the effect of specimen length on tensile strength the statistical and structural size effects are equidirectional and tend to reinforce each other. By contrast, the two size effects have opposing influences when considering the influence of specimen width on tensile strength, as clearly shown in the regression analyses for measured and standardized test values in Figures 5 and 7. The effect of width, as suggested in the European standards, is seen to be almost negligible.

For visually graded timber there is a distinct dependence of the statistical size factor on wood quality. For machine graded timber the size effect is considerably less pronounced and relatively independent of wood quality. This may be explained by the fact that the size factor was already implicitly taken into account when determining the settings of the grading machine.

The tests reported here confirm that tensile strength is mainly being affected by the length of a structural member rather than its width. In general, no relationship exists between the length and width for structural elements under tension load, in contrast to the relationship between length and height assumed for structural elements under bending load.

An influence of length is particularly evident in short structural elements only. It decreases with increasing length of the element. The economic advantage of higher design values in tension for shorter structural members on account of material savings is negligible. Moreover, it would then be necessary to also consider the counter-effect of the greater probability that extreme load values will occur in smaller loading areas.

Based on the results and reflections of this study there appears to be no justifiable need to consider a size factor as required by Eurocode 5 in the design of timber constructions. The influence of test length on tensile strength should, however, be taken into consideration in the determination of characteristic strength values. In particular, a uniform length of specimens for tensile strength tests should be stipulated in the test standards.

Similar relationships, i.e. a major influence of the length of structural elements, can be assumed for load in bending. If a size factor appears to be necessary in this context, it should be discussed whether a length factor would perhaps be more suitable than a height factor. This would remove the necessity for a step-wise design process as now required when dealing with a height factor.

References

- AICHER, S.; REINHARDT, H.W.; 1993:
Einfluß der Bauteilgröße in der linearen und nichtlinearen Holzbruchmechanik
Holz als Roh- und Werkstoff 51, 1993, S. 215-222
- AICHER, S.; REINHARDT, H.W.; KLÖCK, W.: 1993:
Nichtlineares Bruchmechanik-Maßstabsgesetz für Fichte bei Zugbeanspruchung senkrecht zur Faserrichtung
Holz als Roh- und Werkstoff 51 1993, S. 385-394
- BARRETT, J.D.; FEWELL, A.R.; 1990:
Size factors for the bending and tension strength of structural timber
Proc. Int. Counc. Build. Res. Stud. Doc., Work. Comm. W18A - Timber Structures, Meeting 23, Lisbon, Portugal, 1990
- BARRETT, J.D.; GRIFFIN, H.; 1989:
Size effects for Canadian dimension lumber
Proc. Int. Counc. Build. Res. Stud. Doc., Work. Comm. W18A - Timber Structures, Meeting 22, Berlin, Germany, 1989
- BARRETT, J.D.; LAM, F.; LAU, W.; 1992:
Size effects in visually graded softwood structural lumber
Int. Counc. Build. Res. Stud. Doc., Working Commission W18 - Timber Structures, Meeting 25, Åhus, Sweden, 1992
- BECHTEL, F.K.; 1988:
A model to account for length effect in the tensile strength of lumber
Proc. Int. Conf. Timb. Eng., Vol. 1, Seattle, USA, 1988, S. 355-362
- BUCHANAN, A.H.; 1983:
Effect of member size on bending and tension strength of wood
IUFRO Wood Engineering Meeting, Proceedings, Madison, Wisconsin, USA, 1983
- BURGER, N.; 1995:
Normierung streuender Meßwerte in Abhängigkeit streuender Einflußgrößen
Interner Bericht 95508, Institut für Holzforschung, Universität München, 1995
- CLINE, M.; HEIM, A.L.; 1912:
Tests of structural timber
US Department of Agriculture, Forest Service, Bulletin 108, 1912
- GLOS, P.; 1990:
Vergleichende Berechnungen für Bauteile und Verbindungsmittel auf der Grundlage des neuen Sicherheitssystems - EUROCODE 5 - Holzbauwerke - Teilprojekt I: Baustoffe
Bericht 89501, Institut für Holzforschung, Universität München, 1990
- GLOS, P.; BURGER, N.; 1995:
Einfluß der Holzabmessungen auf die Zugfestigkeit von Bauschnittholz
Bericht 91501, Institut für Holzforschung, Universität München, 1995, 127 S.
- GRAF, O.; EGNER, K.; 1938:
Über die Veränderlichkeit der Zugfestigkeit von Fichtenholz mit der Form und Größe der Einspannköpfe der Normenkörper und mit Zunahme des Querschnitts der Probekörper
Holz als Roh- und Werkstoff 1, 1938, S. 384-388
- JOHNSON, L.A.; EVANS, J.W.; GREEN, D.W.; 1989:
Volume effect adjustments for the in-grade data, In-grade testing of structural lumber
Proceedings 47363, Forest Products Research Society, Madison, Wisconsin, USA, 1989
- LAM, F.; VAROGLU, E.; 1990:
Effect of length on the tensile strength of lumber
Forest Products Journal 40 (5), 1990, S. 37-42

- MADSEN, B.; 1978:
In-grade testing: Problem analysis
Forest Products Journal 28 (4), 1978, S. 42-50
- MADSEN, B.; 1992:
Structural behaviour of timber
Timber Engineering Ltd., 1992, 405 S.
- MADSEN, B.; BUCHANAN, A.H.; 1986:
Size effects in timber explained by a modified weakest link theory
Canadian Journal of Civil Engineering 13 (2), 1986, S. 218-232
- MISTLER, H.L.; 1979:
Die Tragfähigkeit des am Endauflager unten rechtwinklig ausgeklinkten Brettschichtträgers
Dissertation, Lehrstuhl für Ingenieurholzbau und Baukonstruktionen, Techn. Univ. Karlsruhe, 1979
- NEWLIN, J.A.; TRAYER, G.W.; 1924:
Form factors of beams subjected to transverse loading only
Nat. Adv. Comm. Aero., Report No. 181, 1924 ; reprinted as USDA Forest Service, Forest Products Laboratory, Report No.1310, 1941, 19 S.
- PIERCE, F.T.; 1926:
Tensile tests for cotton yarns
Journal Text. Inst. 17, 1926; S. T355-T368
- ROUGER, F.; FEWELL, T.; 1994:
Size effects in timber: Novelty never ends
Int. Counc. Build. Res. Stud. Doc., Working Commission W18 - Timber Structures, Meeting 27, Sydney, Australia, 1994
- SCHNEEWEIß, G.; 1969:
Der Einfluß der Abmessungen auf die Biegefestigkeit von Holzbalken
Holz als Roh- und Werkstoff 27 (1), 1969, S. 23-29
- SHOWALTER, K.L.; WOESTE, F.E.; BENDTSEN, B.A.; 1987:
Effect of length on tensile strength in structural lumber
USDA For. Ser., For. Prod. Lab., Research Paper FPL-RP-482, 1987
- TANAKA, F.; 1909:
V. Kongreß des Internationalen Verbandes für die Materialprüfungen der Technik, Kopenhagen, 1909, Rückblick auf den Kongreß, II. Abt.: Die Kongreßverhandlungen, S. 190-191
- TAYLOR, S.E.; BENDER, D.A.; 1991:
Stochastic model for localized tensile strength and modulus of elasticity in lumber
Wood and Fiber Science 23 (4), 1991, S. 501-519
- TUCKER, J.; 1927:
A study of the compression strength dispersion of materials with applications
J. Franklin Institute 204; 1927; S. 751-781
- WEIBULL, W.; 1939a:
A statistical theory of the strength of materials
Roy. Swed. Inst. Eng. Res., Bull. No. 151, Roy. Tech. Univ., Stockholm, Sweden, 1939
- WEIBULL, W.; 1939b:
The phenomenon of rupture in solids
Roy. Swed. Inst. Eng. Res., Bull. No. 153, Roy. Tech. Univ., Stockholm, Sweden, 1939
- ZHAO, W.; WOESTE, F.E.; 1991:
Influence of correlation on tensile strength prediction of lumber
Forest Products Journal 41 (2), 1991, S. 45-48

INTERNATIONAL COUNCIL FOR BUILDING RESEARCH STUDIES AND DOCUMENTATION
WORKING COMMISSION W18 - TIMBER STRUCTURES

EQUIVALENCE OF IN-GRADE TESTING STANDARDS

by

R H Leicester
H O Breitingner
H F Fordham
CSIRO
Australia

MEETING TWENTY - NINE

BORDEAUX

FRANCE

AUGUST 1996

EQUIVALENCE OF IN-GRADE TESTING STANDARDS

Robert H. Leicester, Harold O. Breitingger, Heather F. Fordham
CSIRO Division of Building Construction and Engineering, Australia

ABSTRACT

This paper describes the first part of a study to examine the equivalences between various in-grade testing procedures. It covers the bending strength and stiffness of mechanically stress graded 90 x 35 mm radiata pine measured according to European, North American and Australasian standards. The data indicates that small but significant differences of about 20% may occur at both the mean and 5-percentile strength and stiffness due to the test methods used. A simple statistical theory to predict the differences in strength is given; this theory is based on a knowledge of the defect frequency in the timber boards. Eventually, it is hoped to be able to use this theory as a basis for establishing the equivalences between various test procedures.

1. INTRODUCTION

During the past decade there have been millions of dollars invested in measuring the in-grade properties of structural timber. Unfortunately, different methods of measurement have been made in various countries, and the equivalences between these various methods are not apparent. This creates a problem both for technology transfer between countries and for international trade.

The purpose of this paper is to report on the first part of a study to examine procedures for evaluating the equivalence of in-grade testing standards. Other information may be obtained from earlier papers (Leicester and Young 1991; Kallsner and Ditlevsen 1994; Isaksson and Thelandersson 1995).

The differences between standards can be grouped into two major categories as follows;

- (a) the test configuration, and
- (b) the statistical processing of data.

Of these, differences due to the statistical processing does not present a problem if the original test data is recorded. However, methods for overcoming differences in test configurations are still uncertain.

The most important structural properties are strength in bending, tension, compression and shear and also modulus of elasticity. This paper will address primarily the topic of bending strength with some reference to modulus of elasticity measured in the same test. Simple models for use in equivalencing strength data will be discussed, together with some recently obtained experimental data.

1.1 In-grade Evaluation Standards

There are numerous standards and procedures available for evaluating bending strength, but it is useful to focus initially on the following three well defined procedures. All procedures use third point loading configurations as shown in Figure 1.

The European CEN Standards EN 384 and 408 (European Committee for Standardisation 1995), use a span/depth ratio of 18, and state that the worst strength reducing defect be placed within the middle third; a random edge is chosen for the tension edge. For the modulus of elasticity, the deflection of point C relative to B and D is used, Figure 1.

North American practice is best represented by the procedures used for a major in-grade study during the past decade (Green and Evans 1987). Here the specified span/depth ratio was 17, and the worst strength reducing defect was placed at a random location within the test span. For modulus of elasticity the deflection of point C relative to A and E were measured, Figure 1.

Current Australasian practice follows the Standard AS/NZS 4063. Here the specified span/depth ratio is 18, and the test specimen is cut from a randomly chosen portion within the length of the graded board. This procedure is intended to simulate in-service conditions. The modulus of elasticity is derived by measuring the deflection of point G relative to F and H, Figure 1.

From the above it is apparent that the North American procedure lies somewhere between the CEN and the Australasian procedures. In fact, it is identical to AS 4063 if the graded length of the timber is equal to the specimen length; this case is covered by the requirements for non-standard procedures in AS 4063.

In all procedures, the strength is defined in terms of the lowest fifth percentile value.

2. EXPERIMENTAL MEASUREMENTS

The experimental data obtained to date comprises bending strength tests on 90 x 35 mm size F5 and F8 grades of mechanically stress-graded radiata pine. Approximately 150 boards, each 4800 mm long, were tested according to the three in-grade standards.

In addition to the in-grade tests, additional measurements were made that could be useful for equivalencing purposes. These measurements must be simple and rapid to undertake. One obvious measurement relates to the distribution of visible defects, as these form the basis of EN and USA standards. A second proposed measurement is to classify the timber into juvenile and mature wood and treat these separately as their characteristics may be significantly different.

The boards were classified as juvenile wood if at least one end of the board ring radius indicated that the board end was less than 50 mm from the pith. This aspect of the measurements was not rigorously undertaken and will need to be repeated.

To obtain an idea of the distribution of visible defects, the number of knots within each board were counted. In the case of mature wood, these knots were taken to be any knots that would fail to meet Structural Grade No. 2 according to the Australian Standard AS 2858 (Standards Australia 1986). For immature timber, it was taken to be significant knot whorls around the pith.

During the course of developing equivalencing procedures, it became apparent that the within board correlation of defect strength would be a significant parameter. To obtain a rough idea of this effect, two test specimens were cut from each board in the AS/NZS test; this was possible since the AS/NZS test procedure allows for a random location of test specimens. Treating the left hand side and right hand side specimens as two different populations, a correlation coefficient was measured. Note that the correlation between the strengths of defects would be considerably higher than the correlation of the strength of test specimens, because the strength of the tested specimens were not always defect controlled.

3. TEST DATA

Data on measured bending strength and modulus of elasticity are summarised in Tables 1 and 2. Note that the information has been broken down in to sub classes of juvenile and mature wood. The modulus of elasticity in the USA and AS/NZS data do not contain any correction for shear strength. Cumulative frequency plots on the total in-grade data for

each grade are given in Figures 2–4. A plot of the knot frequency for defects in the mature timber is given in Figure 8.

Table 1.
Summary of bending strength data

Property	F5			F8		
	Juvenile	Mature	Total	Juvenile	Mature	Total
Number of boards						
EN	97	53	150	39	111	150
USA	102	48	150	38	111	149
AS/NZS	60	90	149	31	119	150
Mean value (MPa)						
EN	30.8	31.6	31.1	35.6	46.5	43.7
USA	37.2	36.7	37.1	48.3	51.9	51.0
AS/NZS	35.4	40.5	38.5	54.8	52.8	53.2
5-percentile value (MPa)						
EN	13.5	13.6	13.6	16.3	20.6	20.1
USA	15.4	11.9	14.7	24.3	23.4	23.8
AS/NZS	17.8	16.1	17.0	29.1	25.1	26.3
Coefficient of variation						
EN	0.43	0.43	0.43	0.37	0.41	0.42
USA	0.50	0.40	0.47	0.38	0.37	0.37
AS/NZS	0.36	0.47	0.44	0.32	0.38	0.37
Correlation coefficient						
AS/NZS	0.36	0.15	0.21	0.14	0.34	0.30
Mean spacing of knots (m)						
	1.0	1.3		1.1	1.9	

Table 2.
Summary of modulus of elasticity data

Property	F5			F8		
	Juvenile	Mature	Total	Juvenile	Mature	Total
Number of boards						
EN	97	53	150	39	111	150
USA	102	48	150	38	111	149
AS/NZS	60	90	149	31	119	150
Mean value (GPa)						
EN	7.84	7.58	7.75	10.04	10.74	10.55
USA	9.95	9.60	9.84	11.96	12.33	12.24
AS/NZS	8.97	9.83	9.49	12.26	11.98	12.04
5-percentile value (MPa)						
EN	4.50	4.19	4.35	6.56	5.57	5.85
USA	6.88	4.02	6.67	9.71	9.44	9.44
AS/NZS	5.95	6.22	6.11	9.83	8.94	8.97
Coefficient of variation						
EN	0.31	0.28	0.30	0.27	0.30	0.30
USA	0.26	0.23	0.25	0.15	0.15	0.15
AS/NZS	0.23	0.26	0.26	0.15	0.16	0.16
Correlation coefficient AS/NZS	0.48	0.57	0.51	0.54	0.63	0.60
Mean spacing of knots (m)	1.0	1.3		1.1	1.9	

4. DISCUSSION ON TEST DATA

4.1 Strength Properties

The strength properties shown in Figures 2 and 3 indicate that a significant difference of about 20% at the 5-percentile level can occur between in-grade test procedures. As expected the USA data is somewhere between the EN and AS/NZS. Generally, the data

for the USA and AS/NZS are not far apart; however at the 5-percentile level the USA data is closer to the EN data than the AS/NZS data in the case of F5 grade material.

To obtain a further understanding on material characteristics, Figures 5–7 show comparisons between the properties of mature and clear wood for the EN and AS/NZS data. Figure 5 shows that the difference between EN and AS/NZS data is greatest for the F8 juvenile wood, i.e. it is easiest to pick out the worst defect for this type of timber. Figure 6 shows the interesting feature that the juvenile wood in the EN data is the same for both the F5 and F8 grades, while it is well differentiated in the AS/NZS data. This would be consistent with having the same defects in both grades, but with a better quality of clear wood in the F8 grade. Figure 7 shows that for the F8 mechanically stress-graded timber, the EN method would give a different result in mean value depending on the ratio of juvenile to mature wood of the timber mix.

4.2 Modulus of Elasticity

The data in Figure 4 and Table 2 shows that there can be differences of 20% in the in-grade stiffness values, both at the mean and 5-percentile level, depending on the type of in-grade measurement.

As expected, the data of the USA and AS/NZS procedures are fairly close. Unexpectedly however, the USA data shows slightly higher stiffnesses than does the AS/NZS data; this matter is currently under further investigation.

4.3 Defect Spacing

Figure 8 shows a plot of the number of defects within a board length of 4800 mm of mature timber. For comparison, the expected values for a Poisson distribution are also shown in the figure; the data indicates that the true defect spacings are similar but slightly more regular than would be expected of a Poisson distribution.

5. BASIC STATISTICAL MODELS FOR STRENGTH

5.1 General

The statistical models used will focus on the influence of visible strength reducing defects, Figure 9. If these defects are not visible, or if they do not control strength, then all procedures will give essentially the same result.

For practical purposes, statistical models must be simple to apply. They are first fitted to the available test data for one test procedure and then used to predict the expected results for other types of test procedures.

In the following it will be assumed that the lower tail of the strength distribution has been fitted to a Weibull distribution, and it is this tail that is the concern of equivalencing procedures.

5.2 Weibull Distribution of Strength

Strength of both clear wood and defects will be assumed to follow Weibull distributions; hence $G(x)$, the probability of strength exceeding a value x is given by

$$G(x) = \exp[-\phi(x/X_{\text{mean}})^m] \quad (1)$$

where X_{mean} is the mean value, and the constants ϕ and m are related to the coefficient of variation V approximately by

$$\phi = 0.555 + 0.445 V \quad (2a)$$

$$m = V^{-1.09} \quad (2b)$$

5.3 Poisson Distribution of Defects

It will be assumed that defects are dispersed according to a Poisson distribution. Hence, $P(n)$, the probability of finding exactly n defects within a reference length is given by

$$P(n) = \beta^n \exp(-\beta) / \Gamma(n + 1) \quad (3)$$

where β denotes the mean number of defects within the reference length and Γ denotes a gamma distribution.

5.4 Correlation Coefficient of Strength

If the strength of defects within a board are correlated, then the total coefficient of variation V_{total} is roughly given by

$$V_{\text{total}}^2 = V_w^2 + V_B^2 \quad (4)$$

where V_w and V_B denote the variability within and between boards respectively. The within board variability is roughly given by (Leicester 1985)

$$V_w^2 = (1 - r) V_{\text{total}}^2 \quad (5)$$

where r denotes the correlation coefficient between pairs of defects within the same board.

5.5 Effective Span of the Test Specimen

It is convenient to replace L_{span} the span for third point loading by L_{eff} , an equivalent span which would have the same strength if loaded by a uniform moment. Assuming that the within board variability is about the same as the defects, this leads to (Leicester and Breitingner 1991)

$$L_{\text{eff}} = L_{\text{span}} (1 + m_w/3)/(1 + m_w) \quad (6)$$

where
$$m_w = 0.555 + 0.445 V_w \quad (7)$$

The notation for these spans are illustrated in Figure 9.

5.6 Strength of the Weakest Defect

Where strength depends on the weakest defect in a set of n defects within a given board, then $G_d(x,n)$, the probability of the strength exceeding a value x is given by (Leicester and Breitingner 1991)

$$G_d(x,n) = \exp[-\phi(\alpha x/X_{\text{mean}})^{m_t}] \quad (8)$$

where
$$m_t = 0.555 + 0.445 V_{\text{total}} \quad (9)$$

and
$$\alpha = n^{1/m_w} \quad (10)$$

5.7 Modelling of Test Procedures

EN 1 Model

As an extreme case, assume that the test operator can detect the presence of strength reducing defects, but cannot estimate their relative strengths. It is assumed that at least one defect will be in the test specimen. For this case $G_{\text{EN1}}(x)$, the complementary distribution function of the specimens tested according to EN 384 and EN 408 is given by

$$G_{EN1}(x) = \left[\sum_{n=1}^{\infty} P_{\text{eff}}(n) G_d(x,n) \right] / [1 - P_{\text{eff}}(0)] \quad (11)$$

where $P_{\text{eff}}(n)$ denotes the probability of getting exactly n defects in L_{eff} and $G_d(x,n)$ refers to the strength of the weakest of n defects.

EN2 Model

As another extreme case, assume that the test operator has a perfect ability to estimate the relative strengths of defects. For this case $G_{EN2}(x)$, the complementary distribution function of the test specimens is that of the weakest defect within the board and this is given by

$$G_{EN2}(x) = P_{\text{board}}(0) G_{\text{clear}}(x) + \sum_{n=1}^{\infty} P_{\text{board}}(n) G_d(x,n) \quad (12)$$

where $P_{\text{board}}(n)$ denotes the probability of finding exactly n defects within the total board length and $G_{\text{clear}}(x)$ refers to the strength of clear wood.

AS/NZS Model

The complementary distribution function $G_{AS/NZS}(x)$ for the strength of specimens tested according to the Australasian Standard AS/NZS is given by

$$G_{AS/NZS}(x) = P_{\text{eff}}(0) G_{\text{clear}}(x) + \sum_{n=1}^{\infty} P_{\text{eff}}(n) G_d(x,n) \quad (13)$$

5.8 Example

As an example, consider 90 x 35 mm boards of length 4800 mm. This gives $L_{\text{board}} = 4800$ mm and $L_{\text{span}} = 1620$ mm. Assume that on average, there are 4.0 defects per board. Assume that the defects have an average strength of 40 MPa, a coefficient of variation $V_{\text{total}} = 0.3$ and a correlation coefficient $r = 0.5$. Assume that the clear wood has a mean value of 70 MPa and a coefficient of variation $V_{\text{clear}} = 0.25$. For this case, the cumulative distribution functions computed according to equations (11)–(13) are shown in Figure 10.

The large variability of the AS/NZS model is due to the influence of clear wood for test specimens that have no major defects. Further refinements would be required to improve the prediction and comparisons at the higher percentile. However, at the important low percentiles, the model appears to be adequate for practical application.

6. DISCUSSION

An inherent difficulty in modelling the EN procedure is that it requires modelling not only of timber properties but also modelling of the ability of the testing operator to select the weakest defect. However, if the testing operator cannot recognise defects then both the EN and AS/NZS results became identical and the difficulty vanishes.

This is the case for many species. For example, in a recent study of 800 tested pieces of Victorian Ash (Leicester and Seath 1994), it was not possible to develop a visual procedure for ranking the pieces on the basis of strength. Furthermore, application of the existing visual grading rules to 190 x 45 mm sizes according to the Standard AS 2062 (Standards Australia, 1979) were found to incorrectly rank the stress-grades.

An advantage of the AS/NZS procedure is that it simulates a typical in-service loading configuration and as such provides data that can be used directly for design codes without the application of modification factors to take account of the test procedure. It is of interest to note that the early in-grade studies in North America used the AS/NZS procedure (Doyle and Markwardt 1966, Madsen 1992). It is probable that the current North American test procedures developed as a compromise between the conflicting requirements of in-grade testing and testing for quality control purposes.

The philosophy of the AS/NZS test procedure makes it very simple to develop test methods for any structural component. For example, the in-service design strength of finger jointed timber elements depends not only on the strength of individual joints, but also on the frequency and the correlation of these strengths and the length of the structural member. The use of a simulated in-service test configuration eliminates the necessity of compensating for these complex matters in the interpretation of the test data as would be the case if the finger joints are tested one at a time.

7. CONCLUSIONS

Within this limited study of bending strengths and stiffness it has been established that there are small but significant differences between the in-grade properties of structural timber established according to European, North American and Australasian standards. A

simple statistical model has been proposed, which is adequate for establishing equivalences for the limited data obtained to date. In practice, the procedure would be to fit a model to the data derived from one test method, and then to use it to predict information from other methods.

The additional data required for the model is a simple counting of defect frequency; however, as the project is expanded to include additional sizes or other types of tests (such as tension tests), it may be necessary to extend the number of input parameters used for the model.

This paper does not describe a model for establishing the equivalences between standards with respect to data on the modulus of elasticity. This will be done at a later date. However, it should be noted that because of the relatively low variability of this property, mean values of the modulus of elasticity can be established on the basis of very limited testing; thus it is quite feasible to obtain the equivalence between test procedures by direct measurement for any given stress-grade of timber.

8. REFERENCES

Doyle, D.V. and Markwardt, L.J. 1966. Properties of Southern Pine in relation to strength grading of dimension lumber. Research Paper FPL-64, US Forest Service, Forest Products Laboratory, Madison, USA, July, 62 p.

European Committee for Standardisation. 1995. EN 384: Structural timber – Determination of characteristic values of mechanical properties and density. Brussels, Belgium, February, 13 p.

European Committee for Standardisation. 1995. EN 408: Timber structures — Structural timber and glued laminated timber — Determination of some physical and mechanical properties. Brussels, Belgium, 27 p.

Green, D.W. and Evans, J.W. 1987. Mechanical properties of visually graded lumber, 1, A summary. USDA Forest Products Laboratory, Madison, USA, 59 p.

Isaksson, T. and Thelandersson, S. 1995. Effect of test standard, length and load configuration on bending strength of structural timber. In Proceedings of 28th Meeting of CIB Working Commission W18, Copenhagen, Denmark, April, 17 p.

Kallsner, B. and Ditlevsen, O. 1994. Lengthwise bending strength variations of structural timber. Proceedings of IUFRO/S5.02 Timber Engineering Meeting, July 5–7, Sydney, Australia.

Leicester, R.H. 1985. Configuration factor for the bending strength of timber. In Proceedings of Forest Products Research International – Achievements and the Future, Pretoria, South Africa, Paper No. 3–8, 4, April, 13 p.

Leicester, R.H. and Breitingger, H.O. 1991. A discrete co-relationship with Weibull. In Proceedings of 1991 International Timber Engineering Conference, London, UK, September, 2, pp.151–157.

Leicester, R.H. and Seath, C.A. 1994. Regrowth Victorian Hardwood — 2, New grading systems. DBCE Doc. 94/119(M), CSIRO Division of Building, Construction and Engineering, Melbourne, Australia, December, 102 p.

Leicester, R.H. and Young, F.G. 1991. Equivalence of characteristic values. In Proceedings of 24th Meeting of CIB W18A — Timber Structures, Oxford, UK, September, 9 p.

Madsen, B.M. 1992. Structural behaviour of timber. Timber Engineering Ltd, Vancouver, Canada, 440 p.

Standards Australia, 1979. AS 2082: Visually stress-graded hardwood for structural purposes. Sydney, Australia.

Standards Australia, 1986. AS 2858: Timber-softwood-visually stress-graded for structural purposes. Sydney, Australia, 34 p.

Standards Australia/Standards New Zealand, 1992. AS/NZS 4063: Timber-stress-graded-in-grade strength and stiffness evaluation. Sydney, Australia, 15 p.

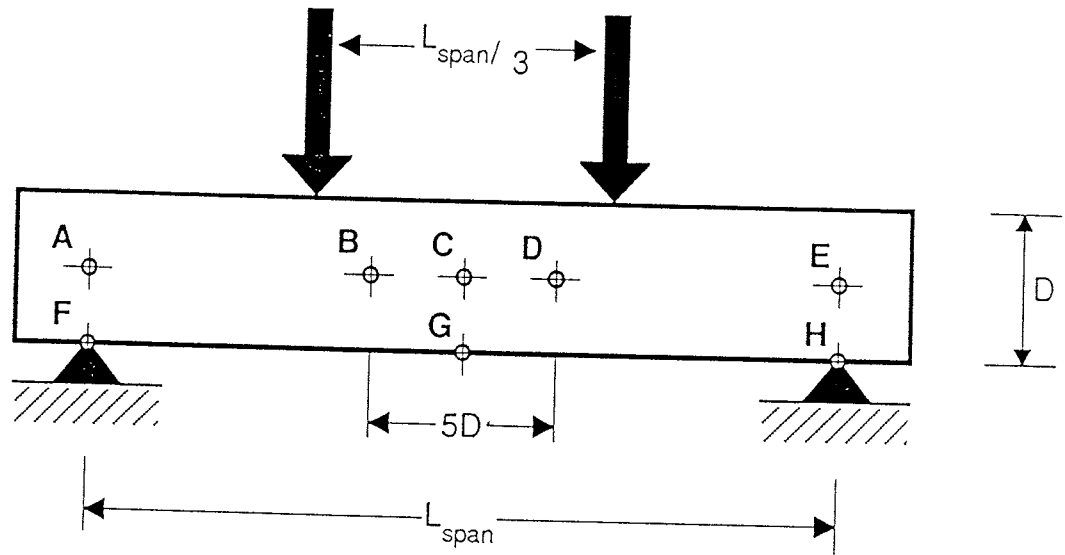


Figure 1. Schematic illustration of loading configurations.

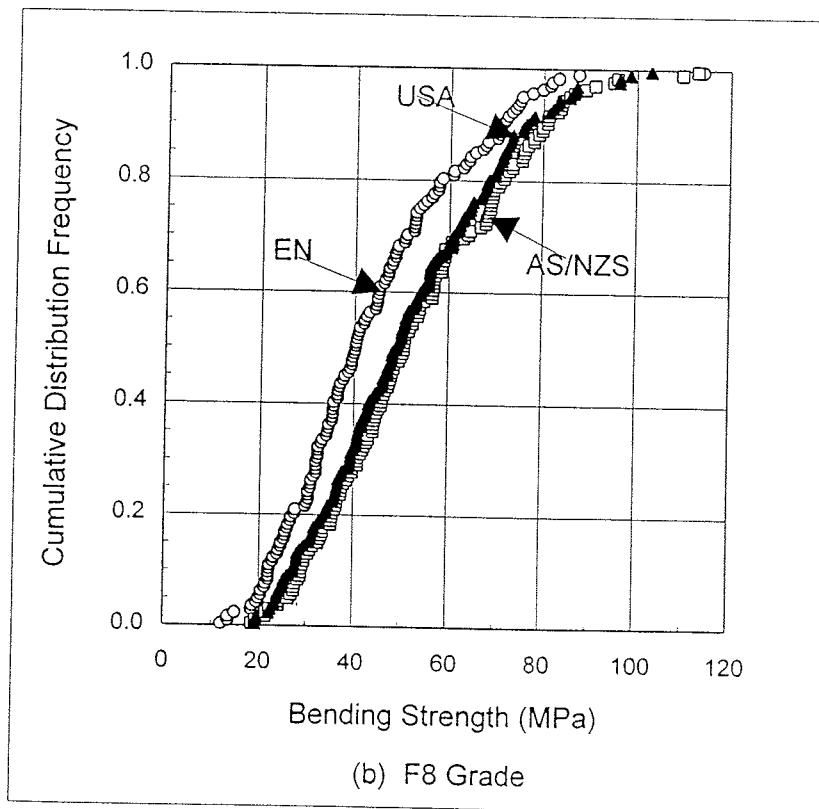
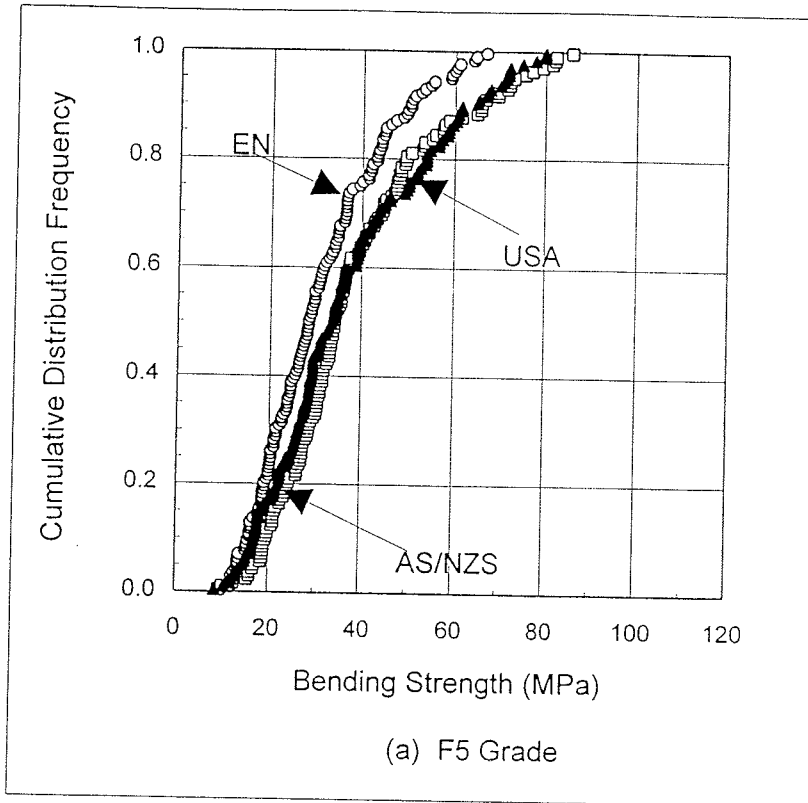


Figure 2. Measured bending strength (total distribution).

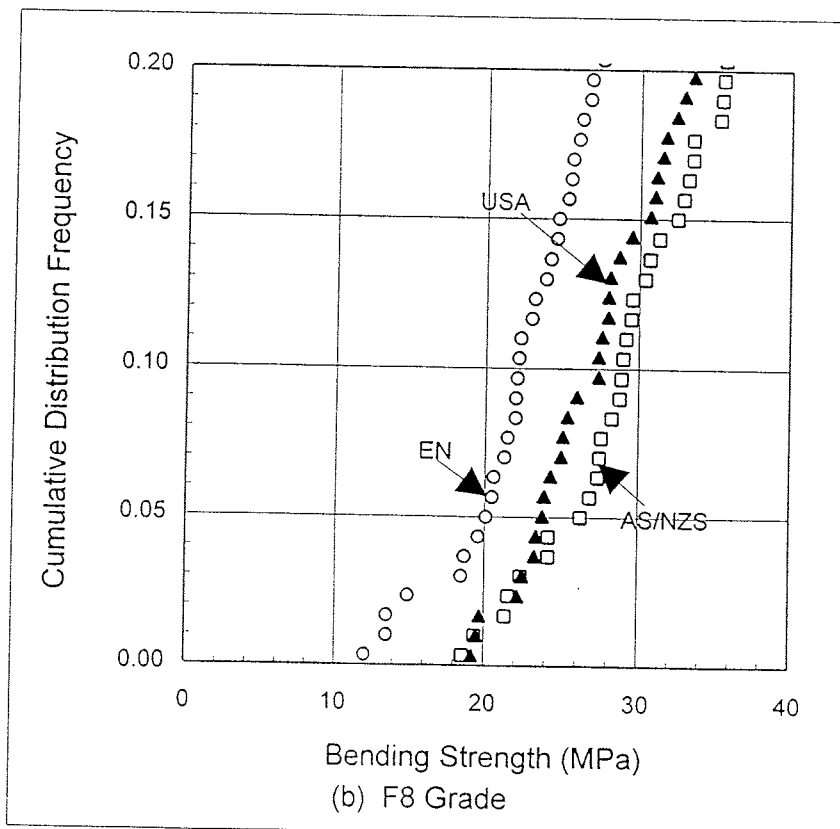
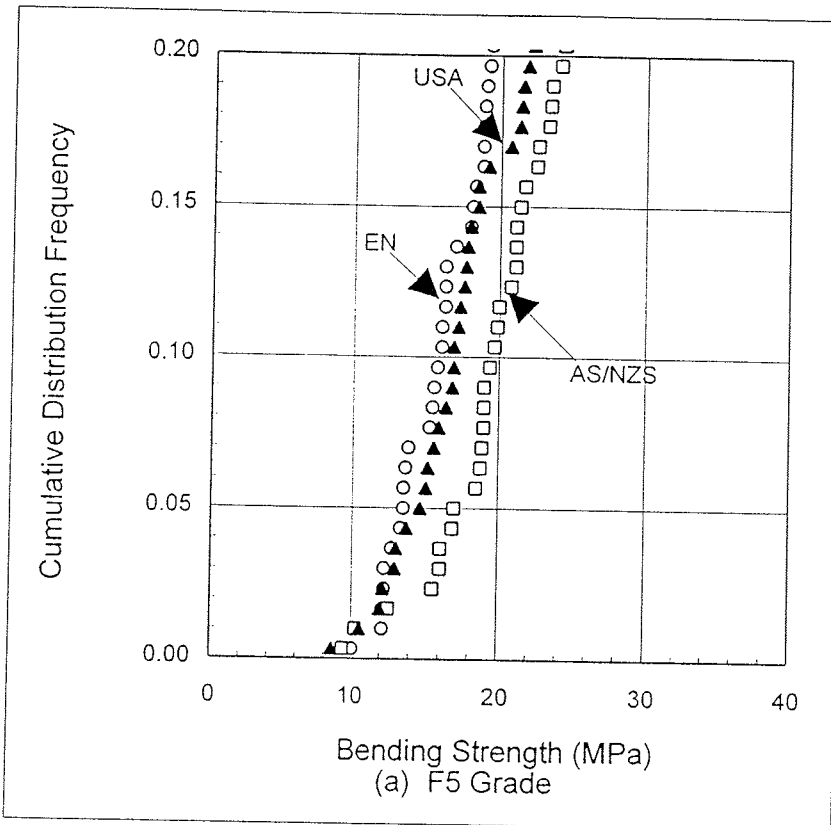


Figure 3. Measured bending strength (lower tail).

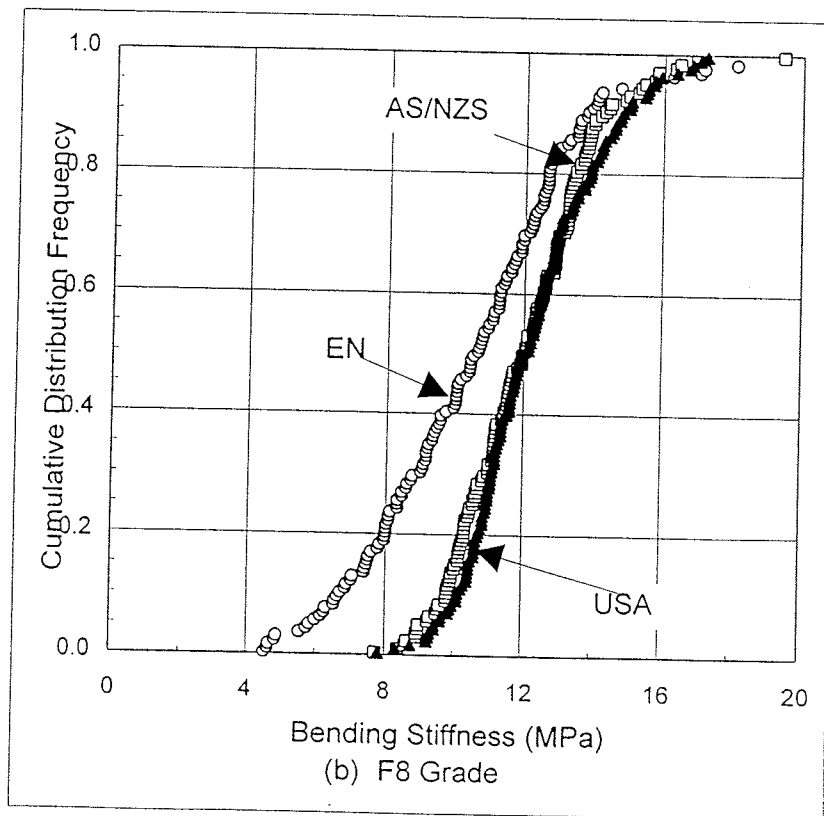
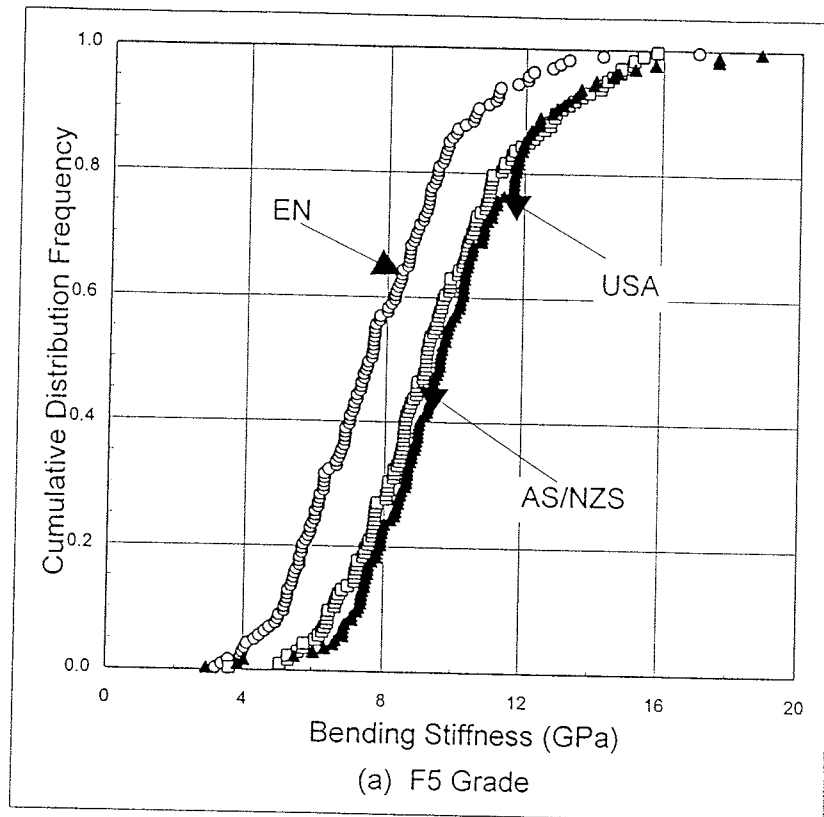


Figure 4. Measured modulus of elasticity (total distribution).

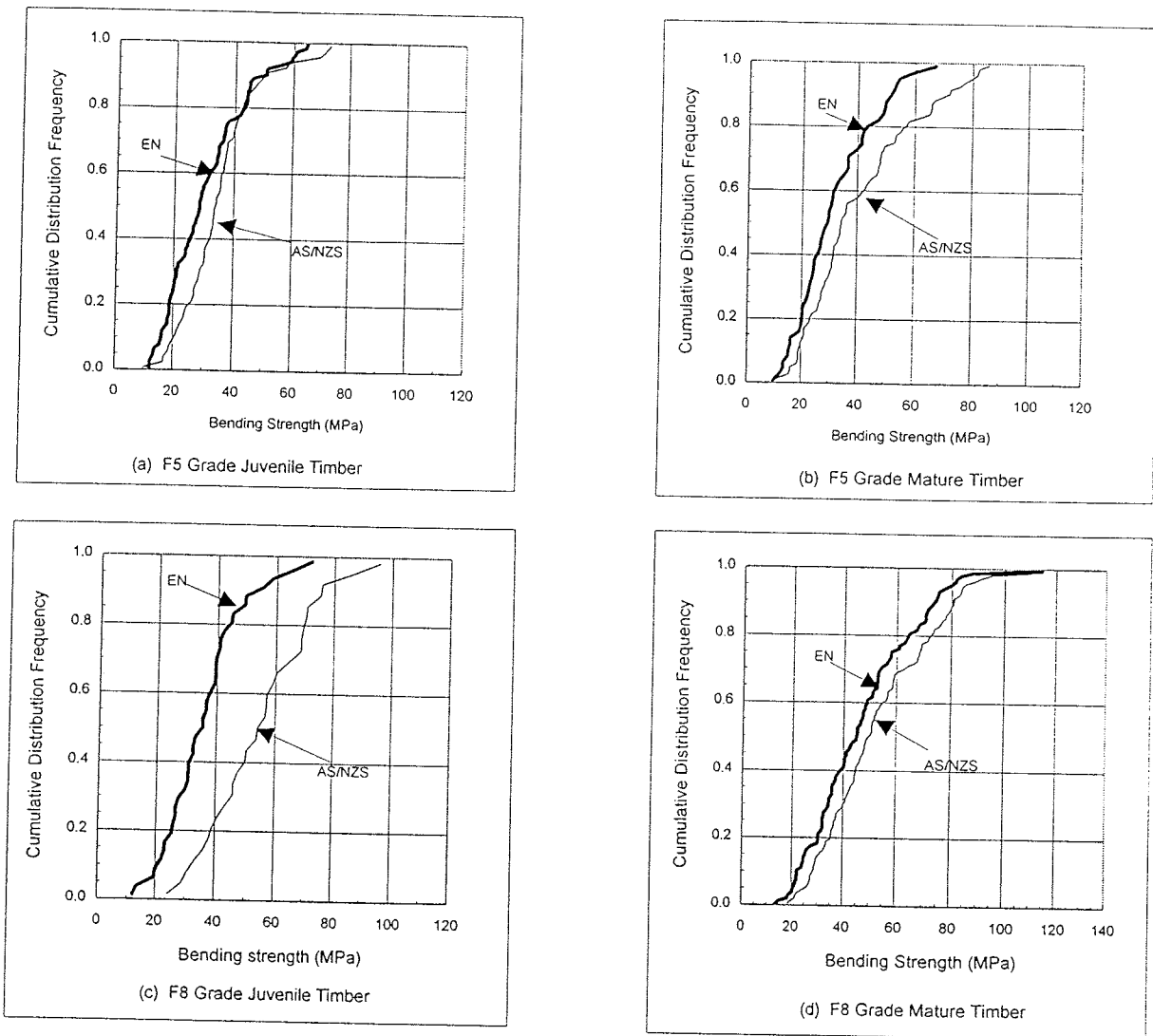


Figure 5. Detailed comparison between EN and AS/NZS procedures.

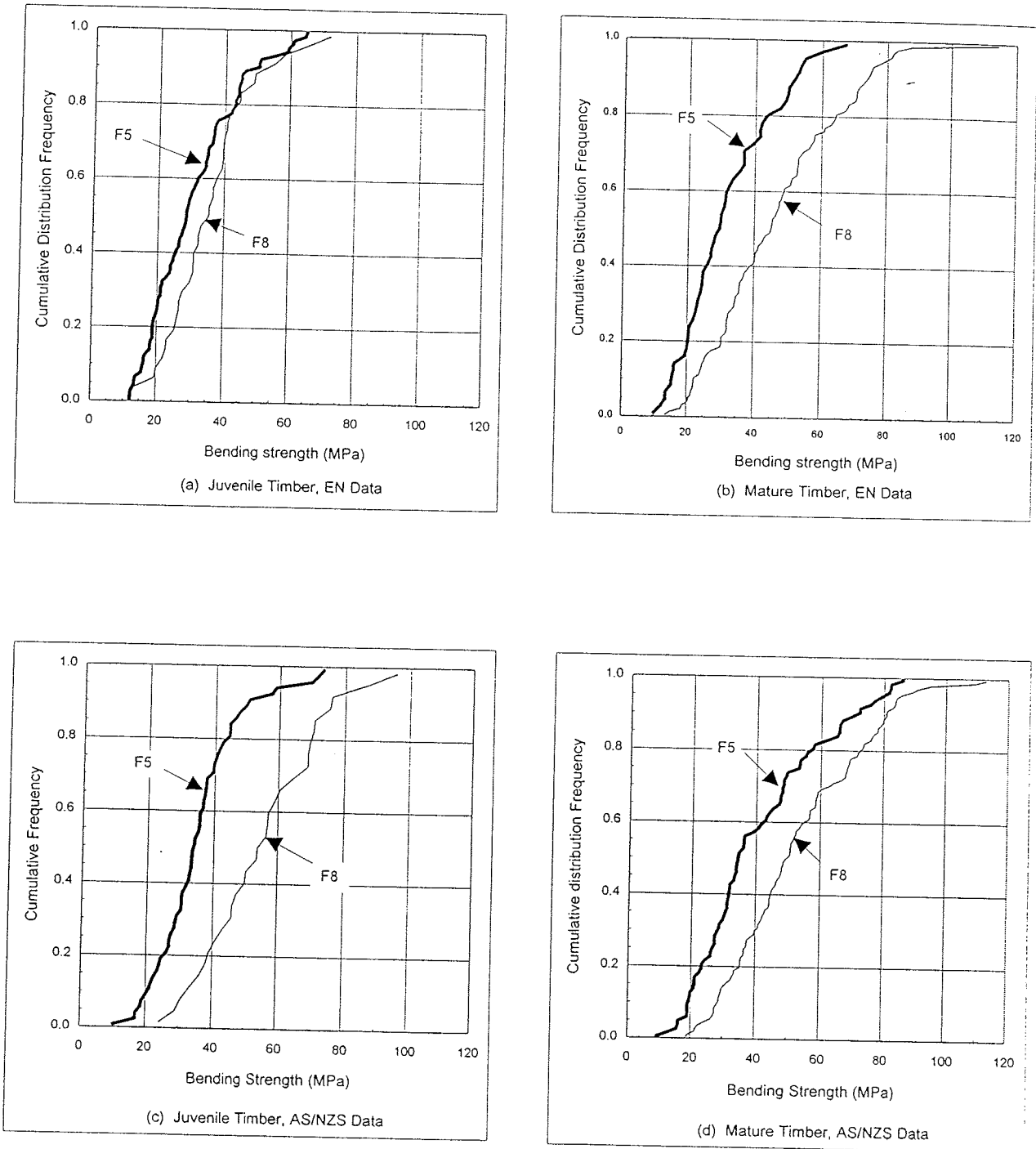


Figure 6. Detailed comparison between F5 and F8 grade timber.

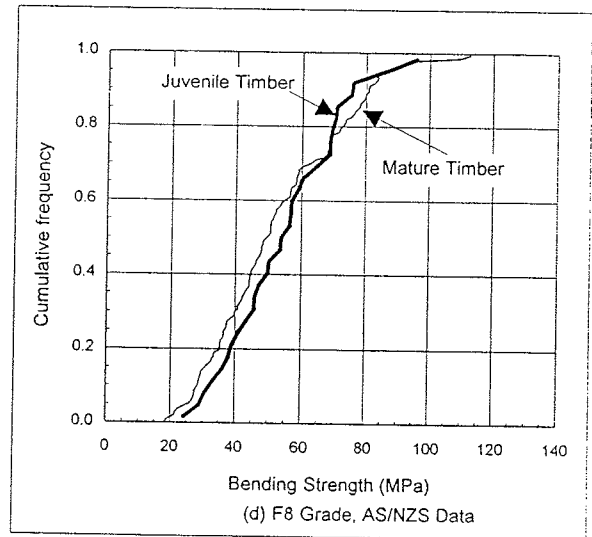
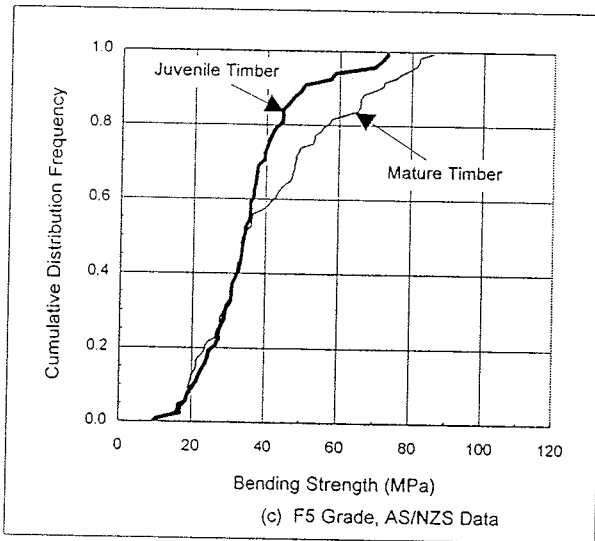
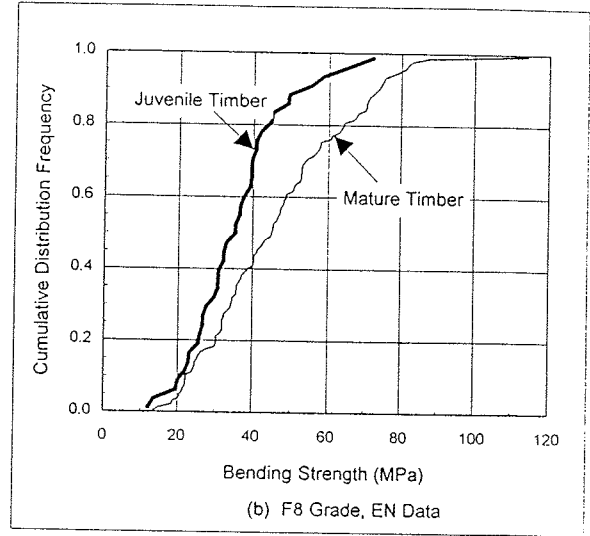
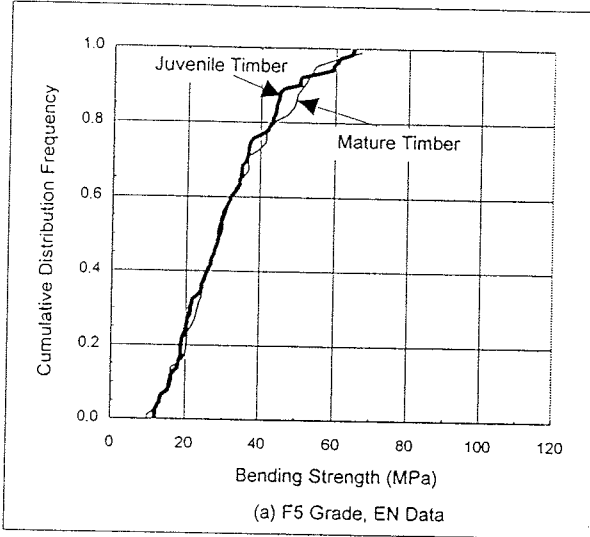


Figure 7. Detailed comparison between juvenile and mature timber.

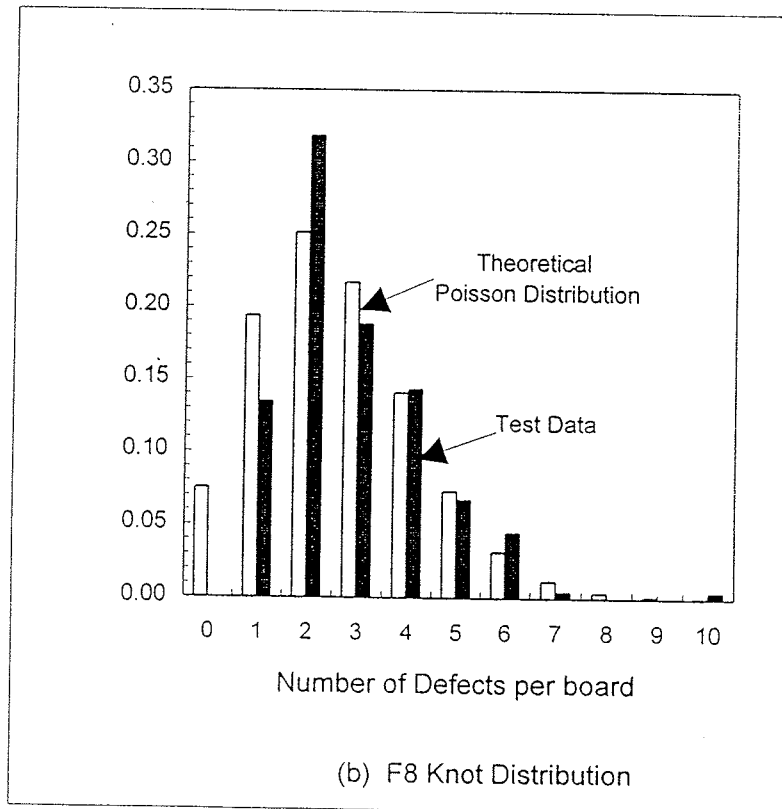
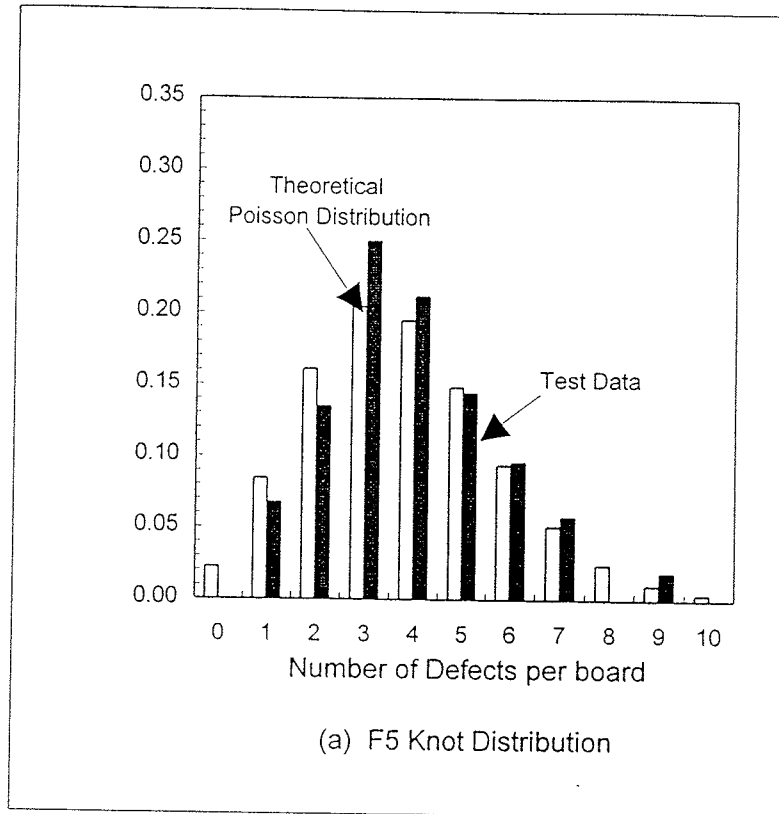


Figure 8. Distribution of number of defects in 4800 mm board of mature wood.

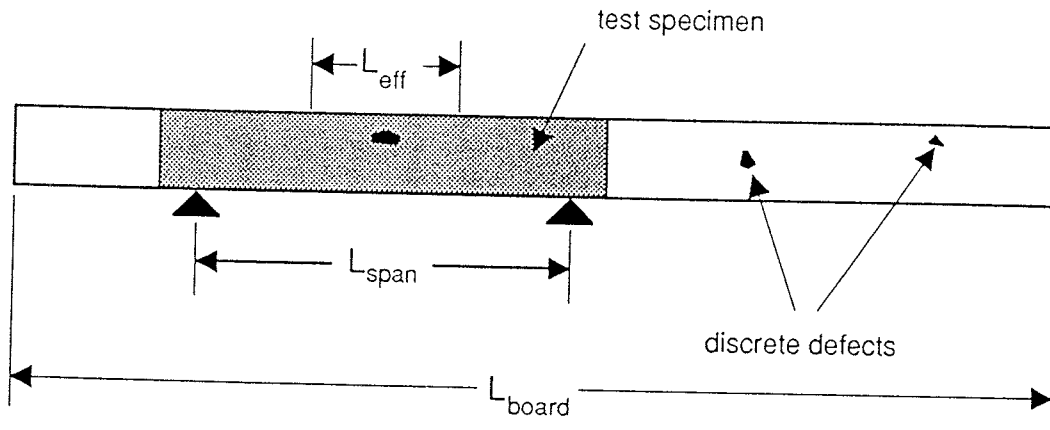


Figure 9. Illustration of notation used for various spans.

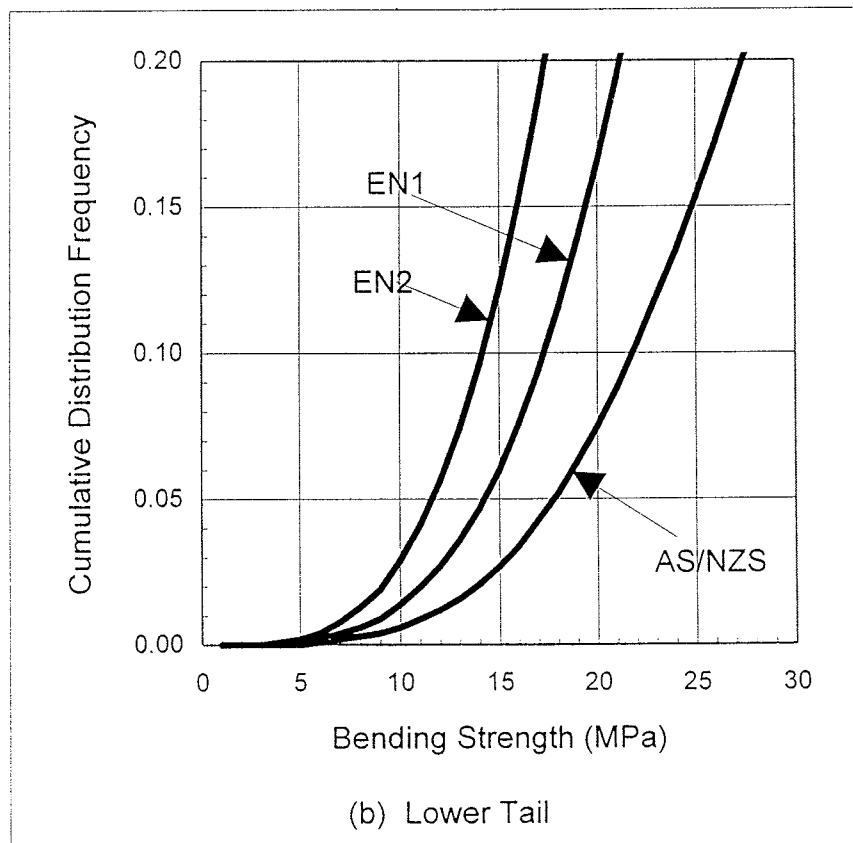
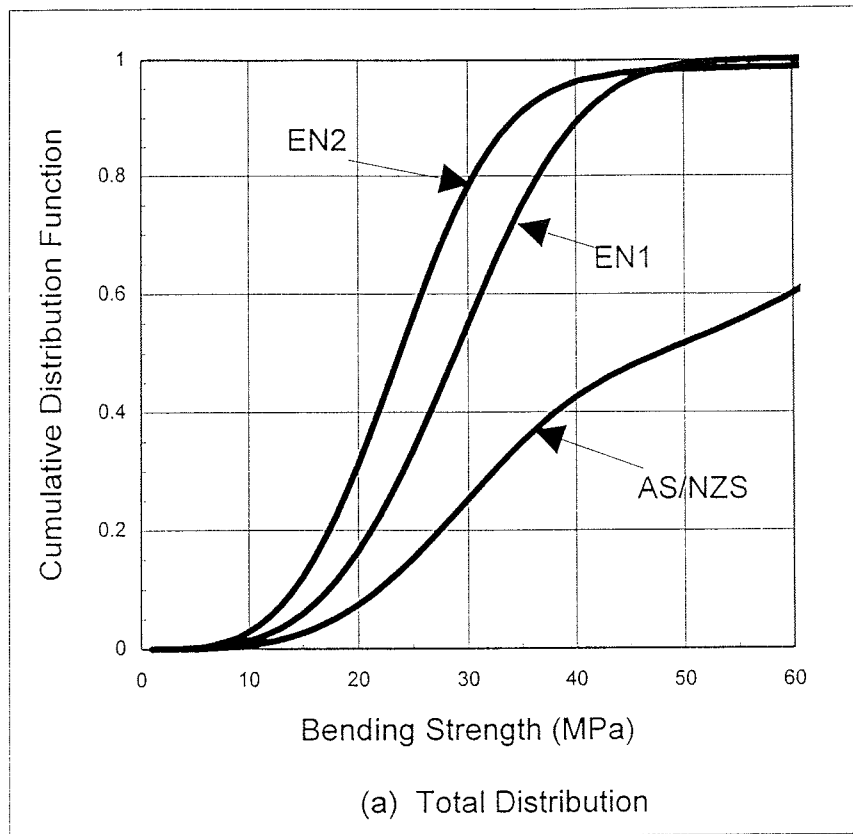


Figure 10. Results of computation for a theoretical sample of timber.

**INTERNATIONAL COUNCIL FOR BUILDING RESEARCH STUDIES AND DOCUMENTATION
WORKING COMMISSION W18 - TIMBER STRUCTURES**

**A SIMPLE METHOD FOR LATERAL LOAD-CARRYING CAPACITY OF DOWEL-
TYPE FASTENERS**

by

J Kangas
J Kurkela
VTT Building Technology
Finland

MEETING TWENTY - NINE

BORDEAUX

FRANCE

AUGUST 1996

A SIMPLE METHOD FOR LATERAL LOAD-CARRYING CAPACITY OF DOWEL-TYPE FASTENERS

Jorma Kangas and Juha Kurkela
VTT Building Technology, Finland

Abstract

The design load-carrying capacity per shear plane per dowel-type fastener, for timber-to-timber and panel-to-timber joints in Eurocode 5 should be taken as the smallest value found from the group of six formulae in single shear and four formulae in double shear.

In this paper a method is presented, on how the group of the complicated formulae can be replaced by two simple formulae, with two new coefficients obtained by two nomographs: one is determined by the relations of two thickness and embedding strength values, the other by the thickness and the embedding strength values of the timber member to be fastened, the thickness and yield moment of the fastener and by the relations of two embedding strength values. The calculated capacities deviate from the theoretical values only by the reading accuracy of the nomographs.

1. Introduction

For the design of the load-carrying capacity of joints made with dowel-type fasteners Eurocode 5 gives groups of comprehensive formulae. They are based upon a theory developed by Johansen and are rather complicated to be used without prewritten programs, for example in the case of different panels in various load-duration and service classes. This makes the design of the timber joints some times laborious and may give room for other materials to replace timber.

The threshold to design timber structures is rather high because of many different and varying material properties and numerous types of fasteners. People are used to simple design formulae or to take the design values from tables. The Finnish government office, as in case of many other countries, favor to increase the usage of timber in building. Last winter, the government funded finance to find out the possibilities to simplify the design of the joints with mechanical fasteners. That initiated our interest in this problem and the results are presented in this paper

2 Eurocode 5 method

The design load-carrying capacity per shear plane per dowel-type fastener, for timber-to-timber and panel-to-timber joints in Eurocode 5 should be taken as the smallest value found from the following formulae where each formula corresponds to its own failure mode:

Design load-carrying capacities for fasteners in single shear:

$$R_d = \min \left\{ \begin{array}{l} f_{h,1,d} t_1 d \quad (6.2.1a) \\ f_{h,1,d} t_2 d \beta \quad (6.2.1b) \\ \frac{f_{h,1,d} t_1 d}{1 + \beta} \left[\sqrt{\beta + 2\beta^2 \left[1 + \frac{t_2}{t_1} + \left(\frac{t_2}{t_1} \right)^2 \right]} + \beta^3 \left(\frac{t_2}{t_1} \right)^2 - \beta \left(1 + \frac{t_2}{t_1} \right) \right] \quad (6.2.1c) \\ 1,1 \frac{f_{h,1,d} t_1 d}{2 + \beta} \left[\sqrt{2\beta(1 + \beta) + \frac{4\beta(2 + \beta)M_{y,d}}{f_{h,1,d} d t_1^2}} - \beta \right] \quad (6.2.1d) \\ 1,1 \frac{f_{h,1,d} t_2 d}{1 + 2\beta} \left[\sqrt{2\beta^2(1 + \beta) + \frac{4\beta(1 + 2\beta)M_{y,d}}{f_{h,1,d} d t_2^2}} - \beta \right] \quad (6.2.1e) \\ 1,1 \sqrt{\frac{2\beta}{1 + \beta}} \sqrt{2M_{y,d} f_{h,1,d} d} \quad (6.2.1f) \end{array} \right.$$

Design load-carrying capacities for fasteners in double shear:

$$R_d = \min \left\{ \begin{array}{l} f_{h,1,d} t_1 d \quad (6.2.1g) \\ 0,5 f_{h,1,d} t_2 d \beta \quad (6.2.1h) \\ 1,1 \frac{f_{h,1,d} t_1 d}{2 + \beta} \left[\sqrt{2\beta(1 + \beta) + \frac{4\beta(2 + \beta)M_{y,d}}{f_{h,1,d} d t_1^2}} - \beta \right] \quad (6.2.1j) \\ 1,1 \sqrt{\frac{2\beta}{1 + \beta}} \sqrt{2M_{y,d} f_{h,1,d} d} \quad (6.2.1k) \end{array} \right.$$

The various failure modes are illustrated in figure 1.

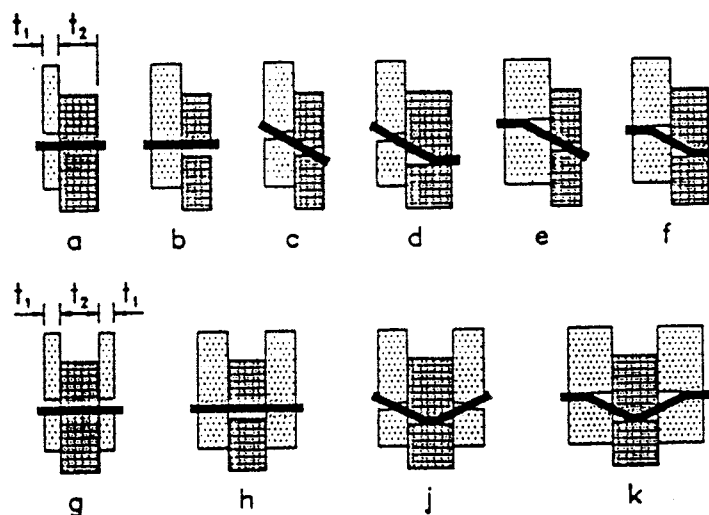


Figure 1 Failure modes for timber and panel joints. The letters correspond to the relevant formula reference.

For the calculation of the formulae the following symbols are to be chosen or they should to be calculated:

d	fastener diameter
k_{mod}	modification factor for service class and duration of load
t_1 and t_2	timber or board thickness or fastener penetration;
$f_{h,1,d}$ and $f_{h,2,d}$	design embedding strengths in t_1 and t_2
$M_{y,d}$	fastener yield design moment
β	$f_{h,2,d} / f_{h,1,d}$
γ_M	partial coefficient for material properties

3 Simplified formulae with nomographs

3.1 Nomograph 1 for both single and double shear joints

Nomograph 1 (figure 2) is made by the formulae, which are common to both single and double shear joints. A new coefficient k_1 is used and it contains symbols mentioned above. It is the relation of the properties of the timber member to be fastened and the properties of the fastener:

$$k_1 = \frac{t_1 \sqrt{f_{h,1,d}}}{\sqrt{M_{y,d} / d}} \quad (1)$$

Formulae (6.2.1a) and (6.2.1d) are then rewritten by coefficient k_1 as formulae (6.2.1a') and (6.2.1d'):

$$R_d = k_1 \sqrt{M_{y,d} f_{h,1,d} d} \quad (6.2.1a')$$

$$R_d = \frac{1,1 k_1}{(2 + \beta)} \left[\sqrt{2\beta(1 + \beta) + \frac{4\beta(2 + \beta)}{k_1^2}} - \beta \right] \sqrt{M_{y,d} f_{h,1,d} d} \quad (6.2.1d')$$

Formulae (6.2.1a'), (6.2.1d') and (6.2.1f) are then written as one uniform formula:

$$R_d = k_2 \sqrt{M_{y,d} f_{h,1,d} d} \quad (2)$$

Coefficient k_2 gives the lowest value of formulae (6.2.1a'), (6.2.1d') and (6.2.1f) and it is drawn in figure 2 as nomograph 1, where on the x-axis is coefficient k_1 and the other parameter to be determined beforehand is the relation β of the embedding strength values.

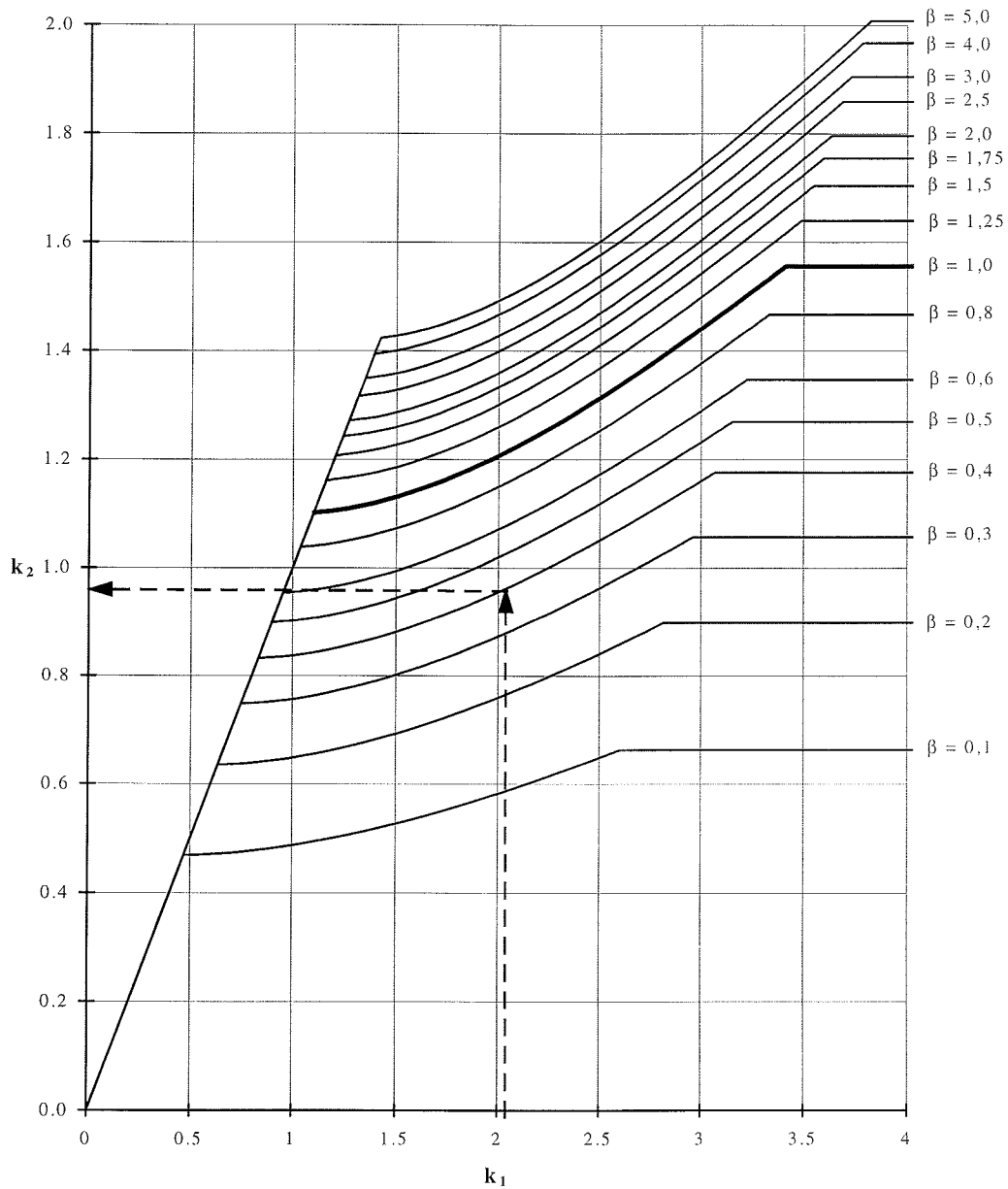


Figure 2 Nomograph 1 of the coefficient k_2 for both single and double shear joints. It covers the failure modes a, d and f (g, j and k) of figure 1. Determination of the value of coefficient k_2 in the given example is shown.

3.2 Nomograph 2 for single shear joints

Nomograph 2 (figure 3) is made by the formulae (6.2.1a), (6.2.1b) and (6.2.1c) of single shear joints. They are written as one uniform formula:

$$R_d = k_3 f_{h,1,d} t_1 d \quad (3)$$

Coefficient k_3 will give the smallest value from the formulae (6.2.1a), (6.2.1b) and (6.2.1c) and is drawn in figure 3 as nomograph 2. In the nomograph there is the dash border line. Formula (6.2.1e) does not need to be taken into account on the range above it and underneath it formula (6.2.1e) should be checked separately (see chapter 3.3). There are marked two points a) and b) where the formulae (6.2.1a - f) are calculated and they are plotted in figure 5. In case of b) there are small area ($11,5 < t_1/d < 14,5$) where formula (6.2.1e) gives smallest values.

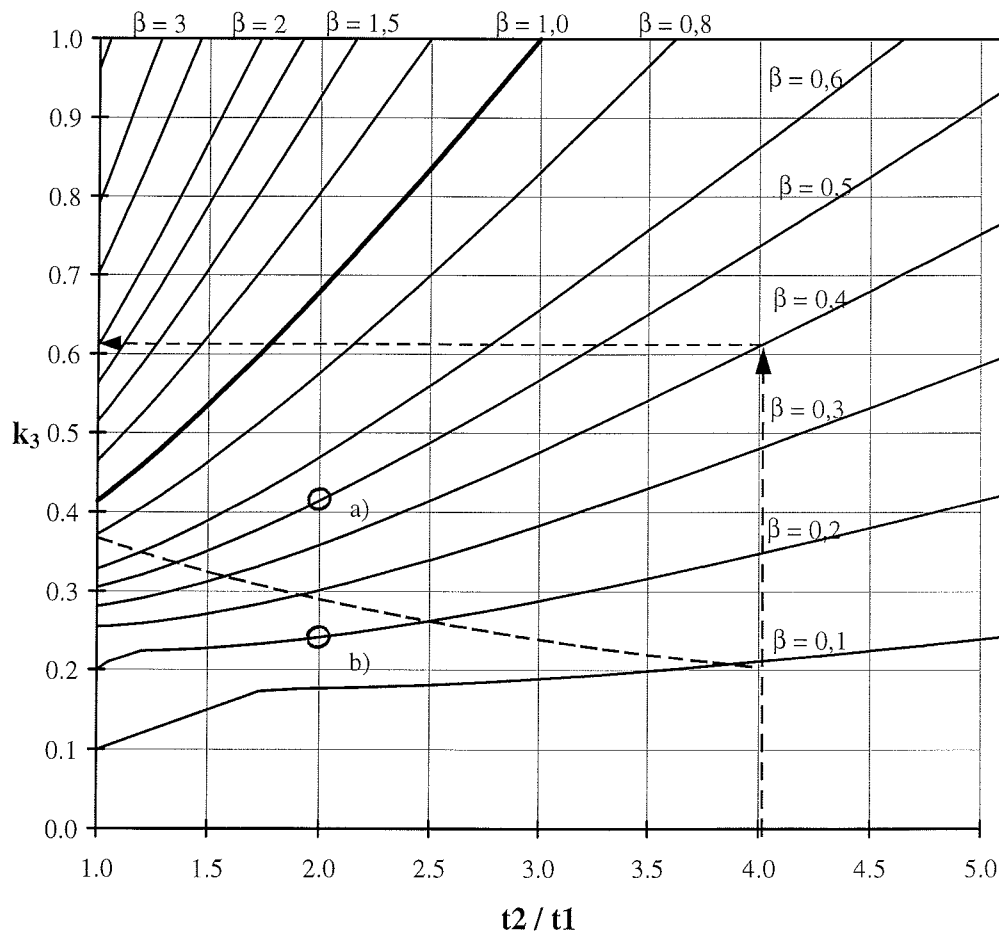


Figure 3 Nomograph 2 of coefficient k_3 for single shear joints. It covers the failure modes a, b and c of figure 1. Above the dashed border line only formulae (2) and (3) are to be checked and underneath it formula (6.2.1e) should be checked in addition to formulae (2) and (3). In marked two points a) and b) the formulae (6.2.1a - f) are calculated in an example joint and they are plotted in figure 4. Determination of the value of coefficient k_3 in the given example is shown.

3.3 Effect of formula (6.2.1e)

Formula (6.2.1e) can not be situated in the nomographs 1 and 2, because it has the parameters k_1 and t_2/t_1 . The nomographs can have only one of those parameters. However, it can be noticed, when formula (6.2.1e) shall be checked separately.

Let us contemplate nomograph 1 with also formulae (6.2.1c) and (6.2.1e) drawn in it. Their locations in it depend on the relation t_2/t_1 . If the graph of formula (6.2.1e) is above the graph of formula (6.2.1c) when it is also beneath formulae (6.2.1f), then formulae (6.2.1c) is always decisive and it is not necessary to check formula (6.2.1e). If the condition above is not fulfilled, formula (6.2.1e) is to be checked.

When the condition is fulfilled can be found out from the section points of the graph of formulae (6.2.1c) and (6.2.1e) with the graph of formula (6.2.1f). If the section of formula (6.2.1c) with formula (6.2.1f) is further from the origo than formula (6.2.1e) has, then the graph of formula (6.2.1e) is also above the graph of formula (6.2.1c). In that case it is not necessary to check formula (6.2.1e).

The section points of formulae (6.2.1c) and (6.2.1e) with formulae (6.2.1f) can be found by setting formulae (6.2.1c) and (6.2.1f) equal and then setting (6.2.1e) and (6.2.1f) equal. The section point of formulae (6.2.1c) and (6.2.1f) on the direction of x-axis is

$$k_1 = \frac{t_1 \sqrt{f_{h,1,d}}}{\sqrt{M_{y,d} / d}} = \frac{1,1\sqrt{4\beta(1+\beta)}}{\sqrt{\beta + 2\beta^2 \left[1 + \frac{t_2}{t_1} + \left(\frac{t_2}{t_1} \right)^2 \right] + \beta^3 \left(\frac{t_2}{t_1} \right)^2 - \beta \left(1 + \frac{t_2}{t_1} \right)}} \quad (a)$$

The section point of formulae (6.2.1e) and (6.2.1f) on the direction of x-axis is

$$k_1 = \frac{t_1 \sqrt{f_{h,1,d}}}{\sqrt{M_{y,d} / d}} = \sqrt{\frac{2\beta}{(1 + \frac{1}{2}\beta - \sqrt{\beta+1})(\beta+1)}} \frac{t_1}{t_2} \quad (b)$$

Setting the formulae (a) and (b) equal the following formula will be written:

$$\frac{1,1\sqrt{4\beta(1+\beta)}}{\sqrt{\beta + 2\beta^2 \left[1 + \frac{t_2}{t_1} + \left(\frac{t_2}{t_1} \right)^2 \right] + \beta^3 \left(\frac{t_2}{t_1} \right)^2 - \beta \left(1 + \frac{t_2}{t_1} \right)}} - \sqrt{\frac{2\beta}{(1 + \frac{1}{2}\beta - \sqrt{\beta+1})(\beta+1)}} \frac{t_1}{t_2} = 0 \quad (c)$$

The graph of the left side of the formula (c) is drawn in figure 4. As the solution of the formula (c) the value of β will be obtained as a function of the relation t_2/t_1 , by which the section points of formulae (6.2.1c) and (6.2.1e) with formulae (6.2.1f) are situated on the same place. By inserting the above solved pair of parameters (β , t_2/t_1) in formula (6.2.1c), the obtained graph (dashed curve) can be drawn in nomograph 2. If the value of coefficient k_3 obtained from nomograph 2 is above the dashed curve, it is not necessary to check formula (6.2.1e).

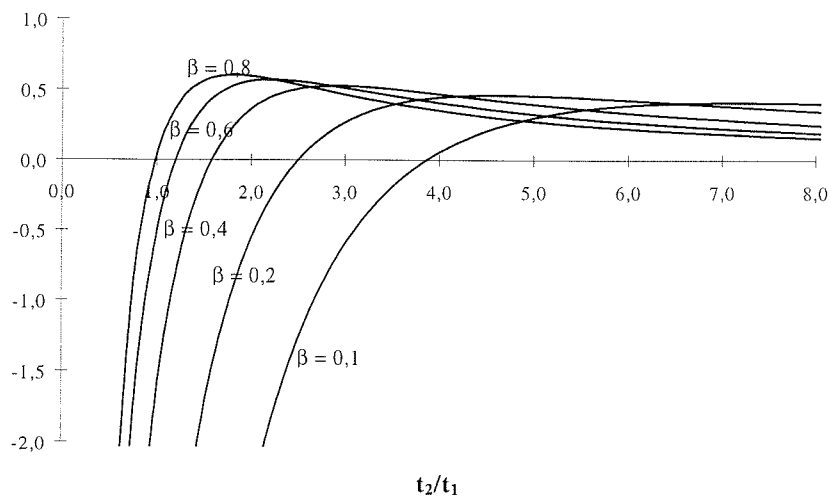
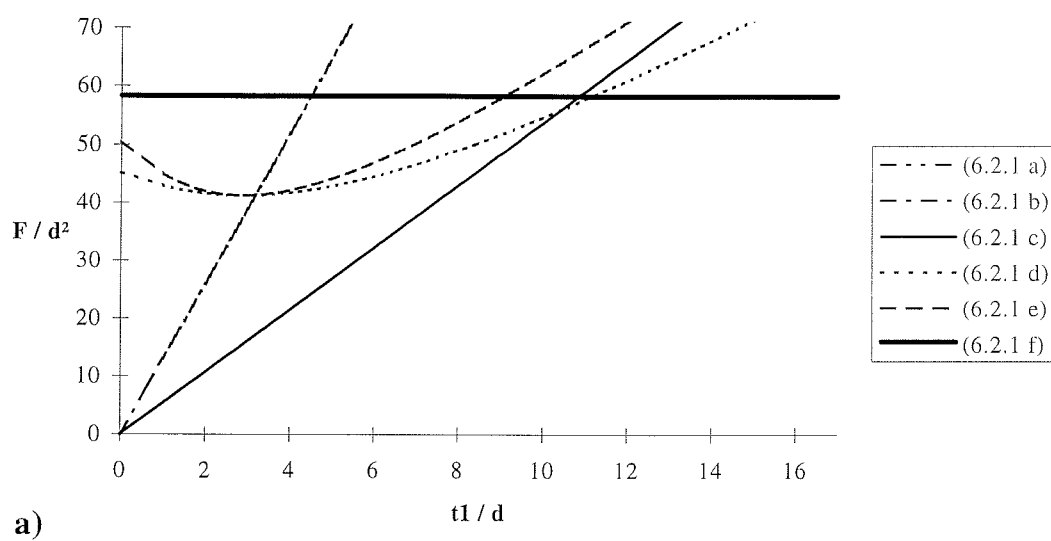
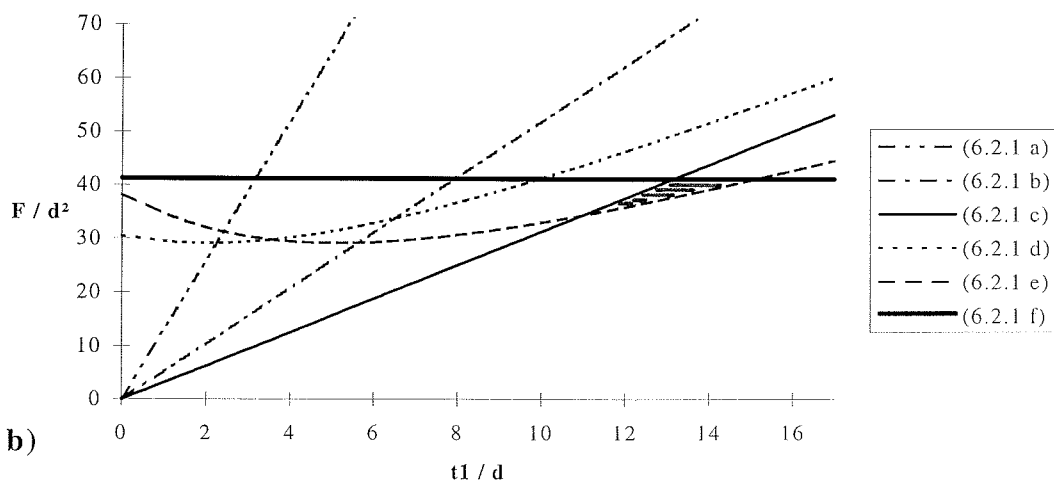


Figure 4 Left side of formulae (c) drawn as a function of the relation t_2/t_1 with different values of β .



a)



b)

Figure 5 Formulae (6.2.1a - f) are graphed in the case of nailed single shear joints with $d=2.8$ mm and $t_2/t_1=2$. The relation β is **a)** 0.5 and **b)** 0.2. The cases are marked in figure 3. They are in different places in relation to the border line in nomograph 2. In the case of **b)** (6.2.1e) gives the lowest values on the shaded area.

4 Design procedure

At first the dimensions of the joint and the material properties will be chosen or calculated as in Eurocode 5:

d	fastener diameter
k_{mod}	modification factor for service class and duration of load
t_1 and t_2	timber or board thickness or fastener penetration, $t_1 \leq t_2$ in single shear joints for the simplification of nomograph 2
$f_{h,1,d}$ and $f_{h,2,d}$	design embedding strengths in t_1 and t_2
$M_{y,d}$	fastener yield design moment
β	$f_{h,2,d} / f_{h,1,d}$
γ_M	partial coefficient for material properties

A new coefficient k_1 is calculated by using the above symbols:

$$k_1 = \frac{t_1 \sqrt{f_{h,1,d}}}{\sqrt{M_{y,d} / d}} \quad (1)$$

4.1 Single shear joints

The coefficients k_2 and k_3 are determined from the nomographs 1 and 2. The design load-carrying capacity per shear plane per dowel-type fastener, for timber-to-timber and panel-to-timber joints should be taken as the smallest value found from the following two formulae:

$$R_d = \min \begin{cases} k_2 \sqrt{M_{y,d} f_{h,1,d} d} & (2) \\ k_3 f_{h,1,d} t_1 d & (3) \end{cases}$$

If the value of parameter k_3 will be underneath the dash line in the nomograph 2, formula (6.2.1e) should be checked separately, which can easy be avoided e.g by changing the relation of timber thickness.

$$R_d \leq 1,1 \frac{f_{h,1,d} t_2 d}{1 + 2\beta} \left[\sqrt{2\beta^2(1 + \beta) + \frac{4\beta(1 + 2\beta)M_{y,d}}{f_{h,1,d} d t_2^2}} - \beta \right] \quad (6.2.1e)$$

4.2 Double shear joints

Coefficient k_2 is determined from the nomograph 1. The design load-carrying capacity per shear plane per dowel-type fastener, for timber-to-timber and panel-to-timber joints should be taken as the smallest value found from the following two formulae:

$$R_d = \min \begin{cases} k_2 \sqrt{M_{y,d} f_{h,1,d} d} & (2) \\ 0,5 f_{h,1,d} t_2 d \beta & (6.2.1.h) \end{cases}$$

4.3 Design example

Nailed plywood-to-timber single shear joint

Plywood thickness of 10 mm nailed to timber C24 thickness of 100 mm by nails $d \times l$
 $= 2,1 \times 50$ mm,

no preboring, $k_{\text{mod}} = 0,8$

$$\rho_k = 350 \text{ kg/m}^3$$

$$\rho_{k,\text{plywood}} = 650 \text{ kg/m}^3$$

Design:

$$f_{h,1,k} = 0,11 \rho_k d^{0,3} = 0,11 * 650 * 2,1^{-0,3} = 57,2 \text{ N/mm}^2 \text{ (plywood)}$$

$$f_{h,1,d} = k_{\text{mod}} f_{h,1,k} / \gamma_M = 0,8 * 57,23 / 1,3 = 35,2 \text{ N/mm}^2$$

$$f_{h,2,k} = 0,082 \rho_k d^{0,3} = 0,082 * 350 * 2,1^{-0,3} = 23,0 \text{ N/mm}^2 \text{ (timber)}$$

$$f_{h,2,d} = k_{\text{mod}} f_{h,2,k} / \gamma_M = 0,8 * 23,0 / 1,3 = 14,1 \text{ N/mm}^2$$

$$\beta = 14,1 / 35,2 = 0,40$$

$$M_{y,k} = 270 d^{2,6} = 270 * 2,1^{2,6} = 1860 \text{ Nmm}$$

$$M_{y,d} = M_{y,k} / \gamma_M = 1860 / 1,1 = 1690 \text{ Nmm}$$

$$t_1 = 10 \text{ mm}$$

$$t_2 = 50 - 10 = 40 \text{ mm (nail point penetration)}$$

$$k_1 = \frac{t_1 \sqrt{f_{h,1,d}}}{\sqrt{M_{y,d} / d}} = \frac{10 \sqrt{35,2}}{\sqrt{1690 / 2,1}} = 2,09$$

nomograph 1 gives $k_2 = 0,97$

$$t_2 / t_1 = 40 / 10 = 4$$

nomograph 2 gives $k_3 = 0,61$

$$R_d = \min \begin{cases} k_2 \sqrt{M_{y,d} f_{h,1,d}} = 0,97 * \sqrt{1690 * 35,2 * 2,1} = 343 \text{ N} \\ k_3 f_{h,1,d} t_1 d = 0,61 * 35,2 * 10 * 2,1 = 450 \text{ N} \end{cases}$$

$$R_d = \underline{343 \text{ N}}$$

Exact solution according to Eurocode 5 by formula (6.2.1d):

$$R_d = 343,3 \text{ N}$$

5 Concluding remarks

For the design of the load-carrying capacity of the joints made with dowel-type fasteners Eurocode 5 gives groups of comprehensive formulae, which are rather complicated to be used without prewritten programs e.g. in the case of different panels in various load-duration and service classes. The whole group of formulae shall be checked anew, when one parameter value will be changed. That may be in some cases too high threshold to design timber structures and may give room for other materials to replace timber.

The method presented in this paper predicts accurate design values for joints with dowel-type fasteners by two simple formulae and easy to use nomographs. Sometimes one complicated original formula will be necessary to be used for single-shear joints. However, that case can be seen directly from the nomograph 2, which also can help to avoid the use of that formula.

The new nomograph method presented in this paper, is easy to use and it is useful in optimization of the joint. It is easy to see directly the effect of the change of different parameter values on the capacity of the joint and how to reach e.g. the optimal yielding of the fastener.

It is the opinion of the authors that because of the easiness and clarity of the proposed design procedure, this method can be added as an increment for 6.2.1 (5) in Eurocode 5 or it could be given as an ANNEX.

References

Eurocode 5, 1993. Design of timber structures - Part 1 - 1: General rules and rules for buildings. ENV 1995-1-1:1993. European Committee for Standardization. Brussels, Belgium.

Hilson, B. O. (1995). Joints with dowel-type fasteners - Theory in: Blass, H. J. Timber Engineering STEP 1, STEP lecture C3, Centrum Hout, The Netherlands.

**INTERNATIONAL COUNCIL FOR BUILDING RESEARCH STUDIES AND DOCUMENTATION
WORKING COMMISSION W18 - TIMBER STRUCTURES**

NAIL PLATE JOINT BEHAVIOUR AT LOW VERSUS HIGH LOAD LEVEL

by

T Poutanen
Tampere University of Technology
Finland

MEETING TWENTY - NINE

BORDEAUX

FRANCE

AUGUST 1996

Nail plate joint behaviour at low versus high load level¹

by

T. Poutanen²

Abstract

Timber trusses exhibit elastic behaviour at low load level and, in many cases, also at high load level. Thus, an elastic design is justified at least in the serviceability design. Plastic behaviour can be observed often in some joints at the ultimate load level. A problem is whether the failure design should be made by the use of elastic or plastic theory.

Timber trusses with nail plate joints were tested to observe joint behaviour at low versus high load level. Measurements were made by use of an automatic equipment enabling measurements to be taken up to the failure.

Three joint failure types were observed:

- a) Anchorage (lateral resistance, no steel yielding),
- b) steel failure on the joint line with steel yielding without friction between adjacent timber members and
- c) steel failure on the joint line with steel yielding with friction between adjacent timber members.

Test results were compared with the theoretical results based on the elastic theory (linear tooth-timber interface, eccentricities considered, joint moments considered, solid plate behaviour assumed, stiffness parameters adjusted to correspond to the load).

In the case of anchorage failure (a) the linear elastic theory corresponds well with the test i.e. the measured chord resultant location (eccentricity) correlates well with that calculated.

Steel yielding in the joint line (b, c) makes a considerable difference. Compound steel yielding and friction (case c) increases joint stiffness and reduces eccentricity compared to case a. The steel yielding with no friction (case b) produces the opposite effect and the eccentricity is increased.

Thus, the joint behaves according to elastic theory if anchorage failure occurs. If steel yielding occurs the eccentricity may be higher or lesser corresponding to friction. The elastic behaviour is an intermediate between different plastic behaviours.

It is concluded that the semi-elastic design (elastic design with load dependant stiffness parameters) can be used in the failure state, and that the plastic design (steel yielding and plastic stress distribution in the joint line) is questionable.

¹Paper CIB-W18A/29-7-2 prepared for presentation in CIB-W18 meeting in Bordeaux, France, August 26-29, 1996

²T. Poutanen, Dr.Tech., Director, Wood Institute, Tampere University of Technology, P.O. Box 600, FIN-33101 Tampere, Finland, tel +358-31-3162111, fax +358-31-3466456

INTRODUCTION

Preamble

Truss tests were recently undertaken which offer information on the following topics:

- . A procedure for truss testing.
- . Consequences induced by plastic steel yielding in truss joints.
- . The design procedure of trusses: the elastic versus plastic theory.

These tests are presented, discussed and conclusions drawn.

Truss design at the failure state, elastic versus plastic design

It is clear that at a low load level (i.e. serviceability design, deflection calculation) the design should be based on the elastic theory.

Plastic behaviour can be observed often at the ultimate load level. However, plastic behaviour does not occur always, especially in cases of joint anchorage failures and timber failures. Furthermore, though plastic behaviour occurs in the truss it usually takes place only in a few joints and most of the joints (and in most cases all members, too) stay elastic. At present some design codes favour the plastic design over the elastic design at nail plate joints, e.g. in [EUROCODE 5] all given design formulas are based on the plastic theory. The plastic design is favoured, apparently, for the following reasons:

- . The plastic design is quite easy (as the approximation of ignoring deformations is made).
- . Plastic design leads to small nail plates and low joint cost.
- . In truss tests joints often exhibit steel yielding in joint lines i.e. they have plastic behaviour; it may be believed that, for this reason, the plastic theory is more correct than the elastic theory.
- . It is the aim that the timber trusses are ductile in order to avoid brittle failures. Thus, it is believed that by making the joints plastic the whole truss becomes plastic (unbrittle). It may even be believed that making the design using the plastic theory secures ductile truss failure.

However, these arguments are questionable:

- . The plastic analysis is easy only if the displacement characteristics are disregarded (according to the basic principle of the plastic theory). It is justified to disregard displacements in statically determinate structures. The displacements may also be disregarded in indeterminate structures in some restricted cases, especially in cases of special yielding conditions are fulfilled and cases where there is no risk of buckling failures. In indeterminate structures deformation characteristics must generally be considered. Timber trusses are statically indeterminate, they do not have yielding capacity in some failure types and there is a risk of buckling failures³. In timber truss design the displacement characteristics should be considered, and, if so the plastic analysis is complicated, far more complicated than the elastic. The approximation of ignoring the displacement characteristics may result in large errors even in some

³ The limitations on the use of the plastic design are well defined in steel codes, e.g. in [EUROCODE 3], similar limitations should be added to timber codes e.g. [EUROCODE 5], too.

normal common cases as shown by the author [1995] and as demonstrated later in this paper⁴. The errors are due to joint modelling.

- The plastic design leads to small nail plates and low joint cost. However the joint cost is a minor part appr. 5-10%, of the total cost. The major cost appr. 50%, lies in timber. Present trusses fail more or less always at joints. This indicates that the strength of joints is too low. By increasing joint strength the overall load carrying capacity can be increased at negligible cost (as the joint cost is low) as concluded e.g. by [Mtenga 1992] and the author [1995]. Furthermore the author believes that the increased joint efficiency (increased strength and stiffness) causes secondary favourable effects, e.g. better overall distribution of stresses. Thus, the plastic theory is questionable from the economic point of view. It minimises a minor cost (joint cost) and pays little attention to the major cost (timber cost). Optimisation of compound joint and member cost is not possible in the present plastic theory as this theory does not have a relevant link between the joint and the member (timber) behaviour. Sometimes, deflection is more governing than failure. Increased joint efficiency is justified in these cases, too.
- In modelling a plastic joint the plastic hinge should be set to the actual plastic hinge (usually to the joint line, sometimes to the centre of anchorage area). This way of applying the plastic theory would be theoretically more correct⁵. However, this principle is not followed in present plastic joint modelling but, on the contrary, it is believed the plastic hinge can be set more or less anywhere as advised e.g. in [EUROCODE 5]. It is believed (according to the general principle of plasticity) that there is freedom in selecting the analysis model and also any error due to this approximation is negligible. However, this is not the case as shown by the author [1995] and as demonstrated later in this paper.
- It is believed that joint yielding leads to favourable effects:
 - redistribution of stresses, levelling of stress peaks and
 - avoidance of brittle failures.
 These kinds of favourable effects really occur in steel structures with yielding capacity all over the structure. However, timber structures with yielding joints and nonyielding members do not exhibit similar favourable effects with the effects in timber structures being random. The favourable and the unfavourable consequences have more or less equal probability⁶ as demonstrated later in this paper.
- Conducting the design using the plastic theory does not ensure that the truss failure is ductile, as explained later in this paper.
- The present plastic truss joint codes are not well defined, inducing variability in design. Different designers end up with significantly different results in the same design task. This variability may cause confusion.
- Plasticity causes variability in other ways, too. Steel yielding changes joint behaviour considerably. The direction of this change (favourable, unfavourable) can not be defined in advance in the design stage. The increased variability should be compensated

⁴ These errors may really be characterised as significant. According to [Poutanen 1995] and also according to the tests presented here plastic models may estimate the governing stress appr. 50% unsafe; that is, the total design safety (of appr. 2) is required for the error of the design model. Further, the plastic models may consist of a big safe error, and according to [Poutanen 1995], the governing stress may be overestimated by a magnitude of three...four.

⁵ However, it does not always work well, not e.g. in present trusses.

⁶ In the trusses presented here the unfavourable effects are dominant. Plasticity tends to increase eccentricities and stresses especially at chords which are most critical in truss economy. Therefore the unfavourable consequences are dominant more generally, not only in this special case.

by an increased safety factor. The plastic design should have a (penalty) factor compared to the elastic behaviour (of no excess variability due to steel yielding). Sometimes this excess variability will be large (as in the present trusses). Thus the (penalty) factor should also be large.

This paper will supply data on these topics.

Modes of plasticity

If load deformation relationship is linear⁷ we may call the behaviour elastic and otherwise plastic.

A timber truss with nail plate joints is clearly elastic at low load levels. As load increases plastic behaviour may be observed in four ways:

1. *Plate plasticity*: The joint lines of the nail plates may have steel yielding, this behaviour is clearly plastic. It is the most difficult from a design point of view. This plasticity occurs most often in present trusses, and can be avoided if strong or big enough plates are used. Plasticity has some advantageous effects (ductility, increased strength). However, it also has unfavourable consequences (excess timber stresses, increased variability, difficult analysis, excess overall cost) meaning that the overall behaviour is disadvantageous.
2. *Anchorage plasticity*: The increased load in the plate timber interface causes a nonlinear load-slip relation due to nail yielding and timber crushing adjacent to nails. This plasticity occurs more or less always in present truss joints. Such plasticity can not be avoided but can be reduced by strong or big plates. The anchorage plasticity differs only a little from the elastic behaviour.
3. *Contact plasticity*: Contact connections of adjacent compressed timber members may cause timber crushing, which may be called contact plasticity. This plasticity can be reduced or even fully avoided by large or effective plates. Such plasticity is of minor importance.
4. *Timber plasticity*: Occurs in some cases in compressed timber members. This topic is beyond the scope of the present paper.

From a design point of view the anchorage plasticity and the contact plasticity can be handled with reasonable accuracy by using one and the same model from low to high load level, and by only adjusting relevant stiffness values. This kind of truss behaviour, including the elastic stage and the anchorage and contact plasticity, is called here *semi-elastic*.

Usually contact connections have a minor role in the overall behaviour of a truss [Poutanen 1995, Nielsen 1996] and in most cases a relevant design can be made by ignoring these connections in the analysis of internal stresses⁸. Consequently it is justified to ignore the contact plasticity at least in most cases⁹.

The plate plasticity is different. If steel yielding does not occur a good approximation is to assume that the plate (and the joint line) is undeformable. If yielding occurs in the joint

⁷ By sufficient accuracy from the point of view of design accuracy induced by the physical behaviour, geometric nonlinearity may be elastic or plastic.

⁸ However, in some special cases contact may have a considerable effect on stress distribution.

⁹ However, contact connections must be utilised in strength design, as present nail plates do not have sufficient efficiency to transmit full timber compression capacity over the joint (from one timber member to another). Contact forces increase variability. Thus, increased use of contact forces cause increased variability. If contact is utilised, in a refined truss design there should be a special (penalty) factor which takes into account the degree of utilisation of contact forces.

line the deformation usually is large, normally larger than deformation induced by other reasons. The steel yielding means that the physical function of the joint changes considerably. The author doubts whether it is possible to make a practical truss design model which would cover both cases. Therefore two models (one to cover the solid plate behaviour and the other to cover the case of the yielding joint line) are needed creating excess difficulty.

TESTS

Tests were carried out by M.Sc. T. Turunen [1996]. There were four trusses altogether. The used test procedure is accurate and its variation is small¹⁰. Therefore conclusions can be drawn even though the number of tests is small. Test trusses with measurement results are shown in appendices 1-4 with some photos in appendix 5.

Test method

The test method used has been explained earlier by the author [e.g. 1988a, 1995]. However, it is explained in short in the following (see figure 1).

Measurement is based on resultant location measurements in timber cross sections. The resultant is located at a fixed place e measured from the cross section centre. It is preferable to use a relative (normalised, dimensionless) eccentricity e_r to measure the resultant location (instead of the absolute eccentricity e):

$$e_r = \frac{e}{h} \quad (1)$$

The measurement consists of the following steps:

- Measurement cross sections along the truss are selected. Increased number of measurement cross sections increase relevant test data. Cross sections without defects are preferred as having the best accuracy. It is preferable to select cross sections in such way joint behaviour can be measured as it is most unknown in trusses.
- Two strains ε_1 , ε_2 are measured in each cross section. Strain measurements should be as far as possible apart (preferably at the edges) to achieve the best accuracy.
- The measured resultant location $e_{r,m}$ (relative eccentricity) is calculated from:

$$e_{r,m} = \frac{\varepsilon_2 - \varepsilon_1}{6(\varepsilon_1 + \varepsilon_2)} \quad (2)$$

- The corresponding theoretical eccentricity is obtained from the calculated normal force N_c and moment M_c :

$$e_{r,c} = \frac{M_c}{h N_c} \quad (3)$$

¹⁰ Actually, the number of tests is larger. In the eccentricity test method each cross section measurement denotes an independent test. From this point of view there were 10 tests.

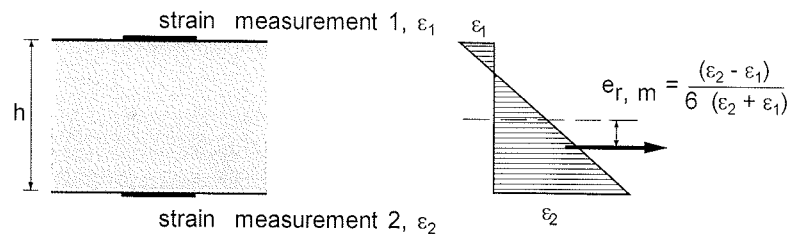
$e_{r,m}$ and $e_{r,c}$ are compared with each other. They should be the same within relevant limits if the calculation is correct and corresponds with the test¹¹.

The author has concluded that the error in the eccentricity measurement is small $\Delta e_{r,m} \leq 0.03$ i.e. 3% in spite of large variations in timber properties, e.g. defects, modulus of elasticity. Normally various calculations based on different design models show far bigger differences in $e_{r,c}$. Therefore it is possible to make conclusions on the correlation between the test and the analysis though only a small number of tests (even one test) are performed. This test method can effectively reveal whether the current analysis model is right or wrong.

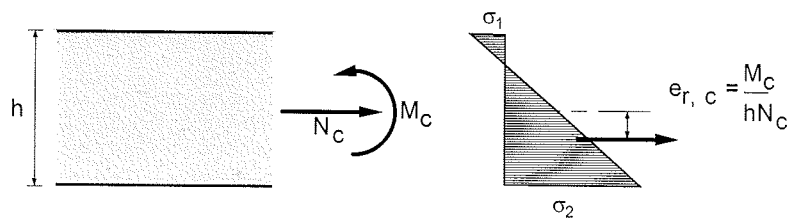
Figure 1

Test principle, the cross section resultant location is obtained by eccentricity $e_{r,m}$ measurement (top) and it is also obtained by calculation $e_{r,c}$. These eccentricities are compared with each other and they should be the same within relevant limits (10% in the author's opinion).

Eccentricity defined by measurement $e_{r,m}$



Eccentricity defined by calculation $e_{r,c}$



Test trusses

Test trusses with loading arrangement and measurement cross sections are shown in appendices 1-5. All test trusses were designed to be symmetrical. Bottom chords did not have any lateral loading. If the bottom chords exhibit some eccentricity (and moment), that is if the resultant is outside the centre line of the chord, it is fully due to end joints. There is a direct correlation between the bottom chord eccentricity and the joint behaviour.

Timber was normal sawn spruce timber used for trusses in Finland. Moisture and density was measured at chords and tensile diagonals, these values were $\omega=8 - 14\%$, $\rho_0=420 - 520 \text{ kg/m}^3$. The average modulus of elasticity was estimated at appr. 10.000 MPa. Variation in the timber properties was rather large. As far as this test is concerned only the ratio of

¹¹ The author [1995] concluded that $|e_{r,m} - e_{r,c}| \leq 0.1$. If this criterion is not fulfilled the analysis model is wrong as the model selects incorrect timber grade. Nail plate joints in present trusses exhibit natural variability Δe_r which may have the same magnitude (± 0.1 i.e. $\pm 10\%$) in the semi-elastic stage. Steel yielding increases this variability and (nearly) doubles the variability. The total design variability is cumulated from effects of physical behaviour and errors in theoretical calculations. The author concluded in [Poutanen 1995], that the design accuracy (and design variability) of $\Delta e_{r,d} \leq 0.1$ is possible to obtain in practical semi-elastic design. The joint behaviour variability may be decreased by disregarding the plasticity in the design. This variability may be decreased further by increasing joint anchorage stiffness and by decreasing use of contact.

timber stiffness and plate (anchorage) stiffness has a relevant effect on the result (eccentricity). It may be estimated that this ratio varies in the test trusses by appr. $\pm 20\%$. A theoretical study shows that variation of this magnitude has a negligible effect on the relative eccentricity, appr $\pm 3\%$ in the present trusses.

The strain gage strips were of type KC-120-A1-11 and X60 adhesive was used. The relative eccentricity was calculated by use of the actual bottom chord depth at each measurement cross section (nominal depth 98 mm, actual 93-97 mm).

The nail plates were Top-91 plates which were widely used in Finland. The plate has thickness 1.2 mm, nail length 12 mm and high steel quality $f_y \geq 360$ MPa.

Trusses 1 and 2 were made and tested first. The joint line and anchorage failure were designed equally governing (however anchorage a little more critical). Both trusses failed in anchorage in the diagonal connection. Truss 1 had effective contact in timber members in all joints whereas truss 2 had appr. 3 mm gap in bottom chord joints. Trusses 3 and 4 were similar to 1 and 2 respectively, but the nail plate of the bottom chord joint was increased to avoid the anchorage failure¹² (however, truss 4 had appr. 5 mm gap in the horizontal joint line at the top of the bottom chord).

The measurement results have been plotted in the form in which the data was collected by an automatic recording device (by use of a spread sheet and graph program) without any human manipulation. Load was increased to obtain the failure in appr. 10 min. In tests 2, 3 and 4 down load was applied as seen in the result graphs. The recording device was adjusted to record of 5 second intervals (in some cases 10 seconds). Trusses were loaded by human operated hydraulic jacks, the velocity of load increase was not fully uniform. This explains the small irregularities in the curves. Deflection measurements were made at the mid span (manually in tests 1, 2 and 3 and automatically in test 4, results not presented here having minor relevance).

Results

The results are presented in relative eccentricity (of bottom chord) versus load graphs. As the bottom chord depth is nearly 100 mm (nominal 98 mm actual 93-97), the relative eccentricity in % almost equals the actual eccentricity in mm (the actual eccentricity denotes the location of the bottom chord resultant above the centre line).

Failures

Trusses 1 and 2 failed at anchorage in the bottom chord plate and tension diagonal connection. The failure may be characterised as brittle. As seen in the graphs in appendices 1 and 2 the capacity is lost suddenly.

Trusses 3 and 4 failed at the joint line along the top of the bottom chord. In truss 4, before the final joint failure there was a timber compression-bending crack at the top chord close to the centre joint, and timber tension-bending failure crack occurred at the bottom chord close to one joint. Though, both cracks were clearly visible, load was not decreased and the final failure took place at the bottom chord joint (the test was terminated due to excess deflection).

¹² The tension diagonal was also increased to increase the anchorage resistance.

DISCUSSION

Test accuracy

The author has concluded in [Poutanen 1995] that the measurement accuracy of the eccentricity test method is $\Delta e_{r, m} \leq 3\%$, and, in good laboratory conditions (proper equipment, skilful and experienced staff), a better accuracy should be obtained. All trusses were symmetric and should behave symmetrically, too. In all trusses the bottom chord should have uniform eccentricity¹³. Two or three cross sections were measured in each truss. These measurements should be approximately the same in each truss and the ultimate difference should be less than 6% ($=\pm 3\%$, the ultimate error of the eccentricity test method). This criterion is fulfilled. Measurements were made in good laboratory conditions¹⁴ and in most cases the differences are far less than 6% as expected.

A dark area has been drawn at the top of the graphs denoting the ultimate accuracy of 6%. The location of this area has been set by human estimation on the actual behaviour of the joint based on average measurements (down load phase is excluded). It is emphasised that the breadth of this area denotes the maximum measurement error of 6% ($=\pm 3\%$). Thus, this breadth defines the actual joint behaviour “for sure”. The design result should fall close to this area, not further than 10% [Poutanen 1995].

Truss 3 clearly is asymmetric and the eccentricity measurements in this truss are not the same. The asymmetry is apparently due to contact in the joints. It is known from other tests, e.g. [Poutanen 1987, Laasonen 1988], that contact causes a significant variation in the joint behaviour.

Error in plastic design models

The plastic design models are not well defined. In these cases several models may be applied. For simplicity only two plastic models drawn in figure 2 are studied:

1. “simple” model, top and
2. “centre line” model, centre,

both of which are widely used and e.g. accepted by [EUROCODE 5]. It is general practice in plastic joint modelling that the rotational stiffness of the joint is disregarded.

In appendices 2 and 4 stress distribution has been presented at the load level of 12 kN (which approximately denotes the failure load) in five cases:

- . Measurement, lower accuracy boarder ($e_{r, m} - 3\%$).
- . Measurement, higher accuracy boarder ($e_{r, m} + 3\%$).
- . Calculation based on the semi-elastic analysis (figure 2 bottom).
- . Plastic calculation using model 1.
- . Plastic calculation using model 2.

¹³ The eccentricity is not quite precisely uniform, with the deflection and the tension force (secondary effect) causing a little variation. However, in this case it is small and can be disregarded. This second order effect is taken into account in the theoretical calculations presented in appendices 2 and 4.

¹⁴ The tests were carried out by a student who did not have any experience of the eccentricity test, but he seemed to carry them out well.

The plastic analysis 1 does not show any eccentricity in these trusses and the critical governing stress used in design to select the timber grade and cross section is 6 MPa. However, the test shows that this stress is at least 13-15 MPa. Thus the plastic model 1 is seriously unsafe. All cumulated safety factors of appr 2 are needed to compensate this kind of error¹⁵ induced only by the incorrect design model. There is no safety left for variation and other errors. On the other hand the plastic model 2 is very much safe at the bottom chord, the governing stress is 24 MPa, but the test shows it is not bigger than 15-17 MPa. However this model is badly unsafe at diagonals. So, both plastic models are unsafe.

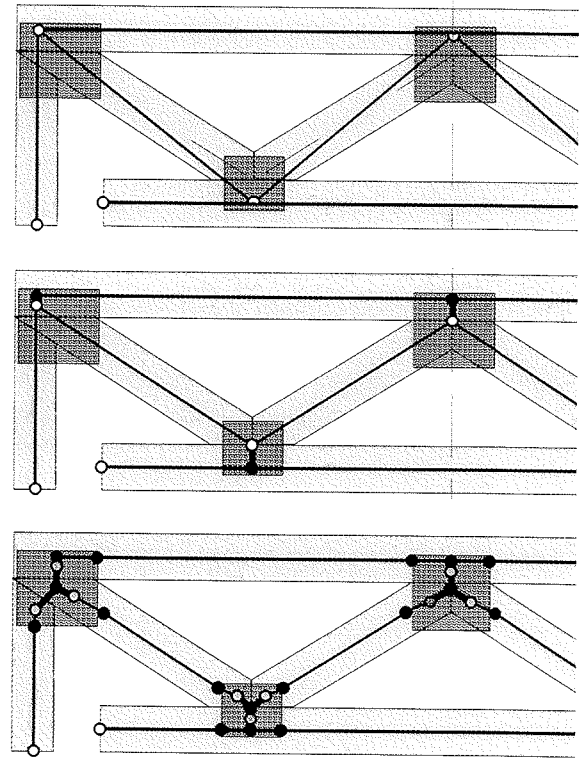


Figure 2

Plastic model 1, "simple model", top, model 2, centre line model, centre (semi-)elastic model, bottom.

Accuracy of the semi-elastic design

The theoretical calculations were made using a semi-elastic theory and a computer program disclosed in [Poutanen 1995].

In appendices 2 and 4 calculated results obtained from a semi-elastic calculation are presented at load level 6 and 12 kN. Theoretical calculation on trusses 1 and 3 where contact occurred between the adjacent timber members are not presented. As seen in the results, contact did not have a big effect except for the ultimate failure. There is little data what kind of contact stiffness values should be used in the calculation. By adjusting the stiffness parameters it would be possible to have full correlation between the test and the calculation.

Trusses had Top-91 plates. Accurate stiffness data on this plate was not available. However, the stiffness may be concluded approximately from other data. Nail plate anchorage translation stiffness is usually in a short term test appr. 10 N/mm^3 ($=k_x=k_y$). Variation is large, probable appr. $\pm 5 \text{ N/mm}^3$. The stiffness of Top-91 is rather poor and therefore the calculation was made using the value of 10^{16} N/mm^3 at low load level, $F=6 \text{ kN}$. At load level 12 anchorage stiffness is reduced and in truss 2 stiffness 7 N/mm^3 and truss 4 stiffness 9 N/mm^3 was used. The stiffness reduction is less in truss 4 as it has a 43% bigger bottom chord joint plate (172×135 versus 120×135), which is most critical to the bottom chord eccentricity. Lesser data is available on rotation stiffness. It is apparent that the rotation

¹⁵ Actually, in truss 2 the safety factor of 2 is not sufficient to compensate the error induced only by the analysis model.

¹⁶ To have better accuracy (contrary to general praxis) the calculations were based on cross areas (no reductions applied in anchorage areas), cross stiffness of 10 N/mm^3 corresponds to net stiffness of appr. 9 N/mm^3 .

stiffness is smaller than the translation stiffness. Therefore in all calculations 30% less rotation (than translation) stiffness was used ($0.7k_x=0.7k_y=k_\phi$)¹⁷.

The semi-elastic calculation falls into the measurement accuracy area fully (truss 2) or nearly (truss 4).

Increased variability by steel yielding

Truss joint has a variability according to these tests under the load level of steel yielding of appr. $\Delta e_r \leq 20\%$ ($\pm 10\%$). Steel yielding in the joint line almost doubles this value. In truss 3 the eccentricity was decreased appr. 7% and in truss 4 increased appr. 9%. The excess variation of 16% is caused by steel yielding and contact. The variation was the same as in author's earlier tests [Poutanen 1988b] where similar variation induced by steel yielding was observed.

Redistribution of stresses due to plasticity

The timber bottom chord does not have any yielding capacity; thus the test illustrates the actual behaviour of these trusses and there can not be any further behaviour modes. If the bottom chord had yielding capacity e.g. if it was made of steel, there would be a secondary behaviour mode with a hinge at the chord. This chord hinge is needed for a favourable redistribution of stresses.

Test 4 discloses that steel yielding does not mean a favourable redistribution of stresses in a timber truss. On the contrary the redistribution is unfavourable at the most critical member. The governing bottom chord timber stress is increased due to steel yielding from 14 MPa to 17 MPa i.e. 20%¹⁸.

Thus, joint plasticity in timber trusses does not induce favourable redistribution of stresses.

Ductile failure

Joint anchorage failure and timber tension failure are brittle. The author does not know any rational means of avoiding such brittle failures in trusses. Thus, these failure types can not be avoided. Plastic joint behaviour causes (favourable) ductile joint line failures but does not exclude other failure modes.

As brittle failures in timber trusses can not be avoided it is of minor reason to favour the plastic design due to ductility.

Joint behaviour at down load

Change in the eccentricity is large at the down load. The eccentricity increases which can be explained due to the decreased plate stiffness. These observations call for further tests.

¹⁷ The calculation is based on the assumption of solid plate. This approximation causes increased error as plate size increases. The error can be compensated by reducing k_ϕ -value further at joints of pig plates. This reduction should be made for truss 3 and 4 and if so the correlation between the test and the semi-elastic analysis would be better.

¹⁸ The plastic theory produces small and inexpensive nail plates but it causes excess cost in timber, according to this example the timber stresses should be reduced by 20% i.e. the penalty factor of the plastic theory in timber design should have the magnitude of 1.1 (1.05-1.2).

CONCLUSIONS

1. The *eccentricity test method* is a valid method in truss testing, and can effectively reveal errors in truss analysis models.
2. The plastic models for truss joint design are questionable:
 - They may include significant unsafe errors. The whole safety factor of appr. 2 may be needed to compensate for these errors leading to unsafe design.
 - They may also include substantial safe errors, leading to uneconomic design.
 - The plastic models can not be used for optimisation (as they include large errors).
3. Steel yielding in the joint line may cause a considerable excess joint variability.
4. Steel yielding in joints does not always cause favourable (but random) redistribution of stresses in timber trusses (as opposed to steel trusses).
5. It apparently is not possible (economic) to obtain ductile timber trusses. The requirement of ductile truss behaviour is questionable.
6. Making the truss design using a plastic model does not secure that the actual truss behaves ductile.
7. Increased contact in a nail plate joint increases variability in joint behaviour.

Acknowledgements

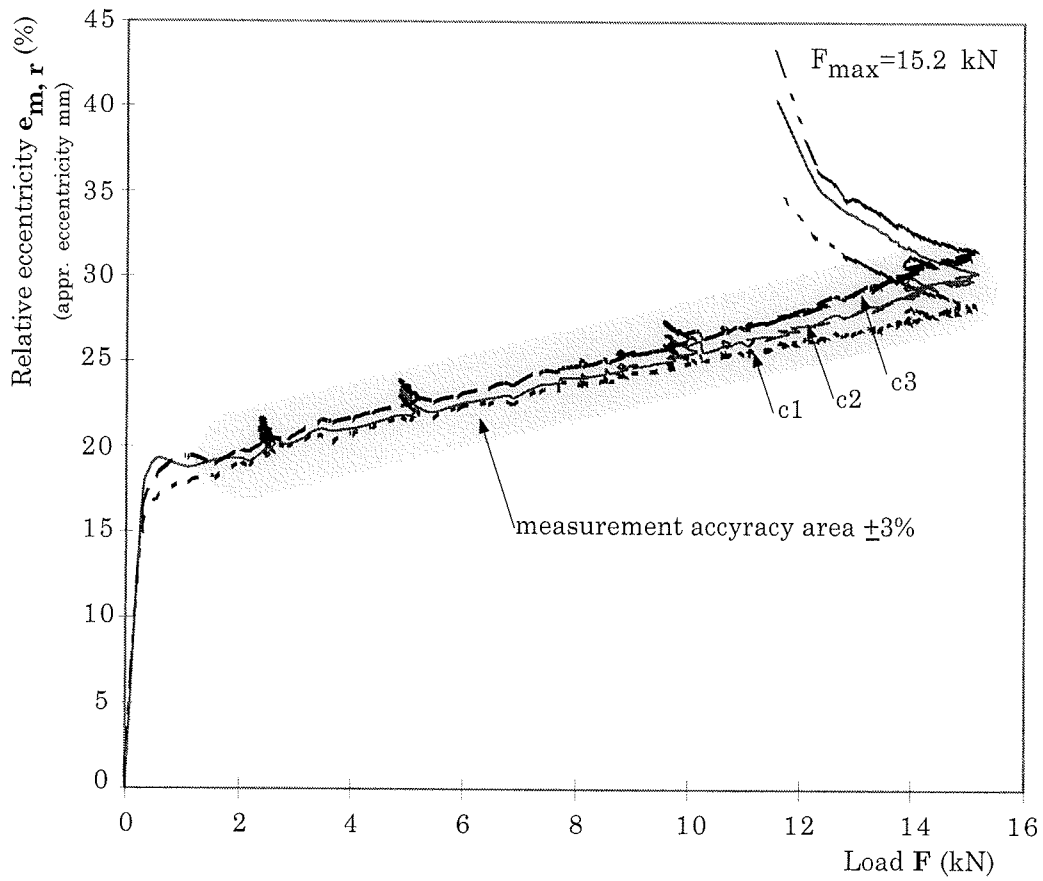
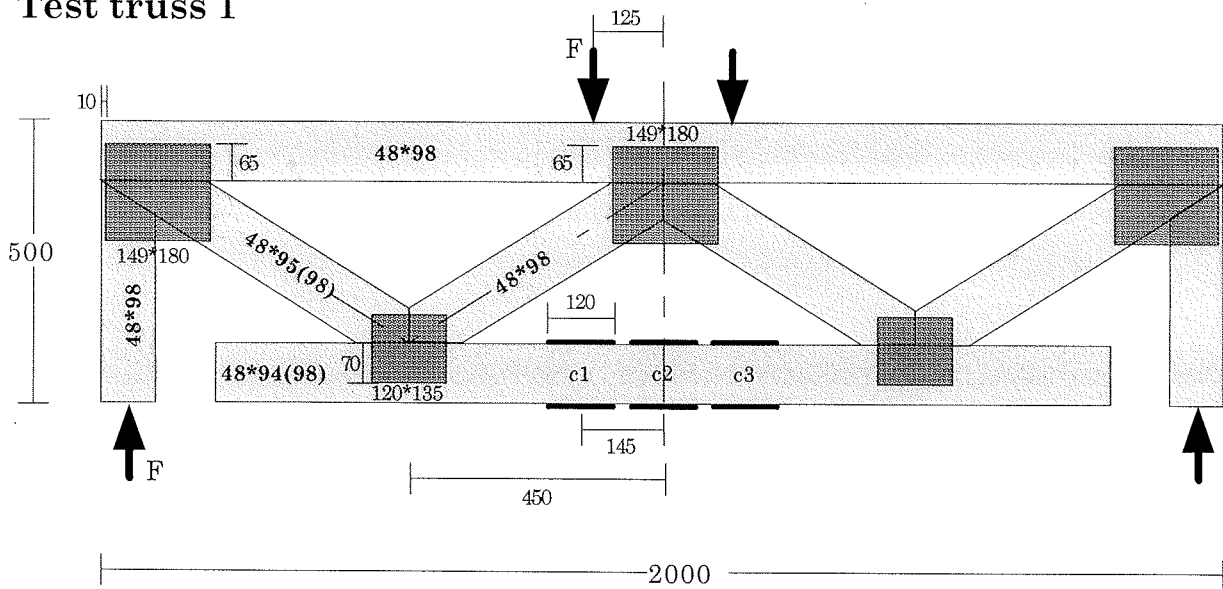
The practical tests were carried out by M.Sc T. Turunen as an exercise work of his timber engineering studies. M.Sc. P. Javanainen and M.Sc. J. Suoniemi assisted in the preparations of this paper mainly in the numerical calculations.

References

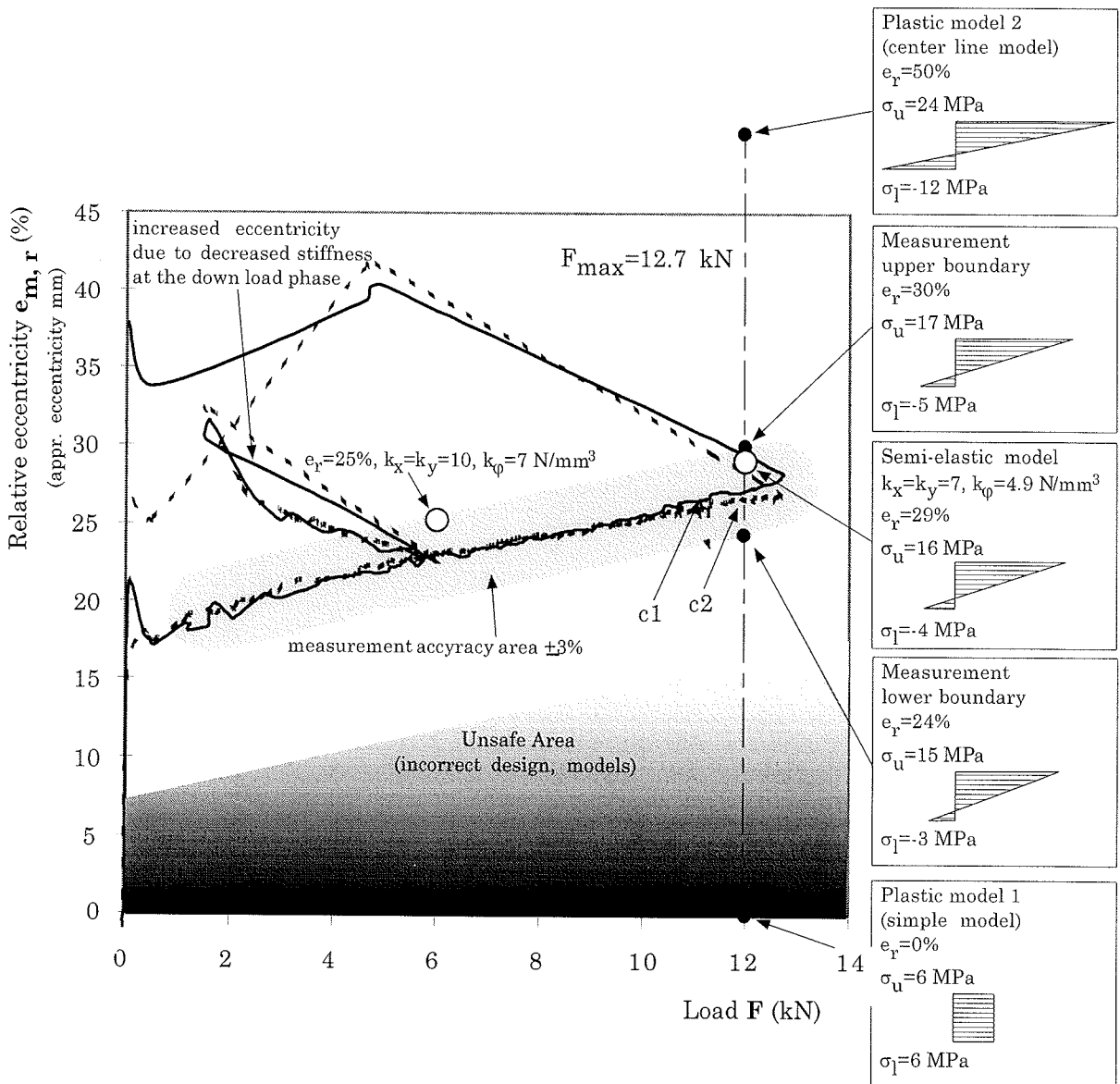
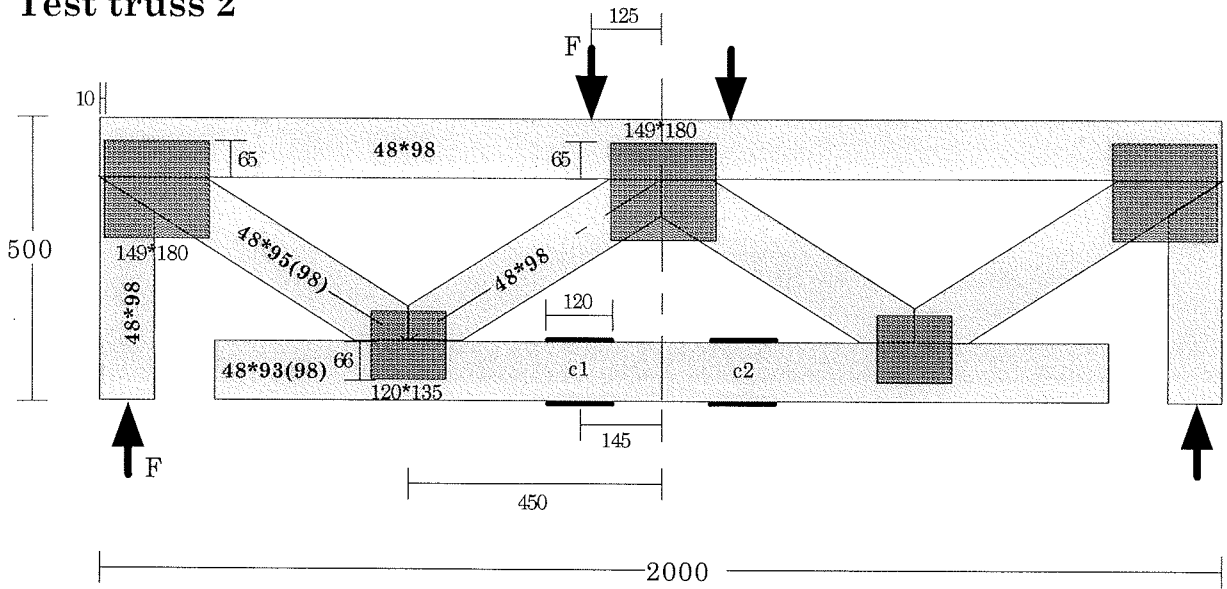
- Eurocode 5. 1993. Design of Timber Structures, European Committee for Standardisation
- Eurocode 3. 1993. Design of Steel Structures, European Committee for Standardisation
- Laasonen M., Leivo M. 1988. Naulalevyrakenteiden koekuormituksia (Timber nail plate component tests). Espoo, Finland. Report nr 842, VTT (in Finnish)
- Mtenga P. V. 1991. Reliability performance of light-frame wood roof systems, USA, University of Wisconsin
- Nielsen J. 1996. Stiffness analysis of nail-plate joints subjected to short-term loads, Structural paper 2, Aalborg University, Denmark
- Poutanen, T. 1987. Moment distribution in trussed rafters, CIB-W18/20-14-1, Dublin Ireland
- Poutanen, T. 1988a. A method for moment measurement in timber cross section, IUFRO, Turku, Finland
- Poutanen, T. 1988b. Nail Plate Joint under Shear Loading, CIB-W18/21-7-3, Vancouver, Canada
- Poutanen, T. 1995. Analysis of timber nail plate components. Tampere University of Technology. Tampere, Finland
- Turunen, T. 1996. Naulalevyristikoiden koekuormitukset (Tests on trusses with nail plate joints), exercise work, Tampere University of Technology (In Finnish)

Appendix 1

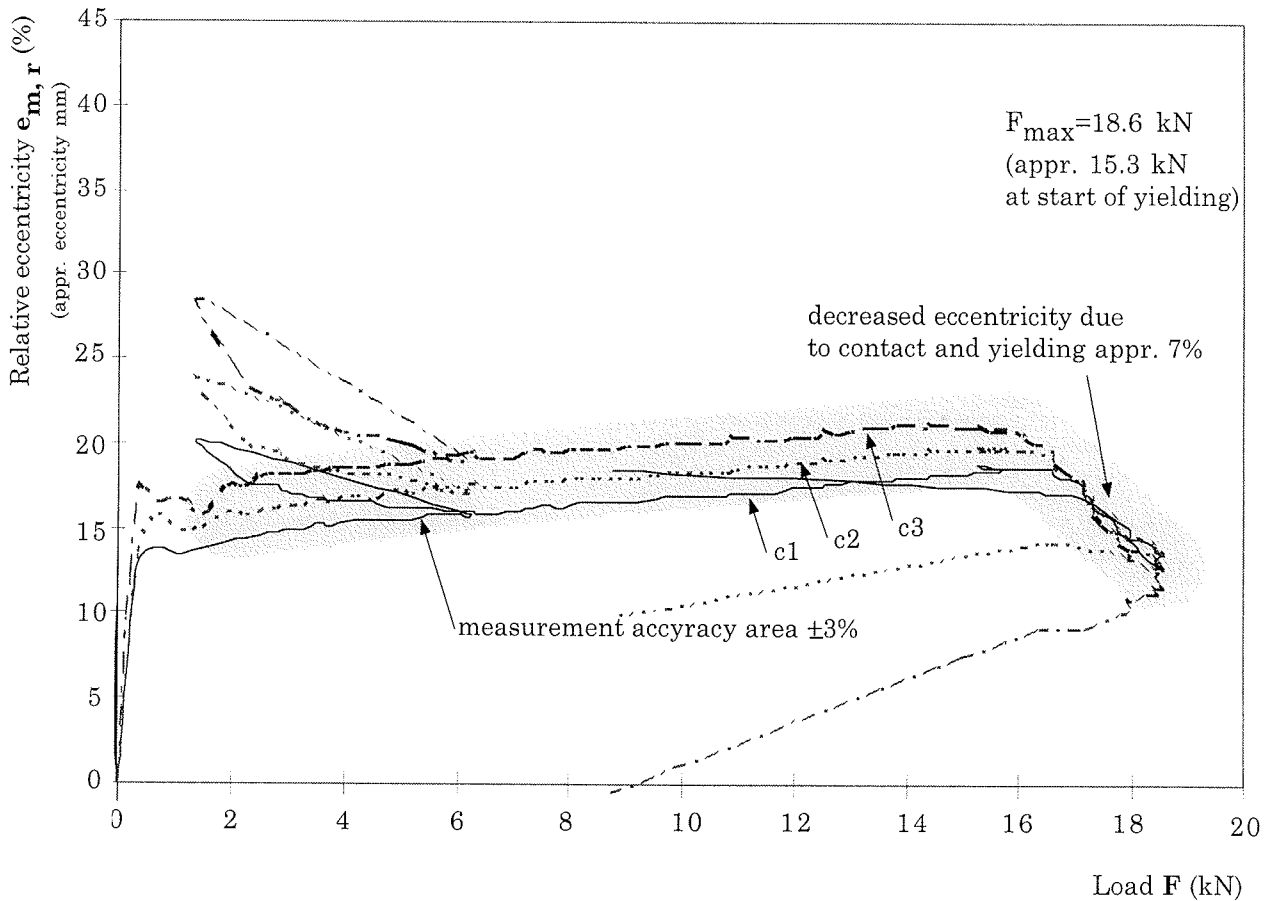
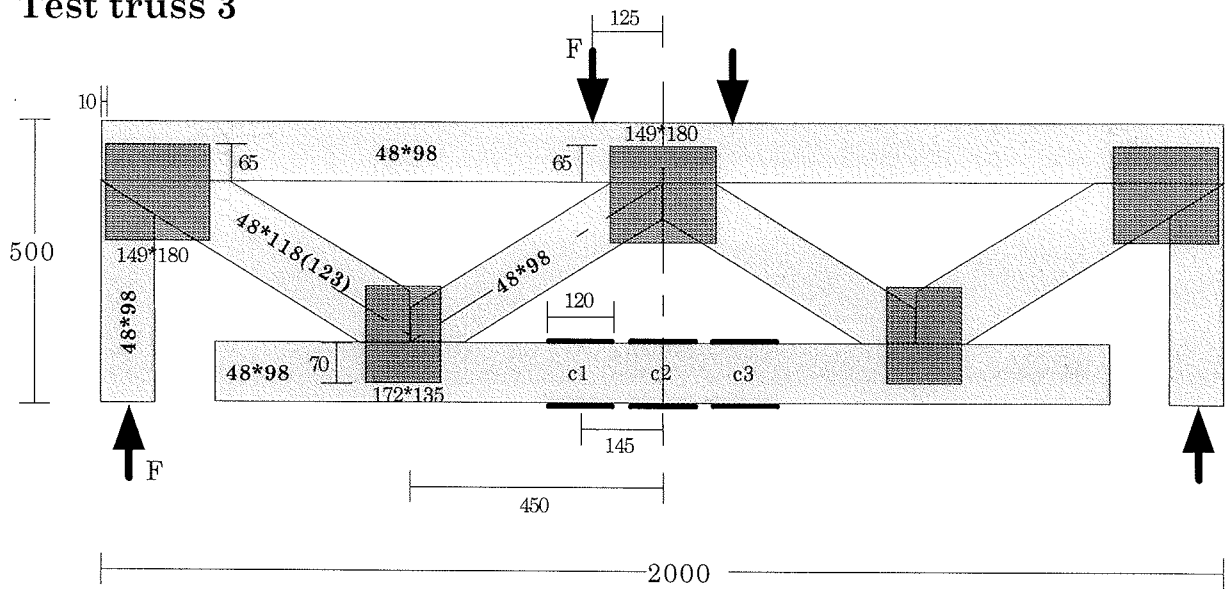
Test truss 1



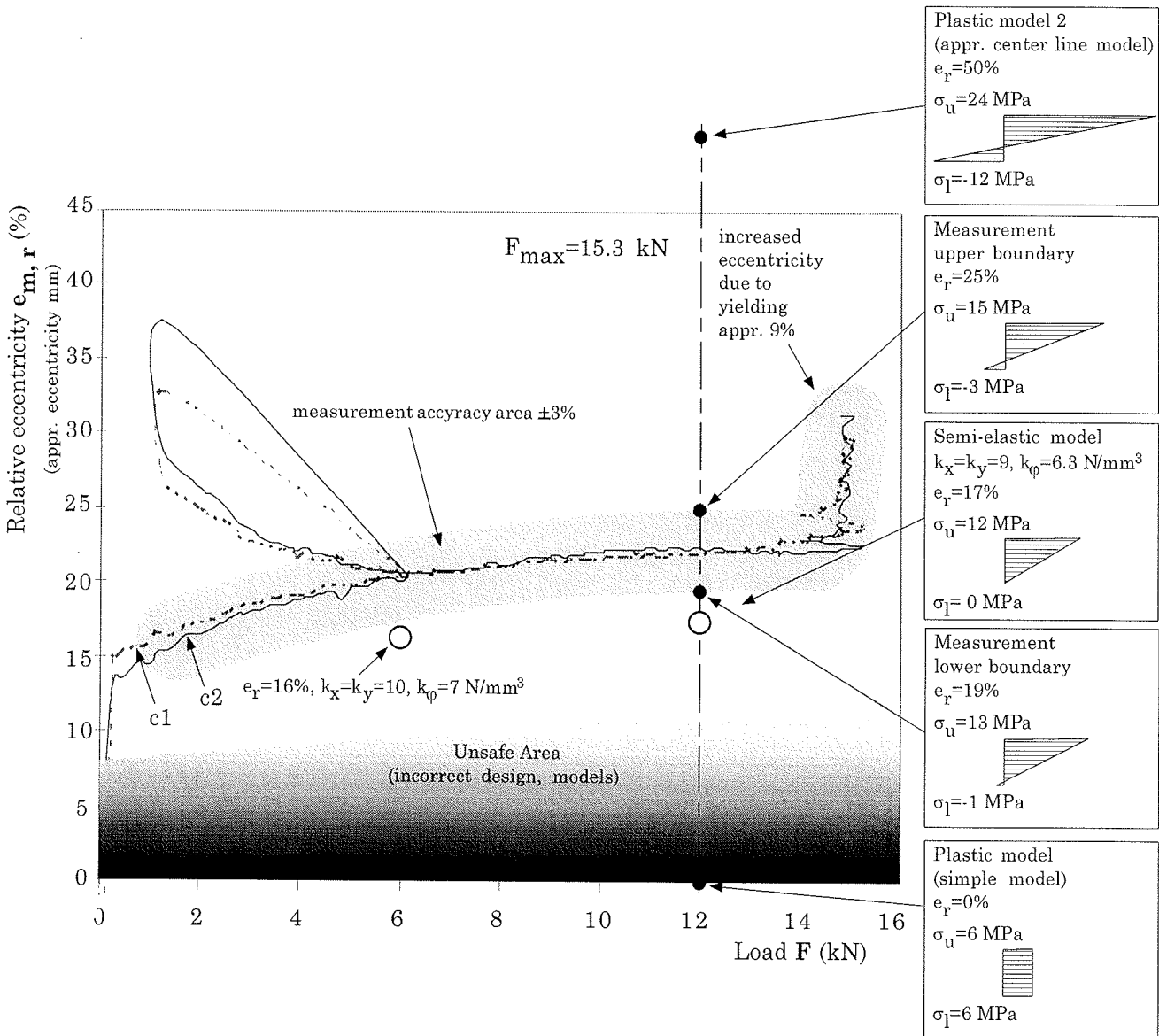
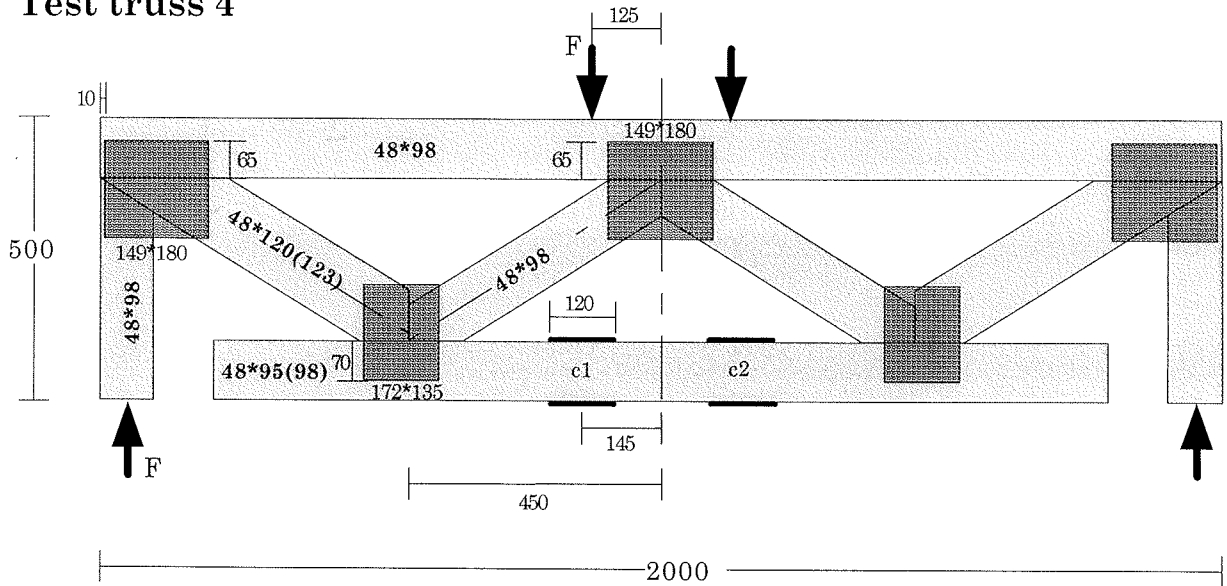
Appendix 2
Test truss 2



Appendix 3
Test truss 3



Appendix 4 Test truss 4



Appendix 5

Figure 5-1

Test apparatus, truss 3 at failure.

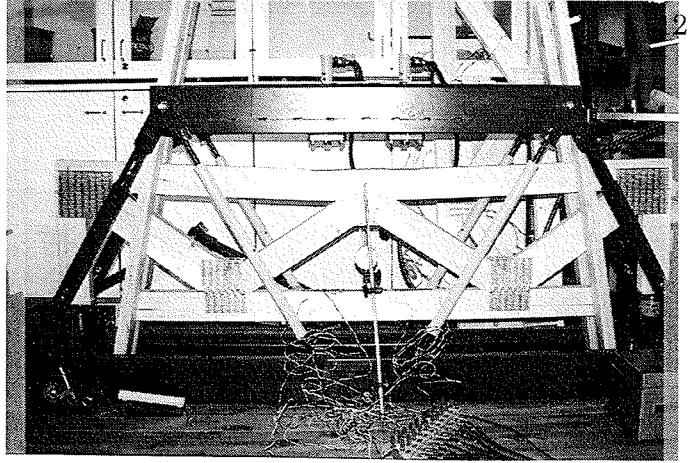


Figure 5-2

Joint anchorage failure of truss 2.

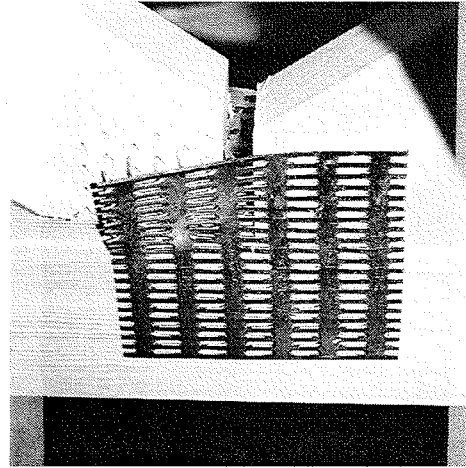


Figure 5-3

Joint line failure of truss 3.

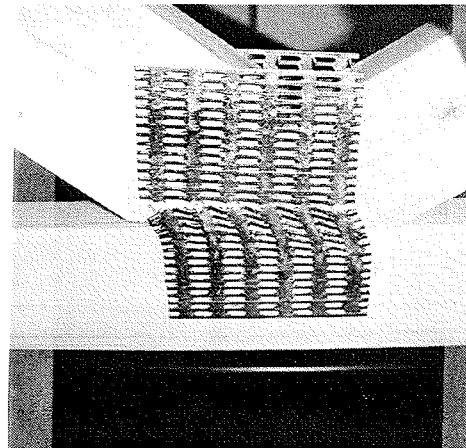
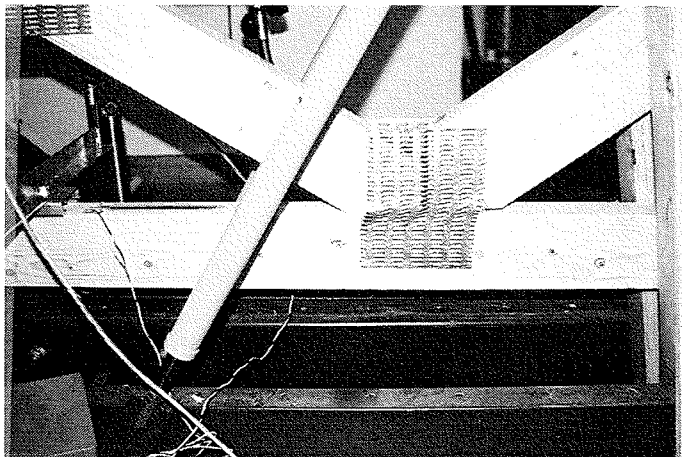


Figure 5-4

Joint line failure of truss 4.



INTERNATIONAL COUNCIL FOR BUILDING RESEARCH STUDIES AND DOCUMENTATION
WORKING COMMISSION W18 - TIMBER STRUCTURES

**THE MOMENT RESISTANCE OF TEE AND BUTT - JOINT NAIL PLATE TEST
SPECIMENS - A COMPARISON WITH CURRENT DESIGN METHODS**

by

A Reffold,
L R J Whale
Gang-Nail System Ltd.
England
B S Choo
University of Nottingham
England

MEETING TWENTY - NINE

BORDEAUX

FRANCE

AUGUST 1996

1. Introduction

Eurocode 5 establishes a method of designing for the effects of moments in the joints of nail-plated structures. This paper compares the experimental performance of such joints with the design method given in Eurocode 5 and with the proposed plastic design method by Noren et al [1].

Typically trussed rafters have joints that resist a combination of axial force and moment, where the ratio of axial stress to bending stress is high. The inclusion within Eurocode 5 of a joint design method that accounts for the effects of moments provides designers with a tool for analysing more indeterminate structures and for designing structures with joints at positions of high moment. It is the desire for flexibility of form and potential new markets arising from this ability that provides the motivation for the analyses and test results presented here.

The paper starts by analysing the moment anchorage capacity of 20 standard shear tests and 20 beam tests carried out by Bettison et al. [2]. The anchorage capacities from a further 160 moment tests on Butt and Tee joint specimens encompassing a wide range of bending moment, axial force and shear force combinations are then presented and compared with the design methods.

2. Materials

2.1 Timber

All the joint specimens featured in this paper were manufactured from European Whitewood, (*Picea Abies*) M75 grade trussed rafter material. The timber was visually selected, cut as required and, where appropriate, matched ends were jointed by the nailplates to form the specimens. The specimens were held in a conditioning room prior to testing. The mean moisture content at the time of testing was 13.2% within a range of 8.5% to 17.5%. The mean dry density of the specimens was 435 kg/m³ within a range of 337 kg/m³ to 569 kg/m³ and Young's Modulus varied from 9.09 to 15.15 kN/mm². The laboratory mean temperature and relative humidity were 20.5°C and 58% respectively.

2.2 Nailplates

Gang-Nail GN20 plates were used throughout the test series. The plates are nominally 1mm thick with 9.5mm long nails. Figure 1 shows a typical GN20 nail plate.

3. Test Series

3.1 General

All the testing was carried out at The University of Nottingham, England. The test arrangements and procedures are described briefly here and more detail is available in CIB Paper 29-7-4. [2].

The test series had two main objectives:-

- i) to carry out tests similar to those performed by Kevarinmaki et al [3] and to compare the anchorage load carrying capacities with the current Eurocode 5 design method and other theories. Two types of joint were tested:
 - standard shear tests in accordance with prEN1075 [4] (joint type J5).
 - beam specimens (joint type J6) similar to those used by Kyrkjeeide et al [5].
- ii) to carry out tests on specimens representing a wide range of practical situations in which the ratios of applied moment to direct load were varied and to compare the anchorage load carrying capacities with Eurocode 5 and other theories. Two principle types of joint were tested:
 - Butt joint specimens in which axial load and shear forces were applied in addition to the bending force (joint type JT1 and JT3).
 - 'Tee' joint specimens in which the bending and direct force ratios were varied (joint type JT2 and JT4).

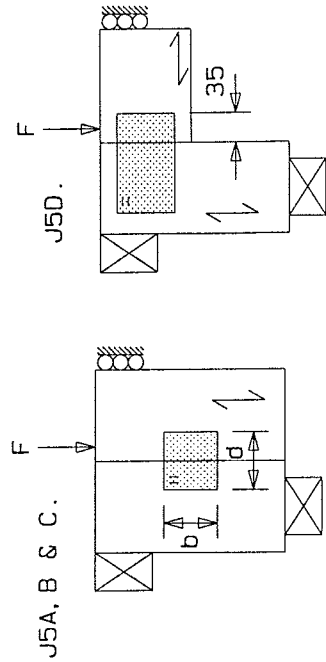
Table 2 gives a summary of the test configurations for the shear test and beam test specimens and Tables 3 and 4 give a summary of the test configurations for the butt joint and tee joint specimens respectively.

3.2 Ultimate Joint Strength and Timber Densities

It is generally accepted that there is a correlation between timber density, moisture content and joint strength. Other researchers [Kevarinmaki et al] have adjusted the test result values using a method that takes account of the specimen density and moisture content, with the aim of making all the results correspond to a datum density. The adoption of a similar adjustment was considered here. However, it was very difficult to see a correlation between ultimate strength, density and moisture content in our moment test results. The application of a density correction factor similar to that applied by Kevarinmaki et al would have made a significant change to some results (up to 25%) and in view of the apparent absence of a clear trend in the test results it was decided not to apply a density adjustment to the ultimate loads.

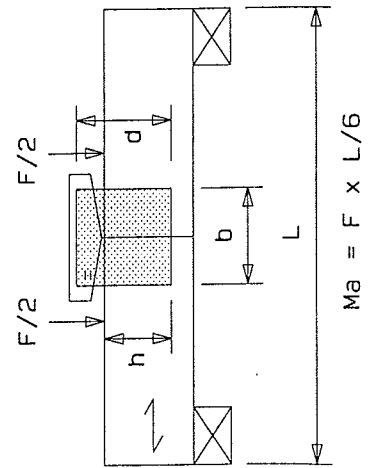
TABLE 2: SUMMARY OF STANDARD SHEAR TESTS AND BEAM TESTS

SHEAR TESTS



Joint Type	n	Plate Size		Orientation		Mean Fmax (kN)	Failure Mode A = Anchorage
		d	b	α	β		
J5A	5	76	71	0	0	10.55	A
J5B	5	76	71	90	0	10.36	A
J5C	5	76	71	45	0	9.88	A
J5D	5	76	185	90	90	10.87	A

BEAM TESTS



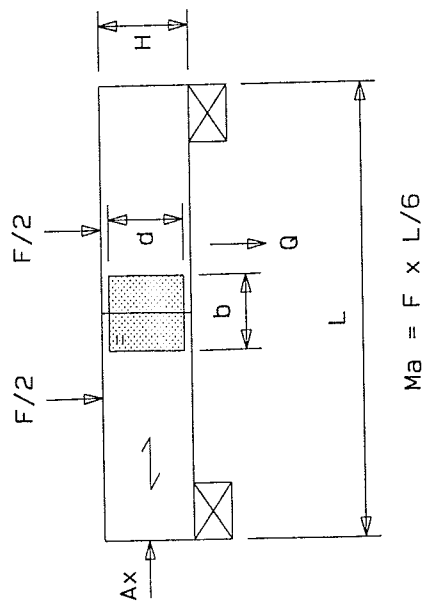
Joint Type	n	Plate Size		Bite h	Angle of plate to grain	Mean Ma max (kNm)	Failure Mode A=Anchorage
		d	b				
J6A	5	127	129	92	0	1.040	A
J6B	5	127	129	90	90	0.900	A
J6C	5	152	157	112	0	1.916	A
J6D	5	152	157	112	90	1.499	A

TABLE 3: SUMMARY OF BUTT JOINT TESTS

Joint Type	n	Plate Size d x b		Angle of Plate to Grain	Timber Size B x H		Axial Force*AX (kN)	Shear Force Q (kN)	Mean Ma max (kNm)	Failure mode A=Anchorage S=Steel
J1T1	5	101	99	0	35	120	0	0	1.12	A
J1T2	5	101	99	0	35	120	-5.4	0.45	0.76	A
J1T4	5	101	99	0	35	120	5.4	0.45	1.00	A
J1T6	5	101	99	90	35	120	-5.4	0.45	0.79	A
J1T8	5	101	99	90	35	120	5.4	0.45	0.89	A
J1T9	5	152	343	0	35	169	0	0	3.44	S
J1T10	5	152	343	0	35	169	-8.0	0.45	2.94	S
J1T12	5	152	343	0	35	169	8.0	0.45	3.46	S
J3T1	5	101	142	0	35	120	0	0	1.47	A
J3T2	5	101	142	0	35	120	5.4	0.45	1.69	A
J3T3	5	101	142	0	35	120	-5.4	0.45	1.13	S
J3T4	5	101	142	0	35	169	0	0	1.82	A
J3T5	5	101	142	0	35	169	5.4	0.45	1.92	A
J3T6	5	101	142	0	35	169	-5.4	0.45	1.71	A
J3T7	5	101	142	30	35	169	0	0	1.62	A
J3T8	5	101	142	30	35	169	5.4	0.45	1.62	A
J3T9	5	101	142	30	35	169	-5.4	0.45	1.63	A

* Axial Force Ax: minus sign (-) denotes compression force.

BUTT JOINTS



TEE JOINTS

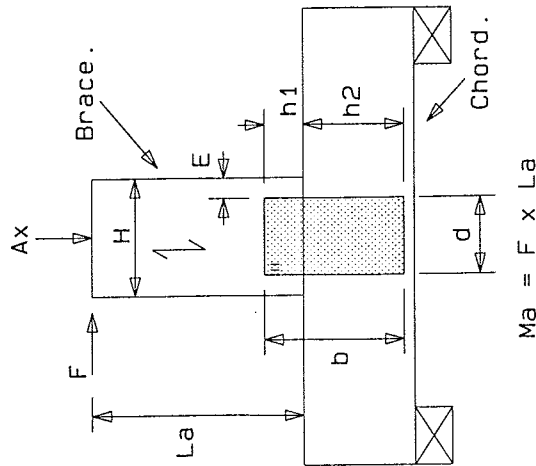


TABLE 4: SUMMARY OF TEE JOINT TESTS

Joint Type	n	Plate Size d x b	h1	h2	Timber size B x H	Edge Dist. E	Axial Force * Ax (kN)	Mean Fmax (kN)	La (m)	Mean Ma max (kNm)	Angle of plate to brace	Mode of failure A = Anchor S = Steel T = Timber
J2T1	5	101 x 99	=	=	35 x 120	9.5	-5.4	1.2	0.9	1.08	0	T
J2T2a	3	101 x 99	=	=	35 x 120	9.5	0	1.16	0.9	1.05	0	T
J2T2b	2	101 x 99	=	=	35 x 120	9.5	0	2.86	0.3	0.86	0	T
J2T3	5	101 x 99	=	=	35 x 120	9.5	5.4	0.83	0.9	0.75	0	T
J2T5	5	101 x 99	=	=	35 x 120	10.5	-5.4	1.02	0.9	0.92	90	S
J2T7	5	101 x 99	=	=	35 x 120	10.5	5.4	0.71	0.9	0.64	90	T
J2T9	5	152 x 343	=	=	35 x 169	8.5	-8.0	2.27	0.9	2.05	0	S
J2T10	5	152 x 343	=	=	35 x 169	8.5	0	2.44	0.9	2.20	0	S
J2T11	5	152 x 343	=	=	35 x 169	8.5	8.0	2.26	0.9	2.04	0	S
J4T1	5	101 x 185	52	133	35 x 155	27	0	8.8	0.15	1.32	0	A
J4T4	5	101 x 185	52	133	35 x 155	27	0	1.43	0.9	1.29	0	A
J4T5	5	101 x 185	52	133	35 x 155	27	5.4	1.08	0.9	0.98	0	A
J4T6	5	101 x 185	52	133	35 x 155	27	-5.4	1.46	0.9	1.32	0	A
J4T8	5	101 x 185	52	133	35 x 169	5	5.4	0.99	0.9	0.89	0	S
J4T9	5	101 x 185	52	133	35 x 169	5	-5.4	1.19	0.9	1.08	0	S
J4T11	5	101 x 185	52	133	35 x 155	49	5.4	1.34	0.9	1.21	0	A
J4T12	5	101 x 185	52	133	35 x 169	63	-5.4	2.04	0.9	1.84	0	S
J4T7a	5	101 x 185	52	133	35 x 169	5	0	6.87	0.15	1.03	0	S
J4T8a	5	101 x 185	52	133	35 x 169	5	0	3.74	0.30	1.12	0	A
J4T9a	5	101 x 185	52	133	35 x 169	63	0	14.7	0.15	2.21	0	S

* Axial Force Ax: - minus sign (-) denotes compression force
T = Tension perpendicular to grain failure

3.3 Shear Test and Beam Test - Analysis of Results

The shear test and beam test analyses are given in table 5. Figure 2 shows the effective plate areas adopted to calculate the geometric plate properties used in the analysis.

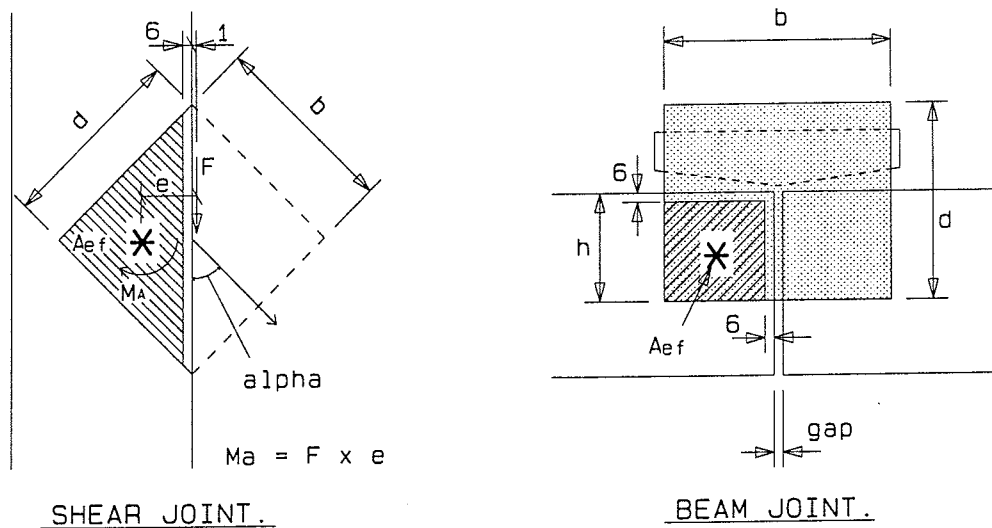


Figure 2 - Effective plate areas for shear tests and beam tests

The presented F_{max} in table 5a (shear tests) is the lesser value of either the ultimate F_{max} or the F_{max} recorded at 6mm shear displacement (despite sizing the plates to ensure an anchorage failure occurred, large shear deformations were observed in some shear tests before an anchorage failure resulted). A 6mm deflection limit was chosen as this is the criteria given in prEN1075 for the determination of steel shear failure in nailplate joint tests.

The ultimate test loads have been compared with the Eurocode 5 [6] method (EC5) and with Norens methods (plastic *noren*) as well as the true theoretical plastic method (plastic *theor*). The resulting stresses have been determined using the following equations:-

$$\tau_f = \frac{F_{max}}{2A_{ef}} \quad (4a)$$

$$\tau_{m_{ec5}} = \frac{M_{a_{max}}}{2z_{polar}} \quad (4b)$$

TABLE 5 RESULTS OF COMPARISON STUDY
Shear Tests and Beam Tests

Table 5a - Shear Tests (J5)

Joint Type	Mean Fmax (kN)	Resulting Stresses				EC5				Plastic Noren		Plastic Theory	
		τ_{f}	$\tau_{m_{ec5}}$	$\tau_{m_{noren}}$	$\tau_{m_{theor}}$	Vcal (1) eqn4e	$\frac{F_{max}}{Vcal}$ (1)	Vcal (2) eqn4f	$\frac{F_{max}}{Vcal}$ (2)	Vcal (3) eqn4g	$\frac{F_{max}}{Vcal}$ (3)	Vcal (4) eqn4g	$\frac{F_{max}}{Vcal}$ (4)
J5A	10.55	2.32	4.11	2.74	2.61	7.51	1.41	6.43	1.64	7.68	1.37	7.91	1.33
J5B	10.36	2.31	3.69	2.47	2.36	8.20	1.26	6.77	1.53	7.13	1.45	7.26	1.43
J5C	9.88	2.24	5.48	3.39	2.63	5.28	1.87	4.96	1.99	6.27	1.57	7.35	1.35
J5D	10.87	2.42	3.88	2.58	2.47	8.20	1.33	6.77	1.61	5.64	1.93	5.7	1.91
Mean							1.47		1.69		1.58		1.51
Standard Deviation							0.275		0.20		0.24		0.27

Table 5b - Beam Tests (J6)

Joint Type	Mean Mmax (kNm)	Resulting Stresses			EC5				Plastic Noren		Plastic Theory	
		$\tau_{m_{ec5}}$	$\tau_{m_{noren}}$	$\tau_{m_{theor}}$	Mcal (1) eqn4e	$\frac{M_{max}}{Mcal}$ (2)	Mcal (2) eqn4f	$\frac{M_{max}}{Mcal}$ (2)	Mcal (3) eqn4g	$\frac{M_{max}}{Mcal}$ (3)	Mcal (4) eqn4g	$\frac{M_{max}}{Mcal}$ (4)
J6A	1.04	6.46	4.31	4.03	0.47	2.21	0.63	1.65	0.63	1.65	0.67	1.54
J6B	0.90	5.89	3.93	3.67	0.45	2.01	0.59	1.50	0.59	1.50	0.64	1.40
J6C	1.916	6.10	4.07	3.80	0.92	2.08	1.23	1.55	1.23	1.55	1.32	1.45
J6D	1.499	5.10	3.40	3.18	0.86	1.74	1.15	1.30	1.15	1.30	1.23	1.22
Mean						2.01		1.50		1.50		1.40
Standard Deviation						0.198		0.147		0.147		0.134

$$\tau m_{noren} = \frac{2Ma \max}{Aef(d)} \quad (4c)$$

$$\tau m_{theor} = \frac{Ma \max}{2Wp_{theor}} \quad (4d)$$

where:

$$z_{polar} = (I_{xx} + I_{yy})/r_{max}$$

$$d = \text{"diagonal" according to Noren [1]}$$

$$Wp_{theor} = (Aef \times r) \text{ da (See Kevarinmaki [7])}$$

The presented maximum loads (V_{cal} and M_{cal}) in Table 5 are calculated from the following criteria:

$$\text{Eurocode 5} \quad \{\tau m_{ec5} \leq 2. fa9090 \quad (4e)$$

$$\{\tau f + \tau m_{ec5} \leq 1.5. fa00 \quad (4f)$$

$$\text{Plastic method} \quad \left(\frac{\tau f}{fa\alpha\beta} \right)^2 + \left(\frac{\tau m_{pl}}{fa00} \right)^2 \leq 1.0 \quad (4g)$$

where:

τm_{pl} is either τm_{noren} or τm_{theor} as appropriate.

3.4 Butt Joint and Tee Joint - Analysis of Results

The butt joint and the joint analyses are given in Table 6. Figure 3 shows the effective plate areas adopted to calculate the geometric properties used in the analysis.

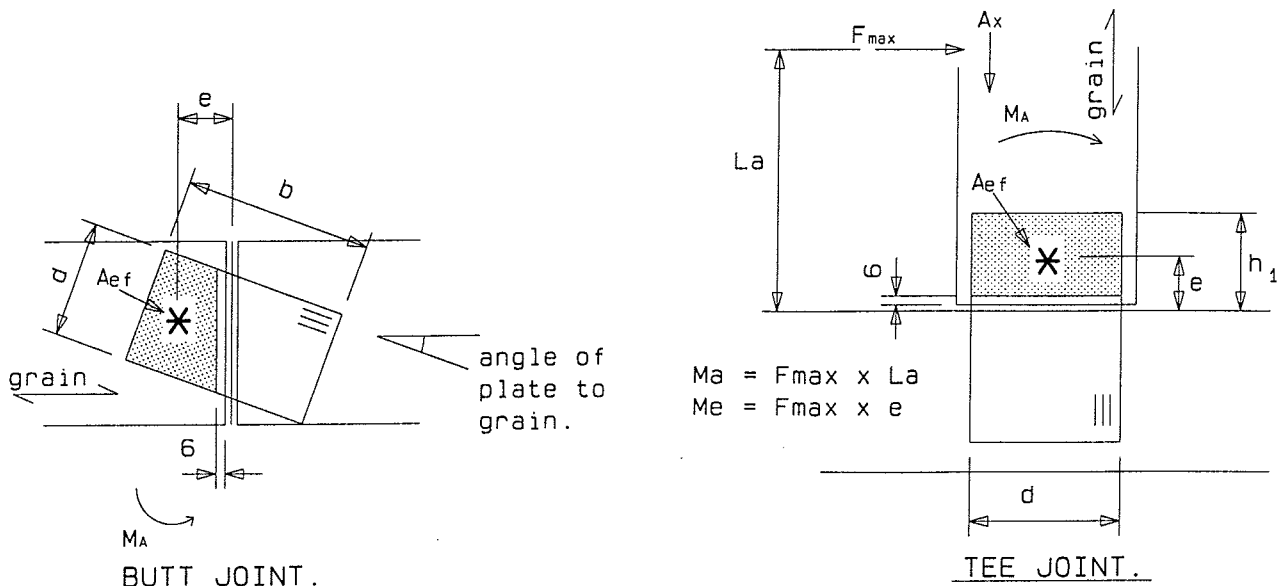


Figure 3: Effective Plate Areas For Butt and Tee Joints

TABLE 6 - RESULTS OF COMPARISON STUDY - BUTT JOINTS AND TEE JOINTS

Joint Type *	Resulting Stresses				EC5 Stress Index		Plastic Noren Stress Index $\frac{\tau f}{fa\alpha\beta} + \frac{\tau mnoren}{fa00}$ **	Plastic Theory Stress Index $\frac{\tau f}{fa\alpha\beta} + \frac{\tau mtheor}{fa00}$
	τf	τm_{ec5}	τm_{noren}	τm_{theor}	$\frac{\tau m}{2fa9090}$	$\frac{\tau f + \tau m}{1.5 \cdot fa00}$		
Butt Joints	J1T1	0.0	6.95	4.64	4.41	2.38	1.77	1.69
	J1T2	0.31	6.76	4.51	4.29	2.31	1.80	1.76
	J1T4	0.61	8.25	5.5	5.24	2.82	2.26	2.24
	J1T6	0.31	7.00	4.68	4.45	2.39	1.86	1.84
	J1T8	0.61	7.62	5.10	4.85	2.60	2.10	2.14
	J3T1	0.0	5.59	3.73	3.49	1.91	1.43	1.33
	J3T2	0.41	7.69	5.13	4.80	2.63	2.06	1.99
	J3T4	0.0	6.92	4.62	4.32	2.37	1.76	1.65
	J3T5	0.41	8.56	5.71	5.34	2.93	2.29	2.20
	J3T6	0.21	7.77	5.18	4.84	2.65	2.03	1.93
	J3T7	0.0	6.91	4.44	3.89	2.36	1.76	1.49
	J3T8	0.42	8.28	5.32	4.69	2.83	2.22	1.95
	J3T9	0.21	8.36	5.37	4.71	2.85	2.18	1.88
	J4T1	0.95	9.16	6.11	5.80	3.13	2.58	2.86
J4T4	0.15	7.75	5.16	4.90	2.65	2.01	1.98	
J4T5	0.59	5.88	3.92	3.73	2.01	1.65	1.65	
J4T6	0.33	7.93	5.28	5.02	2.71	2.10	2.06	
J4T8a	0.40	7.15	4.76	4.53	2.44	1.92	2.06	
J4T11	0.60	7.21	4.81	4.56	2.46	1.99	1.98	
			Mean		2.55	1.98	2.05	1.93
			Standard Deviation		0.305	0.266	0.329	0.327

* Only comparisons for test specimens failing in anchorage are included here. However, many specimens with steel or timber failure exceeded the calculated anchorage strength. For example joint type J2T1 to J2T5 inclusive all failed in the timber, but the anchorage stress indices were all in the range 1.4 to 2.0

** The proposed verification for the plastic design methods is $\left(\frac{\tau f}{fa\alpha\beta}\right)^2 + \left(\frac{\tau m_{plastic}}{fa00}\right)^2 \leq 10$. However, since all these test results give a value greater than 1.0, the 'squared' term gives a misleading effect to the comparison. The stress indices in the table are numerically the same as presenting M_{max}/M_{cal} as used in Table 5.

The resulting stresses (τ_f , $\tau_{m_{ec5}}$, $\tau_{m_{noren}}$, $\tau_{m_{theor}}$) have been determined using equations 4a to 4d inclusive. The presented stress indices in Table 6 (EC5, plastic *noren*, plastic *theor*) are determined from equations 4e to 4g inclusive and are all directly comparable to the maximum load/calculated load ratios given in Table 5.

4. Discussion

4.1 Beam Specimens

The relative performance of the beam tests when the ultimate strengths are compared with calculated resistances was very similar to those analysed by Kevarinmaki et al. It is notable that for the EC5 method the τ_f equation (4e) is considerably more conservative than the $\tau_f + \tau_m$ equation (4f), giving mean conservatism ratios (M_{max}/V_{cal}) of 2.01 and 1.50 respectively. The plastic methods give the best correlation with mean conservatism ratios (M_{max}/V_{cal}) of 1.50 for Noren's method and 1.40 for the true theoretical method.

By comparison, mean conservatism ratios of 1.43, 1.34, 1.34 and 1.24 for EC5 (eqn 4e), EC5 (eqn 4f), plastic *noren* and plastic *theor* respectively were derived from work carried out by Kevarinmaki et al [3].

One anomaly worth noting is that beam joints with nail plates perpendicular to the grain (J6B and J6D) are only 82% as strong as with nailplates parallel to the grain (J6A and J6C). This phenomenon is not recognised in the design methods (equations 4e, 4f and 4g) since $\tau_f = 0$ and the angle of plate to grain is given no significance in the design methods.

4.2 Shear Specimens

The shear tests all exhibited anchorage failures although some of these were recorded after considerable shear deflection had taken place. The presented F_{max} values are the lesser of either the ultimate F_{max} or the F_{max} recorded at 6mm shear displacement as described earlier. Even so, the mean conservatism ratios (F_{max}/V_{cal}) for the Eurocode 5 method, plastic *noren* and plastic *theor* methods are 1.69, 1.58 and 1.51 respectively. In the case of the shear tests the Eurocode $\tau_f + \tau_m$ equation (4f) is the most onerous since τ_f is relatively high (about 0.85 of τ_f characteristic). The conservatism ratios are higher than those observed by Kevarinmaki et al [3] who presented values of 1.13, 1.07 and 1.02 for the Eurocode 5, plastic *noren* and plastic *theor* methods respectively.

Care was exercised in selecting small nailplates (76mm x 71mm) where the anchorage strength was much less than the shear strength to precipitate an anchorage failure. This need to size the nailplates to avoid shear failure imposes severe restrictions on the nailplate size (and resulting A_{ef}) and aspect ratio (d/b) that may be selected for testing. In our case the width of effective plate perpendicular to the joint line was; $(76/2)-6=32$ mm. The observed shear displacements suggest this figure should have been nearer to 25mm (about 4 rows of

teeth). It seems questionable whether moment anchorage capacities of nailplates should be verified from such artificially small effective areas. For this reason it may be possible that the shear test arrangement is not universally suitable for determining the moment anchorage strength with all nailplate types. Indeed, this view may even be upheld by the results of Kevarinmaki, Kangas CIB paper 25-14-1 [8] in which moment anchorage capacities for eleven nailplate types were evaluated using the shear test method. Some nailplate types had consistent mean conservatism ratios similar to those presented here.

4.3 Butt Joints

The butt joint tests (joint types J1 and J3) introduced constant axial and shear forces into specimens in which a varying bending force was applied until an anchorage failure was recorded. Timber contact occurred in all specimens. When comparing the ultimate strengths of the butt joints with the Eurocode 5 design method, equation 4e (2.Fa9090) was always more onerous than equation 4f (1.5.fa00) with mean conservatism ratios of 2.51 and 1.96 respectively. The plastic *noren* method (equation 4g) gave a mean conservatism ratio of 1.99 and the plastic *theor* method gave a mean conservatism ratio of 1.85. The conservatism ratios given here are considerably higher (30%) than those given earlier for the beam tests (emulating Kyrkjeelde et al). Much of this difference can be attributed to the occurrence of timber contact which modifies the moment rotational behaviour of the joint.

Joints with a compression force generally had a lower bending strength than joints with a tension force.

4.4 Tee Joints

The tee joints (J4) introduced a varying shear force (inducing a τ_f and τ_{m_e} -see figure 3) together with a varying bending force (M_a) created by the lever arm (L_a). By changing the lever arm length it was possible to alter the ratios of applied force (F_{max}) to bending force (M_{max}). The longest lever arm (900mm) produces a low force to moment ratio ($\tau_f=0.41$) whilst the shortest lever arm (150mm) produces a higher force moment ratio ($\tau_f=0.67$) but these only represent 15% and 45% of the relevant characteristic anchorage strengths compared with 85% observed in the shear tests.

Considering joint types J4T1 (150 L_a) and J4T4 (900 L_a) and referring to table 4, it would appear that the external anchorage moments are fairly similar (1.32 kNm and 1.29 kNm respectively). However, when the effects of the internal moment (M_e in figure 3) are considered in the analysis the resulting stress indices are markedly different; J4T1 indices are 3.13, 2.58, 2.98 and 2.86 whilst J4T4 indices are 2.65, 2.01, 2.08, 1.98 for the EC5 (equation 4e), EC5 (equation 4f), plastic *noren* and plastic *theor* respectively.

The stress indices for J4T1 are between 18% and 40% more conservative than those of J4T4. A further study of the analysis shows that for joint J4T1 the total anchorage stress comprises; 76% from M_a , 15% from M_e and 9% from F_a (shear induced). This compares with 95% from M_a , 3% from M_e and 2% from F_a (shear induced) for joint J4T4.

This may suggest that the internal moment (M_e) may not have the same effect on nailplate behaviour as the external moment (M_a).

Another feature that was varied in the tee joint tests was the nailplate to timber compression edge distance (E , in table 4). Whilst some of these specimens produced a steel failure (even though the nailplates were sized using EC5 criteria to produce an anchorage failure) it is worth considering joint types J4T7a and J4T9a in table 4. Both joint types had 150mm lever arms. J4T7a had a distance $E=5$ mm, whilst in J4T9a $E=63$ mm. Joint J4T7a resisted an applied moment of 1.12 kNm ($\tau_{m_{ec5}}=6.96$) and joint J4T9a resisted a moment of 2.21 kNm ($\tau_{m_{ec5}}=15.75$) before a steel failure resulted. The design methods predict the same ultimate anchorage strengths for each joint (and incidentally the same ultimate steel capacities). The observed higher anchorage resistance (and steel strength) of joint type J4T9a is believed to be due to timber contact once again.

The mean stress indices of all the tee joints presented in table 6 for the Eurocode 5 design criteria (equations 4e to 4f) are 2.23 and 2.04 respectively.

The mean stress indices for the plastic *noren* and plastic *theor* methods are 2.18 and 2.09 respectively.

4.5 Overview

A summary of the mean nailplate anchorage conservatism ratios for the four joint types tested and analysed in this study together with comparable conservatism ratios observed by Kevarinmaki et al are given in table 7.

Joint Type	DESIGN METHOD			
	EC5		Plastic <i>Noren</i>	Plastic <i>Theor</i>
	Eqn 4e	Eqn 4f		
Shear (J5)	1.47 (-)	1.69 (1.13)	1.58 (1.07)	1.51 (1.02)
Beam (J6) no contact	2.01 (1.43)	1.50 (1.34)	1.50 (1.34)	1.40 (1.24)
Butt (J1,J3) contact	2.54	1.96	1.98	1.85
Tee (J4) long lever arm, low shear	2.45	1.93	2.01	1.91
Short lever arm, high shear	2.78	2.25	2.54	2.46

values in parenthesis are mean conservatism ratios presented by Kevarinmaki et al [3] for similar style tests.

Table 7 Mean Conservatism Indices

In summary, the shear tests did not correlate as well with the design methods as those carried out by Kevarinmaki et al. This may be due in part to difficulty in obtaining anchorage failure in the specimens without excessive shear deflection. This in turn indicates that the shear test method may not be suitable for all nailplate types as a means of verifying moment anchorage capacity.

The conservatism ratios of the beam tests were similar to the values recorded by Kevarinmaki et al with the exception of the Eurocode 5 equation 4e where a conservatism ratio of 2.01 was recorded.

The butt and tee joints correlated least well with the design methods with the short lever arm (high shear) being the most conservative. Much of this conservatism is probably due to timber contact.

Figure 4 shows a graph of limiting anchorage stress for the Eurocode 5 design criteria equations 4e and 4f. Plotted on the graph are the relevant positions of some of the test results presented here together with the relevant positions of some of the analysis carried out by Kevarinmaki et al. Figure 5 shows a similar graph for the plastic *noren* method in the case where α and $\beta=0$. (Unlike Eurocode 5 which takes no account of α and β when considering moments, the plastic design method would require a different trace for each value of α and β .) Figure 5 has the relevant positions of some analyses plotted as described for figure 4.

Figures 4 and 5 serve to illustrate that all the testing done to date has been concentrated in two main areas:

- i) areas of low direct force (τ_f) and high moment (τ_m).
- ii) areas of moderate direct force and moderate moment.

In the case of ii) above, the direct force is induced by shear and the moment is totally a result of eccentricity.

It is clear that there are large parts of the τ_f/τ_m surface that have not been explored, either in this study or in the studies of Kevarinmaki et al. Much of the nailplate anchorage design method in Annex D of Eurocode 5 is therefore still unverified.

5. Conclusions

The shear and beam tests were carried out with the intention of following the work of Kevarinmaki et al and providing a bench mark against which to compare the butt and tee joint tests. The butt and tee joint tests were intended to represent a range of typical joints that might be designed in practice. The aim was to observe how the ultimate strength of such joints compared with the design theories which were themselves validated from shear tests.

The test series sought to probe the effects of varying direct force to moment ratios as well as observe the effects of timber contact on moment resistance.

- Legend for conservatism ratios:
- 1 denotes mean of butt joints with no axial force. J1T1,J3T1/4.
 - 2 denotes mean of butt joints with compression force. J1T2/6,J3T6.
 - 3 denotes mean of butt joints with tension force. J1T4/8,J3T2/5/8.
 - 4 denotes J4T1
 - 5 denotes J4T4
 - 6 denotes J4T5
 - 7 denotes J4T8a
 - 8 denotes J4T11
 - 9 denotes mean of all J5
 - 10 denotes mean of all J6
 - 11 denotes mean of shear tests[4]
 - 12 denotes mean of beam tests[4]

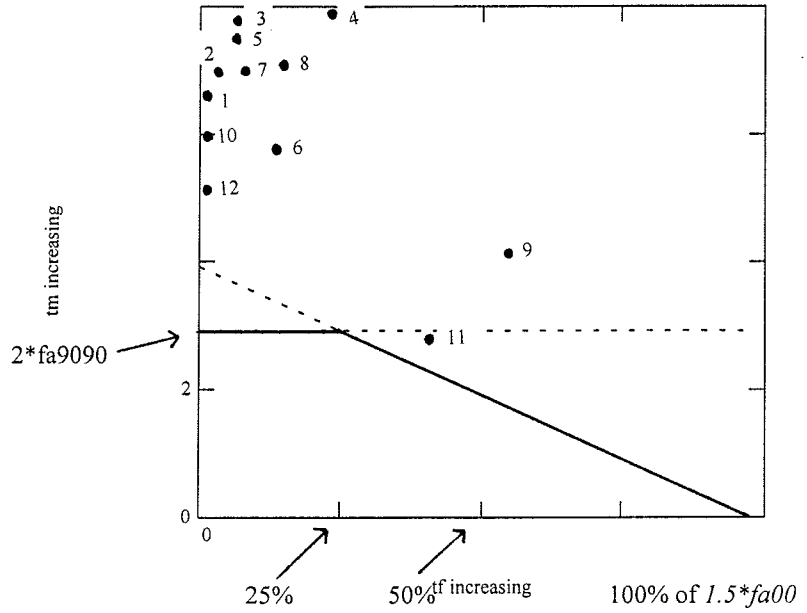


Figure 4.- τ_f, τ_m failure surface for Eurocode 5 (eqn. 4e&4f)

- Legend for conservatism ratios:
- A denotes mean of butt joints (J1) where α & $\beta=0$
 - B denotes mean of joint type J5A,B & C
 - C denotes mean of joint type J6
 - D denotes mean of shear tests[4] where α & $\beta=0$
 - E denotes mean of beam tests[4]

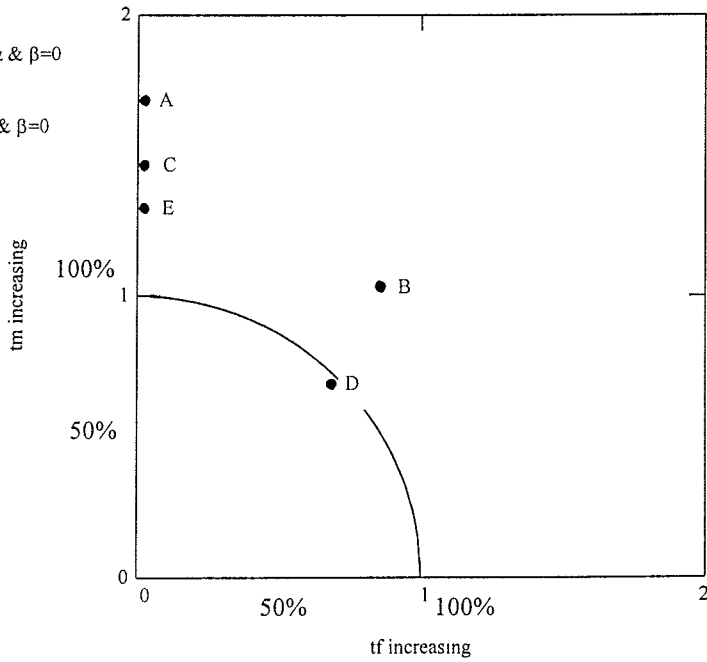


Figure 5.- τ_f, τ_m Failure surface for Plastic Noren (eqn. 4g) design method when $f_{a\alpha\beta} = f_{a00}$.

After considering the various analyses the following conclusions are drawn:-

- 1) The shear test method does not appear to be suitable for all nailplate types.
 - It imposes severe restrictions on nailplate area.
 - It imposes severe restrictions on nailplate aspect ratio (d/b)
 - It gives a fixed τ_f to τ_m ratio which is heavily weighted toward τ_f .
 - All τ_f and τ_m are implied by shear.

- 2) The existing design methods do not correlate well with the ultimate bending strengths of practical joints. (See table 7).
 - timber contact modifies joint behaviour and is a major influence on joint strength.
 - external moments (M_a) and internal moments (M_e) have a different effect on joint strength.
 - angle of nailplate to grain affects joint strength but is given no significance in pure moment joints.

- 3) The design methods are still largely untried over much of the τ_f/τ_m surface.

6. Recommendations

1. There is a need to undertake more testing and analysis to validate the efficacy of the design methods across the τ_f/τ_m surfaces.
2. Consideration should be given to deriving an anchorage design method that takes account of timber contact.
3. Further design criteria should be introduced to account for the 18% moment strength change due to angle of plate to grain in pure bending joints.
4. Further studies are needed to explore the relationship between external moment (M_a), internal moment (M_e) and their effect on joint strength.
5. Collaboration between interested parties would greatly assist in carrying out the above studies and lead to a greater understanding of the behaviour of nailplate joints.

7. References

1. Noren B. - Design of Joints with Nailplates. CIB W18. 14-7-1. 1981.
2. Bettison M., Choo B.S., Whale L.R.J. - A Critical Review of the Moment Rotation Test Method Proposed in prEN1075. CIB W18. 29-7-4. 1996.
3. Kevarinmaki A., Kangas J. - Moment Anchorage Capacity of Nailplates. CIB W18. 26-14-2.1993.

4. prEN1075. Timber Structures - Test Methods. Joints made with punched metal plate fasteners. ENTC 124.116:1992.
5. Kyrkjeeide O., Aune P. & Aasheim E. - Spikerplater med momentpakjenning. Universiteti Trondheim. 1992.
6. Eurocode 5: Design of Timber Structures. Part 1.1. Annex D. DD ENV 1995-1-1:1994.
7. Kevarinmaki A. - Solution of Plastic Moment Anchorage Stress in Nailplates. CIB W18. 26-14-4. 1993.
8. Kevarinmaki A., Kangas J. - Moment Anchorage Capacity of Nailplates in Shear Tests. CIB W18 25-14-1.

**INTERNATIONAL COUNCIL FOR BUILDING RESEARCH STUDIES AND DOCUMENTATION
WORKING COMMISSION W18 - TIMBER STRUCTURES**

**A CRITICAL REVIEW OF THE MOMENT ROTATION TEST METHOD PROPOSED
IN PREN 1075**

by

M Bettison

B S Choo

University of Nottingham

England

L R J Whale

Gang-Nail System Ltd.

England

MEETING TWENTY - NINE

BORDEAUX

FRANCE

AUGUST 1996

A Critical Review of the Moment Rotation Test Method Proposed in prEN1075

M Bettison and B S Choo
University of Nottingham, England

L R J Whale
Gang-Nail Systems Limited, England

1. INTRODUCTION

It is estimated (by the authors) that some 400 million nailplates (30 000 tonnes) are used annually throughout the European Community. This requirement is satisfied by well over 20 different plate types, supplied by over 10 manufacturers. Each plate type will presently be the subject of separate national testing and accreditation procedures to provide the necessary design data.

It is clear that there is a need for a European Standard which lays down standardised test procedures and interpretation rules for such products. PrEN1075⁵ is the draft for such a standard, setting out test procedures to determine the anchorage, tension, compression and shear capacity of nailplate joints, as well as their rotational stiffness characteristics.

This paper describes tests carried out in accordance with prEN1075 to determine the rotational stiffnesses of nailplate joints from shear tests. Two other series of tests were carried out, bending tests on beams in which the shear force was zero, and bending tests on tee joints in which the shear force was varied. The rotational stiffnesses obtained for these more practical joint configurations are then compared with the rotational stiffnesses from the shear tests.

2. TEST SPECIMENS

The test pieces, shown in Table 1, were manufactured using structural timber (European Whitewood) and Gang Nail nailplates type GN20, with a thickness of 1.0 mm. There were five specimens in each set of test pieces.

The timber properties were as follows:

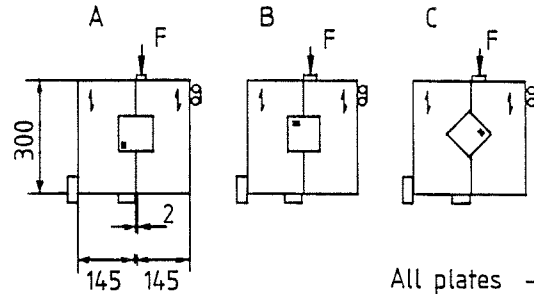
Density	-	mean = 435 kg/m ³ ,	range = 354 to 514 kg/m ³
Moisture content	-	mean = 13.2%,	range = 9.9 to 17.5%

Before testing the specimens were held in a curing room at 20°C ± 1°C and 65% relative humidity. During the test procedure in open laboratory conditions the temperature and relative humidity means and ranges were as follows:

Temperature	-	mean = 20°C,	range = 16 to 25°C
Relative humidity	-	mean = 55%,	range = 43 to 66%

Table 1. Test Specimens

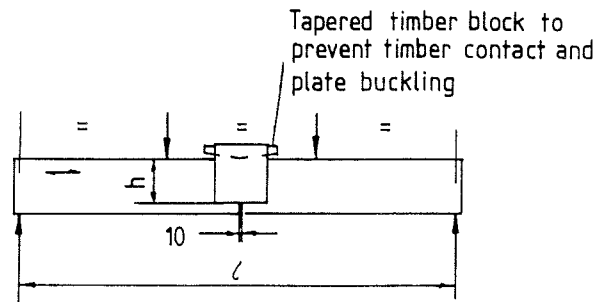
Test series	A	B	C
Plate size	76 x 71	76 x 71	76 x 71
Force/Plate angle α	0	90	45
Force/Grain angle β	0	0	0
Plate/Grain angle	0	90	45



All plates - GN-20
All timber - 35 x 145

Shear test specimens - Joint type J5

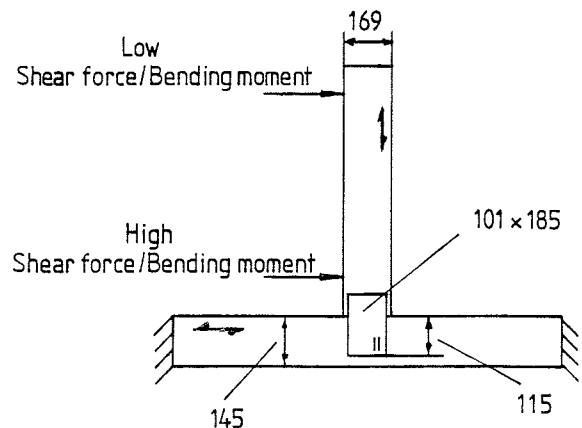
Test series	A	B	C	D
Plate size	127 x 129	127 x 129	152 x 157	152 x 157
Bite (h)	87	89	115	115
Plate/Grain angle	0	90	0	90



All plates - GN-20
All timber - 35 x 120

Beams - Joint type J6

Plate type	GN20	GN20
Plate orientation		
Test series	T1	T4
SF/BM	High	Low



Tee joints - Joint type J4

3. TEST PROCEDURE AND APPARATUS

Various apparatus were fabricated and assembled in order to carry out the tests.

For the shear tests and beam tests the apparatus shown in Figures 1 and 2 were installed in a screw driven universal test machine and loaded directly by the moving crosshead. Note that in the beam tests the central deflection of the beam was measured using additional deflection transducers mounted on the fabricated frame.

The tee joints were tested using a rotating arm mechanism as shown in Figure 3. In this arrangement the chord of the tee joint was fixed and the vertical web was loaded by the rotating arm. By changing the point of application of the bending load it was possible to change the shear force/bending moment ratio.

In all the tests, displacement measurements were made using linear potentiometers and the loads were measured using load cells. As far as possible the tests were conducted in accordance with EN26891¹ and prEN1075 and in the manner described by Kevarinmaki and Kangas² and Kyrkjeeide, Aune and Aasheim³.

A data logging system, linked to a PC, was used to record the various transducer outputs during the tests.

4. PRESENTATION OF TEST RESULTS

The determination of rotational stiffnesses from the test results, obtained for each of the three nailplated joint types, is based on the methods given in EC5 1995-1-1: 1994 Annex D⁴ and prEN1075⁵. The methods, using elastic theory only, are summarised below.

Shear Tests

$$\text{Rotational stiffness } K_{\phi \text{ el}} = 0.4 \tau_{M \text{ el max}} / \theta_{i \text{ mod}}$$

where $\tau_{M \text{ el max}}$ is the elastic moment anchorage stress at F_{max}

F_{max} = maximum applied force on effective plate area A_{ef}

$$\theta_{i \text{ mod}} = \frac{4}{3} (\theta_{0.4} - \theta_{0.1})$$

$\theta_{0.4}$ is the rotation angle between the plate and the timber at $0.4 F_{\text{max}}$

$\theta_{0.1}$ is the rotation angle between the plate and the timber at $0.1 F_{\text{max}}$

The moment anchorage stresses $\tau_{M \text{ el max}}$ were calculated as follows:

$$\tau_{m \text{ el max}} = \frac{M_{\text{max}} r}{I_p}$$

where M_{max} is the maximum internal bending moment induced on effective plate area A_{ef}

= F_{max} x distance from joint line to centroid of the effective plate area

I_p = polar moment of inertia of A_{ef} about the centroid

r = distance from centroid to the furthest point of the effective area

The effective area A_{ef} was obtained from the measured dimensions together with allowances for gaps and ineffective fixing at the joint line (6 mm).

Bending Tests (Beams)

The determination of rotational stiffness was similar to that for the shear tests except

$$\text{that } M_{\max} = \frac{F_{\max}}{2} \times \frac{l}{3} = \frac{F_{\max} l}{6}$$

where F_{\max} = maximum applied force
 l = distance between supports

An additional rotational stiffness based on the member total rotation was also determined; with the rotation angle calculated as shown below:

$$\theta_{t \text{ mod}} = \frac{4}{3} (\theta_{t0.4} - \theta_{t0.1})$$

where $\theta_t = \frac{\text{Beam central deflection}}{\frac{1}{2} \text{ span}}$, at $0.1 F_{\max}$ and $0.4 F_{\max}$

Bending Tests (Tee Joints)

The analysis was performed in a manner similar to that for the previous two joint types except that

$$M_{\max} = F_{\max} l + F_{\max} e \text{ (i.e. external moment + internal moment)}$$

where F_{\max} = force between the rotating arm and the web
 l = distance between the line of action of the force and the joint line
 = 900 mm in the low shear force tests and 150 mm in the high shear force tests
 e = distance from the joint line to the centroid of the effective plate area

Figures 4, 5 and 6 show plots of load against displacement using typical results obtained from the shear and bending tests.

The rotational stiffness values etc. obtained from the analysis of the test results are given in Tables 2, 3 and 4.

5. DISCUSSION OF RESULTS

Failure Modes

At ultimate load, the joints showed signs of distress, usually nail extraction and shear deformation at the joint line in the case of the shear test specimen, and nail extraction, plate buckling and plate tearing in the beam and tee specimens. The rotations at the ultimate load were in the range 5 - 10°.

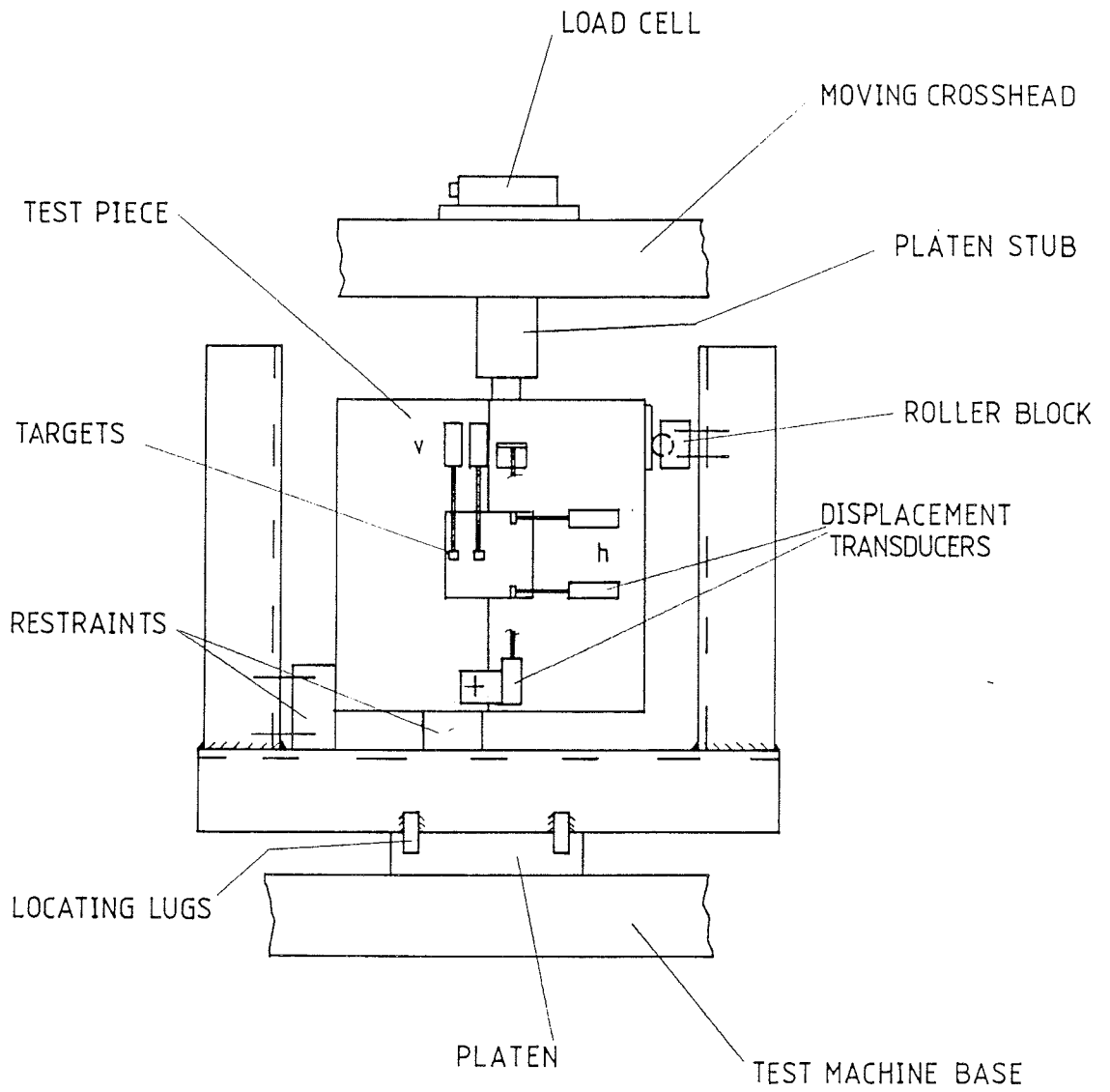
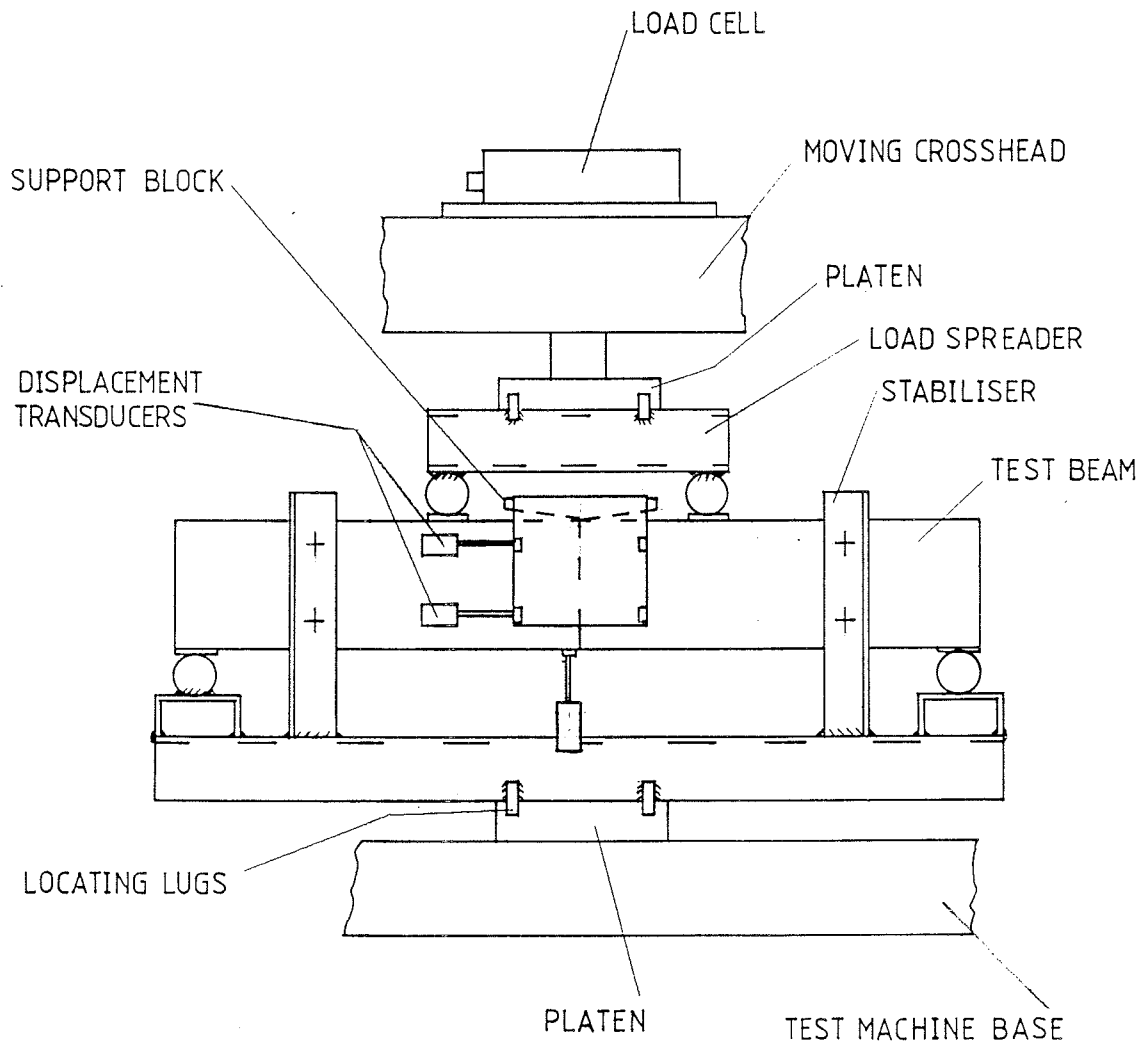


Figure 1. Shear Test Arrangement



SUPPORT SPAN $l = 900$
 LOAD SPAN $= 300$

Figure 2. Beam Test Arrangement

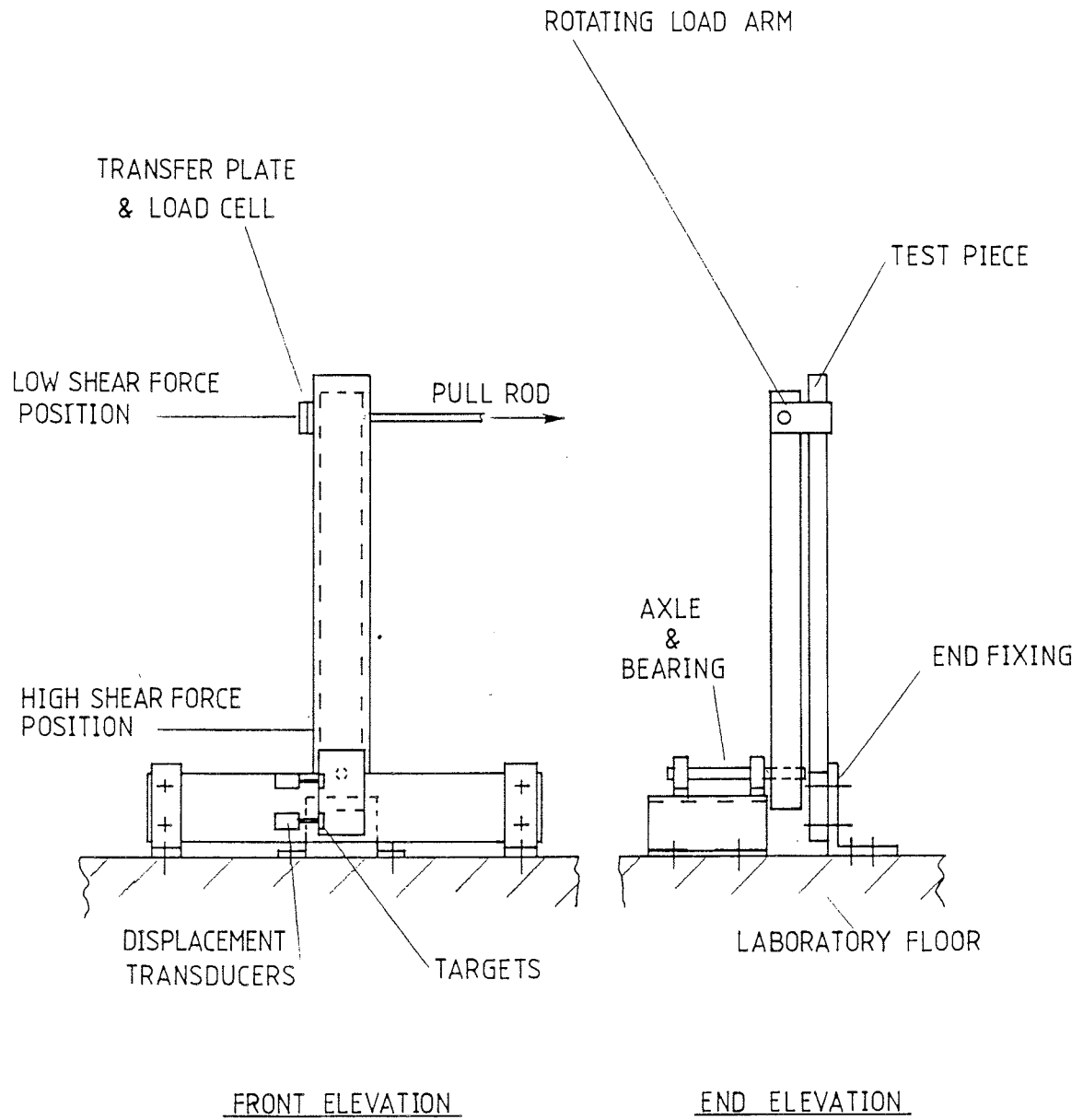


Figure 3. Tee Joint Test Arrangement

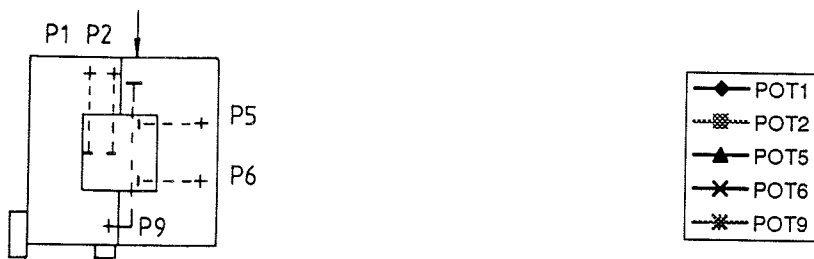
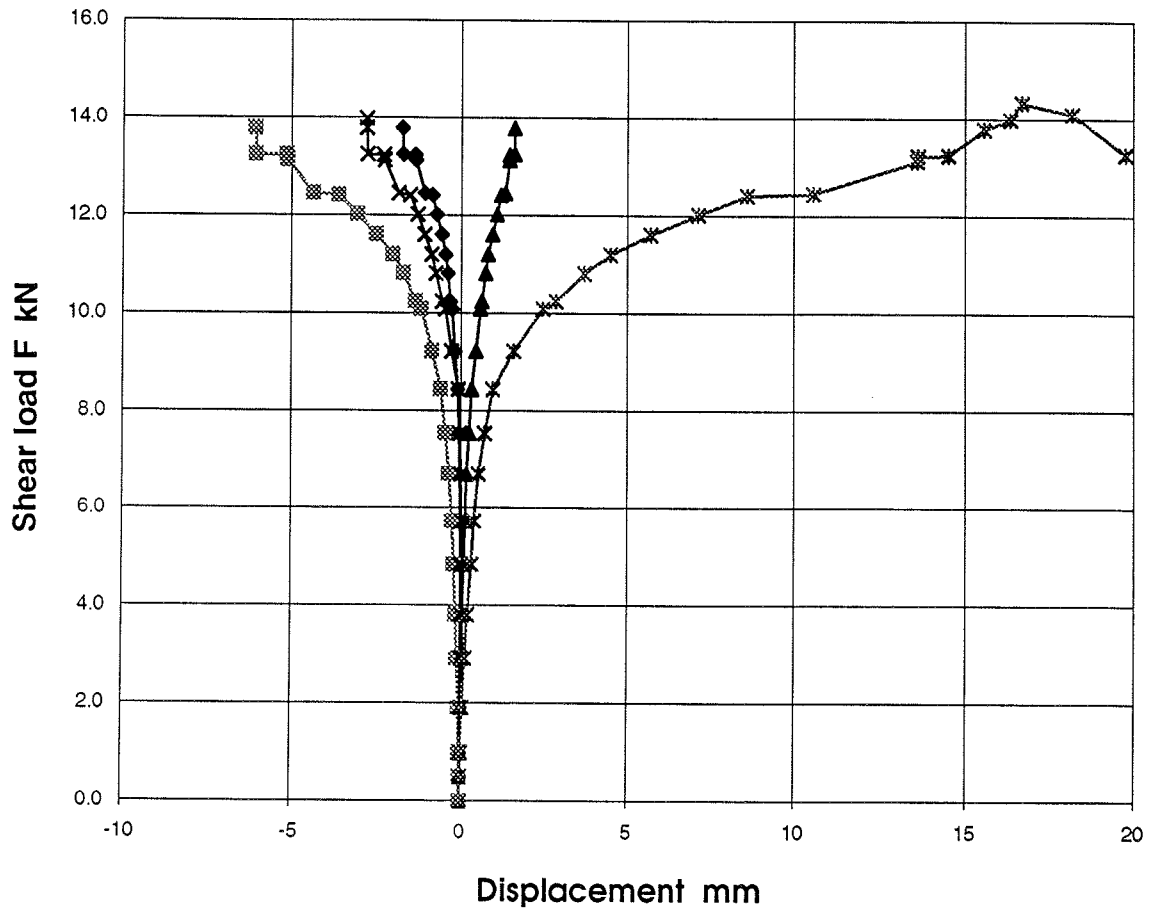


Figure 4. Graph Showing Shear Test Result for Joint Type J5A (Specimen 1)

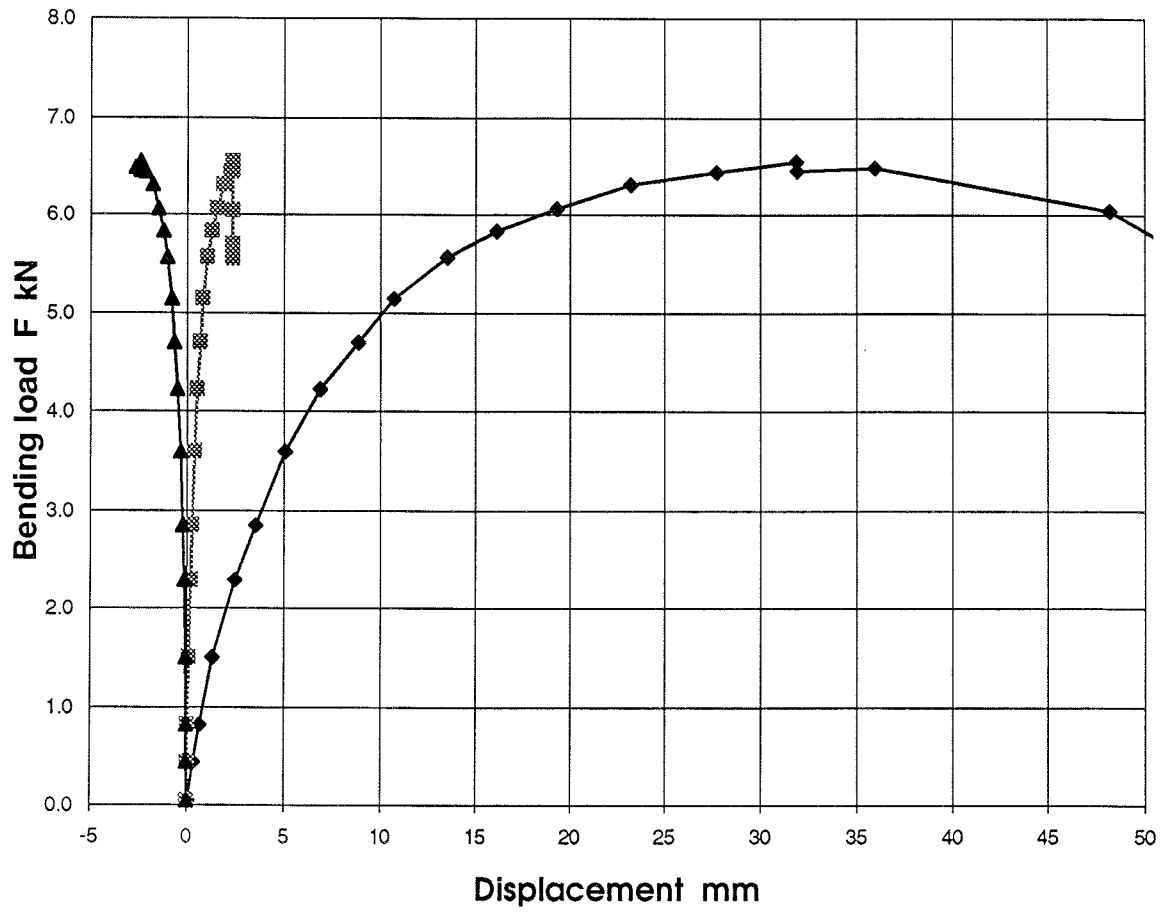


Figure 5. Graph Showing Bending Test Result for Joint Type J6A (Specimen 1)

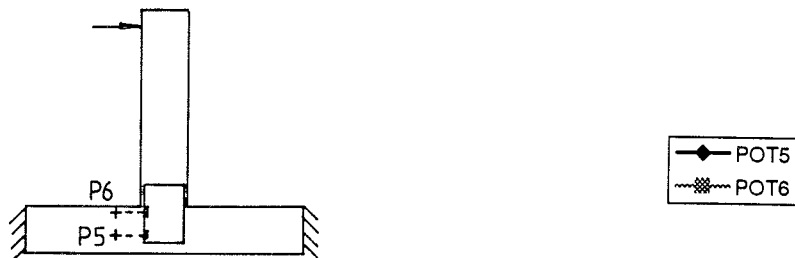
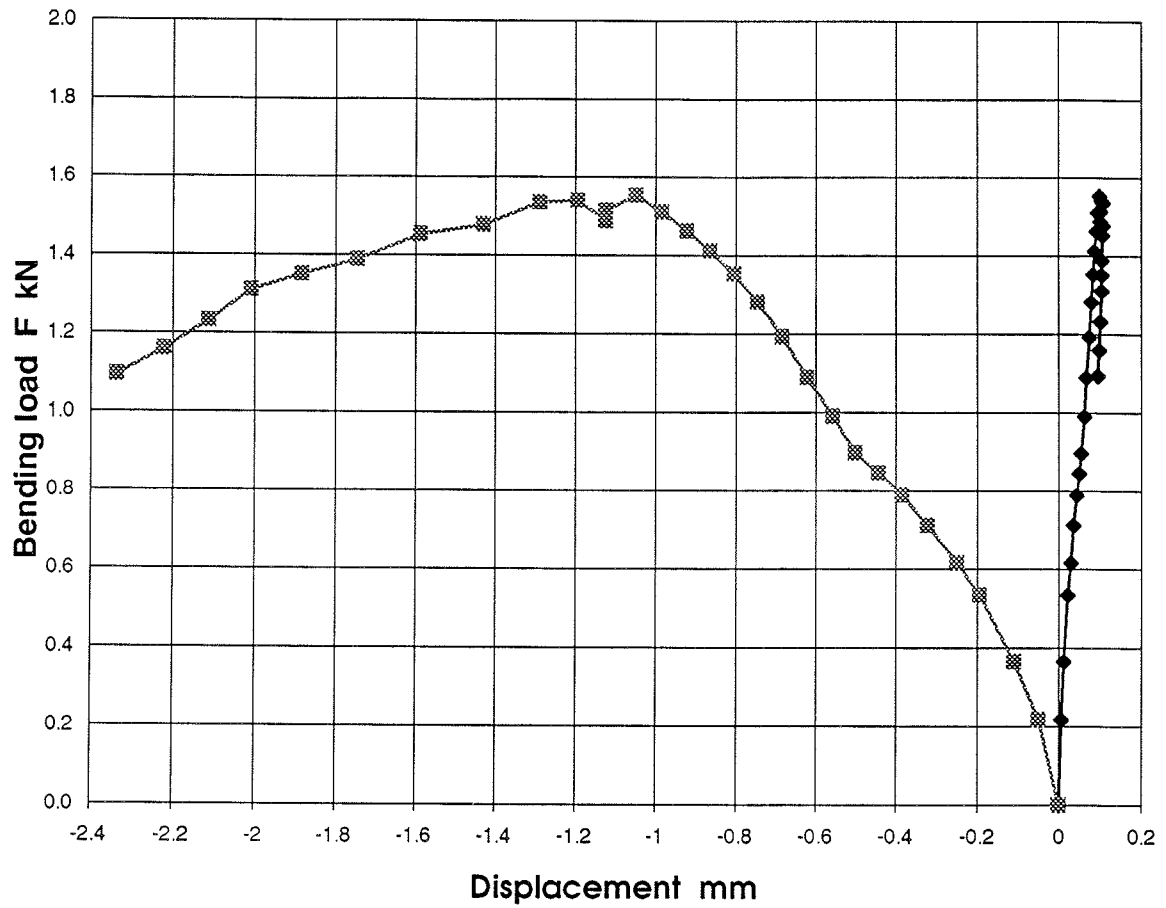


Figure 6. Graph Showing Bending Test Result for Joint Type J4T4 (Specimen 2)

Table 2. Mean results for the Shear Tests

Joint Type	α Deg	$K_{F,red}$ N/mm ³	$0.4F_{max}$ kN	$0.4\tau_{F,max}$ N/mm ²	$0.4\tau_{M,el,max}$ N/mm ²	$K_{\phi,h,el}$ N/mm ² /rad	$K_{\phi,v,el}$ N/mm ² /rad	$K_{\phi,el}$ N/mm ² /rad
J5A	0	9.34	5.04	1.119	1.874	352	266	204
J5B	90	10.32	4.30	0.965	1.597	359	425	319
J5C	45	*	3.95	0.973	2.315	399	749	-

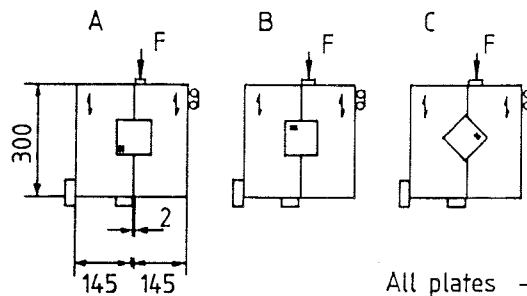
$K_{F,red}$ - displacement modulus per unit plate area A_{ef} determined from anchorage tests

$K_{\phi,h,el}$ - rotational stiffness determined using rotation calculated from the displacements measured with the horizontally mounted transducers. See Figure 1.

$K_{\phi,v,el}$ - rotational stiffness determined using rotation calculated from the displacements measured with the vertically mounted transducers. See Figure 1.

$K_{\phi,el}$ - rotational stiffness determined using the displacements measured at the joint line and corrected for shear translation of the joint

* -displacement modulus not available



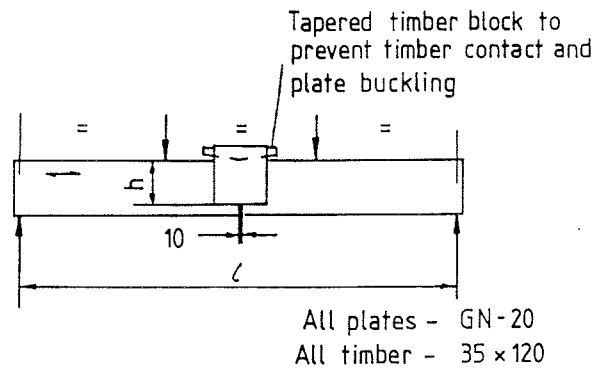
All plates - GN-20
All timber - 35×145

Test series	A	B	C
Plate size	76 × 71	76 × 71	76 × 71
Force/Plate angle α	0	90	45
Force/Grain angle β	0	0	0
Plate/Grain angle	0	90	45

Table 3. Mean results for the Bending Tests

Joint Type	$0.4 M_{\max}$ kNm	$0.4 \tau_{M.el.\max}$ N/mm ²	$K_{\phi.el}$ N/mm ² /rad	$K_{\phi.el\ total}$ N/mm ² /rad
J6A	0.415	2.52	312	276
J6B	0.358	2.30	526	408
J6C	0.761	2.30	338	277
J6D	0.600	1.96	452	321



$K_{\phi.el\ total}$ - rotational stiffness determined using the measured total rotation of the timber member

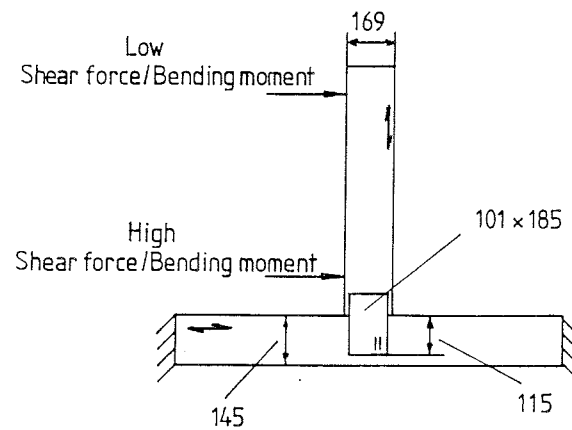


Test series	A	B	C	D
Plate size	127×129	127×129	152×157	152×157
Bite (h)	87	89	115	115
Plate/Grain angle	0	90	0	90

Table 4. Mean results for the Bending Tests on the Tee Joints.

Joint Type	$0.4 M_{\max}$ kNm	$0.4 \tau_{F \max}$ N/mm ²	$0.4 \tau_{M.el.\max}$ N/mm ²	$K_{\phi.el}$ N/mm ² /rad
J4T1 High Shear	0.726	0.157	1.367	457
J4T4 Low Shear	0.617	0.030	1.162	446

Plate type	GN20	GN 20
Plate orientation		
Test series	T1	T4
SF/BM	High	Low



At test loads close to $0.4 F_{\max}$ the rotations were approximately 0.5° and there were no signs of distress at the joint.

Stiffness Comparisons

The rotational stiffness values K_ϕ obtained by the various test methods were in the range 204 - 526 N/mm²/rad.

For similar joint configurations greater rotational stiffnesses were found in those joint types where the plates were fixed perpendicular to the grain. In the case of joint types J5A and J5B for example the rotational stiffness $K_{\phi,el}$ of J5B (plate perpendicular to grain) was 319 N/mm²/rad and that of J5A (plate parallel to grain) was 204 N/mm²/rad.

The rotational stiffnesses obtained from shear tests are generally smaller than the rotational stiffnesses obtained from bending tests. For example, in the tests on joint type J5B, the shear method, the rotational stiffness was 359, 425 or 319 N/mm²/rad, whilst the rotational stiffness by the pure bending method on joint type J6B was 526 N/mm²/rad. This result is different to that obtained by Kevarinmaki and Kangas.

The bending tests on the tee joints gave rotational stiffnesses of 457 and 446 N/mm²/rad, which are greater than those from the shear tests and similar to those from the beam bending tests. Although the rotational stiffnesses obtained in the tee joint tests with the high shear force and low shear force applications are practically the same, the results generally indicate a decreasing rotational stiffness with increasing shear force.

The rotational stiffnesses determined from the beam bending tests, given in Table 3 for joint types J6A to D, as well as being generally greater than those obtained in shear tests, also show the effect of using either the plate to timber rotation or the member total rotation in the calculations. Depending on the plate size and orientation, the rotational stiffnesses, $K_{\phi,el,total}$ based on member rotations, are between 12% and 29% less than the rotational stiffnesses, $K_{\phi,el}$ based on plate to timber rotation. It is considered that the larger total member rotation is a consequence of plate deformation across the joint line.

Shear Tests - Effects of Transducer Orientation

It is seen that the rotational stiffness values obtained with the horizontally and vertically positioned displacement transducers in the joint tests J5C are very different. The horizontal value $K_{\phi,h,el}$ at 399 N/mm²/rad is similar to that obtained from the tests on specimens 5A and 5B but $K_{\phi,v,el}$ at 749 N/mm²/rad is significantly higher. A far smaller, but significant variation was also observed in test series J5A and J5B.

The reason for the difference is not clear as the plates are fixed symmetrically across the joint line and at all stages during the tests the plate distortion and nail extraction were fairly evenly distributed. The extent of the nail extraction and fixing in the plate at the end of the test and the relative positions of the transducer targets are shown in Figure 7. It is possible that the positioning of the targets on plate areas with varying degrees of disturbance is causing the discrepancy in the measured rotations.

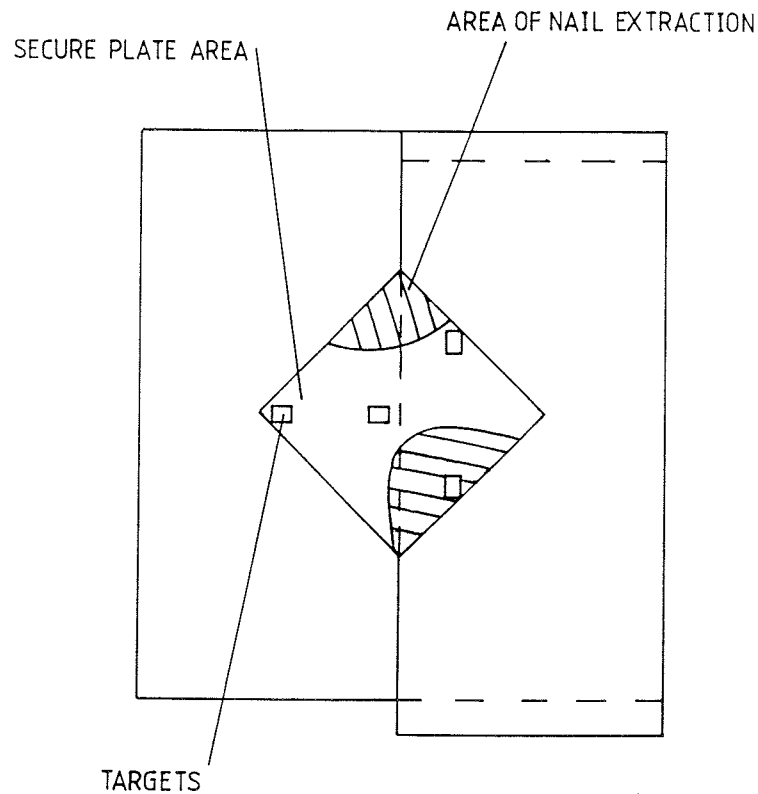


Figure 7. Transducer Target Positions Relative to Plate Disturbance

6. CONCLUSIONS

1. The tests have shown that different values of rotational stiffness can be obtained by different test methods for the same type of nailplate. Although it is not clear which particular values are the most accurate, because of the directness of the measurements, particularly that for rotation, in the authors' opinion the beam test results are probably the most acceptable.
2. All the rotational stiffnesses calculated from the test results were of the same order of magnitude, but generally, where shear forces existed the rotational stiffnesses were reduced. For example, the rotational stiffness for J6B (beam and no shear force) was $526 \text{ N/mm}^2/\text{rad}$ and that for J5B (shear specimen) was $319 \text{ N/mm}^2/\text{rad}$, a reduction of approximately 40%.

3. When considering the shear and bending test methods as a whole, with reference to EN26891, prEN1075 and the proposals by Kevarinmaki and Kangas, and Kyrkjeide, Aune and Aasheim, no particular technical difficulties are foreseen, although the results may be affected by the targeting of the displacement transducers, see Figure 7. The shear method requires a stiffness modulus obtained from other tests, in order to calculate the rotational stiffness. The definition and derivation of this stiffness modulus could be clarified in prEN1075. Resulting shear slip corrections applied in this study amounted to about 40% of the total deformation measured. Conversely, the bending method provides all the data required and rotations are measured directly.

REFERENCES

1. EN 26891:1991. Timber structure - Joints made with mechanical fasteners - General principles for the determination of strength and deformation characteristics.
2. Kevarinmaki and Kangas (August 1993) 'Rotational Stiffness of Nail Plates in Moment Anchorage', International Council for Building Research Studies and Documentation Working Commission W18A - Timber Structures, Meeting Twenty-six, Athens, USA.
3. Kyrkjeide, Aune and Aasheim 'Spikerplater med momentpakgenning'. Universitet i Trondheim, 1992, 85p.
4. Eurocode 5: Design of Timber Structures, 1995-1-1: 1994 Annex D.
5. prEN1075. 'Timber Structures - Test Methods - Joints made With Punched Metal Plate Fasteners'. February 1995.

INTERNATIONAL COUNCIL FOR BUILDING RESEARCH STUDIES AND DOCUMENTATION
WORKING COMMISSION W18 - TIMBER STRUCTURES

**EXPLANATION OF THE TRANSLATION AND ROTATION BEHAVIOUR OF
PRESTRESSED MOMENT TIMBER JOINTS**

by

A J M Leijten
University of Technology Delft
the Netherlands

MEETING TWENTY - NINE
BORDEAUX
FRANCE
AUGUST 1996

EXPLANATION OF THE TRANSLATION AND ROTATION BEHAVIOUR OF PRESTRESSED MOMENT TIMBER JOINTS

by

Ad. J. M. Leijten
Delft University of Technology,
the Netherlands

SUMMARY

With traditional fasteners it is doubtful to predict the behaviour of a multiple fastener moment joint by extrapolation of a single fastener tension joint. It is demonstrated that this statement is no longer valid for the densified veneer wood (dvw) reinforced joints. The investigation presented aims at verifying the behaviour of dvw moment transmitting joints by means of a model prediction based on a single fastener joint. Results show that the behaviour with respect to rotation and the translation can fully be explained.

INTRODUCTION

In structural timber design timber joints with dowel type fasteners are very popular but also are regarded as a necessary evil. Non of the existing types of joints have a high strength nor stiffness capacity combined with a reliable ductility. This limits the application of moment transmitting joints in portal frames undoubtedly. Even today, the emphasis of research on timber joints focus only on strength and no body seems to care about stiffness and ductility. This is probably due to the old allowable stress calculation method which disregards the structural behaviour at the Ultimate Limit State. However, as the ULS method is more and more adopted over the world, also for the structural analyses of timber structures, the combination of strength, stiffness and ductility becomes more and more important. The ULS method also enables the designer to apply plastic theory provided certain requirements as minimum rotation capacity is satisfied. Concrete and steel joints have past this stage decades ago and structural analyses on the bases of plastic theory has become a standard procedure with all the positive economic aspects which go with it. Now it becomes time timber pass this threshold as well. Therefore, it is required to improve the strength, stiffness and ductile capacity of timber joints as well as the reliability of the properties. So all three key properties should be addressed simultaneously. Attempts to reinforce timber joints is a topic which attracts more and more attention.

A solution is to reinforce the joint with densified veneer (ply)wood combined with a novel prestressing fastener (expanded tube fastener) as outlined in CIB/W18/28-7-1.

BACKGROUND AND AIM OF THE TEST PROGRAMME

A well known feature of non-reinforced timber joints is the inability to deduce the behaviour of moment joints with multiple fasteners with a single fastener joint. Or to say it in other words, the global and local behaviour are not compatible.

To verify whether this deficiency is also apparent for the dvw reinforced joint a number of tests were conducted. The tension and four point bending tests are considered as basic tests, figure 1 type a) and b). These tests provided information regarding minimum edge and end distances and some other parameters. In principle both tests series provide sufficient information to set up some design guidelines. With

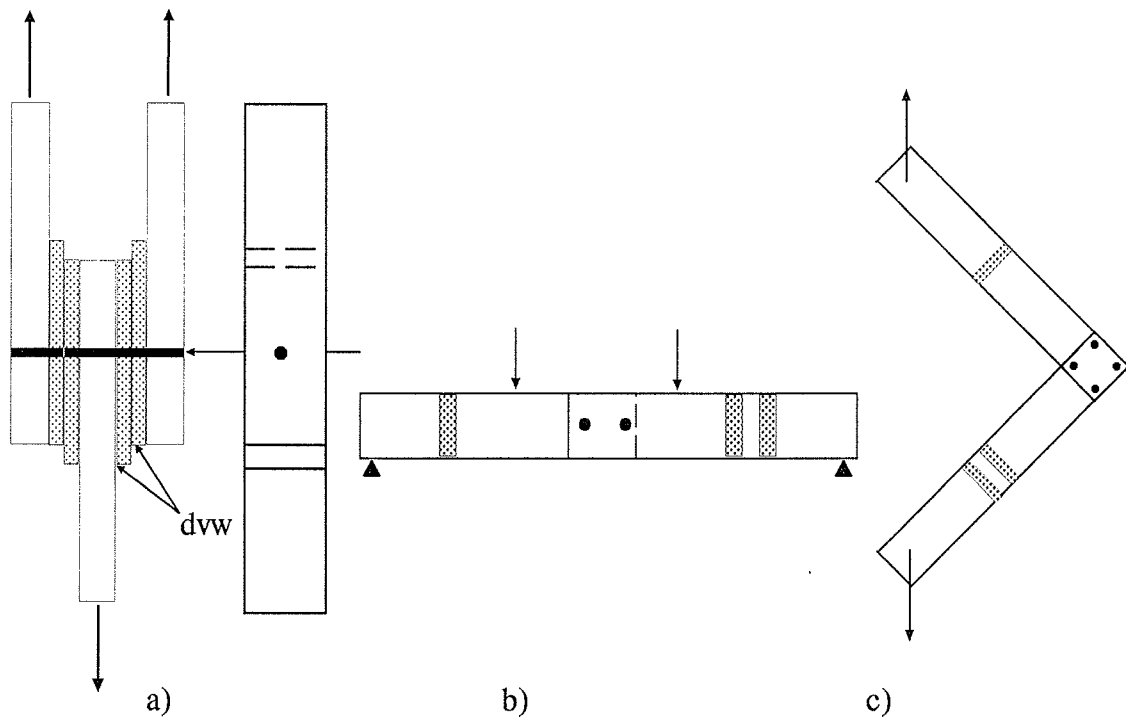


Fig. 1.: Test specimens of Werner and Weersink a) , Rodd b) and Leijten c)

the aid of the results, the translation as well as the moment rotation behaviour of moment joints, type c, can be predicted.

To do so the non-linear load-slip curves of both tension and four point bending tests are characterized by a curve fitting equation in which the parameters have a physical meaning.

Curve fitting models

The models described in literature can be classified into four main categories:

A: Curve fitting

B: Simplified analytical models

C: Mechanical models

D: Finite element analysis

Although purely empirical the advantage of the curve fitting models (A) is the capacity to represent any shape of load-slip curve with great accuracy. These models have the inability to recognize that, depending on the geometrical and material parameters, the behaviour as well as the contribution of each component to the overall joint response may change significantly. The simplified analytical models (B) can be defined as to reflect the main characteristic values of the load-slip or moment-rotation curves such as initial and post yield stiffness, plastic and ultimate load or moment. For the mechanical and finite element models (C and D) it is required to have knowledge about the behaviour of all components of the joint represented as a set of rigid or deformable elements.

For the joints considered in this paper the simplified analytical model of Richard-Jaspart [1] is considered appropriate because all knowledge required to apply the models C and D is not yet available.

Jaspart's-curve fitting model, figure 2, is presented as:

$$M = \frac{(k_i - k_y) \phi}{\left\{ 1 + \left[\frac{(k_i - k_y) \phi}{M_y} \right]^c \right\}^{1/C}} + k_y \phi$$

in which:

ϕ is the rotation

k_i the initial stiffness (a)

k_y the post yield stiffness (b)

M_y is the transition bending moment (c)

C a curve parameter (d)

The parameters of this regression model can of course easily be substituted to describe the load–slip curve instead of a moment–rotation curve with constants a, b, c, and d as indicated above.

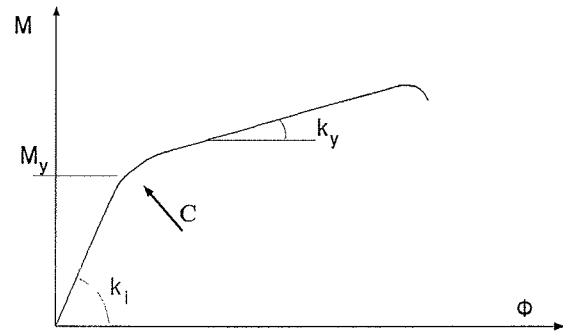


Fig. 2: Model parameters

TEST PROGRAMME

Test Setup

The moment joint specimens tested consist of a double side member connected to one central or middle member, type c) in figure 1. Two test series are set up to accommodate two tube sizes, 18 and 35 mm diameter. Four tubes are located at the corners as shown in figure 3. The glued laminated timber middle members range in dimension from 80x300 mm (10 specimens) to 110x600 mm (8 specimens) The thickness of the side members is half the middle member. The member length is 1650 and 2100 mm for the small and big specimens respectively. The wood species is Spruce; mean density 430 kg/m³ ranging from 350 to 550. The characteristic bending strength of the glulam is 30 MPa.

The densified veneer wood (dvw) is cross-wise layered and the density range is 1075 to 1270 kg/m³ for the joints with 18 mm tubes and 1300 to 1380 kg/m³ for the large joints with 35 mm tubes. The thickness of the timber members and dwv sheets correspond with the dimensions of earlier tension and four point bending tests. The end and edge distance in both test series is 2.5D or 3.5D (D=diameter of the tube). The test procedure corresponds with EN 26891 (ISO 6891).

Device For Translation and Rotation Measurements

The translation and rotation measurements should be taken in one point, preferably at the intersection of the system lines. Therefore, a special accurate purpose built rotation–translation device was developed able to provide the required information. Figure 3 shows schematically this equipment. Through a big hole in the side members a small threaded rod (8mm) is positioned in a 8 mm side member hole. As its length is bigger than the jointed section it

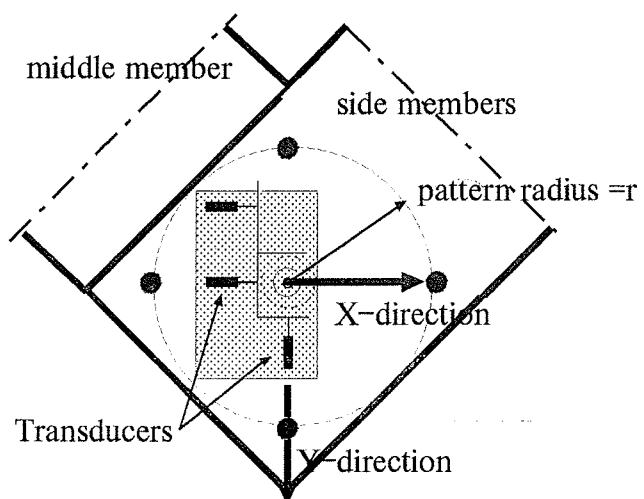


Figure 3: Principle of measuring device

sticks out on both sides. In this way the movement of the middle member is lifted above the surface of both side members. A square is fixed to both rod ends. The transducers are fixed on the side members. One transducers provide information about the translation in X and the other in Y-direction. A third one takes account of the rotation. The readings can easily be separated into pure rotation and translation in X and Y-direction. More information is given in Leijten et al.[2].

Second Order Effect

The test results are corrected for the following second order effect. When the legs of the specimen, as shown in figure 1c, are pulled apart, the timber members bend and the joint opens. This cause the lever arm to shorten and requires correction of the imposed bending moment. All data presented is corrected as such.

THE TEST RESULTS OF THE MOMENT TRANSMITTING JOINTS

In figure 4, all test results with the large specimens (35 mm tubes) are presented. In this graph also (old) results are presented of the same specimens size not reinforced joints with 24 mm dowels. As the end and edge distance of the tubes is different per series, 2.5 and 3.5 D, consequently, the moment rotation curves are different. The curves finally drop which is not an indication of failure but caused by the end of the stroke length of the hydraulic jack (200 mm). The maximum rotation attained is about 0.07 rad. The traditional joints with dowels clearly show much more scatter while the strength and stiffness capacity is much lower. Note also the bending stresses in the glulam members,

presented at the right hand side of the graph. Such a stress level (30 to 35 MPa) with only four fasteners is quite unique. The transmitted moment exceeds the characteristic bending moment capacity of the timber. With traditional dowels the capacity of such joints is no more than 40% of the timber strength. Once more evidence of the high strength capacity of this type of joint. The translation measurements of the middle member with respect to the side members are given in figure 5.

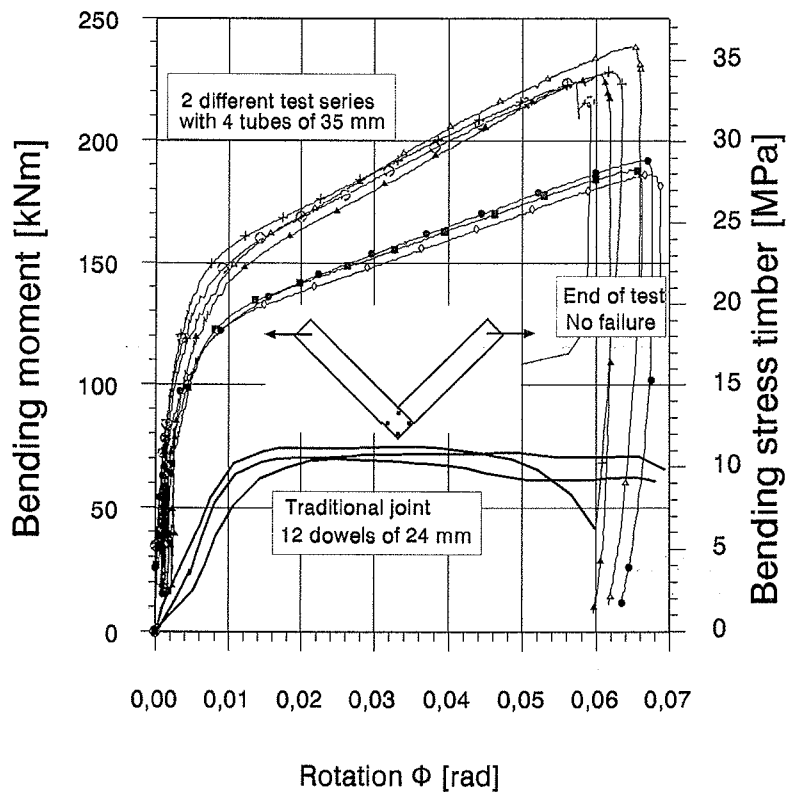


Figure 4: Moment-rotation results of prestressed joints with 35 mm tubes and joints with 24 mm dowels

ANALYSES

In order to compare the moment joints with the elementary tension and four-point bending tests, the moment rotation curves of figure 4, are transformed to load-slip curves. This is possible assuming a centre of rotation which corresponds to the geometrical centre of the pattern of the fasteners. Although not shown here, all curves not only coincide well along the whole load path, the scatter is remarkable small as well. Apparently, based on this visual assessment the assumption stated above, is not bad. This is confirmed by the similarity between the parameters of Jaspert's-model when fitted to all load-slip data. The regression

parameters are given in Table 1 for both tube sizes (18 and 35 mm) and per test series. The tension tests with 18 mm tubes should for all kinds of reasons not be considered as valid data. It can be concluded that the parameters correspond well over the test series per tube size. Apparently, the load to grain angle dependency of strength and stiffness, which is prominent for traditional joints, is now vanished.

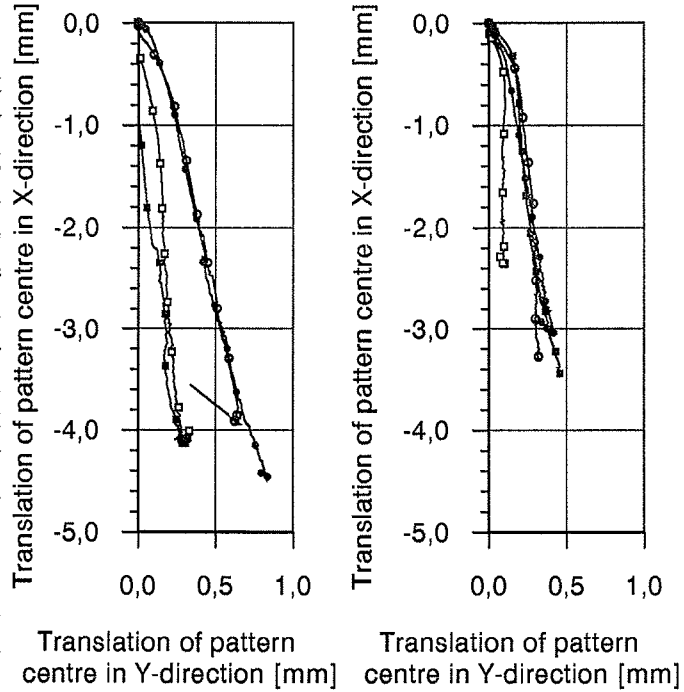


Figure 5: Translation results of the joints with 35 mm tubes. Left, the series with 2.5D end/edge distance, right 3.5D series.

Explanation of the Translation Measurements

The translation measurements, of the middle member with respect to the side members are given in figure 5. The X-translation readings of 3 to 4 mm can not be caused by the shear force only. The highest shear load at test is 12.5 kN/shear plane/per fastener. The expected slip at this load level is about 0.1 mm, as the tension joint data shows. Are these readings false or can they be explained by an other phenomenon?

Table 1: Regression parameters of Jaspert's-model

Comparison of regression equation parameters of Jaspert's-model						
$F = (k_x - k_y) \cdot \delta / (1 + ((k_x - k_y) \cdot \delta / M_y)^C)^{1/C} + k_y \cdot \delta$						
Test type dvw thickness	Joints with tubes 35 mm			Joints with 18 mm tubes		
	Tension 12/18	Moment 18mm	Four point bending 14/18 mm	Tension 10/12	Moment 12mm	Four point bending 12mm
k_x	98.2	125.8	89.9 [kN/mm]	15.02	37.4	36.6 [kN/mm]
k_y	1.45	1.63	1.49 [kN/mm]	0.706	1.21	0.57 [kN/mm]
M_y	61.0	67.6	62.8 [kN]	24.1	24.1	30.2 [kN]
C	1.71	1.02	1.33	2.83	1.79	1.49

The loads imposed on the fasteners by shear and bending moment are visualized in figure 6. Obviously, the tube at the inner corner is the highest loaded one as both moment and shear vector have the same direction. On the opposite corner the lowest loaded tube is situated. It will be clear that the centre of rotation lies underneath the centre of the tube pattern on the y-axis. The rotation centre is defined as the position where only rotation exists and no translation. In case the load-slip behaviour of the fastener is linear elastic this rotation centre is fixed. As long as this rotation centre does not correspond with the geometrical centre, the rotation contributes to the X-direction readings. Because the load-slip behaviour is highly non-linear the rotation centre will move and its contribution to the translation readings change correspondingly. This effect should be taken into account in trying to understand the X-translation readings.

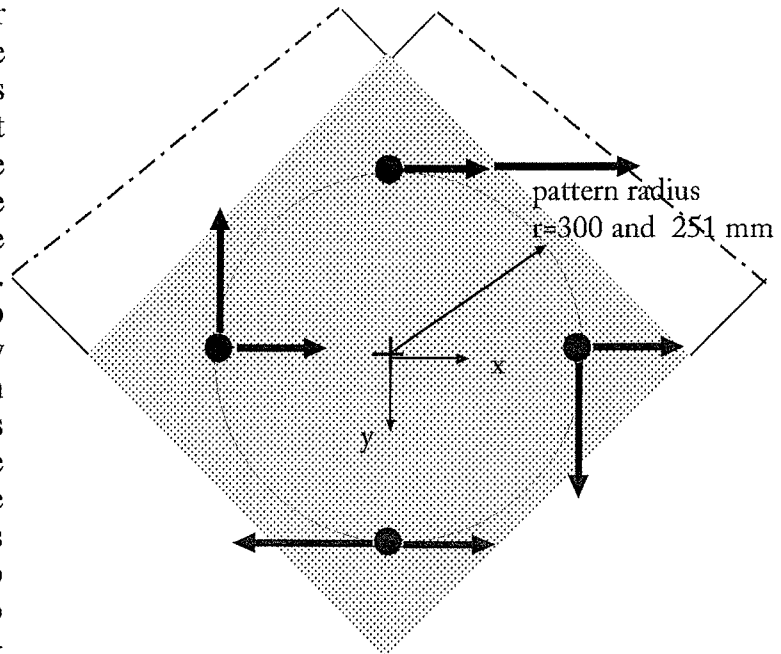


Figure 6: Forces caused by shear and moment. Jaspert's model parameters of tension and four point bending tests are used to predict the movement of the rotation centre along the Y-axis versus the rotation of the joint. The result is presented in figure 7. Two lines are drawn. The top one is based on the assumption that the joint is made with only two tubes, one at the inner corner and one at the opposite outside corner. Although not relevant for our case but illustrative, is the movement and the eccentric position of the rotation centre on the Y-axis. The bottom line reflects the actual situation of four 35mm tubes with a edge/end distance of 2.5D. The contribution of the rotation to the X-direction translation readings corresponds with the area underneath the lines. In case of the top line, the X-dir. reading caused is 8.91 mm. For the fig. 5 left test set the results is 4.0 mm. For the

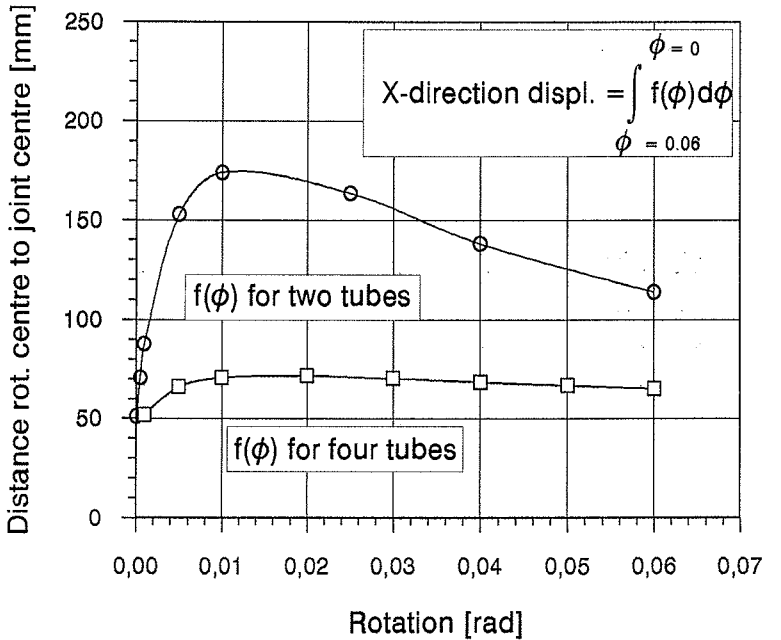


Figure 7: Movement of the rotation centre for joints with 35 tubes with 2.5D end distance.

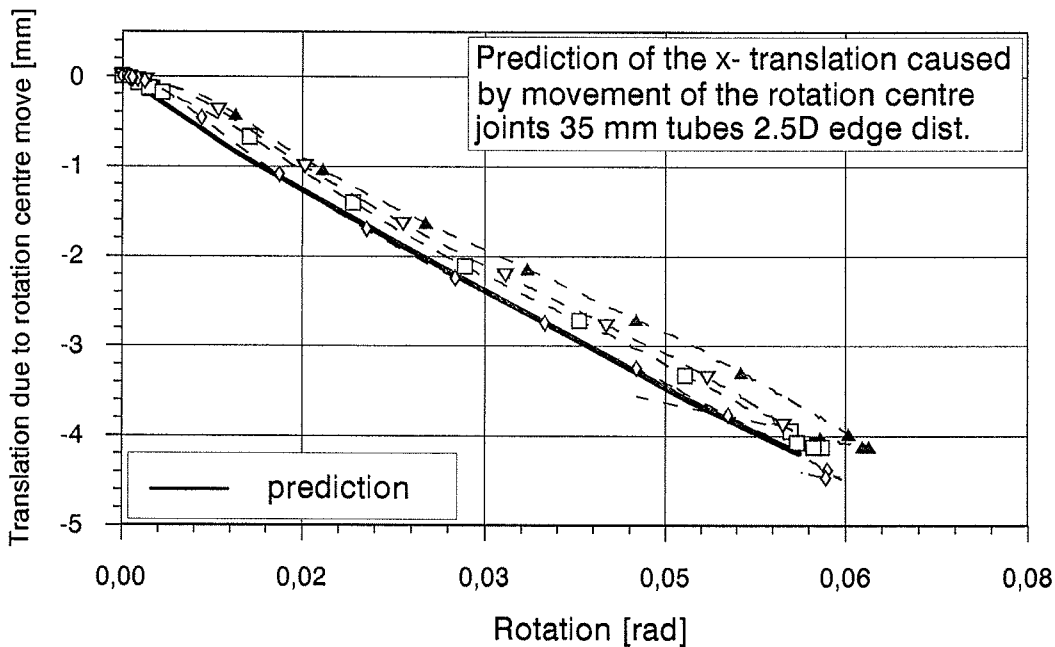


Figure 8: X-translation versus rotation

right one 3.1 mm which corresponds very well with the data. Another way to compare and to present the test results with the model prediction is reflected by figure 8 and 9. Notice how well the test data compares with the model, based on the load-slip results of the elementary tests.

The readings in Y-direction are small, about 0.1 to 0.9 mm. There is a second order effect which explains this movement as well as the general slope of the figure 5 curves. During the course of the test the side members on which the transducers are fixed, rotate with respect to the direction of the applied (shear) load. This means that in the rotated situation any movement in X- or Y- direction affect the readings of both transducers which originally corresponded with the X and Y-coordination system. If so, than there is a relation between both readings. When the X-reading is 4.0 mm at an rotation of 0.06 rad, the Y reading caused is $0.06 \times 4.0 = 0.24$ mm. The Y-readings of the tests vary from 0 mm to 0.75 mm. In some cases 0.25 mm is found. This variability can be caused by all kinds of small errors.

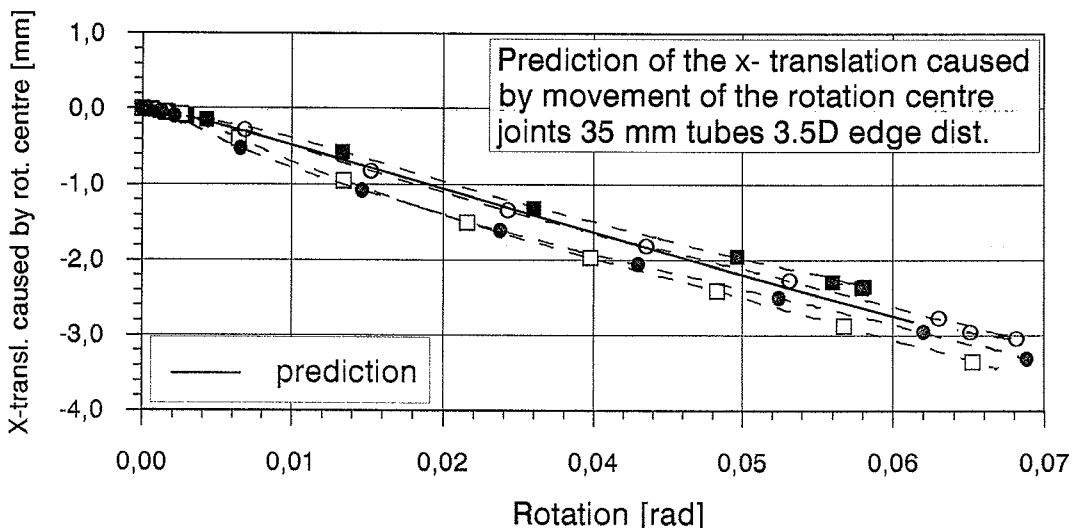


Figure 9: X-translation versus rotation

CONCLUSIONS

The local behaviour of single dowel type fastener joints can not be extrapolated to predict the global behaviour of multi fastener joints. Recently, a new type of joint is developed, the prestressed DVW reinforced joints with expanded tubes. This requires to check the local and global behaviour of the new joint. For this purpose single fastener tension test were performed as well as four point bending tests. The results were used to predict the global behaviour of a multi fastener moment transmitting joint .

- It is concluded that prestressed DVW reinforced joints with expanded tubes are, strong, stiff and ductile.
- It is shown that the behaviour of the moment transmitting multi fastener joints can be predicted and described by the behaviour of a single fastener joints.

Not only the moment rotation behaviour but also the slip of the timber members caused by shear loads. Therefore, it is concluded that the load-slip behaviour of these type of joints is independent of the load to grain direction angle.

ACKNOWLEDGEMENT

The authors wish to acknowledge the research partners, A. Ceccotti (Firenze,Italy), H.M. Cruz (LNEC, Portugal), P.D. Rodd (Brighton, United Kingdom), H.Werner (Karlsruhe, Germany) as well as the industrial partners, Lignostone International (NL) and De Groot Vroomshoop (NL) and the Firm Holzbau (Italy) as well as the European Commission for their financial contribution of this research project within the R&D progame FOREST.

REFERENCES

- [1] Jaspart, J.P. and Maquoi, R.(1994). Prediction of the semi-rigid and partial-strength properties of structural joints, Proceedings of the Annual Technical session, SSRC, Lehigh, U.S.A., June 20, 1994, p. 177-192.
- [2] Leijten A.J.M., Ceccotti, A., Cruz, H.M., Rodd, P.D., Werner, H., Viridi, K.S.(1994). Physical and mechanical properties of densified veneer wood for structural applications, Stevin report EC4-1994, Faculty of Civil Engineering, University of Technology Delft, the Netherlands.

**INTERNATIONAL COUNCIL FOR BUILDING RESEARCH STUDIES AND DOCUMENTATION
WORKING COMMISSION W18 - TIMBER STRUCTURES**

DESIGN OF JOINTS AND FRAME CORNERS USING DOWEL-TYPE FASTENERS

by

E Gehri
Chair of Wood Technology
ETH Zürich
Switzerland

**MEETING TWENTY - NINE
BORDEAUX
FRANCE
AUGUST 1996**

Design of joints and frame corners using dowel-type fasteners

Prof. E. Gehri, Chair of Wood Technology, ETH Zürich

1. Introduction

The design of joints is an important part of the design of timber structures. Basis of this design should be in the European Countries the Eurocode 5 – Part 1–1. Unfortunately chapter 6 – Joints – deals quite only with fasteners and not with joints. Therefore even simple joints like a moment splice in a beam cannot be treated with this Code.

Furthermore the assumptions used for the derivation of the load-carrying capacity of dowel-type fasteners can only partially and under certain conditions be fulfilled, which means that design of joints using Eurocode 5 may be erroneous.

In addition structural detailing plays a major role on the behaviour of the joint. Tolerance problems may strongly affect the strength of the joint. Tolerances on the dowel diameter are given actually with $-0/+0,1$ mm; the pre-bored holes in the timber should have a diameter not greater than the dowel. No values are given about tolerances between connecting pieces.

2. Johansen's equations for a single dowel and k_{sys}

2.1 Introduction

The ultimate load equations for laterally loaded joints with dowel-type fasteners given in Eurocode 5–1–1 are based on Johansen's equations [Johansen, 1949], which assume that both the dowel and the timber behave like ideal rigid-plastic materials. This approximation simplifies the analysis but leads to values greater than in reality.

Due to the deformation of the fasteners and caused by friction between the fastener and the timber a higher resistance has been stipulated by different authors [Werner H., 1993; Ehlbeck J. and Larsen H.J., 1993; Hilson B.O., 1994]. Based on these works the Eurocode 5 has taken the above mentioned effect into account by enhancing the resistance by 10 per cent (except for wood failure modes).

In the preliminary comments to the Madrid meeting of TC 250/SC5, November 1992, the Swiss representative had exposed different views. In fact it must be expected that the values given by the Johansen's equations represent always an upper bound which only under special conditions (eg. for a single dowel) may be reached.

In the following (see 2.3) it will be shown that the derivation of k_{sys} on the research work made by Werner (1993) is based on an erroneous comparison: test values using dowels with about 50 % higher effective yield moments, than the nominal values, where simply compared with values derived from Johansen's equations but using there only the lower nominal values. For a more complete study see Gehri (1994).

2.2 Basis of design in Eurocode 5–1–1

The load-carrying capacities given in Eurocode 5–1–1 are valid for:

- joints up to 6 dowels in line with the load, without any reduction;
- joints with humidity up to about 20 % (for soft woods) without any reduction, since the k_{mod} factor for service class 1 and 2 is the same;
- joints with "normal" imperfections (in alignment or in spacing), which means that distribution of load on the dowels may be uneven.

Werner has based his conclusions on research made only on a single dowel (see Werner H., 1993, page 1–2).

It has been shown by Doyle [1964], Gehri [1992, 1994], Yasumura [1993] that the influence of the number of dowels in a row may be important, the reduction depending mainly upon the ductility of the single dowel. The reduction can be greater than 30 to 40 per cent for a joint with 6 dowels in line with the load, when compared with the resistance for a single dowel.

It can therefore not be understood – since the Eurocode 5–1–1 is valid for 6 dowels in line – why the research work done by Werner on a single dowel can be the basis for the introduction of a so-called system factor $k_{sys} = 1,1$.

2.3 The system factor k_{sys}

Werner (1993) has introduced the system factor to "correct" Johansen's equations, since he found in his tests and his simulation work higher values than those given by Johansen's equations. The system factor is given by

$$k_{sys} = \frac{R_{k,Werner}}{R_{k,Johansen}}$$

It has to be noted that the values of $R_{k,Werner}$ are those obtained by tests or by simulation with the real strength characteristics for f_h and M_y , whereas for $R_{k,Johansen}$ nominal strength values were introduced.

For slender dowels the characteristic load-carrying capacity is proportional to $\sqrt{M_{y,k} \cdot f_{h,k}}$. Therefore it can be written for k_{sys} :

$$k_{sys} = \sqrt{\frac{(M_{y,k} \cdot f_{h,k}) \text{ test or simulation}}{(M_{y,k} \cdot f_{h,k}) \text{ nominal}}}$$

We obtain for k_{sys} a value of 1,18 when using test results or 1,14 when using simulation results. Those factors result directly from the higher yield moments M_y of the dowels used in the tests (about 40 to 50 % higher compared to the nominal value using the EC5 formula given by clause 6.5.1.2(2)). The so-called system strength factor results therefore from an erroneous comparison. Johansen's equations need no correction when using a single dowel.

2.4 Conclusions

The simulation study made by Werner was based on the effective strength properties (the yield moment of the dowels was about 40 % higher than the nominal strength values) whereas the load-carrying capacities calculated from Johansen's equations were based on the nominal strength values.

From the results and the study made by Werner on a one dowel joint no system factor k_{sys} can be justified, therefore a value equal to unity has to be introduced.

As mentioned in 2.2 the study of Werner gives no justification for the load equations in Eurocode 5, since he considers only a one dowel joint and timber with moisture content of 12 %. In contrast with this the loads given by Eurocode 5 must be valid for joints up to 6 dowels in line with load direction and "normal" imperfections of fabrication as well as for timber with moisture content up to about 20 %. The reductions observed in testing larger joints and/or joints exposed to higher moisture contents may be very important. The design of dowel-type joints will be in these cases on the unsafe side.

3. Group effect

3.1 General

From studies going back to 1920 it is known that the load-carrying capacity of a joint will be less than the sum of the individual fasteners capacity. The reduction depends on geometry of the joint, type of connectors or fasteners used. In existing Codes the reduction is normally given for the type of fastener and the number in a row in line with the load direction. In Eurocode 5, clause 6.5.1.2(3) reads:

"For more than 6 dowels in line with the load direction the load-carrying capacity of the extra dowels should be reduced by 1/3, i.e. for n dowels the effective number n_{eff} is $n_{\text{eff}} = 6 + \frac{2}{3}(n-6)$."

For joints using stiff and brittle connectors like shear plates larger reductions are obtained (Erki/Huggins, 1983). The same is valid for dowelled joints when using stocky dowels. As mentioned before by Doyle (1964) and Gehri (1992) the reduction depends mainly on the ductility of the joint.

3.2 Verification of EC5

In STEP publications the derivation of Johansen's equations is given but not the background, e.g. which requirements must be fulfilled that the assumption of ideal rigid-plastic behaviour of the materials is acceptable (see STEP C3). STEP C6 and C7 deal with dowelled joints. Example 3 – Dowelled steel-to-timber joint was used as basis for the verification (see STEP C7, page 5).

Example 3: Dowelled steel-to-timber joint

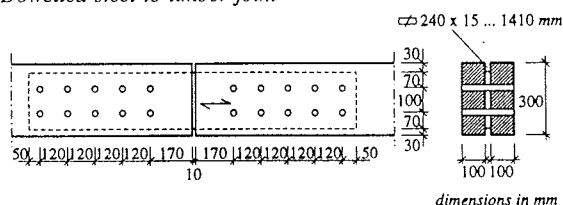


Figure 3 Dowelled joint with centre member of steel. Dimensions in (mm).

Dowel $d = 24 \text{ mm}$

Glued laminated timber according to prEN 1194:

GL 24

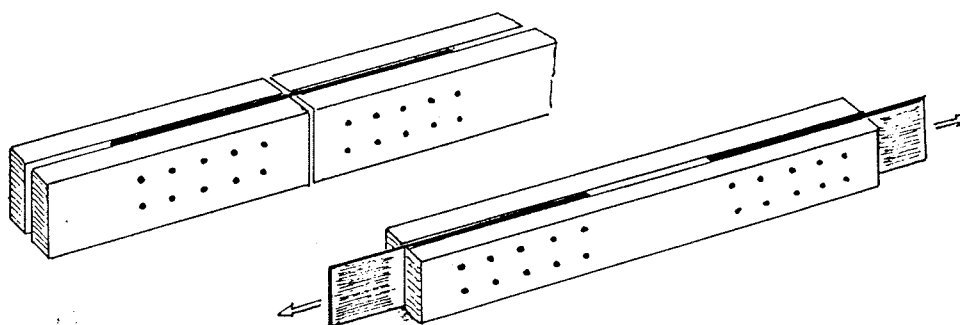
Steel plate

$f_{u,k} = 360 \text{ N/mm}^2$

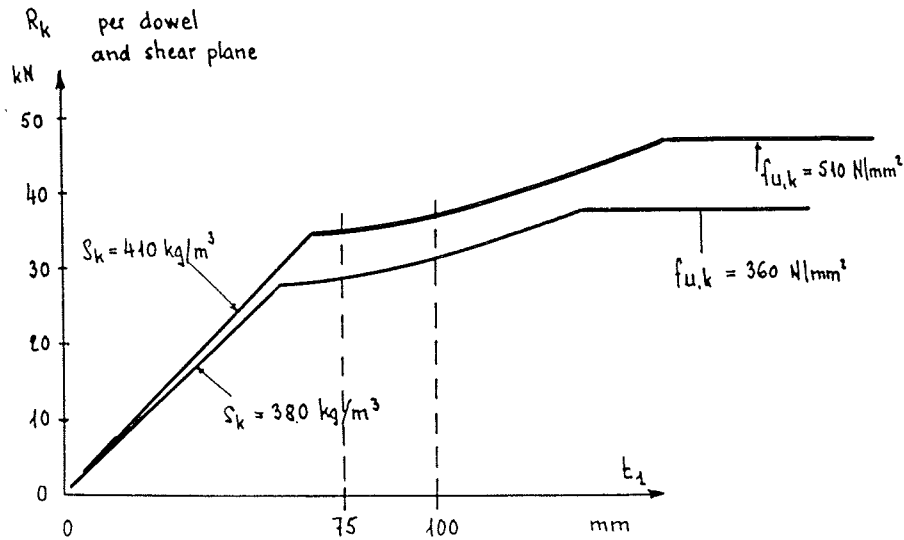
$\rho_k = 380 \text{ kg/m}^3$

$t = 15 \text{ mm}$

For the experiment, the joint was slightly modified, as seen below:

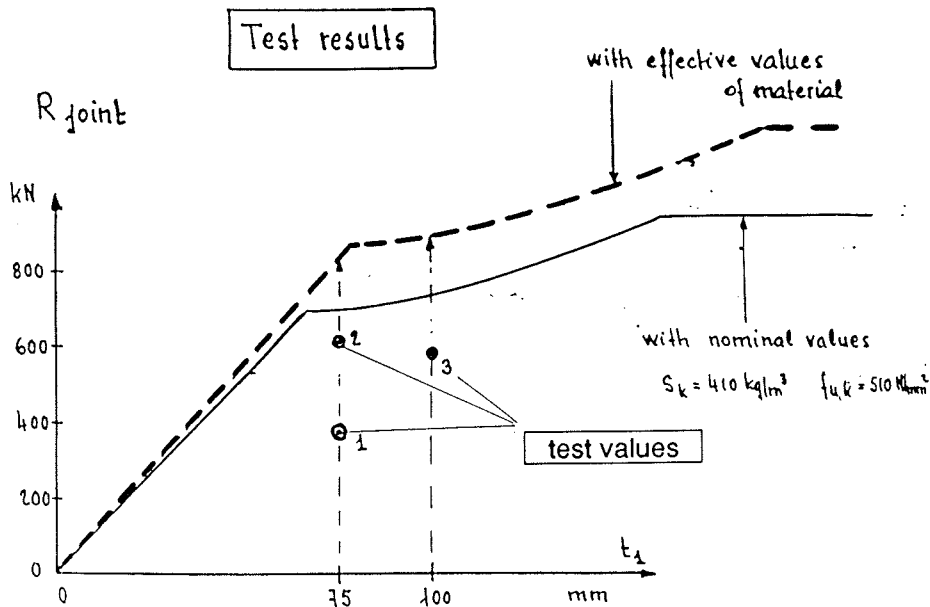


Furthermore for the glued laminated timber quality GL 28 with $\rho_k = 410 \text{ kg/m}^3$ (instead of GL 24) and dowels with $f_{u,k} = 510 \text{ N/mm}^2$ (instead of 360 N/mm^2) were used. Below are compared the load-carrying capacities for the materials used in STEP C7 and those foreseen for the verification, in function of the thickness t_1 of the timber.



As can be seen, differences between timber thickness $t_1 = 75 \text{ mm}$ and 100 mm are small.

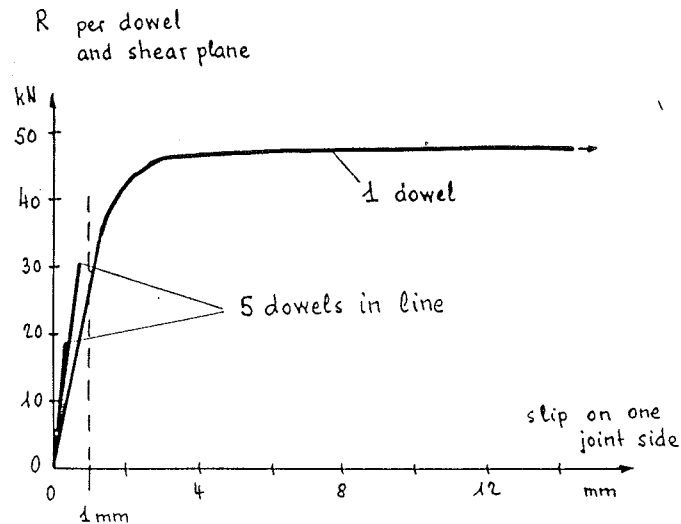
The material properties for the 5 specimens fabricated were directly established and used for the comparison. Only 3 tests were performed (material for 2 tests is still existing and tests may be done on requirement) and showed the following results.



Compared are the test results with the nominal characteristic values and with the measured values of the properties (dashed line). The test values are alarmingly low; dowelled steel-to-timber joints designed according to the actual proposals of EC 5-1-1 are really unsafe.

3.3 Individual dowel – dowels in a row

Tests were performed on individual dowels. Using the same material the individual dowel performed as foreseen by the Johansen's theory and ultimate strength was correctly established. In the same graph are represented the results for a row of 5 dowels. No plastification – neither of the dowel, they remained straight after the test, neither of the timber hole – could be realised: the timber elements failed by splitting after very small deformations of the joint of only 0,4 to 0,7 mm. These values are of the same magnitude of fabrication tolerances.



3.4 Conclusions

From this simple verification and only based on 3 tests, it could be shown:

- the actual approach given in EC 5-1-1 for steel-to-timber dowelled joints is alarmingly on the unsafe side;
- the actual approach starting from an individual dowel (see Werner 1993), even disregarding the so-called factor k_{sys} , cannot reflect the real behaviour of the joint;
- besides fulfilment of ductility conditions for the individual dowel, fabrication tolerances must be considered.

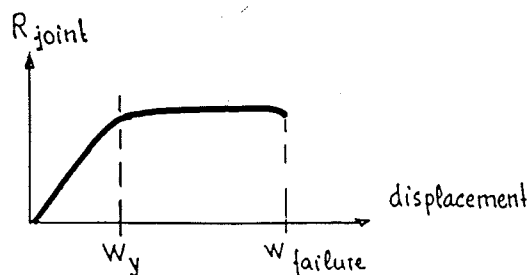
4. Proposal taking into account joint geometry

4.1 General

Based on earlier research work it was clear that for the use of Johansen's equations additional requirements must be fulfilled; otherwise the assumption of plastic behaviour of the material involved cannot be warranted. The additional requirements must be deduced from the joint behaviour and not from the behaviour of a single dowel.

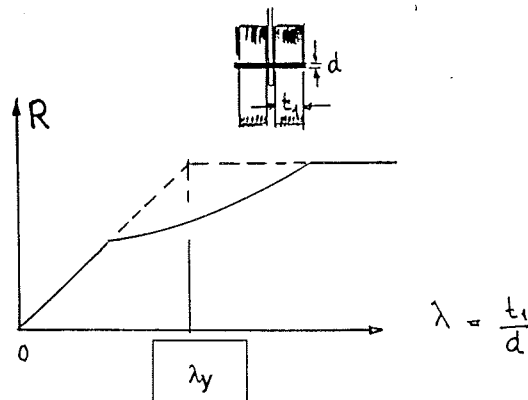
As a result the following approach was formulated (Gehri, 1992):

- Mechanical joints should be designed in such a way that they develop a large plastic deformation before failure



- avoid brittle joint
- high ductility of joint
- use of connector with large deformation capacity

- Fasteners of dowel-type should develop plastic hinges on the dowel. This condition may be considered fulfilled, when using a fastener slenderness higher than λ_y .



- In dowel-type joints with more than 2 fasteners in line with the load direction the effective number n_{ef} should be taken as:

$$n_{ef} = 2 \left(\frac{n}{2} \right)^{0,8 \cdot \lambda_r} \quad \lambda_r \leq 1$$

where $\lambda_r = \frac{\lambda_{ef}}{\lambda_y}$ ← effective slenderness
 ← "yield" slenderness

4.2 Evaluation of test results

It can be assumed of general knowledge, that

- in the elastic range, distribution of loads in a row, is very uneven; this is not only affected by the stiffness conditions but also by (small) fabrication tolerances;
- by plastification of the interconnecting elements a more even distribution can be achieved; this is valid only under the assumption that the basic material does not fail before load redistribution (e.g. by splitting).

Based on the above an empirical approach was made, introducing a yield slenderness λ_y and a relative slenderness λ_r , as the relationship of the effective slenderness divided by the yield slenderness. To account for fabrication tolerances a reduction factor was introduced. For good workmanship a value of 0,8 seemed reasonable.

Above is shown an evaluation of the tests made by Doyle (1964), on steel-to-timber connections with 4 dowels in a row. According to Eurocode 5-1-1 only reduction should be foreseen for $n > 6$.

Type	Value per dowel		Empirical formula	
	tested individually	in group of four	proposed by Gehri (1992)	Slenderness λ_{ef}
3/4 "	100 %	67 %	73 %	4,33
1/2 "	100 %	86 %	87 %	6,5

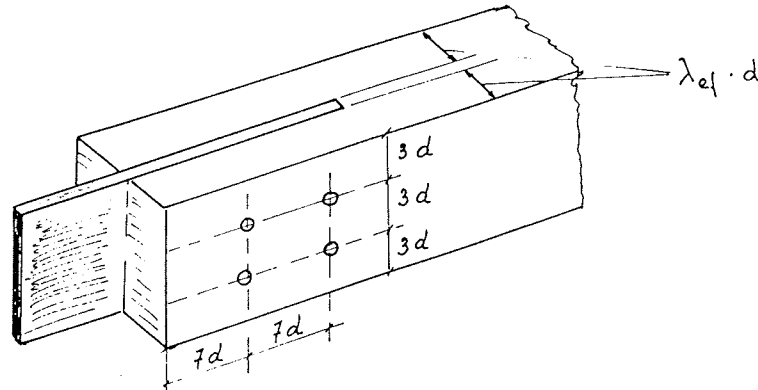
The proposed empirical approach helps to understand the behaviour of the joint. For more informations see Gehri (1993).

4.3 Eurocode 5-2

In Eurocode 5-2 a new proposal for dowelled joints has been introduced which takes in account joint geometry and fabrication tolerances. The approach is still based on the load-carrying capacity for a single dowel as given in Eurocode 5-1-1.

The following should be changed:

- the k_{sys} – values should be taken unity (instead of 1,1);
- the basal values should be taken from tests executed on joints with at least 2 dowels in a row and two rows.



The actual test procedures not even reflect the behaviour of an individual dowel, since f_h is based on stocky (rigid) dowels and M_y is based on an empirical approach, starting from the tensile ultimate strength of the dowel material.

The proposed test should be made on test elements as show above. Therefore basic spacings and distances can be considered and fabrication tolerances can be included. For that it will be important to use the same manufactor proceedings. Joints on test elements are too often fabricated in the laboratory and therefore usual fabrication tolerances may not be reflected.

The results of such a test would directly give the value needed for the empirical approach of 2 dowels in line:

$$n_{ef} = 2 \left(\frac{n}{2} \right)^x = 2 \cdot 1^x = 2$$

5. Joints on multiple shear

5.1 The BSB-multiple shear joints

The multiple shear joint developed by H. Blumer about 20 years ago fulfills many of the conditions mentionned before. Since most of the tests where made at the Federal Institute of Technology at Zurich, we dispose of data over 400 tests made on large specimens.

During the years research was made to optimize the multiple shear joints. Only two aspects related with ductility requirements will be shown here.

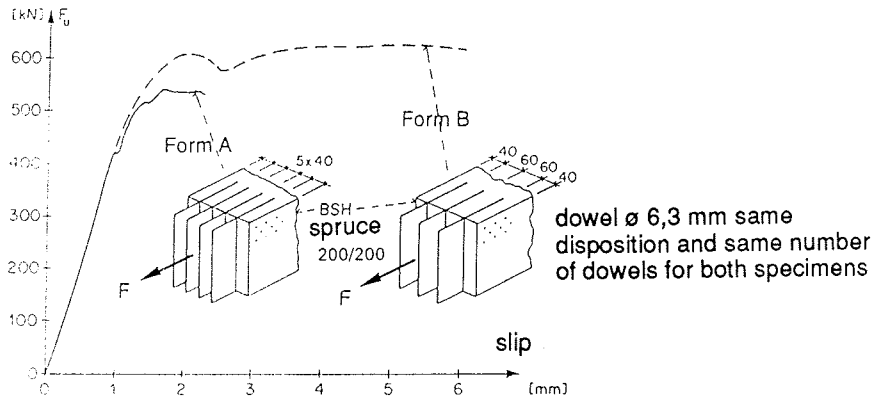
5.2 Influence of effective slenderness on the load-carrying capacity of the joint

Tests on BSB-joints with low glulam timber strength had shown:

- too low efficiency of the joint
- low efficiency per dowel and shear plane, as compared to single dowel
- very little ultimate deformation and brittle failure of the joint

By reducing the number of shear planes to 3/4 (3 steel plates instead of 4) we obtained for the same timber dimensions and quality:

- higher efficiency of the joint
- more than 40 % increase of load-carrying capacity per dowel and shear plane
- large ultimate deformation and ductile behaviour of the joint.

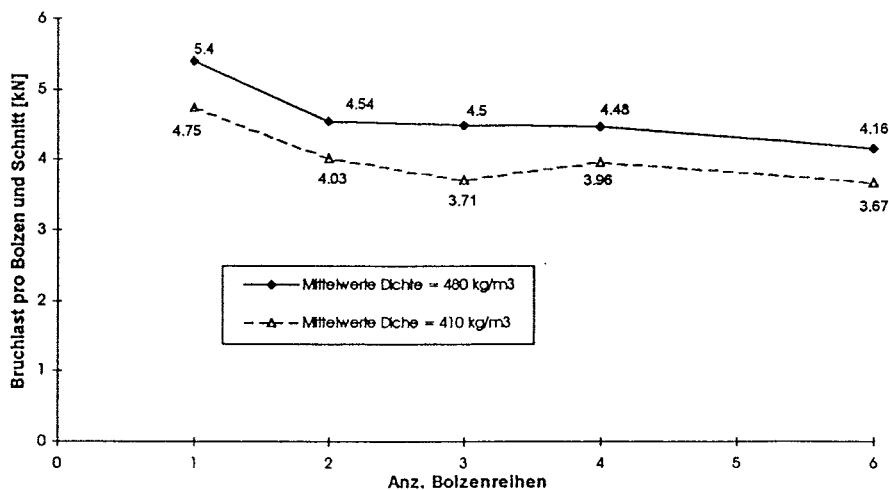


The initial results were supported by a large number of tests.

5.3 Group effect

For the BSB-system the group effect should be small, since the relative slenderness is high and furthermore very small tolerances are achieved with the fabrication procedure used.

For two well defined densities of glulam (the laminations were graded to density before gluing) with ρ_{mean} of 410 and 480 kg/m³ tests were made for 1, 2, 3, 4 and 6 dowels in a row. The test specimens of section 200/200 mm had normally 9 rows of dowels; for more than 2 dowels in a row, normally the number of rows had to be reduced, to avoid timber failure.



[Taken from Indermühle, D./1996]

The group effect can clearly be seen.

Since tests made with the BSB-system are normally made with 3 dowels in a row, the test results take account of the group effect. Only when using more dowels a small reduction must therefore be considered.

6. Frame corners with moment–resisting dowelled joints

6.1 General

Based on EC 5–1–1, Racher (1995) has developed a design procedure in STEP (lectures C16 and D8). Basically the design considers: the strength of the highest loaded dowel and the shear strength of the timber in the joint area. By optimisation of the dowels, e.g. by using slender dowels of higher strength, Racher has shown, that the frame corner can reach about 80 % of the bending capacity of the members to be jointed at the corner. This is an astonishing high performance.

6.2 Verification of the design procedure

To show up the validity of the procedure, the calculated resistance will be compared with test results published by Kolb (1970).

Tests X3 and X4 had a column section of 2 x 70/830 mm; the glulam strength corresponds to GL 28. The frame corner collapsed with the following forces acting on the column:

$$V_{c,u} = 75 \text{ kN} \qquad N_{c,u} = 115 \text{ kN} \qquad M_u = 273 \text{ kNm}$$

For the glulam quality GL 28 the following characteristic values are given:

$$f_{m,g,k} = 28 \text{ N/mm}^2 \qquad f_{v,g,k} = 3,0 \text{ N/mm}^2 \qquad f_{t,90,g,k} = 0,45 \text{ N/mm}^2$$

Assuming a coefficient of variation for bending of 0,12, for shear of 0,20 and for tension perpendicular to grain of 0,25, the mean values would be:

$$f_{m,g} \cong 35 \text{ N/mm}^2 \qquad f_{v,g} \cong 4,5 \text{ N/mm}^2 \qquad f_{t,90,g} = 0,77 \text{ N/mm}^2$$

The shear value obtained in both tests was of 3,2 N/mm². This value is slightly higher than the characteristic value on shear of the glulam, but about 70 % of the estimated mean value.

We may therefore estimate, that the proposed design procedure overestimates the strength of the frame corner by about 40 %. The performance of an optimised design would in that case be of less than 60 % of the bending capacity of the individual members.

It has to be noted that failure occurred on tension perpendicular to grain (splitting starting from the ends).

6.3 Why the discrepancy?

Maybe that the assumed glulam strength – assumed corresponding to GL 28 – was not achieved (the tests were made in the 60^{ties}), but even so, the large discrepancy can not be explained.

Maybe that the design model is not adequate to explain the real behaviour of the dowelled frame corners. The failure seen by all the tests was a splitting of the timber members, e.g. a tension failure perpendicular to grain, and not a shear failure.

Therefore the strength model for the timber in the joint area should – besides of shear strength – take in account the tensile strength perpendicular to grain, otherwise the design may be unsafe.

It is interesting to remark that P. RACHER published the analytical results of a similar frame corner, where he showed up the stresses on shear and perpendicular to grain. For a circular pattern of the dowels he found the relationship of maximum values

$$\frac{\sigma_{t,90}}{\tau} \cong 0,2$$

For glulam the same relationship based on the material characteristics given in 6.2 would be 0,13 (based on characteristic values) or 0,17 (based on mean values). That means that the failure should occur by splitting of the members, at a load about 70 % of the calculated ultimate load based on the shear strength.

It has also to be noted, that based on the test results, KOLB had proposed in 1970 the introduction of a reduced shear strength for the design of frame corners. The reduced shear value was of 3/4 of the regular design shear value. The design procedure used at that time (see HEMPEL, 1967) was the same as published by P. RACHER in 1995, only that nowadays the reduction – when using only a shear failure criterion – went forgotten.

6.4 Frame corner strength model by Gehri (1976)

To avoid inconsistency between verification of the timber only on shear and the observation that failures occurred on tension perpendicular to grain, a more appropriate design procedure was set up (see GEHRI/1976), which takes in account the tensile strength perpendicular to grain of the glued laminated material.

Basically the corner is reduced to a circular joint area. In this area the general state of stresses can be calculated, assuming a regular transfer of forces between the connected members. Splitting or failure will occur when the condition

$$\sigma_{m,\alpha} = \frac{f_m}{\frac{f_{t,0}}{f_{t,90}} \cdot \sin^2 \alpha + \cos^2 \alpha}$$

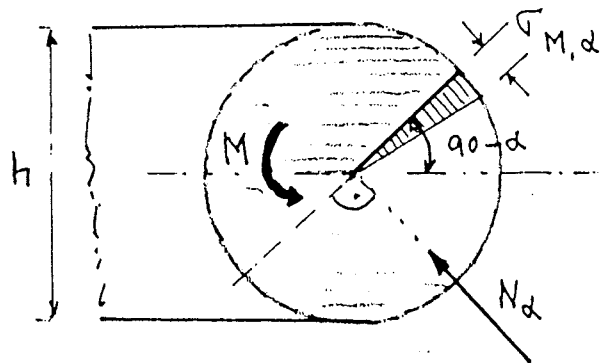
will be fulfilled.

The above formula corresponds to a more generalized Hankinson–formula, which has been introduced in the Swiss Code SIA 164 (1981) and proposed, but not general introduced into EC 5–1–1. See for that clauses 5.1.5(2) and 5.2.3(3).

Based on the proposal the critical stress can be calculated

$$\sigma_{M,\alpha} = \frac{M}{W} \cdot \frac{90 - \alpha^\circ}{180}$$

$$\sigma_{N,\alpha} = \frac{N_\alpha}{b \cdot h}$$



N_α component \perp to section

It can be shown, that the condition will be best fulfilled for the half angle of intersection. For tests X3 and X4 that would be about 52° . The value changes only slightly when using 45° which simplifies the failure condition to

$$\sigma_{m,45} = \frac{f_m}{0,5 \left(1 + \frac{f_{t,0}}{f_{t,90}} \right)}$$

with $f_{t,0} = 0,7 \cdot f_m$ we obtain for $f_{m,\alpha}$: on characteristic value basis $1,26 \text{ N/mm}^2$; on middle value basis $2,13 \text{ N/mm}^2$ and taking account of small (local area) area on tension perp. to grain with increased values $f_{t,90,g} \equiv 1,2 \text{ N/mm}^2$ the value of $3,27 \text{ N/mm}^2$.

The failure condition is therefore very sensitive to the strength perpendicular to the grain or quite directly related to it.

For the tests X3 and X4 we obtain, at failure load,

$$\sigma_{m,45} = \sigma_{M,\alpha} - \sigma_{N,\alpha} = 4,25 - 1,28 = 2,97 \text{ N/mm}^2 \cong 3 \text{ N/mm}^2$$

|
material outside the circle
will reduce value

With a local strength perpendicular to grain of about 1 N/mm^2 the condition would be satisfied.

Tests X1 and X2 with only one circular pattern of dowels showed lower strength. This is explained by:

- reduced end–distance of only $4d$ instead of $7d$ which caused an early beginning of splitting at $2/3$ of the ultimate load
- less regular transfer of forces in the joint area which causes higher stresses
- higher loaded individual dowels
dowels loads where at failure about 15 % higher, than for X3 and X4, introducing therefore higher local stresses
- no overhang of the ends
therefore also reduced strength capacity to shear and tension perpendicular to grain

The capacity of the frame corners with only circular pattern and no overhang (too short end–distances) was about 70 % of the previously shown configuration.

6.5 Conclusions

To establish the resistance of frame corners formed by overlapping the following conditions should be verified:

- for the dowels
 - strength of the highest loaded dowel based on elastic calculation; under certain conditions, where high ductility of the connection may be achieved, a plastic redistribution can be considered
- for the timber in the joint area
 - shear strength
 - tensile strength perpendicular to grain

In case of frame corners built up with glued-laminated timber and of only use of the shear strength criteria, as proposed 1967 by HEMPEL, the shear resistance should be reduced to $3/4$ of the usual design value, (see KOLB (1970)), to take in account, that failure will occur earlier by splitting.

The proposed approach by GEHRI (1976) takes in account both strength criteria for the timber joint area. It may be improved. More important is, that it shows up simple ways to optimize frame corners.

HEMPEL (1967) understood the behaviour of the dowelled frame corners. He not only showed up the calculation which is still used in the STEP lectures, but he also formulated the following recommendations:

- 1 – The pattern of the dowels has a large influence on the resistance of the joint. The best results are achieved when using a circular pattern.
- 2 – The double or paired column is to be verified on shear due to shear force and to splitting (tension perpendicular to grain).
[By using for the paired column the half thickness of the rafter, the failure normally initiates on the column]
- 3 – The paired column should if possible be made of material with cross plies, since this material presents higher resistance to shear and tension perpendicular to grain than glued laminated timber.
[The fact that only one element has higher resistance and stiffness enables not full use but may be enough to increase the ultimate load]

7. Conclusions

For the design of joints and frame corners using dowel-type fasteners the following has to be taken into consideration:

❑ *The general stress state in the joint area*

Failure may be originated by splitting, due to high stresses perpendicular to the grain, and by shear, long before the load-carrying capacity of the dowel is attained. This will cause brittle failure of the joint, even the individual dowel has a high ductility.

❑ *The relative slenderness of the dowel*

When requiring ductile joints only failure modes, where plastic hinges in the dowels are achieved, are acceptable. The relative slenderness should therefore always be chosen greater than unity.

❑ *Fabrication tolerances*

Fabrication tolerances reduce the ability of plastic redistribution of the dowels. This results in a larger reduction in the efficiency of the joint.

❑ *Johansen's equations*

Johansen's equations give the upper bound of values for a single dowel. The factor $k_{\text{SYS}} = 1,1$ used in EC 5-1-1 should therefore be reduced to unity. The equations are also valid for multiple-shear joints: therefore the clause 6.2.3(1) should be deleted.

When using Johansen's equations for joints, restrictions must be made about ductility, group effect and fabrications.

Literature

- Doyle, D.V.: Performance of joints with eight bolts in laminated Douglas-fir. U.S. Forest Service Research Paper, FLP 10, 1964.
- Ehlbeck, J., Larsen, H.-J.: Grundlagen der Bemessung von Verbindungen im Holzbau nach dem Eurocode 5. Bauen mit Holz, 1993, S. 821 – 840.
- Erki, M.-A. / Huggins M.: Load capacity of row of shear plate connectors. Journal Structural Engineering, Vol. 109, No. 12, December 1983.
- Gehri, E. (1976): Verdübelte oder verbolzte Rahmenecken, in "Bemessung und Ausführung von Brett-schicht-Konstruktionen" p. 130 – 139. Schweiz. Arbeitsgemeinschaft für Holzforschung, 1976.
- Gehri, E.: Swiss proposals for new formulations and comments on Eurocode 5 – Part 1. Nov. 1992.
- Gehri, E.: Grundlagen der Verbindungstechnik. In "Holzwerkstoffe auf Furnierbasis". SAH-Fortbildungskurs 1993.
- Gehri, E.: Joints with dowel-type fasteners. A system factor or a systematic error? Paper prepared for CIB-Meeting in Sydney, 1993.
- Hempel, G. (1967): Rahmenecken mit Dübelanschluss. Bauen mit Holz, 1967, p. 77 – 81.
- Hilson, B.O.: Joints with dowel-type fasteners – Theory. STEP-Lecture. 1993.
- Johansen, K.W.: Theory of timber connections. IABSE, Publ. Nr. 9, 1949.
- Kolb, H. (1970): Festigkeitsverhalten von Rahmenecken, Bauen mit Holz, 1970, p. 387–392.

- Mischler, A.: Untersuchungen an BSB-Verbindungen. 1991 – 1996. Interner Bericht Professur für Holztechnologie, ETH Zürich [Auszug in D. Indermühle. Diplomarbeit SISH].
- Racher, P. (1995): Biegesteife Verbindungen. STEP 1, lecture C16.
- Racher, P. (1995): Frame corners. STEP 2, lecture D8.
- Werner, H.: Tragfähigkeit von Holz-Verbindungen mit stiftförmigen Verbindungsmitteln unter Berücksichtigung streuender Einflussgrößen, 1993. Berichte der Versuchsanstalt für Stahl, Holz und Steine der Uni Karlsruhe. 4. Folge – Heft 28.
- Yasumura, M.: Japan overview: design concept and prospect of bolted joints and nailed joints. Int. Workshop on Wood Connectors. Forest Products Society 1993.

INTERNATIONAL COUNCIL FOR BUILDING RESEARCH STUDIES AND DOCUMENTATION
WORKING COMMISSION W18 - TIMBER STRUCTURES

QUASI-STATIC REVERSED-CYCLIC TESTING OF NAILED JOINTS

by

E Karacabeyli
A Ceccotti
Forintek Canada Corporation
Canada

MEETING TWENTY - NINE

BORDEAUX

FRANCE

AUGUST 1996

QUASI-STATIC REVERSED-CYCLIC TESTING OF NAILED JOINTS

By

Erol Karacabeyli¹ and Ario Ceccotti²

ABSTRACT

Nailed joints provide platform frame wood structures with most of their ductility and energy dissipating characteristics which, in turn, make these wood frame structures a very suitable choice, especially for areas with high seismic activity. There are a number of standards, either developed or proposed, for testing joints under a quasi-static reversed-cyclic displacement protocol. Results from a seismic research program at Forintek Canada Corp., including testing of nailed joints according to the above mentioned standards are presented here with particular emphasis on establishing yield point and envelope curves and quantifying ductility and impairment of strength. Differences in those characteristics arising from utilization of different standards are discussed.

INTRODUCTION

There are a number of test standards which are under development for quasi-static reversed-cyclic testing of timber joints with mechanical fasteners (CEN 1995, ASTM 1993, AS 1995). The International Standards Organization's Technical Committee on Timber Structures (ISO TC 165) established a Working Group (WG 7) for the development of an international standard for reversed-cyclic testing of joints for earthquake loading (ISO 1995). There is an opportunity, to a certain extent, to harmonize these standards into an international standard.

There have been number of investigations on the different testing protocols and their implications on cyclic performance of joints (Ceccotti 1994, Chui et. al. 1995, Foliente 1994, RILEM 1994). The following characteristics appear to be important for cyclic testing of joints for earthquake loading: cyclic displacement protocol (the magnitude and number of cycles, constant frequency or constant velocity, duration of the test), procedure for defining yield point and ductility, ultimate load, strength degradation, and assessment of stiffness and energy dissipation capability of the joint. The purpose of this paper is to provide additional technical data for nailed joints on these characteristics.

MATERIALS AND METHODS

The test matrix for the nailed connections presented in this paper is given in Table 1. These five test groups are part of a larger test matrix which was designed to investigate the effect of variables such as grain direction (for lumber and panels), wood species, panel type (plywood, oriented strand board, gypsum wall board), and test configuration (end fixity, number of nails, number of side members,

¹ Wood Engineering Scientist, Forintek Canada Corp.

² Visiting Scientist, Forintek Canada Corp.

specimen geometry), loading direction (tension versus compression) and cyclic displacement protocols. Matching between the test groups were performed based on the clear wood density. The statistics in Table 1 indicates that the matching between the groups was reasonable.

Table 1. Test matrix and relative density of the lumber.

GROUP NO.	TEST DESCRIPTION	N	RELATIVE	
			Mea	Std. Dev.
2	Static (Ramp) - Tension	6	0.44	0.05
40	ASTM-SDP procedure	6	0.43	0.05
39	CEN-long procedure	6	0.45	0.03
38	CEN-short procedure	6	0.45	0.06
29	Forintek (FCC) - Cyclic	6	0.44	0.05

A schematic of the test specimen and jig is shown in Figure 1. The lumber main member of each specimen was cut from a 2x4 (38 mm by 89 mm) SPF (spruce, pine, fir) piece, and the plywood side member was cut from 9.5 mm thick CSP (Canadian Softwood Plywood Sheathing Grade CSA O151-M). The grain direction of lumber member and the surface veneer of plywood were parallel to the applied load. These two members were connected by **two common nails** (63.5 mm long, diameter of 3.1 mm). The average bending yield strength of five randomly selected nails was determined using the ISO/CD 10984-1.2 standard (ISO 1995b), and found to be 770 MPa. Conditioning and testing were performed at ambient laboratory conditions where the average moisture content of both the lumber and the plywood were approximately 9 percent. The time period between the assembly and the testing of the joints was approximately half an hour.

A total of five types of displacement schedules were employed. The first one is a static test with a slip rate of 2.5 mm/minute. Each of the other four groups were subjected to one of the following four cyclic displacement protocols:

- 1) ASTM SDP (Sequential Phased Displacement Procedure, ASTM 1993, Dolan, 1993). A constant frequency of 1 Hz is specified.
- 2) CEN-Long Cyclic Procedure (CEN 1995). A constant velocity between 0.02 and 0.2 mm/second is specified.
- 3) CEN-Short Cyclic Procedure (CEN 1995). A constant velocity between 0.02 and 0.2 mm/second is specified.
- 4) FCC (Forintek) Cyclic Procedure. A constant frequency of 0.5 Hz is specified.

The cyclic displacement schedules are shown in Figure 2. For simplicity, in this paper, the authors used a slightly modified yield and ultimate definition for the ASTM-SPD procedure.

An examination of these protocols suggest that the possible differences in the test results may be due to the rate of displacement or the frequency, the recovery of the wood on the previously loaded side of the joint, and the fatigue of the nails.

TEST RESULTS

The results are given for the entire connection which include **two nails**. The load-slip data for the static ramp test group are shown in Figure 3. The load versus time data obtained from the corresponding cyclic displacement protocol (Figure 2) are shown in Figure 4. Examples of load-slip data are shown in Figure 5 for each of the four cyclic test protocols. The envelope curves for the first cycle and third cycle peak loads are shown in Figures 6a and 6b for ASTM-SPD, in Figures 7a and 7b for CEN-Long, and Figures 8a and 8b for FCC-Cyclic protocols. The first, second, and third envelope curves for one FCC-Cyclic specimen are shown in Figure 9 along with the mean static test data (shown with a dashed line).

INTERPRETATION OF THE DATA

Stabilized Envelope Curves

The data were analysed to determine an appropriate envelope curve to be used as the stabilized curve. The CEN-Short specimens were tested to failure after being subjected to five (instead of three as specified in the CEN 1995) displacement cycles (Figure 2). In Figures 4 and 5, the load values for one of the CEN-Short specimens are plotted against the time and slip data, respectively. These data suggest that the majority of the strength degradation occurs between first and second cycles, and differences between the peak loads obtained in second, third, fourth and fifth cycles are relatively small. Test data obtained on other cyclic test protocols in Figures 4 and 5 also support this observation. For the nailed joint investigated in this paper, the test results suggest that three consecutive cycles are sufficient to achieve the stabilized envelope curve.

Cyclic Displacement Protocol and Failure Modes

In order to detect the differences in load-slip data between different cyclic displacement protocols, we plotted the first and third cycle envelope curves for each of the protocols (Figures 6, 7 and 8). These data show minimal differences between the three cyclic protocols up to approximately 10 mm slip. After this level, the ASTM-SPD specimens exhibit a sharper decline in load carrying capacity (see item "a" below for possible reasons). From the standards harmonization point of view, this observation is quite promising if this drop in load carrying capacity can also be observed for other configurations and fasteners.

The failure mode is one of the important factors in selecting an appropriate cyclic test protocol for earthquake loading. It is desirable that the failure mode obtained in testing be similar to that observed under earthquake loading.

A close examination of tested specimens after 15 mm slip revealed three types of failure modes:

1) nail failures (the rupture of a nail through the shear plane); 2) nail pull-through failure; and 3) nail withdrawal failure. We made the following observations with regards to failure modes:

- a) Nail failures were non-existent in static-ramp tests and CEN-short tests, but most dominant in ASTM-Cyclic tests. This may be attributed to the fast rate of displacement as a consequence of the 1 Hz frequency specified in the ASTM standard. It is the authors' opinion that these nail failures may be due to excessive fatigue, and may not be one of the dominant failures under earthquake loading. The fast rate may also be difficult to achieve in some test facilities.
- b) Pull-through failures were the dominant failure mode in static-ramp tests and most (four out of six specimens) FCC-Cyclic tests. We suspect that a thicker and denser panel product would have resulted in higher ultimate loads and less pull-through failures. The CEN-Long Cyclic tests resulted in a mixture of pull-through and nail failures.
- c) Withdrawal failure mode was observed together with pull-through failure only for CEN-short Cyclic tests.

In testing nailed shear walls, we also observed nail tear-out failures where the edge distance was relatively small, and the nail forces perpendicular to the edge were significant (Karacabeyli and Ceccotti 1996). Future cyclic and shake table tests on nailed shear walls will help to select the appropriate cyclic testing procedure with regard to failure mode.

Impairment of Strength

There is a common displacement level among the three cyclic protocols where the first envelope curves of all the cyclic test specimens were similar to those obtained for the ramp test specimens (Figure 9). After that displacement level, however, the first envelope curves for the cyclic test specimens, with the exception of CEN-Short specimens, showed a rapid decline. The impairment of strength values obtained for FCC-cyclic specimens are given in Table 2. The average impairment of strength at a slip level of 5 mm in the second and third envelope curves relative to the first envelope curve were found to be less than 20 percent. The impairment of strength was slightly larger for tension loading than compression loading. This may be attributed to loading this particular group on the first cycle in tension (the reverse cycle was the compression cycle).

Yield Displacement and Ductility

The yield and ultimate displacements are defined differently in various standards. Examples of four approaches are shown in Figure 10. They are also linked differently to the seismic design procedures in their respective building codes. Although the ductility is consistently defined as the ratio of ultimate to yield displacements in all these standards, one may expect differences in ductility

Table 2. Impairment of strength (%) at various displacement levels.

Displacement (mm)	-9	-8	-7	-6	-5	-4	-3	-2	2	3	4	5	6	7	8	9
Specimen 291																
Load (kN) at 1st Envelope Curve	-1.632	-1.737	-1.853	-1.997	-2.142	-2.098	-1.993	-1.778	1.624	1.811	1.933	2.044	2.032	2.023	2.020	2.017
Impairment (%) 3rd vs. 1st	31	26	23	20	17	15	12	10	11	12	15	23	25	27	34	44
Impairment (%) 2nd vs. 1st	n/a	n/a	17	14	12	9	9	7	8	8	11	17	20	22	28	37
Specimen 292																
Load (kN) at 1st Envelope Curve	-1.820	-1.809	-1.788	-1.735	-1.683	-1.605	-1.508	-1.323	1.613	1.772	1.849	1.944	2.009	2.073	2.081	2.074
Impairment (%) 3rd vs. 1st	25	22	19	18	16	14	12	12	12	11	14	17	21	24	26	28
Impairment (%) 2nd vs. 1st	18	16	14	13	11	9	8	9	8	8	10	13	16	19	21	22
Specimen 293																
Load (kN) at 1st Envelope Curve	-1.662	-1.745	-1.817	-1.850	-1.883	-1.781	-1.684	-1.497	1.519	1.726	1.891	2.063	2.149	2.235	2.180	2.053
Impairment (%) 3rd vs. 1st	n/a	n/a	22	19	17	13	11	11	10	11	14	20	27	33	36	38
Impairment (%) 2nd vs. 1st	23	19	16	12	9	7	7	6	8	8	9	12	19	25	28	30
Specimen 294																
Load (kN) at 1st Envelope Curve	-1.983	-2.090	-2.178	-2.208	-2.239	-2.146	-1.989	-1.727	1.776	2.024	2.136	2.283	2.318	2.352	2.312	2.241
Impairment (%) 3rd vs. 1st	24	23	22	19	16	13	11	10	12	12	16	23	27	31	33	34
Impairment (%) 2nd vs. 1st	19	18	17	14	11	9	8	7	8	9	12	15	20	24	26	27
Specimen 295																
Load (kN) at 1st Envelope Curve	n/a	n/a	-2.086	-2.152	-2.219	-2.166	-2.064	-1.809	1.666	1.853	1.982	2.106	2.145	2.185	2.078	1.932
Impairment (%) 3rd vs. 1st	n/a	n/a	21	18	15	13	11	10	12	11	16	23	32	40	48	55
Impairment (%) 2nd vs. 1st	n/a	n/a	19	14	10	9	8	6	7	8	11	16	24	31	39	47
Specimen 296																
Load (kN) at 1st Envelope Curve	n/a	n/a	-1.917	-1.980	-2.043	-1.993	-1.909	-1.713	1.776	1.962	2.053	2.187	2.230	2.274	2.185	2.041
Impairment (%) 3rd vs. 1st	n/a	n/a	22	20	18	14	12	10	12	12	15	20	27	34	41	49
Impairment (%) 2nd vs. 1st	n/a	n/a	13	13	12	10	7	7	7	8	10	14	21	27	33	41
Average																
Load (kN) at 1st Envelope Curve	n/a	n/a	-1.940	-1.987	-2.035	-1.965	-1.858	-1.641	1.662	1.858	1.974	2.105	2.147	2.190	2.143	2.060
Impairment (%) 3rd vs. 1st	n/a	n/a	22	19	17	14	12	11	12	12	15	21	27	32	36	41
Impairment (%) 2nd vs. 1st	n/a	n/a	16	13	11	9	8	7	8	8	11	15	20	25	29	34

values determined by these standards because of the differences in definition of yield and ultimate displacements. Examples of differences in the yield displacement and ductility values between the four standards are presented in Table 3. For example, we calculated these properties for the average ramp test data, and for the first envelope curve of one of the FCC-Cyclic test specimen. Despite the differences in definitions, the yield displacement for ASTM, CEN, and FCC-cyclic methods, and the ductility values for CEN and ASTM methods were quite similar. The ductility value determined utilizing the Australian standard was significantly greater because of lower yield displacement. The ductility value calculated with FCC method is lower because of the smaller ultimate displacement used (Figure 10).

For this FCC-cyclic specimen which was analysed in detail, we made the following observations. The yield displacements for first envelope curve were found to be greater than those found for the third envelope curve. Because of relatively greater ultimate displacements, the ductility values for ramp test data were found to be greater than those found for first envelope curve. Yield displacement and ductility values for tension and compression cycles appear to be similar.

In an international standard, it would be difficult to define ductility which is in harmony with different building codes. On the other hand, presentation of impairment of strength versus slip would give the necessary information required for the evaluation of the joint behaviour according to individual design codes.

Table 3. Examples of yield displacement and ductility values.

Specimen No.	Envelope Curve	Tension (+) or Comp. (-)	Yield Displacement				Ductility			
			AS	ASTM	CEN	FCC	AS	ASTM	CEN	FCC
Average	Ramp	+	0.7	1.3	0.9	0.9	23	13	19	13
FCC-Cyclic-No.3	1st	+	0.8	1.3	1.1	1.3	15	9	11	6
	1st	-	0.8	1.1	1.1	1.1	14	10	10	5
	3rd	+	0.7	0.9	0.9	0.9	12	10	10	6
	3rd	-	0.6	1.1	0.9	0.9	15	8	11	6

Stiffness Degradation, Equivalent Viscous Damping

The initial and cyclic stiffness, and equivalent viscous damping (EVD) may be used for comparing the behaviour of different joints. In order to study the stiffness degradation, one can calculate the cyclic stiffness as a function of the slip as described by Dolan (1993). The definition of EVD is the same in all the standards. It would be useful, however, to agree on the specific envelope curve from which these properties are determined.

FUTURE WORK

The damage on the joint can be related to the work done by the joint, and this may be used as one of the parameters in selecting an appropriate cyclic displacement protocol. The work done on the joint may be estimated by calculating the hysteretic energy dissipated by the joint. For a fixed ultimate displacement level, this can be done for cyclic tests as well as simulated earthquakes. For example, the behaviour of a nailed joint under an earthquake loading is shown in Figure 11. The closest dissipated energy to the simulated earthquake may be a selection parameter for an international cyclic test protocol.

ACKNOWLEDGEMENTS

This work forms part of Forintek's research program on the seismic resistance of timber structures, and is being carried out under a contract funded by Canadian Forest Service. We would like to thank our colleagues Mr. W. Deacon, Mr. C. Lum, Mr. H. Fraser, and Mr. L. Stroh and Mr. L. Olson for their contributions to this work.

REFERENCES

- AS 1995. Australian Standard (Draft). Timber-Methods of test for mechanical joint systems. Standards Australia.
- ASTM 1993. American Society for Testing and Materials. Proposed standard test method for dynamic properties of connections assembled with mechanical fasteners (3rd draft). ASTM Philadelphia, Pa, U.S.A.
- Ceccotti, A. 1994. Timber connections under seismic actions. Timber Engineering STEP 1. Centrum Hout, The Netherlands.p:c17/1-10.
- CEN 1995. Comite' Europeen de Normalisation. Timber structures- test methods- cyclic testing of joints made with mechanical fasteners. (Draft). EN TC 124.117, European Committee for Standardization, Brussels, Belgium.
- Chui, Y., H., Smith, I., Daneff, G. 1995. On protocols for characterising "dynamic" properties of structural timber connections. Seventh Canadian Conference on Earthquake Engineering, Montreal, Canada. p:617-624.
- Dolan, J.D. 1993. Proposed test method for dynamic properties of connections assembled with mechanical fasteners. Proceedings of CIB Working Commission W18 Meeting Twenty-Six, Athens, Georgia, U.S.A.
- Foliente, C. G. 1994. Analysis, design and testing of timber structures under seismic loads. Proceedings of a research needs workshop, University of California, Forest Products Laboratory, Richmond, CA, U.S.A.
- ISO 1995a. Report (N182) of the 9th meeting of ISO/TC 165. Paris. Secretariat of ISO/TC 165 Timber Structures. Standards Council of Canada.
- ISO 1995b. ISO/CD 10984-1.2 Timber Structures-dowel type fasteners-Part 1:Determination of bending strength (EN409). Secretariat of ISO/TC 165 Timber Structures. Standards Council of Canada.
- Karacabeyli, E. and A. Ceccotti 1996. Test results on the lateral resistance of nailed shear walls. Prepared for presentation and publication at the International Wood Engineering Conference, New Orleans, U.S.A.
- RILEM 1994. Timber structures in seismic regions, RILEM state-of-the-art report. Materials and Structures, Vol. 27, No. 167. p:157-184.

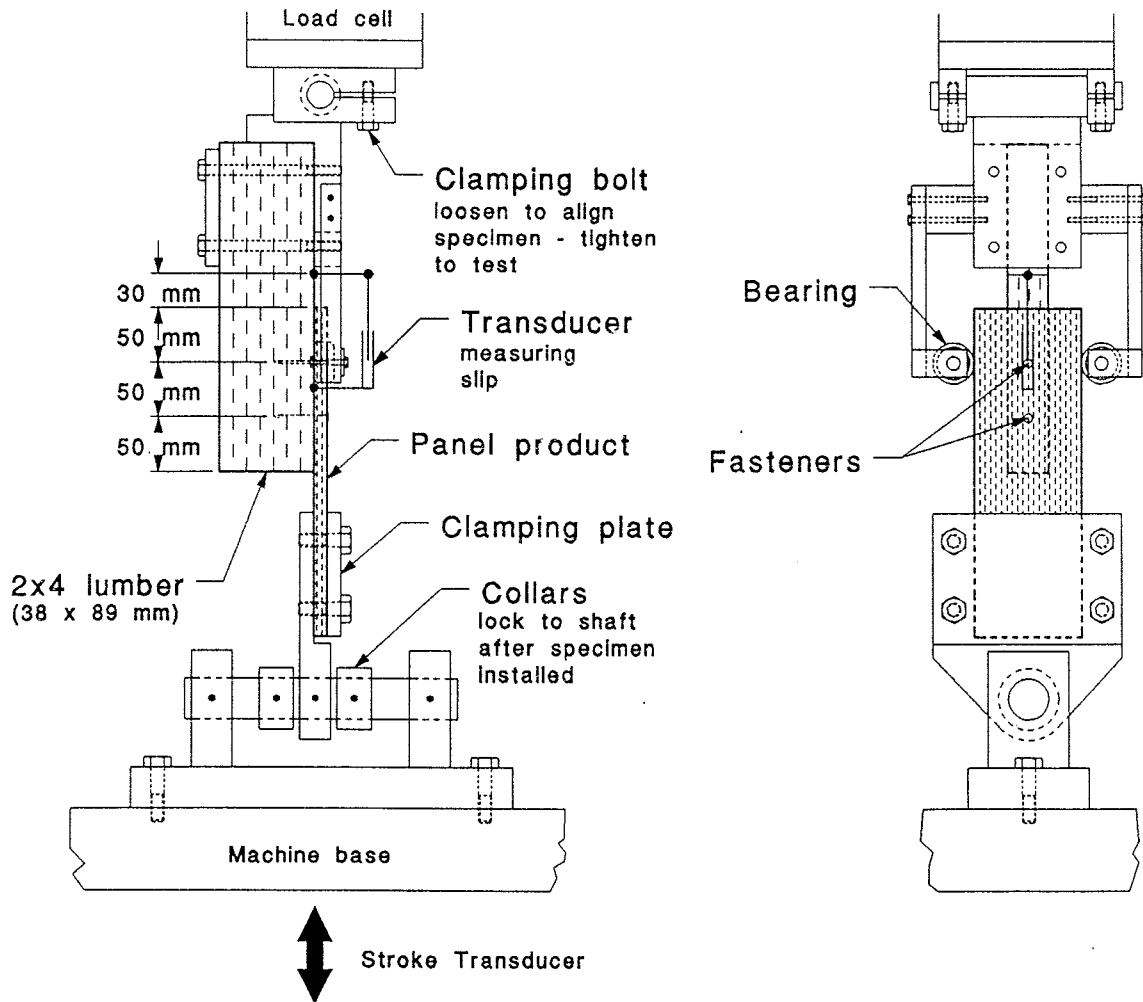


Figure 1. Test set-up for load-slip tests

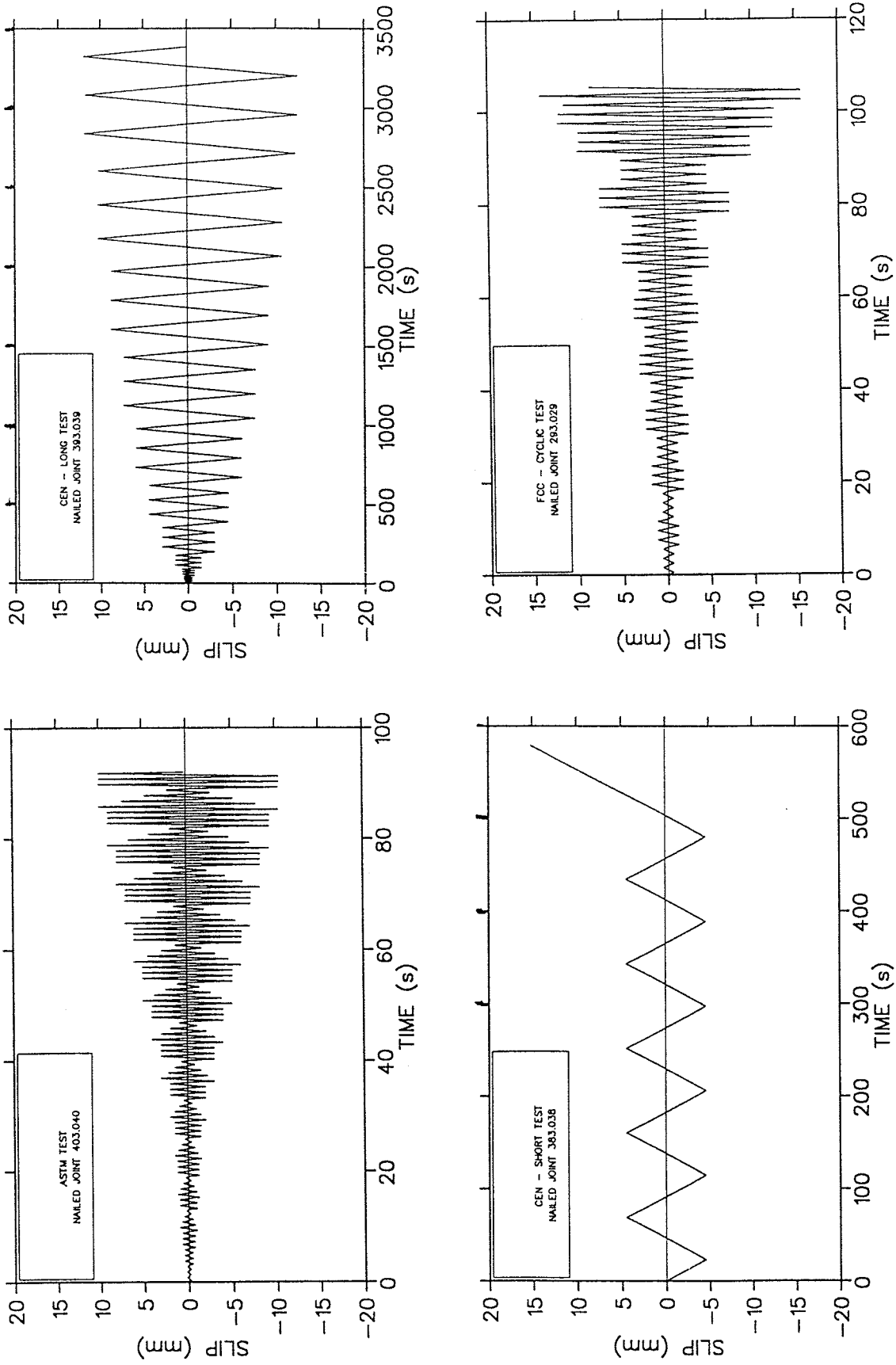


Figure 2. Cyclic displacement protocols for different standards.

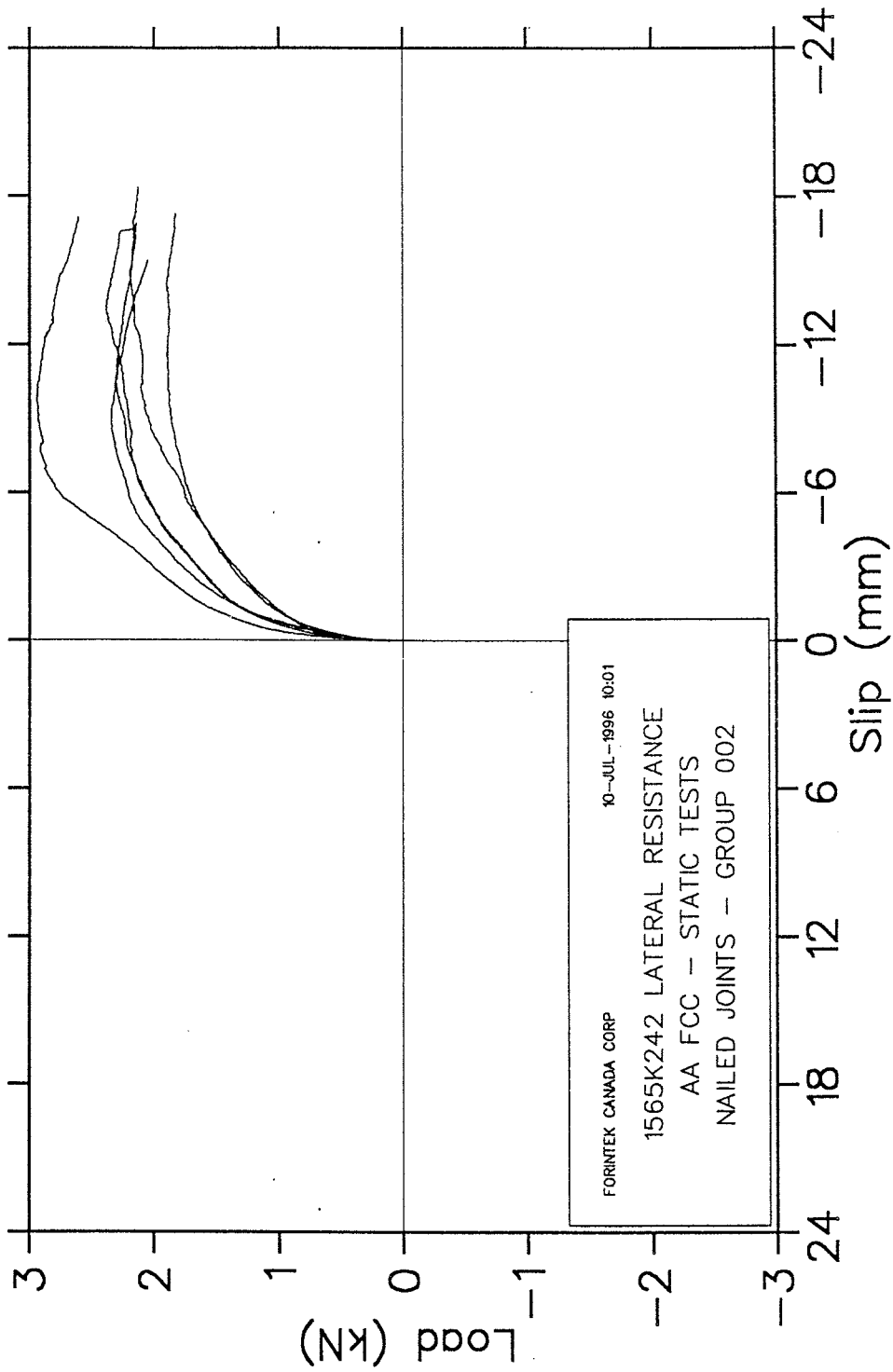


Figure 3. Data from ramp tests.

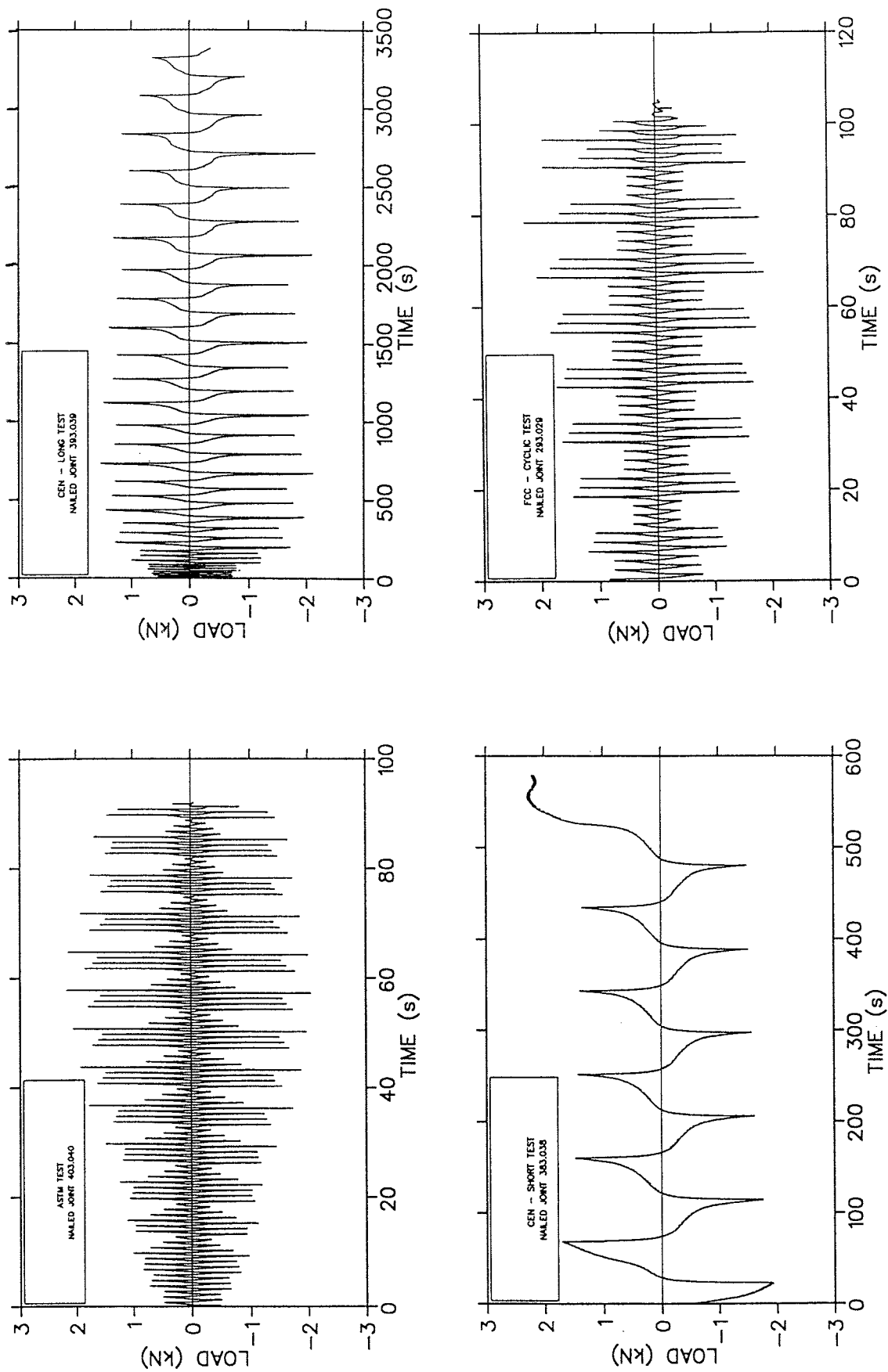


Figure 4. Load versus time data.

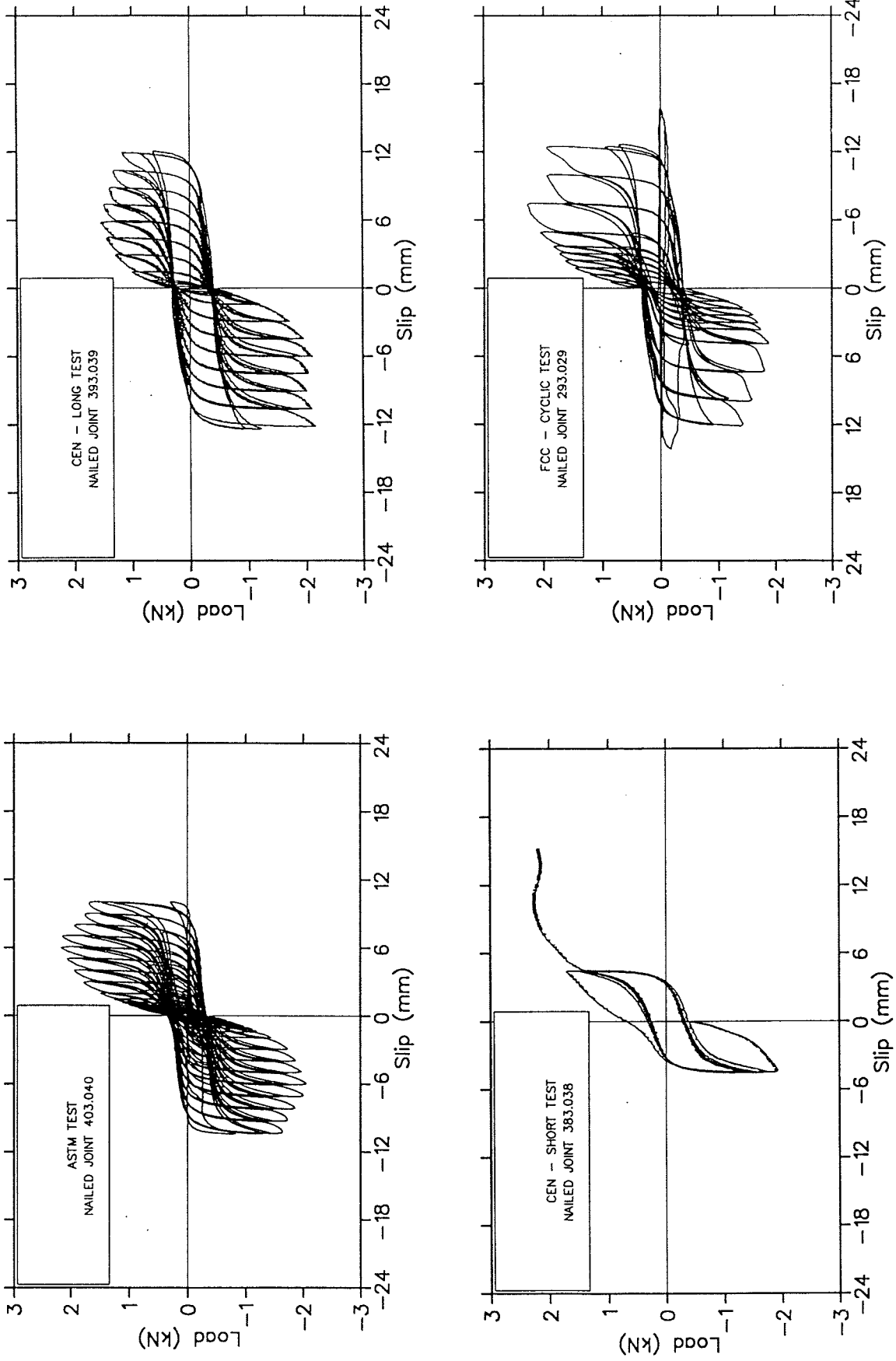


Figure 5. Load versus slip data.

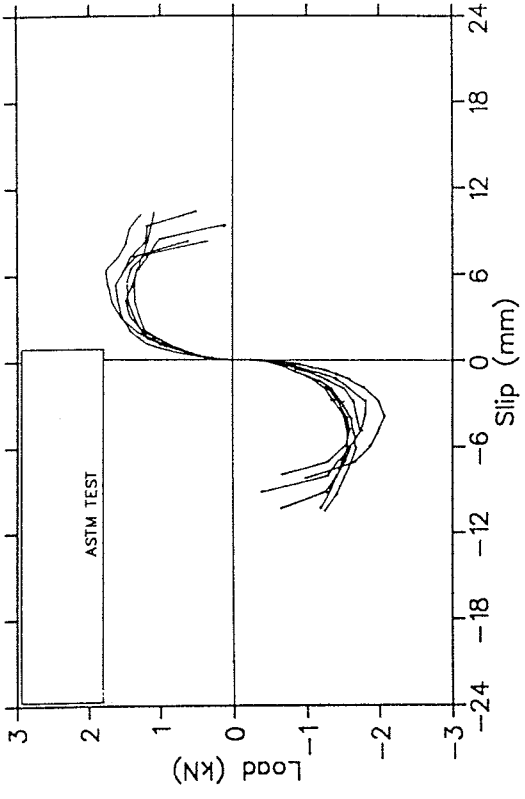


Figure 6a. 1st cycle envelope curves, ASTM-SPD.

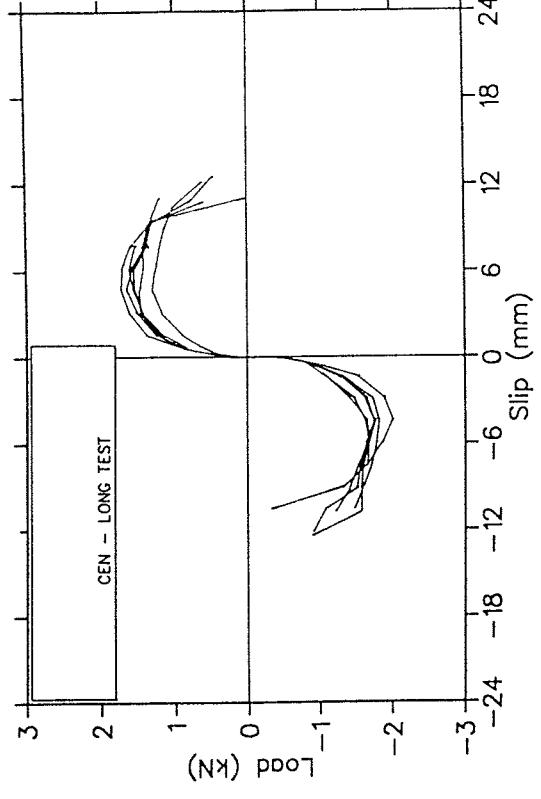


Figure 6b. 3rd cycle envelope curves, ASTM-SPD.

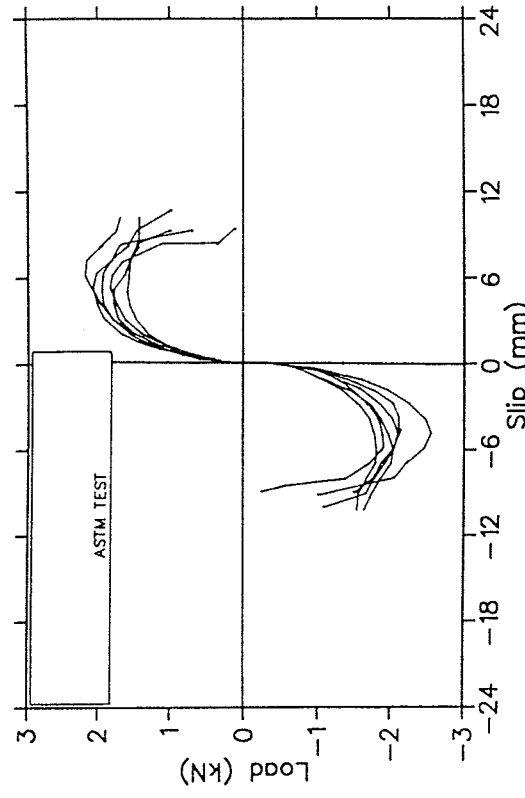


Figure 7a. 1st cycle envelope curves, CEN-long.

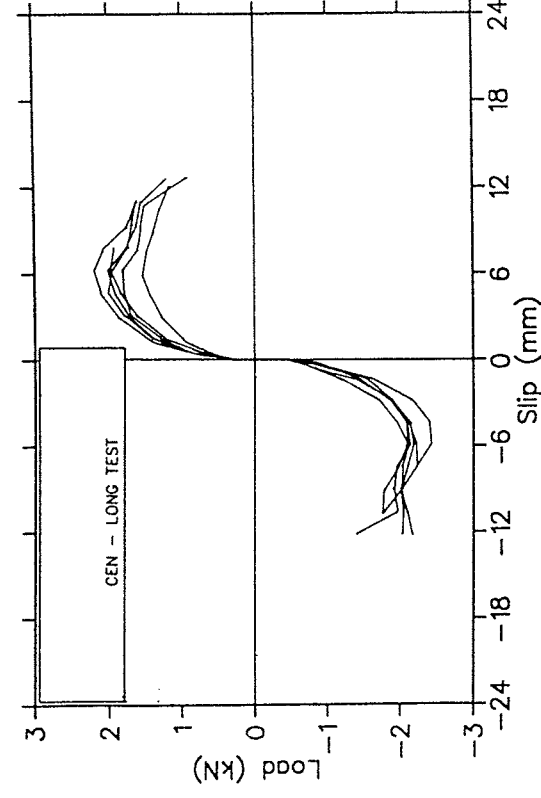


Figure 7b. 3rd cycle envelope curves, CEN-long.

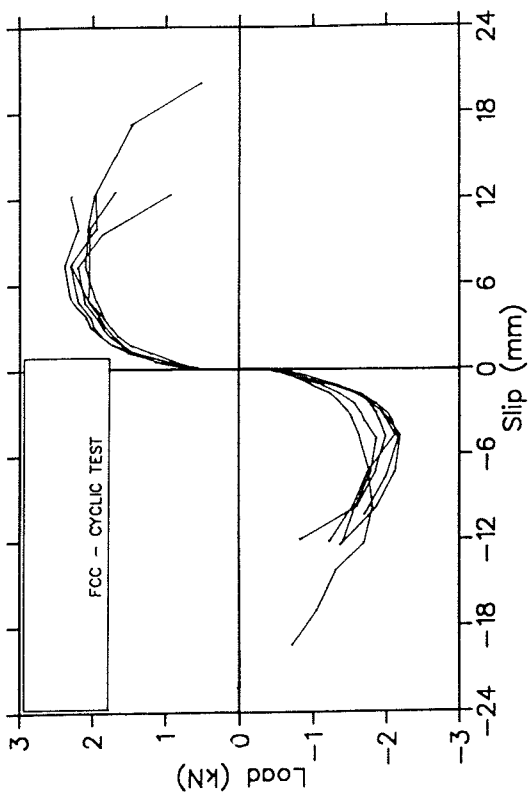


Figure 8a. 1st cycle envelope curves, FCC-cyclic.

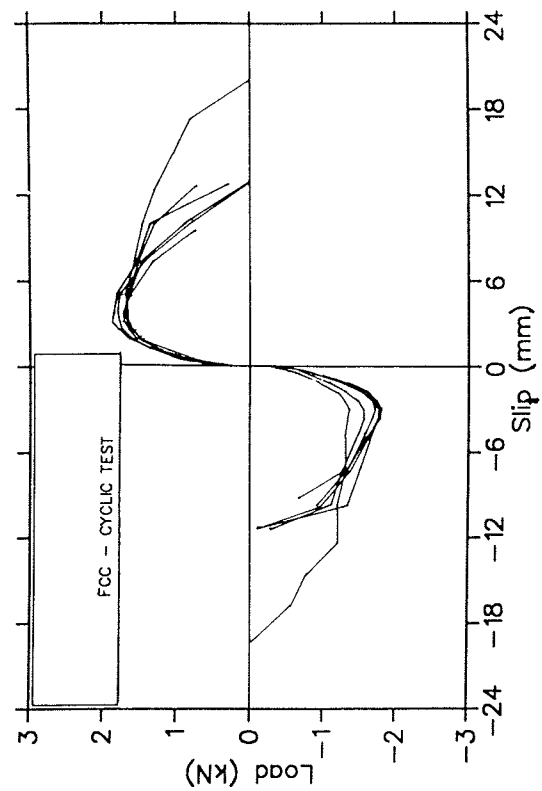


Figure 8b. 3rd cycle envelope curves, FCC-cyclic.

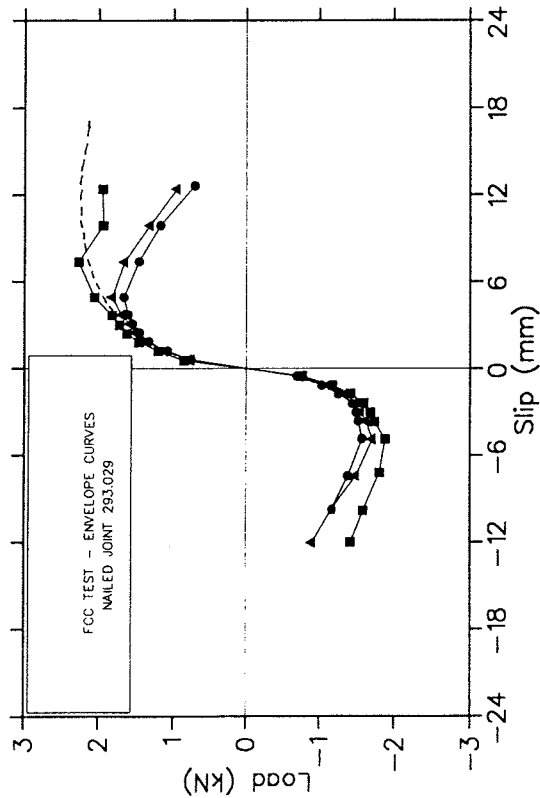


Figure 9. 1st, 2nd, and 3rd envelope curves of one FCC-cyclic specimen and the mean static test data.

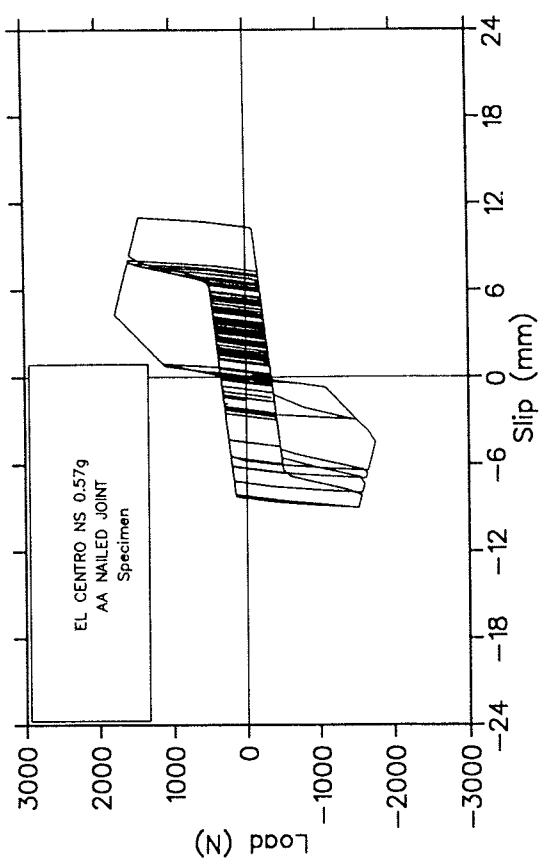


Figure 11. Behaviour of a nailed joint under earthquake loading.

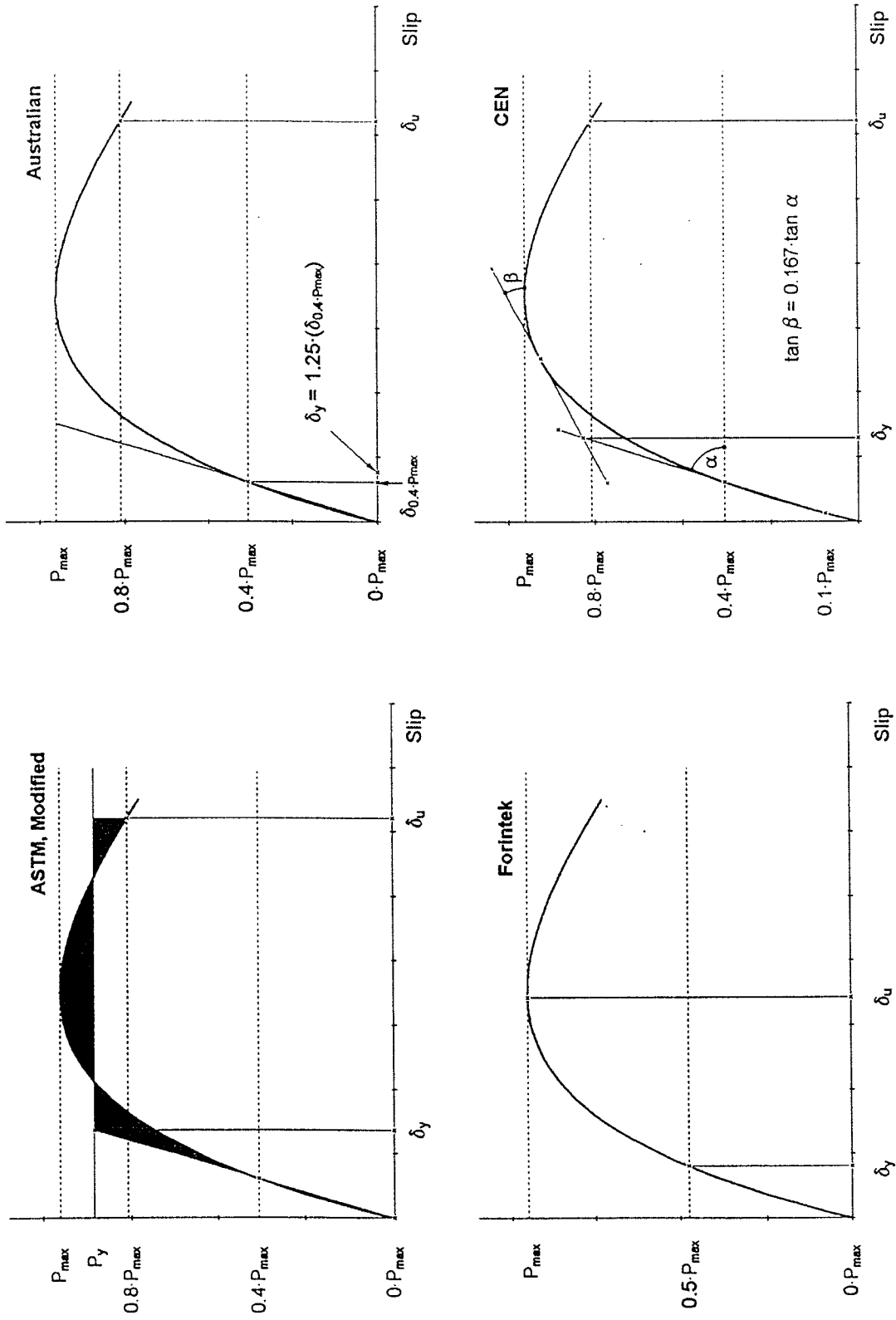


Figure 10. Definition of yield and ultimate displacements for different standards.

INTERNATIONAL COUNCIL FOR BUILDING RESEARCH STUDIES AND DOCUMENTATION
WORKING COMMISSION W18 - TIMBER STRUCTURES

**FAILURE OF BOLTED JOINTS LOADED PARALLEL TO THE GRAIN:
EXPERIMENT AND SIMULATION**

by

L Davenne

L Daudeville

Laboratoire de Mécanique et Technologie

France

M Yasumura

Building Research Institute

Japan

MEETING TWENTY - NINE

BORDEAUX

FRANCE

AUGUST 1996

Failure of Bolted Joints Loaded Parallel to the Grain: Experiment and Simulation

Luc DAVENNE, Laurent DAUDEVILLE

Laboratoire de Mécanique et Technologie, ENS Cachan / CNRS / Univ. Paris 6

61 avenue du Président Wilson, 94235 Cachan, France

E-mail: daudevil@lmt.ens-cachan.fr

Motoï YASUMURA

Building Research Institute, 1 Tatehara, Tsukuba Ibaraki 305, Japan

ABSTRACT

This paper deals with the analysis of failure of joints with dowel-type fasteners in glued laminated timber under static loading. The single bolt loads the wood parallel to the grain. The joint failure is due to a cracking along the grain direction.

An experimental program was carried out on joints for different structural parameters and bolt diameters.

Fracture is analysed by use of linear elastic fracture mechanics concepts. Possible pure or mixed modes of fracture are investigated. The crack propagation condition is assumed to be based on a comparison of the energy release rate with a critical value. An analysis of elastic stresses is carried out for the prediction of the onset of cracking.

The critical energy release rate value was obtained from experimental results of fracture tests under three point bending. The comparison between experimental and numerical results for the simulation of fracture in joints shows that the linear elastic fracture mechanics provides a good approximation of load-bearing capacity of bolted joints and may help improve design codes.

INTRODUCTION

The calculation methods for the design of mechanical joints with dowel-type fasteners proposed in codes like (Eurocode 5, 1993) do not take into account damage mechanisms of wood like fracture parallel to the grain. In the Eurocode 5 standard, only the calculation of notched beams is based on Linear Elastic Fracture Mechanics (LEFM) concepts.

The aim of that paper is an experimental and numerical analysis of failure of dowel-type joints when cracking of wood is the main mode of damage. Only joints with a single dowel are examined but this work can be extended to industrial joints. The loading conditions and the parameters of this study are given in Figure 1.

The structural parameters are the bolt diameter d , the end-distance e_1 and the edge-distance e_2 . The thickness b is chosen with the intention of avoiding bending of the dowel ($b/d = 2$).

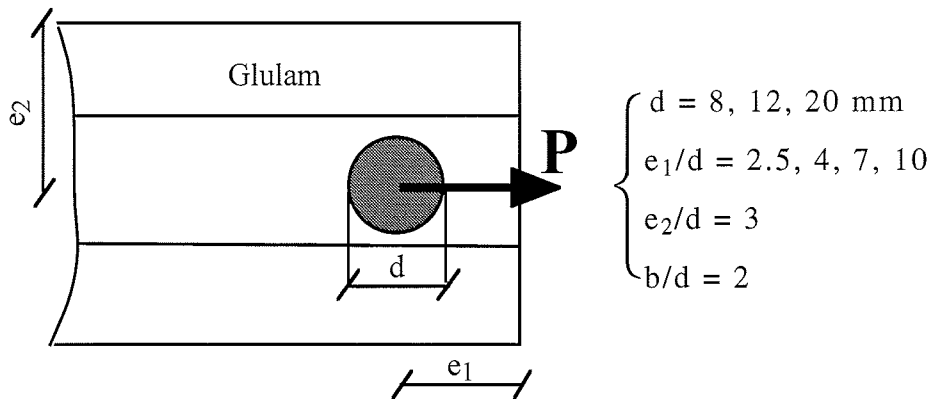


Figure 1 - Glued laminated specimens loaded parallel to the grain (b is the thickness)

Experimental results are presented. Tests were performed at the Building Research Institute (BRI) of Tsukuba, Japan.

The failure mode is a propagation of a crack parallel to the grain (L direction) that is the weakest plane of wood. Some plasticity may appear due to the embedding of the bolt into the wood.

A simplified analysis is proposed, plasticity phenomena are not considered in this study. The crack initiation and the crack propagation are analysed separately. Both problems are solved with the Finite Element (FE) code CASTEM 2000 under the assumptions of elastic bodies and of plane stress states.

The crack initiation analysis is essentially carried out for the determination of the onset location. The crack propagation is analysed with the LEFM approach. Application of fracture mechanics to wood has principally concerned test specimens for the evaluation of fracture properties (Valentin et al., 1991).

For the analysis of mechanical joints, fracture mechanics methods have been scarcely applied. LEFM assumes that all damage phenomena are concentrated at the crack tip. Non Linear Fracture Mechanics (NLFM) or Damage Mechanics (DM) consider a process zone where non linear damage phenomena occur (Daudeville et al., 1996).

For this problem, the size of the process zone can be neglected compared with the dimensions of the crack and of the structure. In such a case the LEFM approach is valid.

The energy release rate G_{Ic} value is issued from experimental results (Daudeville et al., 1996). The fracture energy G_f of white wood was obtained with three point bending tests proposed in (Larsen and Gustafsson, 1989). It is assumed $G_{Ic} = G_f$.

In the case of a parallel to the grain load, the stress state is a combination of shear and tensile stresses perpendicular to the grain. Thus a possible mixed mode of fracture (mode I and II) is investigated.

If the crack propagates along the plane of symmetry of the specimen, the fracture mode is a pure mode I.

In the latter case, the energy release rate can be computed by the compliance method, that is a global method. In the case of a mixed mode of fracture, a partition of modes is necessary and the two energy release rates G_I and G_{II} are computed by the local crack closure method.

The friction at the wood and bolt contact is considered.

The load-bearing capacity of joints was computed for each combination of structural parameters. Comparisons between experimental and numerical results for studied single bolted joints are presented.

EXPERIMENT

Specimens consist of glued laminated spruce (*Picea* spp.). Two thick steel plates connected with steel dowels load the wood member. The diameter d is the same for the fastener and the wood.

Specimens were tested to failure in stroke displacement control with a head speed of 0.5 mm/mn. Rather than the stroke displacement, the displacement between the steel plates and wooden member was measured with four electronic transducers.

Some specimens were tested with a higher speed (x2). We did not notice any important effects on the maximum load of these specimens.

The mean density was about 410 kg/m³. The wood member thickness was $b = 2d$, the end-distance e_1 varied from 2.5 d to 10 d and the edge distance e_2 was fixed to 3 d (see Figure 1). Figure 2 shows the different patterns of fracture that were observed. The test was stopped just after the load has reached its maximum value.

The pattern A corresponds to a pure tensile mode I of fracture. It is the main mode of damage. The pattern B is combination of shear and tensile modes is essentially possible for large diameters ($d = 20$ mm).

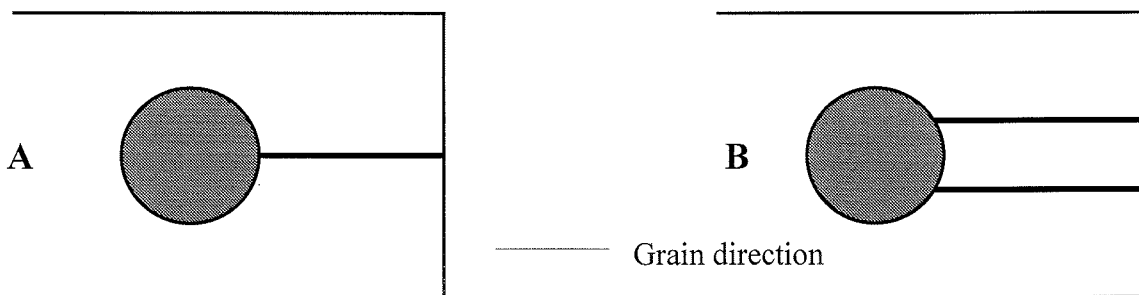


Figure 2 - Fracture patterns

The following table gives the mean maximum load value per unit width. CV denotes the coefficient of variation.

The coefficient of variation is quite important. That may be due to plasticity that is observed on a large part of specimens. Note the mean density was a little lower for $d = 20$ mm.

d (mm)	e_1/d	P_m / b (kN/m) (CV)	Nb	Mode A	Mode B	A & B
8 (421 kg/m ³)	2.5	138 (9)	5	3	0	2
	4	162 (10)	5	5	0	0
	7	156 (15)	5	5	0	0
	10	168 (13)	5	5	0	0
12 (416 kg/m ³)	2.5	284 (41)	5	5	0	0
	4	317 (32)	5	4	0	1
	7	315 (19)	5	4	1	0
	10	316 (12)	5	4	1	0
20 (380 kg/m ³)	2.5	225 (14)	5	4	0	1
	4	270 (23)	5	1	1	3
	7	426 (32)	5	3	1	1
	10	375 (9)	5	3	1	1

Table 1 - Experimental results of bolted joints

MODELING

Assumptions

The modeling assumptions are:

H1 : Plane stress state

H2 : Wood is linear-elastic to failure

H3 : The bolt is a rigid body

H4 : The wood and bolt contact is made with friction.

H5 : The transverse T and radial R directions are not distinguished, i.e. the wood is transversally isotropic

The structure is modelled by finite elements. Because of symmetries, 1/4 of the structure is studied (Figure 3).

H2 assumption can be considered as a coarse assumption because plasticity phenomena due to the embedding of the bolt in the wood are observed.

In a plane stress problem, the radial R and transverse T directions cannot be distinguished so a mean behaviour is considered . The elastic moduli were chosen by extrapolation of results

(Guitard, 1987) with respect to the actual density. x direction corresponds to the L direction (Figure 3).

$$\begin{cases} E_x = 15000 \text{ MPa} , E_y = \frac{E_T + E_R}{2} = 600 \text{ MPa} \\ G_{xy} = \frac{G_{RL} + G_{TL}}{2} = 700 \text{ MPa} , \nu_{xy} = 0.5 \end{cases} \quad (1)$$

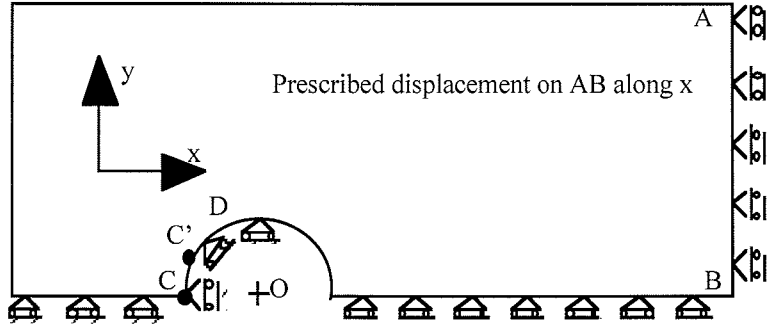


Figure 3 - 1/4 of structure and boundary conditions

Initiation

Due to the orthotropy, the stress state is mainly a tensile one in the y direction around point C (Figure 3), while the maximum shear stress is around point D. The initiation of cracking may occur at point C in mode I, where a high stress gradient exists. But the crack may also start in mixed mode somewhere between C and D.

Different fracture criteria for wood exist in the literature (Rathkjen, 1993). They are expressed in terms of stresses in a co-ordinate system coinciding with the directions of orthotropy. For those particular tests, the failure is due to a cracking parallel to the grain, thus the chosen criterion is expressed as a polynomial function of the elastic stresses $\sigma_{yy} = \sigma_{TT}$ and $\sigma_{xy} = \sigma_{LT}$:

$$\left(\frac{\sigma_{TT}}{Y_t} \right)^2 + \left(\frac{\sigma_{LT}}{S_x} \right)^2 = 1 \quad \text{and} \quad \sigma_{TT} \geq 0 \quad (2)$$

The material constants are $Y_t = 5 \text{ MPa}$ and $S_x = 8 \text{ MPa}$ (C.T.B.A., 1995). The previous values were obtained from shear and tensile tests on French wood.

In the present paper, rather than the initiation load, (2) will be used to obtain information about the location of the onset of cracking.

The maximum of the criterion (2), for every simulation (with different d values), is near point C, at point C'. The friction at the bolt and wood contact has an influence on the location of the onset of cracking.

An other approach for the determination of the location of the cracking initiation consists in the application of LEFM concepts for the initiation problem by assuming a pre-existing sharp crack. This approach was applied to wood in (Sobue, 1989).

Propagation

The existence of a crack at the point C or C' is now assumed (Figure 3). The propagation analysis is carried out by use of classical LEFM i.e. all damage phenomena are assumed to occur at the crack tip.

The energy release rate is:

$$G(P,a) = G_I + G_{II} = -\frac{1}{b} \frac{\partial W}{\partial a} \quad (3)$$

With: P is the applied load, W is the potential energy, a is the crack length, b is the specimen width.

As said before, the location of the plane of propagation is difficult to evaluate accurately. Thus two cases are considered:

- A propagation in the mid plane: angle (OC, OC') = 0, that is a pure mode I of fracture
- A propagation in another plane: angle (OC, OC') ≠ 0, that is a mixed mode of fracture

If the crack propagates from C under a pure mode I ($G_{II} = 0$). A Griffith criterion (Griffith, 1920) is chosen:

$$\begin{cases} G(P,a) < G_{Ic} & \text{No crack propagation} \\ G(P,a) = G_{Ic} & \text{Possible crack propagation} \end{cases} \quad (4)$$

and,

$$\begin{cases} \frac{\partial G}{\partial A}(P,a) \geq 0 & : \text{unstable propagation} \\ \frac{\partial G}{\partial A}(P,a) < 0 & : \text{stable propagation} \end{cases} \quad (5)$$

G_{Ic} is the critical energy release rate in pure mode I. (4) and (5) give some information about the ultimate load by a stability condition of the structure.

During tests, most of fracture planes took place in the mid plane (initiation at point C). In the latter case, the fracture mode is a pure mode I. The fracture analysis is then based on (4) and (5).

According to the numerical results concerning the location of the cracking initiation, the crack may propagate from C' (near C). In such a case, a mixed mode is present. It was decided to study that case.

When the crack initiates at point C', a Griffith criterion does not hold because the critical energy release rate G_{IIc} is much higher than G_{Ic} due to the orthotropy of wood. A partition of modes is then necessary. The following criterion is generally proposed in the literature (Valentin et al., 1991; Wu, 1967):

$$\left(\frac{G_I}{G_{Ic}}\right)^m + \left(\frac{G_{II}}{G_{IIc}}\right)^n \leq 1 \quad (6)$$

(<1 no crack propagation, =1 possible crack propagation).

Coefficients m and n are chosen equal to 1 for simplicity purpose.

The computation of the energy release rate is quite easy in pure mode I. In this case (onset of the crack at point C), $G(P,a)$ is computed by the compliance method which is a global method. The crack propagation is modelled by separating two connected lines. Thus for two F.E. computations 1 and 2:

$$\frac{G}{P^2} = \frac{1}{2b} \frac{1}{\Delta a} \left(\frac{1}{k_2} - \frac{1}{k_1} \right) \quad (7)$$

With $\Delta a = a_2 - a_1$ and $\Delta a \ll a$

In the second case (crack starting at point C' under a mixed mode), G_I and G_{II} are obtained separately with a local method, the crack closure technique.

G_I and G_{II} are computed with the necessary work to close the crack during a propagation Δa (Figure 4):

$$G_I = \frac{1}{2b} \frac{F_x \cdot \Delta u}{\Delta a}, G_{II} = \frac{1}{2b} \frac{F_y \cdot \Delta v}{\Delta a} \quad (8)$$

Where F_x and F_y are the forces in the x and y directions respectively (obtained in the first FE computation). Δu and Δv are the relative displacements of the released node in the x and y directions (second FE computation).

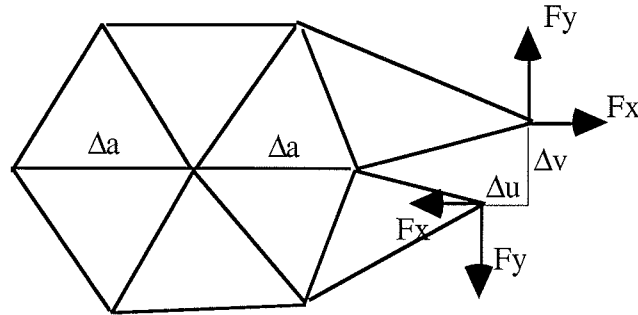


Figure 4 - Crack closure technique

In the both local and global methods for the computation of the energy release rates, the mesh refinement at the crack tip is constant during the crack propagation.

In order to verify the validity of both methods, the local crack closure method was applied to a situation of a pure mode I of cracking. The results of both methods (7) (8) were compared, they were exactly similar.

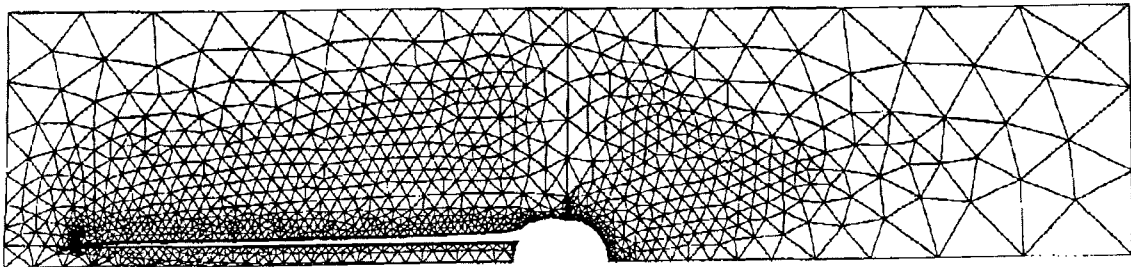


Figure 5 - Finite element mesh in the case of a mixed mode of propagation

Determination of the ultimate load

An important problem consists in the choice of material parameters G_{Ic} and G_{IIc} .

For the studied problem, i.e. the analysis of fracture in a mechanical joint, the process zone size is assumed to be small compared with the crack length and the structure size. Hence the influence of the process zone is negligible and LEFM assumptions are valid.

Classical fracture tests (DCB, SEN) allow the determination of the critical energy release rates G_{Ic} and G_{IIc} corresponding to the *onset* of propagation of an *artificial* initial crack (with no process zone). A distinction may be necessary with the problem of the *propagation* of a *natural* crack. In the latter situation the energy release rate G_p (propagation) is defined. An estimation of G_p can be obtained by considering the global fracture energy dissipated during a test. The fracture energy G_f of white wood was obtained with three point bending tests proposed in (Larsen and Gustafsson, 1989). It is then assumed (Daudeville et al., 1996):

$$G_{Ic} = G_f = 200 \text{ Nm/m}^2 \quad (9)$$

No tests were performed for the determination of the G_{IIc} value. According to the literature (Valentin et al., 1991; Mansfield-Williams, 1995; Petersson, 1995) the G_{IIc} value can be obtained with:

$$G_{IIc} = 3.5 G_{Ic} \quad (10)$$

For a given critical energy release rate G_{Ic} it is possible to compute the strength of the specimen. The two propagation criteria can be written (4) (6) (10):

$$\frac{G_{Ic}}{P^2} = g(a) \quad (11)$$

The ultimate load corresponds to the minimum value of $g(a)$. For this minimum value:

$$\frac{\partial g}{\partial a}(a_c, P_c) = 0 \text{ and } G(a_c, P_c) = G_{Ic} \quad (12)$$

When the crack length a and the load P reach the critical values a_c and P_c , the crack becomes unstable. P_c is the computed strength of the specimen.

Note that absolutely no parameter is identified by comparison between the experimental results of joints and the FE ones.

RESULTS

Initiation

The criterion (2) was applied for determining the location of cracking. For every simulation, the angle (OC,OC') (Figure 3) was under 20 degrees. That result is confirmed by experimental observations (see Table 1).

As said before LEFM can also give information about the initiation location. The length of the initial defect was chosen equal to $a_0 = 3$ mm. Different simulations with an initial crack starting at a point C' with different angles (OC,OC') ranging from 0 to 50 degrees were performed. The results are in accordance with the first approach, i.e. the initial crack which corresponds to the initiation (P_{mini}) is located at an angle of about 10 degrees.

Joint strength

As said before, it is difficult to determine accurately the plane of cracking. The previous initiation study concluded that it was very close to the mid plane. Thus, two cases were considered:

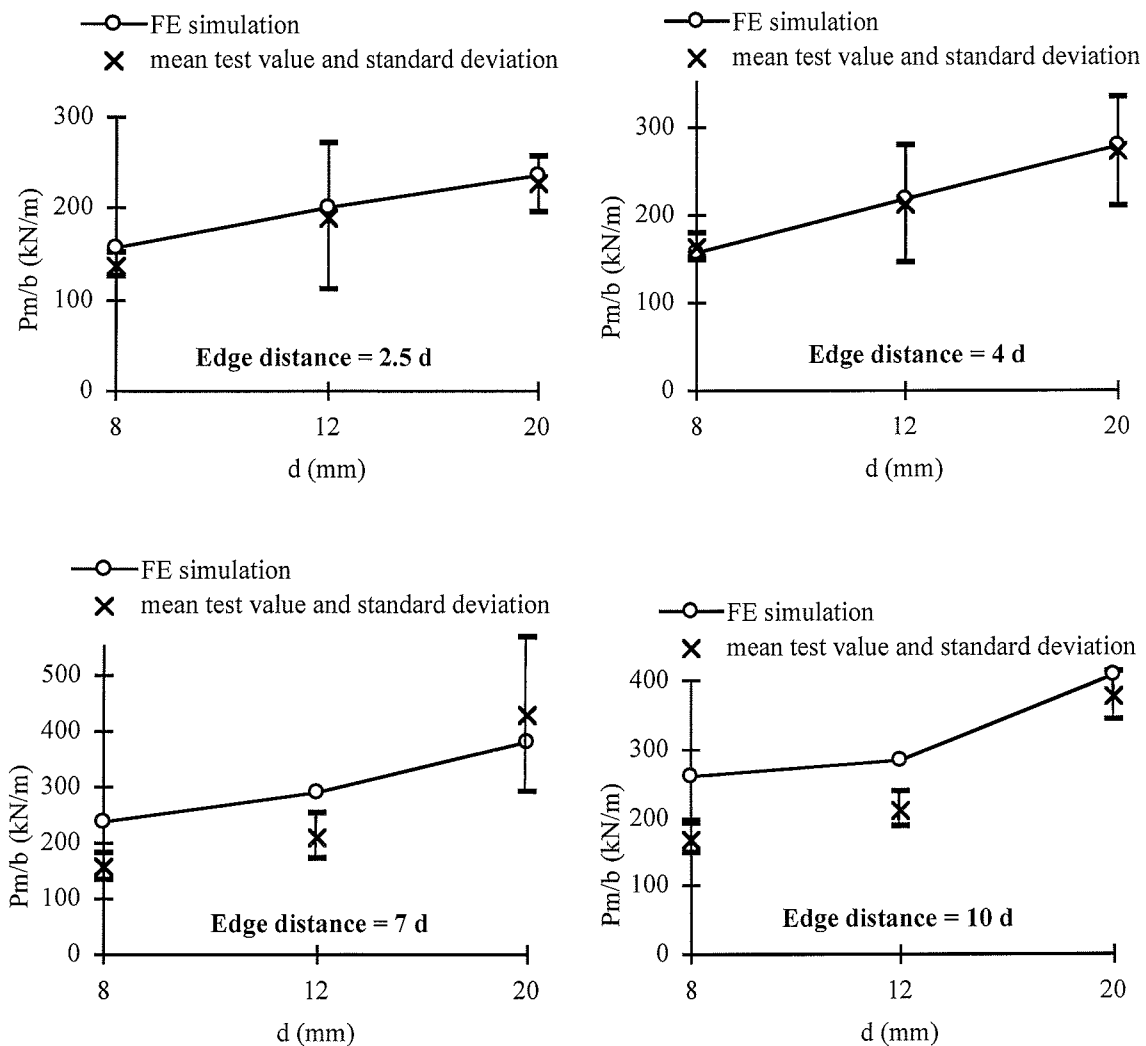
- cracking in the mid plane (angle $(OC, OC') = 0$)
- cracking in the plane such that the angle $(OC, OC') = 10$ degrees.

For the both cases a Coulomb friction at the wood and dowel contact was taken into account. Two friction coefficients f were considered in each situation ($f = 0.1$ and $f = 0.2$).

The following results were obtained with a cracking in the mid plane and $f = 0.2$ which give the best comparison with the experimental results.

The following figures give the comparison between the maximum loads obtained experimentally and numerically. The influences of the bolt diameter and of the end-distance are shown.

According to the numerical results, a stable propagation is possible on a very short distance. This stable propagation was scarcely observed experimentally.



Figures 6, 7, 8, 9 - Influence of the bolt diameter on the maximum load

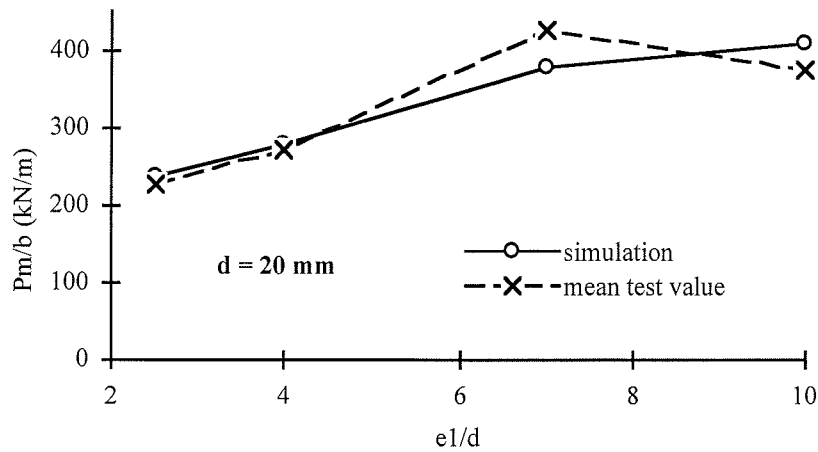


Figure 10 - Influence of the end-distance on the maximum load

The comparison between experimental and simulation results is very good for low end-distances ($e_1/d = 2.5, 4$) and for each bolt diameter (Figures 6, 7). That may be due to the few plasticity observed in such cases. For large end-distances (Figures 8, 9) plasticity phenomena occur that are not taken into account in the modelling especially for $d = 8, 12$ mm.

For $d = 20$ mm, the embedding is less important than for lower diameters. Thus the comparison is quite good for each end-distance e_1/d . The influence of e_1/d is very important for low values ($e_1/d < 7$) but can not be neglected for large end-distances ($e_1/d \geq 7$) (Figure 10).

CONCLUSION

LEFM is a simplified approach consisting in the comparison of the energy release rate with a critical value. This method has been applied for the determination of the load carrying capacity of a mechanical joint with a single bolt. The loading was parallel to the grain. The fracture mode that leads to failure is the mode I of opening. The critical energy release rate was chosen equal to the fracture energy value issued from bending tests. Comparisons of the load carrying capacity obtained experimentally and numerically with the Finite Element method is encouraging by considering the coarse assumptions of the simplified approach.

Adjust this simplified approach for calculation rules might provide an improvement for the determination of the ultimate load in the design of bolted or nailed joints.

ACKNOWLEDGEMENTS

The authors would like to thank O. Taland in Master's courses of ENS Cachan for his help in the numerical work.

REFERENCES

- C.T.B.A. 1995. Étude des Caractéristiques Mécaniques du Sapin et de l'Épicéa - France Entière, Rapport interne
- Daudeville, L.; Yasumura, M; Lanvin, J.D; 1996. Experiment and simulation of fracture parallel to grain. IWEC'96. New-Orleans.
- Daudeville, L; Yasumura, M. 1996. Failure analysis of timber bolted joints by fracture mechanics. *Materials and Structures*. 29 (to appear).
- EUROCODE 5. 1993. Design of timber structures. ENV 1995-1-1. Brussels, CEN.
- Griffith, A. 1920. The phenomena of rupture and flow in solids. *Philosophical Transactions of the Royal Society of London, Series A*, 221: 163-198.
- Guitard, D. 1987. *Mécanique du matériau bois et composites*. Cépadues-Editions, ISBN 2.85428.152.7.
- Larsen, H.J.; Gustafsson, P.J. 1989. Design of end-notched beams. CIB-W18 Meeting; Berlin DDR: paper 22-10-1.
- Mansfield-Williams H.D. 1995. A new method for determining fracture energy forward shear along the grain. CIB-W18 Meeting, Copenhagen, Denmark: paper 28-19-2.
- Petersson H. 1995. Fracture design analysis of wooden beams with holes and notches. CIB-W18 Meeting, Copenhagen, Denmark: paper 28-19-3.
- Rathkjen, A. 1993. Failure criteria for wood. Failure criteria of structured media, Boehler (ed.), Balkema, Rotterdam The Netherlands, ISBN 9.06191.179.6.
- Sobue, N. 1989. Scientific report for the grant-in aid scientific research. n°62560174, Ministry of Education, Science and Culture, Japan.
- Valentin, G; Boström, L; Gustafsson, P.J; Ranta-Maunus, A; Gowda, S. 1991. Application of fracture mechanics to timber structures. RILEM state-of-art Report. Technical Research Centre of Finland, Espoo Finland. Research Notes 1262. ISBN 951.38.3891.1
- Wu, E.M. 1967. Application of fracture mechanics to anisotropic plates. *Journal of Applied Mechanics, Series E*, 34(4): 967-974.

**INTERNATIONAL COUNCIL FOR BUILDING RESEARCH STUDIES AND DOCUMENTATION
WORKING COMMISSION W18 - TIMBER STRUCTURES**

TIME DEPENDENT LATERAL BUCKLING OF TIMBER BEAMS

by

F Rouger
Centre Technique du Bois et de l'Ameublement
France

MEETING TWENTY - NINE

BORDEAUX

FRANCE

AUGUST 1996

Time dependent lateral buckling of timber beams

F. ROUGER¹

Introduction.

In 1994, Le Govic&al. [4] reported the results of a research program dealing with long term behavior of timber beams (solid timber and glulam). All along this program, beams had been tested in external protected conditions at three stress levels (2 MPa, 5 MPa, 15 MPa) corresponding to three average stress ratios (10%, 20%, 60%) with respect to the average short term characteristic strength. Whereas for low stress ratios (10%, 20%) the beams did not fail, a high percentage of failures due to lateral instabilities was observed at the highest stress level (60%). These percentages ranged from 50% for solid timber to 100% for glulam. A simple reliability calculation based on Eurocode 5 formulas [3] lead to equivalent probabilities of failure ranging from 10% for solid timber to 25% for glulam. These calculated values were obviously much too low and justified further investigation.

In this paper, finite elements analysis combined with Eurocode 5 concepts have been done. In a first part, Timoshenko formulas are compared with finite elements results. They show a very good accordance and justify the use of finite elements concept for further analysis. In a second part, critical stresses are calculated for the tested specimens. They lead to the evaluation of probabilities of failure which are compared with the experimental values. In a third part, Eurocode 5 formulas are analysed and a new design proposal is given.

Critical moments for different loading configurations.

In this chapter, different critical moments leading to lateral buckling are calculated. The reference case given by Timoshenko&Gere [5] deals with constant moment bending. The formulas are given and calculations for different cross-sections are illustrated. This reference case is further used for deriving critical moments in three and four points bending. The influence of the loads location is studied, as well as second order effects.

Constant moment bending.

The critical moment leading to lateral buckling in the case of a beam subjected to a constant bending moment is given by TIMOSHENKO & GERE :

$$M := \frac{\pi}{L} \sqrt{E_0 \cdot I_y \cdot G \cdot J} \quad (1)$$

with, in the case of rectangular cross-sections,

$$I_y := h \cdot \frac{b^3}{12} \quad (2)$$

$$J := h \cdot \frac{b^3}{16} \left[\frac{16}{3} - 3.36 \cdot \frac{b}{h} \left[1 - \frac{1}{12} \cdot \left(\frac{b}{h} \right)^4 \right] \right] \quad (3)$$

¹CTBA, Dept of Timber Engineering, PARIS, FRANCE

where

- h is the beam depth,
- b is the beam width,
- L is the beam span,
- E_0 is the beam Young's modulus,
- G is the beam shear modulus.

According to these formulas, the critical moment is calculated for three beams geometrical configurations (see Table 1).

TABLE 1 : *Critical moments for different beam configurations ($E_0 = 11000 \text{ MPa}$, $G = 700 \text{ MPa}$)*

b (mm)	h (mm)	L (mm)	M (kN.m)
40	100	1800	4.47
40	400	7200	5.0
100	400	7200	74.1

In the following sections, the critical moments (M_{cr}) are compared with this reference moment (M) according to the following formula :

$$M_{cr} := \frac{M}{m} \quad (4)$$

Three points bending.

This configuration was used to validate the finite elements model. Foulon [2] gives the critical loads for different locations of the loading points (see Figure 1). These critical loads are compared with Timoshenko results in the case where loads are applied on neutral fiber (see Table 2). They show a very good accordance and justify the use of finite elements approach in further investigations.

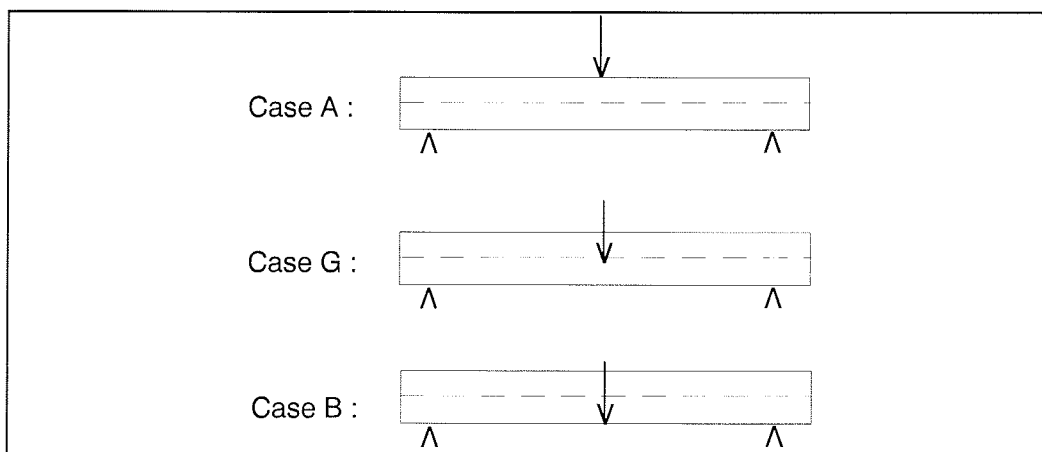


FIGURE 1 : *Loading points configurations (Case A : Compressive edge, Case G : Neutral fiber, Case B : Tensile edge).*

TABLE 2 : Comparison of critical loads according to Timoshenko and finite elements
(Loading case G)

Beam Configuration	Critical Load (kN)		Difference
	Finite elements	Timoshenko	
40*100*1800 mm	13.312	13.4	+0.7%
40*400*7200 mm	3.74	3.7	-1%
100*400*7200 mm	55.305	55.317	+0.02%

In table 3, the critical moments (M_{cr}) as well as the correction factors (m) are given for the three beams configurations and for the three loading conditions. These moments are calculated by finite elements. They are deducted from the critical loads according to :

$$M_{cr} := P_{cr} \cdot \frac{L \cdot 1000}{4} \quad (5)$$

TABLE 3 : Critical moments (in kN.m) in three points bending.

Beam Configuration	Loading case A		Loading case G		Loading case B	
	M_{cr}	m	M_{cr}	m	M_{cr}	m
40*100*1800 mm	5.29	0.845	5.99	0.746	6.795	0.658
40*400*7200 mm	6.03	0.83	6.73	0.743	6.98	0.716
100*400*7200 mm	88.65	0.836	99.54	0.744	108.8	0.68
Mean value		0.84		0.744		0.68

It should be noted here that the location of the loading point has a strong influence on the critical moment. If the load is located on the compressive edge, the critical moment is much lower than if it is located on the tensile edge. The value of m for loading case G is in excellent agreement with the value given by Choo [1].

One of the concerns with the creep experiment was to investigate if the creep deflections tended to increase or to decrease the critical moment. In order to assess this assumption, a calculation was performed with an initial curved shape of the beam.

The initial shape is given by :

$$w(x) := A \cdot \sin\left(\pi \cdot \frac{x}{L}\right) \quad (6)$$

with $A = 0.05 \cdot L$

The calculation was performed for loading case G. The results are reported in Table 4. They show that the initial curvature tends to stabilize the beam and to increase the critical moment. Therefore, this effect will not be considered in the following sections.

TABLE 4 : Influence of an initial curvature on the critical moment (in kN.m)

Beam Configuration	Initial straight beam		Initial curved beam	
	M_{cr}	m	M_{cr}	m
40*100*1800 mm	5.99	0.746	6.84	0.65
40*400*7200 mm	6.73	0.743	8.62	0.58
100*400*7200 mm	99.54	0.744	129.8	0.57
Average		0.744	129.8	0.6

Four points bending.

In this case the distance between the loads and the supports are (1/3; 1/3; 1/3). The critical moment is deducted from the critical load (half of the total applied load) according to :

$$M_{cr} := P_{cr} \frac{L \cdot 1000}{3} \quad (7)$$

They are reported in Table 5, as well as the correction factors, for the three beams configurations and the three loading points locations.

TABLE 5 : Critical moments (in kN.m) in four points bending.

Beam Configuration	Loading case A		Loading case G		Loading case B	
	M_{cr}	m	M_{cr}	m	M_{cr}	m
40*100*1800 mm	4.44	1.0	5.09	0.88	5.59	0.8
40*400*7200 mm	5.25	0.95	5.73	0.87	6.22	0.8
100*400*7200 mm	77.3	0.96	85.9	0.86	92.5	0.8
Average		0.97		0.87		0.8

As in three points bending, the critical moment increases as the loads move from the compressive edge to the tensile edge. Since the experiments have been performed according to loading case A, the corresponding values of m will be considered in the following sections.

Calculation of the critical stresses.

The critical stress is deduced from the critical load according to :

$$\sigma_{cr} := 2 \cdot P_{cr} \cdot \frac{L \cdot 1000}{b \cdot h^2} \quad (8)$$

which, in combination with equations (1), (4) and (7) gives :

$$\sigma_{cr} := \frac{6 \cdot \pi \cdot \sqrt{E_0 \cdot I_y \cdot G J}}{m \cdot L \cdot b \cdot h^2} \quad (9)$$

For rectangular beams, equations (2) and (3) can be used, which gives :

$$\sigma_{cr} := \frac{\pi \cdot b^2 \cdot E_0 \cdot \sqrt{\frac{G}{E_0}} \cdot \sqrt{1 - 0.63 \frac{b}{h}} \cdot \left[1 - \frac{1}{12} \left(\frac{b}{h} \right)^4 \right]}{m \cdot L \cdot h} \quad (10)$$

The specimens used in the experiments have strength and stiffness properties given in Table 6.

TABLE 6 : *Strength and stiffness properties of the specimens.*

	Strength Class	E_{mean} (MPa)	$f_{m,k}$ (MPa)
Solid Timber	C22	10 000	22
	C30	12 000	30
Glulam	GL 24	10 800	24
	GL 30	12 000	30

The 5% lower fractile of E is deduced from E_{mean} (= E) according to :

$$E_0 := 0.67E \quad (11)$$

The shear modulus G is deduced from the E_{mean} (= E) according to :

$$G := \frac{E}{16} \quad (12)$$

Both solid timber strength classes correspond to cross-section 40*100 mm, glulam corresponding to cross-sections 40*400 mm and 100*400 mm.

The permanent critical stress is deducted from the instantaneous one according to :

$$\sigma_{cr,permanent} = \frac{\sigma_{cr}}{1 + k_{def}} \quad (13)$$

with $k_{def} = 2.0$ (according to EC5, Permanent, Service Class 3)

The critical stresses are reported in Table 7.

TABLE 7 : *Critical stresses (in MPa) for the different test specimens.*

Beam Configuration	Strength Class	Critical stress (MPa)	
		Instantaneous	Permanent
40*100*1800 mm	C30	58.96	19.65
	C22	49.1	16.38
40*400*7200 mm	GL 30	4.54	1.51
	GL 24	3.92	1.31
100*400*7200 mm	GL 30	26.7	8.91
	GL 24	23.1	7.7

Calculation of the probabilities of failure.

Since the beams can fail either by lateral buckling or by classical bending failure, both aspects are investigated. The resulting probability of failure of the beam is the result of a series system calculation.

Probability of failure by lateral buckling.

This calculation is performed for an applied stress of 15MPa, and assuming that the critical stresses (given in Table 7) have a normal distribution, with a coefficient of 30% for solid timber and 20% for glulam. The safety index β is given by :

$$\beta := \frac{\mu_R - S}{\sigma_R} \quad (14)$$

where μ_R and σ_R are the mean value and the standard-deviation of the critical stress, S is the applied stress.

The probability of failure is deducted from the safety index according to :

$$P_{fl} := 1 - \text{cnorm}(\beta) \quad (15)$$

where $\text{cnorm}(x)$ is the cumulative Gaussian distribution.

The calculated probabilities of failure are reported in Table 8.

TABLE 8 : *Probabilities of failure by lateral buckling.*

Beam Configuration	Strength Class	Probability of failure	
		Instantaneous	Permanent
40*100*1800 mm	C30	0.006	0.215
	C22	0.01	0.39
40*400*7200 mm	GL 30	1.0	1.0
	GL 24	1.0	1.0
100*400*7200 mm	GL 30	0.014	1.0
	GL 24	0.04	1.0

It can be noted that the time effect is considerable. The probabilities of failure are multiplied by a factor of at least 25.

Probability of failure in bending.

The calculation is performed by assuming a log-normal distribution for the strength. The mean strength value is deduced from the 5% lower fractile (f_{mk}) and the coefficient of variation (cv) according to :

$$f_m := \exp \left[\ln(f_{mk}) + \left(\frac{1}{2} \cdot cv^2 + 1.65 \cdot cv \right) \right] \quad (16)$$

The mean value of the permanent strength is deduced from the instantaneous one according to :

$$f_m := k_{mod} \cdot f_m \quad (17)$$

with $k_{mod} = 0.50$ (according to EC5, Permanent, Service class 3)

Probabilities of failure are calculated according to equations (14) and (15), replacing the critical stress by the bending strength. The values are reported in Table 9.

TABLE 9 : *Probabilities of failure in bending.*

Beam Configuration	Strength Class	Probability of failure	
		Instantaneous	Permanent
40*100*1800 mm	C30	0.009	0.059
	C22	0.022	0.177
40*400*7200 mm	GL 30	$6.0 \cdot 10^{-4}$	0.036
	GL 24	$3.0 \cdot 10^{-3}$	0.16
100*400*7200 mm	GL 30	$6.0 \cdot 10^{-4}$	0.036
	GL 24	$3.0 \cdot 10^{-3}$	0.16

Calculation of the combined probability of failure.

The failure of a beam, either by lateral buckling or in bending, constitutes a series system. The combined probability of failure has two bounds. The lower bound (P_{fi}) and the upper bound (P_{fs}) are given by :

$$P_{fi} := \min(P_{f1}, P_{f2}, P_{f1}) \quad (18)$$

$$P_{fs} := 1 - (1 - P_{f1}) \cdot (1 - P_{f2}) \quad (19)$$

The values are reported in Tables 10 and 11.

TABLE 10 : *Lower bound for combined probability of failure.*

Beam Configuration	Strength Class	Probability of failure	
		Instantaneous	Permanent
40*100*1800 mm	C30	0.009	0.215
	C22	0.022	0.39
40*400*7200 mm	GL 30	1.0	1.0
	GL 24	1.0	1.0
100*400*7200 mm	GL 30	0.014	1.0
	GL 24	0.04	1.0

TABLE 11 : *Upper bound for combined probability of failure.*

Beam Configuration	Strength Class	Probability of failure	
		Instantaneous	Permanent
40*100*1800 mm	C30	0.015	0.261
	C22	0.032	0.498
40*400*7200 mm	GL 30	1.0	1.0
	GL 24	1.0	1.0
100*400*7200 mm	GL 30	0.015	1.0
	GL 24	0.042	1.0

These values are very close to the experimental ones (50% for solid timber and 100% for glulam) which validates the approach.

Proposals for revising Eurocode 5.

The calculation of the probability of failure according to Eurocode 5 is performed by the following approach :

--> Calculation of the relative slenderness (§5.2.2, Application rule (2), Equation (5.2.2a))

$$\lambda_{rel} = \sqrt{\frac{f_{mk}}{\sigma_{cr}}} \quad (20)$$

where f_{mk} is the characteristic bending strength
 σ_{cr} is the critical stress (calculated according to equation (10))

It should be noted that the critical stress must take into account the time effect (see equation (13)), whereas the bending strength is the instantaneous value. Eurocode 5 should be revised according to this remark.

The values of λ_{rel} are reported in Table 12.

TABLE 12 : *Relative slenderness* λ_{rel} .

Beam Configuration	Strength Class	Relative slenderness λ_{rel}	
		Instantaneous	Permanent
40*100*1800 mm	C30	0.713	1.236
	C22	0.67	1.159
40*400*7200 mm	GL 30	2.57	4.452
	GL 24	2.473	4.284
100*400*7200 mm	GL 30	1.059	1.835
	GL 24	1.019	1.766

--> Calculation of k_{inst} (§5.2.2, Application rule (4), Equations 5.2.2c to e)

$$k_{inst} := \begin{cases} 1 & \text{if } \lambda_{rel} \leq 0.75 \\ 1.56 - 0.75 \lambda_{rel} & \text{if } 0.75 < \lambda_{rel} \leq 1.4 \\ \frac{1}{\lambda_{rel}^2} & \text{if } \lambda_{rel} > 1.4 \end{cases} \quad (21)$$

The values of k_{inst} are reported in Table 13.

TABLE 13 : *Instability factor* k_{inst}

Beam Configuration	Strength Class	Instability factor k_{inst}	
		Instantaneous	Permanent
40*100*1800 mm	C30	1.0	0.633
	C22	1.0	0.691
40*400*7200 mm	GL 30	0.151	0.05
	GL 24	0.163	0.054
100*400*7200 mm	GL 30	0.765	0.297
	GL 24	0.795	0.321

--> Calculation of the probability of failure.

The calculation is performed according to equation (14), replacing μ_R by :

$$\mu_R := k_{inst} \cdot f_m \quad (22)$$

This is justified by §5.2.2, Application rule (3), equation (5.2.2b)

The combined probabilities of failure are reported in Table 14.

TABLE 14 : *Probabilities of failure according to EC5.*

Beam Configuration	Strength Class	Probability of failure	
		Instantaneous	Permanent
40*100*1800 mm	C30	0.009	0.293
	C22	0.022	0.561
40*400*7200 mm	GL 30	1.0	1.0
	GL 24	1.0	1.0
100*400*7200 mm	GL 30	0.003	1.0
	GL 24	0.013	1.0

By comparing these values with the ones given in Table 11, especially the instantaneous ones, it is obvious that equation (21) should be revised. If we adjust the probabilities of failure to Table 11, we should get the values of k_{inst} given in Table 15. The comparison between these values and the ones of EC5 are illustrated in Figure 2.

TABLE 15 : *Expected values of k_{inst}*

Beam Configuration	Strength Class	k_{inst}	
		Instantaneous	Permanent
40*100*1800 mm	C30	0.83	0.66
	C22	0.9	0.72
40*400*7200 mm	GL 30	0.151	0.05
	GL 24	0.163	0.054
100*400*7200 mm	GL 30	0.62	0.297
	GL 24	0.67	0.321

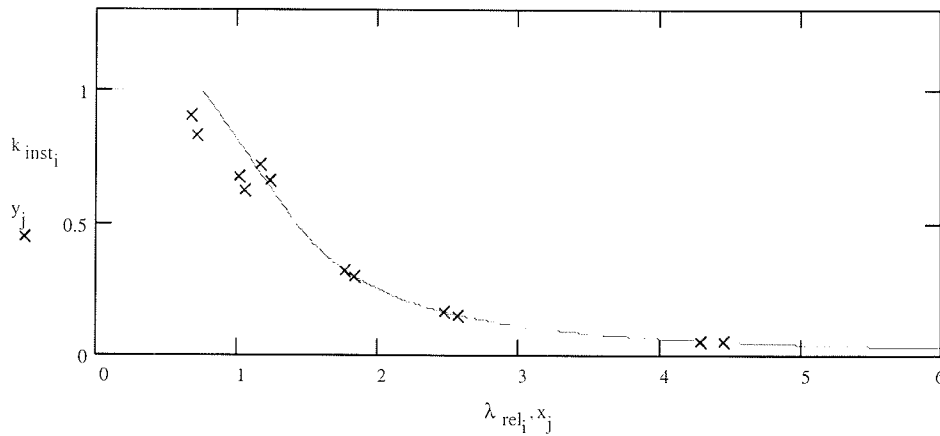


FIGURE 2 : k_{inst} versus λ_{rel} (x's represent the expected values, solid line represents EC5)

Revision of EC5 equations 5.2.2c to e

If we wish to maintain $k_{inst} = 1/\lambda_{rel}^2$ for $\lambda_{rel} > 1.4$, the best fit is given by :

$$k_{inst} := \begin{cases} 1 & \text{if } \lambda_{rel} \leq 0.5 \\ 1.26 - 0.53 \lambda_{rel} & \text{if } 0.5 < \lambda_{rel} \leq 1.4 \\ \frac{1}{\lambda_{rel}^2} & \text{if } \lambda_{rel} > 1.4 \end{cases} \quad (23)$$

This is illustrated in Figure 3.

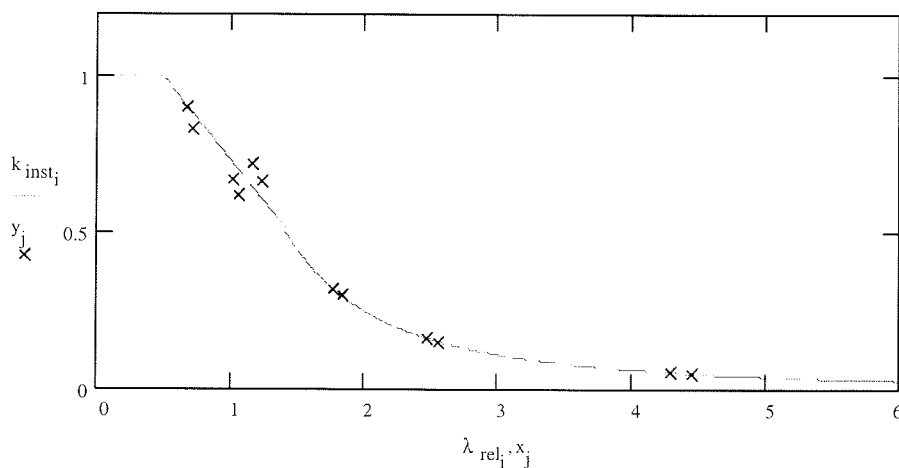


FIGURE 3 : k_{inst} versus λ_{rel} (x's represent the expected values, solid line represents equation (23))

If we skip this option, the best fit is given by :

$$k_{inst} := \begin{cases} 1 & \text{if } \lambda_{rel} \leq 0.56 \\ \frac{1.55}{\lambda_{rel}^2 + 1.24} & \text{if } \lambda_{rel} > 0.56 \end{cases} \quad (24)$$

It is illustrated in Figure 4.

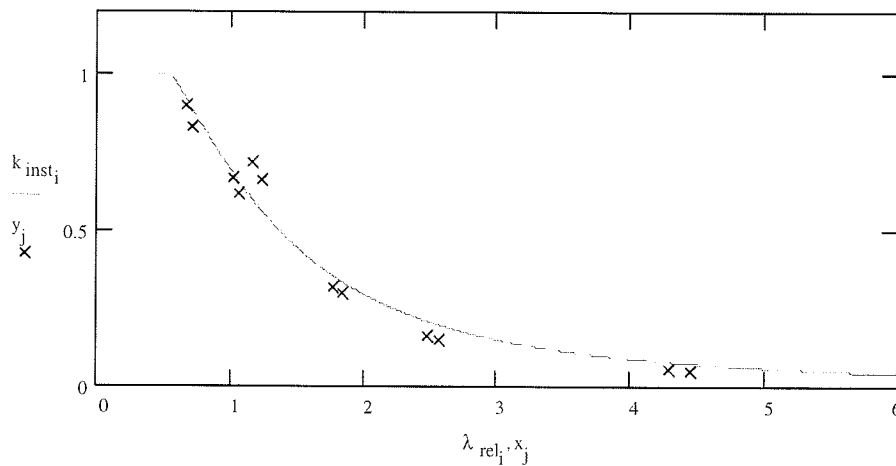


FIGURE 4 : k_{inst} versus λ_{rel} (x 's represent the expected values, solid line represents equation (24))

The corresponding values of k_{inst} and corresponding probabilities of failure are reported in Tables 16 and 17.

TABLE 16 : Values of k_{inst} according to equation (24)

Beam Configuration	Strength Class	k_{inst}	
		Instantaneous	Permanent
40*100*1800 mm	C30	0.886	0.56
	C22	0.918	0.6
40*400*7200 mm	GL 30	0.198	0.074
	GL 24	0.211	0.079
100*400*7200 mm	GL 30	0.656	0.336
	GL 24	0.68	0.356

TABLE 17 : Probabilities of failure according to equation (24)

Beam Configuration	Strength Class	Probability of failure	
		Instantaneous	Permanent
40*100*1800 mm	C30	0.013	0.428
	C22	0.029	0.75
40*400*7200 mm	GL 30	1.0	1.0
	GL 24	1.0	1.0
100*400*7200 mm	GL 30	0.01	1.0
	GL 24	0.039	1.0

These values are in very good accordance with Table 11 and with experiments, at least on the conservative side. In addition, equation (24) is simpler than the current equations of EC5.

Conclusions.

A numerical method has been compared with the classical theory of Timoshenko and shows a very good accordance. It was therefore applied for deriving critical moments and subsequent critical stresses. From these results, probabilities of failure have been calculated and show a very good agreement with the experiment. EC5 equations have been investigated. A revision is proposed in two points :

- (1) Calculate the relative slenderness with the time dependant critical stress,
- (2) Use another equation for k_{inst} vs λ_{rel} .

This approach is easily applicable to columns behavior. In §5.2.1, application rule (2), equations (5.2.1c) and (5.2.1d), the MOE values should be divided by $(1 + k_{def})$.

By adopting this approach, the long term instability problems can be easily solved.

References.

- [1] Choo B.S., 1995 - Bending - STEP Lecture B3
- [2] Foulon T., 1995 - Flambement élastique et viscoélastique de poutres en bois. Masters Thesis, University of Technology of Compiègne, France.
- [3] Eurocode 5, 1993 - Design of Timber Structures. Part 1-1 : General rules and rules for buildings.
- [4] Le Govic C., Rouger F., Toratti T., Morlier P., 1994 - Creep behavior of timber under external conditions. 27th CIBW18 Meeting, Sydney, AUSTRALIA.
- [5] Timoshenko S., Gere J.M., 1961 - Theory of elastic instability, Mc Graw Hill Book Co. Inc. New York, NY., 2nd edition

INTERNATIONAL COUNCIL FOR BUILDING RESEARCH STUDIES AND DOCUMENTATION
WORKING COMMISSION W18 - TIMBER STRUCTURES

**DETERMINATION OF MODULUS OF ELASTICITY IN BENDING ACCORDING TO
EN 408**

by

K H Solli
Norwegian Institute of Wood Technology
Norway

MEETING TWENTY - NINE

BORDEAUX

FRANCE

AUGUST 1996

DETERMINATION OF MODULUS OF ELASTICITY IN BENDING ACCORDING TO EN 408

Kjell Helge Solli, Norwegian Institute of Wood Technology

August 1996

Background

The test method for determination of the modulus of elasticity is given in the European standard EN 408 [1]. According to EN 408:8.2 the test piece shall “...be symmetrically loaded in bending at two points over a span of 18 times the depth as shown in figure 1.”

And the “...deformation shall be measured at the centre of a central gauge length of five times the depth of the section.”

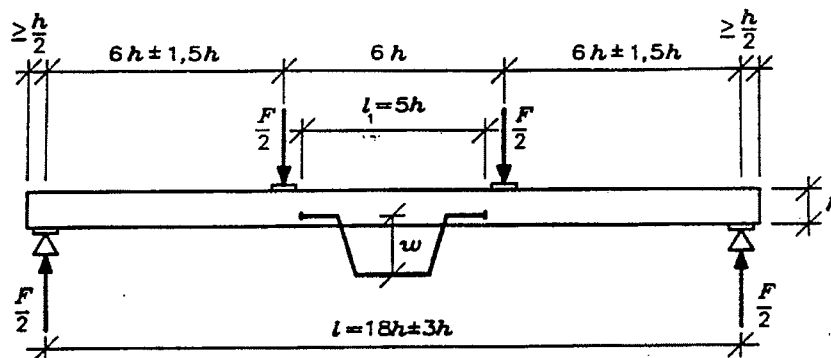


Figure 1: Test arrangement for measuring modulus of elasticity in bending.

Figure 1. Description of the test method (copy from EN 408).

The description of some of the details in the test method are, however, not precise enough. Examples of questions which might come up before testing are:

- At which point of the depth shall the deformation be measured?
Shall the transducer be fixed at the tension edge, compression edge or the neutral axis? Or does it not matter at all where it is measured? EN 408 does not give an exact answer.
- Is it good enough to measure the deformation with one transducer fixed on one side of the cross section? Or is it necessary to measure the deformation on both sides and then calculate the mean deformation value? EN 408 does not give an exact answer.

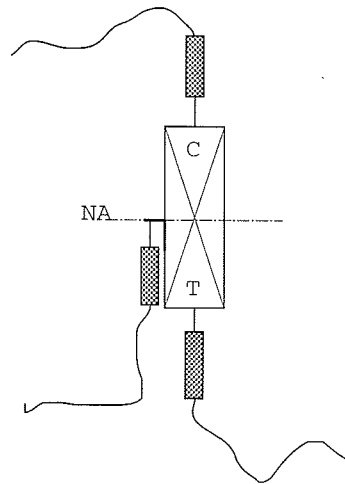


Figure 2. Where shall the deformation be measured?
 (C = Compression edge, T = Tension edge, NA = Neutral Axis)

These questions about how to measure the deformation came up during a meeting in one of the TC124/WG 2 groups. The members in this group were asked about their own practice in this matter. The answers showed clearly that there were no absolute method or practice. Some countries referred that they were measuring on the compression edge, some on the tension edge, some on both side of the neutral axis and some on one side of the neutral axis.

These facts raise the following questions:

- *Do these differences in method of measuring the deformation cause any difference in the final result, i.e. the value of MOE?*

And if YES:

- *Should EN 408 be revised as soon as possible to ensure that the values from different laboratories are based on the same criteria?*

In order to ensure that our test routines were reliable and eventually give a contribution to a solution of the mentioned questions, a small project was established at the Norwegian Institute of Wood Technology. The purpose of this project was to compare the results from measuring the deformation on one and two sides of the neutral axis.

Materials to the test

The materials used in this test were spruce (*Picea abies*) with a moisture content corresponding to +20 °C and 65 % relative humidity. The dimensions of the test pieces were 36 x 148 mm (ca. 50 %), 36 x 198 mm (ca. 25 %) and 48 x 148 mm (ca. 25 %). The test program involved totally 95 test pieces.

The quality of the test pieces was chosen to represent the whole span of natural variation of Nordic structural timber. Some were straight with no visual defects, other had big knots and/or heavy distortion.

Test procedure

The test procedure was according to EN 408. The deformation was measured on both sides of the cross section but with separately reading of data from the two transducers (see Figure 3).

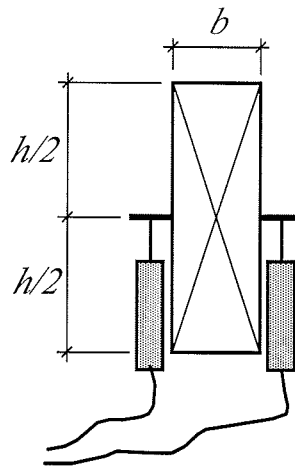


Figure 3. Deformation was measured by two symmetrical located transducers.

To eliminate that the measured differences were caused by the measuring equipment, two measurements were done where the transducers changed place in the second reading. This was done on about 40 of the test pieces. No systematic difference between the two transducers was shown.

The ratio between load and deformations was registered approximately continuous up to a bending stress of 15 N/mm², i.e. about one third of the expected mean value of the ultimate bending stress for this sample.

Test results

Each test piece gave two values of the ratio between load and deformation, i.e.

$$K_1 = \frac{\Delta F}{\Delta \delta_1} \text{ and } K_2 = \frac{\Delta F}{\Delta \delta_2}.$$

This K-values are proportional to the modulus of elasticity in bending:

$$E_m = \frac{a \cdot l_1^2}{16 \cdot I} \cdot K_n$$

where

a = the distance between a loading position and the nearest support
(i.e. 6h in this test)

l₁ = gauge length for measuring the deformation
(i.e. 5h in this test)

For each test piece the following expression was calculated:

$$\left(\frac{K_{\max}}{K_{\min}} - 1 \right) \cdot 100\%$$

where

K_{\max} = the highest K-value for the actual test piece independent of which side or by which transducer it was measured

K_{\min} = the lowest K-value for the actual test piece independent of which side or by which transducer it was measured

The results given in ranked order are shown in *Figure 4*.

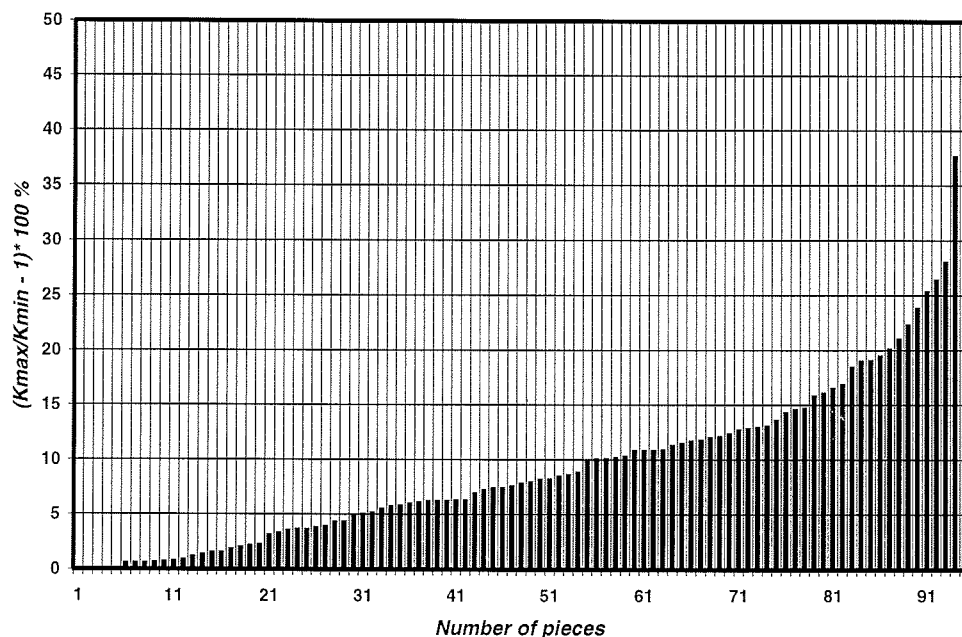


Figure 4. The relation between K_{\max} and K_{\min} for 95 test pieces

Comment on the results

Most probably the shown deviations are caused by a smaller or bigger rotation of the cross section during the loading/measuring procedure. Since the maximum deformation normally is very small (i.e. 1,0 - 1,5 mm) a quite small rotation can cause a considerable influence on the registered MOE.

Theoretical and idealised example:

Dimensions: 48 mm x 148 mm

$MOE_{\text{real}} = 12000 \text{ N/mm}^2$

$\Delta F = 6000 \text{ N}$ (corresponds to a bending stress of $\Delta\sigma_m \approx 15 \text{ N/mm}^2$)

The corresponding deformation will then be $\delta_m \approx 1,17 \text{ mm}$.

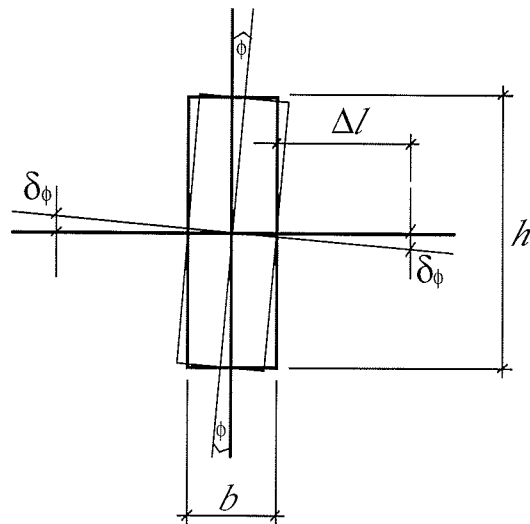


Figure 5. Rotation of the cross section during testing

If the centre of the rotation in this idealised example is identical with the centre of gravity the situation will be as shown in Figure 5.

If the transducer measures the deformation at a point with distance $\Delta l = 15$ mm from the surface of the test piece and the rotation angle is $\phi = 0,5^\circ$, the deformation caused by the rotation is calculated as:

$$\delta_{\phi} = \left(\frac{b}{2} + \Delta l \right) \cdot \tan \Phi = \left\{ \left(\frac{48}{2} + 15 \right) \cdot \tan 0,5^\circ \right\} mm = 0,34 mm$$

This deformation will be added to the vertical deformation caused by the bending moment. By using just *one* transducer the registered value of MOE will depend on which side the transducer is fixed:

$\delta_{\max} = \delta_m + \delta_{\phi} = (1,17 + 0,34) mm = 1,51 mm$ which corresponds to a MOE value given as $MOE_{\min} = 9310$ N/mm², i.e. 76% of $MOE_{\text{real}} = 12000$ N/mm².

$\delta_{\min} = \delta_m - \delta_{\phi} = (1,17 - 0,34) mm = 0,83 mm$ which corresponds to a MOE value given as $MOE_{\max} = 16940$ N/mm², i.e. 141% of $MOE_{\text{real}} = 12000$ N/mm².

In this illustration the relation $\left(\frac{K_{\max}}{K_{\min}} - 1 \right) \cdot 100\%$ is given as 82 %.

By using *one* transducer it will be random either the maximum or minimum value is registered as a MOE-value of this test piece.

By using *two* transducers and the mean value of their deformation values the described effect from rotation should be eliminated:

$\delta_{mean} = \delta_{max} + \delta_{min} = \frac{(1,51 + 0,83)}{2} mm = 1,17 mm$ which will correspond to the “true value” $MOE_{real} = 12000 N/mm^2$.

Potential consequences

In a normal bending sample where the tension edge according to EN 384:5.2 [2] is selected at random, it should be expected that the same number of pieces were registered with the maximum value as with the minimum value when just one transducer is used. If the target information is the sample *mean value of MOE* one might expect that the result should be approximately correct. However, the mean value will probably be some what higher than “the correct value” since the effect of Φ is stronger on the maximum values. *Figure 6* shows how MOE will change compared with the angle (the figure is directly related to the previous example).

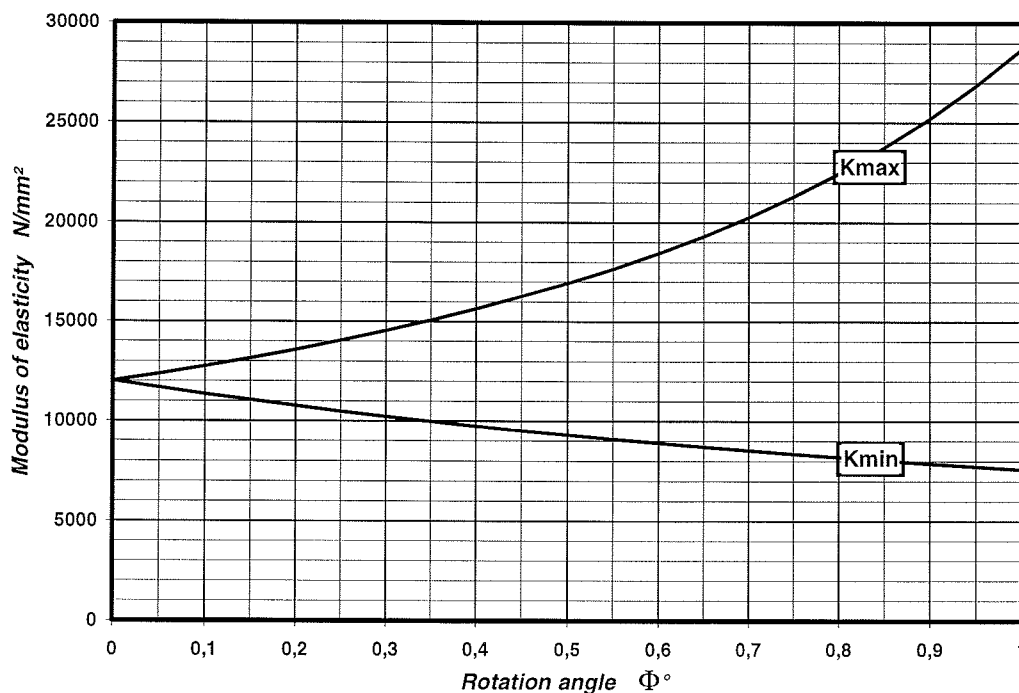


Figure 6. MOE depending on the rotation Φ .

In EN 338:6.2.2 [3] the mean modulus of elasticity parallel to the grain is one of three main criteria which must be fulfilled before a sample can be assigned to a certain strength class. On this background it is important to define which accuracy the mean value MOE shall have, and then compare this accuracy with the uncertainty caused by the use of one side measuring of deformation.

However, sometimes it is not good enough with an “approximately correct” mean value of a sample. Sometimes it is necessary to have each individual value as exact as possible. For instance when a strength grading machine shall be approved according to EN 519 [4]. In EN 519:7.2.5 it is stated that:

“The relation between the bending modulus of elasticity E_m as measured in EN 408 and the machine’s indicating property shall have a coefficient of determination of not less than 0,5.”

The experiences from such approval tests show that this requirement may be difficult to fill for some machines. When using a MOE-value with an accuracy of plus/minus 10 % caused by the testing method the requirement of $r^2 \geq 0,5$ might be impossible to reach.

Conclusion

The test method for determination of the modulus of elasticity given in EN 408 opens for various practice. This paper shows examples of inaccuracy which can occur when the deformation is measured in the neutral axis at one side of the cross section.

As an average it was detected about 10 % higher values on one side compared to the opposite. In two extreme cases (out of 95 pieces) the MOE-value measured on one of the sides was almost 40 % higher than the value measured on the opposite side.

The modulus of elasticity is one of the most important material properties of structural timber. Based on this fact it is strange that the details in the method of measuring this property is as vague as given in EN 408. Statements from several laboratories in Europe prove that this actual method in EN 408 are practised quite differently.

The definition of which method gives the *correct* MOE in bending is important. Far more important is it, however, to have a standard which ensures that everyone who are involved in this type of testing follows *the same procedure*.

We will therefore make a suggestion that EN 408 is revised to ensure that the values from different laboratories are based on the same criteria.

References

- [1] EN 408 Timber structures - Structural timber and glued laminated timber - Determination of some physical and mechanical properties. (January 1995)
- [2] EN 384 Structural timber - Determination of characteristic values of mechanical properties and density. (February 1995)
- [3] EN 338 Structural timber - Strength classes. (February 1995)
- [4] EN 519 Structural timber - Grading - Requirements for machine strength graded timber and grading machines. (February 1995)

**INTERNATIONAL COUNCIL FOR BUILDING RESEARCH STUDIES AND DOCUMENTATION
WORKING COMMISSION W18 - TIMBER STRUCTURES**

ON DETERMINATION OF MODULUS OF ELASTICITY IN BENDING

by

L Boström
Swedish National Testing and Research Institute
Sweden
S Ormarsson
O Dahlblom
Lund Institute of Technology
Sweden

MEETING TWENTY - NINE

BORDEAUX

FRANCE

AUGUST 1996

On determination of modulus of elasticity in bending

Lars Boström¹, Sigurdur Ormarsson², Ola Dahlblom²

Abstract

The European standard EN 408 does not clearly specify the method and position of the deformation measurement. This paper presents experimental and theoretical results showing the influence of the position of the deformation measurement when determining the modulus of elasticity according to EN 408.

1. Introduction

European standard EN 408 includes a method for the determination of modulus of elasticity, MOE, in bending. The standard specifies the geometry of the test set-up and gauge length for deformation measurements (see Fig 1), but it does not specify method or position for the gauge. In other words, the measurement can be made anywhere on the beam as long as it is centred between the loading points.

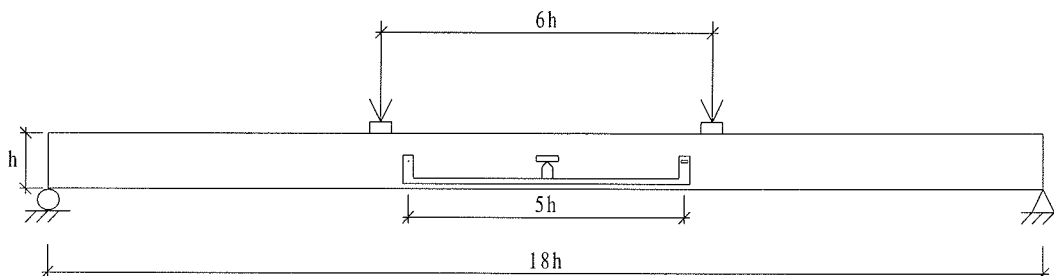


Figure 1 Test arrangement for determination of MOE in bending.

Tests performed on the same specimens at two laboratories resulted in MOE values that differed by more than 10% (Johansson 1996). The deformations were measured at different positions of the beams. The purpose of this study was to investigate how the position of the gauge affects the determination of MOE. Theoretical simulations as well as experimental studies of the influence of position have been performed. Nine beams have been studied experimentally and five of these beams were chosen for theoretical analysis.

2. Cross-sectional MOE distribution

In the following sections theoretical and experimental studies are presented, where values of apparent MOE are determined. Theoretical simulations require information about material parameters as input data. Furthermore, it is of interest to compare the values of the apparent MOE evaluated from bending obtained from simulations and experiments with the MOE obtained from experiments where the variation over the cross-section has been considered.

¹ Building Technology, Swedish National Testing and Research Institute, Box 857, S-501 15 Borås, Sweden

² Structural Mechanics, Lund Institute of Technology, Box 118, S-221 00 Lund, Sweden

Nine pieces of timber were selected, with the planed dimensions 45x95 mm². The timber was free from defects, and it was taken from five different positions in the log (see Fig 2). Two beams from each position were tested, except for the beam with annual rings parallel to the wide face and the pith far from the face, where only one beam was tested. The beams were conditioned in a climate chamber (20°C, RH 65%) to a moisture content of 12% and thereafter tested according to EN 408 for determination of the MOE in bending.

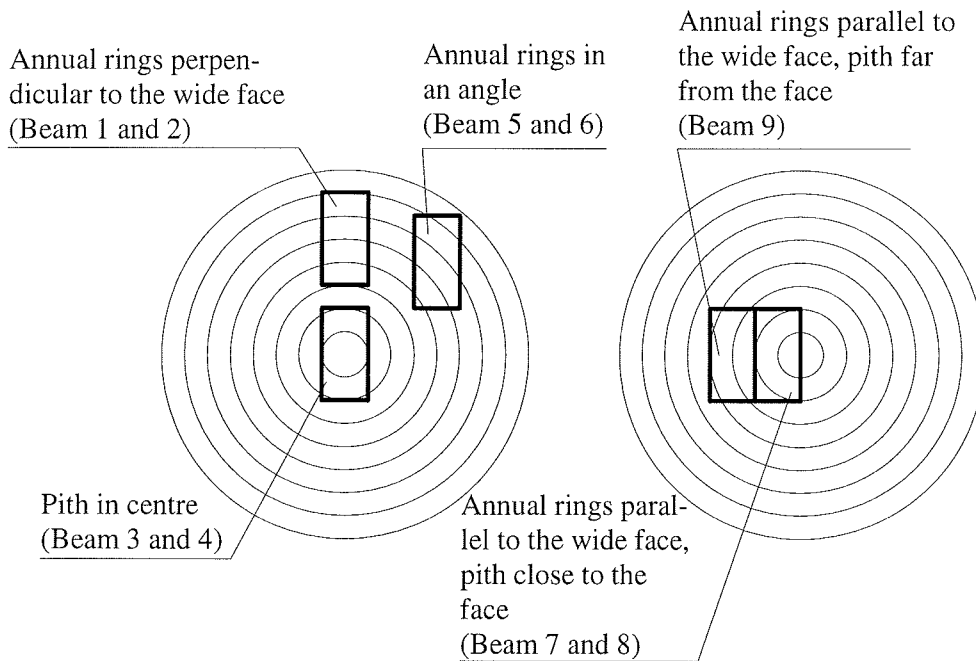


Figure 2 Location in the log where the specimens were taken.

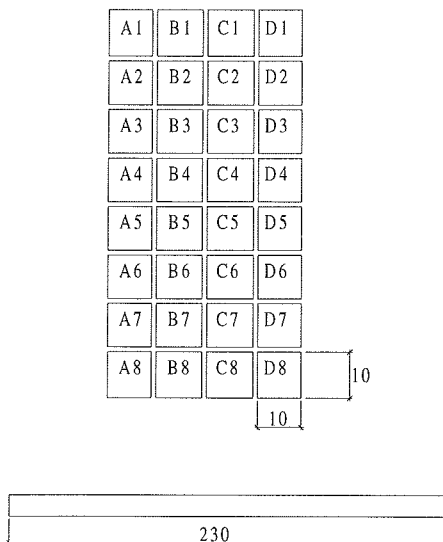


Figure 3 Cutting pattern for the sticks used for determination of variation of MOE over the cross-section.

After performing bending tests (cf. Sec. 4), the longitudinal MOE was determined using a dynamic method. The MOE was determined from the velocity of an ultrasonic pulse and the density as

$$E = v^2 \cdot \rho_{12,12} \quad (1)$$

where E is the MOE, v is the velocity of an ultrasonic pulse, and $\rho_{12,12}$ is the density at 12% moisture content. This was performed on specimens with the dimensions 10x10x230 mm obtained by splitting up a part of the central section of the beams tested (see Fig 3). The results for the individual specimens are presented in Appendix.

According to elementary beam theory the bending stiffness is given by $\int_A Ey^2 dA$. By dividing the bending stiffness by the moment on inertia $I = \int_A y^2 dA$ a weighted value of the MOE, E^* , is obtained, i.e.

$$E^* = \frac{\int_A Ey^2 dA}{\int_A y^2 dA} \quad (2)$$

which has been calculated as

$$E^* \approx \frac{\sum_{i=1}^n E_i y_i^2 A_i}{\sum_{i=1}^n y_i^2 A_i} \quad (3)$$

The MOE shows a considerable variation with the distance from the pith. Using the least-square method, a linear relation

$$\bar{E} = E_0 + E_1 r \quad (4)$$

between MOE, \bar{E} , and the distance from the pith r has been determined.

The values obtained for the nine cross-sections examined are given in Table 1.

Table 1 MOE of a central section of the tested beams.

Beam position in log	Beam	E^* (MPa)	E_0 (MPa)	E_1 (MPa/m)	Note
Annual rings perpendicular to the wide face	1	16460	17560	- 15850	
Annual rings perpendicular to the wide face	2	15370	11700	55620	Simulated
Pith in centre	3	16230	8170	105100	
Pith in centre	4	20220	7690	330000	Simulated
Annual rings at an angle	5	16060	14290	24560	
Annual rings at an angle	6	14970	13670	18420	Simulated
Pith near face, annual rings parallel to wide face	7	17420	11980	99910	Simulated
Pith near face, annual rings parallel to wide face	8	16530	11590	88490	
Pith far from face, annual rings parallel to wide face	9	15620	9690	87220	Simulated

3. Theoretical simulations

Theoretical simulations of bending tests have been performed using the finite element method. Three-dimensional simulations have been performed and eight-node isoparametric solid elements with eight integration points have been utilised. A mesh with $10 \times 20 \times 76$ elements for the wood as shown in Fig 4 have been used. The mesh also includes elements for steel plates at the supports and at the positions of load application. The steel plates are assumed to have full coupling with the wood material. In the computation, the orthotropic structure of the wood has to be considered. The influence of annual ring orientation and spiral grain on the orthotropic directions are taken into account. The computations have been performed using a commercial computer code (Hibbitt et al. 1994), supplemented with special-purpose routines for constitutive model and coordinate transformation specific to wood (see Ormarsson 1995).

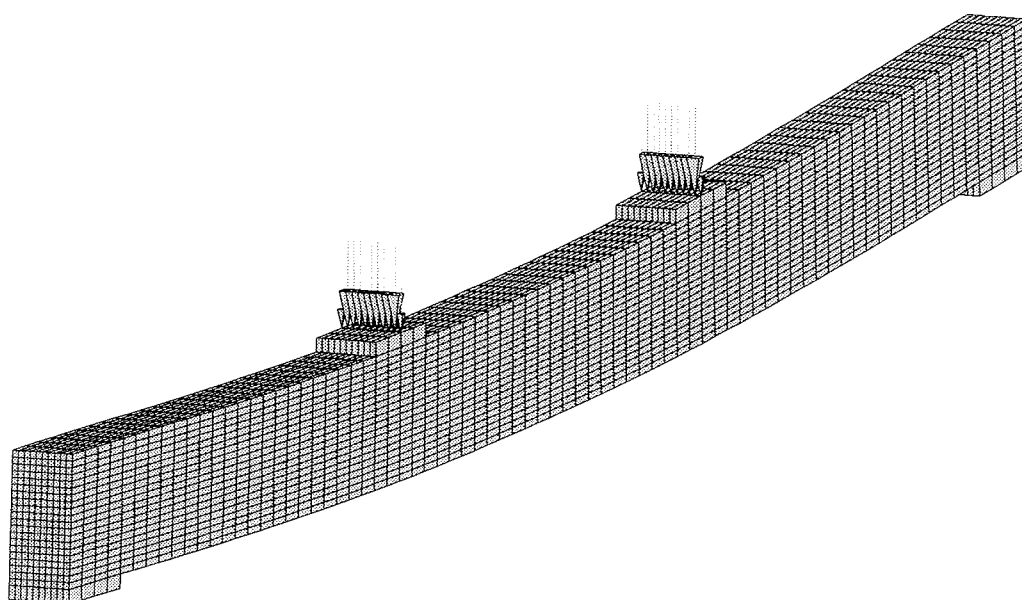


Figure 4 The finite element mesh used in the theoretical simulations.

In addition to the cross-sectional MOE distribution given in Table 1 (cf. Sec. 2) the material properties given in Table 2 have been assumed. The spiral grain angle, θ , is defined as the angle, in the longitudinal/tangential plane, between the pith direction and the fibre direction (see Ormarsson 1995). The function chosen is based on experimental investigations on Norway spruce (Dahlblom and Petersson 1996).

Table 2 Material properties used in theoretical simulation. (r is the distance from the pith in [m])

Spiral grain, θ	E_R	E_T	G_{LR}	G_{LT}	G_{RT}
4 - 40 r	500 MPa	280 MPa	500 MPa	500 MPa	50 MPa

Static analyses were performed and the total load $P = 7.0$ kN was applied as several nodal loads in a transversal line on the upper face of the steel plates. The supports were modelled by assuming zero vertical displacement of a transversal line under one steel plate and zero vertical displacement of the central point under the other steel plate.

The computation simulates determination of MOE from bending tests. The purpose of the simulation is to investigate the influence of position of deformation measurement. One advantage of theoretical simulation is that the results are not affected by the inaccuracies in measurements and uncontrolled imperfections in the material studied which may affect experimental investigations.

The computational results are evaluated in the same manner as bending tests, i.e. an apparent MOE is calculated according to

$$E = \frac{P \cdot L_a \cdot L_1^2}{16 \cdot I \cdot w} \quad (5)$$

where P is the load, L_a is the distance between support and load, L_1 the gauge length, I is the moment of inertia and w is the relative vertical displacement given by

$$w = \frac{1}{2} (u(-L_1/2) + u(L_1/2)) - u(0) \quad (6)$$

where $u(0)$ is the vertical displacement at the mid-point and $u(-L_1/2)$ and $u(L_1/2)$ are the vertical displacements at the end-points of the gauge.

Assuming $L_a = 6h$, $L_1 = 5h$ and $I = bh^3/12$, where h and b are the cross-sectional height and width respectively, yields

$$E = 112.5 \frac{P}{b \cdot w} \quad (7)$$

Evaluation of the results obtained from simulations of five different cross-sections have been performed and evaluated according to Eq. (7) at eight different positions around the cross-section (see Fig 5). This corresponds to different locations of gauge in an experiment.

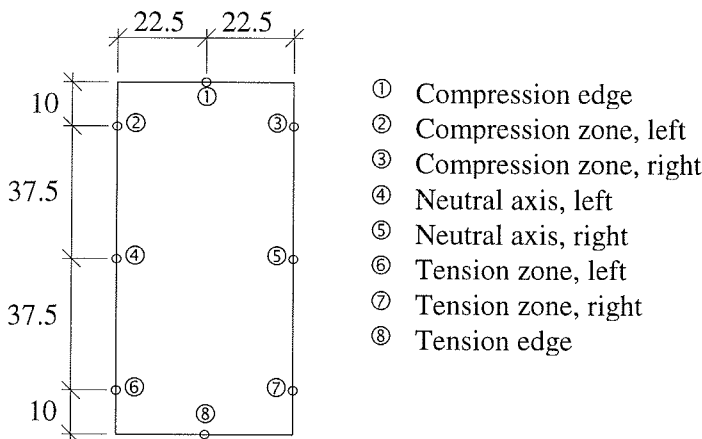


Figure 5 Positions on the beam where apparent MOE has been determined.

The results obtained are shown in Table 3. It may be noted that the apparent MOE obtained is affected by the position of determination of deformation. The results show that the obtained value of the apparent MOE increases from the tension zone to the compression zone. The difference between the neutral zone and the compression zone is greater than between the

tension zone and the neutral zone. This difference develops due to local deformations near the loading point which leads to greater value of the apparent MOE in that point.

The values for one cross-section vary by about 5 - 9% depending on position of deformation determination. The results also show that the annual ring orientation affects the apparent MOE.

Table 3 Comparison of apparent MOE from theoretical simulation and weighted MOE.

Position of the deformation measurement (see Fig 5)	Beam 2		Beam 4		Beam 6		Beam 7		Beam 9	
	E_{FEM}	$\frac{E_{FEM}}{E^*}$	E_{FEM}	$\frac{E_{FEM}}{E^*}$	E_{FEM}	$\frac{E_{FEM}}{E^*}$	E_{FEM}	$\frac{E_{FEM}}{E^*}$	E_{FEM}	$\frac{E_{FEM}}{E^*}$
	MPa		MPa		MPa		MPa		MPa	
Compression edge	15220	0.990	20260	1.002	15490	1.035	17780	1.021	16430	1.052
Compression, left	14930	0.972	19780	0.978	15230	1.017	17420	1.000	16060	1.028
Compression, right	14990	0.975	19620	0.970	14920	0.997	17260	0.991	15970	1.022
Neutral axis, left	14560	0.947	18900	0.934	14610	0.976	16560	0.950	15360	0.983
Neutral axis, right	14560	0.948	18990	0.939	14540	0.971	16500	0.947	15340	0.982
Tension zone, left	14460	0.941	18700	0.925	14920	0.997	16370	0.940	15240	0.976
Tension zone, right	14460	0.941	18830	0.931	14460	0.966	16350	0.938	15210	0.974
Tension edge	14440	0.940	18740	0.927	14460	0.966	16360	0.939	15220	0.975

To investigate to what extent the values of transversal MOE, shear moduli and spiral grain angle affect the obtained value, a parameter study has been performed for beam 9. The results of the study are presented in Table 4. Computations have been performed where one of the elastic or shear moduli has been given a value twice as large as in the reference computation. For the cross-section studied, the largest influence (about 2%) is obtained for a change in G_{LT} . The assumption of zero spiral grain also affects the results. The influence is then about 1%.

Table 4 Parameter study of beam 9.

Position of the deformation measurement	E_{ref}	$\frac{E(E_{R,1000})}{E_{ref}}$	$\frac{E(E_{T,1000})}{E_{ref}}$	$\frac{E(G_{LR,1000})}{E_{ref}}$	$\frac{E(G_{LT,1000})}{E_{ref}}$	$\frac{E(G_{RT,100})}{E_{ref}}$	$\frac{E(\theta=0)}{E_{ref}}$
	MPa						
Compression edge	16430	1.000	0.986	0.996	1.011	0.992	1.012
Compression, left	16060	0.999	0.991	0.990	1.018	0.994	1.012
Compression, right	15970	1.000	0.990	1.006	1.008	0.995	1.013
Neutral axis, left	15360	1.000	1.001	0.996	1.019	1.002	1.011
Neutral axis, right	15340	0.999	1.002	1.003	1.014	0.998	1.012
Tension zone, left	15240	1.000	1.003	0.999	1.018	1.003	1.011
Tension zone, right	15210	1.000	1.005	1.002	1.020	1.000	1.012
Tension edge	15220	1.000	1.004	1.000	1.019	1.002	1.011

4. Experimental study

In the four-point bending test the deformation was measured at three different positions on the side of the beam, 10 mm below the upper edge, i.e. in the compression zone, at the neutral axis, and 10 mm above the lower edge, i.e. in the tension zone. These measurements were

made on both sides of the specimens, referred to below as left and right gauge. The deformation was also measured on the lower edge of the beam (see Fig 6).

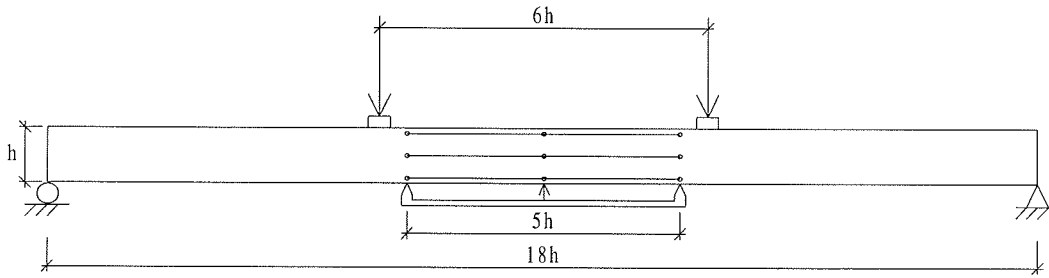


Figure 6 Positions for deformation measurements.

The beams were loaded with a constant movement of the cross-head at a rate of 8 mm/min. The load-deformation measurements were recorded up to a load of 8 kN, and thereafter the specimen was unloaded. Each beam was tested eight times in the following order:

- deformation measured in the compression zone
- deformation measured at the neutral axis
- deformation measured in the tension zone
- deformation measured at the neutral axis.

Each test was done twice. In all tests the deformation was also recorded on the lower edge with a special cradle hanging under the specimen.

The experimental results show a dramatic effect of the position of the gauge on the determined MOE. In Figs 7 and 8 all results for beam 1 and 4 respectively are presented. The figures clearly show a decreasing MOE from the compression zone to the tension zone. They also show the large differences found between the two sides (left and right gauge). In beam 4 the MOE measured in the compression zone is more than 60% higher than in the tension zone.

Two tests were carried out each time the gauges were moved on the beam. The diagrams show that repeatability is good.

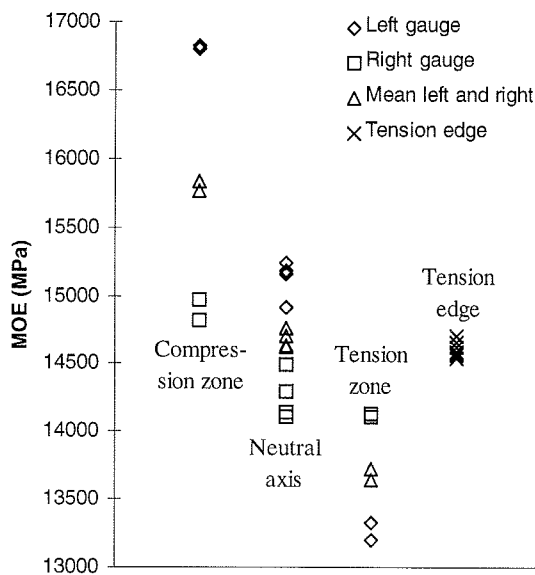


Figure 7 MOE for all tests on beam 1.

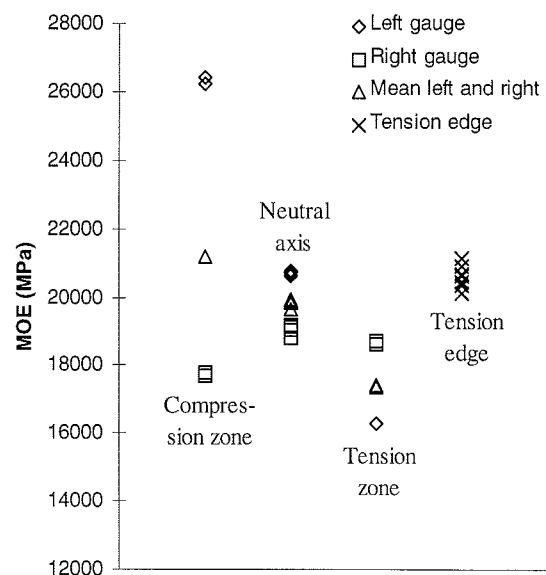


Figure 8 MOE for all tests on beam 4.

The MOE determined at different positions on the beams is presented in Table 5. All values used are the mean value between the two gauges, except for the tension edge where only one gauge was used. The table also presents the maximum deviation at the different positions from the mean MOE determined at the neutral axis. The mean value for the neutral axis, $\bar{E}_{\text{neutral axis}}$, has been calculated from four tests. $E_{\text{compression}}$, $E_{\text{neutral axis}}$, $E_{\text{tension zone}}$ and $E_{\text{tension edge}}$ are the values that differ most from the mean in the neutral axis in the compression zone, the neutral axis, the tension zone and at the tension edge respectively.

In all beams except 5, 6 and 7 the MOE decreases from the compression zone to the tension zone. A peculiar phenomenon is that the MOE measured on the tension edge is significantly higher than the MOE measured on the side of the beam in the tension zone. Only beam 7 contradicts this result. The measurements made on the tension face were made with a different cradle, attached under the beam by using rubber bands, which can be an explanation to the different results between the values obtained in the tension zone on the side of the beam and the values obtained on the tension face under the beam.

Table 5 Experimentally determined MOE and the effect of position of gauge on the measurement.

	Mean MOE (MPa)				Maximum deviation from mean MOE at the neutral axis (%)			
	Compression zone	Neutral axis	Tension zone	Tension edge	$\frac{E_{\text{compression}}}{\bar{E}_{\text{neutral axis}}}$	$\frac{E_{\text{neutral axis}}}{\bar{E}_{\text{neutral axis}}}$	$\frac{E_{\text{tension zone}}}{\bar{E}_{\text{neutral axis}}}$	$\frac{E_{\text{tension edge}}}{\bar{E}_{\text{neutral axis}}}$
<i>Annual rings perpendicular to the wide face</i>								
Beam 1	15800	14680	13680	14610	14.6	-4.0	-10.1	-1.0
Beam 2	16520	15250	14150	14730	13.6	5.9	-7.9	-4.7
<i>Pith centred in the beam</i>								
Beam 3	15930	15690	14970	16520	9.1	-2.9	-11.8	7.4
Beam 4	21190	19840	17390	20580	33.0	-5.5	-18.1	6.4
<i>Annual rings at an angle</i>								
Beam 5	15530	16320	14980	15800	-13.1	2.5	-14.1	-3.7
Beam 6	13460	14150	13270	13980	-11.8	-4.0	-11.2	-3.6
<i>Pith outside but close to the wide face, annual rings parallel with the wide face</i>								
Beam 7	14000	13920	14100	13180	2.9	-1.9	4.9	-8.3
Beam 8	18260	17240	16080	16570	14.4	-1.8	-12.4	-7.5
<i>Pith outside far from the wide face, annual rings parallel with the wide face</i>								
Beam 9	14170	13910	13520	14200	8.5	5.0	-3.6	3.7

In Table 6 the difference between measurements on the two sides is presented, as well as the coefficient of variation for the measurements made on the tension edge. The largest difference between left and right gauge is obtained in the compression zone and the smallest in most cases in the neutral axis.

The measurements made at the tension edge show good repeatability. The largest value for the coefficient of variation is 2.5%.

Table 6 Difference between measurements on the two sides of the beams (%). The value given for the tension edge is the coefficient of variation for all eight tests.

	Compression zone		Neutral axis		Tension zone		Neutral axis		Tension edge
	Test 1	Test 2	Test 3	Test 4	Test 5	Test 6	Test 7	Test 8	COV (%)
<i>Annual rings perpendicular to the wide face</i>									
Beam 1	12.3	13.5	2.9	6.6	6.1	6.8	7.6	7.2	0.4
Beam 2	9.2	9.5	4.3	2.0	0.3	1.1	0.3	0.4	0.7
<i>Pith centred in the beam</i>									
Beam 3	14.4	15.0	4.5	4.5	17.5	15.7	5.0	3.4	1.6
Beam 4	49.5	47.6	9.1	9.7	14.9	14.4	8.0	8.4	1.6
<i>Annual rings at an angle</i>									
Beam 5	20.0	20.2	4.8	3.3	14.5	14.3	3.7	4.0	0.4
Beam 6	16.3	16.2	1.1	2.3	10.3	12.8	5.4	2.6	2.1
<i>Pith outside but close to the wide face, annual rings parallel with the wide face</i>									
Beam 7	3.1	3.8	1.1	1.2	6.4	5.8	2.5	2.5	2.5
Beam 8	15.1	13.0	2.2	2.8	13.8	12.2	3.1	3.1	2.3
<i>Pith outside far from the wide face, annual rings parallel with the wide face</i>									
Beam 9	13.8	11.9	8.6	9.5	0.7	1.3	6.8	8.7	1.3

5. Comparison between theoretical and experimental results

The effect of position of the gauges on the MOE is more pronounced in the experimental results than in the theoretical simulations. However, the same tendencies can be found in the simulations as in the experiments, i.e. the MOE decreases from the compression zone to the tension zone. Fig 9 gives an example of the differences between the experimental and theoretically obtained MOE for beam 4. The experimental data is represented by crosses. The diamonds represent values obtained on the left side of the beam by the theoretical simulation, the squares represent the values for the right side, and the triangles the mean values for respective position.

In Table 7 the simulated and the experimentally determined MOE for the beams in the neutral axis are compared. The theoretically simulated values are within 10% of the experimentally determined ones, except for beam 7.

A comparison has also been made between the theoretically calculated MOE of the beam and the weighted MOE calculated from the cross-sectional distribution of the MOE obtained from tests with the small sticks. The theoretically calculated value is 2 - 6% lower than the weighted MOE. A corresponding comparison between experimentally determined MOE and weighted MOE yields the difference 1 - 20%.

Table 8 presents ratios between the MOE values obtained by theoretical simulations and experiments. In most cases the simulation yields a higher value than the experiments. Only in beams 2 and 4 in the compression zone, the neutral axis and at the tension edge did the simulations give a lower value.

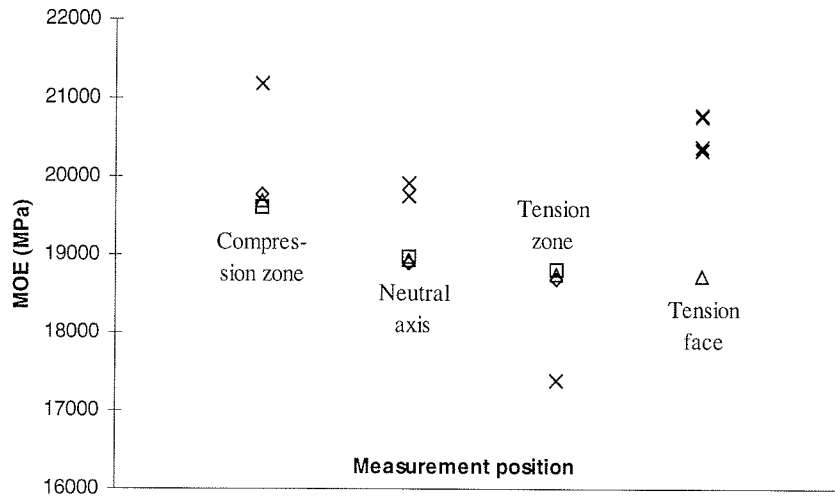


Figure 9 Comparison between theoretically and experimentally determined MOE at different positions on a beam with the pith in the centre, beam 4. Crosses represent experimental data.

Table 7 Comparison between theoretically simulated and experimentally determined MOE.

Grain orientation	Beam	$E_{NA,sim}$	$E_{NA,exp}$	E^*	$\frac{E_{NA,sim}}{E_{NA,exp}}$	$\frac{E_{NA,sim}}{E^*}$	$\frac{E_{NA,exp}}{E^*}$
		(MPa)	(MPa)	(MPa)			
Annual rings perpendicular to the wide face	2	14560	15240	15370	0.955	0.947	0.992
Pith in centre	4	18940	19840	20220	0.955	0.937	0.981
Annual rings at an angle	6	14570	14150	14970	1.030	0.973	0.945
Pith near face, annual rings parallel to wide face	7	16530	13920	17420	1.188	0.949	0.799
Pith far from face, annual rings parallel to wide face	9	15350	13910	15620	1.103	0.983	0.890

Table 8 Ratio between theoretically simulated MOE and experimentally determined MOE at different positions on the beams. Columns headed left and right are valid for the gauges on the respective sides of the beam.

	Compression zone			Neutral axis			Tension zone			Tension edge
	Left	Right	Mean	Left	Right	Mean	Left	Right	Mean	
Beam 2	0.863	0.947	0.906	0.948	0.962	0.955	1.026	1.019	1.022	0.981
Beam 4	0.752	1.107	0.930	0.912	0.997	0.955	1.149	1.009	1.079	0.910
Beam 6	1.217	1.026	1.120	1.046	1.013	1.030	1.186	1.031	1.108	1.035
Beam 7	1.223	1.253	1.238	1.179	1.196	1.187	1.195	1.125	1.160	1.241
Beam 9	1.066	1.196	1.130	1.060	1.148	1.103	1.133	1.120	1.126	1.072

6. Conclusions

The following conclusions can be drawn from the present study:

- The position of the deformation measurement strongly affects the obtained value of MOE. The highest values are obtained in the compression zone, and the value decreases when going down towards the tension zone. Both the theoretical simulation and the experiments yield this effect. One source of the effect is local deformations near the loading points. The magnitude of the effect of position is smaller in the theoretical simulation than through experiments.
- The MOE is higher when measurements are made on the tension face, under the beam, than when measuring the MOE in the tension zone on the side of the beam. Of all specimens there is only one exception.
- When measuring the deformation on one side only, and in the compression zone or the neutral axis, the highest MOE is obtained for the inside face (the face closest to the pith). When measurements are made in the tension zone the outside face usually gives the highest MOE. Therefore it is important that the deformation is measured on both sides of the beam, and a mean value between the two measurements is used for the determination of MOE.
- A theoretical parameter study shows that for one cross-section the shear modulus, G_{LT} , and the spiral grain both affect the results, while the effects of the elastic moduli E_R and E_T , and the shear moduli G_{LR} and G_{RT} are negligible.

References

- Dahlblom O., Petersson H. (1996): A study of engineering properties of spruce. In preparation
- EN 408 Timber structures - Test methods - Solid timber and glued laminated timber - Determination of some physical and mechanical properties.
- Hibbitt, Karlsson & Sorenson, Inc (1994): ABAQUS, Version 5.4. Pawtucket, Ri.
- Johansson C-J. (1996) Personal communication.
- Ormarsson S. (1995): A finite element study of the shape stability of sawn timber subjected to moisture variations. Report TVSM-3017, Lund Institute of Technology, Sweden

Appendix: Cutting pattern and distribution of MOE

In Figs A1-A9 the cutting pattern and the distribution of the MOE over the cross-section for a central part of all beams are presented.

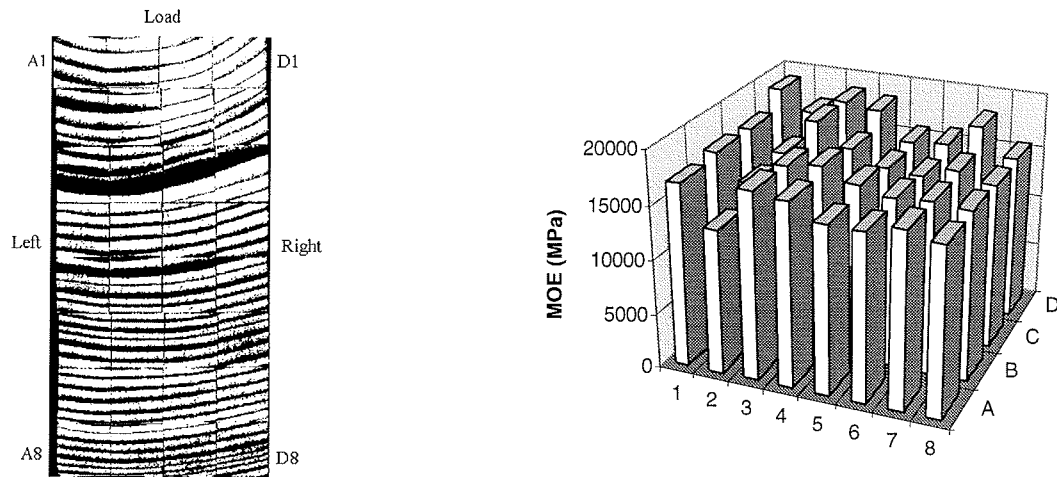


Figure A1 Cutting pattern and cross-sectional distribution of MOE of beam 1.

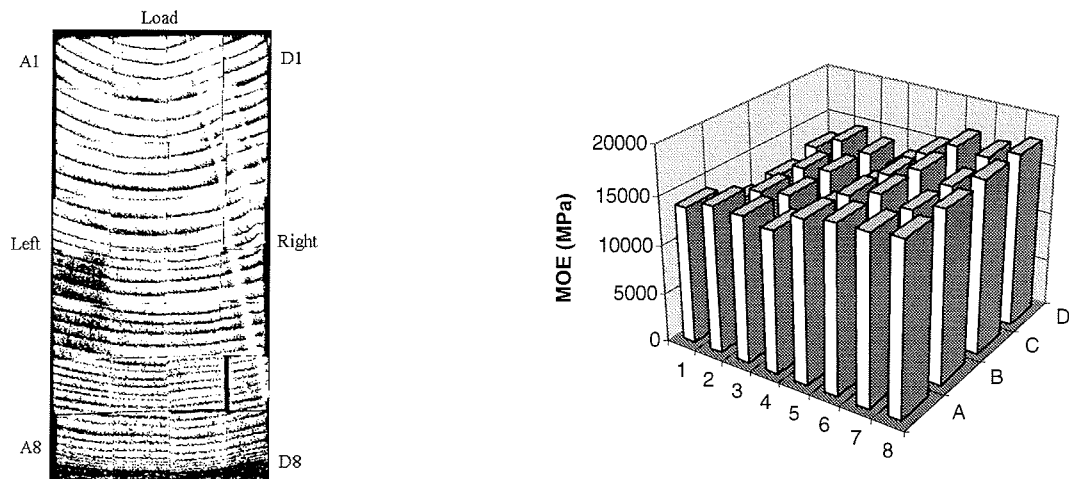


Figure A2 Cutting pattern and cross-sectional distribution of MOE of beam 2.

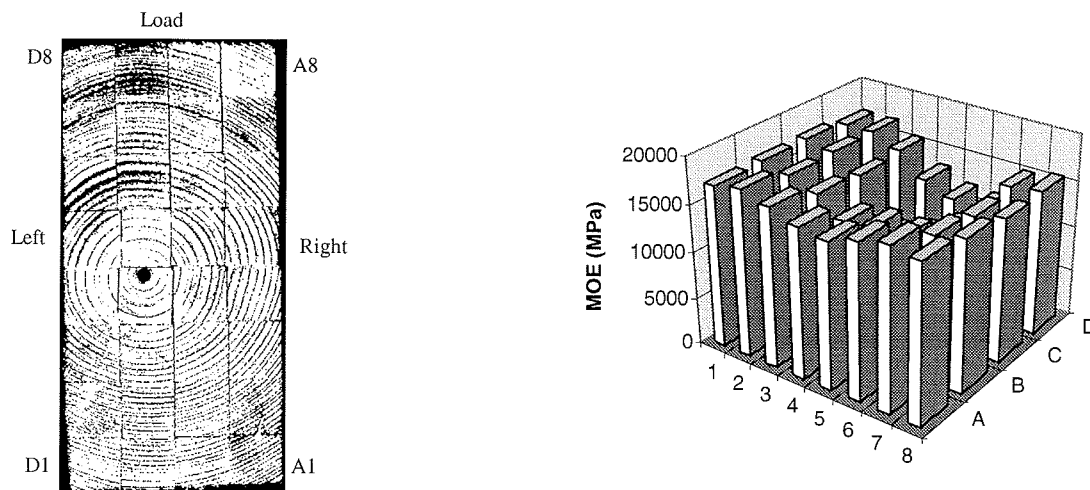


Figure A3 Cutting pattern and cross-sectional distribution of MOE of beam 3.

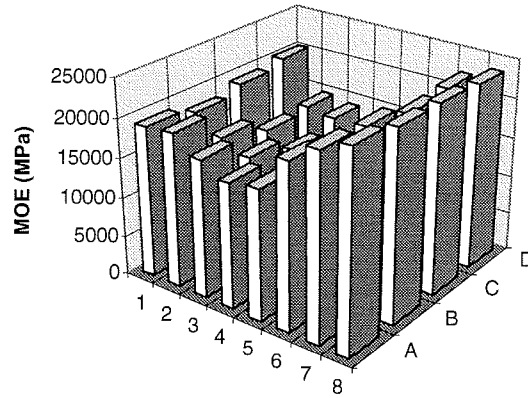
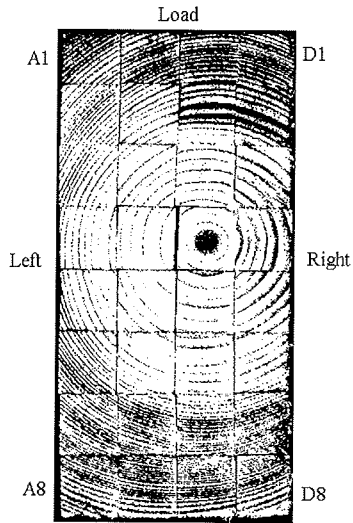


Figure A4 Cutting pattern and cross-sectional distribution of MOE of beam 4.

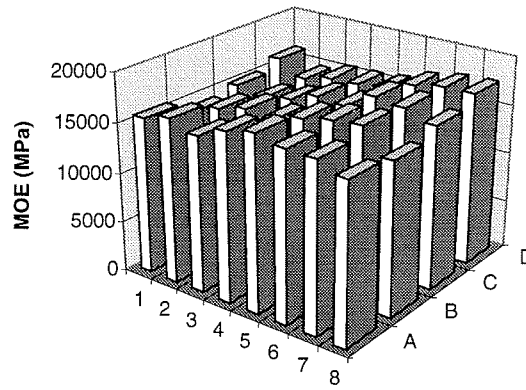
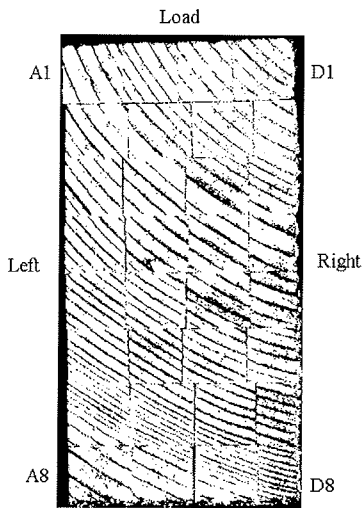


Figure A5 Cutting pattern and cross-sectional distribution of MOE of beam 5.

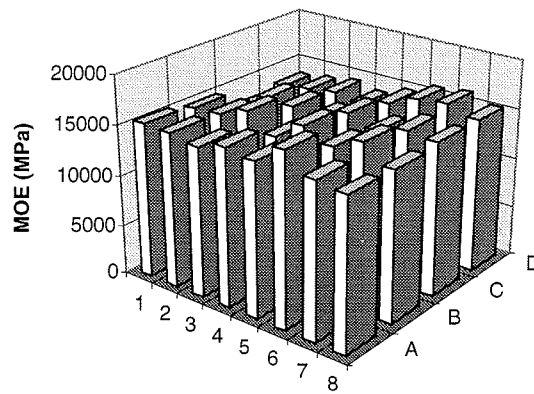
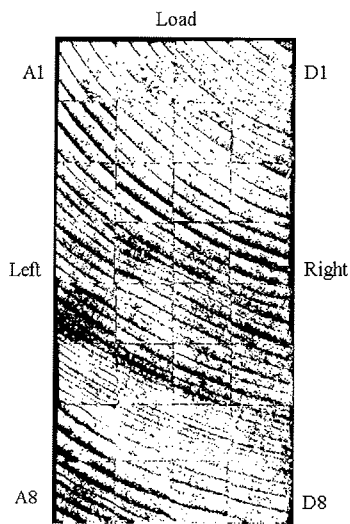


Figure A6 Cutting pattern and cross-sectional distribution of MOE of beam 6.

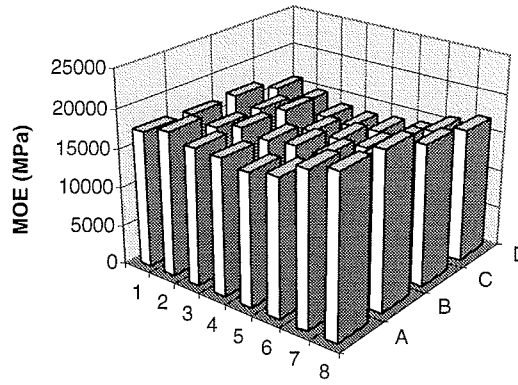
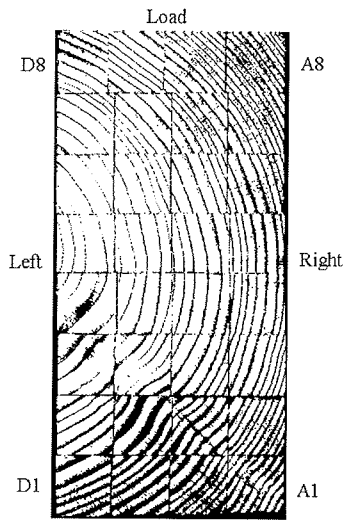


Figure A7 Cutting pattern and cross-sectional distribution of MOE of beam 7.

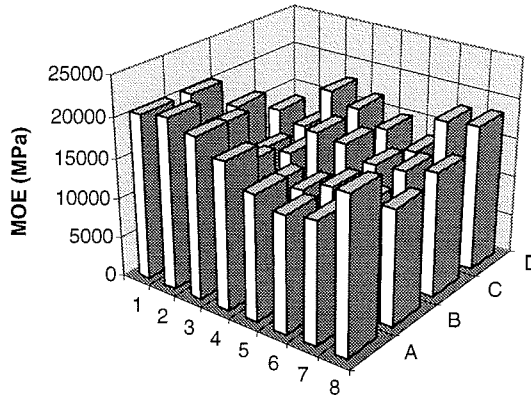
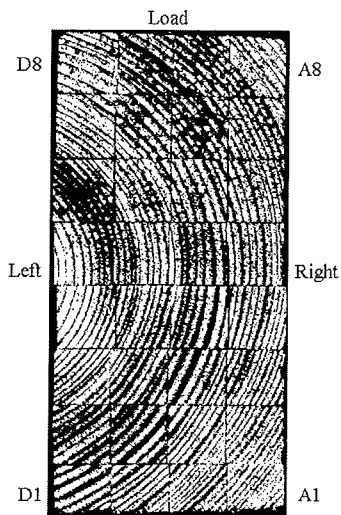


Figure A8 Cutting pattern and cross-sectional distribution of MOE of beam 8.

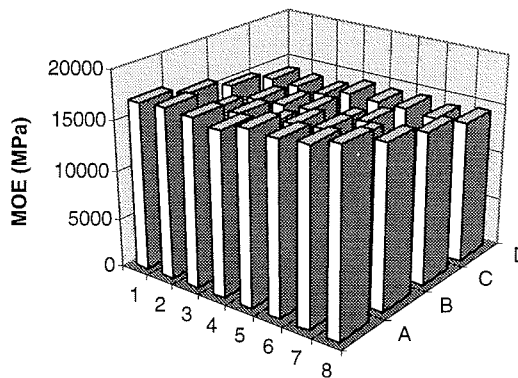
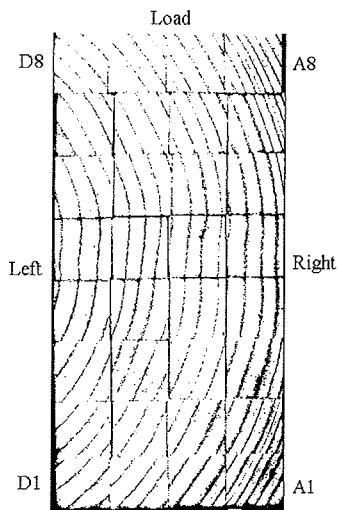


Figure A9 Cutting pattern and cross-sectional distribution of MOE of beam 9.

INTERNATIONAL COUNCIL FOR BUILDING RESEARCH STUDIES AND DOCUMENTATION
WORKING COMMISSION W18 - TIMBER STRUCTURES

**RELATION OF MODULI OF ELASTICITY IN FLATWISE AND EDGEWISE
BENDING OF SOLID TIMBER**

by

C J Johansson

Swedish National Testing and Research Institute

Sweden

A Steffen

University of Hamburg

Germany

E W Wormuth

Germany

MEETING TWENTY - NINE

BORDEAUX

FRANCE

AUGUST 1996

Relation of Moduli of Elasticity in Flatwise and Edgewise Bending of Solid Timber

by

C.-J. Johansson¹⁾, A. Steffen²⁾ and E. W. Wormuth³⁾

Abstract

The moduli of elasticity determined in edgewise and in flatwise bending were compared on 45x170 mm² and 67x195 mm² Norway spruce timber. Sections of the timber were cut into 300 mm long specimens with 9x9 mm² cross section. The modulus of elasticity of these small specimens was determined by means of the ultrasonic pulse technique to study the variation of the modulus of elasticity over the cross section. The results of the static bending tests showed that the edgewise modulus of elasticity was distinctly higher than the flatwise modulus of elasticity, even when shear deformations were considered. The modulus of elasticity of the small specimens varied considerably over a timber cross section. Normally, the value increased from the pith outwards. The difference was as large as a factor 2. This explained an important part of the difference between the edgewise and the flatwise modulus of elasticity.

1 Introduction

Johansson (1992) obtained a difference of 23 % between the moduli of elasticity (MOE) in edgewise bending according to EN 408 and flatwise three point bending. When shear deformations are taken into account, a difference of 7 to 12 % remains. 58x120 mm² Norway spruce timber was studied. The flatwise MOE was determined in a strength grading machine with a span of 900 mm.

The purpose of the study presented here was to explain the difference between the edgewise and flatwise MOE of Norway spruce timber. The edgewise and flatwise MOE have been determined both in knotty and in knot free sections of the timber. In addition to this the MOE and density distribution over the timber cross sections were determined. Detailed results are given by Wormuth (1992).

¹⁾ *Department of Building Technology, Swedish National Testing and Research Institute, P.O. Box 857, S-501 15 Borås*

²⁾ *Department of Wood Technology, University of Hamburg, Leuschnerstrasse 91, D-21031 Hamburg*

³⁾ *Dr. Wolman GmbH, D-76545 Sinzheim*

2 Material

Norway spruce (*Picea abies*) timber from the southern part of the province Västergötland in Sweden was selected. Two dimensions, 45x170 mm² (8 pieces) and 67x195 mm² (5 pieces), were chosen. Timber pieces with narrow or wide growth rings as well as different positions of the pith were selected. Two cross sections are shown in Figure 1.

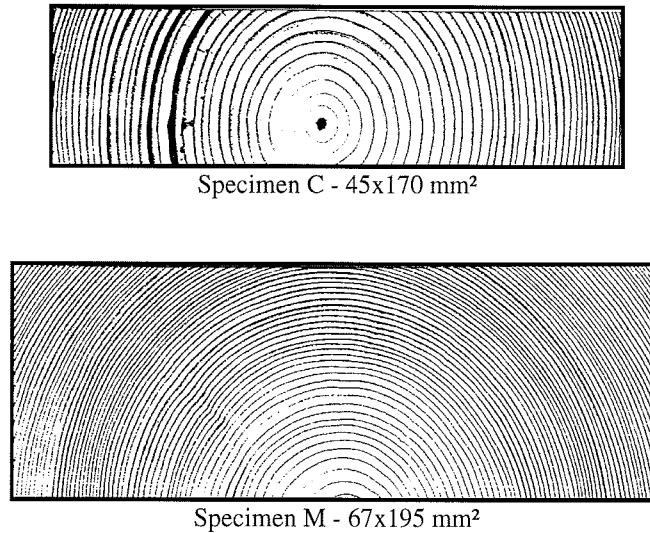


Figure 1 Examples of cross sections

3 Experimental methods

On each of the specimens the edgewise MOE was determined according to EN 408 with a span-to-depth ratio of 18. This was done on two sections in each specimen, one knotty and one knot free. The flatwise MOE (span = 900 mm) was determined on the same sections in a three point bending test, where the determination of the MOE was based on the mid span deflection. After this, a 400 mm long piece was cut out of the knot free sections. One 45 mm long part of that piece was used to determine density and moisture content, the remaining part was reduced to 300 mm in length and cut into 9x9x300 mm³ specimens. This resulted in a total of 1980 such specimens on which the tensile MOE was determined by means of an ultrasonic pulse device 'Pundit' by C.N.S. Electronics. The device measured the velocity of the ultrasonic pulse in the material operating with a frequency of 54 kHz. The dynamic MOE was calculated according to

$$E_{dyn} = c_L^2 \cdot \rho \quad (1)$$

where c_L is the ultrasonic pulse velocity and ρ is the density of the material.

Dynamic and static tensile MOE were determined on 70 specimens for calibration purposes. In the static test, the rate of loading was adjusted to correspond to the conditions in the edgewise and flatwise bending tests. The relation between static and dynamic MOE was $E_{t,static} = E_{dyn} / 1.056$ with a correlation coefficient of 0.92. With

Eq. 1 and this correction factor the static tensile MOE of the 9x9x300 mm³ specimens was calculated.

4 Test results

The results of the static bending tests are presented in Table 1 together with density, knot area ratio etc.

Table 1 Summary of test results. Moisture content, annual ring width and density have been obtained from the knot free sections.

Specimen	Moisture content (u)	Annual ring width (mean)	Density ($\rho_{0,u}$)	KAR	$E_{edge,test} / E_{flat,test}$	
	(%)		(kg/m ³)		Knotty section	Knot free section
45 x 170 mm²						
A	14.1	2.5	416	0.24	1.23	1.17
B	13.9	3.1	433	0.26	1.13	1.18
C	13.8	2.2	357	0.19	1.22	1.25
D	13.8	2.3	460	0.35	1.17	1.11
E	13.3	1.9	431	0.19	1.42	1.33
F	13.6	1.8	388	0.20	1.23	1.31
G	13.6	2.4	374	-	-	1.13
H	13.9	2.6	409	0.25	1.14	1.15
<i>Mean</i>	<i>13.8</i>	<i>1.9</i>	<i>408</i>	<i>0.24</i>	<i>1.22</i>	<i>1.20</i>
67 x 195 mm²						
I	12.0	2.1	393	0.18	1.36	1.32
J	10.6	3.4	357	0.31	1.34	1.27
K	11.5	1.4	435	0.13	1.52	1.41
L	12.2	1.2	441	0.12	1.63	1.59
M	12.1	1.5	433	0.10	1.60	1.48
<i>Mean</i>	<i>11.7</i>	<i>1.9</i>	<i>411</i>	<i>0.17</i>	<i>1.49</i>	<i>1.41</i>

The following conclusions are drawn:

- The average difference between edgewise and flatwise MOE is 22 % for the knotty sections of the 45 x 170 mm² and 49 % for the 67 x 195 mm² timber. In the knot free sections the differences are slightly smaller. The differences are in the same order as those reported by Boström (1994), but higher than those obtained by Burger and Glos (1995).
- The edgewise/flatwise MOE ratio seems to increase with decreasing knot area ratio and with increasing edgewise MOE, see Figures 2 and 3. Results obtained by Boström (1992) show the same tendency.

Typical examples of density and MOE distributions over the timber cross sections are shown in Figures 4, 5 and 6. In general, both the density and the MOE increase from the

pith outwards. In a few cases, the density is almost homogeneously distributed, but the MOE still varies with a factor of more than 2, see Figures 4 and 5.

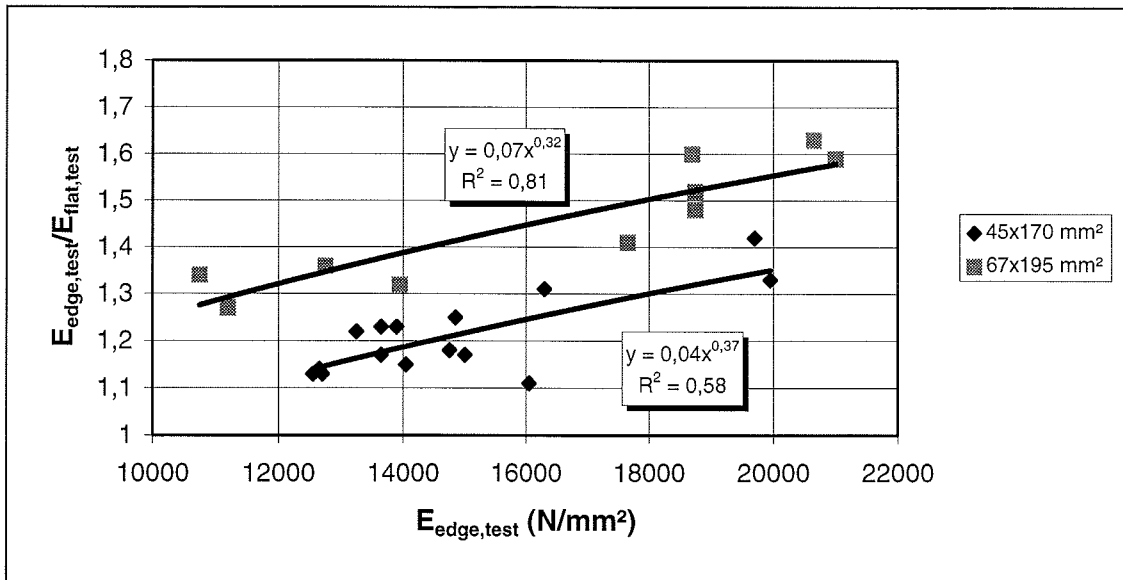


Figure 2 Relation between the ratio $E_{edge, test} / E_{flat, test}$ and the EN 408 edgewise MOE.

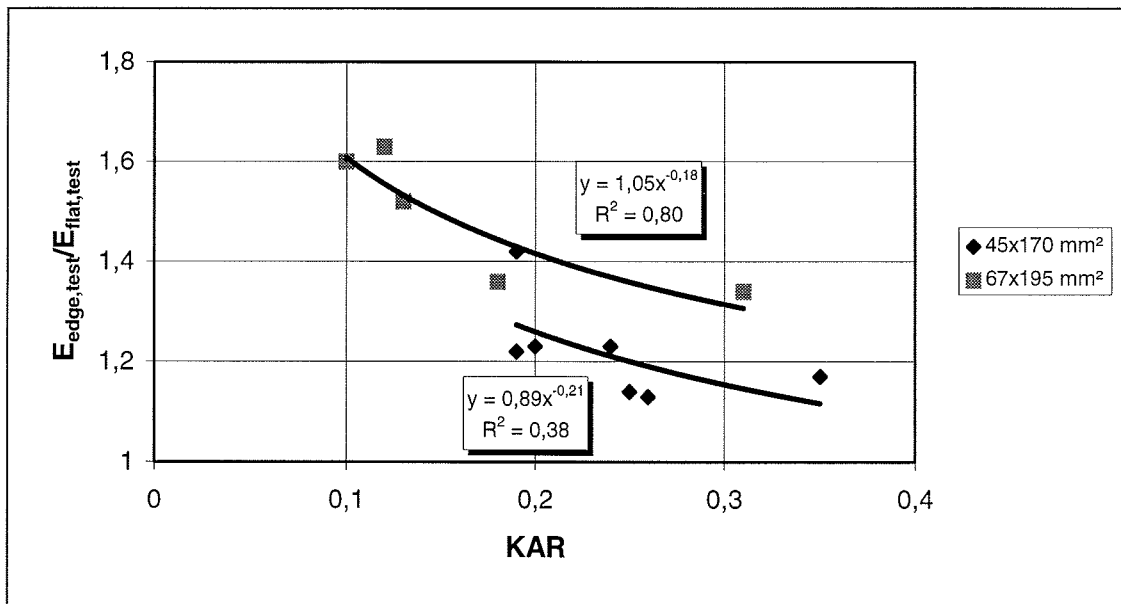


Figure 3 Relation between KAR and the EN 408 edgewise MOE.

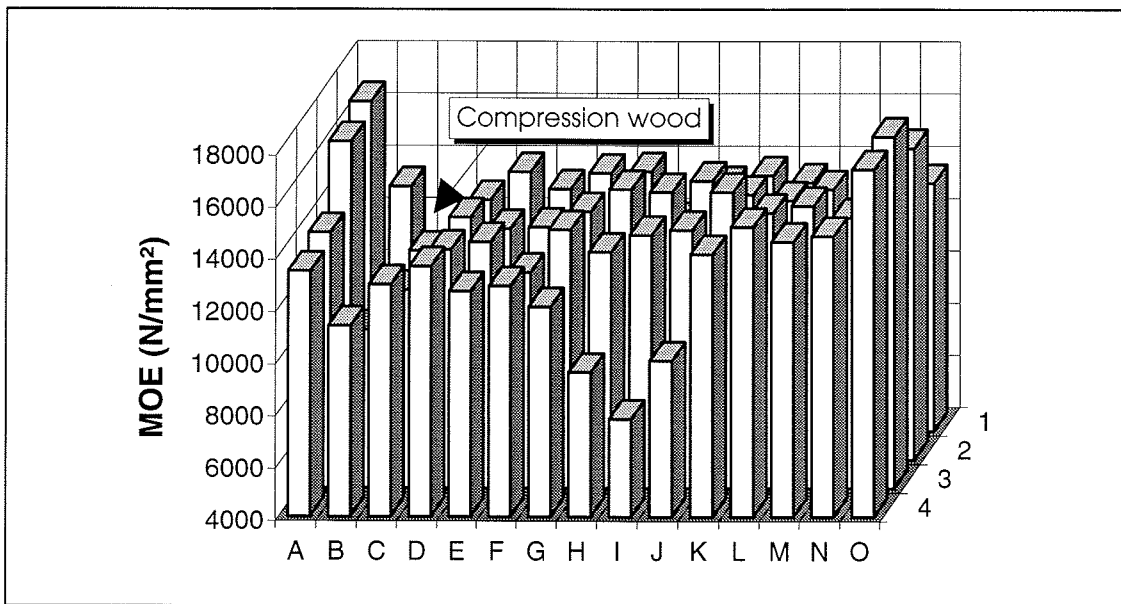
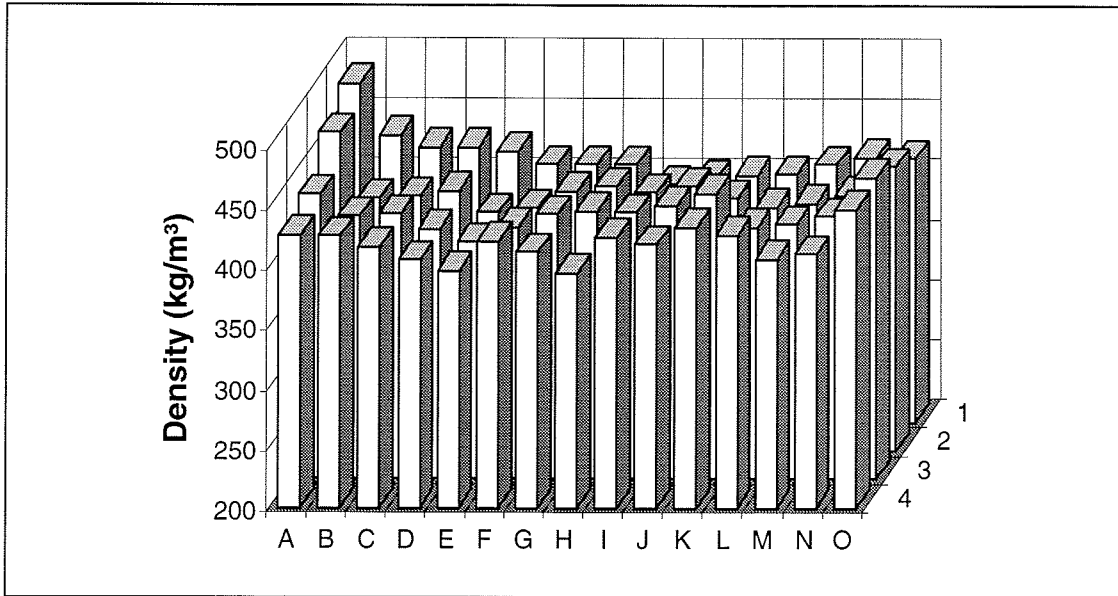
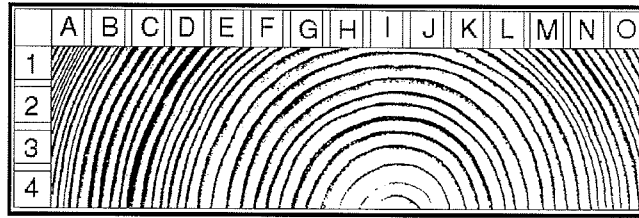


Figure 4 Density ($\rho_{0,u}$) and MOE distribution in specimen A.

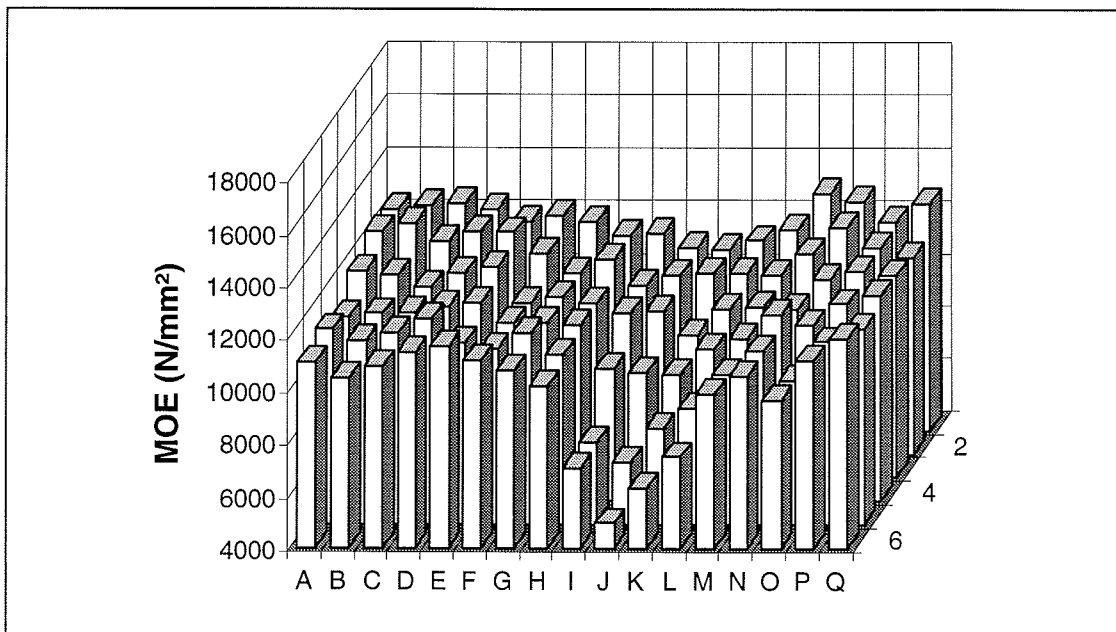
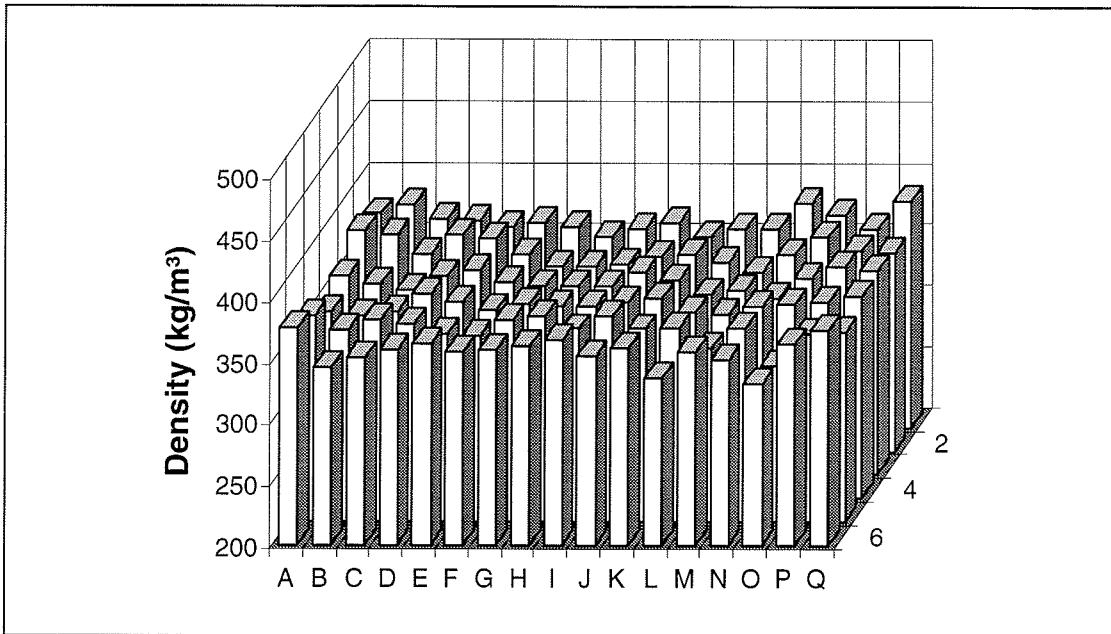
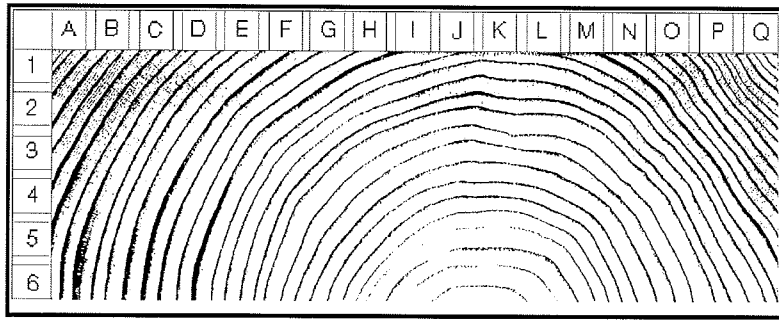


Figure 5 Density ($\rho_{0,u}$) and MOE distribution in specimen J.

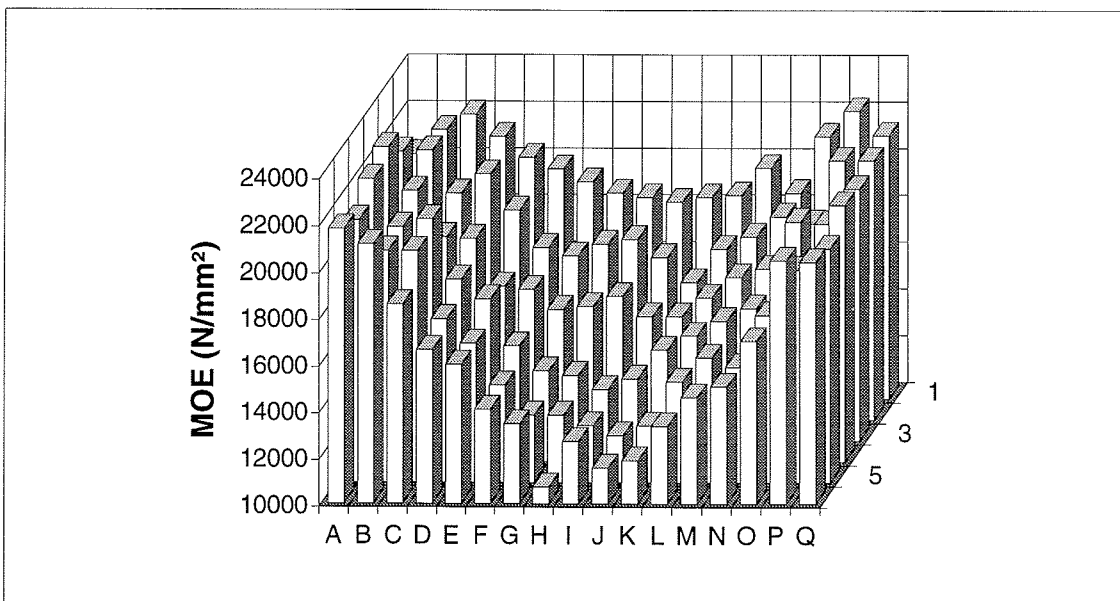
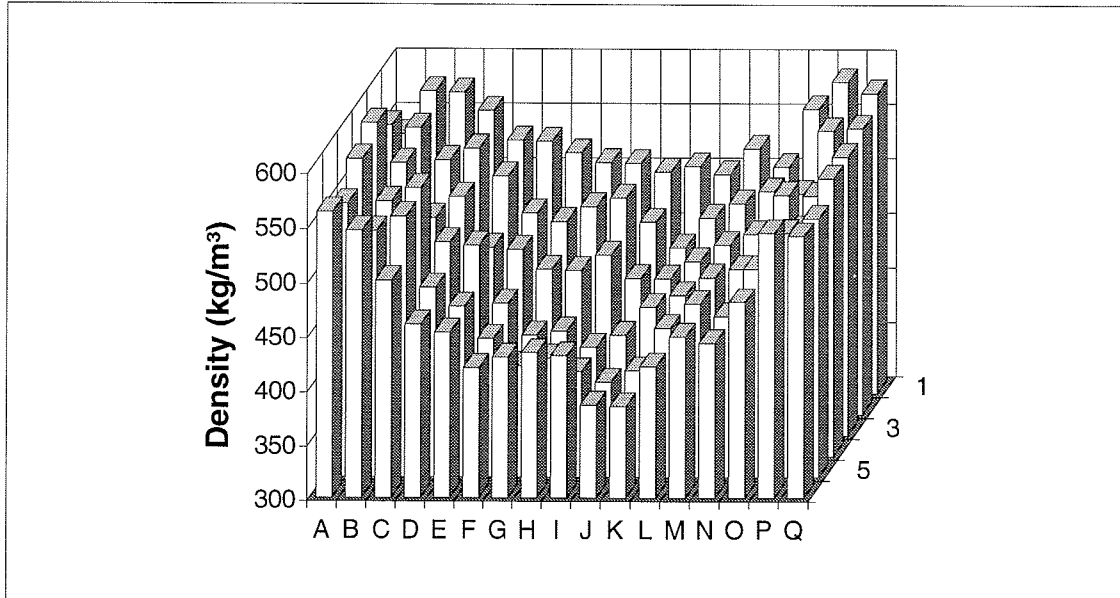
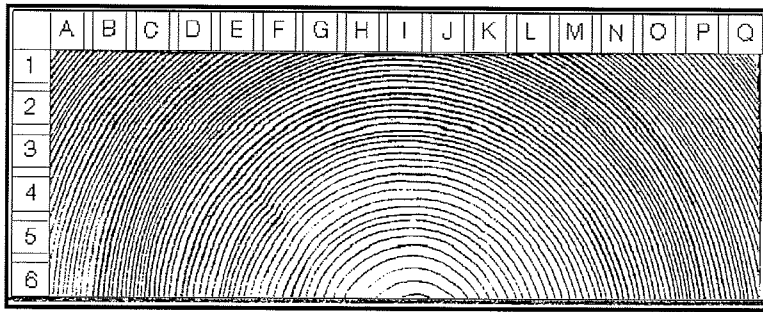


Figure 6 Density ($\rho_{0,u}$) and MOE distribution in specimen M.

5 Edgewise and flatwise MOE based on dynamic MOE

Based on the MOE values from the 9x9x300 mm³ specimens the edgewise and flatwise $E_{edge,calc}$ and $E_{flat,calc}$ have been calculated according to

$$E_{calc} = \frac{\sum_{i=1}^n E_i I_i}{\sum_{i=1}^n I_i} \quad (2)$$

where E_i is the MOE of the 9x9x300 mm³ specimen and I_i is the moment of inertia of the specimen cross section in relation to the neutral axis. The calculated MOE values are presented in Table 2 together with the values obtained from the bending tests.

Table 2 Calculated (based on dynamic MOE measurements) and actual (static bending test) MOE values. Note that $E_{flat,calc}$ has no influence from shear deformation.

Specimen	$E_{flat,stat}$	$E_{flat,calc}$	$\frac{E_{flat,calc}}{E_{flat,test}}$	$E_{edge,test}$	$E_{edge,calc}$	$\frac{E_{edge,calc}}{E_{edge,test}}$	$\frac{E_{edge,calc}}{E_{flat,calc}}$
	(N/mm ²)	(N/mm ²)		(N/mm ²)	(N/mm ²)		
45 x 170 mm²							
A	11700	13200	1.13	13650	13650	1.00	1.03
B	12500	14700	1.18	14750	15750	1.07	1.07
C	11850	14000	1.18	14850	15200	1.02	1.09
D	14450	16300	1.13	16050	17100	1.07	1.05
E	14950	17000	1.14	19950	18950	0.95	1.11
F	12400	14100	1.14	16300	15500	0.95	1.10
G	11200	12550	1.12	12700	12650	1.00	1.01
H	12250	13850	1.13	14050	14350	1.02	1.04
<i>Mean</i>	<i>12650</i>	<i>14450</i>	<i>1.14</i>	<i>15300</i>	<i>15400</i>	<i>1.01</i>	<i>1.06</i>
67 x 195 mm²							
I	10600	13200	1.25	13950	14150	1.01	1.07
J	8800	10650	1.21	11200	11450	1.02	1.08
K	12550	15700	1.25	17650	16850	0.95	1.07
L	13200	17050	1.29	21000	18650	0.89	1.09
M	12700	16900	1.33	18750	18700	1.00	1.11
<i>Mean</i>	<i>11550</i>	<i>14700</i>	<i>1.27</i>	<i>16500</i>	<i>15950</i>	<i>0.97</i>	<i>1.09</i>

The following conclusions are drawn:

- The calculated and actual edgewise MOE is, as can be expected, almost the same, as there is no shear deformation to be considered. The correlation between calculated and actual values is high, see Figure 7 and 8. For the flatwise MOE it is extremely high. This means that the calculation based on the dynamic MOE gives an accurate estimate of both the edgewise MOE determined according to EN 408 and the flatwise MOE without shear deformation influence.

- For the 45 x 170 mm² timber the calculated edgewise MOE is 6 % higher than the calculated flatwise MOE (without shear deformation influence). The corresponding value for the 67 x 195 mm² timber is 9 %. These differences are close to what Burger and Glos (1995) found and can be explained by the MOE variation over the timber cross section as exemplified in Figure 4, 5 and 6.
- The differences between calculated and actual flatwise MOE are 14 and 27 %, respectively, for the two dimensions. These differences cannot be explained entirely by the shear deformations, which, if an E/G ratio of 30 is assumed would account for 9 and 20 % respectively (Ehlbeck (1967) obtained mean E/G ratios of 22.5 to 32.5 using European coniferous timber.). The remainder is possibly due to compression perpendicular to grain at the supports.

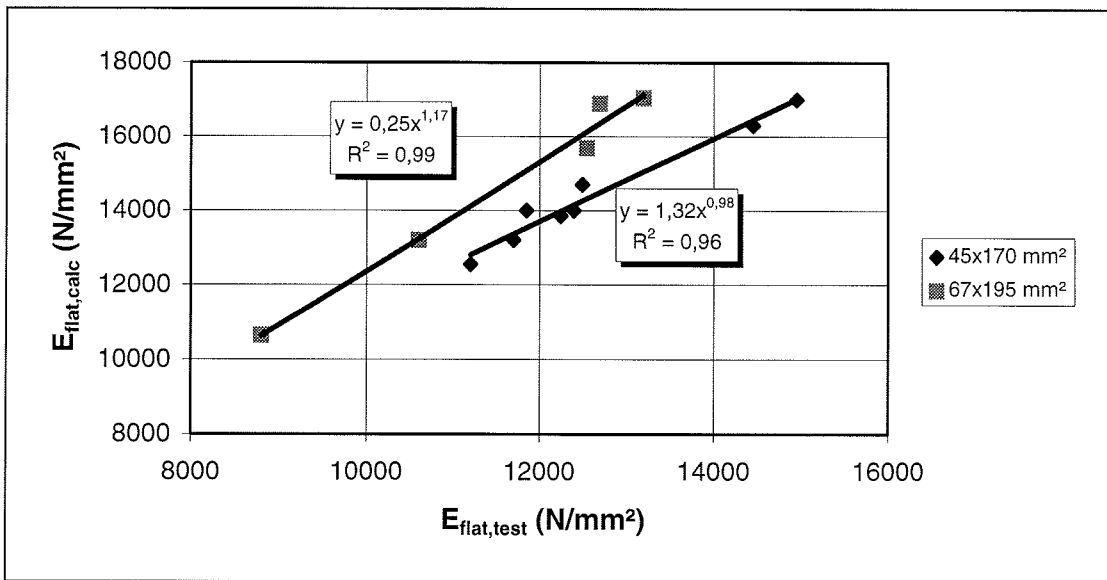


Figure 7 Relation between calculated flatwise MOE and tested flatwise three point loading MOE.

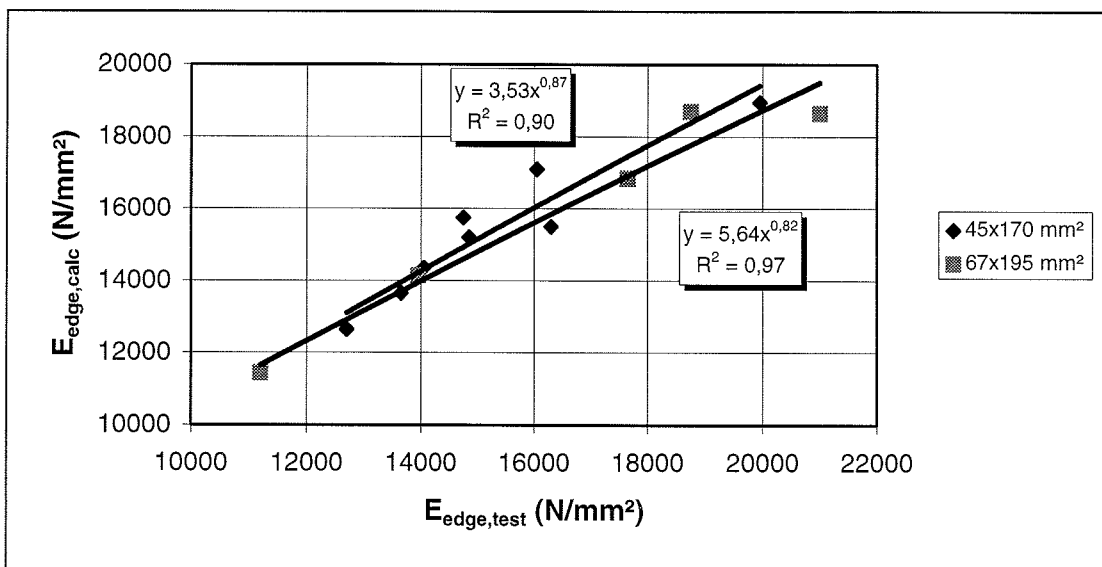


Figure 8 Relation between calculated and EN 408 edgewise MOE.

6 Conclusions

- The difference between edgewise MOE according to EN 408 and flatwise MOE determined in a three point bending test was 22 and 49 % respectively for the 45x170 and 67x195 mm³ timber, which was greater than obtained in other investigations.
- The difference between edgewise MOE and flatwise three point bending MOE seemed to increase with increasing edgewise MOE and to decrease with increasing knot area ratio.
- Density and MOE varied considerably over the timber cross section. In most cases both the density and the MOE had a minimum close to the pith and then increased in the radial direction.
- Edgewise and flatwise MOE based on dynamic MOE measurements were highly correlated with the static bending MOE. In addition, the calculated edgewise MOE was almost on the same level as the EN 408 edgewise MOE.
- The shear deformations and the MOE variation over the timber cross section explained a major part of the difference between the EN 408 edgewise MOE and the flatwise three point bending MOE.

7 Symbols

c_L	ultrasonic pulse velocity
E_{dyn}	modulus of elasticity based on ultrasonic pulse velocity measurements
$E_{edge,calc}$	edgewise modulus of elasticity calculated based on E_{dyn}
$E_{edge,test}$	edgewise modulus of elasticity determined according to EN 408
$E_{flat,calc}$	flatwise modulus of elasticity calculated based on E_{dyn}
$E_{flat,test}$	flatwise modulus of elasticity determined in three point bending test with a span of 900 mm
E_i	= $E_{t,static}$ for a 9x9x300 mm ³ specimen
$E_{t,static}$	modulus of elasticity obtained in static tension test
$\rho_{0,u}$	density on the basis of the wood mass at 0% and the volume at u m.c.
KAR	Knot Area Ratio
I	moment of inertia
G	shear modulus

8 Literature

Boström, L.(1994) Machine Strength Grading. Comparison of Four Different Systems. SP Report 1994:49, Swedish National Testing and Research Institute, Borås, Sweden.

- Burger N. and Glos P.(1995) Relationship of Moduli of Elasticity in Bending of Solid Timber. CIB. W18/28-5-2, Copenhagen/Denmark.
- Ehlbeck, J. (1967) Durchbiegung und Spannungen von Biegeträger aus Holz unter Berücksichtigung der Schubverformung. Disseration, Lehrstuhl für Ingenieurbau und Baukonstruktion, TH Karlsruhe.
- Johansson, C.-J. (1992) Stress grading of Swedish and German Timber. A comparison of machine stress grading and three visual grading systems. SP Report 1992:23, Swedish National Testing and Research Institute, Borås, Sweden
- Wormuth E. (1992) Untersuchungen des Verhältnisses von flachkant zu hochkant ermitteltem Elastizitätsmodul von Schnittholz zur Verbesserung der maschinellen Festigkeitssortierung, Universität Hamburg, Fachbereich Biologie.

INTERNATIONAL COUNCIL FOR BUILDING RESEARCH STUDIES AND DOCUMENTATION

WORKING COMMISSION W18 - TIMBER STRUCTURES

**LOAD DURATION EFFECT ON STRUCTURAL BEAMS UNDER VARYING
CLIMATE INFLUENCE OF SIZE AND SHAPE**

by

P Galimard

P Morlier

Laboratoire Rhéologie du Bois de Bordeaux

France

MEETING TWENTY - NINE

BORDEAUX

FRANCE

AUGUST 1996

LOAD DURATION EFFECT ON STRUCTURAL BEAMS UNDER VARYING CLIMATE INFLUENCE OF SIZE AND SHAPE

Philippe GALIMARD¹
Pierre MORLIER²

ABSTRACT

The Duration Of Load effect has been of increasing interest for either the understanding of wood or wood products in long term behaviour and for the determination of safety factors for engineering purposes. Many kinds of testing, mainly in bending, have been made but the large amount of configurations have always been reduced to few moisture contents and load histories. However, it is still not easy to compare all the results for the protocol of testing and presenting the results is not yet a standard [BARRETT, 1996].

Different attempts of evaluating the stress level have been done and their accuracy depends on what is wanted to be shown. The methods are applied on 2 meter LVL beams subjected to bending in natural environment. Fourty beams are stepwise loaded in an open shed in the Laboratoire de Rhéologie du Bois de Bordeaux in order to have a failure of 80% of the beams within two months. The step levels are from 50% to 90% of the average short term strength. Two beam depths (100 & 150 mm) are tested. The beams can be sealed or unsealed. The curvature, the time-to-failure and the climatic conditions are monitored.

A rank method is used to show the main trends of the duration of load results: the time-to-failure are not affected by daily or short time variations of hygrothermal conditions, but by the two month mean variation of the moisture content.

The long term strength reductions are evaluated and finally compared to standard (EC5) ones. This work is a part of a European AIR-Project which has been set to have experimental data on DOL of LVL and glulam straight, notched and curved sized beams.

Key-words: Duration Of Load Representation - LVL beams - Stepwise loading in bending -

INTRODUCTION

For all building materials, it can be said that failure occurs when some criterion reaches a limit value; for wood mechanics we know problems when the criterion seems

- to be the stress :

longitudinal stress for straight beams in bending,

transverse stress for curved beams in bending,

- or to be a fracture mechanics criterion (stress intensity factor K, strain energy release G, rice

¹ Philippe GALIMARD *Lecturer* - Laboratoire Rhéologie du Bois de Bordeaux tel:(33) 57.97.91.02
Domaine de l'Hermitage
33610 CESTAS GAZINET - FRANCE

email galimard@lrbb3.pierroton.inra.fr

² Pierre MORLIER *Professor* - Laboratoire Rhéologie du Bois de Bordeaux tel:(33) 57.97.91.08
Coordinator of AIR Project CT94-1057 email morlier@lrbb3.pierroton.inra.fr

integral J) : notched beams are a good example.

The stress or K (or G or J) depends on the mechanical and/or climatic history of the load and on the history of the material itself (through constitutive laws), the strength or K_{JC} depends on the current conditions of temperature and moisture content but also on the damage accumulated in the material, including ageing, i.e. once more on its history, probably on the scale. For simplification, the long term strength of timber beam depends on :

- present parameter size, shape, temperature, relative humidity, rate of changing of this two parameters,
- history depending parameters which are two types
 - parameters that the present knowledge masters and the modeling of which is possible (moisture transfert, rheological behavior),
 - hidden parameters like damage.

The present parameters are (are not) standard ones (constant temperature of 20°C, constant relative humidity of 65%, "loading rate" chosen for a failure occurring in 5 minutes) ; if they are not, it is possible to write, regardless the partial security coefficient :

$$\begin{aligned} \text{strength} &= \text{standard strength (includes scale effect)} \\ &\quad \times \text{stress distribution effect (from modeling)} \\ &\quad \times \text{damage parameters (a priori unknown)} \\ &= k_{mod} \times \text{standard strength (according to EUROCODE 5)} \end{aligned}$$

I - A EUROPEAN PROJECT : AIR CT94-1057

In order to find answers to different unsolved questions, a so called "duration of load effect on different sized timber beams" was accepted by European Community and has been running for 18 months at the time being.

Shape effect - three different problems are studied :

- A - bending of straight beams,
- B - bending of notched beams,
- C - bending of curved beams, including tension perpendicular to grain tests.

Material and size effect - to reduce the variability it was decided to limit investigations to LVL and glulam which are much more homogeneous than solid wood ; it was estimated that samples of unless 10 specimens were statistically representative. Transverse sizes of beams are between

- 45 x 100 and 75 x 300 for A (LVL)
- 45 x 100 and 140 x 445 for A (glulam)
- 45 x 100 and 75 x 100 for B (LVL)
- 50 x 100 and 90 x 300 for B (glulam)
- 90 x 600 and 140 x 600 for C (glulam).

For testing such beams we were obliged to build (or rebuild) a quantity of rigs in each laboratoty (see Annex I).

Various climatic history are (to be) used :

- *constant climate* or constant mean moisture content for sealed specimens tested in the laboratory or outdoor,
- a *cyclic relative humidity*, the period of which is one month, between 55% and 90% R.H. (see Annex II)
- *natural climate* : experiments are performed outdoor under shelter, in Bordeaux, Lund or Stuttgart.

Two different loading histories

- creep experiments with constant load capable of giving 50% of failure in a sample within 3 months
- slow step by step loading : the experiment begins at a predefined stress which is maintained for a month, then the load is increased in a step wise manner with a new period of equal duration for the unbroken specimens, ... the experiments are stopped when more than 50% of specimens have failed.

The experimental campaign has the role to obtain a significative level of failure at 3 months for different sized beams in each problem and different climates :

- a 3 months period corresponds to a typical seasonal climate in Bordeaux for instance (see Annex II) ;
- on a logarithmic timer scale 3 months is just between 5 minutes (standard tests) and 10 years.

II - LOAD DURATION REPRESENTATION

MADSEN [1994] has shown that the increase of moisture content reduces the long term strength of clear wood. The higher is the grade of the wood, the greater is the influence of the duration effect. Therefore, we can imagine the same influence on homogenized wood as glulam or L.V.L..

However, it is important to detail and try to standardize the variables used

- to compare Duration Of Load results,
- to present the results and to study the sensitivity of some parameters,
- to assess mathematical, phenomenological or physical models and
- to assess the strength reduction factors used in the Eurocode 5 for medium and long term.

Many reviews on previous studies have already been made. They enlight the large amount of testing configurations, although, for experimental problems, the range of the studies is very narrow compared to in-service climatic and loading conditions.

We present in the references the most recent studies on Duration of Load. The topics are:

- *surveys*
- *straight beams* : DOL experiments on structural lumber and LVL beams.
- *notched beams*
- *curved beams and tension perpendicular to grain*,
- *numerical analysis*,
- *methodology*.

II-1 - Definition of the Variables

1-1 Loading history

The origin of the time is simple as far as the applied stress is constant; all these kinds of results can be compared. However, as the stress history is variable, an equivalence must be found. In stepwise loading, the stress increase for each step has to be large enough to assume there is no damage accumulation before the last step [HOFFMEYER 1995], unless no effective damage measurement is available. Therefore, in stepwise loading analysis, the origin of the time could be stated as the beginning of the last step, when the failure occurred.

1-2 Stress Level

For high grade lumber or homogeneous wood product, the Modulus Of Rupture may not be estimated for each long term tested beam from its MOE or from its side beam. As the standard deviation of the distributions is quite small, we can assume that the mean value is enough to design the stress level.

LEBATTEUX [1995] has demonstrated that this estimation (and the use of MOE) does not give as good results as the ranking method proposed by MADSEN in 1973. This method is assuming that, in a sample, the failure rank of a beam would be the same in a short term test as in a long term test. Therefore, the short term strength, through its distribution, can be estimated for every beams.

1-3 Strength reduction factors

They are deduced from a straight line joining the short term test point. The straight line can be drawn using:

- an interpolation between all the datas, or
- the point defined by the time and stress level of the 50% failure according to HOFFMEYER.

As the k_{mod} factor of the Eurocode 5 is a coefficient applied the characteristic value, we can think to draw the reduction line of the 5-percentile. Unfortunately, as it can be seen on figure 1, the tails of the distributions are not as stable as the mean values. Thus the mean value evolution is conservative in regard with the 5-percentile when the moisture content is increasing.

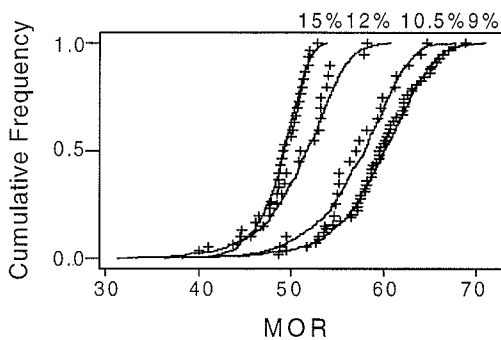


Figure 1 - Strength distribution of LVL structural beams (2mx100mmx45mm) at four moisture contents (HOFFMEYER 12% & 10.5%, LEBATTEUX 15% & 9%)

When the moisture content does not remain constant throughout the test, it must be considered that the short term strength distributions are not equal for every moisture contents. The long term tests should be referred to the short term distribution corresponding to the moisture content in the beam when the failure occurs. In a first analysis, the mean value of the moisture content in the cross section is considered, rather than the moisture at the highest stressed point.

III - D.O.L. EFFECT ON STRAIGHT STRUCTURAL BEAMS

The results, presented below, come from the experimental part of the AIR Project carried out in Bordeaux on straight LVL beams in outdoor conditions.

Two-meter span LVL straight beams were loaded in four point bending at the same time, for a minimum period of two and a half months. Half of the beams are coated with a moisture barrier paint.

- 20 small beams that have a cross section of 45x100 mm²
- 20 large beams that have a cross section of 45x150 mm²

III-1 - Short Term Characteristics

Two samples of sixty LVL beams have been previously tested to characterize the long term beams at two moisture contents: 9% and 15%. Thus, ten beams have been tested up to failure at the beginning of each long term test season. See Table 1.

	Section mm ²	MOR MPa	Nb	CV %	MOE GPa	Nb	CV %	MC %
Spring 95	45x100	50,6	6	6	11,6	32	3	14
	45x150	56,8	4	7	12,0	24	7	14
Summer 95	45x100	61,9	6	10	13,1	32	4	11
	45x150	58,2	4	9	13,4	24	7	11
Autumn 95	45x100	53,3	6	6	12,8	32	4	13
	45x150	52,1	4	7	11,4	24	5	13
Winter 95	45x100	45,7	6	5	12,4	32	5	17
	45x150	47,0	4	5	12,1	24	4	16
February 95	45x100	60,0	30	7	12,8	30	4	9
	45x150	59,7	30	8	12,5	30	5	9
February 96	45x100	49,0	30	6	12,3	30	7	15
	45x150	50,3	30	6	12,7	30	7	15

Table 1 - Short term mechanical characteristics

Rather than the standard deviation, Table 1 includes the coefficient of variation (CV) of the MOE and MOR.

The normal distribution (as well as the Weibull distribution) fitted well with the dry beam modulus of elasticity (MOE) and modulus of rupture (MOR) data (fig. 2&3).

The Weibull distribution gave slightly better results for the small wet beams (fig. 4). No size effect could be statistically proved.

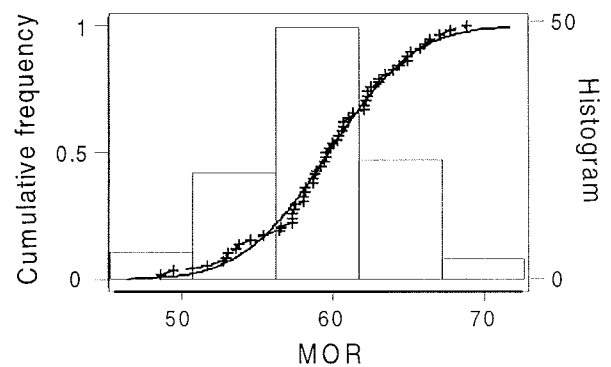


Figure 2 - Normal strength distribution for small and large beams at MC=9%

These distributions (figures 2 and 3) have been used for evaluating the stress level applied to long term tested beams, as is explained below. However, neither the side beam, nor the MOE or the density were good estimators of the short term strength of each. The coefficients of correlation MOE/MOR are 0.02 and 0.28 respectively for the small and the large cross sections.

The mechanical characteristics of L.V.L., as a homogenous wood product, have high characteristic values (5th percentile) because of their small variations. There was no evidence of a size effect between the small and the large beams.

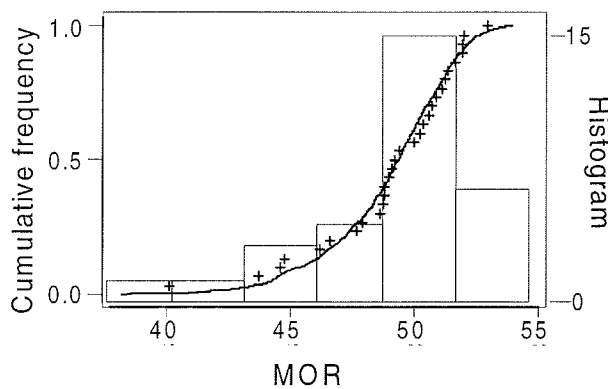


Figure 3 - Weibull strength distribution of the large beams (45x100 mm²) at MC=15%.

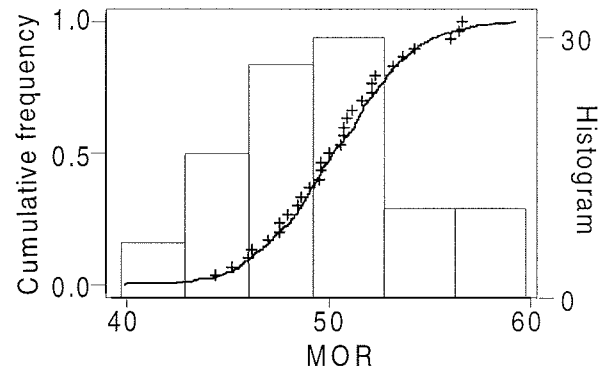


Figure 4 - Normal strength distribution of the small beams (45x150 mm²) at MC=15%.

III-2 - Influence of Moisture Content Variations

As explained above, we have taken the moisture content at the beginning of the first step as the reference because of the lack of short strength distributions at every needed moisture content. The trends of results have been only studied with a linear interpolation of the long term data, without any point corresponding to short term (WOSTR). *This representation is accurate to study the trends of the results.*

As with deflection, the main factor is the trend of the average moisture content. There was no difference between coated and uncoated beams in summer (Fig 5). In autumn, as the average moisture content increases, the uncoated beams failed earlier than the coated ones (Fig 6). Similar results were obtained in spring: the uncoated beams had greater times to failure as the moisture content decreased.

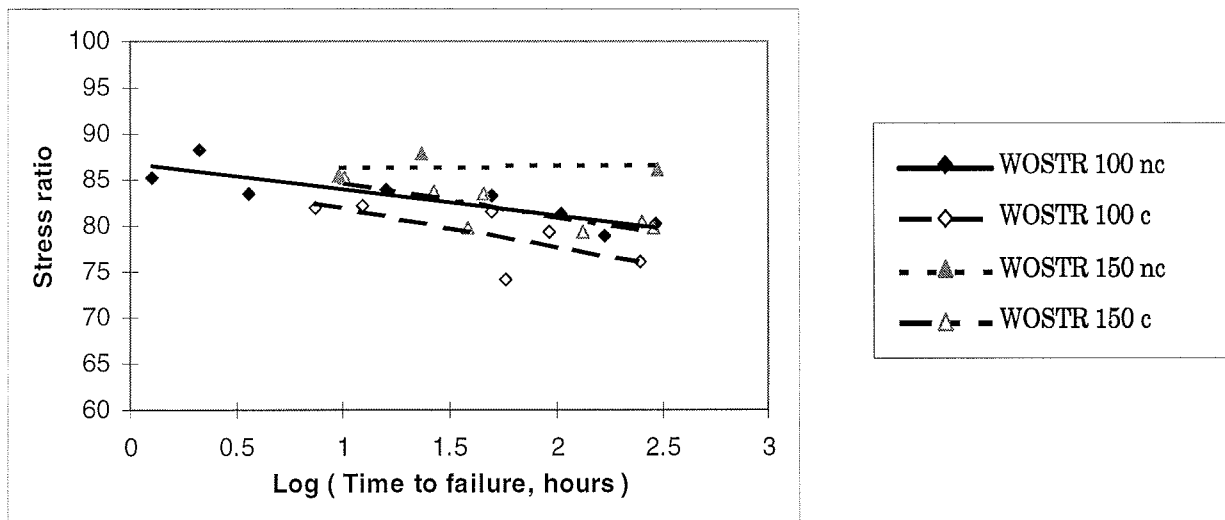


Figure 5 - Summer time-to-failure results.

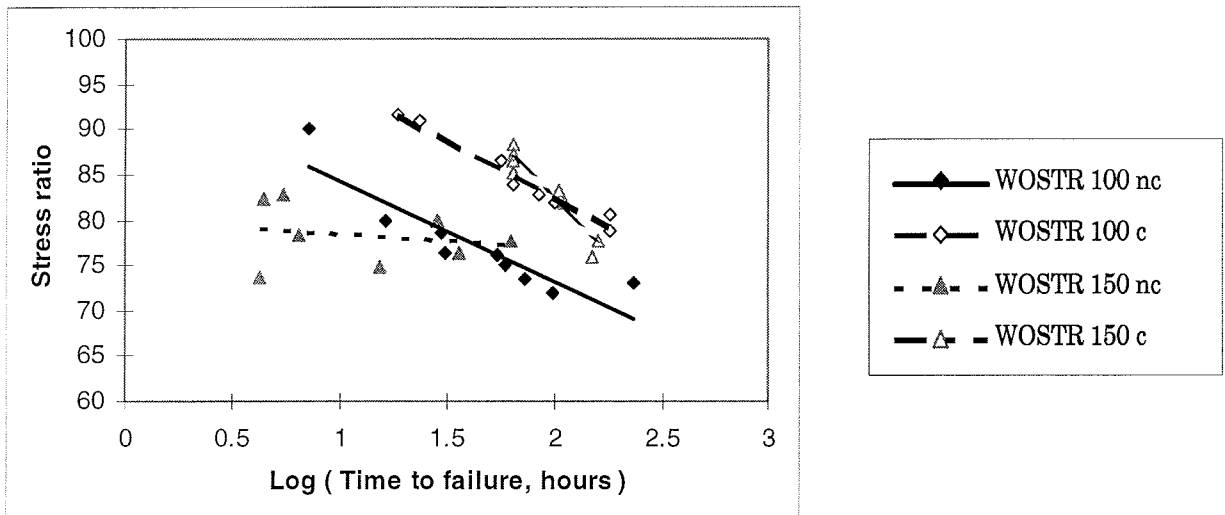


Figure 6 - Autumn time-to-failure results.

The study of short term hygrothermal variations have not emphasized any influence on the DOL results. The summer results (Fig 5) were very similar, whether the beams are coated or not. Therefore, there was no particular time at which the occurrence of failure was increased. Thus, the appearance of the final failure, characterized by a fast increasing of strain rate before failure, cannot be linked to the short term MC variations. Fig 7 shows, for a high, slightly decreasing moisture content, the same kind of results.

Comparing Fig 5, 6 and 7, it appears that the material was sensitive to the moisture content and its long term variation. This result is in accordance with part of previous studies [MADSEN, 1992], which have shown that the higher the grade of timber, the greater the effect of moisture on long term behaviour.

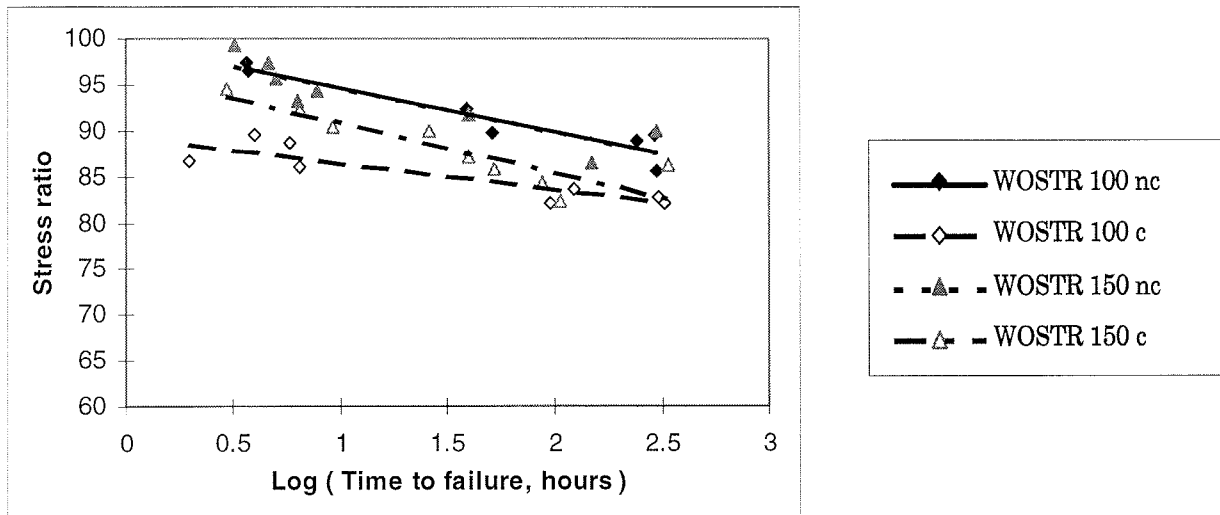


Figure 7 - Winter time-to-failure results.

The linear interpolation gave good results on these data: the regression coefficient was
 $0.65 < R^2 < 0.82$

Size effect

The diffusion of moisture inside the different cross sections may have some influence. In the summer results (Fig 5) there was no evidence of size effect: the results of the small and large sections are the same. However, autumn and winter climate seem to have more influence on the large beams. It can be noticed that the linear extrapolation to short term strength (5 minutes) had given stress levels in a range of 90% to 120% for the small section but in a much wider range for the large section. This representation cannot be used for the estimation of DOL strength factors.

III-3 - Ten Year Strength Reductions due to Load Duration

The following curves only considered the duration of load effect: the ranking method was applied, using the short term strength distributions in the moisture content of the beginning of the season. Fig 8, 9 and 10 are showing:

- the datas of the small coated and uncoated sections,
- the linear interpolations between the ranked datas but including the short term point (With Short Term Reference) at the beginning of the loading,
- the straight line given by the short and the average failed beam (beam #50%) according to HOFFMEYERS' presentation. #50% beam has been chosen when it has not failed during a reloading. In this case, #50% beam would be the last failed beam of the previous.

The slopes of the lines were significantly different from the presentation of figures 5, 6 & 7. It can be seen on figure 9 where the without short term reference (WOSTR) line of the uncoated beams remains. It seems that the time to failure was affected by the previous steps.

The D.O.L. reduction factors have been extrapolated to ten years from the two lines and compared on table 2.

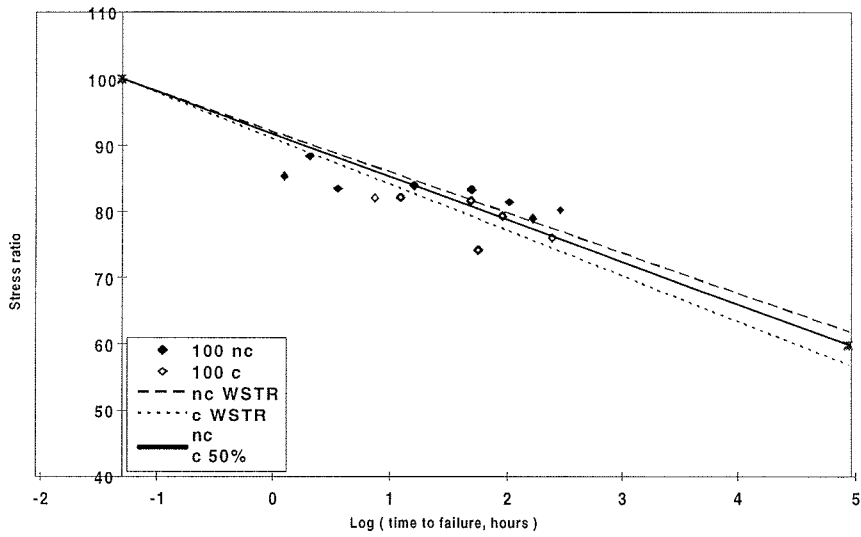


Figure 8 - Summer strength reduction.

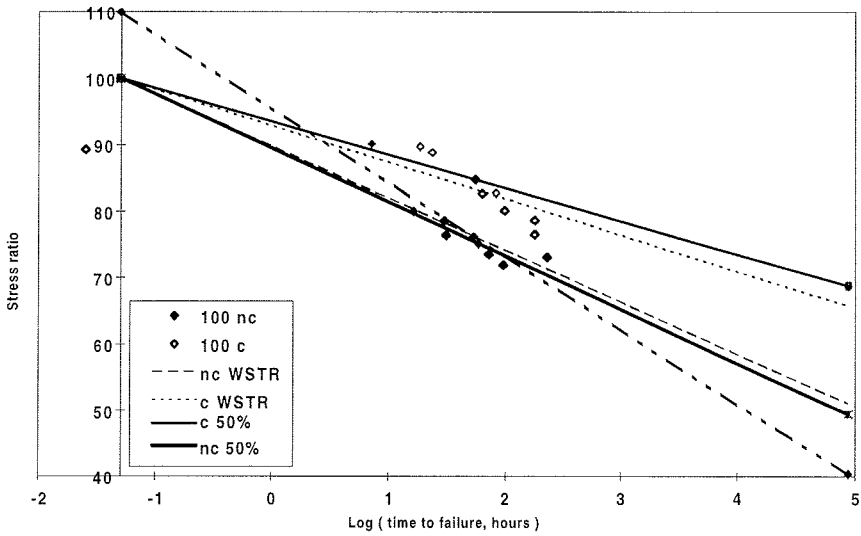


Figure 9 - Autumn strength reduction.

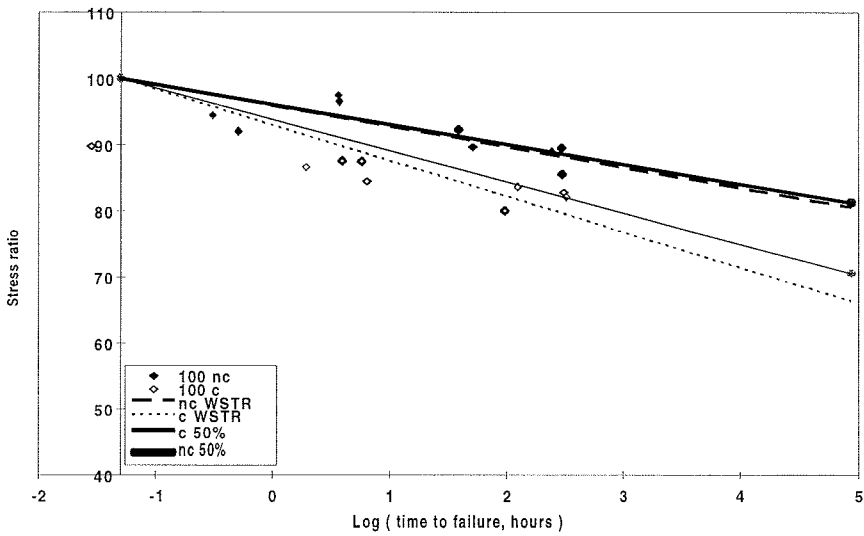


Figure 10 - Winter strength reduction.

	autumn		spring		summer		autumn		winter	
	MC= 12 - 15% ref. MC = 15%		MC= 14 - 11% ref. MC = 15%		MC = 11% ref. MC = 9%		MC = 12 - 15% ref. MC = 9%		MC = 16 - 14% ref. MC = 15%	
	rank	50%	rank	50%	rank	50%	rank	50%	rank	50%
100 nc	81	79			62	60	51	49	81	81
100 c			65	69	57	59	66	69	66	71
150 nc	80	73	96	100	70	71	42	37	83	98
150 c			84	80	64	65	67	68	73	77

Table 2 - D.O.L. strength reduction depending on the short term reference and on the interpolation method: with all the whole ranked datas or with #50% beam.

- There is little difference between the two ways of drawing the strength reduction line. As it is much more easy, the beam #50% method from HOFFMEYER can be kept.
- The strength reduction is very effected by the Moisture Content reference. It is a real problem as the Moisture Content varies.
- The strength reduction is lower for high Moisture Content. It is opposite with the previous observations on the same datas. However, it is confirmed by other studies [HOFFMEYER, 1995, MADSEN, 1992].
- There is no evidence of size effect on the D.O.L. strength reduction factors. The sizes may not be different enough to enlight an effect of the moisture gradient.

III-4 - Comparison to EC5 Coefficients k_{mod} .

The k_{mod} coefficient from the Eurocode 5 depends on the moisture content in service and on the duration of the loads. It is deduced from the above D.O.L. reduction factors and from the moisture content. The three service classes of the Eurocode 5 can be found in the moisture conditions of the seasons. See Annex II.

- Service Class I (RH<65%)
summer coated and non coated beams / autumn coated beams
- Service Class II (RH<85%)
autumn non coated beams
- Service Class III (RH>85%)
winter coated and non coated beams

To design the k_{mod} factors for ten year loads, we must adjust the strength reductions according to the moisture content. We make the assumption that the short term strength at MC=9% is the good reference strength. Therefore, the reduction coefficients of Class I & II remain unchanged. The short term reference winter moisture content was MC=15% which mean strength value is 50 MPa. The strength reduction has to be affected by (Table 4) the following coefficient : $c = 50/60$.

**Table 4 - Strength reduction due to moisture and Duration Of Load/
 k_{mod} EC5.**

Service Class	I	II	III
k_{mod} tests	62%	51%	61%
k_{mod} EC5	60%	60%	40%

For service class I, the results are the same. The EC5 seems optimistic for service class II. The results for service class III show that the EC5 is too conservative. These kind of results have been previously enlightened by HOFFMEYER [1995].

IV - LOAD DURATION EFFECT ON NOTCHED BEAMS

In a second task devoted to the L.R.B.B., notched beams are studied in short term and stepwise long term tests (see Annex I).

Beam size : 1mx45mmx100mm

IV-1 Short term results

Half of beams have the notch sealed. The short term experiments have shown that the increase of moisture content makes the load failure rise, as previously noticed in other studies.

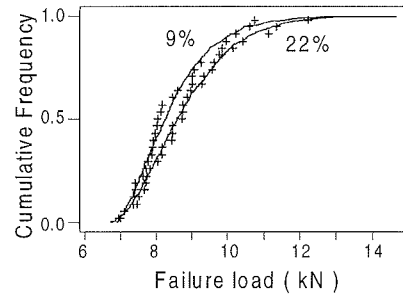


Figure 11 - Failure load distributions of notched beams at MC = 9 & 22 %

IV-2 Load duration trends

The long term tests have been carried out in the shelter used for the straight beams (see Annex D). The moisture content of short term distribution reference, used for the four seasons, is 9%. The linear interpolations, presented on the figures below, were determined without any short term reference. That does not make any great difference, as it does for straight beams. It can be seen on the figures 12, 13, 14 & 15 that the strength reduction effect is much smaller for the notched beams than for the straight beams. For example, the autumn results give a long term strength coefficient of 95%. The difference between sealed and unsealed notches are still to be explained.

It is obvious that extra analysis has to be made e.g. on the influence of the moisture content reference, on #50 beam, or on the EC5 k_{mod} factor.

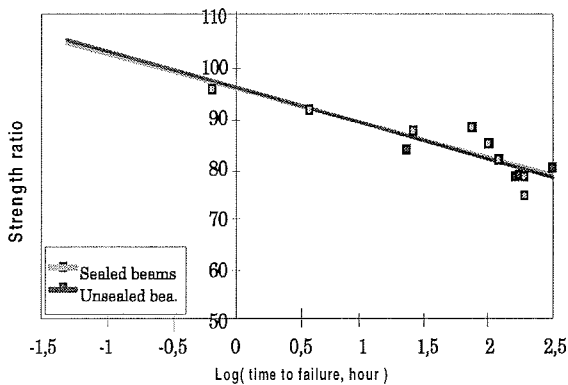


Figure 12 - Long term strength reductions (rank method) for notched beams in spring.

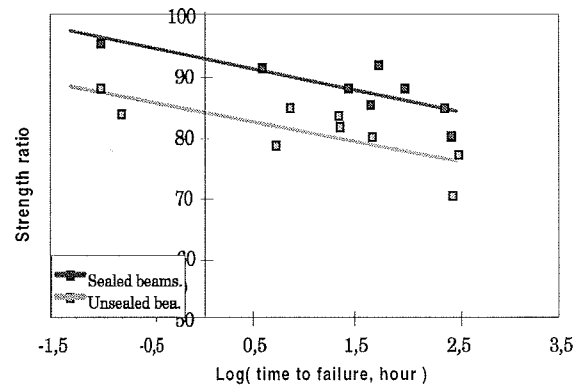


Figure 13 - Long term strength reductions (rank method) for notched beams in summer.

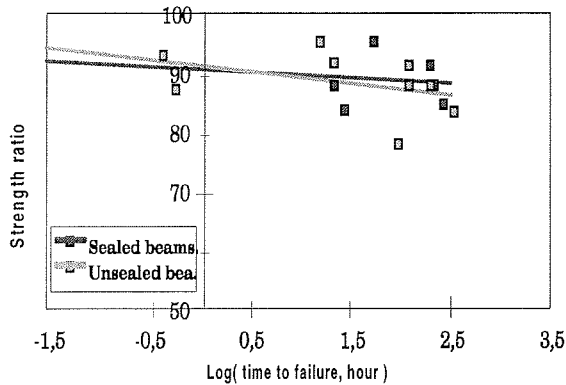


Figure 14 - Long term strength reductions (rank method) for notched beams in autumn.

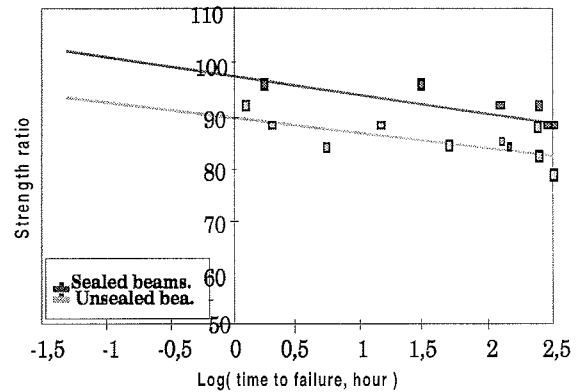


Figure 15 - Long term strength reductions (rank method) for notched beams in winter.

CONCLUSION

- We have shown, on straight LVL beams, that opposite conclusions can appear from the same datas depending on the way of presenting the results.
- However, the influence of the general changing of the climate was more important than the absolute moisture content.
- The strength reduction estimation has roughly given the same results from the two tested methods; so #50% beam can be accurately used.
- The short term strength has been influencing the results in a large scale, because of the moisture content reference and of the definition of the stress level.
- The duration of load effect is fairly depending on the tested shape: it is more important on straight beams than on notched beams.
- The EC5 k_{mod} factor, for LVL beams, seems to be optimistic for EC5 Service Class 2 and conservative for EC5 Service Class 3.

A protocol of Duration Of Load test and analysis is still needed [BARRETT, 1996] because of the numerous testing configurations, the variability of the result analysis, the influence of the analysis on the conclusions that can be contradictory.

REFERENCES

Surveys

J. D. BARRETT

Duration of Load - The past, present and future
COST 508 Final Conference, Stuttgart, 1996

P. MORLIER

Introduction of Air project : Duration of load effect
on different sized timber beams
COST 508 4th Workshop, Espoo, 1994

P. MORLIER, G. VALENTIN, T. TORATTI

Review of the theories on long term strength and
time to failure
COST 508 4th Workshop, Espoo, 1994

R.C. TANG

Overview of duration of load research on lumber and
wood composite panels in North America
COST 508 4th Workshop, Espoo, 1994

T. TORATTI

Load duration of timber in a varying climate
COST 508 3d Workshop, Limerick, 1993

G. VALENTIN, P.J. GUSTAFSSON, L.
BOSTROM, A. RANTA-MAUNUS,
S. GOWDA

Application of fracture mechanics to timber
structures, a RILEM state-of-the-art,
VTT Report 1262, 1991

Straight beams

P. HOFFMEYER

Failure of wood as influenced by moisture and load duration

CEC Contract MA1B-0042DK, final report, 1990

P. HOFFMEYER, M. VESTERGAARD

Duration of load properties of LVL made of sitka spruce

COST 508 5th Workshop, Watford UK, 1995

M. LEBATTEUX, P. GALIMARD

Duration of load in LVL : interpretation of step loading truncated creep experiments in variable environment

European Workshop on application of Statistics and Probabilities in Wood Mechanics, Bordeaux, 1996

T. TORATTI

Short and long term bending experiments on LVL

COST 508 4th Workshop, Espoo, 1994

Notched beams

P.J. GUSTAFSSON

A study of strength of notched beams

CIB W 18 A meeting 21, Vancouver, 1988

S.K. JENSEN, P. HOFFMEYER

Mechano-sorptive behavior of notched beams in bending

COST 508 final conference, Stuttgart, 1996

C. JOURDAIN, P. RACOIS, G. VALENTIN

Delayed fracture of spruce notched beams

COST 508 4th Workshop, Espoo, 1994

Curved beams and tension perpendicular to grain

G. DILL-LANGER, S. AICHER, H.W. REINHARDT

Creep of glulam in tension perpendicular to grain at 20°C 65%RH and at sheltered outdoor climate conditions

COST 508 final conference, Stuttgart, 1996

S. GOWDA, A. RANTA-MAUNUS

Curved cambered glulam beam

part I - short term load tests, VTT Res. #150, 1993

part II - long term load tests, VTT Res. #171, 1994

A. RANTA-MAUNUS

Long term strength of curved glulam beams at cyclically varying climate

COST 508 4th Workshop, Espoo, 1994

Numerical analysis

J.D. BARRETT, R.O. FOSCHI

Duration of load and probability of failure in wood part I : modelling creep rupture

Canadian J. of Civ. Eng. 5(4), 1978

A. HANHIJARVI, A. RANTA-MAUNUS

Computational analysis of factors affecting the bending DOL behavior of LVL

COST 508 5th Workshop, Watford UK, 1995

J. LU, R.H. LEICESTER

Deformation and strength loss due to mechano-sorptive effects

Pacific Timber Engineering Conference, Gold Coast-Australia, 1994

L. NIELSEN

Wood as a cracked viscoelastic material

part I : theory and applications

Copenhagen University, Technical Report 153, 1985

A. RANTA-MAUNUS

Impact of mechano-sorptive creep to the long term strength of timber

Holz als Roh und Werkstoff, 48, 1990

A. RANTA-MAUNUS

The influence of changing state of stress caused by mechano-sorptive creep on the duration of load effect

COST 508 final conference, Stuttgart, 1996

T. TORATTI

Creep of timber beams in a variable environment

Doctoral dissertation, Helsinki University of Technology 1992

Methodology

B. MADSEN

Structural behavior of timber, Chapter VI : duration of load

Timber Engineering LTD, 1992

P. VIGNOLLES

Effets de la vitesse et de la durée de charge sur la résistance en flexion du pin maritime

Thèse n°413 Université Bordeaux I, 1989

M. LEBATTEUX, Ph. GALIMARD

Duration of Load of structural L.V.L. Beams in Natural Environment

International Wood Engineering Conference, New-Orleans, 31 October 1996.

APPENDIX I List of participants to the european Project: AIR 2-CT94-1057

LAB1	LRBB - France.	P. MORLIER (Coord.) & G. VALENTIN Laboratoire de Rhéologie du Bois de Bordeaux
LAB2	VTT - Finland.	A. RANTA-MAUNUS Technical Research Centre of Finland Building Technology
LAB3	LBM - Denmark.	P. HOFFMEYER Laboratory of Building Materials Technical University of Denmark
LAB4	FMPA BW - Germany.	S. AICHER Forschungs und materialprufungs anstalt Baden Wurttemberg
LAB5	DSM LUND - Sweden.	P. J. GUSTAFSSON Division of Structural Mechanics Lund Institute of Technology
LAB6	CEBTP - France.	J. M. QUILLACQ Centre Expérimental de Recherches et d'Etudes du Bâtiment et des Travaux Publics

Comments on the photographs (next pages)

Photo 2 : 40 rigs (airjack - straight beams in LAB1) - external

Photo 3 : 18 rigs (dead load - notched beams in LAB1) - external

Photo 5 : 8 rigs (hydraulicjacks - curved beams in LAB2) - climatic room

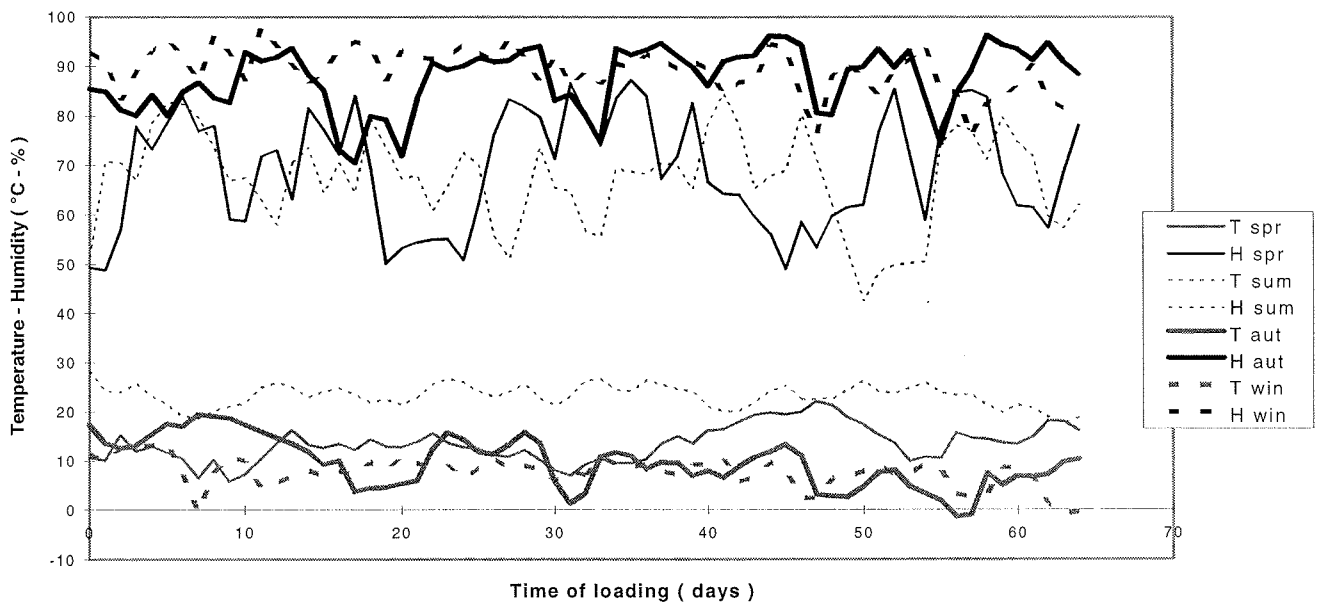
Photo 6 : 10 rigs (hydraulicjacks - straigh beams in LAB2) - climatic room

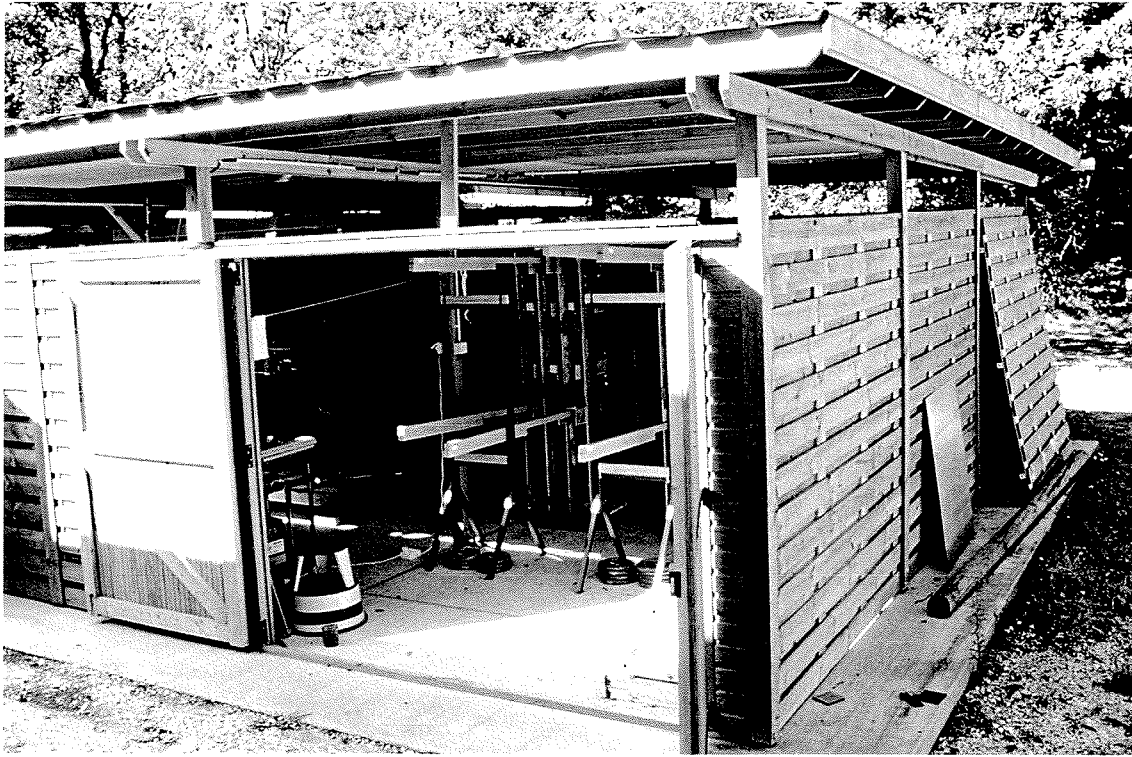
Photo 8 : 60 rigs (dead load - notched beams in LAB5) - external

These rigs were designed in LAB3 where 45 are working in a climatic room

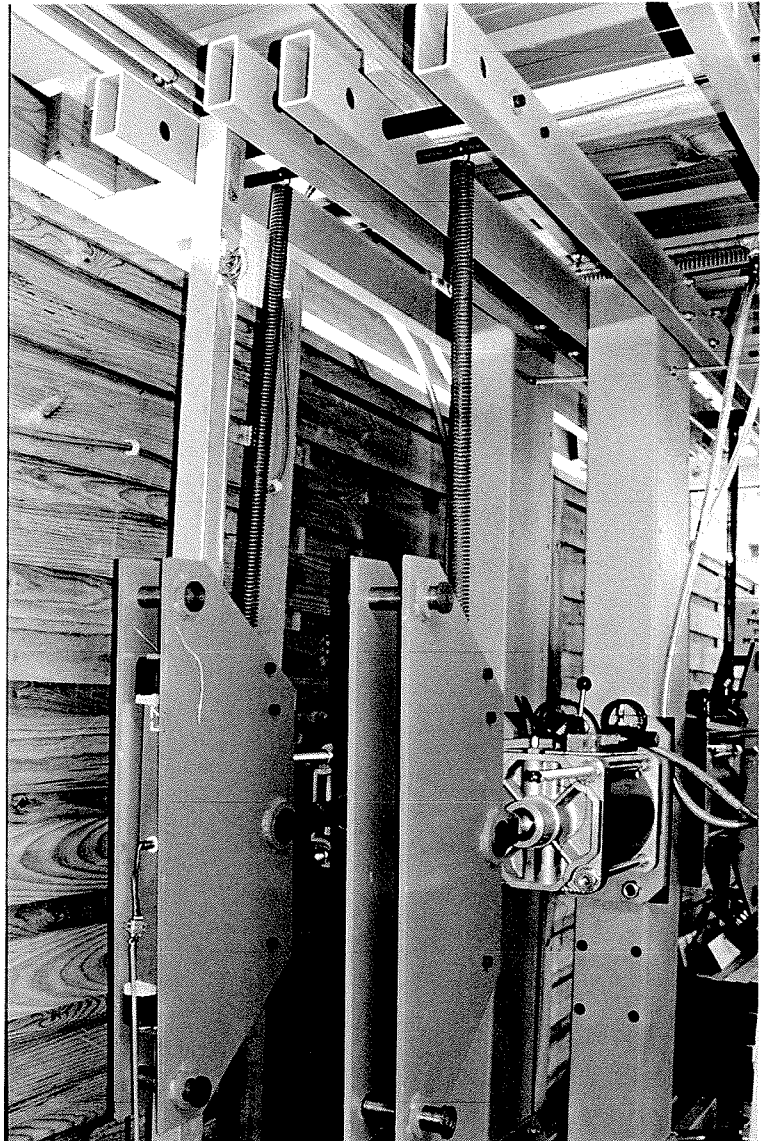
Photo 9 : 24 rigs (dead load - tension ⊥ grain in LAB4) - external and climatic room

APPENDIX II Monitored hygrothermal conditions in the open shelter in Lab 1.

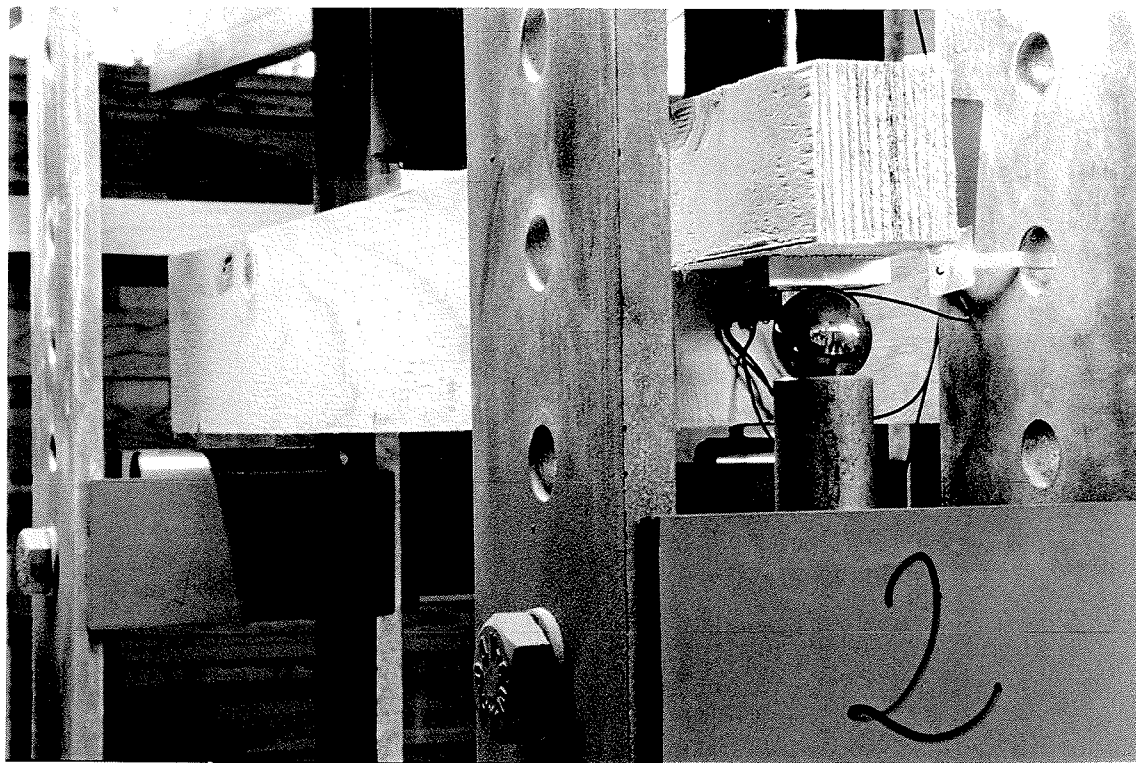
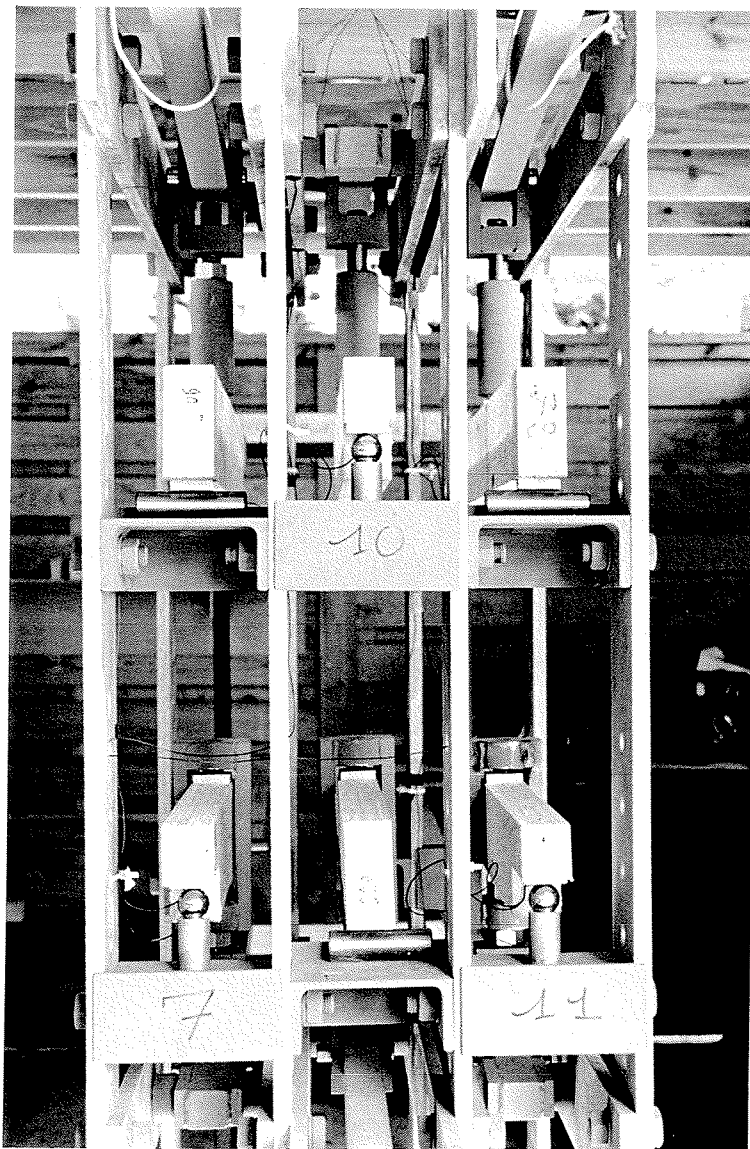




Upper Photo (n° 1) :
Shelter under which experiments
are performed in Lab 1

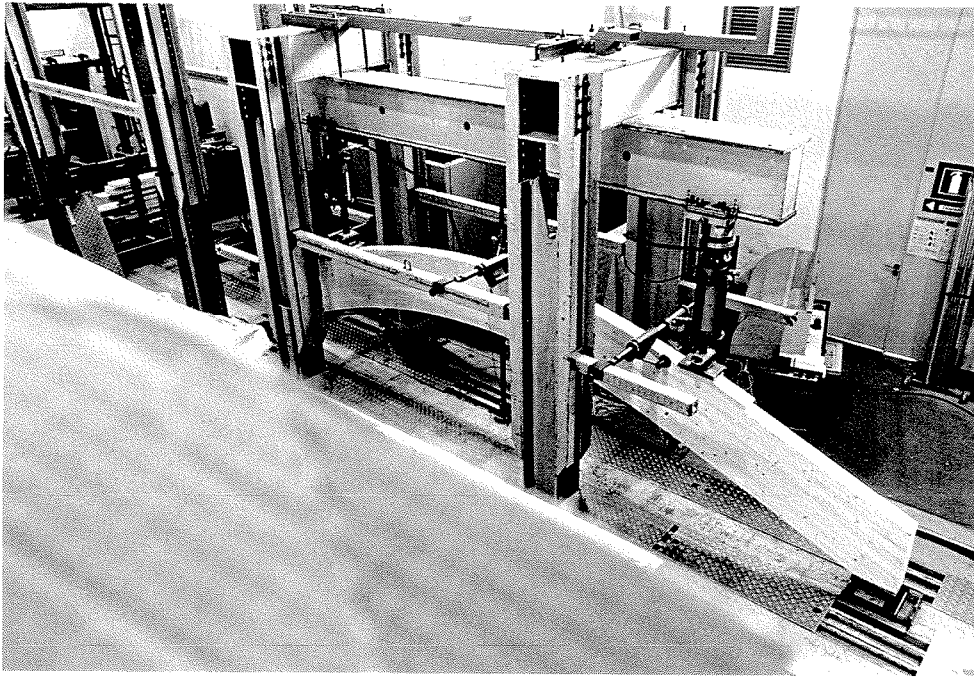


Lower Photo (n°2) :
rigs for straight beams with air jacks
in Lab 1



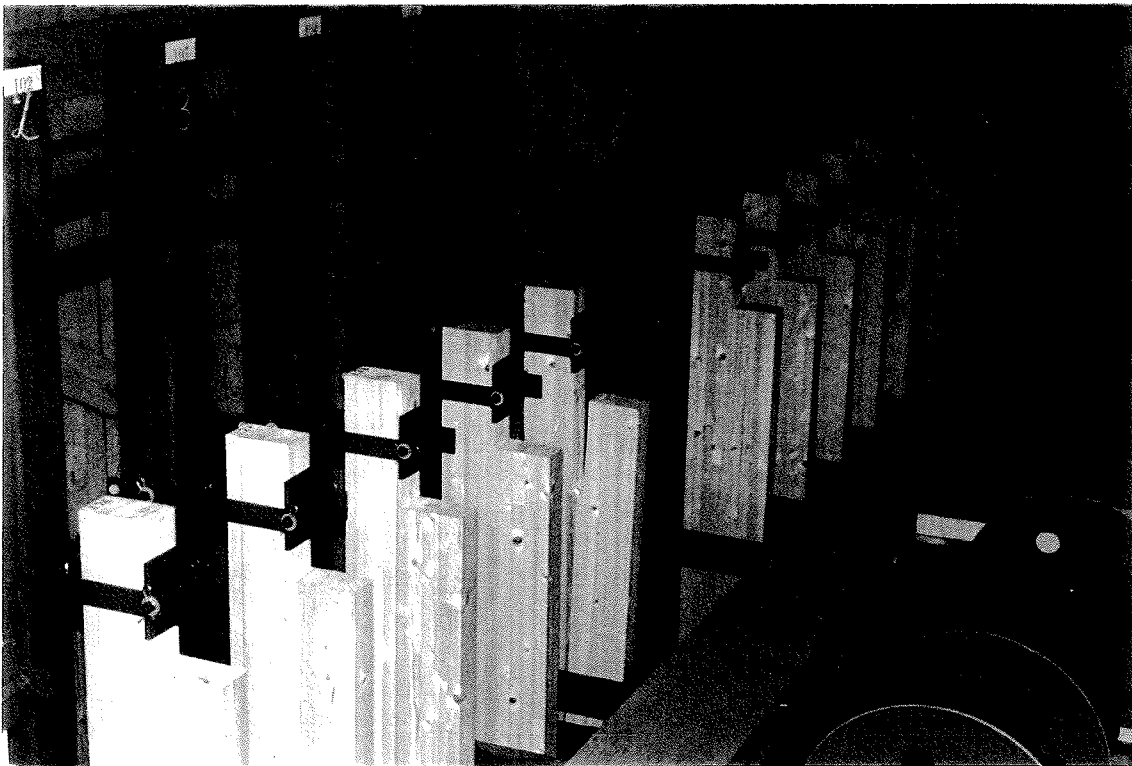
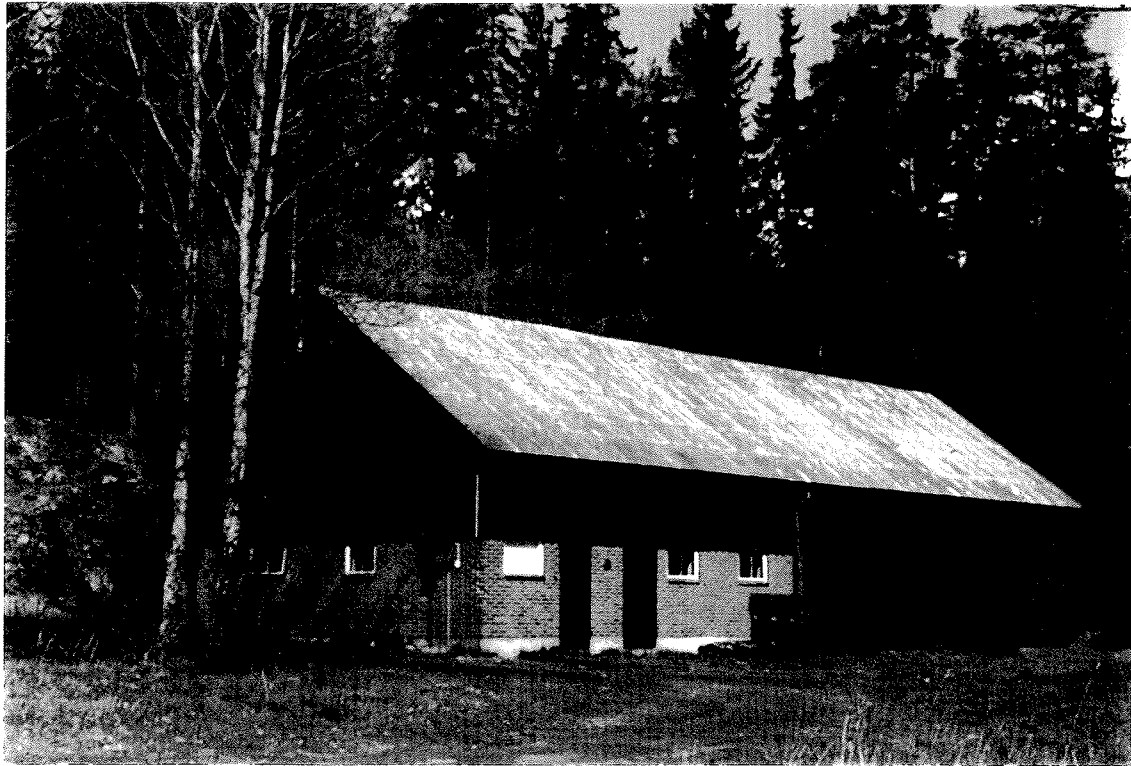
Upper Photo (n°3) : rigs for notched beams in Lab 1

Lower Photo (n°4) : details of the supports for notched beams



Upper Photo (n° 5) : short term test of curved beams in Lab 2

Lower Photo (n° 6) : rigs for straight or curved beams in Lab 2



Upper Photo (n°7) : place where the tests are made in ASA - Lab 5 -

Lower Photo (n°8) : long term tests for notched glulam beams in Lab 5

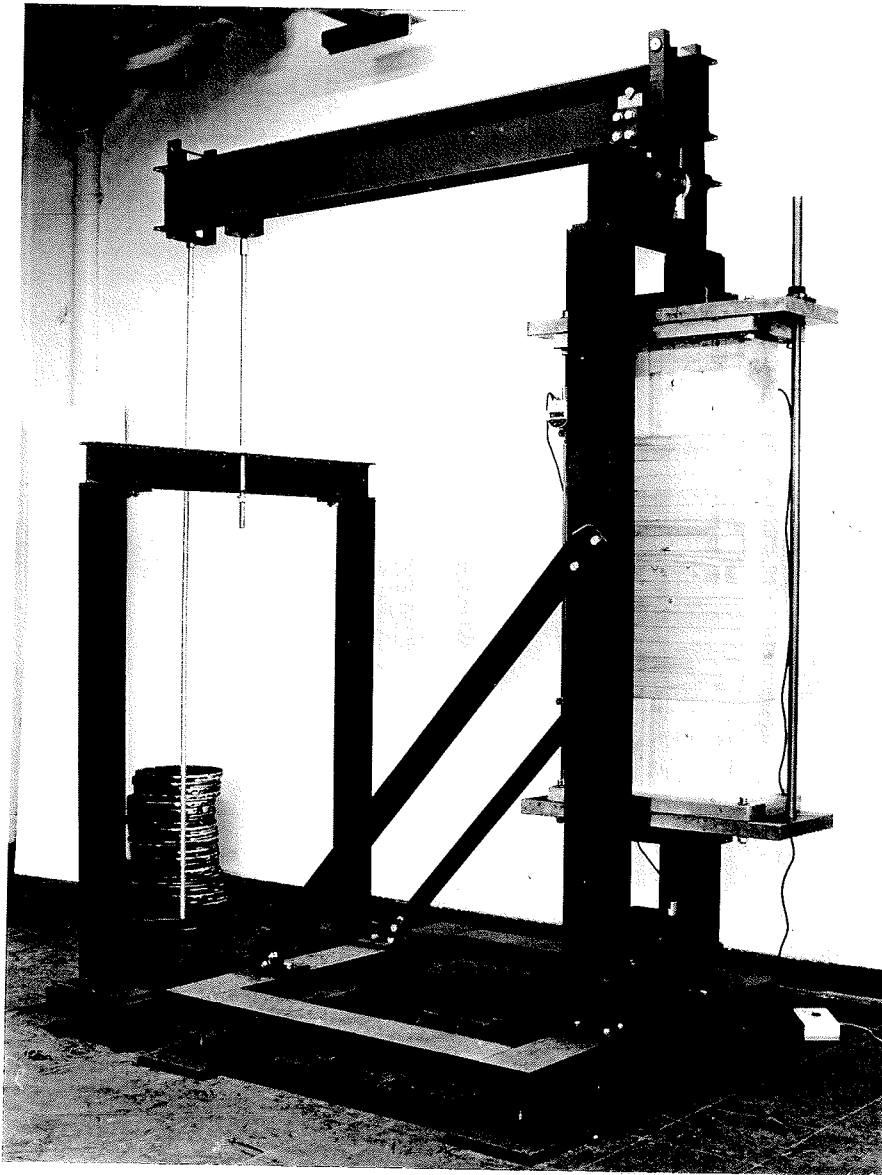


Photo (n°9) : One of the rigs for glulam transverse characteristics (Lab. 4)
rigid clamping via glued-on steel plate

**INTERNATIONAL COUNCIL FOR BUILDING RESEARCH STUDIES AND DOCUMENTATION
WORKING COMMISSION W18 - TIMBER STRUCTURES**

DEVELOPMENT OF EFFICIENT GLUED LAMINATED TIMBER

by

G Schickhofer
Technical University of Graz
Austria

MEETING TWENTY - NINE

BORDEAUX

FRANCE

AUGUST 1996

Development of Efficient Glued Laminated Timber

G. Schickhofer

Abstract

Within most of the European countries the grading of timber as well as its classification results from visual obvious characteristics of quality. The inaccuracy of such visual grading, as far as strength and stiffness of timber are concerned, causes an insufficient utilisation of the material timber itself. Special mechanical grading methods working by means of accurate grading parameters to determine stiffness are a basic requirement to classify the respective strength of boards used for the production of GLULAM timber. We give you a survey of the results from mechanical grading relating to the particular grading classes and point out which characteristics constitute mechanically graded boards. Finally we define the efficiency of mechanically graded boards within the field of GLULAM members, considering also the quality of finger joints respectively interdependent grading scales and qualities of products and their effects on GLULAM timber quality.

1.0 Introduction

Actually in Austria, according to the wording of the Austrian Standards ÖNORM B4100/part 2, valid for the time being, there exists only one grade to define the standard of quality, the so-called 'Good Timber' ('GBH' - 'Gutes BauHolz'). A fact which permits, of course, only the production of one single kind of GLULAM timber quality. The European Conception of Standards, however, provides nine grades of stiffness for conifers (C14 to C40), according to ÖNORM EN 338 [2]; the ÖNORM prEN 1194/April, 1995 [6] provides even 11 main grades of stiffness (GL18 to GL38) to classify GLULAM timber. The visually graded 'GBH' falls into the class C24, following an European instruction of classification (Code ÖNORM EN 1912 E). Producing a GLULAM beam by that means, we reach GL26h as stiffness class, according to the draft of ÖNORM prEN 1194/April, 1995 [6], and only GL24 basing on the previous draft.

Extensive comparative calculations were made, based on three typical types of GLULAM beams. The findings resulted in a foreseeable deterioration of 10% to 15% compared to the conception of dimensioning, ÖNORM B4100/part 2, concerning the dimensions of cross sections. At the instance of these facts the research work started, entitled: 'Development of efficient glued laminated timber with the application of mechanical stress graded timber'.

Only an extensive mechanical stress grading of timber and of the boards used to produce GLULAM beams can meet the requirements of the production of GLULAM timber corresponding to the classes GL30 to GL38, according to the ÖNORM prEN 1194/April, 1995 [6]. Having realized these demands we knew that the aim had to be the production of efficient GLULAM components by means of mechanically graded boards. The grading of the timber (about 150 m³ of boards) obtained from 18 Austrian sawmills, was conducted with the help of a stress grading machine, developed in Germany, classifying the scales MS7, MS10, MS13 and MS17. Extensive testing of the boards (regarding tension and bending strength) determined the characteristics of the 'material'. Above all the tension strength of the boards of a bending stressed beam is very important.

Moreover 12 Austrian GLULAM producing firms made available not only more than 200 beams, but also more than 1000 finger joint test specimen. Also those finger joint test specimen were subjected to extensive testing (tension, bending), according to their classifications. As above we notice, that first of all the tension strength is of high importance for the quality. It has to be mentioned, that Austrian firms are able to produce finger joint GLULAM beams of elevated quality. Since both facts - quality of the boards and quality of the finger joints - determine the final quality of GLULAM beams. We wanted to make evident the influence of these two facts, taking into consideration also the grading classes MS10,

MS13 and MS17, on the quality of a GLULAM component. Conclusively we can say, that an extensive mechanical grading of the boards is showing its effects on the quality of the beams.

2.0 Material and grading

2.1 Material

A basic requirement of any scientific work is the convenient selection of the specimen. To fulfil the claim to representative random samples of timber is very difficult, since the multiple influences which have to be observed. Timber used for the test was taken from 18 Austrian sawmills. The essential data of the respective amount of random samples, 150 cubic metres, was registered by means of registration forms, which referred to forestry and sawing.

- Forestry geographical position
 felling date
 quality of the round timber
- Sawing storage of the round timber
 pregrading of the round timber
 method of cutting
 grading of the timber
 method of desiccating

The information resulting of the registration forms was that Austrian timber is convenient and typical to the production of GLULAM timber.

- Specie: spruce
- Dimension of the boards: thickness / width / length = 38 mm / 175 mm / 4000 mm
- Moisture: 12%, $\pm 2\%$

On this basis of boards' width almost all the Austrian firms producing GLULAM components fabricate their pieces of a width of 160 mm and a lamella thickness of 33 mm.

2.2 Grading

The mechanical grading was effected by a grading machine corresponding to the ÖNORM DIN 4074/part 3 [1], the so-called Eurogrecomat, which works according to the following principles: In a pass through procedure the local bending E-modulus flatwise gets defined (span of 700 mm). Density, size and position of knots get determined by X-rays.

2.2.1 Grading in phase 1 and phase 2

The grading of the timber is effected in two steps. During the mechanical grading - in phase 1 of the project - the values of strength and stiffness of the boards didn't reach the nominal values by far, so to speak it was an insufficient grading. Only during the second phase of the project - during a second grading, after a new adjustment of the identification values of the machine, the relations could be made clear.

Additional to that mechanical grading with the Eurogrecomat (MS7, MS10, MS13, MS17) in phase 2 we conducted an extensive ultrasound grading (US7, US10, US13, US17) with 3200 boards. The relations we found out you can take from the parts [12] and [13] within our literature.

2.2.2 Grading for the following project

After we had finished that project and with the existing results we adjusted the setting of the machine, since the value of tensile strength of the MS17₂ boards, which we had discovered during the examination, was not high enough, so that we would be able to reach with our following

tests also the strength classes GL36 respectively GL 38, which we thought be possible because of the set formulas and their correlation. During an actually adopted following project a total of 2745 boards 36 mm / 155 mm / 4000 mm again were being graded mechanically. Table 1 sums up the grading results and brings them face to face.

Table 1. Output. Phase 1, phase 2 und following project

Grading class according to ÖNORM DIN 4074/part 1¹⁾	Def.* rejects and MS7	MS10	MS13	MS17
Phase 1 ²⁾	1%	7%	16%	76%
Phase 2³⁾	5%	26%	31%	38%
Following project ⁴⁾	7%*	44%	36%	13%
Strength classes according to ÖNORM EN 338 ⁶⁾	C16 ⁵⁾	C24 ⁵⁾	C35 ⁵⁾	C40⁵⁾

- 1.) The Austrian Engineering Standards Committee FNA012 for wooden structures has adopted DIN 4074/part 1, part 3 and part 4 unchanged as ÖNORM DIN 4074/part 1, part 3 and part 4.
- 2.) First grading from 22nd and 23rd of July, 1994.
- 3.) Second grading from 3rd of December, 1994 after adjusting of the machine - starting situation for the project.
- 4.) Grading for the following project, 13th of May, 1996, after the termination of the research project, a supplementary adjustment of the machine and an attestation of the suitability by DIN CERTCO.
- 5.) Related according to P. Glos [16], [17];
- 6.) Strength classes according to ÖNORM EN 338 [2];

After the second grading 38% consequently reached the highest grading class, according to ÖNORM DIN 4074/part 1 [1]. Which characteristic values we reached with this class out of this grading will be pointed out in the following. Beforehand we can say that the present grading was a very distinct one. To take into account the existing differences concerning the characteristic values between the 2nd grading and the last grading, we extend the designation of the grading classes in the following with an index.

Table 2. Designation of the grading classes

Phase 1	MS7 ₁	MS10 ₁	MS13 ₁	MS17 ₁
Phase 2¹⁾	MS7₂	MS10₂	MS13₂	MS17₂
Following project ²⁾	MS7	MS10	MS13	MS17

- 1.) Designation of the grading class in phase 2 of the research project.
- 2.) Designation of the grading class according to ÖNORM DIN 4074/part 1 for the grading used within the following project.

It has to be mentioned, that in spite of differing grading results, every data between the first and the second grading is of scientific interest, because independent of the quality of the grading all essential characteristic values have been found out and therefore correlations do exist!

3.0 Experimental conceptions

Necessarily the whole test was executed in two phases, because phase 1 - first grading - showed an insufficient grading. Nevertheless within this phase we made 841 single tests - 120 boards (tension), 120 boards (bending), 541 finger joints (tension) and 60 beams (bending, h = 320 mm) - which results wont be of any interest for the report. The experimental conceptions of phase 2 were corresponding to a large extent to

those of phase 1, however, some extensions were made, first of all with regard to the series of beams. Table 3 and 4 show the conceptions of phase 2.

Table 3. Conception phase 2. Boards (L) and finger joints (f_j)

Test	L/f _j Total	MS7 ₂ 1)	MS10 ₂ 1)	MS13 ₂ 1)	MS17 ₂ 1)	f	E	ρ	Laboratory
Tension	L 228	14	70	70	74	✓	✓	2)	ETH Zurich E. Gehri
Bending edgewise	L 89	0	29	30	30	✓	✓	✓	ÖHFI Vienna R. Mauritz
Bending flatwise	L 66	0	22	20	24	✓	✓	✓	ÖHFI Vienna R. Mauritz
Tension 8 firms	f_j 200	0	0	0	200	✓	×	✓	ETH Zurich E. Gehri
Tension firm B	f_j 135	0	50	45	40	✓	×	✓	ETH Zurich E. Gehri
Bending flatwise firm B	f _j 133	0	50	45	38	✓	✓	✓	ÖHFI Vienna R. Mauritz
	851³⁾								

- 1.) Second grading from 3rd of December, 1994.
Designation of the grading class with index 2: MS7₂, MS10₂, MS13₂, MS17₂;
- 2.) The determination of the density was taken from the whole specimen and was reduced to small specimen of reference.
- 3.) The evaluation neglects slight differences of the quoted number of pieces.

Table 4. Conception phase 2. Beams

Tests	Σ	1010 ₂ hom ¹⁾	1313 ₂	1717 ₂	1310 ₂ comb ²⁾	1713 ₂	f	E	ρ	LAB
h = 300 mm 8 firms	40	0	0	0	0	40	✓	✓	✓	ÖHFI Vienna
h = 300 mm firm B	115	23	30	20	20	22	✓	✓	✓	ÖHFI Vienna
h = 600 mm firm B	28	10	0	18	0	0	✓	✓	✓	SZA Vienna
	183									

- 1.) f.e.: 1010₂ means that the layup of the beam homogeneously consists only of MS10₂ boards.
- 2.) f.e.: 1310₂ means that the layup of the beam combines MS13₂ boards in the section of tension and MS10₂ boards in the remaining cross sectional part.

In the following will have a close look at the results of the tension tests we made with boards and finger joints, another crucial point will be the tests we made with GLULAM beams according to table 3 and 4.

4.0 Boards

4.1 Test specimen, experimental conceptions, conditions of reference

The tension test in phase 1 was based on boards with a cross section of 32 mm / 160 mm, in phase 2 they showed a cross section of 36 mm / 170 mm. The free length of examination was 3220 mm, at which the minimum length, according to the ÖNORM EN 408 [5] has to be 9 times the largest cross sectional measure. We determined the tension E-modulus in the middle of a measured length of 800 mm, without looking for the obvious worst point, which also corresponds to the ÖNORM EN 408 [5], which demands that the measurements of deformations ought to be based on a minimum length of 5 times the largest cross sectional measure.

The following data essentially has to be seen as pure results of examinations. We did not define conversion factors for the values of strength we found out, because in parts those factors are mostly disputed. Like the influence of length and width at the tension test. The quoted E-modulus values have been corrected according to the ÖNORM EN 384 [3] to a moisture of reference of 12%. Another correction concerns the density in relation to the moisture of reference of 12%, according to the ÖNORM EN 384 [3], and even, if necessary, we adopted a division with 1.05 of the values of density we had found out, if we had determined the value on the whole specimen. By that we reached a reduction of the density to a punctilious specimen without knots and 'mistakes'.

4.2 Results of the tension test and the measuring of the density

In the following table 5 and 6 we present the results of phase 1 and phase 2. Phase 2 was based on a distinct grading, a fact which is shown in the results of the test.

Table 5. Results of phase 1

Grading classes ¹⁾	MS7 ₁	MS10 ₁	MS13 ₁	MS17 ₁	All ₁ ⁴⁾
Tension strength ²⁾ $f_{t,0,l,k}$ [N/mm ²] - (L)	-	8.9	11.5	15.1	12.7
Tension E-modulus ³⁾ $E_{0,l,mean}$ [N/mm ²] - (G)	-	8900	10400	12800	12100
Density ³⁾ ρ_k [kg/m ³] - (G)	-	340	345	365	360

1.) First grading from 22nd and 23rd of July, 1994.

Designation of the grading class with index 1: MS7₁, MS10₁, MS13₁, MS17₁;

2.) (L) - Log-Normal-Distribution;

3.) (G) - Gauß-Normal-Distribution;

4.) The description of these results gets used to compare with the basic totality.

Table 6. Results of phase 2

Grading classes ¹⁾	MS7 ₂	MS10 ₂	MS13 ₂	MS17 ₂	All ₂ ⁵⁾
Tension strength $f_{t,0,l,k}$ [N/mm ²] - (L) ²⁾	-	11.6	17.5	21.9	14.3
$f_{t,0,l,k}$ [N/mm ²] - (Z) ³⁾	-	11.7	18.1	22.2	13.6

Table 6. Results of phase 2

Grading classes ¹⁾	MS7 ₂	MS10 ₂	MS13 ₂	MS17 ₂	All ₂ ⁵⁾
Tension-E-modulus⁴⁾ E _{0,l,mean} [N/mm ²] - (G)	-	10100	12300	14900	12800
Density ⁴⁾ ρ _k [kg/m ³] - (G)	-	345	360	380	355

- 1.) Second grading from 3rd of December, 1994.
Designation of the grading class with index 2: MS7₂, MS10₂, MS13₂, MS17₂;
- 2.) (L) - The Log-Normal-Distribution describes the tension strength best.
- 3.) The Countingmethod (Z) without any distribution is very sensible as far as small deviations within a smaller test are concerned.
- 4.) (G) - Gauß-Normal-Distribution;
- 5.) The description of these results gets used to compare with the basic totality.

In the following we analyse the correlations of the single tests. We emphasise only the tension tests, in special their relation to the density. The density is defined as a dimension which derives from the tension E-modulus and the strength of tension..

Table 7. Lines of regression and coefficient of correlation

Y	=	a	+	b	*	X	Annotations	r
f _{t,0,l}	=	-12	+	3.2	*	E _{t,0,l}	(E in 1000)	0.78
f _{t,0,l}	=	-23	+	0.11	*	ρ	ρ=(f _{t,0,l} +23)/0.11	0.43
E _{t,0,l}	=	-6200	+	43	*	ρ	ρ=(E _{t,0,l} +6200)/43	0.65

We notice an obvious correlation between tension strength and the tension E-modulus. The influence of the density on the tension strength appears less. All the examinations show an influence of the density across the E-modulus, the most important criterion of grading. Moreover we point out the relations between the tension and the bending tests. You find these results, which regarded the factors of dimension according to ÖNORM EN 384 [3], which orders a relation of the fifth percentile of the tension and bending strength to a height of reference respectively to a width of reference of 150 mm, in table 8.

Table 8. Correlation tension strength : bending strength³

	MS7 ₂	MS10 ₂	MS13 ₂	MS17 ₂	All ₂	Mean
f _{t,0,l,k} /f _{m,k,edgewise} ¹⁾	-	0.60	0.72	0.70	0.64	0.67
f _{t,0,l,k} /f _{m,k,flatwise} ²⁾	-	0.61	0.79	0.70	0.68	0.70

- 1.) (1/0.975)/(1/0.975) = 1.000;
- 2.) (1/0.975)/(1/1.330) = 1.364;
- 3.) Please take the experimental values of the tests edgewise and flatwise from our literature [23].

According to ÖNORM EN 338 [2] we introduce f_{t,0,l,k} as derived size f_{t,0,k} = 0.60*f_{m,k}. This factor is about mean 0.70 at both of the bending tests, flatwise and edgewise as well.

5.0 Finger joints

Apart from the tension strength and the tension E-modulus of the boards it is first of all the tension strength of the finger joints which is of essential importance for the bending strength and the bending E-modulus of a bending stressed GLULAM beam. That was also the reason we made examinations of the finger joints on all the three classes of strength for boards.

As you can see from table 3 and 4, not only most of the laminated timber beams - 143 beams of 7 series - but also most of the finger joints - 135 finger joints of three classes - had been produced by the firm B. So we could avoid deviations because of the spread inside the firm within our final results.

5.1 Test specimen, experimental conceptions, conditions of reference

The pieces of specimen for the finger joints were taken during the production of the beams. The production was lead in such a way, that for the bending tests the same boards were joined to each other as for the tension tests (they had been numbered before). The joints were shaped according to the I-15-profile defined by the ÖNORM EN 385 [4] (15.0/3.8/0.3). The glue used was resorcin resin glue. The tension tests were based in phase 2 on a cross section of 33 mm / 160 mm. The free length of examination amounted on 200 mm, according to the prescriptions made in ÖNORM prEN 1194/April, 1995 [6].

The data presented followingly are mainly based on testing! The strength properties we found out were not converted with particular factors, because they are still being disputed on. This refers to the influence of width on the tension test, the factors k_q , k_v and k_s according to ÖNORM EN 384 [4] and also the factor k_f according to ÖNORM EN 385 [5]. We expected more fractures within the class MS10₂, which made us test a higher quantity of that specimen.

5.2 Results of the finger joint tension test and the measuring of the density

In table 9 you find the results of the tension test made on the finger joints of firm B.

Table 9. Results of the tension test on finger joints. Firm B

Grading classes ¹⁾	MS7 ₂	MS10 ₂	MS13 ₂	MS17 ₂
Number of all the tested pieces ^{2a)}	-	50	45	40
Number of all the evaluated pieces ^{2b)}	-	40	42	37
$f_{t,j,k}$ [N/mm ²] ³⁾ - (G)	-	24.7	24.0	34.8
$f_{t,j,k}$ - Z [N/mm ²] ³⁾ - (Z)	-	25.9	21.4	33.3
Density ⁴⁾ ρ_k [kg/m ³] - (G)	-	365	375	390
Finger joints (A)⁵⁾	-	80%	60%	40%
Finger joints (D)⁵⁾	-	20%	40%	60%

1.) Second grading from the 3rd of December, 1994.

2a) Within the grading class MS10₂ we had expected more fractures, which made us raise the number of specimen.

2b) A lot of A-fractures is a sign for an inferior quality of the timber. We did not sum up in our results those fractures caused only by the timber. The evaluation neglects slight differences of the tested number of pieces.

3.) The tension strength of finger joints is well defined by the Gauß-Normal-Distribution (G). Countingmethods (Z), corresponding to ÖNORM EN 384 [3] without any distribution is here even more sensible against small deviations than the boards themselves (one bad board used for a finger joint fractiles 40 tests).

4.) This value corresponds to the mean value of the fifth percentile of both of the halves.

Annotation: The desiccated specimen material was taken from both of the halves, as close to the site of fracture as possible, which we converted then according to DIN 52182 [7] into 12%. Moreover we know the density of the total weight. The converting factor of the denisty for flaw-less specimen is fxd in the ÖNORM EN 384 [3] with 1.05. We define it here inferior for all the three grading classes with 1.02, because of the length of 800 mm.

5.) Finger joints (A) - Failures at the base of the finger joint.

Finger joints (D) - Failures in the flank - extraction of a finger joint.

The higher the grading class, the more the number of timber fractures decrease.

In phase 1 and in phase 2 there were produced moreover by 8 Austrian GLULAM timber producing firms respectively 45 and 25 finger joints. The tested material of phase 1 showed a characteristic tension strength of 15.1 N/mm^2 (Log-Normal). The material of phase 2 showed 21.9 N/mm^2 (Log-Normal). Usually the cut is made on a flaw-less point of the timber, which means that the grading is only secondary to the tension of the finger joints. The same is valid also for the density. The difference of the boards within their grading classes MS17₁ und MS17₂, which we notice at the density, doesn't influence on the tension strength of the finger joints in the same extent. An determining influence on the quality of finger joints, however, seems obviously to be found within the production deviations. Table 10 gives you the results of all of the 8 firms (every firm got a capital letter as a sign: A, D, E, G, I, J, K, L), as well compared to the firm B as compared between phase 1 and phase 2 within the respective firm.

Table 10. Tension strength of the finger joints, without fractures of timber, in $[\text{N/mm}^2]$

Firm	A	B ¹⁾	D	E	G	I	J	K	L	All
$f_{t,j,\text{mean}}$ Phase 1 ²⁾	35.8	42.5	43.7	42.5	39.7	43.9	39.5	42.0	39.3	41.7
$f_{t,j,k}$ Phase 1 ²⁾	21.9	31.4	26.5	26.4	28.8	27.6	30.8	29.1	28.5	28.6
$f_{t,j,\text{mean}}$ Phase 2 ²⁾	44.4	47.8	40.2	36.4	32.8	49.0	43.3	49.5	43.4	42.4
$f_{t,j,k}$ Phase 2 ²⁾	32.6	34.8	31.8	26.1	26.7	30.7	33.7	40.0	31.2	31.6
$f_{t,j,\text{mean}}$ Diff. 2:1 ³⁾	+24%	+12%	-8%	-14%	-17%	+12%	+10%	+18%	+10%	+2%
$f_{t,j,k}$ Diff. 2:1 ³⁾	+49%	+11%	+20%	-1%	-7%	+11%	+9%	+37%	+9%	+10%

- 1.) We chose firm B for the production of 143 GLULAM beams, that means 7 series.
- 2.) Designation of the grading class MS17₁ (phase 1 -> index 1) and MS17₂ (phase 2 -> index 2).
- 3.) The mean value is moving between -17% and +18%, the fifth percentile is moving between -7% up to +37%. The value of +49% can not be seen as a productional deviation, since this firm because of its bad values during the tests in phase 1 was told to improve its working methods. The corrections which were made on the geometry of the profile didn't be in vain (+24% in the mean, +49% with the fractile value).

5.3 Correlations

The demands made for the finger joints in the ÖNORM prEN 1194/April, 1995 [6] concerning the tension strength amounts on 80% of the bending strength of GLULAM timber. If we want to reach the highest level of strength, given in the draft of the ÖNORM prEN 1194/April, 1995 [6], defined in the class of strength for GLULAM timber GL38, we have to reach a minimum of tension strength with the finger joints of $f_{t,j,k} \geq 30.4 \text{ N/mm}^2$ ($f_{t,j,k} \geq 30.0 \text{ N/mm}^2$ in consideration of the factor k_w). Looking at table 10 you will notice that 7 of nine of those firms were able to meet the conditions of tension of the highest quality of GLULAM timber. The following comparison will make clear that the characteristic tension strength of the finger joints partly was obviously superior to the tension strength of the basic material.

Table 11. Tension strength of fj : Tension strength of boards

Grading classes ¹⁾	MS7 ₂	MS10 ₂	MS13 ₂	MS17 ₂
$f_{t,j,k}/f_{t,l,0,k}$	-	2.11	1.35	1.57

- 1.) Second grading from 3rd of December, 1994.

2.) $f_{t,j,k}$ - Gauß-Normal-Distribution : $f_{t,1,0,k}$ - Log-Normal-Distribution;

6.0 GLULAM beams

We aimed with our tests on beams in phase 1 and phase 2, based on mechanical stress graded boards - MS10₂, MS13₂ und MS17₂ - at producing efficient GLULAM beams on the one hand, and on the other, at the same time, we wanted to find a classifying system for GLULAM timber.

6.1 Test specimen, experimental conceptions, conditions of reference

All the beams talked about in the following had been produced by one Austrian firm for GLULAM timber - the so-called firm B. The series 1 to 5 had a cross section of 160 mm / 297 mm (9*33 mm), the series 6 und 7 showed one of 160 mm / 594 mm (18*33 mm). In the whole we fractured 115 beams within the first five series of examination. 73 of those beams were homogeneously built, 42 were built in a combined unsymmetrical way. We used another 28 homogeneously built beams in the series 6 and 7. Please take the information about the layup of the beams used during the tests from the figure 1 below.

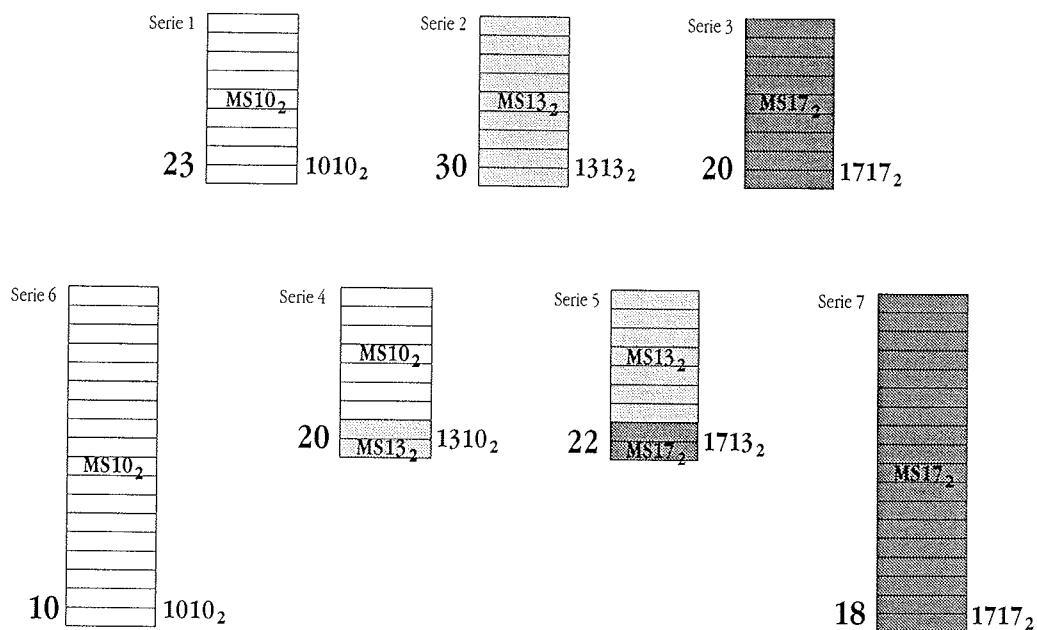


Figure 1. Serials of examination in phase 2 - firm B

The experimental conception was effected according to the ÖNORM EN 408 [5]. Only the series 6 and 7 - $h = 594$ mm (18*33 mm) - were based on a reduced length of beams, still accordingly to the quoted normation, to $17 \cdot h$. Those reductions were made, to use the existing cubature of timber for the production of an elevated number of beams.

The used data has to be seen as pure results of examinations! When we defined the strength properties, we did not use any converting factors - $k_1 (= 1.01!)$ according to the ÖNORM EN 384 [3]. We determined the strain on the base of M/W . The mean E-modulus of every serie was corrected by means of the respective average value of the moisture of timber, accordingly to ÖNORM EN 384 [3], to a moisture of reference of 12%. To specify the density we took a tiny specimen out of the belowmost tension lamella. We also adopted a correction according to the ÖNORM EN 384 [3] to a moisture of reference of 12%.

6.2 Results of the bending test and the measuring of the density on beams

Looking at the failure of the examined bending beams at the test, it becomes very obvious, that first of all two factors are essential for the bending strength of a GLULAM beam. Those qualities are the tension strength of the finger joints and the quality of the board itself, above all the quality of the outermost lamella of pressure in that part of the beam that gets exposed to the tension. The following table 12 gives you a survey of the results evaluation of the 7 quoted series of examination.

Table 12. Results - phase 2 - firm B

	Serie 1 1010 ₂ hom. ¹⁾	Serie 2 1313 ₂	Serie 3 1717 ₂	Serie 4 1310 ₂ comb ²⁾	Serie 5 1713 ₂	Serie 6 1010 ₂	Serie 7 1717 ₂
Bending strength							
$f_{m,g,k}$ - [N/mm ²] - (G) ³⁾	22.4	26.2	32.5	22.5	32.9	21.5	31.2
$f_{m,g,k}$ - [N/mm ²] - (Z) ³⁾	22.5	26.6	33.2	24.9	32.0	19.5	30.0
Bend.-E-modulus - G⁴⁾							
$E_{g,0,mean}$ - [N/mm ²]	10400	11900	14600	10600	13100	10600	14300
Density ⁵⁾	MS10 ₂	MS13 ₂	MS17 ₂	MS13 ₂	MS17 ₂	MS10 ₂	MS17 ₂
ρ_k - [kg/m ³] - (G)	350	355	385	375	380	340	390
Failure timber⁷⁾	91%	89%	61%	98%	75%	95%	76%
Failure finger joints	9%	11%	39%	2%	25%	5%	24%

- 1.) f.e.: 1010₂ means that the layup of the beam is homogeneous with MS10₂ boards.
- 2.) f.e.: 1310₂ means a combined built beam with MS13₂ boards in the tension stressed zone and MS10₂ boards for the other parts of the cross section.
- 3.) The bending strength gets defined quite well by the Gauß-Normal-Distribution (G). To refer to the nominal value seems to be rather problematical, since the number of pieces of specimen is small.
- 4.) (G) - Gauß-Normal-Distribution;
- 5.) The value of the density of the boards is, however, a value which doesn't suit a comparison with the **ÖNORM prEN 1194/April, 1995 [6]**; same situation as with the tension test.

6.2.1 Bending strength

Looking at the table 12, which gives you the values of bending strength, you may notice an increase within the series 1010₂ and 1313₂ of 18% within the series 1010₂ and 1717₂ the rise amounts on 48% - with high beams is also 54%. Among the combined GLULAM beams we also notice an obvious graduation between the series 1310₂ and 1713₂, with a percentage of 29%. Another essential fact is that the difference of the bending strength between homogeneously built and unsymmetrically combined series might be neglected, if the quality of the outermost lamellas is the same one. The coefficient of variation within the beams of the series 1 to 5 is on the mean at 0.14 respectively at 0.11 within the series 6 & 7.

6.2.2 Bending E-modulus

At the same time also the graduation of the bending E-modulus among the single classes is obvious. We notice an increase of the mean value from serie 1010₂ to serie 1313₂ of 15%, within the serie 1010₂ to 1717₂ the rise differs from 35% (h = 600 mm) to 41% (h = 300 mm). If we compare the homogeneously built series, 1313₂ respectively 1717₂, to the combined unsymmetrically built ones 1310₂ respectively 1713₂ (in the zone of tension MS13₂ respectively MS17₂), we notice a difference in the quality of the boards, in contrast to the bending strength, in a decline of the mean bending E-modulus of 10%, as far as homogeneous series are concerned.

6.2.3 Types of fractures and analyses of fractures

Analysing the 23 1010₂ beams we notice that only in 10% of all fractures the finger joints were the reason for the failure. Concludingly we can say that 90% of all fractures find their reasons in the quality of the timber itself. In 65% of the fractures the number of knots is generally or at least partly the fracture-causing weak point. The size and the position of the knots (flat knots at the edges) turned out to be very essential for the phenomenon of fractures. Moreover accumulations of knot, square fibres, deviation of fibres (in the most cases in connection with knots), the position of pith inside the board, respectively very near to the board. And extreme high or low extent of the single annual rings were further reasons for fractures of the timber. Like within the 20 1010₂ beams within the serie 1 (h = 300 mm), also within the serie 6 (h = 600 mm) there exists only a small number of fractures (about 5%) where the finger joints cause the fractures themselves. Also at those examinations we found the knots - knots at the edges, accumulation of knots - responsible for the fractures.

At the serie 1313₂ (h = 300 mm) we found a similar situation as within the serie 1010₂. Only ~10% of the beams fractures are caused by the finger joints. We have to stress that at ~90% of the fractures that an essential criterion for the fractures is the number respectively the extent of knots.

The characteristic tension strength of the finger joints was rising less with an elevated quality of timber than the characteristic tension strength of the board. After we had analysed the present 20 1717₂ beams (h = 300 mm) we found out that ~40% of the reasons for the fractures were based on the finger joints. Nevertheless the timber was the main fact which created the fractures. The 18 1717₂ beams (h = 600 mm) of serie 7 showed us that the three mostbelow lamellas of tension featured about in ~20% of the finger joints within all of the three lamellas.

It is quite difficult, to give a reliable and exact statement on the factor which really causes the fracture, it's the more problematical the higher a beam is, since in the zone of tension a larger volume gets stressed.

6.3 Influence of the size of the beams

Many publications and projects of research [8], [9], [21], a. o. have been working on the problem of influence of the size. Most of the projects of research and their resulting correlations, first of all those which referred to the influence of the height, are however based on examinations of solid timber blanks with a maximum height of h = 300 mm. Some of those publications point out that the effect of height in fact is an effect of the volume. That's why the one dimensional problem of the influence of height generally gets a problem of the influence of volume. Hence it becomes necessary to consider not only the height of a beam, but also the width and the length of that beam.

The present results make it possible to state facts, based on the variable heights within the series 1 and 6, respectively 3 and 7, with the same construction of the beams, on the influence of the height of a beam, according to the ÖNORM prEN 1194 [6]. We compare the series in tab. 13.

Table 13. Factor of height k_h of the series 1010₂ and 1717₂

	Serie 1 1010 ₂	Serie 6 1010 ₂	k_h	Serie 3 1717 ₂	Serie 7 1717 ₂	k_h
Height of the beam 9*33, 18*33 [mm]	297	594		297	594	
Bending strength¹⁾ $f_{m,g,mean}$ [N/mm²] - (G)	27.9	25.3	1.10	43.0	39.4	1.09
Bending strength¹⁾ $f_{m,g,k}$ [N/mm²] - (G)	22.4	21.5	1.04	32.5	31.2	1.04

1.) (G) - Gauß-Normal-Distribution;

Concludingly we can define the same factor of height as well for the series 1010₂ as for the series 1717₂. Basing on these results we can conclude that independent of the various classis of strenght and also independent of the grading classes of the boards, it's always the same valid factor. It's a fact that the mean value of the factor of height is about 1.10 and that one of the fifth percentile is about 1.05.

6.4 Correlations

In the following table 14 gives you an impression of the essential correlations, like bending E-modulus and bending strength, and also how both of those previous are connected with the density. Moreover we refer more closely to the so-called model of beams. That means the correlation between the values of the characteristic tension strength $f_{t,0,1,k}$ of the boards which are used to built up the beam and the resulting characteristic values of bending strength of the beam $f_{m,g,k}$.

Table 14. Lines of regression and coefficient of correlation

Y	=	a	+	b	*	X	Annotation	r
Series 1 to 5 $f_{m,g}$	=	-6.3	+	3.5	*	$E_{0,g}$	(E in 1000)	0.71
Series 6 and 7 $f_{m,g}$	=	-13.4	+	3.6	*	$E_{0,g}$	(E in 1000)	0.92
Series 1 to 5 $f_{m,g}$	=	0	+	0.086	*	ρ		0.40
$E_{0,g}$	=	4700	+	18	*	ρ		0.40
$f_{m,g,k}$ ¹⁾	=	9.3	+	0.97	*	$f_{t,0,1,k}$ ²⁾	n = 11! ³⁾	0.83

1.) Gauß-Normal-Distribution.

Considering also the factor of width k_w and the factor of height k_h , corresponding to the newly revised second draft of the prEN 1994/April, 1996.

2.) Log-Normal-Distribution.

Considering also the factor of width k_w and the factor of length k_l , according to newly revised second draft of the prEN 1194/April, 1996.

3.) n = 11: Additional to the 9 series (7 series of firm B and two series of all the firms) we took also two Norwegian series with the respective factor of correction into consideration (see also index 1 and 2).

We found out a good correlation between the bending E-modulus and the bending strength. The correlation between density and bending strength as bending E-modulus is rather small. However you should consider that the density was determined by only a tiny specimen of the mostbelow lamella. The bending E-modulus, in contrast to that, is an integral value of the whole beam.

7.0 Summary and relation to the revised second draft of prEN 1194

Having finished the project of research and in front of the interpretation of the results it seemed to be logical, that a statement against the second draft of the ÖNORM prEN 1194/April, 1995 [6] was necessary, because of various reasons. In the following we give you a summary based on the present results to the single steps of the Austrian comment [22], also in relation to the revised second draft of the prEN 1994/April, 1996.

7.1 Boards - criteria of the grading according to the strength and stiffness

Based on the results of the present project of research we have to point out, that first of all the tension strength and the tension E-modulus of the boards are essential for the bending strength and the bending E-modulus of a GLULAM beam. That's why you should define the following both values as the criteria to classify the boards:

$$f_{t,0,1,k}$$

$$E_{t,0,mean}$$

We should not take the density as a criterion of classification!

A classification by means of the bending attributes according to the ÖNORM EN 338 [2] is not valid for boards used to produce GLULAM timber. Neither the flatwise bending tests nor those edgewise ones give us respective values. The bending test flatwise gives us an unsuitable value of the bending E-modulus, since the zone of measuring is too small for the boards, that's why a problematical 'knot-bending-modulus'. The bending test edgewise doesn't correspond to the usual stress of a board within any component of GLULAM timber. The most opportune test turned out to be the tension test, on which you should take the following measurements of reference (w_R , l_R) for the examined pieces of specimen to determine their characteristic values:

width of the boards $w_R = 150$ mm
 free length of examination l_R with a minimum of $9 \cdot w$, according to the ÖNORM EN 384 [3]

If you work on other measurements you should take into consideration the influence of length and width as follows:

$$f_{t,0,1,k} = f_{t,0,1,k,test} \cdot (w/w_R)^{0.1} \cdot (l/l_R)^{0.1}$$

Within the normative supplement A of the prEN 1194/April, 1996 the correlations of GLULAM timber are indicated. There you can see that the most essential needs of a board are the tension strength and the tension E-modulus. The density of the board doesn't exist as a classifying criterion itself.

The determination of the tension strength has to be made accordingly with the ÖNORM EN 408 [5] and the ÖNORM EN 384 [3]. In the following the conditions of reference have to be:

width of the board $w_R = 150$ mm
 free length of examination $l_R = 2000$ mm

If the width respectively the length of the tested piece deviates from 150 mm respectively from 2000 mm, you have to adopt corrections in the following way:

$$f_{t,0,1,k} = f_{t,0,1,k,test} \cdot (w/150)^{0.1} \cdot (l/2000)^{0.1}$$

7.2 Finger joints

Within the present examinations the finger joints have not been the weak point. The characteristic strength of the finger joints partly are clearly elevated - ~35% to ~110% - compared to the strength of the material they are based on themselves. Above all within the grading class MS10₂ we noticed lots of fractures (type of fracture B) and net finger joint fractures (type of fracture A). Therefore we can conclude that the quality of the timber defines a limiting factor. The requirements to the finger joints according to the ÖNORM prEN 1194/April, 1995 [6] could be met. Another interesting fact is that the influence of the density on the finger joints was rather small ($r(\rho:f_{t,j}) = 0.34$). Moreover we have to admit that the tension test of the finger joints gives more evidence than the bending test, since the cross sectional part which gets under tension stress is about twice as big and at the bending test only a small part at the edge of the cross section is exposed to the high stress. Moreover the finger joints wedge themselves during the bending test within the stressed zone, which gives reason to a certain value of strength of the not-glued finger joints. The tension test is more sensible. It also shows an elevated coefficient of variation, and it describes much better the state of tension stress of finger joints within the beam.

According to the revised second draft of the prEN 1194/April, 1996 the following requirements are to meet of the finger joints:

$$f_{t,j,k} \geq 5.0 + f_{t,0,1,k}$$

$$f_{m,j,k} \geq 8.0 + 1.4 \cdot f_{t,0,1,k}$$

The testing of the characteristic tension strength of the finger joints has to be made in accordance with the ÖNORM EN 408 [5], with a fee

length of examination of 200 mm as a maximum. The testing of the bending strength of the finger joints flatwise has to be made in accordance with the ÖNORM EN 386.

If you take $f_{t,0,l,k} = 26 \text{ N/mm}^2$ - the demanded tension strength of boards for the highest class of strength of laminated timber GL36 - there result the following demands to the finger joints:

$$f_{t,j,k} = 5.0 + 26.0 = 31.0 \text{ N/mm}^2$$

$$f_{m,j,k} = 8.0 + 1.4 * 26.0 = 44.4 \text{ N/mm}^2$$

Both of the characteristically values have been reached in the present project of research. From the table 10 you can see that there exists a characteristic value of tension strength for all the firms of $f_{t,j,k} = 31.6 \text{ N/mm}^2$. Please take the values of bending strength of the finger joints from the literature [23].

7.3 GLULAM beams

It's an essential fact, that the distinct grading of the boards finds its corresponding values within the beams. The increase of the bending strength respectively of the bending E-modulus between the series 1010₂ to 1717₂ is rather high. Please take those facts from capture 6. Analogous to the decisive criterions of classification for boards - $f_{t,0,l,k}$ and $E_{0,l,mean}$ - also the classification of the GLULAM timber should correspond to the classes of strength according to the ÖNORM prEN 1194/1995 [6]. The decisive criterions are:

$$\frac{f_{m,g,k}}{E_{0,g,mean}}$$

The density should not be adopted as a main criterion of classification, since it leads to a declassification of the 'light' GLULAM timber.

According to the present pieces of research we can reach with the highest class of grading in phase 2 - MS17₂ ($f_{t,0,l,k} = 21.9 \text{ N/mm}^2$, not corrected) - a characteristically bending strength of about 31 N/mm^2 to about 32 N/mm^2 . Departing from the model of beams of the ÖNORM prEN 1194/April, 1995 [6]

$$f_{m,g,k} = 9.0 + 1.20 * f_{t,0,l,k}$$

you get - confronted to the examination of beams (A/SUI - tests of beams with $h = 600 \text{ mm}$) - ~15% to ~20% values of calculation which are too high. Also at the first tests with $h = 300 \text{ mm}$, with which we had like at the beams with a height of 600 mm the values of tension strength, we found out similar results, as soon as the influence of height gets registered closely.

Based on the present results of our examinations we should fix a model of beams for a new draft of ÖNORM prEN 1194. It also would be necessary to base the new model of beams on a reproducible curve of examinations. The following diagram - figure 2 - gives you an impression of the correlation $f_{t,0,l,k}$ and $f_{m,g,k}$ within the 11 series of timber beams - two Norwegian series and 9 series A/SUI. Moreover three kind of models of beams:

$$f_{m,g,k} = 9.0 + 1.20 * f_{t,0,l,k} \text{ (ÖNORM prEN 1194/April, 1995 [6])}$$

$$f_{m,g,k} = 7.0 + 1.15 * f_{t,0,l,k} \text{ (F. Colling/R. Falk)}$$

$$f_{m,g,k} = 9.5 + 1.00 * f_{t,0,l,k} \text{ (G. Schickhofer/A. Steinberger/C. Seiner)}$$

get illustrated and compared to each other. The model $f_{m,g,k} = 9.5 + 1.00 * f_{t,0,l,k}$ gives the best fit to the 11 series. You will find corrected to a measurement of reference, in this case, the tension strength of the boards as well as the bending strength of the GLULAM timber with a factor of size according to the prEN 1194/April, 1996.

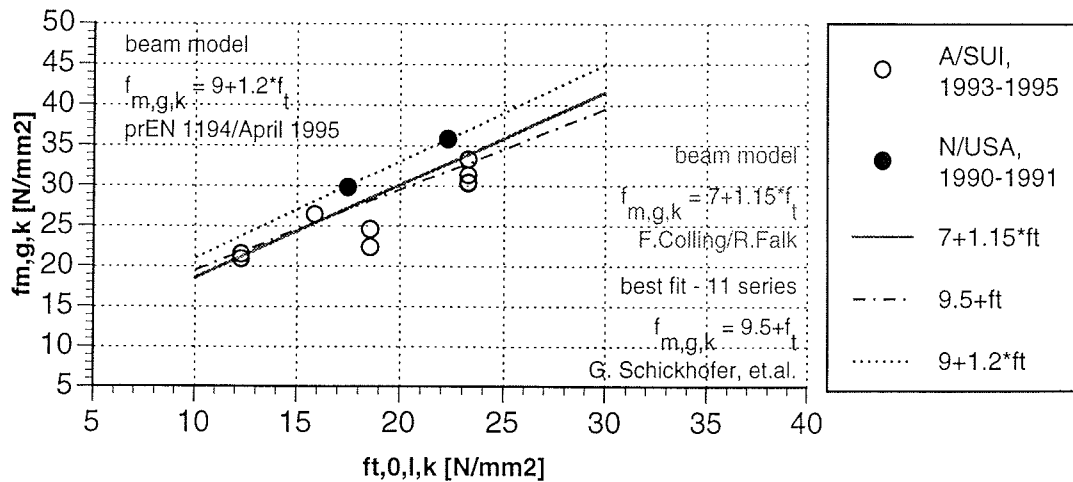


Figure 2. Test data and beam models

The base for the system of classification of strength, table 1 and 2, prEN 1194/April - GL24, GL28, GL32, GL36 - is the model of beams:

$$f_{m,g,k} = 7.0 + 1.15 \cdot f_{t,0,l,k}$$

The difference between the model of beams of F. Colling/R. Falk and that one which is basic for the model of the 11 series amount on -1% to 4%. The very slight difference and the fact that behind this model we suppose a lot of series of American und European examinations as well as many calculations of simulations is the reason for the acceptance of this model of beams into the prEN 1194/April, 1996.

The height of reference for the present characteristic values of the ÖNORM prEN 1194/April, 1995 is $h = 600$ mm. We could not confirm the correlation of the factor of height

$$k_h = (600/h)^{0.2}$$

A reduction of this factor is necessary. According to the examinations of E. Aasheim and K.H. Solli (N) [8] and A/SUI [23], [24] it gets quite obvious, that we have to depart from rather small height influence from $h = 300$ mm to $h = 600$ mm.

Table 15. Influence of size k_h

	prEN 1194/ April, 1995	A/SUI	(N)
Beam $h = 300$ mm k_h	1.15	1.05	1.07

Based on these examinations it's reasonable to reduce the influence of the beams heights in the following way:

$$k_h = (600/h)^{0.1}$$

Additional to that you have also to take into consideration the influence of width. We got to that result by comparing the project of research N/USA, 1990/1991 [11] - width of the beam $w = 90$ mm - and our own examinations - width of the beam $w = 160$ mm. It turned out clearly that the tension strength of the board, which influenced on the model, also showed an influence of width. Hence it seems to be logical, that this fact also valid for the GLULAM beams.

$$k_w = (150/w)^{0.1}$$

The prEN 1194/April, 1996 gives the following measurements of reference for the tested beams:

Height of the beam $h_R = 600$ mm

Width of the beam $w_R = 150$ mm

If smaller cross sectional dimensions get adopted for the examined beam, the results change in the following way:

$$f_{m,g,k} = f_{m,g,k,test} * (w/150)^{0.05} * (h/600)^{0.1}$$

We have to consider not only the height of a beam but also its width, because it is possible to compare experimental series with different cross sectional measurements

8.0 Final considerations and prospects

By means of this present project, which we made together with the Austrian industry of wood, with centres of research on wood and the institute of Wood technology of the ETH Zurich, we are able to enlarge the amount of knowledge in two essential parts. On the one hand we enabled for the first time an insight into the actual standards of quality of the Austrian industry of timber, on the other hand we created by our work, an extensive amount of basic materials, which together with the results of the Norwegian examinations can be taken as a first step for further European projects of research. We also have to point out that this project of research was an essential base for a new revision of the prEN 1194/April, 1996.

If we want to take further advantage out of the European normative standards of classes of strength, it's a fact that a mechanical grading is indispensable. The present results make clear, that an improvement of the value of timber can be reached. Another fact is, however, that an improvement of the mechanical grading remains still a field of further activities. See the optimising of the output of various methods of grading, the finding of optimal criterions for grading classes respective to the operational field of the graded timber, and so on. Of great consequence, however, beside the scientific field of research is a realisation of the knowledge (research and standardisation) of the economic partners.

9.0 Definitions

• Main Symbols

f	Strength (of a material)	h	High (or depth of a beam)
k	Coefficient; Factor (always with a subscript)	ρ	Density
COV	Coefficient of Variation	MOE	Modulus of elasticity

• Subscripts

c	Compression	g	Properties of glued laminated timber
j	Properties of finger joints	k	Characteristic values (5%)
l	Properties of laminations	m	Bending
mean	Mean value (50%)	t	Tension
v	Shear	0	Parallel to grain

10.0 References

- [1] ÖNORM DIN 4074/1.Juni 1996:
Teil 1: Sortierung von Nadelholz nach der Tragfähigkeit - Nadelschnittholz
Teil 3: Sortierung von Nadelholz nach der Tragfähigkeit - Sortiermaschinen, Anforderungen und Prüfung
Teil 4: Sortierung von Nadelholz nach der Tragfähigkeit - Nachweis der Eignung zur maschinellen Sortierung
- [2] ÖNORM EN 338/1.Mai 1995:
Bauholz für tragende Zwecke - Festigkeitsklassen
- [3] ÖNORM EN 384/1.Mai 1995:
Bauholz für tragende Zwecke - Bestimmung charakteristischer Festigkeits-, Steifigkeits- und Rohdichtewerte
- [4] ÖNORM EN 385/1.Mai 1995:
Keilzinkenverbindungen in Bauholz - Leistungs- und Mindestanforderungen an die Herstellung
- [5] ÖNORM EN 408/1.März 1995:
Holzbauwerke - Bauholz für tragende Zwecke und Brettschichtholz - Bestimmung einiger physikalischer und mechanischer Eigenschaften
- [6] ÖNORM prEN 1194/April 1995:
Holzbauwerke - Brettschichtholz - Festigkeitsklassen und Bestimmung zusätzlicher physikalischer und mechanischer Eigenschaften
- [7] DIN 52182/September 1976:
Prüfung von Holz - Bestimmung der Rohdichte

- [8] Aasheim, E., Solli, K.H.: 'Size Factor of Norwegian Glued Laminated Beams', CIB-W18/28-12-2, Kopenhagen (DK), April 1995.
- [9] Colling, F.: 'Biegefestigkeit von Brettschichtholzträgern in Abhängigkeit von den festigkeitsrelevanten Einflußgrößen - Einfluß der Trägergröße und der Belastungsart', Holz als Roh- und Werkstoff 48 (1990), Seite 321-326.
- [10] Falk, R.H., Colling, F.: 'Laminating Effects in Glued-Laminated Timber Beams', Journal of Structural Engineering, Page 1857-1863, December 1995.
- [11] Falk, R.H., Solli, K.H., Aasheim, E.: 'The performance of glued laminated beams manufactured from machine stress graded norwegian spruce, Forest Products Laboratory & Norwegian Institute of Wood Technologie, Oslo, 1990-1991.
- [12] Gehri, E.: 'Sortierung mittels Ultraschall', Tagungsband zur Grazer Holzbau-Fachtagung 1995, Seite C/1-1-C/1-9, 22. Juni 1995.
- [13] Gehri, E.: 'Festlegung der US-Werte für die Sortierung von BSH-Lamellen', Professur für Holztechnologie, ETH Zürich, Interner Bericht 1994.
- [14] Glos, P., Diebold, R.: 'Maschinelle Sortierung: DIN 4074 zugelassen - Neue Chancen für den Holzbau', mikado 7-8/94, Seite 79-83.
- [15] Glos, P., Diebold, R.: 'Prüfbericht Nr. 92514 - Kurzfassung', Prüfung der Euro-GreComat-Gütesortiermaschine Typ 704 nach DIN 4074 Teil 3; Sortierung von Fichten-Brettlamellen in die Sortierklassen MS10, MS13 und MS17, November 1993.
- [16] Glos, P., Diebold, R.: 'Prüfbericht Nr. 94504 - Kurzfassung', Prüfung der Euro-GreComat-Güte-Sortiermaschine Typ 704, Register-/Baumusternr. 5E001 nach DIN 4074 Teil 3; Sortierung von Schnittholz für geleimte Querschnitte in die Sortierklassen MS7, MS10, MS13 und MS17, Dezember 1995.
- [17] Glos, P.: 'Qualitätsbauschnittholz als unternehmerische Notwendigkeit', bauen mit holz 6/95, Seite 502-508, 1995.
- [18] Palm, K.: 'Maschinelle Festigkeitssortierung von Massivholz', Schweizer Holzbau 9-1995, Seite 45-47, 1995.
- [19] Palm, K.: 'Maschinelle Holzsortierung mit dem Euro-Grecomaten', Tagungsband zur Grazer Holzbau-Fachtagung 1995, Seite B/1-1-B/1-8 + 8 Seiten, 22. Juni 1995.
- [20] Peterson, J.: 'The effect of width on the bending strength of glulam beams', Forest Products Journal, Vol. 43, No.3, March 1993.
- [21] Rouger, F., Fewell, T.: 'Size effects in timber: Novelty Never Ends', CIB-W18/27-6-2, Sydney, July 1994.
- [22] Schickhofer, G., Steinberger, A., Seiner, Ch.: 'Austria's Comment on prEN 1194', TU Graz, 5 Pages, July 1995.
- [23] Schickhofer, G., Pischl, R., Seiner, Ch., Steinberger, A., Gehri, E., Mauritz, R.: 'Development of Efficient Glued-Laminated Timber with the Application of Mechanical Stress-Graded Timber', Summary of the FFF-Research Project, Graz-Zurich-Vienna, 36 Pages, 1993-1995.
- [24] Schickhofer, G.: 'Entwicklung leistungsfähiger Holzleimbauteile - Ergebnisse & Auswertung - Träger - Betrieb B', Tagungsband zur Grazer Holzbau-Fachtagung 1995, Seite E/4-1-E/4-34, 22. Juni 1995.

INTERNATIONAL COUNCIL FOR BUILDING RESEARCH STUDIES AND DOCUMENTATION

WORKING COMMISSION W18 - TIMBER STRUCTURES

**LATERAL RESISTANCE OF WOOD BASED SHEAR WALLS WITH OVERSIZED
SHEATHING PANELS**

by

F Lam

H G L Prion

M He

Department of Wood Science

Faculty of Forestry

University of British Columbia

Canada

MEETING TWENTY - NINE

BORDEAUX

FRANCE

AUGUST 1996

LATERAL RESISTANCE OF WOOD BASED SHEAR WALLS WITH OVERSIZED SHEATHING PANELS

by

F. Lam¹, H.G.L. Prion¹ and Ming He²

Abstract

This paper summarizes the results from the first phase of a study to develop a database comparing the structural performance of shear wall systems built with regular and nonstandard large dimension oriented strand board panels under monotonic and cyclic loading conditions. Different types of nail connectors have also been investigated. The results indicate that under monotonic loading, a substantial increase in both stiffness and lateral load carrying capacity can be achieved by shear walls built with oversized panels when compared to regular panels. Defining ductility as the ratio between wall displacements at maximum load and at 50% of the maximum load during monotonic testing, a slight increase in ductility has been observed for the shear walls built with oversized panels. Examining the dissipated energy as the area under the load deformation curve, it seems that the walls built with the regular panels can dissipate more energy under cyclic loading when compared to the walls built with oversized panels. The failure modes in the shear walls have been shown to be substantially different under monotonic (nail withdrawal) and cyclic (nail fatigue) test conditions. It seems that further investigation of the adopted cyclic load schedule in relation to the dynamic response of the shear wall is needed to fully understand and characterize the failure modes in shear walls.

Introduction

Changes in North American demographics and industry restructuring to value-added products have caused the Canadian wood product industries to try to expand from the traditional residential construction market into the commercial construction market while trying to maintain and protect the current competitive advantage in residential construction. A key element in wood based construction is the shear wall and diaphragm system which efficiently provides the building with its three major load carrying components to resist (i) vertical loads, (ii) transverse wind loads and (iii) in-plane lateral forces imposed by wind and seismic loading. These systems typically are composed of lumber framing members sheathed with 1.2 x 2.4 m plywood or oriented strand board panels and connected using nails. These systems have a history of excellent performance against lateral loading especially in residential applications. For example, in the recent 1995 Kobe earthquake in Japan, there is evidence that residences built with North American wood based shear wall techniques (2x4 platform construction) have survived

¹ Assistant Prof., Dept. of Wood Sci., Univ. of British Columbia, Van., B.C. Canada V6T 1Z4.

² Graduate Res. Assistant., Dept. of Wood Sci., Univ. of British Columbia, Van., B.C. Canada V6T 1Z4.

major seismic forces with relatively little damage even in sites of serious liquefaction of the supporting ground.

In the past there has been much experimental work on the structural behavior of wood based shear walls and diaphragms. Typically experimental studies were conducted under either static or dynamic loading with the majority of earlier research efforts focused on the static case. Full size shear walls and diaphragms were tested to quantify the ultimate load carrying capacity of the system under static loads (Tissel and Elliott 1977, COFI, 1979, TECO 1980 and 1981, Atherton 1982 and 1983, and Adams 1987). Experimental studies were also conducted to evaluate the performance of full size shear walls and diaphragms under dynamic (Stewart 1987 and Dolan 1989) and pseudo dynamic (Kamiya 1988) test conditions. Finally, full scale testing of buildings under lateral loads were also conducted (Sugiyama *et al.* 1988, Boughton 1988, and Stewart *et al.* 1988). Recently Forintek Canada Corp. has started a major research program to evaluate the lateral resistance of shear walls under static and cyclic loading.

All of these research efforts have focused on walls and diaphragms built with standard 1.2 x 2.4 m size panels as sheathing material. The discontinuity between panels, as dictated by standard panel dimensions, has a significant impact on the performance and load carrying capacity of the shear walls. In cases where the sheathing panels are oriented horizontally, blocking components are typically installed to provide shear continuity between panels. In cases where the long axes of the sheathing panels are oriented vertically, nail spacings are halved along the seams. Although these construction details increase the lateral load carrying capacity and stiffness of the walls, failure always occurred along the panel edges and it was expected that shear walls built with continuous panels would be stronger and stiffer than common wall assemblies. Preliminary finite element analyses comparing the load carrying capacity of 2.4 x 7.3 m shear walls modelled with standard dimension panels and with oversized panels supported this hypothesis, provided the failure modes in both structural systems would be consistent.

In Canada some oriented strand boards mills have the capability to produce panels of up to 3.3 x 7.3 m in size. Currently these large panels are cut into standard sizes for conventional building practice. Potential structural advantages of using the larger dimension panels need to be investigated and quantified especially for commercial construction where building geometry such as height, length, and width typically exceeds those in residential construction. Here, larger lateral forces will be introduced into the building systems and the use of prefabricated shear wall systems using the large nonstandard panels is especially well suited. Furthermore, with a comprehensive database and verified model, optimization of the wall assembly is possible through reduction of panel thickness, redistribution of the nailing pattern, and shortening of the required length of wall while achieving the same lateral capacity as walls built with regular size panels.

The overall objectives of the research program are:

- 1) to experimentally investigate and quantify the structural performance of shear wall systems built with nonstandard large dimension oriented strand board panels under

static and dynamic lateral loading to take advantage of the reduced discontinuity compared to standard size panels.

- 2) to develop analytical and design procedures for the seismic performance of wood based shear wall systems built with nonstandard large dimension panels.

In the first phase of the research program, an experimental study was conducted to develop a database on the structural performance of shear wall systems built with nonstandard large dimension oriented strand board panels under monotonic and cyclic loading conditions. This paper reports: 1) the development of a test facility for shear walls of up to 1.2 x 7.3 m in dimension where both lateral and vertical loading can be applied simultaneously onto the wall assembly and 2) a summary of experimental results from the first test series comparing the monotonic and cyclic responses of shear walls built with standard and oversized panels and different types of nail connectors.

Experimental Studies

Test Facilities

Figure 1 shows the schematics of a typical shear wall test specimen with staggered regular size sheathing panels. The test specimen was mounted in the load assembly with variable in-plane lateral load applied by a 222 kN servo-controlled hydraulic actuator along the top of the wall through a load distribution beam that was bolted to the wall. The actuator with an inline load cell was mounted onto the reaction frame through a pin connection 2.5 m from the ground. A MTS Micro-controller (458.10) and Material Testing Function Generator (Exact-340) were used to drive the actuator in a displacement control mode to develop the required lateral loading pattern.

To facilitate the set-up procedure, the test wall specimen was first mounted between load distribution beam and base beam using 12.7 mm diameter class 5 steel bolts at a spacing of 0.4 m. W150 x 22 steel I beams, 7.6 m in length, were used as the load distribution beam and base beam. After erection, the base beam was attached to the test floor and the load distribution beam was connected to the hydraulic actuator at one end. Out-of-plane support systems were provided at the two ends of the load distribution beam.

Six hydraulic jacks, each with a working pressure capacity of 17.24 MPa, were mounted to the test floor at the base and attached through 2.1 m long steel rods (diameter 12.7 mm) to the top of load distribution beam. Three jacks were mounted on each side of the wall and symmetrically placed about the center of the wall with a spacing of 2.4 m. These jacks provided a static uniformly distributed vertical load on the wall through the top of the load distribution beam. In all of the tests a vertical load of 9.12 kN/m was used which represented a gravity load of 5.0 kPa over an area of 7.3 x 7.3 m, supported by 4 walls.

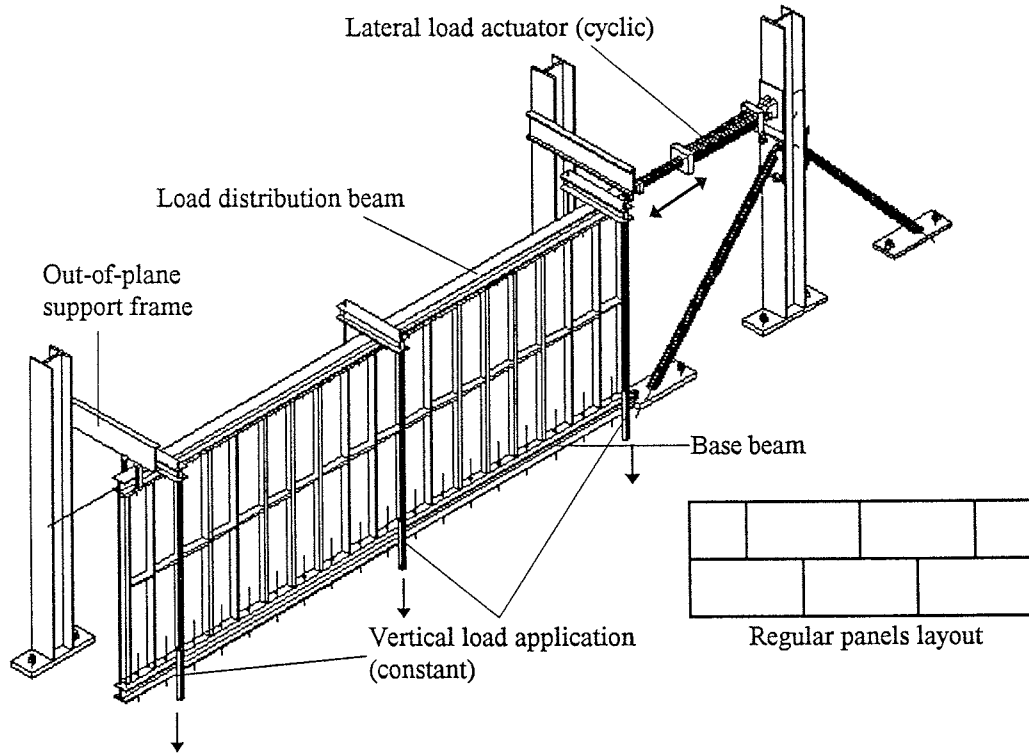


Figure 1 The scheme of the shear wall test setup assembly

A 386/25 personal computer data acquisition system with 16 A/D channels and LabTech Notebook data acquisition software were used to collect the experimental data which included the lateral load, vertical load, actuator displacements, lateral displacements at the top of the shear wall, uplift at the base of the shear wall, and relative movements between panel and frame at various locations. The sampling frequencies were 1 Hz for the monotonic load condition and 10 Hz for cyclic load conditions.

Test Wall Configurations

Shear walls, 2.4 x 7.3 m in dimension, were tested. In each wall, No. 2 and better Spruce Pine Fir 38 x 89 mm lumber were used as framing members and connected by a Bostitch-N80CB air driven nail gun with coil fed 76 mm common nails. The stud members (2.4 m in length) were spaced 400 mm apart. The top plate and the end studs consisted of double members while the bottom plate and the interior studs consisted of single members. Performance Rated W24 oriented strand boards (CSA-0325.0-M88), 9.5 mm thick, were used as sheathing panels. The sheathing panels were connected to the framing members with 50 mm common and spiral nails at a spacing of 150 mm along the panel edges and 300 mm for the interior attachment of the sheathing panel to the frame members.

Seven shear walls were tested with one replicate per test type (Table 1). In tests 2, 3, 5, and 6, 2.4 x 7.3 m oversized panels were used. In tests 1, 4, and 7, regular 1.2 x 2.4 m panels were used. In these cases the regular size sheathing panels were staggered and

oriented with the long axis of the panels parallel to the length of the wall as shown in Figure 1. At mid-height of the walls, continuous blocking components were installed in cases 1 and 4 and staggered blocking components were installed in case 7. The installation of the continuous blocking components was done by end-nailing one end of the blocking and toe-nailing the other end to the framing member. The installation of staggered blocking involved only end-nailing. Two types of nails were considered for the sheathing to frame connection: Bostitch-N80CB air driven coil fed 50 mm spiral nails and hand driven 50 mm common nails. The total number of nail connections between panel and framing were 424 (375 for staggered blocking) and 281 for the walls with regular and oversized panels, respectively.

Table 1. Shear wall test program

Wall	Panel size (m)	Blocking	Nails for sheathing	Lateral load Type	No. of nails
1	1.2 x 2.4	Continuous	Spiral (Gun)	Monotonic	424
2	2.4 x 7.3	No	Spiral (Gun)	Monotonic	281
3	2.4 x 7.3	No	Spiral (Gun)	Cyclic	281
4	1.2 x 2.4	Continuous	Spiral (Gun)	Cyclic	424
5	2.4 x 7.3	No	Common (Hand)	Monotonic	281
6	2.4 x 7.3	No	Common (Hand)	Cyclic	281
7	1.2 x 2.4	Staggered	Spiral (Gun)	Monotonic	375

Loading Scheme

Two types of loading scheme were used: monotonic loading for walls 1, 2, 5 and 7 and cyclic loading for walls 3, 4 and 6. The loading rate for the monotonic tests was approximately 7.8 mm/min based on recommendations in the ASTM Standard E564-73 and in compliance with tests done previously by Forintek Canada Corp.

The testing schedule for cyclic loading consisted of a sequence of sinusoidal cycle groups, with each cycle group consisting of three identical cycles. The amplitude of each cycle group was taken as a percentage of the nominal yield displacement (δ_y). This nominal yield point was defined as the displacement at a load level equal to half of the maximum load obtained during a monotonic test. To obtain consistent results for both monotonic and cyclic tests and for the ease of actuator control, the values for the yield points were taken from the displacement of the hydraulic cylinder, instead of that of the shear wall. The yield points, cycle frequencies and other parameters for shear walls 3, 4 and 6 are listed in Table 2.

Table 2. Basic parameters for cyclic testing

Wall	Maximum monotonic test load, P_{max} (kN)	Maximum monotonic test displacement, (mm)	δ_y (mm)	Loading rate	
				Cycle group	Cycle frequency (Hz)
3	82.2	45.0	6.0	1 to 23	0.25
4	62.7	80.0	10.0	1 to 19 20 to 22	0.25 0.083
6	71.1	42.0	6.0	1 to 13 14 to 23	0.25 0.125

The amplitudes of cycle groups as a percentage of the yield point (Am_{per}) for these walls are listed in Table 3. The displacement amplitudes of these cycle groups are also graphically illustrated in Figure 2. It can be noted that the Am_{per} schedule is identical for the various walls up to cycle group 18. Typically at this cycle group, the maximum load had already been well exceeded. Both the Am_{per} schedules and the cycle frequencies were adjusted beyond cycle group 18 so that the hardware data storage capability was not exceeded.

Table 3. Displacement amplitude schedule of various cycle groups as a percentage of δ_y .

Cycle Group	Wall No. 3	Wall No. 4	Wall No. 6	Cycle Group	Wall No. 3	Wall No. 4	Wall No. 6	Cycle Group	Wall No. 3	Wall No. 4	Wall No. 6
1	25%	25%	25%	11	200%	200%	200%	21	450%	700%	450%
2	50%	50%	50%	12	300%	300%	300%	22	600%	800%	600%
3	25%	25%	25%	13	250%	250%	250%	23	750%		700%
4	100%	100%	100%	14	350%	350%	350%				
5	50%	50%	50%	15	300%	300%	300%				
6	150%	150%	150%	16	400%	400%	400%				
7	100%	100%	100%	17	350%	350%	350%				
8	200%	200%	200%	18	450%	450%	450%				
9	150%	150%	150%	19	400%	500%	400%				
10	250%	250%	250%	20	500%	600%	500%				

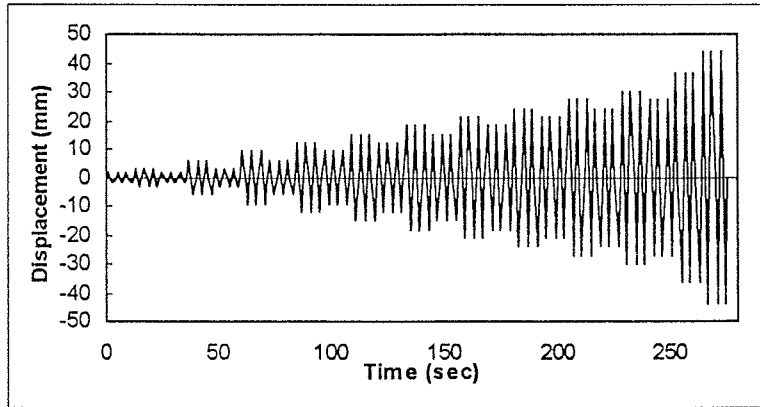


Fig. 2 Typical displacement amplitudes for cycle testing

Results and Discussions

Wall Performance

The load-displacement curves for shear walls 1, 2, 5 and 7 under monotonic lateral load are shown in Figure 3. Here the displacement is taken as the lateral displacement of the top corner of the wall. Figures 4 to 6 show the static envelope curves and the cyclic load displacement curves for walls 3, 4, and 6, respectively.

In compliance with ASTM Standard E 564-76 and the calculation methods used by Forintek Canada Corp., the following parameters (shown in Table 4) were obtained:

- P_{max} : the maximum load carrying capacity of shear wall, kN.
- δ_{max} : total displacement of shear wall at failure, measured at the top plate of shear wall, which includes both the shear deflection of the wall and deflections caused by the anchorage system, mm.
- $\delta_{P_{max}}$: displacement of shear wall at the maximum load, mm.
- $\delta_{0.5 P_{max}}$: the displacement of shear wall at half of the maximum load, mm.
- S_u : ultimate shear strength of shear wall, N/m.

$$S_u = \frac{P_{max}}{L}$$

where: L = length of shear wall measured parallel to the loading direction.

- G' : shear stiffness of shear wall obtained from test, N/m.

$$G' = \frac{P_{max} H}{2 \delta_{0.5 P_{max}} L}$$

where: H = height of shear wall = 2.438 m.

- D : ductility factor.

$$D = \frac{\delta_{P_{max}}}{\delta_{0.5 P_{max}}}$$

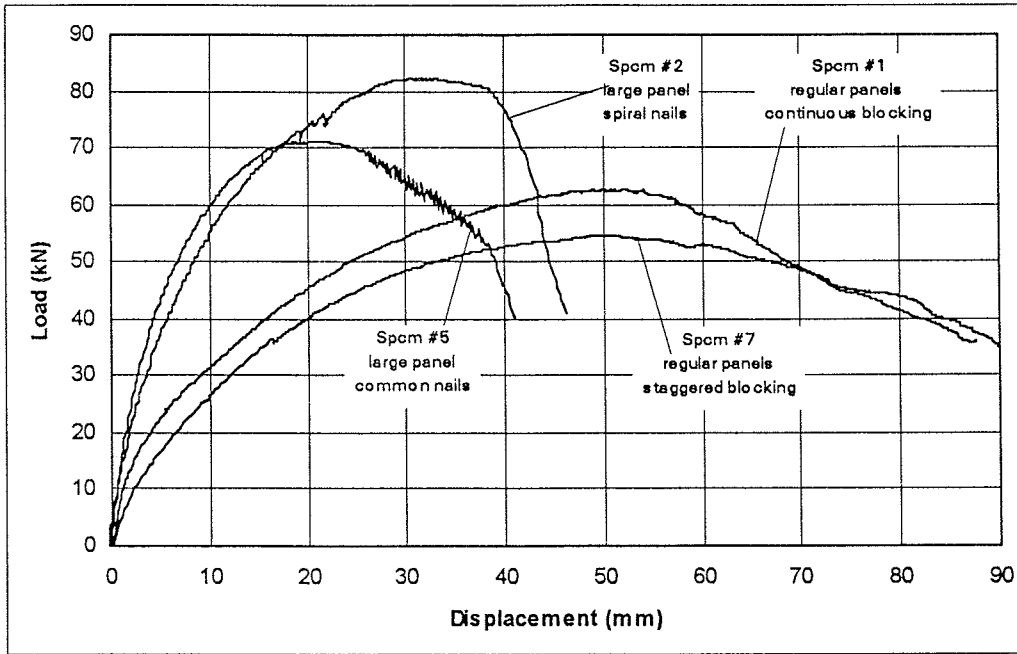


Fig. 3 Load-displacement curves for shear walls 1, 2, 5 and 7

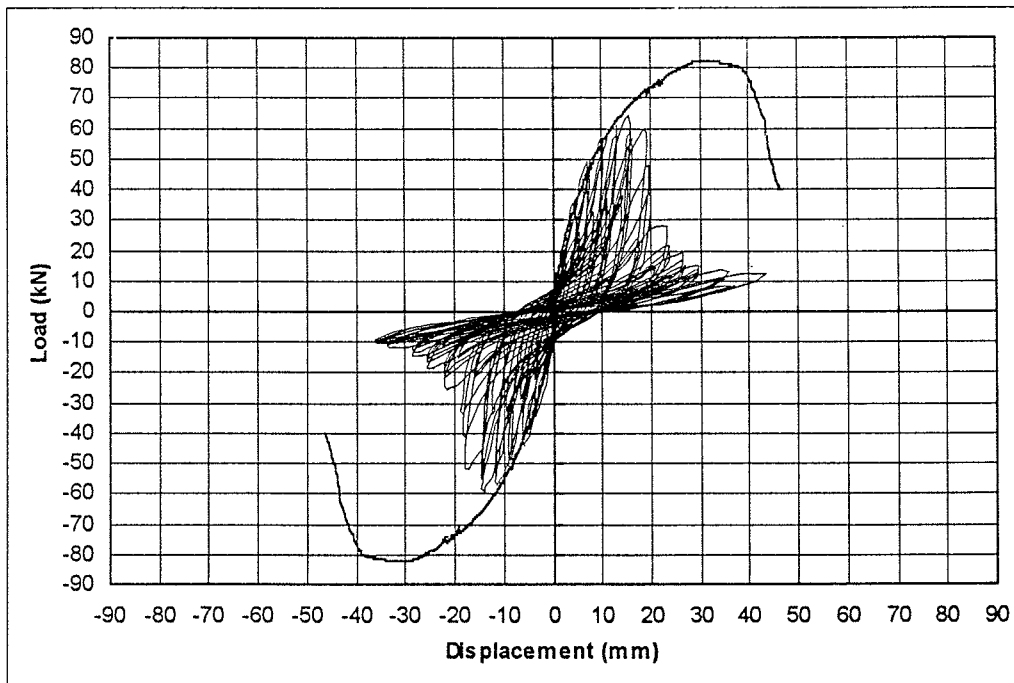


Fig. 4 Cyclic load-displacement curve and the static envelope for wall 3

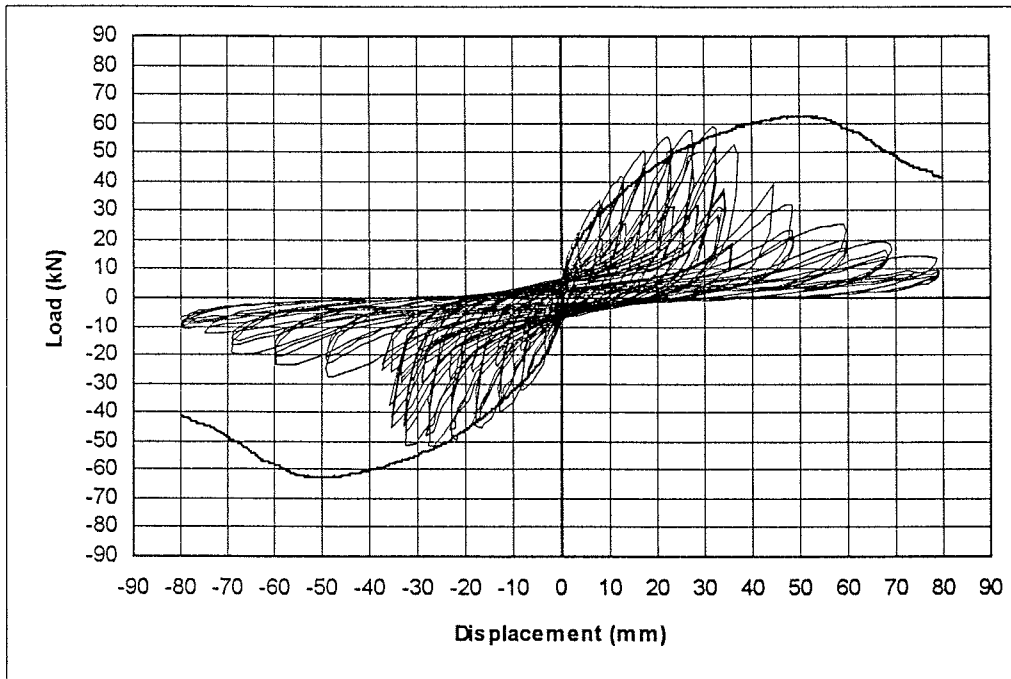


Fig. 5 Cyclic load-displacement curve and the static envelope for wall 4

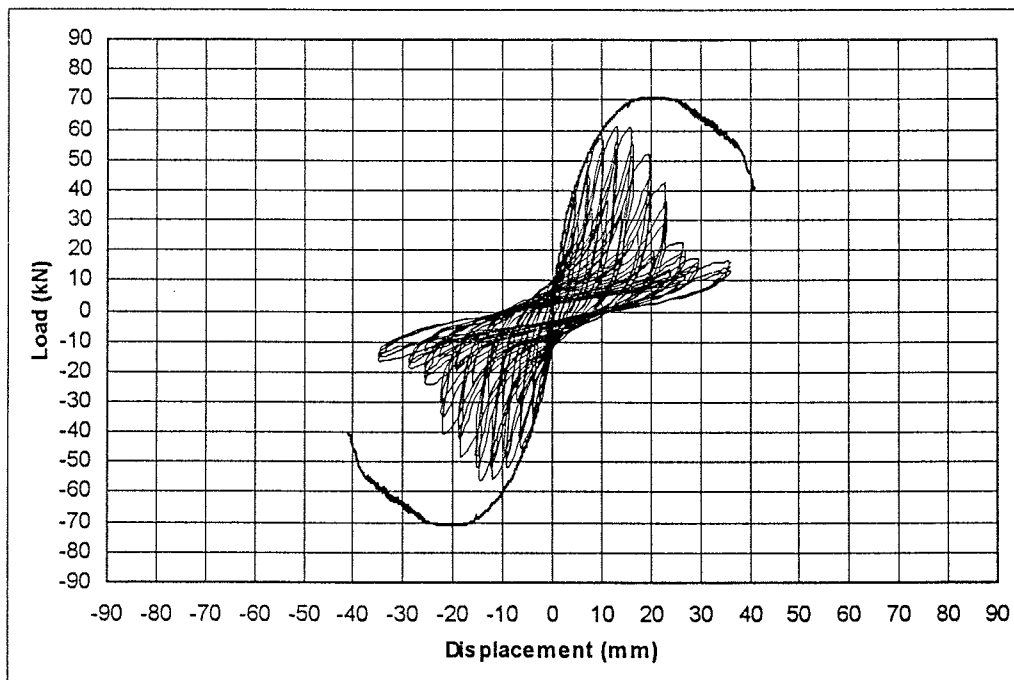


Fig. 6 Cyclic load-displacement curve and the static envelope for wall 6

Table 4. Shear wall summary test results

Wall	P_{max} (kN)	δ_{max} (mm)	$\delta_{P_{max}}$ (mm)	$\delta_{0.5P_{max}}$ (mm)	S_u (kN/m)	G' (MN/m)	D
1	62.77	88	54.04	9.82	8.581	1.07	5.5
4	+59.29, -51.69	80	31.93	12.62	-	-	-
2	82.21	46	33.27	5.88	11.239	2.33	5.7
3	+64.07, -59.40	45	15.60	4.51	-	-	-
5	71.13	42	21.92	3.54	9.724	3.35	6.2
6	+61.25, -56.69	42	15.78	4.56	-	-	-
7	54.73	90	50.97	10.32	7.482	0.88	4.9

Note: + \Rightarrow extension of the hydraulic cylinder, - \Rightarrow contraction of the hydraulic cylinder.

The monotonic test results show that walls 2 and 5 (oversized panels) had higher load carrying capacity, higher stiffness, higher ductility, and lower deformations compared to walls 1 and 7 (regular panels). Common nails were used as panel-to-frame connectors in wall 5 under monotonic test. Wall 5 showed a higher stiffness and a lower strength than wall 2 which implied that the common nails connections were stiffer but weaker than the spiral nail connections. The cyclic test results show that the walls 3 and 6 (oversized panels) had slightly higher load carrying capacity and lower deformations compared to wall 4 (regular panels).

Energy Dissipation

Under cyclic loading, energy dissipation occurred through internal friction, yielding of the nails and non-recoverable deformation (damage) in the wall assembly. A measure of this energy dissipation was obtained by evaluating the area of the hysteresis loops from the load-displacement curves for each load cycle. For walls 3, 4, and 6, the dissipated energy within each cycle group (U_i) and the total dissipated energy at the end of a cycle group (U_{Ti}) are shown in Table 5. Figures 7 to 8 also graphically illustrate the energy dissipation characteristics of the walls. Since slight differences exist in loading schedule, the results are only comparable up to cycle 18. It is clear that more energy dissipation occurred in wall 4 (regular panel) compared to walls 3 and 6 (oversize panel). The maximum amount of energy dissipated within a cycle group occurred in cycle group 14 in all three cases. Figure 9 shows the normalized dissipated energy within a cycle group as a percentage of the peak dissipated energy in cycle group 14. It can be observed that the normalized dissipated energy of all 3 walls was similar until cycle group 14 after which the normalized dissipated energy significantly reduced in wall 3.

Table 5. Dissipated energy in shear wall during cyclic loading.

Cycle Group No. i	Wall 3		Wall 4		Wall 6	
	U_i (N m)	U_{Ti} (N m)	U_i (N m)	U_{Ti} (N m)	U_i (N m)	U_{Ti} (N m)
1	19	19	70	70	17	17
2	99	118	248	318	103	120
3	19	137	60	378	20	140
4	394	531	755	1133	430	570
5	96	627	181	1314	95	665
6	741	1368	1267	2581	816	1481
7	291	1659	451	3032	375	1856
8	1138	2797	1845	4877	1262	3118
9	551	3348	824	5701	666	3784
10	1516	4864	2475	8176	1713	5497
11	837	5701	1227	9403	984	6481
12	1881	7582	2985	12388	1923	8404
13	1103	8685	1662	14050	1073	9477
14	1919	10604	3339	17389	1920	11397
15	778	11382	1977	19366	1100	12497
16	1033	12415	2900	22266	1817	14314
17	531	12946	1950	24216	893	15207
18	765	13711	1837	26053	1260	16467
19	429	14140	2415	28468	765	17232
20	618	14758	2459	30927	1034	18266
21	392	15150	2247	33174	688	18954
22	572	15722	2898	36072	1075	20029
23	536	16258			834	20863

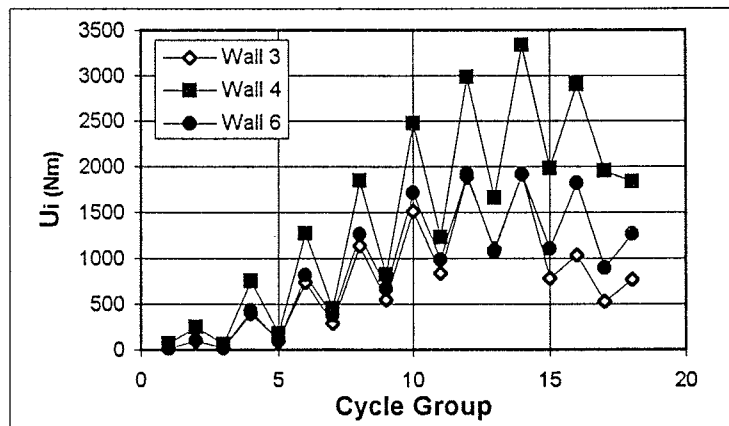


Figure 7 Energy dissipation characteristics within each cycle group (U_i) of walls 3, 4 and 6

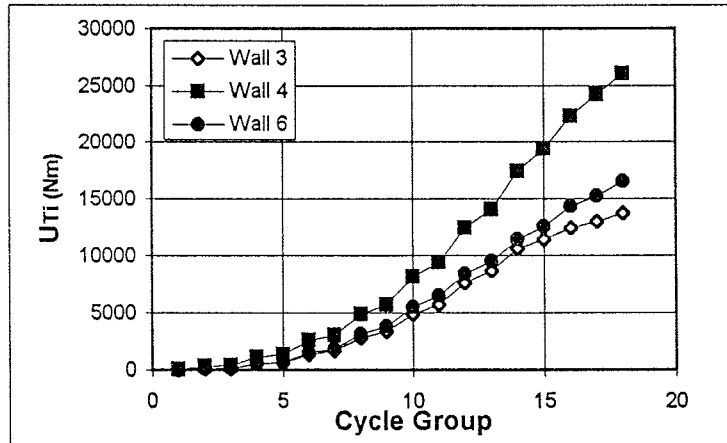


Figure 8 Cumulative energy dissipation (U_{Ti}) of walls 3, 4 and 6

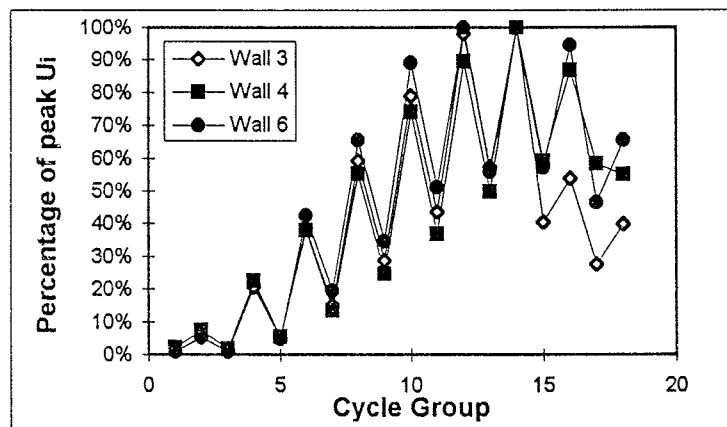


Figure 9 Normalized dissipated energy within a cycle group as a percentage of the peak dissipated energy in cycle group 14

Failure Modes and Locations

In the monotonic tests of walls 1 and 7 (regular panels), connection failures were first observed at the edges of panels along the blocking. The failures were initially in the form of nail withdrawal (Figures 10a and b) from blocking and framing members and eventually from nail heads embedding into and pulling through the panels. In the monotonic tests of wall 2 and 5 (oversized panels) connection failures initiated along the bottom edge of the wall in the form of nail withdrawal (Figures 10a and b) from the framing members and progressed upward towards the mid-height of the wall.

Under cyclic load, the predominant failure mode was different from the monotonic load cases, although failure occurred at the same locations. Instead of nail withdrawal, most connectors failed in low cycle fatigue fracture (Figure 10c) due to reversed bending. For

example, along the bottom edge of walls 4 (regular panel) and 6 (oversize panel), 100% and 84% of the nails failed in fatigue fracture, respectively.

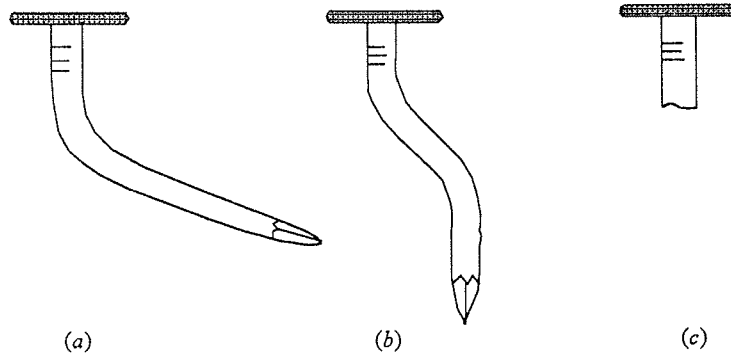


Figure 10 Three deformation patterns of nails

The observed distinct difference in failure mode between monotonic and cyclic loading led to the question of which failure mode should be considered critical for realistic dynamic lateral earthquake and wind loading. Careful correlation between static and dynamic test results is needed to fine tune the static testing schemes and to fully understand and characterize the relevant failure modes in shear walls under earthquake loads.

Conclusions

A database comparing the structural performance of shear wall systems built with regular and nonstandard large dimension oriented strand board panels under monotonic and cyclic loading conditions was reported. Under monotonic loading, a substantial increase in both stiffness and lateral load carrying capacity was observed when comparing shear walls built with oversize and regular panels. Defining ductility as the ratio between wall displacements at maximum load and 50% of the maximum load during monotonic testing, a slight increase in ductility was observed comparing the shear walls built with oversize and regular panels. Examining the dissipated energy as the area under the load deformation curve, walls built with the regular panel dissipated more energy under cyclic loading as compared to walls built with oversized panels. The failure modes in the shear walls were substantially different under monotonic (nail withdrawal) and cyclic (nail fatigue) test conditions. Further investigation of the adopted cyclic load schedule in relation to the dynamic response of the shear wall is needed to fully understand and characterize the failure modes in shear walls.

References

Adams, N.R. (1987) Plywood shear walls. Res. Rep. 105. American Plywood Association, Washington, USA.

Annual Book of ASTM Standards (1991) Standard Method of Static Load Test for Shear Resistance of Framed Walls for Buildings (ASTM standard E 564-76), Vol. 04.07, Philadelphia, USA.

Atherton, G.H. (1982) Ultimate strength of structural waferboard and particleboard diaphragms. Forest Res. Lab., Oregon State Univ., Oregon, USA.

Atherton, G.H. (1983) Ultimate strength of particleboard diaphragms. Forest Prod. J. 33(5):22-26

Boughton G.N. (1988) Full-scale structural testing of houses under cyclonic wind loads. Proc. 1988 Int. Timber Engrg. Conf., Seattle, USA, 2:82-87.

COFI (1979) Douglas-fir plywood diaphragms. Council of Forest Industries of British Columbia, British Columbia, Canada.

Dolan, J.D. (1989) The dynamic response of timber shear walls. Ph.D. Dissertation, Dept. of Civil Engineering, Univ. of British Columbia, Vancouver, Canada.

Kamiya, F. (1988) Nonlinear earthquake response analysis of sheathed wood walls by a computer actuator on-line system. Proc. 1988 Int. Timber Engrg. Conf., Seattle, USA, 1:838-847.

Karacabeyli, E. (1995) Lateral resistance of nailed shear walls subjected to static and cyclic displacements. Proc. FPS 1995 Annual Meeting, Section on Seismic Safety of Timber Structures, Portland, Oregon, USA, pp.6.

Stewart, A.H., J.R. Goodman, A. Kliwer and E.M. Salsbury (1988) Full-scale tests of manufactured houses under simulated wind loads. Proc. 1988 Int. Timber Engrg. Conf., Seattle, USA, 2:97-111.

Stewart, W.G. (1987) The seismic design of plywood sheathed shearwalls. Ph.D. Dissertation, Dept. of Civil Engineering, Univ. of Canterbury, Christchurch, NZ.

Sugiyama, H., N. Andoh, T. Uchisako, S. Hirano and N. Nakamura (1988) Full-scale test of a Japanese type two-story wooden frame house subjected to lateral load. Proc. 1988 Int. Timber Engrg. Conf., Seattle, USA, 2:55-61.

TECO (1980) Summary of racking tests conducted on waferboard sheathing. Report to the Canadian Waferboard Association. TECO, Oregon. USA.

TECO (1981) Racking load test report on 3 application procedures of 7/16 inch waferboard. Report to the Canadian Waferboard Association. TECO, Oregon. USA.

Tissel, J.R. and J.R. Elliott (1977) Plywood diaphragms. Res. Rep. 138. American Plywood Association, Washington, USA.

Wood Reference Handbook (1991) Canadian Wood Council, Ottawa, Canada

Acknowledgments

The authors gratefully acknowledge funding support received from the Structural Board Association and the National Research Council-Industry Research Assistant Program. Ainsworth Lumber Co. is also thanked for providing the testing material. Forintek Canada Corp. and NSERC are acknowledged for providing funding support to the research program of the first author (FSP0166869). Finally the technical contributions from P. Symons, D. Janssens, and E. Karacabeyli in the research program are acknowledged.

INTERNATIONAL COUNCIL FOR BUILDING RESEARCH STUDIES AND DOCUMENTATION

WORKING COMMISSION W18 - TIMBER STRUCTURES

**DAMAGE OF WOODEN BUILDINGS CAUSED BY THE 1995 HYOGO-KEN NANBU
EARTHQUAKE**

by

M Yasumura
Sizuoka University

N Kawai
N Yamaguchi
S Nakajima
Building Research Institute
Japan

MEETING TWENTY - NINE

BORDEAUX

FRANCE

AUGUST 1996

DAMAGE OF WOODEN BUILDINGS CAUSED BY THE 1995 HYOGO-KEN NANBU EARTHQUAKE

M YASUMURA, Sizuoka University

N KAWAI, N YAMAGUCHI, S NAKAJIMA, Building Research Institute,
Japan

Introduction

A strong earthquake occurred in Hanshin area in the early morning of 17 January, 1996. It caused the largest scale of damages since after the second world war. Over 6,300 persons were killed or lost, over 43,000 persons were injured and about 400,000 buildings were damaged. A large number of fatalities were caused by the collapse of wooden houses. Building Research Institute conducted a survey on the damaged wooden houses due to the 1995 Hyogo-ken Nanbu earthquake. This report presents the outline of the damages of wooden houses and discusses the aseismic design of timber structures in Japan.

Outline of earthquake and damage

(1) Outline of earthquake (Announcement of the Meteorological Agency)

Date of occurrence: 17 January, 1995 at approximately 5:46 a.m.

The seismic center: Awaji Island

The depth of the seismic center: 14km

Magnitude: $M=7.2$

(2) Damages (Investigated by the Fire Defense Agency and summing up on 27 December 1995)

Fatality: 6,308 persons (including of the 789 related to this earthquake)

Missing: 2 persons

Seriously injured: 1,883 persons

Slightly injured: 26,615 persons

Under investigation: 14,679 persons

Completely destroyed houses: 100,302 units

Partial destroyed: 108,741 units

Slightly damaged: 222,373 units

Public building: 750 units

Other building: 3,952 units

Number of fires: 294

Damage portions of roads: 9,948

Outline of damage of wooden houses

(1) Classification of wooden houses in Kobe area

Wooden houses in damaged area are briefly classified into the following three types according to the structure and the constructed period.

S1: Wooden houses having the clay wall and heavy tile roof with clay pad. In general they have very few or no diagonal braces.

S2: Wooden houses having the clay wall finished with the lath mortar and tile roof with clay pad. They have a certain amount of diagonal braces and continuous concrete foundation.

S3: Wooden houses having no clay wall sheathed with lath-mortar or sidings. Sometimes thermal insulation is used. Interior walls are generally sheathed with gypsumboard or lathboard. They have slates or tile roof without clay pad, and diagonal braces or plywood-sheathed shear walls.

It is estimated that houses of S1 type were constructed before or just after the World War II. Houses of S2 and S3 types are estimated to be constructed at the period from 1955 to 1975, and after 1975, respectively.

(2) Outlines of Damages

Damages of wooden houses in Nagata, Nada, and Higashinada ward were surveyed. Figs. 1 to 3 show the damages of each type of wooden houses in a block where wooden houses were severely damaged. Fig.1 shows that the number of S1 type houses was the highest in the surveyed area of Nagata ward, and followed by S2 and S3. In Nada and Higashinada ward, the number of S2 type houses was the highest, and followed by S3 and S1. The rate of severely damaged wooden houses was approximately 80% in both types of S1 and S2. In S3 type, the rate of severely damaged houses was 30 to 50%, and smaller than that of S1 and S2 in all the area. Here, the severe damage is defined by the residual story drift of more than $1/20$, the moderate damage is defined by the residual story drift from $1/60$ to $1/20$, and the light damage is defined by the residual story drift of less than $1/60$.

A large number of wooden buildings collapsed or were severely damaged by this earthquake. Most of collapsed buildings were one or two story dwellings in which the structural calculation was not required. The degree and state of the damages depend on the kinds and the construction method.

Photo. 1 shows a typical example of the damaged wooden houses in Nagata ward. Whole the building collapsed completely. This type of damage occurred mainly in old wooden houses constructed before or just after the World War II. Photos. 2 to 5 show the damages of wooden buildings whose first story collapsed. This damage

took place generally in wooden houses constructed of the clay wall and heavy tile roof with clay pad. Some newly constructed wooden houses also collapsed as shown in Photos. 4 and 5. Having a garage in the first story, this building of Photo. 4 did not have the sufficient amount of shear walls, and also the shear walls were placed eccentrically in the first story. The third story of the building of Photo. 5 was extended afterwards, and was lacking the seismic consideration.

Photos. 6 and 7 show the damage of the comparatively new wooden houses having a reinforced concrete garage in the first story. The first level of wooden structure of Photo. 6 collapsed completely. In general these houses have less shear wall in front of the second story, and heavy balconies in the third story.

Photos. 8 and 9 show the damages of the dwellings whose width was very narrow. This type of buildings have generally very few or no shear walls in front of the building. A number of dwellings of this type were damaged. This type of damages were also observed in the buildings having a shop in the first story. Having a large space in the first story and eccentrically placed shear walls, a number of buildings of this type were severely damaged.

Photo. 10 shows the damages of the exterior mortar. The lath-mortar has been used for the exterior in urban area since roughly 40 years ago because of the fire safety. In many houses, the exterior mortar was peeled off because of the inadequate connection between the lath-mortar and sheathings.

Photos. 11 and 12 shows a non-damaged three-story house of conventional wooden post and beam house and a prefabricated house. These buildings designed by the structural calculation showed in general very few or no damages even in high seismic area.

(3) Major causes of typical damages

The majority of the collapsed wooden buildings were old houses of post and beam construction consisting of the clay walls and heavy tile roof with the clay pad. These buildings having no diagonal braces, or very few if any, had comparatively long natural period and insufficient lateral resistance to support the mass of the building. The insufficient reinforcement of the traditional tenon-type joints is also one of the causes of the collapse. In some old houses, the length of the tenon was not sufficient and the members were not connected in adequate way.

Some wooden buildings constructed recently also collapsed or were severely damaged. Most of them were conventional post and beam construction having large openings in the first story. This design appears often in the dwellings whose width is extremely narrow or those whose first floor is a shop. As the shear stiffness of the floor diaphragm of conventional construction is generally low, a large horizontal

displacement occurs in front of the building having very few or no shear walls.

The inadequate application of the diagonal braces is also one of the causes of the damage of wooden buildings. In most cases, braces were connected to the post and horizontal members such as a girder and a sill with only few nails, and the posts and the horizontal members themselves were not connected in an adequate way. These braces do not work sufficiently not only as tension member but also as compressive member.

The second story of some wooden buildings having a reinforced concrete garage in the first story were severely damaged. It is supposed that the first level of the wooden structure was shaken excessively because of the difference of mass and stiffness between the reinforced concrete and the wooden structure, however further study should be done to verify this fact.

Generally speaking, wooden buildings constructed with the North American Wood Frame Construction Method, prefabricated panel structure, three story wooden buildings designed by the structural calculation and well designed conventional wooden post and beam buildings resisted well against the strong earthquake.

Strength of wooden houses and damage grade

One of the main causes of the damage of wooden houses is the lack of the sufficient shear walls. Therefore, thirty one damaged and undamaged houses were investigated precisely.

(1) Mass of the building

The mass of the building was obtained from the following weight of elements;

Roof tiles without clay pad (including of rafter and ceiling): 120kg/m^2

Roof tiles with clay pad (including of rafter and ceiling): 160kg/m^2

Metal roof: 70kg/m^2

Slate roof: 70kg/m^2

Lath-mortar wall: 90kg/m^2

Siding wall: 90kg/m^2

Gypsumboard wall: 40kg/m^2

Floor: 60kg/m^2

The length of eaves was assumed to be 45cm, and a half of the weight of the wall was considered for the opening. the live load was assumed to be 60kg/m^2 .

(2) Shear strength of shear walls

The load-displacement relationship of typical shear walls and non-structural walls were assumed as follows from the experimental results of racking test of wall panels.

Table 1 shear strength of walls (N/m)

Displacement	h/500	h/120	h/40
30x90mm brace	588	2352	3920
45x90mm brace	588	2352	4704
Lath-mortar	784	1568	1960
Clay wall	392	980	1078
Gypsumboard wall	686	1666	2646

h: height of wall

The allowable strength(Q_y) and the maximum strength(Q_u) of the building were obtained from the sum of the product of the wall length and the load for h/120 and h/40 respectively.

(3) Results

Fig. 4 shows the relationship between the shear wall ratio and the damage grade of wooden buildings. Here, the shear wall ratio is the ratio of the total effective length of shear wall(smaller value of total wall length in two directions multiplied by the wall multiplier prescribed in building code) to the required wall length in building code(1). It indicates that the buildings which satisfy the shear wall ratio of 1.0 generally show light damage, and those which do not satisfy the required wall length show comparatively severe damage.

Figs. 5 and 6 show the relation between the ratio of the allowable load (load for h/120 displacement) to the weight of building (Q_y/Mg) and the ultimate load (load for h/40 is considered as ultimate) to the weight of the building (Q_u/Mg) and the damage grade. Fig. 5 shows that the average value of Q_y/Mg of the buildings whose damage grade was 1 and 2 was approximately 0.2, and those of the damage grade 4 were below 0.2. Fig.6 shows that average value of Q_u/Mg of the buildings whose damage grade was 1 or 2 was 0.34, and those of the damage grade 4 was 0.05 to 0.2 except for one. These fact indicate that the building designed with base shear of 0.2 and having the ultimate base shear of 0.34 have less possibility to be damaged by the severe earthquakes. In this study, the effect of small walls, 3D effects, etc. were not included. Further study should be done on these subjects.

References

- 1) M.O.C., Building Standard Law, Enforcement Order
- 2) B.R.I; A Survey Report for Building Damages due to The 1995 Hyogo-ken Nanbu Earthquake, March 1996

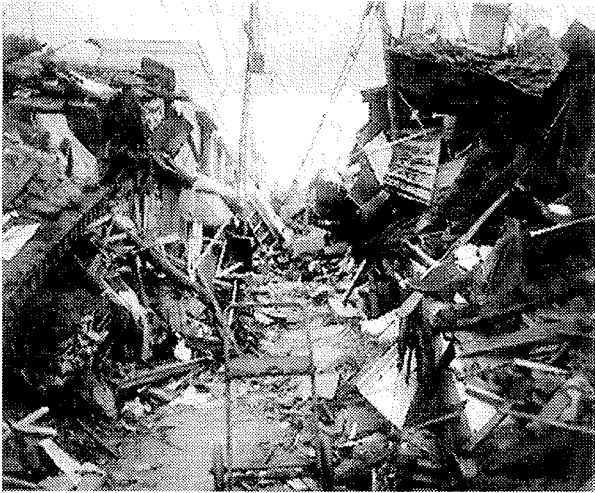


Photo.1 - Collapsed of wooden houses in Nagata ward.

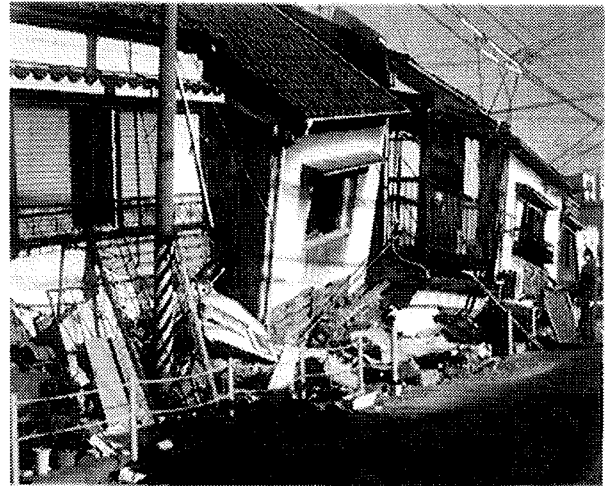


Photo.2 - Houses whose first story collapsed.

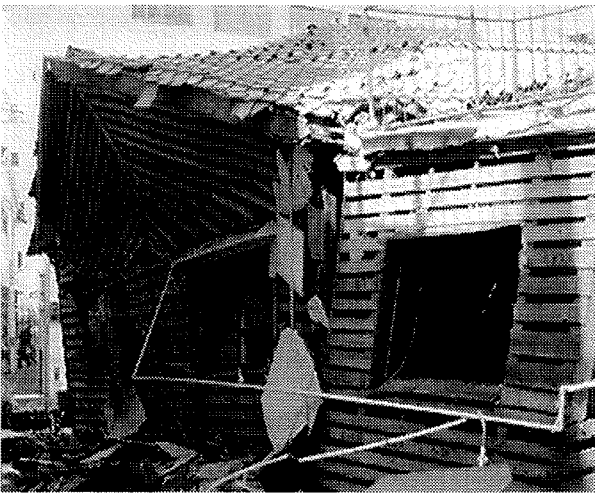


Photo.3 - Collapse of the first story.



Photo.4- Collapse of newly constructed house. The first story was garage and the displacement of shear wall was eccentric.



Photo.5 - Collapse of the first story. The third story was added afterwards.



Photo.6 - Collapse of the second story. The first story was a garage of reinforced concrete.

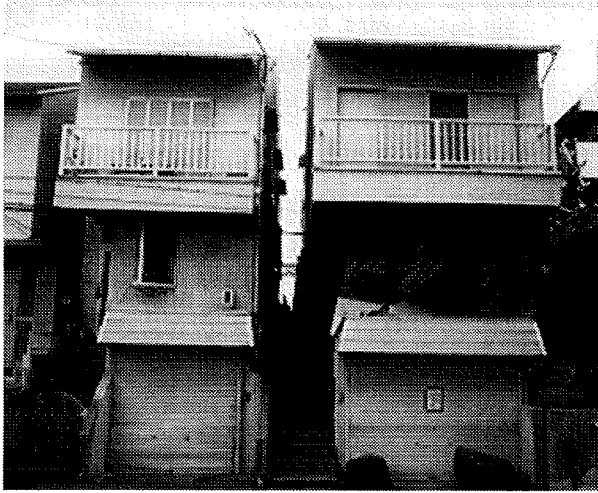


Photo.7 - Damage of the second story. The first story was a garage of reinforced concrete.



Photo.8 - Damage of the first story. No shear walls were placed in front of the house.

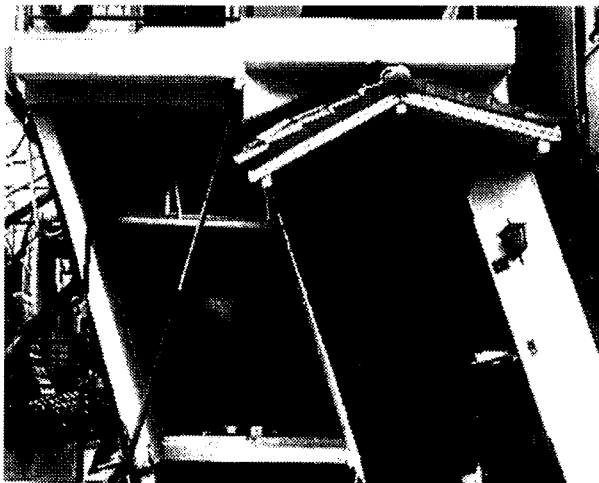


Photo.9 - Very narrow house with few shear walls.

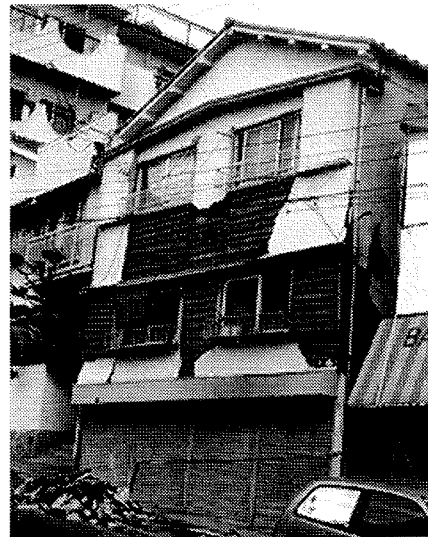


Photo.10 - Damage of the exterior mortar.



Photo.11- Three story conventional wooden house without damage. Well designed houses had no or few damages.

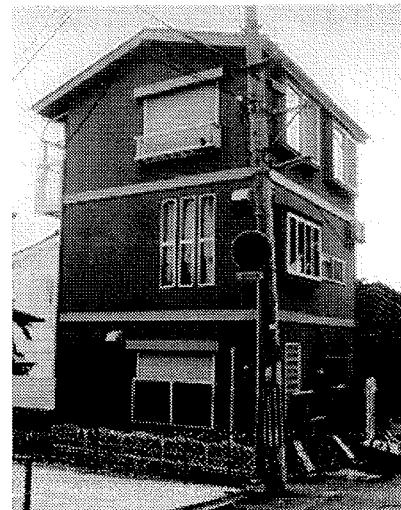


Photo.12 - Three story prefabricated wooden panel house without damage.

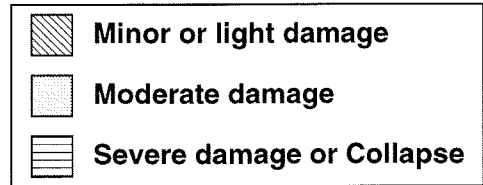
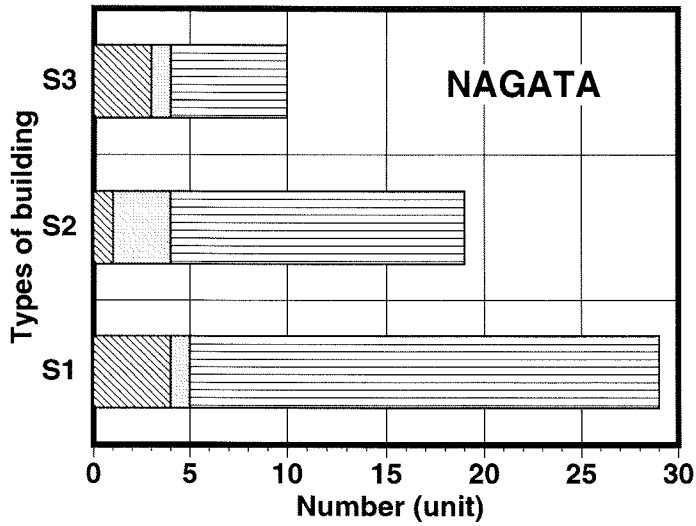


Fig.1 Damage of wooden houses in Nagata ward.

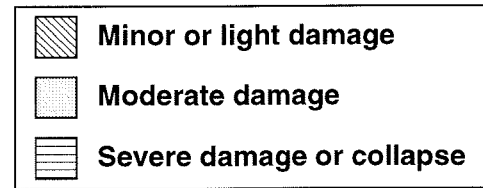
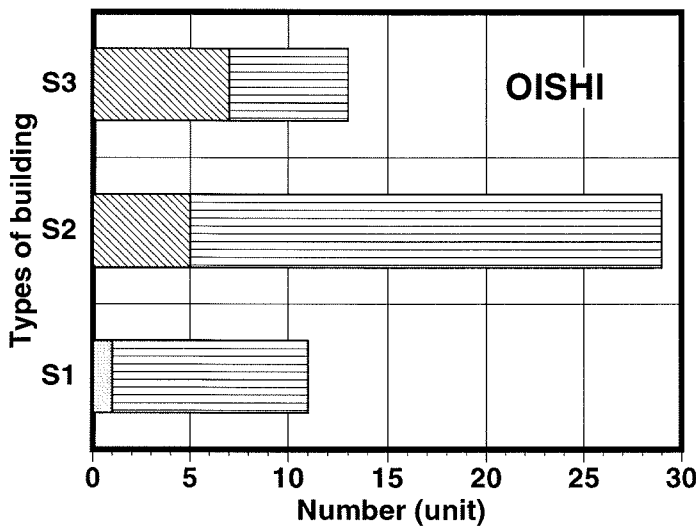


Fig.2 - Damage of wooden houses in Nada ward.

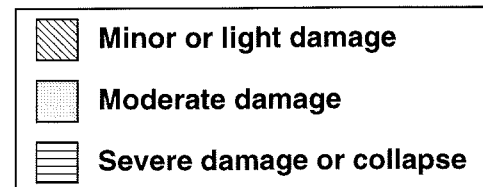
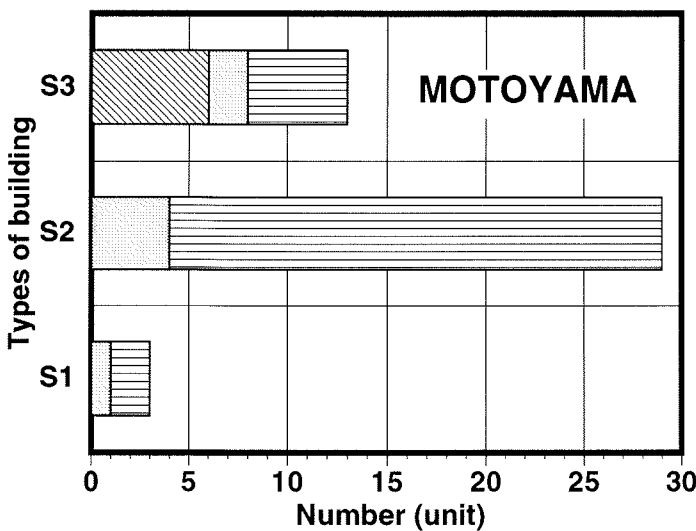


Fig.3 - Damage of wooden houses in Higashi-nada ward.

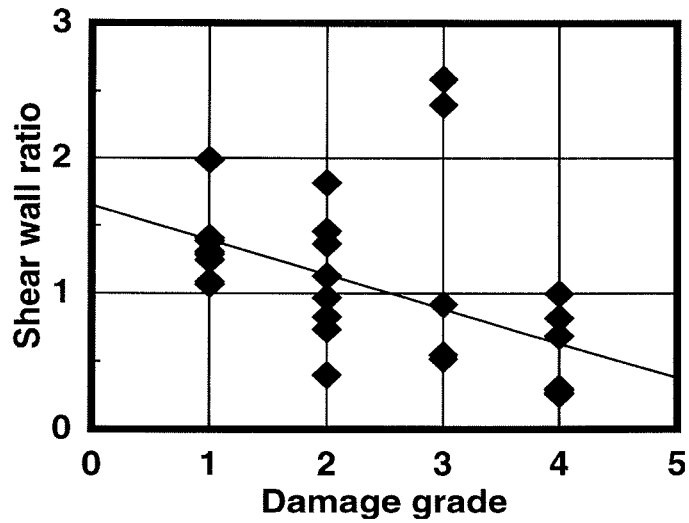


Fig.4 - Relationship between damage grade and shear wall ratio

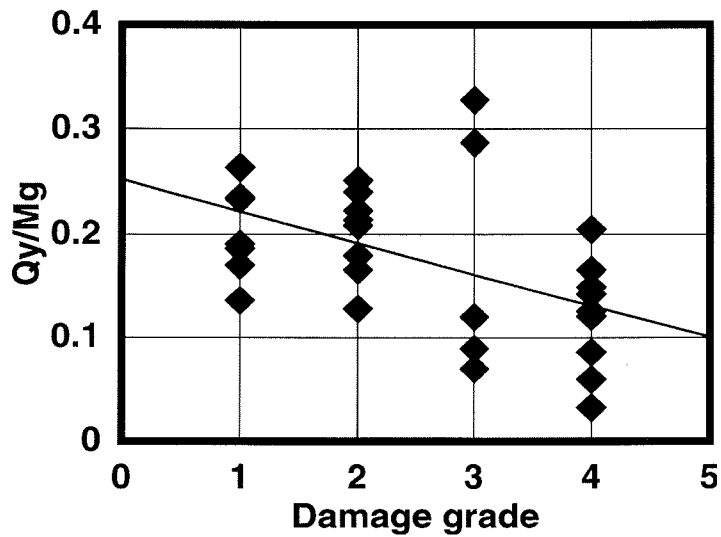


Fig.5 - Relationship between damage grade and the ratio of allowable strength to the weight of building

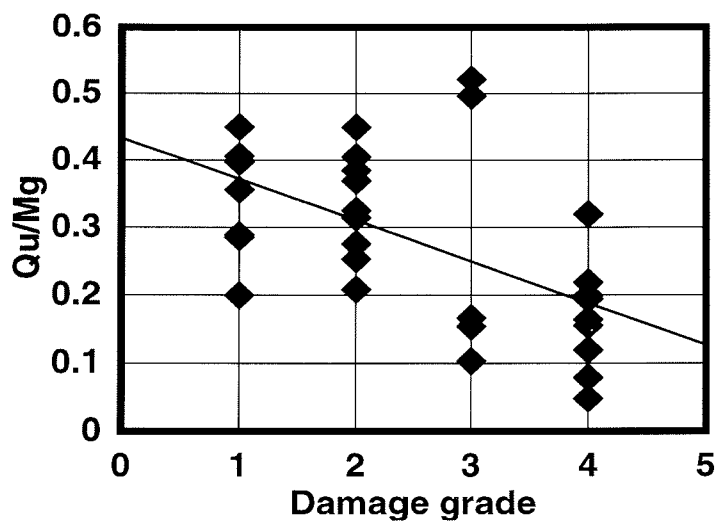


Fig.6 - Relationship between damage grade and the ratio of ultimate strength to the weight of building

Damage grade 1: almost no damage 2: little damage 3: moderate damage 4: severe damage 5: collapse

INTERNATIONAL COUNCIL FOR BUILDING RESEARCH STUDIES AND DOCUMENTATION

WORKING COMMISSION W18 - TIMBER STRUCTURES

**THE RACKING RESISTANCE OF TIMBER FRAME WALLS:
DESIGN BY TEST AND CALCULATION**

by

D R Griffiths

University of Surrey

C J Mettem

TRADA Technology Ltd

V Enjily

Building Research Establishment

P J Steer

Consulting Engineer

United Kingdom

MEETING TWENTY - NINE

BORDEAUX

FRANCE

AUGUST 1996

The Racking Resistance of Timber Frame Walls: Design by Test and Calculation

**by Dr D R Griffiths, University of Surrey, UK
Mr C J Mettem, TRADA Technology Ltd, UK
Dr V Enjily, Building Research Establishment, UK
and Mr P J Steer, Consulting Engineer, UK**

Abstract

This paper introduces work carried out over many years in the UK, on timber frame wall design. It explains why the work was necessary for the national acceptance of timber frame, and demonstrates how knowledge gained is now helping in considering designs for medium-rise timber frame buildings of up to six storeys. Alternative design and test methods are considered, and a justification is given for a top loading test, which leads to an empirically-based design method. This paper is written in preparation for a UK initiative to find a suitable design method for racking resistance to limit-state design principles. The importance of correctly modelling the timber frame behaviour under load is noted, and short design examples are included.

Introduction

Rapid developments of timber frame in the form of prefabricated platform frame panels took place in the UK in the 1960's (Enjily and Mettem, 1996). Historically, the UK had good experience of the use of timber in building. Nevertheless, platform frame was a new form, and the building authorities required it to be fully engineered, even for domestic-scale construction. Consequently, a design method linked to a new test approach was developed, and was first published in Code form in 1988 (BSI, 1988) having been used unofficially in evolving formats for a number of years (Robertson and Griffiths, 1981). In developing the test and design methods, many alternatives were considered, in particular a TRADA approach linked to the ASTM E-72 test. More recently, the test method for timber frame walls has been updated, as a result of European harmonisation. The new EN 594 test for racking resistance (BSI, 1996b) has been published, and has caused the UK code to be updated (BSI 1996a). No changes have been made in the design approach, but the test section has been replaced by one giving guidance on test programmes, and on the reduction of results related to the EN 594 test.

Eurocode 5 (EC5) for the design of timber structures (BSI, 1994) includes a short section on the design of wall diaphragms. This section is not linked to the EN 594 test, and thus no guidance is available on how test results should be reduced for limit-state design. The EC5 method seems to have a similarity to the ASTM/TRADA method. It greatly oversimplifies a timber

frame wall. The method has also been shown to contain design discrepancies, and the UK National Application Document recommends that it shall not be used.

At present, in the UK, the timber frame industry is slowly recovering the share of the domestic market which was suddenly lost as a result of competitor sniping and media hype in 1985. Furthermore, the advantages of prefabricated timber frame have introduced new markets for commercial, residential and industrial developments. Initiatives are underway for medium-rise timber frame buildings, taller than the current commercially constructed maximum of five storeys, and for tall walls with storey heights of up to 4.8m. These initiatives both verify the value of the design code, and present it with a new challenge through the need to increase its scope. Already research has been carried out for tall wall panels (Enjily and Griffiths, 1995) and a programme is being considered for medium-rise projects (Mettem et al, 1996).

It is becoming increasingly important that timber frame research and design is acceptable throughout Europe, and in order to take full advantage of the lead shown by the UK timber frame industry in recent years, the Department of the Environment in conjunction with industry has initiated a "Eurodiaphragms" project. This has the objective of preparing a wall racking design method which is comprehensive in its coverage, yet simple and most importantly, acceptable throughout Europe. This method is to be prepared within the timetable for the revision of Eurocode 5.

General Principles

The general principles underlying the UK design approach to platform frame wall design are as follows:-

- (i) Only the racking resistance (ability to resist horizontal wind forces in the plane of the wall panel) is considered in detail in the relevant section of the design code. Vertical resistance, and horizontal resistance normal to the wall, is covered by standard design methods given in the general code.
- (ii) The racking resistance is assessed for the wall itself, independent of base fixings and return walls, which may either add or detract from overall performance. Normally base fixings should be provided to enable the full wall racking resistance to be achieved.
- (iii) A working stress approach is employed, such that the design value will provide an adequate factor of safety against failure (given that the applied load is short-term), and will ensure that deflections do not exceed 0.003 times the panel height (h).

- (iv) Within a building, both structurally sheathed and semi-structurally lined walls may contribute to racking resistance. The factor of safety applied to linings is increased, and a limitation is placed upon their contribution. Since the true stiffness of walls is not used, the actual distribution of load into the timber frame walls of a building cannot be determined, and three-dimensional effects must be ignored. In general it is adequate to ensure that for the principal wall directions, the design capacity exceeds the applied load. If the make-up of the walls means that there is a major eccentricity between the applied and aggregate resistive forces, the effect on other walls should be checked.
- (v) Brickwork external walls may provide a shielding effect, reducing the load applied to the timber frame, and may also act in conjunction with a structural sheathing, to improve racking resistance. In both cases, the brickwork external and timber internal leaves of the wall must be adequately connected.
- (vi) The design model should reflect as accurately as possible the practical factors which influence racking resistance and which affect test performance, and only practical restraints should be included.
- (vii) In practice, little time and finance is available to consulting engineers for racking checks, due to the types of structure being designed, and the very low occurrence of failures in such structures. It is therefore necessary to keep the design method simple, even though the problem is complex, and the structures themselves are extremely variable.

Racking Resistance Tests

The purpose of the racking test should be to provide information on wall panel strength and stiffness, from which design data can be derived. The method should be capable of covering full-length walls, where the design value will be the performance value for the wall, as well as smaller panels which include all the constituent materials of the walls. In the latter case, the design values can be used as the basis for an empirical design method, which should of course be checked by full-length wall tests.

The most significant requirement for such a test is then to model most accurately the restraints and weakness of the wall or panel in its practical applications. Where the restraints are variable, such as in the base or intermediate fixings of wall units, the test can either take an average situation, or it can take a lower-bound course, and allow strengthening factors to be built in.

Wall racking test proposals involving both horizontal and vertical loading were published in the UK as long ago as 1967, (Lantos). However one of the earliest widely-used wall racking tests was the American ASTM E-72 (ASTM, 1980) procedure. The principle here was to produce pure racking by restricting vertical movement. The leading stud of the wall was therefore

prevented from uplifting by holding-down rods, and as a consequence the base fixings only carried shear forces. Griffiths (unreported) found that the forces generated in the holding-down rods were enormous, and much higher than those identified by applying rules of statical equilibrium to the panel. This was quite simply due to the fact that the panel did not behave as a rigid body.

The holding down enabled high resistance values to be achieved, but placed substantial requirements in actual design conditions upon the panel fixings or top loading. The E-72 test was also problematic, in that it did not measure panel stiffness realistically, and this could not easily be covered, due to the vertical load changing with racking load, and the virtual elimination of vertical slip in the test set up. This had been recognised in the United States, where an alternative E-564 test (ASTM, 1976), had been introduced, involving a zero vertical load procedure.

The UK, unhappy with the E-72 restraints, and after much committee deliberation, adopted the following principles for the BS test method:-

- (i) the base rail is rigidly fixed to the test rig, such that the racking resistance is substantially due to the resistance of the cladding fixings in preventing differential movement of the frame and sheathings or linings.
- (ii) the rest of the frame and claddings are free to move in the plane of the panel.
- (iii) vertical load is applied to the frame, to increase racking resistance.
- (iv) out-of-plane movements are restricted at the top of the panel.

A standard test panel 2.4 m square without openings (see Figure 1) was devised to incorporate the major points of weakness in most normal forms of panel *ie* uplift of sheathings at the connection of the leading stud to the base rail, and sheathings abutting on a common stud. The principal functions of the test procedure were to:

- (i) enable stiffness tests to be carried out at different vertical load conditions, before failing the panel at one vertical load.
- (ii) to measure stiffness over four cycles to 0.002h deflection and the "panel set", *ie* the non recoverable racking deflection, between stiffness cycles.
- (iii) to allow prediction of the load carried by the panel at a deflection of 0.003h, based on the lowest load at 0.002h, and modified if necessary due to unacceptable panel sets.
- (iv) to predict a safe working load, using a factor of safety applied to the maximum load achieved in the failure test, where the deflection rate was no more than 3 mm per minute.

Advice was included in the code on sampling and statistical requirements, and on the reduction of test results to give either a design value for the wall as tested, or a single design value for a zero vertical load condition adequate for both serviceability and strength, noting the UK code to be based on working stress principles. The latter was for use in design within the range of vertical loads for which the panels were tested. The test method was incorporated in the UK timber frame wall code (BSI, 1988).

In 1996, the UK test was replaced by the European EN 594 test. This was identical to the national test in terms of the principles and the standard test panel, but different in its procedures. The new method is based on the standard format for European timber tests, and only allows one vertical load to be considered for each panel. The new test improves on the UK test, in that it is quicker, and it ignores the problem of panel set which imposed a double penalty on weaker sheathings in the UK procedure. However the EN 594 test, being load-based, is more difficult to run, requires a previous knowledge of the estimated failure load, and does not have a suitable approach to the determination of panel stiffness. In the latter case, stiffness is calculated over two cycles, but in setting load limits, the stiffness is seen to increase significantly in the second cycle, and in weaker panels where recovery of the panel on unloading is reduced, the increase in stiffness is amplified, hence a weaker panel records a higher stiffness. The principle adopted in the EN 594 test would be correct, if the panel were to be subjected to load reversal. The EN 594 test standard gives no advice on sampling or use of the test results, and no other Eurocode support document is available to provide any further advice linking the test method with any limit-state design approach. However in the UK, the timber frame code has been adapted (BSI 1996a) to include the new test, and to allow similar reduction procedures to those of the old BS test.

In summary, both the BS and the European test methods can be reduced by the UK procedure, to provide either design values for a particular form of panel, or a lower bound generic design resistance for empirical design purposes. These design loads or resistances are for working stress design, and provide both an adequate factor of safety against failure, and a check that deflections will be limited to $0.003h$. To convert to EC5 philosophy, the methods of reduction would have to be reworked to conform with a limit-state design approach, and in considering the stabilising effects of vertical load, would have to take account of the different load factors, γ_f , for favourable and unfavourable actions.

Further detail on the derivation of data from the UK test methods and on their development is included in a paper accepted for the International Wood Engineering Conference in New Orleans in October 1996 (Griffiths and Wickens, 1996).

History of Design Methods

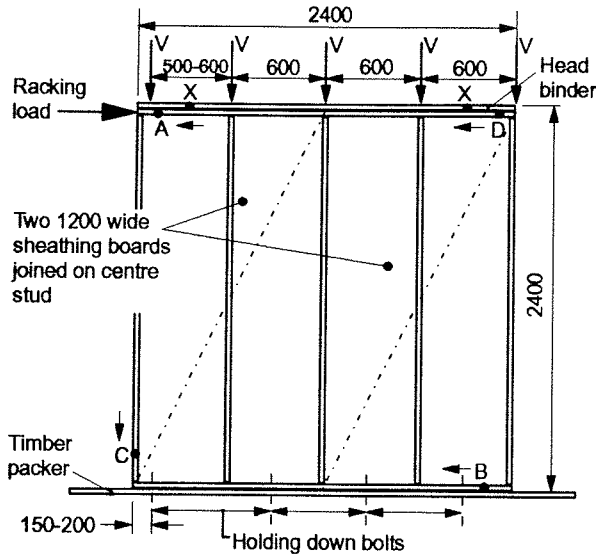
Much empirical design based on the ASTM E-72 was reported by Anderson (1975). Similar procedures were adopted by TRADA for their design manuals, early editions of which were prepared in the 1960's (TRADA 1968). The method was very simple. A racking resistance determined by test as a load per metre run of panel, was applied to the aggregate length of full height panel in a wall to determine its load capacity (see Figure 10). Griffiths (1987) reported in detail on work carried out in the USA and in the UK, on analytical methods related to procedures akin to these ASTM-type tests.

These analytical approaches were complex, due to the number of cladding fixing points in a wall, each of which had a different deformation. The racking load was related to the sum of the fixing resistances, based on an ASTM-type deformation model and, normally a linear elastic fixing response. It was felt that these forms of analysis were too complex for a design method. Furthermore, they did not cover panel stiffness, and they were unlikely to model the ASTM test well, unless they took account of the direction of nail loading and the limited edge- and end-distances required in timber frame walls.

Griffiths also noted the more refined finite element approaches of Gutkowski and Castillo, with their WANELS program, and Foschi with his SADT program. Later, Griffiths adapted the SADT program, and used it to model the UK top loading test (Griffiths, 1987). He demonstrated the importance of modelling nail performances parallel and perpendicular to the framing timber, and in including a failure mechanism for the sheathing material. A plain 2.4m square panel and a similar sized window panel were modelled reasonably accurately for different vertical load cases, covering initial stiffness (deflections up to 5.0mm) and failure (deflections of 40 mm). Further work was needed to refine the model, but it was considered to be purely a research exercise, and not suitable for practical design.

Griffiths' own approach to design had developed from earlier work (Robertson and Griffiths, 1981), and took advantage of the better test information achieved through improvements to the racking test. The wall length and opening factors critical to the design method were based on two major test programmes, covering walls up to 4.8m long.

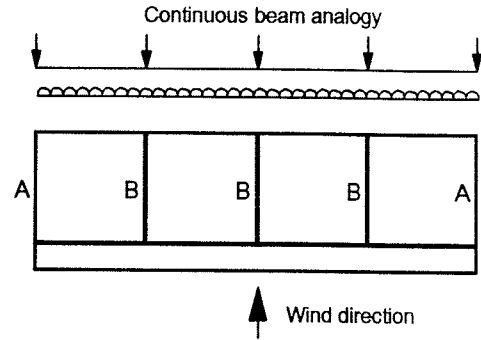
Work was also being carried out on whole-house behaviour, based on testing principles. Griffiths (1987) considered the work of the Cyclone Testing Station at Townsville, Australia to be very significant. They demonstrated the importance of internal walls sheathed with plasterboard, even when poorly fixed, to the overall stiffness and strength of the building. Testing a building where all the external sheathing is broken due to cyclone damage may not seem relevant to UK conditions, but the minimal loss of performance caused by removal of the "structural" component is of great significance. A typical wall layout tested at Townsville is shown in Figure 2.



A, B, C and D are deformation measuring points.
X represents an in-plane stabilisation point.

All dimensions are in millimeters.

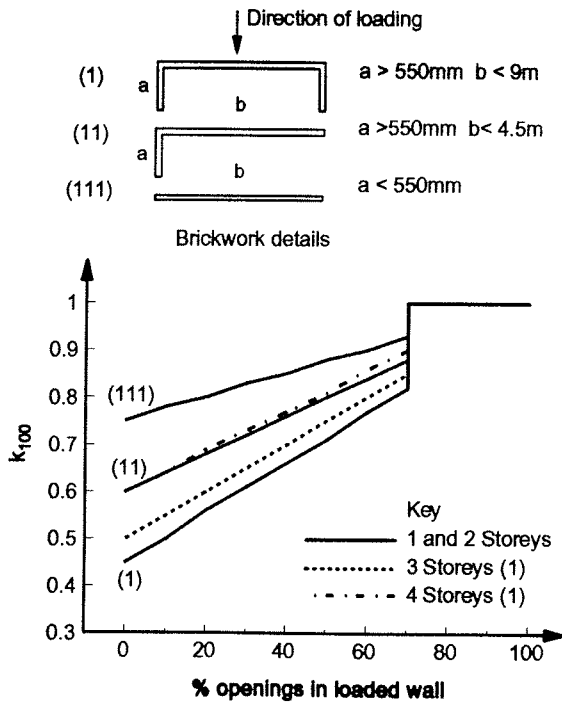
Figure 1 Standard test panel for the UK BS 5268, section 6.1 test.



Wall details

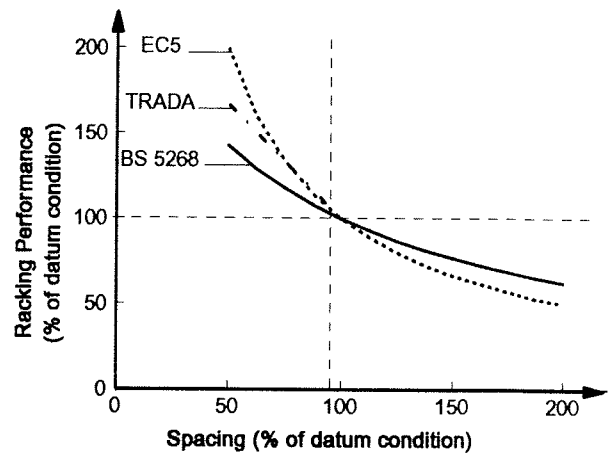
- A External walls; weak due to windows and doors and lay up of sheathing in rectangular sheets around openings. They carry little load in continuous beam analysis but majority of load according to BS 5268 section 6.1.
- B Internal plasterboard walls; strong as few openings and taped sheet joints. They carry the majority of load in continuous beam analysis but little load according to BS 5268 section 6.1 due to potential for poor fixings and accidental damage.

Figure 2 Continuous beam analogy for wall loading in a building using layout typical of Darwin, Australia tested by Cyclone Testing Station.



$$\text{Design wind load} = K_{100} \times \text{Design wind pressure} \times \text{area}$$

Figure 3 The effect of brickwork shielding on applied load.



The datum spacing in all design methods is 150mm along the board perimeter. The spacing on internal studs is not critical to performance and will often be twice the perimeter spacing.

Figure 4 The effect of nail spacing on racking performance.

Griffiths' test work and interpretations were used as the basis for the UK design code (BSI, 1988), together with work on brickwork shielding and racking undertaken at the Polytechnic of the South Bank, London, (Procter, 1986). Rules based on experience, dealing with non-structural wall limitations, were also devised by the Code drafting committee.

More recently in Europe, Eurocode 5 (EC5) on the Design of timber structures, has been introduced (BSI, 1994). The Code follows limit-state principles, and includes a short section on the design of vertical diaphragms. It allows the determination of racking resistance by calculation or by testing of prototype structures, but it does not link with the European wall racking test method of EN 594 (BSI, 1996b).

The Eurocode considers only the strength of panels fixed to a base with holding-down straps on vertical studs, and ignoring vertical load. The latter provides stiffness and strength data for a panel attached to a base by the bottom rail only, such that stiffness and strength will be influenced by vertical load. Kallsner and Lam (1995) have detailed the principles behind the EC5 design method, and have noted the inconsistencies in the text. Kallsner and Lam include a detailed set of recent references. Their test information is at odds with that of Griffiths, but this is likely to be due to the very different test models researched. They also note that the wall diaphragm section is incompatible with the rest of EC5, in terms of edge- and end-distances of fixings.

The UK Design Method

The design method for wall racking in BS 5268 Section 6.1 covers the following functions:

- (i) The applied wind load on the timber frame structure may be reduced in one or more principal wall directions by the shielding effect of the brick outer skin, using the K_{100} modification factor (see Figure 3).
- (ii) The racking resistance for a cladding on one face of a timber frame wall is given by:

$$F_{v,d} = R_b \times K_m \times K_w \times L$$

where R_b is the basic racking resistance

L is the wall length

K_m are materials modification factors K_{101} to K_{103}

K_w are wall modification factors K_{104} to K_{107}

- (iii) The wall is normally considered as a whole, with a reduction in performance applied for openings. However due to the over-simplicity of the openings modification factor, it is also acceptable to break the wall into parts, apply the normal procedures, and sum the parts, if this gives an improved performance.
- (iv) A wall clad on both sides has primary and secondary claddings, whose contribution can be determined separately. This is of major importance when the wall has a structural sheathing on one face, and a semi-structural lining on the other.
- (v) Plasterboard is considered as a semi-structural material, except in the case of party walls, where the thickness of board applied and the greater care and attention given to nailing, allow it to be considered fully structural albeit with a much greater factor of safety applied.
- (vi) The contribution of semi-structural linings should not exceed 50% of the capacity of structural sheathings, for any direction of wind load.
- (vii) Brick walls in the direction of wind load can contribute to racking resistance, but performance is limited to 25% of that of the sheathed wall to which the brickwork is linked. The design is restricted to full wall height brickwork, and follows the principles for horizontal load demonstrated in Figure 10.
- (viii) A whole building interaction factor, K_{108} , of 1.1 can be applied to the total wall racking resistance. Effectively, this will increase all wall contributions, however the Code now advises that it is applied to basic resistance values.

The value of $F_{v,d}$ for a wall can also be determined directly by test, but should be restricted to the values of vertical load tested, although interpolation of results is possible. If a full-scale test should include both sheathing and lining, great care must be taken in interpreting the results to ensure that in the whole building design, the required limitations on structural use of linings are observed.

Basic Racking Resistance

The basic racking resistance, the unique performance value for a combination of materials, is either a test value, or a tabulated value which is a lower bound for a group of similar claddings. It is quoted for a fixed specification of materials, but is given for both primary and secondary use.

The values quoted in the code have been derived from many standard panel tests, and relate in terms of board thickness to the most common use of the board type. The boards are grouped into three categories. Category 1 covers the stronger sheathings, Category 2 the weaker sheathings, and Category 3 the semi-structural linings. The datum values typically will show a

10 to 20% margin of safety, compared with test results from a full five- panel test programme. This allows safety in using materials of the minimum quality permitted in the specification. Limiting the categories and the ranges of the material modification factors has not been a problem in traditional domestic construction, and the Code covers adequately the most common board types.

More recently, the system has been seen to give problems relating to conservatism in dealing with increased board thicknesses, and mid-range boards. In the latter case, typically, high density insulation boards, low density medium boards and some non wood-based building boards are affected. The enormous safety margin imposed on separating wall construction to allow it to be considered fully structural, can be noted in its inclusion as a Category 2 material.

Where the datum code resistance values are considered unacceptably conservative, they can be substituted by values taken from standard panel tests. Then however, the value is only applicable to the configurations of materials tested. Separating walls are an exception in this respect.

Materials Modification Factors

The K_m modification factors are applied only to tabulated R_b values to modify the resistance to that applicable to the configuration of materials in the wall. These factors have been based on a number of different test programmes. Essentially K_{101} , for board thickness, and K_{102} , for nail diameter, show the resistance to be approximately proportional to the area of contact between the nail and the sheathing within a limited range around the datum condition.

Of significant interest is the spacing factor, K_{103} , where the test results showed very clearly that improvement was not directly proportional to the number of fasteners, and was lower than predicted by ASTM and EC5 based analyses (see Figure 4). It is considered that these analyses often over simplify the nail loading, and ignore the problem of end distances. Typically the most heavily stressed fixings in a panel will be those at the windward edge of the unit attaching the cladding to the base rail. Here the vertical loading component due to the sheathing rotating, significantly affects the performance, and the end distance for the fixing is likely to be about 18 mm. The K_{103} factor has recently been reconfirmed in a major test programme (Enjily and Griffiths, 1996).

Table 1 shows some design resistance values for a typical configuration of materials. The boards are at their datum thickness, and the nails are at standard spacing, but the most common nail diameter has been used for the sheathing, requiring the incorporation of the K_{102} factor. The plasterboard has a set requirement for fixings, which does not allow the use of K_{102} and K_{103} factors. 9.0 mm OSB or 12.0 mm chipboard or 9.0 mm medium board could be substituted for the plywood. The table demonstrates several important points, including the limited contribution of the secondary board, the additional factor of safety applied to the use of plasterboard, and the

more significant problem of coupling two boards of different behavioural types.

These values are quoted for the datum wall conditions of the standard panel test.

Wall Modification Factors

The K_w wall factors cover the form of the wall, ie length L , height h , openings, and the vertical load. The datum values which give a unity value relate to the standard test panel ie $h = 2.4\text{m}$ $L = 2.4\text{m}$, no openings and zero vertical load.

The height factor (K_{104}) in the present code is very limited in scope, and is based on a simple analysis which is relatively untested. It assumes the racking to be proportional to the couple resulting from the height and the horizontal force. More recent work (Enjily and Griffiths 1995) confirms this is not true, over a wider range of heights, and suggests a different approach to both height and length modification factors.

The vertical load factor (K_{107}) is the only factor which is not independent of the others. Here the improvement with vertical load decreases with length. The modification factor can take account of uniformly distributed loading, equal stud loads, and variations in stud load. It can also be used to accommodate holding-down ties attached to studs when the short term shear resistance of the tie fasteners can be considered as an equivalent vertical load. The vertical load factor was derived in conjunction with the length factor, from tests on plain wall panels. It was then checked with the test data obtained for perforated panels containing door and window openings.

In reality, the vertical load performance relates to the quality of the materials. A strong combination allows full benefit to be gained as vertical load increases. Weaker combinations are unable to take advantage of the higher vertical loads, as shown in Figure 5. This does not affect design because the basic racking resistance value has been reduced in such a way as to be safe for all vertical loads. Unless otherwise stated, the upper bound will be 5 kN/stud (or its equivalent), which is the normal maximum test loading. It is sensible for weaker claddings to be tested to a lower maximum vertical load, in which case the basic racking resistance must be quoted, together with a limitation on the use of the vertical load factor which relates to the maximum test loading.

Panel Details	
Sheathings:	9.5mm plywood, 3.35mm diameter nails at 150/300mm centres.
Lining:	12mm plasterboard, 2.87mm diameter nails at 150/300mm centres.
Framing:	Minimum of 38 x 72mm SC3 timber.
Primary sheathing only	1.88kN/m
Primary sheathing + secondary sheathing	2.82kN/m
1.88 + 0.94	
Primary sheathing + secondary lining	2.16kN/m
1.88 + 0.28	
Primary sheathing only	0.90kN/m
Primary sheathing + secondary lining	1.35kN/m
0.90 + 0.45	

Table 1 Some examples of wall racking resistance for zero vertical load and 2.4m wall lengths only (Note that 3.35mm is not the datum nail diameter for plywood).

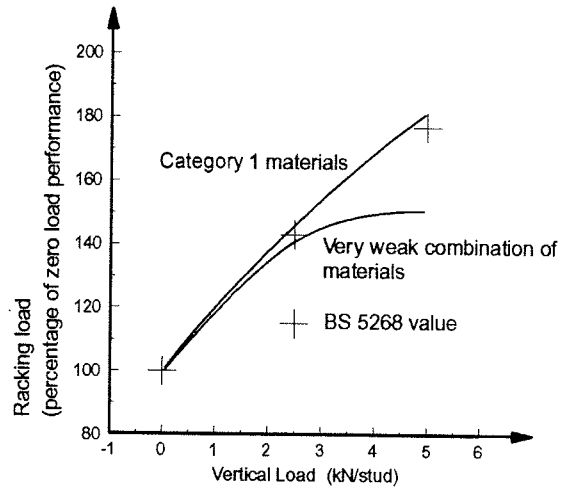


Figure 5 Effect of vertical load on racking performance.

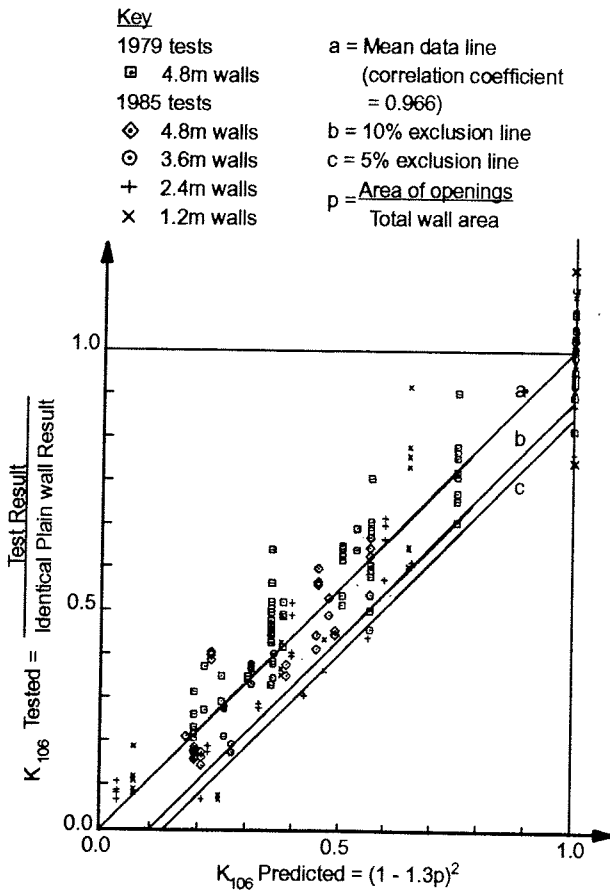


Figure 6 Correlation of openings modification factor with test data based on loads causing 5mm racking deflection.

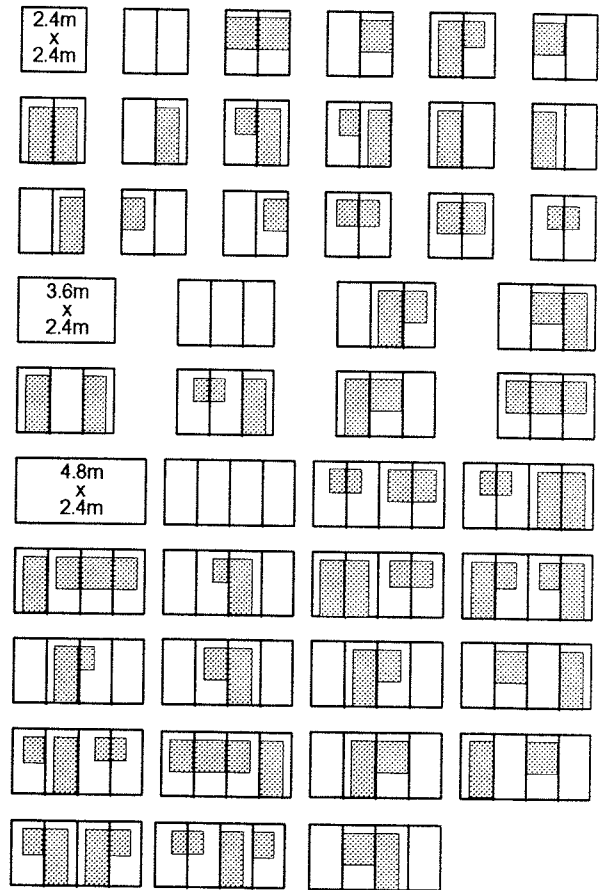


Figure 7 Part range of walls tested to determine the effect of openings.

The length factor is in three parts, as follows:

- (i) For $L < 2.4h$, $K_{105} = L/2.4$; thus for short walls racking performance, $F_{v,d}$, is proportional to L^2 which indicates more a beam type interaction, with the wall acting as a vertical cantilever.
- (ii) For $L > 4.8m$ $K_{105} = 1.32$; thus $F_{v,d}$ is proportional to L , indicating that shear is the governing factor.
- (iii) In between, $2.4 < L < 4.8$, $K_{105} = (L/2.4)^{0.4}$ which is an intermediate case.

The values for K_{105} in (i) and (iii) above have been proven by test in two substantial programmes. (ii) is a lower bound estimate, assuming no further increase in performance for panels longer than 4.8m. It is clear that resistance will tend to a maximum value for longer panels, assuming the load to be carried uniformly into the panel along its length by the horizontal diaphragm. K_{105} in (ii) above gives a lower bound value for this resistance based on the maximum wall length tested.

Figure 8a shows the results of wall tests on plain walls sheathed with either 9.5 mm plywood or 9.0 mm medium density fibreboard, using 3.35 mm diameter nails at standard 150/300 mm centres on standard framing systems. The loads are those to produce a deflection of 5 mm, approximately $0.002h$. A number of failure tests were carried out in the programme, which showed that strength would not be important to design for shorter wall lengths, but could be critical for longer panels and at higher vertical loads. From these results, the design equations were derived. Figure 8b shows the plots for the limiting design conditions of strength, and stiffness, based on a deflection of $0.003h$, together with the design line based on the Code modification factors. The margin of safety again reflects the need to include an allowance for materials that might be of a lower specification than those tested, although still within acceptable tolerance.

The test walls were either made up of combinations of smaller units connected by three M12 bolts across abutting studs, or from one single unit. In the latter case, the sheathings were linked by joining onto common studs. The make-up of the wall was seen to have little effect on performance. Where possible, sheathing widths of 1.2m were used, but in the build up of 0.6m and 1.8m units, a 0.6m sheathing width was necessary. In general, the use of 0.6m width sheathings did reduce the panel capacity, but the losses were not significant. These secondary results allowed the design method to be made independent of panel construction, although it was clear that performance is improved by using wider boards, and that very narrow boards should be avoided. Recent unpublished work at the University of Surrey shows the benefit to racking performance of taping plasterboard type joints, effectively enhancing the width of the sheathing units.

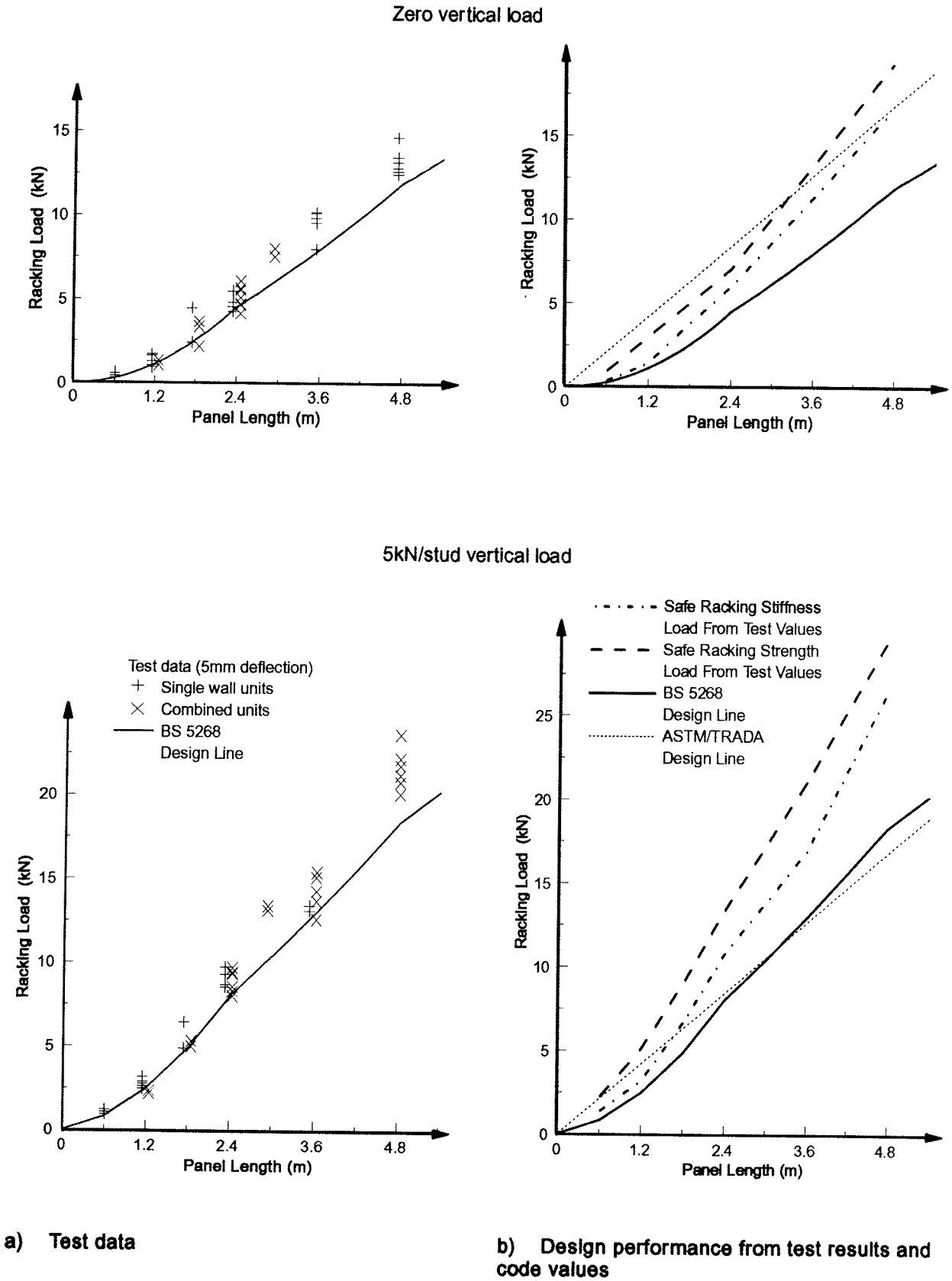


Figure 8 Effect of panel length on vertical load.

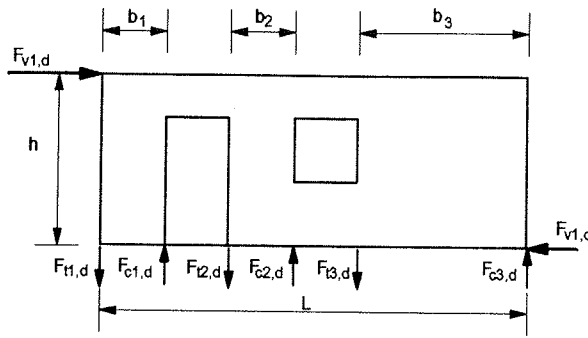
The opening factor, K_{106} , is extremely simplistic in format; $K_{106} = (1-1.3p)^2$ where p is the aggregate area of openings in a wall divided by the total wall area. The factor is independent of the size or form of individual openings, their layout and the direction of load. The code gives limitations on the distance between openings and on the size of small openings considered not to affect racking resistance. It also gives recommendations on dealing with openings closer together than 300 mm.

The factor is based on two major test programmes which covered a very wide range of openings in walls up to 4.8m long (Girths, 1987). Smaller panels with openings often contain very narrow widths of full height panels, thus when a wall is made up of such units there may be few, if any, cladding boards of even 0.6m width. This will weaken the wall in addition to the natural effect of the openings, and may be avoided by using larger wall units. However, this limitation should be included in the derivation of the lower bound opening factor. Because of the narrow full height parts, perforated panels when tested usually are governed by their stiffness. Figure 6 shows how the test results have been reduced to confirm the K_{106} factor. For the wide range of walls and openings tested (see Figure 7), the effect of the opening has been calculated by determining the ratio of the perforated wall performance against that of the same sized plain panel. The results cover two vertical load conditions and relate to the racking load to produce a 5 mm deflection. This ratio is plotted against the design value of K_{106} for the area of opening, and the correlation of data to the direct relationship between the two demonstrates the accuracy of the design factor.

The K_{106} factor is extremely onerous, and it is possible that a wall can be found to have a greater performance if it is designed in parts, particularly if the wall contains either a large length of plain panel, or one with a significantly large opening (see Figure 9). Recent tests (Enjily and Griffiths, 1995) and the stiffness interpretation of the new test method (BS EN 594, 1996) indicate that the panel opening factor should be reviewed, and a desk study is currently underway. This may lead to a less onerous factor being allowable, provided that certain conditions are met, such as the minimum width of full height sheathings.

Comparison of Design Methods

A brief comparison of the design approaches is given below. Figure 9 shows a typical wall, and notes how the racking load would be calculated using BS 5268. The modification factors are not evaluated, and must be derived from the equations given in the code (BSI, 1996a). The racking resistance is dependent on vertical load, and two means of dealing with the openings are shown; the higher racking load may be used. Values of racking resistance will ensure an adequate factor of safety against failure, and will keep deflections below 0.003 times the panel height. The base fixings should be capable of resisting the shear load and overturning, and in so doing, if sensibly spread, will resist the racking load.



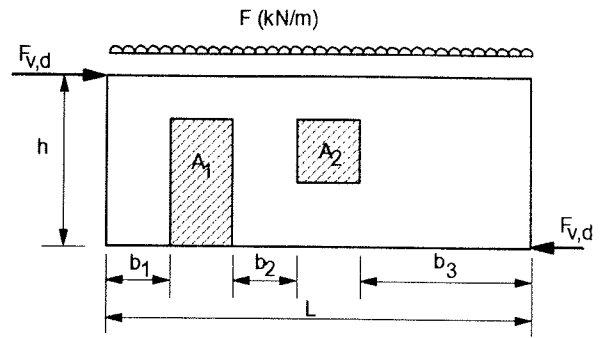
$$F_{v,d} = R_b \times K_m \times K_{104} [f(h)] \times K_{105} [f(L)] \times K_{106} [f((A_1 + A_2)/(h \times L))] \times K_{107} [f(L,F)] \times L$$

or splitting panel into two parts

$$F_{v,d} = R_b \times K_m \times K_{104} \times K_{107} \times \{ \{ K_{105} [f(L-b_3)] \times K_{106} [f((A_1 + A_2)/h(L-b_3))] \times (L-b_3) \} + \{ K_{105} [f(b_3)] \times b_3 \} \}$$

where A1, A2 are opening areas
f represents a function of the terms following it

Figure 9 Wall design example using BS 5268 section 6.1.



$$F_{v,d} = \sum_1^3 F_{v,j}$$

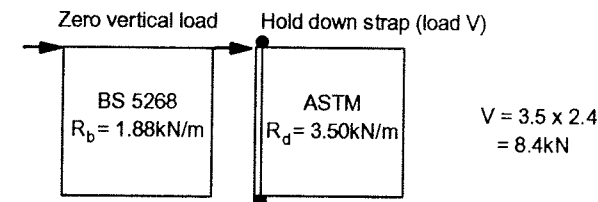
where $F_{v,j} = R_d \times b_j$ by test

or $F_{v,j} = F_{f,d} \times b_j / s$ * by analysis

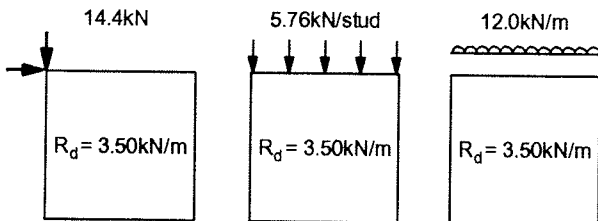
where $F_{f,d}$ is the lateral design capacity of the fastener
s is the fastener spacing
 $F_{s,d} = F_{v,j} \times h / b_j$
 $F_{ci,d} = 0.67 \times F_{v,j} \times h / b_j$ **

* interpretation of EC5 rules which contain inconsistencies.
** EC5 rule for single sheathings.

Figure 10 Wall design approximating to EC5 and ASTM/TRADA design methods.



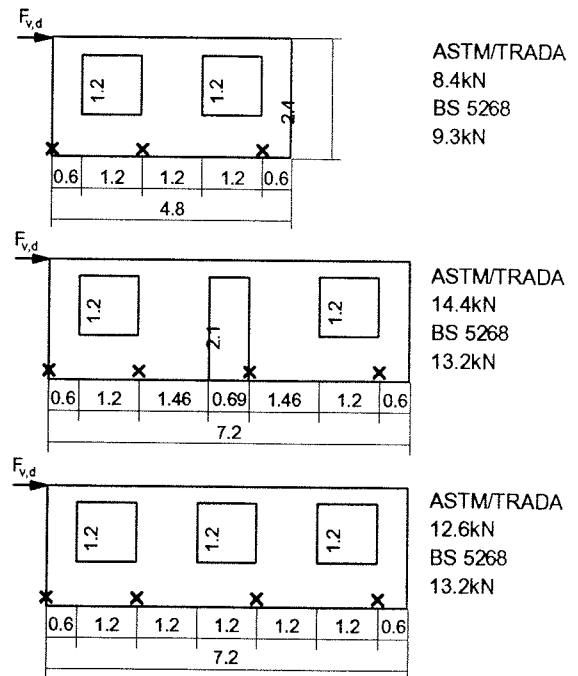
a) Results on standard test panels.



b) BS 5268 test equivalent vertical loads to give resistance similar to ASTM.

All design values are for 9.5mm plywood nailed with 3.35mm diameter nails at 150/300mm centres.

Figure 11 Comparison of BS 5268 and ASTM/TRADA design values for standard test panels



Material details as Figure 11

ASTM/TRADA resistance, $R_d = 3.5kN/m$
BS 5268 basic racking resistance $R_b = 1.88kN/m$

Vertical load: 10kN/m for BS 5268
Holding down: 8.4kN/m at points X for ASTM/TRADA
Openings: 25% of gross area

Figure 12 Comparison of BS 5268 and ASTM/TRADA design values for typical wall panels.

Figure 10 shows the same wall unit and the design approach, approximately, for both the ASTM/TRADA method and the EC5 method. For the same specification of sheathing, where the basic racking resistance in Table 1 was 1.88 kN/m, the ASTM resistance would be 3.50 kN/m (TRADA, 1989). This design value should provide an adequate factor of safety against failure, but does not consider deflection. The racking load is independent of vertical load, and in order that it can be achieved, vertical restraints must be attached to the windward end of plain panels (i.e. $F_{ti,d}$). The base fixing must resist the racking force.

In EC5, the design value will be an ultimate limit-state condition. No advice is given on the racking resistance of the panel; the capacity is determined by the base fixings and in turn determines the anchorage and compression stud requirements.

A further comparison of the ASTM/TRADA and BS 5268 design methods is given in Figure 8. It shows that for plain walls, the ASTM/TRADA design values will be similar to those for a 5 kN/stud vertical loading. To achieve the ASTM/TRADA load, an 8.4 kN hold-down must be provided at the windward end of each length of full-height panel. In a 4.8m long plain wall, this demonstrates a significant difference between the design methods. In the ASTM/TRADA case, a single holding down strap motivating 8.4 kN is required, whereas in the BS 5268 design, to achieve a similar racking load, a stud load of 5 kN is required on each of the nine studs i.e. a total vertical load of 45 kN.

This vertical load effect is demonstrated further in Figure 11 on standard test panels. In part a), the basic racking resistance values are shown with their vertical loading requirements. In part b), three different top load conditions are shown, each of which will give a racking resistance equivalent to the ASTM/TRADA value. The vertical load differences are significant, but it must be recognised that the BS 5268 design method is also ensuring a maximum deflection limit, which the ASTM/TRADA method is not doing.

For panels with openings, the design methods are very different in concept, and make realistic comparison difficult. Three design cases are shown in Figure 12 to illustrate the effects of openings, panel length and vertical load. In general, to achieve the same racking performance, twice the vertical load is required by the BS 5268 design method. However, in all of these comparisons it must be noted that in practice the BS 5268 performance values can be increased by 10% to allow for the K_{108} interaction factor.

Summary and Conclusions

- The principal wall racking test and design method used in the UK was developed to meet a need for the structural appraisal of platform frame housing systems, which when the methods were instigated, represented a new form of domestic building construction. The limitation of deflection was significant to the design objectives. A top-loading test was accepted, after other methods had been seen to model inadequately the complex situation of the real timber frame wall.
- A detailed reduction procedure for the test results linked the test basis to a design method. This entailed the derivation of a single design value, termed the “basic racking resistance” R_b (kN/m). The racking resistance was used with the total wall length, and with modification factors for materials and wall form, to evaluate the safe racking capacity of any practical wall design desired.
- The design method was empirically based. However it was by no means *ad hoc*. Indeed, it was related to the test performance of nearly two hundred wall and panel units. It realistically modelled the timber frame wall, and its practical restraints, but did not take full account of holding-down methods or of return walls, although it has been shown in research projects that these factors can in fact be modelled.
- The UK design approach has rules which allow for the combined use of structural sheathings, and semi-structural linings. These rules preclude the use of a fundamentally-based three dimensional design method, since the high stiffness and strength of internal semi-structurally lined walls must often be ignored.
- Although conceived for working stress design, the UK method could, and probably will be, adapted to a limit-state approach. This will need to look separately at serviceability and ultimate limit-states. This will in turn require a comprehensive re-evaluation of the UK test data. There is a realisation that at present, design values are very much limited by deflection considerations.
- The new EN 594 test reduces the significance of stiffness in design, but at the same time is fundamentally flawed in its evaluation of this parameter. Whilst appealing in their design simplicity, the ASTM-based design methods use an unrealistic test model, and consider only wall strength. The EC5 design method concentrates on external forces, and seems not to consider the racking resistance of the wall itself. Certainly, it does not cover serviceability design, and is restrictive in its requirements for panel fixings.

- It is becoming increasingly important that both timber frame research, and the ensuing design methods are acceptable throughout Europe. In order to take full advantage of the lead shown by the UK timber frame industry, a “Eurodiaphragms” project has just been initiated. This has the objective of preparing a wall racking design method which is comprehensive in its coverage, yet simple. Most importantly, it seeks to establish a basis which will be acceptable throughout Europe. This method is to be prepared within the timetable for the revision of Eurocode 5.
- Completed research on the brickwork outer skin in the UK, both as a contributor to racking resistance, and as a wind shield, could with great benefit be transferred to a limit-state design approach. This would be a fairly substantial undertaking. However, the common between-materials safety format of the Eurocodes would help considerably in such an endeavour. Developments in medium-rise timber frame construction are stimulating a desire to investigate such masonry/timber composite action effects for taller buildings.

Acknowledgement

The new "Eurodiaphragms" project, full title "Efficient Diaphragm Wall Design to the Principles of EC5", in which all of the joint authors of this paper are involved, is co-sponsored by the Department of the Environment, TRADA, and by individual industrial partners. The authors gratefully acknowledge this sponsorship.

References

- Anderson, L.O., 1975 Wood frame house construction (1975 rev) Washington, U.S. Department of Agriculture..
- ASTM E72-80, 1980, Standard methods of conducting strength tests for panels for building construction, American Society for Testing and Materials.
- ASTM E564-76, Standard method of static load test for shear resistance of timber framed walls for buildings. American Society for Testing and Materials.
- BSI, 1988 Structural use of timber, code of practice for timber frame walls, dwellings not exceeding three storeys, BS 5268 Section 6.1. London, British Standards Institution.
- BSI, 1994, Eurocode 5, Design of timber structure, Part 1.1, General rules and rules for buildings, DD ENV 1995-1-1, London, British Standards Institution.
- BSI, 1996a Structural use of timber, code of practice for timber frame walls, dwellings not exceeding four storeys, BS 5268 Section 6.1. London, British Standards Institution.
- BSI, 1996b Timber structures - Test methods - Racking strength and stiffness of timber frame wall panels, BS EN 594, London, British Standards Institution.
- Enjily, V. and Griffiths, D.R., 1995 The racking resistance of large wall panels. Building Research Establishment client report CR119-95, Crown copyright, Watford.
- Enjily, V. And Mettem, C.J., 1996 The Current Status of Medium-Rise Timber Frame Buildings in the UK. International Wood Engineering Conference, New Orleans, Louisiana State University.
- Griffiths, D.R., 1987 The racking resistance of timber frame walls assessed by experimental and analytical techniques, Guildford, Surrey, University of Surrey.
- Griffiths, D.R. and Wickens, H.G., 1996 The derivation of design data from UK timber frame wall racking tests. International Wood Engineering Conference, New Orleans, Louisiana State University.
- Kallsner, B. and Lam, F., 1995 Diaphragm and shear walls. Grundlagen STEP 3 Entwicklungen Ergänzungen, Dusseldorf, Informationsdienst Holz.
- Lantos, G., 1967 Proposed Method of Testing Timber Wall Panels Under Lateral Load (Racking). TRADA Test Memorandum E/TM/71, High Wycombe.

Mettem, C.J., Pitts, G.C. and Enjily, V., 1996, Innovation - the Challenge for Timber Frame 2000. Proceedings of the Second Cardington Conference, Building Research Establishment, Watford.

Procter, S. L., 1986. Structural Performance of Timber Framed / Brick Veneer Construction. CNAA, M Phil Thesis, South Bank Polytechnic.

Robertson, R.A. and Griffiths, D.R., 1981, Factors affecting the racking resistance of timber framed panels. Journal of the Institution of Structural Engineers Vol. 59B No 4, London.

TRADA, 1968, Timber Frame Housing Design Guide, (First edition) High Wycombe.

TRADA, 1989, Timber Frame Housing, Structural Recommendations, (Second Edition), High Wycombe.

INTERNATIONAL COUNCIL FOR BUILDING RESEARCH STUDIES AND DOCUMENTATION

WORKING COMMISSION W18 - TIMBER STRUCTURES

**CURRENT DEVELOPMENTS IN MEDIUM-RISE TIMBER FRAME BUILDINGS IN
THE UK**

by

C J Mettem

G C Pitts

TRADA Technology Ltd

P J Steer

Consulting Engineer

V Enjily

Building Research Establishment

United Kingdom

MEETING TWENTY - NINE

BORDEAUX

FRANCE

AUGUST 1996

Current Developments in Medium-Rise Timber Frame Buildings in the UK

**by C J Mettem and G C Pitts, TRADA Technology Ltd
P J Steer, Consulting Engineer and
V Enjily, Building Research Establishment**

Introduction

This paper addresses the current status of medium-rise timber frame buildings in the UK, and describes some significant developments which have been taking place recently. These have led to a project which involves the full-scale testing of a six-storey prototype, along with many desk-based, component-based and site-driven ancillary exercises.

Throughout Europe, reduced costs, rapid construction times and high build quality are all reasons for the growing interest in timber frame for medium-rise construction. In fact, irrespective of its particular form or size, timber frame can call upon a series of well-established credentials, including the following:-

- Lightness, giving low erection costs and needing only inexpensive foundations
- Excellent thermal performance
- A dry construction process
- An economical and amenable technique for factory pre-fabrication, providing production efficiency and environmental benefits, including waste reduction
- A good environmental image for the constituent materials, backed up by demonstrable whole-life audits

Collectively, these benefits combine to make timber frame an attractive alternative to steel and concrete construction for a wide range of buildings in the four to eight storey range. It is ideally suited to many residential, commercial, hotel, office, and leisure applications. Exploiting the potential of this construction method will give timber frame access to new and extended markets.

In the last four years, in the UK, some sixteen timber framed structures have already been built on a commercial basis, at heights of four storeys plus basements, or with five full storeys in timber. However, there are at present no comprehensive design rules for such buildings, and correcting this deficiency has been the motive for the Research and Technology Developments (RTD) which have been initiated, and which are described in this paper.

Feasibility Study

A collaborative Building Research Establishment (BRE) and TRADA Technology Ltd (TTL) feasibility study, funded jointly with the industry through the DoE Partners in Technology programme, was commissioned in 1994 to review and summarise the construction requirements and existing information affecting medium-rise timber framed buildings in the UK, and to develop proposals for any necessary further research (1).

The partners completed this feasibility study in 1995. The main recommendation was that a programme of both component testing and also a series of full-scale building tests would be required. It was recognised that this should lead to the production of a major, nationally accepted, authoritative Guidance Document on the subject. This would link in turn to codes and standards expected to be coming into force at the time of completion of the recommended work, including of course Eurocode 5 and parts of Eurocode 1.

TF2000 Project

Recently, the same partners have embarked upon Stage 1 of a full-scale project, entitled Timber Frame 2000 (TF 2000). This is intended to fulfil the aims recommended in the feasibility study, namely to generate authoritative guidance, which will ensure a uniform design approach, and encourage "best practice" procedures. All the best design features and fabrication techniques for medium-rise timber frame will be investigated and developed throughout the project. This will entail, amongst other things, designing, constructing and testing a full-scale six-storey test building at the BRE Cardington facility. Figure 1 shows indicative sections, and a plan of the six-storey test building, as conceived at present. The principles of this are discussed in later sections of this paper. However, it should be noted that developments are still occurring in the research programme, and that therefore details of the building itself may change.

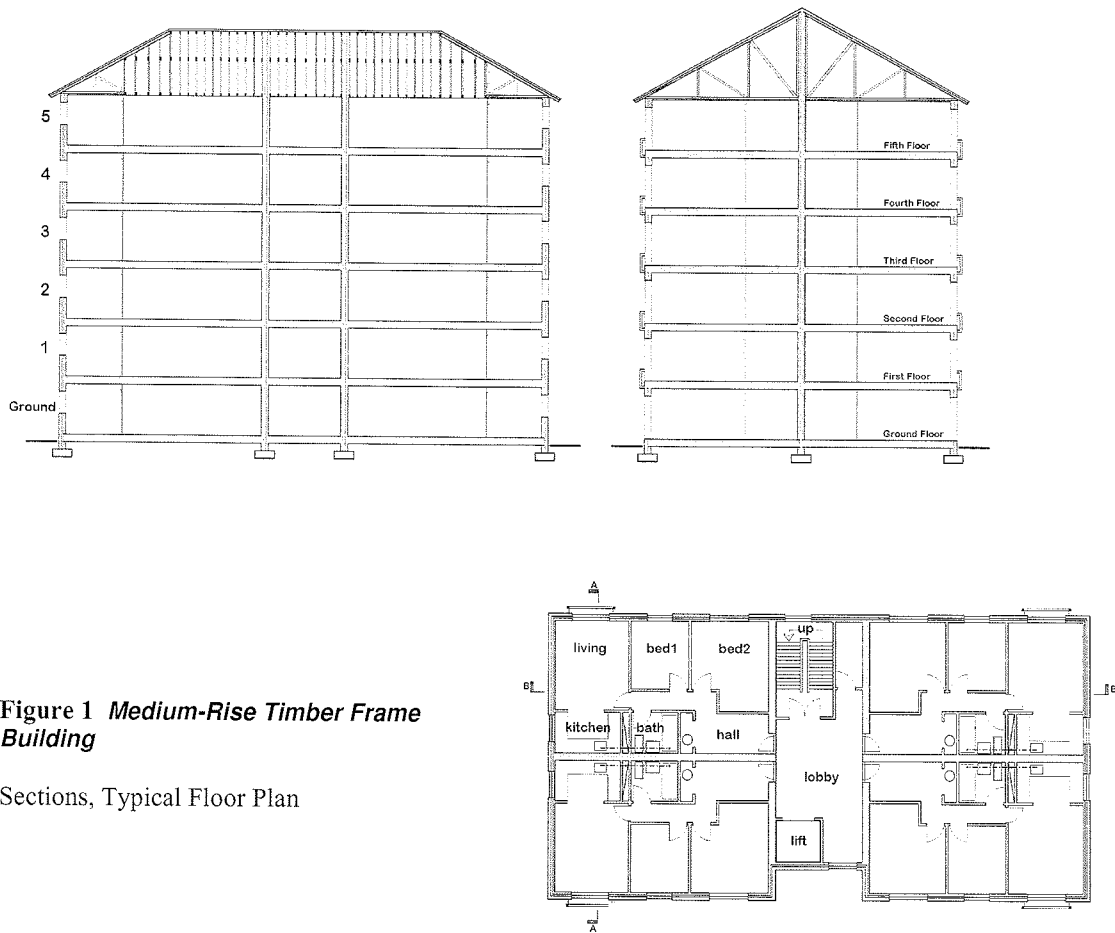


Figure 1 *Medium-Rise Timber Frame Building*

Sections, Typical Floor Plan

Whilst the main purpose of the TF 2000 initiative is obviously to derive a basis for timber frame buildings over four storeys in height, there will clearly be considerable spin-off in a number of areas relevant to all timber frame buildings. This is also regarded as of great importance by the whole industry, and by government.

Primary Issues

As mentioned above, the project TF 2000 is funded through the DoE “Partners in Technology” programme. Such projects are only partially supported from public funds, and new proposals are bid for competitively by all sectors of the building industry. These proposals are reviewed independently and very critically, in order to ensure that they reflect real industry needs. TF 2000 is in fact the largest joint-venture RTD project ever embarked upon by the UK timber frame industry. Two leading English companies, and two equally leading Scottish firms, have been central not only to the technical efforts, but also to a major share of the fund raising, and recruitment of further partners.

Because of this highly competitive element within the project, primary issues were carefully reviewed by both Management and Technical Committees, before deciding upon the design and specification of the test building, and before choosing the core items for the RTD programme in Stage 2. A formal construction management tool, known as SMART Analysis (2), was employed, to clarify the complex choices. This used a consensus approach, incorporating the views of all of the “stakeholders”, in arriving at the key decisions.

Market demand, certainty of success, affordability, and Regulatory acceptance were seen as the main commercial factors, whilst choice of cladding, key construction techniques, and those aspects relating to what Eurocode 5 describes as “mechanical resistance, serviceability and durability” were major technical factors. Building performance requirements, such as thermal and sound insulation, and satisfactory reaction to moisture and temperature effects, were also of course technically very important. Finally, resistance to fire was recognised as another primary requirement, and this was related to a changing Regulatory perception within the UK, which is briefly amplified upon in the subsequent section of this paper entitled **“Regulatory Acceptance”**.

In summary, therefore, the issues of primary concern affecting the decisions relating to the prototype were as follows:-

- Market-related aspects
- Regulatory acceptance
- Key constructional choices
- Cladding
- Mechanical resistance
- Serviceability
- Building performance
- Fire engineering

It can be understood from the above explanation of the aims, and of the industry-led motivations for the project, that the market-related aspects were of paramount importance. It would be improper however to attempt to deal with these more fully, in a technical paper of this nature. Suffice it to say that both the choice of a six-storey prototype, and the decision to use a single, half-brick-thick leaf of cladding, now regarded as “conventional” for timber frame in the UK, (3), were both taken on hard-headed commercial grounds.

Regulatory Acceptance

In order to understand the importance attached to "Regulatory Acceptance", it is necessary to appreciate some of the important, and in the main "deregulatory", changes that have been occurring in the UK in recent years. Whilst these will of necessity be strictly of national relevance only, they may well parallel similar changes elsewhere in Europe. Particularly important are the features relating to fire safety, working practices, and to resistance to accidental damage.

Fire Safety

Improvements in the "England and Wales" Building Regulations with regard to fire safety, mean that timber framed buildings of more than three storeys are now fully permitted, rather than requiring special waivers. The alterations, which occurred in 1991, removed most of the prescriptive limitations on the use of combustible materials. There is now effectively no height limit in the Regulations for timber framed buildings, provided that the relevant fire resistance performance can be demonstrated.

This situation allows, for example, timber framed buildings of up to 20.0 metres to top floor level to be constructed with components framed in timber, provided that they have a fire resistance of at least 60 minutes. Timber floors and walls with this degree of fire resistance have for long been a well-established fact of life for the timber frame industry, and can easily be achieved.

Scotland

The regulatory changes with respect to England and Wales also bring prospects of influencing future editions of the Building Standards for Scotland. These are at present more restrictive in terms of fire safety than the Regulations for England and Wales, even though timber frame is a highly preferred method of construction in Scotland, where climatic conditions are more comparable with those in parts of Scandinavia. The Scottish timber frame industry therefore sees this RTD as especially significant, since it is a means of demonstrating that adequate fire safety can be provided, as well as achieving all the essential requirements for mechanical resistance, serviceability and durability. Obtaining greater harmonisation between the various UK regulations is therefore another important goal for all concerned.

Working Practices

New Health and Safety at Work requirements are affecting timber frame design generally, as well as influencing this project in particular. Traditional 3.6 metre long "two-man lift" wall panels are no longer acceptable. Very small companies or projects may use short panels, or more manpower, but in general, crane erection is now planned in, at the design stage. Encouragement of the use of large, crane-erected panels also reflects the desire to achieve greater factory prefabrication, which is linked in turn to the aim of quality in off-site manufacture.

Perhaps less surprisingly if it is thought about, the size and extent of prefabricated units, including both wall and floor panels, has a considerable bearing upon the achievement of details which are satisfactory in resisting accidental damage, as well as relating to a number of other points concerning "whole-building performance".

Accidental Damage

Ever since the notorious collapse of the Ronan Point building, there have been strict regulatory requirements throughout the UK, with respect to resistance to accidental damage. In more recent years, robust buildings have been required to provide protection for both the occupants, and for those in the surrounding vicinity, in the face of various forms of event, sometimes of a sinister nature.

There are design requirements relating to Accidental Damage for all forms of building covered by both of the main sets of UK Building Regulations, which are more prescriptive than those given in general codes, such as Eurocode 5 Clause 2.1 P(2). At five storeys or more (and this is an important distinction), in addition to the normal vertical and lateral resistance calculations, the designer is obliged to provide formal calculations, following a choice of several alternative assumption philosophies, proving that the structure will remain stable, and will not experience "Disproportionate Collapse" in the event of an accident. The Regulations are couched in such a manner that the nature of the "accident" itself is undefined.

The Feasibility Report included a review of both the Regulatory requirements for resistance to "Disproportionate Collapse", and also of the design assumptions, construction methods and details which are currently employed in medium-rise timber frame, in order to satisfy such requirements in the UK. The report concluded that these are in general satisfactory, but that it is an example of one of the areas in which nationally accepted, harmonised design guidance would be beneficial.

Low-rise experience (4), as well as assessments on completed medium-rise schemes, and feasibility studies on buildings of six to eight storeys, all suggest that adequate robustness is achievable, without major alterations to the engineering basics. Bridging and tying solutions are expected to be adopted, using effectively "modified platform frame construction". Connections between prefabricated units, and amongst the various structural diaphragms, will be required to be more positively "engineered" than is the case in low-rise timber frame buildings. Recent work on defining more formally the resistance of "timber engineering hardware" (5) will pay dividends in this respect.

Thought has already been given to performance requirements in relation to the extent of walls notionally removed in the face of "Accidental Actions". The safety format of the Eurocodes, in formally recognising such actions as being associated with factors different from normal design, is undoubtedly one of the major areas of improvement, in comparison with older national codes. In ENV Eurocode 5 Part 1-1 for example, the design values of accidental actions are defined formally in Table 2.3.2.2 and its associated clauses.

Stabilising the brick cladding may prove something of a challenge. Although it is easy to demonstrate that the timber structure itself remains stable in the event of an accident in which all of the bricks are removed, danger to persons external to the structure should be considered by conscientious designers, if not by Regulations. It is believed however that protection can be achieved by a combination of local reinforcement within the brickwork, together with the normal tying arrangements which are required for other purposes.

Key Constructional Choices

Four broad categories of structural form are recognised (3) as having potential for the general design of modern timber framed buildings of the type required for dwellings, commercial uses, and the other classes of occupancy considered here. These are shown in Figures 2,3,4 and 5 and are as follows:-

- Platform frame (sub-divided into three types)
- Balloon frame
- Post and beam
- Volumetric construction

Platform Frame

Platform frame construction consists of floor to ceiling height stud wall panels with intermediate floors sitting on top of these as a platform. One of its major advantages is ease of erection. Platform frame is likely to be the selected option for the TF 2000 prototype; a choice which can be understood in the light of the commercial decision-making process described above. Platform frame construction has a long and successful record in the UK, extending back at least seventy years (6). It is also the most common "light framing" timber system world-wide. The system has been used for all of the UK five storey buildings which have been constructed to date.

Differential movements in the face of potential moisture content changes have been recognised as a challenge with this system. Aggregated sections of cross-grained timber, summing up all of the joist depths and other transverse sections, become quite considerable as the number of storeys increases. Working against shrinkage in the timber may be the swelling effects of the types of clay brick commonly used for timber frame cladding in the UK. Proposed solutions for the prototype include the use of precision kiln-dried timber, taken to a target moisture content corresponding to Service Class 1 in Eurocode 5.

Figures 2a, 2b and 2c illustrate successive degrees of panelisation and of factory prefabrication, within the range of platform frame options. For the reasons explained above under the heading ***Working Practices***, large, crane-erected panels as shown in Figure 2c will prevail, both in future commercial practices, and hence in the prototype building.

Balloon Frame

Prefabricated balloon frame construction is shown in principle in Figure 3. This method was the basis for most of the mediaeval timber frame construction throughout north western Europe, with green temperate hardwoods such as oak being the normal choice of timber (7). Prefabricated softwood frames in North America were introduced by European settlers, using similar techniques.

The modern version entails stud panel systems of a broadly similar form to platform frame, but with walls of two or more storeys in height. Intermediate floors can be hung internally off the walls, thus obviating some of the difficulties mentioned above in relation to differential movement. Panel heights have until recently been limited both by available timber lengths, and also by perceived transport limitations. It is quite possible that with the growing awareness of the advantages of Structural Timber Composites (STCs) (8), together with the changing attitudes to large factory-made units mentioned above, there could be a revival of interest in balloon frame construction.

Post and beam

Post and beam is another traditional form of long standing, Figure 4. Its use for medium-rise construction with large section solid timber, or even with glulam, would probably not be viable, for a combination of economic and technical reasons. However, post and beam construction using modern materials, including STCs, might become a preferred option where clear spans are desired, for example in medium-rise office accommodation. Lengths of up to 24 metres in laminated veneer lumber (LVL), parallel strand lumber (PSL) and similar STCs are readily available. As well as being obtainable in large sizes, these materials have the additional merits of being of high strength and stiffness; "ultra-dry"; of great dimensional precision, and of demonstrable environmental merit.

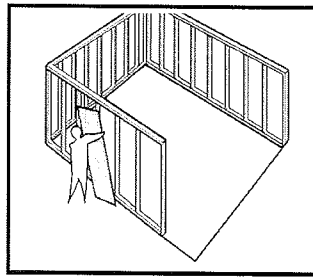


Figure 2 a

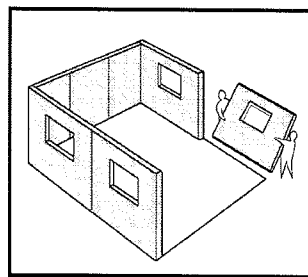


Figure 2 b

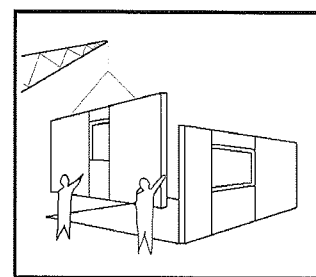


Figure 2 c

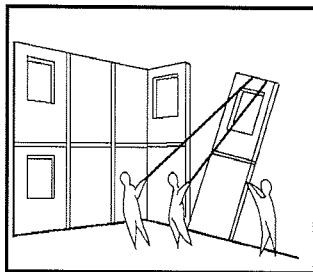


Figure 3

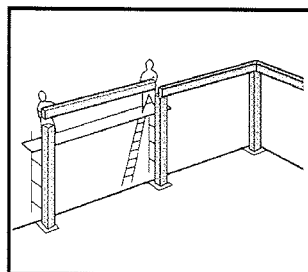


Figure 4

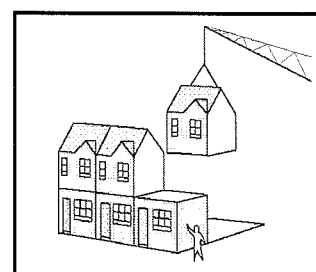


Figure 5

Volumetric Construction

Volumetric construction, Figure 5, represents the maximum added value form of system which can be completed in the factory. Internal finishes, glazing, doors and services can all be fitted, before transporting to site. This method has been used in the UK with considerable success for timber framed construction of up to four storeys. Its main applications have been those where very standardised layout requirements exist, such as hotel extensions, motels, nursing homes and student accommodation. Whilst appealing because of the concept of increased factory prefabrication, along with quality improvement prospects, volumetric construction tends to place too much restriction upon floor layouts for flats and houses. It is also less attractive than the alternatives mentioned here, in relation to differential movement.

Mechanical Resistance and Structural Serviceability

Apart from the specific requirements of being capable of resisting "Accidental Events", as described above in the Section headed **Regulatory Acceptance**, three principal classifications of required "mechanical resistance" exist, each of which can be related to sections of Eurocode 5. In addition, there are a number of Serviceability requirements, which for the purposes of brevity in this paper can all be summarised under a single heading. The three design performance requirements related to ultimate limit states are "*loss of equilibrium of the structure or any part of it, considered as a rigid body*" (Clause 2.2.1.1 (4)), conveniently taken as "Overall Stability", and "*failure by excessive deformation, rupture, or loss of stability of the structure or any part of it*" (same Clause, second paragraph), conveniently covered in the main by the two UK Building Regulations items "Elemental Resistance to Horizontal Forces" and "Normal Vertical Load-Carrying Capacity".

Overall Stability

This is dependent primarily upon the building's plan aspect ratio ("footprint") in relation to its total mass. It is also a function of the technology that can be harnessed to mobilise any necessary anchorages. In general terms, the latter may be based upon existing solutions for timber structures, and therefore simply becomes a question of cost and buildability. All of the available options for structural forms described above can achieve the required overall stability, provided that they have appropriate building "footprints" that permit the desired architectural layouts.

In relation to the preliminary designs for the six-storey TF 2000 test building, calculations have been made concerning overall stability. Two wind loading codes have been compared. The first is BS CP3 Chapter V Part 2, a code regarded by the authorities as obsolescent, but still prevalently that used in the UK for all building structures, and with all materials. The second wind code used has been BS 6399 Part 2, a document frequently giving rise to higher loadings than the former, for the types of structure considered here. In either case, six storey (and even higher) timber framed buildings of "sensible" footprints can be shown to have more than adequate factors of safety against gross overturning.

Elemental resistance to horizontal forces

The ability of a wall panel to resist horizontal forces in the plane of the panel is generally termed "racking resistance". Manufactured sheets and boards used as bracing are called "sheathing".

Since wind forces increase with building height, the sheathing requirements for medium-rise timber frame obviously become more onerous, compared with those for low-rise buildings. For example, thicker sheathing, more layers, and/or closer nailing of the sheathing are likely to be required. In addition, internal walls and compartment walls are often required to be treated as structural diaphragms. The engineer is also likely to wish to take into account the contribution to horizontal resistance and local stability which can be provided by gypsum board or similar linings.

The British Standard code, BS 5268 Part 6 'Code of practice for timber frame walls' makes provision for all of the aspects just mentioned. Eurocode 5 Part 1-1 on the other hand, has been found deficient in this respect more than any other, by British trial designers. The use of the Clauses under 5.4.3 "Wall Diaphragms" is expressly excluded in the UK National Application Document, and collaborative research, intended to be applicable to timber frame constructions of all heights, is in hand.

BS 5268 Part 6 provides tabulated values of what are termed “basic racking resistances”. These are based upon tests, using fully sheathed panel walls 2.4 m square, together with generic framing and sheathing materials. The tabulated values take account of load duration effects, and thus are useable directly as design resistances, in association with unfactored loads. The values are based upon zero vertical load.

To illustrate the approach used in the design of a typical medium-rise structure, consider the values given in Table 1 of this paper. Let it be assumed that the designer is seeking to establish a design resistance greater than 4.6 kN per metre run of diaphragm wall, a typical figure for a six-storey building. Then the thought process follows the steps shown in the table. At Stage 1, a basic resistance of 1.96 kN/m is found, using standard values for the generic sheathing materials, in this case 9.0 mm OSB plus 12.5 mm gypsum plasterboard. Stage 2 seeks improved values from larger diameter fasteners at closer centres. Finally, Stage 3 takes advantage of geometrical factors and the contribution of vertical loads (what Eurocode 5 would term “design effects of stabilising actions”). It can be seen that by reaching Stage 3, a more than adequate resistance is provided. Without each of the stages however, nowhere near sufficient resistance could be achieved.

Table 1 Stages in determining racking resistance for a sheathed timber frame wall in a typical six-storey building design

Stage	Construction	Design Resistance kN/m
1	9.0 mm OSB + 12.5 mm gypsum board	1.96
2	3.35 dia nails at 75 mm c/c	3.14
3	top load & panel length factors	5.38

The decision to use brick cladding on the test building was taken on the grounds of market demand, as explained above, under “**Primary Issues**”. Figure 6 shows a typical section through a brick-clad, timber frame wall, in accordance with well established British practice.

BS 5268 Part 6 provides a method whereby the racking resistance of timber frame walls may be increased to take account of the contribution of masonry cladding, provided that certain conditions are observed. The research upon which this is based was conducted on single storey test walls and upon computer modelling of low-rise building configurations. Design recommendations have subsequently been extrapolated to cover constructions of up to four storeys. At present therefore, there is no basis to extend the concept to medium-rise timber frame construction. Economy of design is likely to be achievable, when research is completed. Whole-building testing, as described later in this paper, will contribute to the knowledge in this field, although it is recognised that other forms of research are also likely to be necessary.

As mentioned above, a number of five-storey real projects have already been built in the UK, and design studies such as those alluded to in connection with Table 1 have been carried out on both these, and taller schemes, including the TF 2000 prototype. These suggest that elemental resistance using the existing concepts of panellised factory pre-fabricated timber wall framing, is achievable with, at the most, improvements and enhancements upon the existing technology, rather than demanding revolutionary changes.

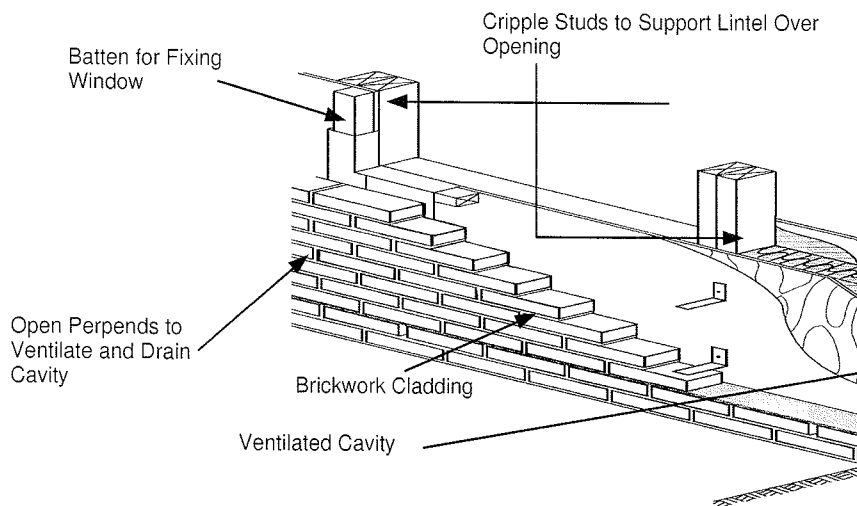


Figure 6 Typical Section, Brick-Clad External Timber Frame Wall

Normal vertical load-carrying capacity

Feasibility design studies on the test building, together with design work and checking on existing constructions of up to five storeys, have both shown that normal vertical load-carrying capacity can readily be assured. Wind loading affects the design of vertical elements such as studs, as well as influencing horizontal action effects, of course.

As mentioned above, there have recently been difficulties expressed by sectors of the British profession, including those concerned with timber structures, over the implementation of a new national wind loading code. This follows a philosophy closer to that being proposed in the drafts of the Eurocode 1 Part 2.4 'Wind loads' rather than that of CP 3 Chapter V Part 2. Preliminary calibration studies have shown however that the national changes are more onerous than the European proposals. In any event, it has also been shown that there are clear benefits in the use of Eurocode 5 Part 1-1, together with its NAD, as opposed to BS 5268 Part 2.

Advantage may be taken of this in completing the design calculations for the test building. It is desired to construct wherever possible with generic, and very "industry standard" materials. The motives for this are associated with the market and commercially-driven aims explained above. There are a number of instances where Strength class C16 (BS EN 338) timber can be used in acceptable sizes, and at logical centres, provided that the design is in accordance with Eurocode 5 Part 1-1.

Serviceability

In 1992, an approach to the control of static deflections in timber structures was published in the CIB W18 proceedings (9). This proposed a basis more similar to the principles of Eurocode 1 Part 1 'Basis of Design' than the application rules provided in ENV Eurocode 5 Part 1-1. The paper generated considerable interest in the UK, and led to further studies of Eurocode 1. A research project was also carried out in which actual measurements of static deflections were made in real timber buildings, and the various criteria for static deflection limitations were examined. This led to the publication of a technical Information Sheet on the subject (10).

Principles broadly as recommended to CIB W18 and as explained in the information note are being adopted in trial designs to Eurocode 5, and in developing comments for future versions. These same principles will be assessed in relation to the six-storey test building calculations, and compared with measurements. Vibrational performance of timber floors will also be checked, as mentioned in the following section of this paper.

Dynamic Testing, and other Measurements

BRE have well-established dynamic testing procedures for whole buildings, and have published results on some sixteen buildings of eight to forty-six storeys in height (11).

Similar techniques will be used on the six-storey timber frame test building. Testing will include structural assessments of the dynamic stiffness of the whole building before and after constructing the cladding and at various other phases of construction. Measured damping will be assessed from forced vibration tests, and a comparative numerical model will be developed.

Floor vibration measurements and acoustical tests will be undertaken. In addition, there will be tests involving the removal of critical parts of the structure, to simulate accidental damage and to prove that there is no risk whatever of disproportionate collapse. Finally “real fire” testing will be undertaken on major compartments within the structure.

Greater consideration of optional (non-regulatory) customer needs is drawing attention to the desirability of achieving excellent acoustical performance, both within and between the timber frame compartments, and in terms of the total building. High performance sound insulation is offered by a number of existing timber floor and wall solutions. The project will be examining how the “whole” structure and envelope performs. Vertical flanking sound transmission across a number of flats or apartments is of special interest in this respect.

It is anticipated that the six storey test building will incorporate a lift and services. It will also be fitted throughout with windows and doors. Those parts of the building to be tested for aspects such as acoustical performance and fire will be fully finished internally. The dimensional accuracy of all of the components and of the complete assembly will be monitored throughout the two-year test programme. Relative dimensional changes will also be continuously measured.

Conclusions

Innovation

The **TF 2000** project will undoubtedly be innovative. Amongst the large number of items in the RTD and information-generation programme for the project, the list of “firsts” includes the following:

- The first full-scale prototype timber frame building of six storeys to have been tested as a complete structure
- The first timber structure of such height in Europe to be fully assessed as satisfying the requirements of ENVs Eurocode 5 Part 1-1 and Eurocode 1 Part 1
- A structure having compartment floors and fire resistant shafts constructed from so-called “combustible” materials, and tested by means of “real” fires
- A unique test bed for many serviceability design enhancements - improved acoustical and vibrational performance, as well as measured stiffness under dynamic loading regimes

Impact

On completion of the full-scale test programme, authoritative guidance will be published to encourage the safe, efficient and economic production of medium-rise timber frame buildings. This aligns directly with national policy. Well thought-out and co-ordinated research and innovation strategies for timber have been developed recently in the UK. These recognise that research must have impact, and create beneficial changes. Such impacts may be:

- **Innovation** - Turning research to commercial and social benefit through new products and processes, or through development of codes of practice and regulations
- **Competitiveness and profitability** - Gaining market share through innovation
- **Environment and Quality of Life** - Improved quality of life, and health and safety

It is also stressed that research impact will not occur without:

- **Knowledge transfer**

Clearly substantial impact in all four of these areas will start to occur, even before the project TF 2000 is completed.

Competitiveness

The timber frame industry in the whole of the UK is convinced that its clients will appreciate the excellent energy efficiency, high comfort levels, and competitive build costs of taller timber frame buildings. The importance of this project and the positive publicity that it will attract, will ensure the highest possible levels of interest in the businesses of all of the participants. Fully developed solutions, proven construction methods and harmonised design guidance will give timber frame access to new and extended markets, whose value has already been calculated. There is also a growing overseas market for factory-engineered timber building solutions, and considerable export potential is foreseen.

Acknowledgements

The authors would like to thank the DoE, TRADA, and the following industrial members of the project TF 2000 for their support:

- Guildway Timber Structures (Meyer International)
- Purpose Built Ltd
- P J Steer, Consulting Structural Engineer
- Stewart Milne Timber Systems
- Walker Timber Ltd

References

1. Enjily, V. & Mettem, C.J. 'Medium-Rise Timber Frame Buildings - Disproportionate Collapse and other Design Requirements - A Nine-Month Feasibility Study.' Joint BRE/TTL Final Project Report for DoE and Industrial Partners, 1995.
2. Popper, S & Green, R 'SMART Methodology,' Value Management, Chartered Institute of Building, 1992.
3. TRADA Technology Ltd. 'Timber Frame Construction'. ISBN 0 901 348 94 5. 2nd Edition 1994. High Wycombe.
4. Mettem, C.J. & Marcroft, J.P. 'Simulated Accidental Events on a Trussed Rafter Roofed Building.' CIB-W18/26-14-6. Athens, Georgia, USA, 1993.
5. TRADA Wood Information 'Timber Engineering Hardware' Section 2/3 Sheet 51, High Wycombe, 1995.
6. Enjily, V. & Mettem, C. J. 'The Current Status of Medium-Rise Timber Frame Buildings in the UK' ITEC New Orleans 1996.
7. Hewett, C. A. 'English Historic Carpentry' ISBN 0 85033 354 7 Phillimore, London & Chichester, 1980.
8. TRADA Technology Ltd. 'Structural Timber Composites' - *A Generic Guidance Document, In Course of Preparation, 1996.*
9. Martensson, A. & Thelandersson, S. 'Control of Deflections in Timber Structures with Reference to Eurocode 5' CIB W18, Ahus, Sweden, Paper 25-102-2, 1992.
10. TRADA Wood Information 'Serviceability Limit States for Timber in Buildings' Section 4 Sheet 24, High Wycombe, 1995.
11. Ellis, B. R. 'Full-scale Measurements of the Dynamic Characteristics of Buildings in the UK' Journal - Wind Engineering and Industrial Aerodynamics 59 pp 382 1996.

INTERNATIONAL COUNCIL FOR BUILDING RESEARCH STUDIES AND DOCUMENTATION
WORKING COMMISSION W18 - TIMBER STRUCTURES

NATURAL FREQUENCY PREDICTION FOR TIMBER FLOORS

by

R J Bainbridge
C J Mettem
TRADA Technology Ltd
United Kingdom

MEETING TWENTY - NINE

BORDEAUX

FRANCE

AUGUST 1996

NATURAL FREQUENCY PREDICTION FOR TIMBER FLOORS

R J Bainbridge and C J Mettem,
TRADA Technology Ltd

Abstract

This paper describes research concerning vibrational performance of timber floors, both domestic and non-domestic, as a component of serviceability limit state design. The paper concludes with a simplified method for natural frequency prediction based on the method presented in Eurocode 5 Part 1.1 (BS DD ENV 1995-1-1:1994) and modified in line with research findings. The paper also describes future items for investigation in this field.

1.0 Introduction

This paper describes research concerning the vibrational performance of timber floors, both domestic and non-domestic, as a component of serviceability limit state design. An overall aim of the research is to produce design guidance on the subject.

The serviceability limit state design method for timber floors given in Eurocode 5 (EC5) [1] requires consideration of the vibrational response with respect to dynamic parameters. Currently, the UK NAD to EC5 contains an alternative method based on a static deflection limit consistent with the current BS 5268: Part 2 [2] design method. It is believed that consideration of a static deflection alone may not be sufficient to ensure adequate vibrational performance, especially in non-domestic applications, and that simplified design equations applicable to UK Floors are required.

This paper details one aspect of this work; namely a method for natural frequency prediction based upon the method presented in EC5, modified in line with research findings to date. The paper also describes other work carried out to date and future items for investigation.

2.0 Code Basis

Eurocode 1 Part 1 "Basis of Design" [3] is intended to be used with all of the design Eurocodes (ENVs 1992 to 1999). As a serviceability limit state which may require consideration, it includes *vibrations which cause discomfort to people, damage to the structure or to the materials it supports, or which limit its functional effectiveness.*

It is nowadays considered important that designers should take steps to ensure the good vibrational performance of timber floors. In most modern timber codes of practice, checks are included as one of a series of serviceability criteria. In a number of instances in the UK, timber floors have been found to vibrate in an unacceptable manner, even whilst complying with static design requirements.

Eurocode 5 states, as a principle, that:

" 4.4.1 P(1) *It shall be ensured that the actions which are anticipated to occur often do not cause vibrations that can impair the function of the structure or cause unacceptable discomfort to users.*"

It also states that floor vibration levels should be estimated by measurements, or by calculation, taking into account the expected stiffness of the floor, and the modal damping ratio. Competent practising structural engineers have no difficulty in estimating the stiffness of a floor, parallel to the direction of the joists, when carrying out a static design check. For such purposes, very simple methods are normally employed, and it is seldom considered necessary, or worthwhile, to allow for effects such as plate action, or the contribution of the flooring and ceiling to the sectional stiffness.

Such simplified methods do not readily lend themselves to making an estimate of the stiffness of the floor transverse to the direction of the joists. In this direction, system effects, and the detailed nature of the floor construction, play a considerable role in influencing the response of the floor to dynamic loading.

There are other difficulties for those familiar with routine static design calculations for floors, but less familiar with the methods required for dynamic design checks. These arise because several new structural parameters and construction-related properties are introduced. Whereas, for example, location and magnitude of maximum deflection can fully describe static serviceability performance, vibrational performance can be described through an array of

parameters (natural frequencies, damping, amplitude, velocity, acceleration etc.) all of which quantify a certain aspect of the complex vibrational response.

When dynamic behaviour of the floor is taken into account, it is found in many cases that the sizes of joists are determined by calculations related to vibration, rather than to strength or static deflection. It is therefore very important to use a design method for vibrational response which produces close approximations (bearing in mind the necessity for simplified equations), and to make a reliable assessment of the design parameters required.

3.0 The Frequency Prediction Method in Eurocode 5:Part 1.1

The Eurocode 5 application rules are currently limited in their range to “residential floors” fulfilling the following criteria:

1. Having a fundamental frequency greater than 8 Hz; *Clause 4.4.3(1)* states that for residential floors with a fundamental frequency ≤ 8 Hz a special investigation should be made.
2. Rectangular floors simply supported on all four edges.

Clause 4.4.3(4) states “For a rectangular floor $\ell \times b$ simply supported along all four edges and with timber beams having a span ℓ the fundamental frequency f_1 may approximately be calculated as

$$f_1 = \frac{\pi}{2\ell^2} \sqrt{\frac{(EI)_\ell}{m}} \quad (4.4.3c)$$

Where

m mass per unit area (kg/m²)

ℓ floor span (m)

$(EI)_\ell$ equivalent plate bending stiffness of the floor about an axis perpendicular to beam direction (Nm²/m)”

The method in EC5 stems from an extensive programme of research into vibrational performance of floors undertaken at Chalmers University of Technology in Sweden [4, 5]

This equation is also known as the Equivalent Beam Method (EBM) for natural frequency estimation and avoids the complex equations of dynamic physics which although covered in scientific texts [6, 7], are too complex for inclusion in general use design codes.

As the equation considers a floor to be a series of beams with connected flanges, it is therefore necessary to quantify the extent to which a bay of a floor behaves as, in the case where there is no ceiling, a ‘T’ beam. By manipulation of test data [8] a value of 1.2 has been derived as an appropriate factor to be applied to the joist stiffness to account for deck action, i.e.

$$(EI)_\ell \approx 1.2 E_j I_j \times 1000/s$$

Where	E_j	=	Mean modulus of Elasticity of the joist	(N/m ²)
	I_j	=	Second moment of the area of the joist	(m ⁴)
	s	=	Joist spacing	(mm)

The UK National Application Document (NAD) to EC5 provides the following alternative recommendation to the residential floors Application Rule of the code:

"f) Clause 4.4.3

For Type 1 residential UK timber floors, as defined in Table 1 of BS 6399: Part 1, which are primarily supported on two sides only and do not have significant transverse stiffness, it is sufficient to check that the total instantaneous deflection of the floor joists under load does not exceed 14 mm or L/333, whichever is the lesser."

In many instances, for commonly occurring domestic floors, this effectively excuses the designer from checking more rigorously against the EC5 principle (4.4.1 P(1)) which has been previously stated and which is quoted from the Eurocode. However, it remains unproven whether or not, in fact, the procedure of checking that the total instantaneous deflection of the joists under load does not exceed 14 mm or L/333 is a sufficient step to ensure that the actions which are anticipated to occur often do not cause vibrations that can impair the function of the structure or cause unacceptable discomfort to the users.

Furthermore, the NAD simplification provides no help for those designing floors for applications other than Type I residential. Clearly, timber floors in buildings other than single occupancy dwellings are of considerable economic importance, and consequently it is also important to ensure their vibrational serviceability.

4.0 Floor Tests

A series of floor tests were carried out on large domestic and non-domestic timber floor designs.

Four main floor configurations were tested under this research programme:

- A. 4.8 m × 4.8 m, C24 whitewood joist floor;
- B. 4.8 m × 7.2 m, C24 whitewood joist floor;
- C. 4.8 m × 4.8 m, Kerto LVL joist floor;
- D. 7.2 m × 4.8 m, Kerto LVL joist floor.

These floor types varied between tests with respect to the following parameters:

- 1. joist spacing;
- 2. imposed design load and corresponding deck material;
- 3. number of sides supported;
- 4. the presence of strutting employed in line with current guidance, versus the absence of strutting.

Figure 1 shows one of the floors during testing.

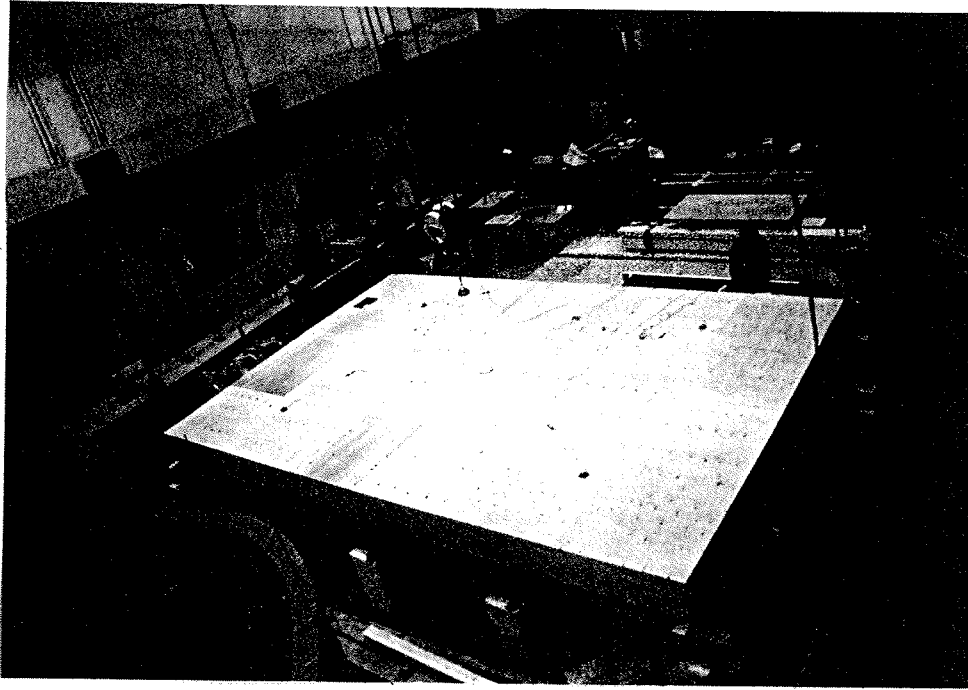


Figure 1 7.2m Span LVL Test Floor

In order to assess dynamic performance, a discrete impulse was induced on each floor. This was achieved by dropping a sand bag, of mass 3 kg, suspended at a height of 1000 mm from an overhead crane, independent of the floor, onto a 200 mm diameter aluminium transfer plate placed in the centre of the floor as shown in Figure 2. Heel drop test and static deflection tests were also carried out [9].

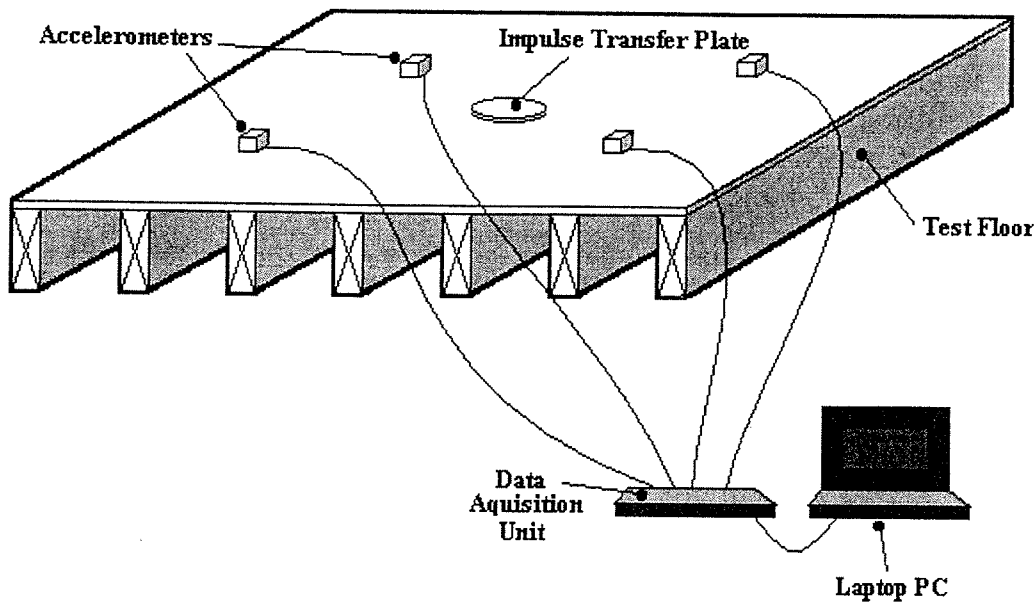


Figure 2 Schematic Representation of Test Equipment

The response was recorded by accelerometers fixed to the deck and relayed to a laptop PC with dedicated software via a data acquisition unit. The software then manipulated the raw

data and displayed the response in terms of a frequency spectrum, with peaks at the natural frequencies (See Figure 3).

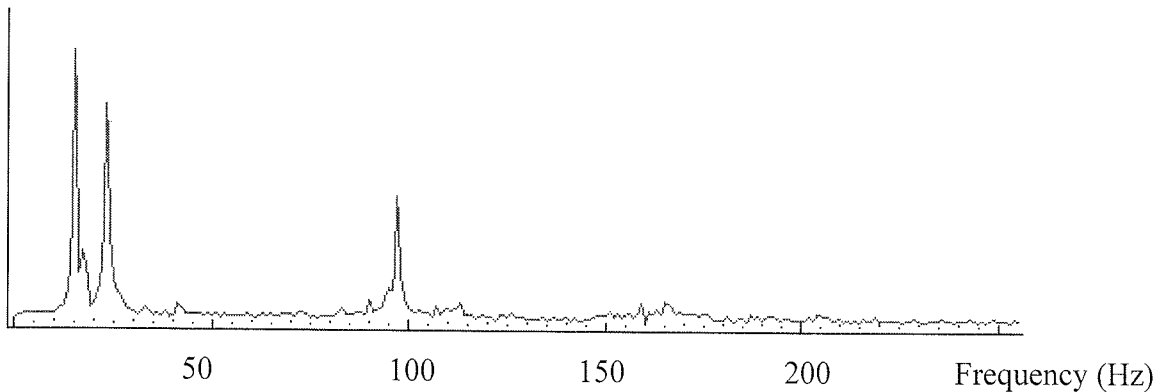


Figure 3 Example frequency spectrum produced from a bag drop test

5.0 Comparison of Test Results and Predicted Frequency

The results of these floor tests and the data presented in other reports [5, 9-15] are compared to the theoretical values obtained using the EBM method in Figure 4. It is emphasised that these data represented generic floor construction of the type described here as “typical UK practice”. Sets were examined from North America, Scandinavia, and New Zealand, hence these comparisons do not relate just to British practice.

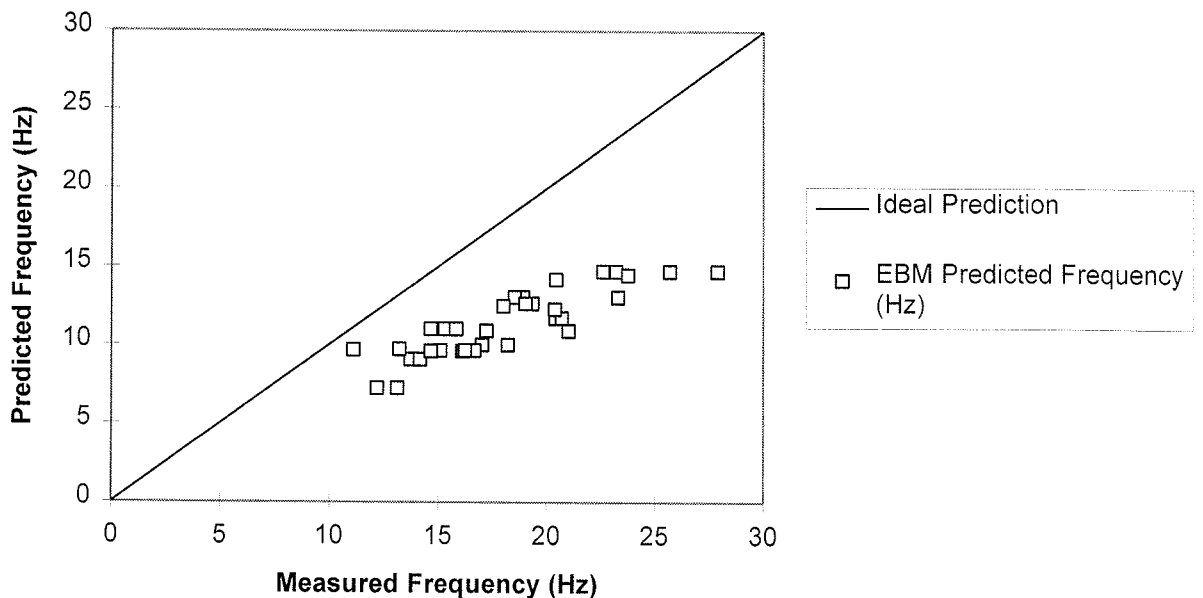


Figure 4 Comparison of EBM predictors and measured values.

The trend shown in these results, i.e. the measured results being noticeably higher than those obtained using the Equivalent Beam Method (EBM), is also in agreement with the findings of research carried out on floors constructed using other materials, including concrete [16].

6.0 Conclusion

As shown in Figure 4, the measured frequency results are consistently higher than predicted values by approximately 50%. Therefore, the suggested modification to the frequency prediction method is as follows:

$$f_1 = \frac{3\pi}{4\ell^2} \sqrt{\frac{(EI)_\ell}{m}}$$

where $(EI)_\ell = 1.2 E_j I_j \times 1000/s$

Predictions using this method are compared to measured results in Figure 5.

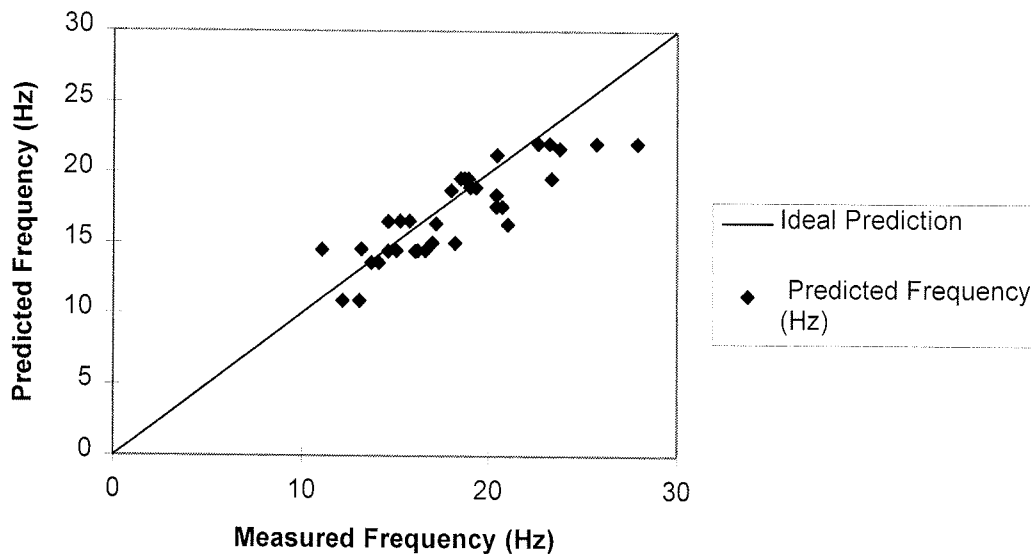


Figure 5 Comparison of Suggested method and Measured Values

7.0 Further Work

As dynamic design methods for timber are an aspect not covered by BS 5268: Part 2, it is likely that designs to EC5 will highlight the importance of this subject.

The prediction of natural frequency forms one of three aspects in the EC5 design method. The issue of unit deflection and response velocity detailed in EC5 have also been incorporated in the research project.

The scope for further investigation in this area is enormous. Some of the many items needing further future investigation include:

- The vibrational performance under periodic excitation (e.g. walking) and design methods to account for the effects of this
- Vibrational performance of engineered timber floor systems
- Further testing to prove/fine tune the suggested method for real floors
- Survey projects to prove/fine tune design limits employed
- Investigation of responses of individual components and the variables associated with these (e.g. proprietary strutting systems, composite joints/box beams, etc.)
- Effectiveness of remedial measures for floors with poor vibrational performance

Acknowledgement

This project was co-sponsored by the Department of the Environment and TRADA. TRADA Technology Ltd. gratefully acknowledges their sponsorship and thanks them for their support.

References

- [1] BSI (1994). *DD ENV 1995-1-1:1994 Eurocode 5: Design of Timber Structures Part 1.1.: General Rules and Rules for Buildings*, British Standards Institution, London, England.
- [2] BSI (1991). BS 5268: PART 2: 1991. *Structural Use of Timber: Part 2. Code of Practice for Permissible Stress Design, Materials and Workmanship*. British Standards Institution, London, England
- [3] BSI (1994), *ENV 1991-1:1994 Eurocode 1 - Basis of Design and Actions on Structures - Part 1 : Basis of Design*. British Standards Institution, London, England.
- [4] OHLSSON, S.V. (1988). *Springiness and Human-induced Floor Vibrations : A Design Guide*, Swedish Council for Building Research, Stockholm.
- [5] OHLSSON, S.V. (1982). *Floor Vibrations and Human Discomfort*. Msc Thesis, Chalmers University.
- [6] BISHOP, R.E.D. and JOHNSON, D.C. (1960) *The Mechanics of Vibration*. Cambridge University Press, Cambridge, UK.
- [7] BARBER, A. (1992) *Handbook of Noise and Vibration Control (6th Edition)*. Elsevier Advanced Technology, Oxford, UK.
- [8] BAINBRIDGE, R.J. (1995). *Vibrational Performance of Timber Floors : Investigation of Results Generated by Computer Programs*, Research Report No PIF119/04a, TTL, UK.
- [9] BAINBRIDGE, R.J. (1995). *Vibrational Performance of Timber Floors :Vibrational Performance Tests on Full Scale Test Floors*, Research Report No PIF119/6b, TTL, UK.
- [10] STARK, J. W. (1993). *The Effect of Lateral Bracing on the Dynamic Response of Wood Floor Systems* MSc Thesis, Virginia Polytechnic Institute and State University.
- [11] RUNTE, D. (1993). *Fundamental Frequencies of I-Joist, Solid-Sawn Joist and Truss Floors based on Tee-Beam Modelling*. Research Report, Virginia Polytechnic Institute and State University.
- [12] SMITH, I. and CHUI, Y. H. (1992). *Construction Methods for Minimising Vibration Levels in Floors with Lumber Joists*. Canadian Journal of Civil Engineering, Volume 19, No.5, pp 833-841.
- [13] HOMB, A., HVEEM, S. AND GULBRANDSEN, O. (1988). *Oscillations in Light-Weight Joist Floors*. Norwegian Building Research Institute.
- [14] THURSTON, S. J. (1993). *Walking Induced Vibrations of Light Timber Floors*. Unpublished report U.P.306, BRANZ, New Zealand.
- [15] CHUI, Y. H. (1986). *Vibrational Performance of Timber Floors and the Related Human Discomfort Criteria*. TRADA, UK.
- [16] WILLIAMS, M.S. and WALDRON, P. (1994). *Evaluation of Methods for Predicting Occupant Induced Vibrations in Concrete Floors*. The Structural Engineer, Volume 72, No 20.

- [17] METTEM, C.J. and BAINBRIDGE, R.J. (1995). *Vibrational Performance of Timber Floors : Study of Design Methods*, Research Report No PIF119/1a, TTL, UK.
- [18] BACHMANN, H. (et al) (1995). *Vibrational Problems in Structures: Practical Guidelines* Birkhauser Verlag Basal Germany.

INTERNATIONAL COUNCIL FOR BUILDING RESEARCH STUDIES AND DOCUMENTATION
WORKING COMMISSION W18 - TIMBER STRUCTURES

MODEL CODE FOR THE PROBABILISTIC DESIGN OF TIMBER STRUCTURES

by

H J Larsen
Danish Building Research Institute
Denmark
and
Lund Institute for Technology
Sweden
S Thelandersson
T Isaksson
Lund Institute for Technology
Sweden

MEETING TWENTY - NINE

BORDEAUX

FRANCE

AUGUST 1996

INTRODUCTION

The Joint Committee on Structural Safety is preparing a probabilistic model code. This code should enable the designer to do a full probabilistic design as an alternative to the partial safety factor design codified for instance in the Eurocodes.

One of the authors was invited to write a section on timber properties and accepted, assuming the advise and assistance of members of CIB W18. It is, therefore, hoped that an ad hoc CIB W18 group could be formed of specialists on the different subjects.

In this paper a first, very rough, draft is presented as a basis for a first discussion of the general format and the structural model to be used. It should also help identify where the necessary data are available or areas where research is needed.

For simplicity's sake, only bending is covered in the following "Draft outline for resistance model for timber". When the principles are established other relevant properties will be included.

DRAFT OUTLINE

RESISTANCE MODELS FOR TIMBER IN BENDING

1. BASIC REQUIREMENT

It shall be verified that the following condition is fulfilled for any member (simply supported or continuous beam) at any time during the intended life of the structure

$$\alpha < 1$$

where α is a parameter expressing the relative damage in the member due to its loading history. $\alpha = 0$ corresponds to undamaged material. $\alpha = 1$ corresponds to failure. ¹⁾

α shall be determined from the following expressions

$$\frac{d\alpha(t)}{dt} = A [\sigma(t)/f_0 - k_0]^b + C \alpha(t) [\sigma(t)/f_0 - k_0]^d \quad \text{for } \sigma(t)/f_0 \geq k_0$$

$$\frac{d\alpha(t)}{dt} = 0 \quad \text{for } \sigma(t)/f_0 < k_0$$

where

- $\sigma(t)$ is the maximum stress in the member at time t ²⁾
- f_0 is the short-term strength, see section 3
- k_0 is a threshold factor given in table 1. It is assumed that no damage accumulates when $\sigma(t) < k_0 f_0$

- b,C,d are factors given in table 1³⁾
- A is a function of f_0 , b, C, d and k_0 to provide model consistency when $\sigma(t)$ is the ramp stress history used to obtain f_{ref} , see section 2.

The parameters A, b, C, d and k_0 are assumed to be constants for a given member, but vary across members.

Table 1 Parameters in the damage model

b		C		d	k_0
mean	c.o.v	mean	c.o.v.		
Species/grade					

Note 1

The damage theory used is the so-called Canadian model, see [Foschi et al., 1989], especially chapter 4. It will probably be necessary to describe the model in an annex indicating also how to calculate more conventional engineering properties, e.g. the residual short-term strength after a load history.

Note 2

The verification is linked to the maximum stress, the stress condition being taken care of by the configuration factor.

Note 3

In [Foschi et al., 1989] values are given for Hemlock and Spruce-Pine-Fir Q1 and Q2. The mean values for b vary between 35 and 160 with c.o.v. between 0.28 and 0.001 (!). For c the mean vary between $1.1 \cdot 10^{-6}$ and $6.6 \cdot 10^{-6}$ with a c.o.v of about 6.7. These big variations require that individual values are given for the different species and grades. For d and k_0 the variations are much smaller and it might be possible to give the same value for all species and grades:

$$d : \text{mean} = 1.2 \quad \text{c.o.v.} = 0.2$$

$$k_0 : \text{mean} = 0.5 \quad \text{c.o.v.} = 0.3$$

2. REFERENCE STRENGTH

The short-term strength is derived from the reference bending strength. The reference strength f_{ref} is the bending strength of a beam with the actual cross-section dimensions⁴⁾ determined by tests in accordance with EN 408 with a test duration of 300 s using test pieces at an equilibrium moisture content resulting from a temperature of 20° and a relative humidity of 65%. If the bending strength is determined by beams with other cross-section dimensions, the following expression should be used to correct the test values

$$f_{ref} = f_{test} \left(\frac{h_{test}}{h_{ref}} \right)^{k_h} \left(\frac{b_{test}}{b_{ref}} \right)^{k_b}$$

where

- h_{test} is the depth of the tested beam
- h_{ref} is the depth of the reference beam
- b_{test} is the width of the tested beam
- b_{ref} is the width of the test beam

and

$$k_b = 0.5$$

$$k_h = 0.2$$

Note 4

Another solution would be to link the reference strength to a standardized cross-section, e.g. 50 x 150 mm as in Eurocode 5.

Note 5

This value is in accordance with the recommendations in [Barret and Lau, 1994].

The distribution of the reference property for the relevant population⁶⁾ corresponds to the higher value⁷⁾ found from:

- a 2-parameter Weibull distribution fitted to the lower 15% of the test values;
- a Normal distribution⁸⁾ fitted to all test values.

Note 6

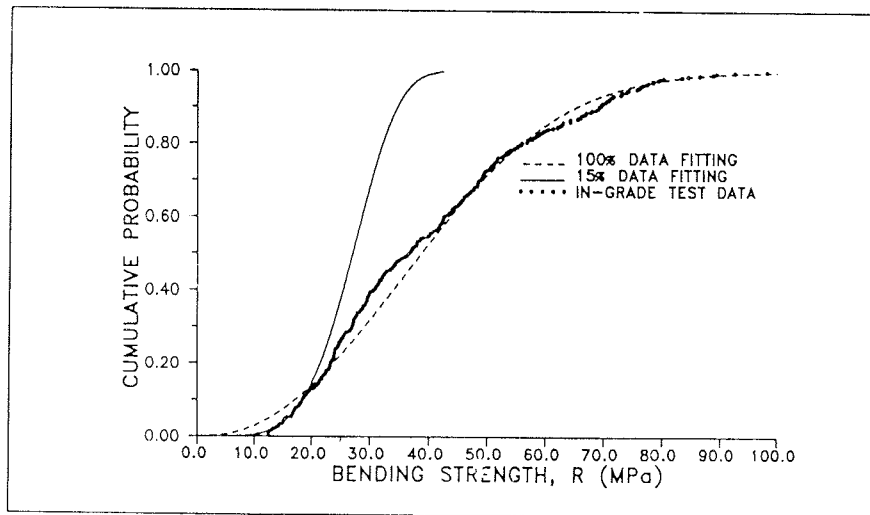
It has to be discussed whether there should be restrictions on the population covered, e.g. requiring a well-known geography or that the material should be graded.

Note 7

This method is proposed in [Foschi, Folz and Yao, 1989] where it is shown that the calculated safety index is very sensitive to the assumed distribution if it is fitted to all test results. The reason being that none of the standardized distributions describe the lower tail adequately: the test values fall below the theoretical distributions, see the figure below. The same trend is found in [Isaksson, 1996]. If the distributions are fitted to the lower part of the test data, the results are much less sensitive to assumptions about the distribution. In parallel with Foschi et al. the truncation is made at 15% and a 2-P Weibull distribution is chosen.

Note 8

The code shall also cover the probabilistic design of systems, where many members interact and for such systems a greater part of the distribution is of importance. For percentiles over about 10% the distribution cannot be described by the truncated distribution. For the central part any of the common distributions - Normal, Log-normal, or Weibull (2- or 3-parameters) - can be used and the simplest, viz. the Normal distribution, is proposed.



2-P Weibull fit to test results from in-grade testing of Douglas Fir. Reproduction of figure 3.2 in [Foschi, Folz and Yao, 1989].

3. SHORT-TERM STRENGTH

The distribution of the short-term strength corresponds to the one for f_{ref} but with a linear affinity in the direction of the abscisse with a factor k . k is a normal distributed variable ⁹⁾ with mean

$$m\{k\} = k_{moist} k_{length} k_{conf}$$

and coefficient of variation ¹⁰⁾¹¹⁾

$$v\{k\} = ?$$

Note 9

Also a log-normal distribution could be prescribed.

Note 10

It is proposed that the variability is assigned to the product. Another possibility is to regard the four partial factors as individual stochastic variables.

Note 11

Another possibility would be to assume k to consist of a deterministic element superimposed by a standard normal (or log-normal) element with mean 0 and a prescribed standard deviation.

k_{moist} takes into account the influence of the moisture content and shall be determined by

$$k_{moist} = \begin{cases} 1 + 6\beta & \text{for } u \leq 6 \\ 1 - \beta(u - 12) & \text{for } 6^2 u \leq 28 \\ 1 - 16\beta & \text{for } 28 < u \end{cases}$$

where u is the moisture content in %, and

$$\beta = ?$$

Note 12

The simplest solution is to give one factor for a species or species combination independent of strength. For softwood in bending, a value of 0.03 may be appropriate taking into account that the geometry at the actual moisture conditions are used for calculating the resistance. Another possibility is in line with [Barret and Lau, 1994] to assume that α depends on the bending strength (f_m) from $\alpha = 0$ for $f_m < 20$ N/mm to 0.035 for $f_m > 80$ N/mm. f_m corresponds either to the mean value of f_{ref} or to the individual value. For softwoods this method might be linked to the strength class system.

k_{length} . This partial factor takes into account the influence of the length and shall be determined from

$$k_{length} = \left(\frac{2.7}{l} \right)^{k_1}$$

where

l is the length in m, and

$$k_1 = 0.2^{13)}$$




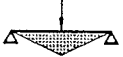



Note 13

This value is in accordance with recommendations in [Barret and Lau, 1994].

k_{conf} . This partial factor takes into account the effect of the configuration (moment distribution). k_{conf} is determined as follows¹⁴⁾

Note 14

One possibility is to calculate the configuration factor assuming that timber is a homogenous material for which Weibull's theory for brittle materials apply. The modification factor can either be given by analytical expressions or as indicated below

BASE	CONSTANT MOMENT AS BASE	3rd POINT LOADING	UDL	RECOMMENDED VALUES FOR CODE PURPOSES
	1.00	0.87	0.84	0.85
	1.15	1.00	0.96	0.95
	1.20	1.04	1.00	1.00
	1.40	1.22	1.17	1.15
	1.40	1.22	1.17	1.15
	1.55	1.35	1.30	1.30
	1.65	1.43	1.38	1.40

Example of table with k_{conf} values. Reproduced from [Madsen, 1992].

in tabular form. A problem with this method is that it is not well suited to handle situations of moment peaks acting over short lengths.

Another possibility is to model timber as a material with weak cross-sections (knots etc.) and assuming that failure takes place only in relation to the weak cross-sections. The spacing of the weak cross-sections and their strength are random variables for which the distribution functions will have to be codified, see e.g. [Canisius, 1994], [Czmoch et al., 1991], [Barrett and Lau, 1994] and [Isaksson, 1996]. If this method is chosen one could of course discuss whether this model should form the basis for the whole code, not only for the configuration effect.

4. CROSS-SECTION

The cross-section dimensions d for a moisture content of $u = 12\%$ may be assumed to be random variables with mean and coefficient of variation as shown in table 3.

Table 3 Cross-section dimensions d . d_0 is target size.

	mean	c.o.v.
Sawn timber in accordance with EN 336		
- Class 1	0.98 d_0	?
- Class 2	0.98 d_0	?
Glued laminated timber in accordance with EN 408	d_0	?
Planed timber	d_0	?

For moisture contents between 6% and 28% the dimensions for moisture contents should be corrected by multiplication by the factor k_u

$$k_u = a_u(u-12)$$

where k_u is 0.002 for softwood and 0.003 for hardwoods ¹⁵⁾.

Note 15

More differentiated values should be given.

REFERENCES

- EN 331 Structural timber, coniferous and poplar - Timber sizes - Permissible derivations. European Committee for Standardization, Brussels.
- EN 390 Glued laminated timber - Sizes - Permissible derivations. European Committee for Standardization, Brussels.
- EN 408 Timber structures - Test methods for solid timber and glued laminated timber - Determination of some physical and mechanical properties. European Committee for Standardization, Brussels.

Barret, J.D. and W. Lau: Canadian lumber properties, Canadian Wood Council, 1994.

Barrett, J.D. and F. Lam: Factors affecting the strength of structural timber. Proc. Pacific Timber Eng. Conf., Gold Coast, Australia, 1994.

Canisius, T.D.G.: Reliability-based configuration factors for timber beams. J. of Structural Safety, 16, 1994.

Czmoch, I., S. Thelandersson and H.J. Larsen: Effect of within member variability on bending strength of structural timber. Proc. CIB/W18A-meeting, Oxford, United Kingdom, paper 24-6-3, 1991.

Foschi, R.O., B.R. Folz and F.Z. Yao: Reliability-design of wood structures. Structural Research Series, Report No. 34, Dept. of Civil Engineering, Univ. of British Columbia, Canada, 1989.

Isaksson, T.: Variability of bending strength within timber elements. Dept. of Struct. Eng., Lund Institute of Technology, Sweden, Report TVBK-1011, 1996.

Madsen, B.: Structural behaviour of timber. Timber Engineering Ltd., Vancouver, Canada. 1992.

